

SEAFLOOR MAPPING OF LONG ISLAND SOUND -

FINAL REPORT: PHASE I PILOT PROJECT

SUBMITTED TO:

THE LONG ISLAND SOUND CABLE FUND STEERING COMMITTEE

STATE OF CONNECTICUT, DEPARTMENT OF ENERGY AND ENVIRONMENTAL
PROTECTION, OFFICE OF LONG ISLAND SOUND PROGRAMS;

STATE OF NEW YORK, DEPARTMENT OF ENVIRONMENTAL CONSERVATION,
BUREAU OF MARINE RESOURCES;

STATE OF NEW YORK, DEPARTMENT OF STATE, OFFICE OF PLANNING AND
DEVELOPMENT;

CONNECTICUT SEA GRANT;

NEW YORK SEA GRANT;

AND

U.S. ENVIRONMENTAL PROTECTION AGENCY, REGIONS 1 AND 2

BY:

LAMONT – DOHERTY EARTH OBSERVATORY COLLABORATIVE
LONG ISLAND SOUND MAPPING AND RESEARCH COLLABORATIVE
NOAA’S OCEAN SERVICE COLLABORATIVE

JUNE 2015

This page intentionally left blank.

Table of Contents

Table of Contents	3
Long Island Sound Cable Fund Steering Committee Organizatons and Members	8
Collaborative Project Teams and Members	9
Acknowledgements	10
Citations	11
Executive Summary	12
Seafloor Topography and Acoustic Intensity	12
Sediment Texture and Grain Size Distribution	12
Sedimentary Environments	14
Benthic Habitats and Ecological Processes: Seafloor & Habitat Characterization	15
Benthic Habitats and Ecological Processes: Infaunal Characterization - LISMARC	16
Benthic Habitats and Ecological Processes: Infaunal Characterization - SBU	17
Benthic Habitats and Ecological Processes: Emergent & Epi-fauna Characterization	18
Benthic Habitats and Ecological Processes: Integrated Ecological Characterization and Habitat Classification	20
Physical Oceanography	21
Data Management	22
1 Introduction	23
2 Seafloor Topography and Acoustic Intensity	26
2.1 Objective	27
2.2 Historical Context	28
2.3 New Data Acquisition	29
2.3.1 NOAA Data Acquisition	30
2.3.2 Stony Brook University Data Acquisition	31
2.4 Integrated Products	35
2.5 Discussion	37
2.6 Summary/Conclusions	37
2.7 References	40
3 Sediment Texture and Grain Size Distribution	60
3.1 Objective	61
3.2 Historical Context	62
3.3 Sediment Sampling and Bottom Photography in Support of Ecological Characterization of Pilot Area	63

3.3.1	Overview	63
3.3.2	Sampling	64
3.3.3	Data processing	64
3.4	Sediment Grab Collection and Analysis	65
3.4.1	Grab Sampling	65
3.4.2	Sediment Grab Sample Processing	67
3.4.3	Chemical Assay	68
3.4.4	Matrix Density	68
3.4.5	Grain Size Analysis.....	68
3.4.6	Revision of SediGraph derived grain size data for LIS13-03 sediment grabs.....	69
3.4.7	Carbon and Nitrogen (CHN) Analysis.....	76
3.4.8	Surface Metal Concentrations and Matrix Density.....	79
3.5	Sediment Texture Interpretations and Other Integrated Products.....	84
3.6	Comparison with Older Data	91
3.7	Summary and Recommendations	91
3.8	References.....	93
4	Sedimentary Environment	95
4.1	Objective	96
4.2	Historical Context	96
4.3	Subbottom Data Collection and Analysis	98
4.3.1	Subbottom Principle.....	98
4.3.2	Data Acquisition	98
4.3.3	Data Processing.....	102
4.3.4	Results.....	102
4.4	Sediment Cores Collection and Analysis.....	106
4.4.1	Sediment Core Collection	106
4.4.2	Sediment Core Processing and Archiving	109
4.4.3	Physical Properties.....	109
4.4.4	Determining Metal Content Using X-ray Fluorescence (XRF).....	109
4.4.5	Sediment Core Descriptions	112
4.5	Sediment Environment Interpretation and other integrated products	112

4.5.1	Sediment Environment Classification.....	113
4.5.2	Interpretation of Different Areas	119
4.5.3	Comparison to Previous Data	121
4.6	Summary and Recommendations	122
4.7	References.....	123
5	Benthic Habitats and Ecological Processes	125
5.1	Objectives and Historical Context	126
5.1.1	Historical Context.....	126
5.1.2	References.....	129
5.2	Seafloor and Habitat Characterization	131
5.2.1	Overview.....	131
5.2.2	Study Area	132
5.2.3	General Approach and Methods	132
5.2.4	Acoustic Analysis by Object-oriented Classification	141
5.2.5	Characteristics of the Acoustic Patches	142
5.2.6	Habitat Analysis by Data Layer Overlay	145
5.2.7	Digital Data Layer Characteristics.....	146
5.2.8	Data Layer Overlay.....	147
5.2.9	Concluding Overview	167
5.2.10	References.....	168
5.3	Infaunal Ecological Characterization - LISMARC.....	171
5.3.1	Field Data Acquisition	172
5.3.2	Infaunal Sample Processing and General Analytical Approaches.....	173
5.3.3	Infaunal Community Characterization and Mapping – October 2012.....	174
5.3.4	Infaunal Community Characterization and Mapping – May 2013	208
5.3.5	Seasonal Changes in Infaunal Communities – Fall 2012 and Spring 2013	230
5.3.6	Historical Comparisons of Infaunal Taxonomic Diversity and Community Composition.....	240
5.3.7	Summary	245
5.3.8	References.....	247
5.4	Infaunal Ecological Characterization - SBU.....	249

5.4.1	Infaunal Sample Acquisition.....	249
5.4.2	Infaunal Sample Processing.....	250
5.4.3	Resulting Infaunal Data	251
5.4.4	Infaunal Data Analysis.....	252
5.4.5	References.....	267
5.5	Emergent and Epi-Fauna Characterization	268
5.5.1	Background and Objectives	268
5.5.2	Image Acquisition & Methods.....	268
5.5.3	Community Structure.....	270
5.5.4	Diversity Measures	271
5.5.5	Species Accounts	273
5.5.6	Inter-seasonal Dynamics.....	273
5.5.7	Historical Analysis: Loss of an Erect Sponge on a Rock Reef at Stratford Shoal..	274
5.5.8	Figures and Tables	280
5.5.9	References.....	371
5.6	Integrated Ecological Characterization and Habitat Classification	376
6	Physical Characterization.....	382
6.1	Objective.....	383
6.2	Historical Context	383
6.3	Physical Characterization.....	384
6.3.1	Physical Oceanographic Data Collection – Time Series Observations	385
6.3.2	Physical Oceanographic Data Collection – Ship Board Observations	386
6.3.3	Resulting Physical Oceanographic Data	387
6.3.4	Physical Oceanographic Analyses	388
6.4	Physical Oceanographic Modeling	388
6.4.1	The Model and Calibration	388
6.4.2	Simulations of the Stratford Shoals Area.....	393
6.4.3	Model Performance Summary	396
6.5	Physical Oceanographic Products.....	397
6.6	Summary and Conclusions	427
6.7	References.....	427

7	Data Management	430
7.1	Objective	431
7.2	LISMARC Data Portal.....	432
7.3	LIS Data Portal and Archive @ LDEO	440
7.3.1	Technical Overview	441
7.3.2	Data System Requirements Described in LIS SOW.....	442
7.3.3	Suggested Guidelines and Workflows to Facilitate Data Management.....	445
7.3.4	How to Browse and Access Data in the LIS Data Portal @ LDEO	446
7.3.5	Data Download Statistics.....	447

Long Island Sound Cable Fund Steering Committee Organizations and Members

US Environmental Protection Agency, Long Island Sound Study
888 Washington Blvd, Stamford, CT 06901
(203) 977-1541

- Mark Tedesco
- Jason Krumholz, Ph.D (NOAA Liaison)

Connecticut Department of Energy and Environmental Protection, Office of Long Island Sound Programs
79 Elm St., Hartford CT 06106
(860) 424-3034

- Brian Thompson
- Peter Francis
- Kate Brown
- Kevin O'Brien

New York Department of Environmental Conservation, Bureau of Marine Resources
205 North Belle Mead Road, Suite 1, East Setauket, New York 11733
(631) 444-0430

- Karen Chytalo
- Charles deQuillfeldt
- Dawn McReynolds
- Sarah Deonarine
- Victoria O'Neill
- Cassandra Bauer

New York Department of State, Office of Planning and Development
One Commerce Plaza Suite 1010, 99 Washington Ave., Albany, NY 12231-0001
(518) 474-6000

- Jeff Herter
- Liz Podowski

Connecticut SeaGrant, University of Connecticut - Avery Point Marine Science Building
1080 Shennecossett Rd, Groton, Connecticut 06340-6048
(860) 405-9128

- Sylvain DeGuise, Ph.D

New York SeaGrant
121 Discovery Hall, Stony Brook University, Stony Brook, NY 11794-5001
(631) 632-6905

- William Wise

Collaborative Project Teams and Members

Lamont-Doherty Earth Observatory of Columbia University Collaborative:

Lamont-Doherty Earth Observatory of Columbia University
61 Route 9W, Palisades, NY 10964
(845) 359-2900

- Frank O. Nitsche, Research Scientist, Ph.D.
- Timothy Kenna, Research Scientist, Ph.D.
- Vicki L. Ferrini, Research Scientist, Ph.D.

Queens College, City University of New York
65-30 Kissena Blvd., Flushing, NY 11367
(718) 997-5000

- Cecilia McHugh, Professor
- Edwige Pichonot Lauture, MA student Queens College, CUNY
- Pariskeh Hosseini, PhD candidate, Graduate Center, CUNY

Stony Brook University
Stony Brook, NY 11794
(631) 632-6000

- Roger Flood, Professor
- Robert Cerrato, Associate Professor
- Glenn Lopez, Professor

Long Island Sound Mapping and Research Collaborative (LISMARC):

University of Connecticut Avery Point, Marine Sciences Department
1080 Shennecossett Rd, Groton, Connecticut 06340-6048
(860) 405-9128

- Ivar Babb
- Peter J. Auster, Ph.D.
- Lauren M. Stefaniak, Ph.D.
- Jim O'Donnell, Ph.D.
- Todd Fake
- Grant McCardell, Ph.D.

University of New Haven
300 Boston Post Rd, West Haven, CT 06516
(203) 932-7000

- Roman Zajac, Ph.D.
- Shannon Penna
- Deena Chadi

- Jaymie Frederick
- Michelle Biegaj

University of Rhode Island
Narragansett Bay Campus, Narragansett, RI 02882-1197
(401) 874-6211

- John King, Ph.D.
- Emily Schumchenia, Ph.D.

US Geological Survey
384 Woods Hole Rd., Woods Hole, MA 02543-1598
(508) 548-8700

- Larry Poppe

National Oceanic and Atmospheric Administration (NOAA) Ocean Service Collaborative:

National Centers for Coastal and Ocean Science (NCCOS):
1305 East West Highway, Silver Spring, MD 20910
(301) 713-3028

- Tim Battista
- Bryan Costa
- Will Sautter
- Gustav Kagesten

Office of Coast Survey (OCS):
1315 East-West Highway, Silver Spring, MD 20910
1-888-990-6622

- CDR James Crocker
- CDR Lawrence T. Krepp

Acknowledgements

This project was made possible by the Long Island Sound Research and Restoration Fund, established by a Memorandum of Understanding among the members of the Policy Committee of the Long Island Sound Management Conference and administered by Long Island Sound Cable Fund Steering Committee.

The Steering Committee would like to thank and acknowledge the following:

- Rob Klee: Commissioner, Connecticut Department of Energy & Environmental Protection
- Joseph Martens: Commissioner, New York Department of Environmental Conservation

- Curt Spalding: Regional Administrator, U.S. Environmental Protection Agency, New England-Region 1
- Judith A. Enck: Regional Administrator, U.S. Environmental Protection Agency, New York-Region 2
- Dr. Kathryn Sullivan: Under Secretary of Commerce for Oceans and Atmosphere and NOAA Administrator
- Northeast Utilities Services Company
- Long Island Power Authority
- Cross Sound Cable, Inc.

Additional thanks to Mark Finkbiener (NOAA Coastal Service Center), Jay Lazar (NOAA Chesapeake Bay Office), Mark Johnson (CT DEEP Fisheries), and Penny Howell (CT DEEP Fisheries) for providing valuable reviews, comments, and suggestions.

Citations

The recommended citations for the overall work and appendices are:

Long Island Sound Cable Fund Steering Committee, eds. (2015). “Seafloor Mapping of Long Island Sound – Final Report: Phase 1 Pilot Project.” (Unpublished project report). U. S. Environmental Protection Agency Long Island Sound Study, Stamford, CT.

Long Island Sound Cable Fund Steering Committee, eds. (2015). “Seafloor Mapping of Long Island Sound – Final Report: Phase 1 Pilot Project Appendices.” (Unpublished project report). U. S. Environmental Protection Agency Long Island Sound Study, Stamford, CT.

The recommended citations for individual sub-sections are provided at the beginning of each section.

Executive Summary

This summary is organized around the thematic topics comprising the structure of the report. The key points listed were extracted from the topical Summary and Conclusion sections where provided; otherwise they were culled from significant points mentioned within sections or communicated by the research teams. Editing for brevity and context was performed.

Seafloor Topography and Acoustic Intensity

- Understanding the geophysical composition and relief of the seafloor is a fundamental precursor for explaining the ecological, physical, sedimentary, and oceanographic components of Long Island Sound.
- While a number of technical approaches can be used to measure the topography and composition of surficial seafloor habitats, given the range of water depth and water clarity within the Pilot Project area, acoustic systems (i.e. ship-mounted multibeam and sidescan systems) were implemented to overcome those challenges.
- Seafloor topography products showing bathymetry and terrain relief are able to depict important features, relief, and seafloor changes. Additionally, acoustics sonars are able to measure the intensity sound reflected off the seafloor to better understand the composition and types of benthic habitats.
- The acoustic products processed for the Pilot Project provided the fundamental spatially organizing information for the analysis conducted in subsequent chapters of the report. The geophysical information contained in the acoustic products conveys important details describing the shape, composition, extent, and composition of surficial features and were used to extract detailed information about benthic habitats, sediment texture, grain size, and sedimentary environments. The acoustic products are used to infer and extract seascape features at a range of spatial scales including fine scale biotopes (Auster et al. 2009) and broader scale geomorphology within Long Island Sound.
- The acoustic products produced a clear demonstration of the value of collaboration. Acquiring data for the size of the Pilot Project area can be a costly endeavor, but close coordination between groups ensured the maximization of the collection area while minimizing data collection duplication so as to produce a valuable product.
- Part of the tasks associated with acoustic data collection included the compilation and evaluation of existing data. While most of the existing data was not used in the final integrated product, it was valuable for planning where field sampling should occur, and identifying locations that would benefit from more contemporary data collections.

Sediment Texture and Grain Size Distribution

- Sediment texture, which includes shape, size and three-dimensional arrangement of sediment particles, is an essential element of any habitat classification.

- In addition to grain size information, the total organic content distribution is of great value for the biological habitat classification since it can be an indicator of biological activity.
- There are abundant old grain size data available, but the seafloor environment is highly variable in places and data several decades old might not reflect the current conditions.
- While acoustic data can provide information on different grain size composition of the seafloor this information does not contain enough details on the composition to discriminate some benthic habitats. Therefore sediment grain size distribution requires analysis of actual samples.
- Data collected include over 300 grab samples (0 – 2cm), along with ~1600 still photos. Video was collected for over ~140 stations by drifting over them along transects ranging from 300 m to 1 km at ~ 0.5m above the bottom.
- Although the initial grain size measurements conducted by LDEO/Queens systematically differed in the clay content from the USGS measurements, this difference was resolved after reexamining the LDEO/Queens data. A comparison of initial sediment grain size distributions obtained from Queens College using a Sedigraph to those obtained from USGS using a Coulter Counter with sample locations in close proximity revealed a significant fraction of fine clay for many samples analyzed with the Sedigraph. This caused a bias towards finer sediment classes in the first interpretative maps. A thorough investigation has revealed that the Sedigraph did not actually measure higher clay content but indicated a high value in the finest fraction which could be corrected through an adjustment of the instruments baseline value.
- The detailed grain size data reveal a larger pattern of grain size distribution with finer sediment in the center west, the north and center east and a patch of finer grain size in the south. Stratford Shoals are dominated by coarser sediments. Sandy sediments are found in the center north and along the southern shore. Despite this larger pattern there are variations on a smaller scale throughout the study area.
- While in most areas the acoustic backscatter data and the grain size data correspond well, there are some locations, e.g. south-east corner, where there sandy sediment do not correspond to high backscatter data. This shows that ground verification is essential for interpreting the acoustic data. Obtaining grain size samples where the biological samples are taken is encouraged to ensure that both data sets are collocated to minimize effects of spatial variability.
- The grain size results can be displayed and visualized in various forms including different classification schemes and interpolated percentages of grain size classes. While for most application it might be useful to use the established, modified Shepard classification scheme some of the additional representations might be useful for other future applications.
- Classification schemes can be useful to highlight major trends in the data, but the distinct boundaries could mask real similarities or differences between the data. Samples with

compositions directly on either side of the boundary could be more similar than samples inside a class.

- Additional analysis on the sediment surface samples including carbon, nitrogen, metals, and matrix density provide valuable, additional information without significant additional cost. In general, we observe higher metal concentration in the northern sections of the study area. The majority of measured lead, zinc, and all copper levels measured in the surface grab samples fall at or below the minimal effects ranges with a small minority of lead and zinc levels falling in the possible effects ranges. No values fell into the probable effect ranges. Lead and zinc surface distribution patterns are quite similar to each other and largely track areas with the highest clay and silt concentrations. To a lesser extent Copper is also elevated in the northern sections. Matrix density is indicative of mineral composition and shows low values in the northwest portion of the study site, while higher values occur in the northwestern portion of the study site.

Sedimentary Environments

- While sediment texture describes the grain size composition, the sedimentary environment describes the processes controlling a certain location such as deposition or erosion. It defines the dynamics of the seafloor in LIS and, therefore, is important for identifying and understanding areas that are stable or changing.
- The sedimentary temporal and spatial record of these processes can be obtained from combining multibeam bathymetry, backscatter, subbottom, and sediment core information.
- Subbottom acoustic surveys collected over 1000 km of survey lines covering nearly all of the pilot area. 23 sediment cores were collected by gravity corer with depths ranging between 45 and 200 cm at an average depth of 125 cm. Another 23 sediment cores were collected by a hydraulic damped corer with depths ranging between 15 and 52 cm at an average depth of 39 cm.
- Subbottom data provide information of the lateral extent of sub-surface layers and changes that enables first order interpretation of the sedimentary environment and allows extrapolation of more detailed information from sediment cores. In addition, subbottom data can also image details of previous anthropogenic changes such as pipelines, cables and dredge channels, which might yield insights on their effects on the environment.
- The high variability of the pilot study area results in many variations of the sedimentary environments. We distinguish several major groups of sediment environments (Depositional, Non-Depositional/Erosional, Dynamic).
- The combination of the different data sets provide insight into the dominant energy levels of the different areas. Based on the composition and type of sediments and layer structure observed in the sediment cores and subbottom data we distinguish High, Moderate/High, Moderate, and Low/Moderate, Low regimes.

- Sediment cores are critical for identifying changes in environments including the temporal distribution of sediments. We found in many of the cores a dramatic change in the sedimentation within 10 to 20 cm down-core. This also means changes in depositional environments and possibly ecosystems within short-time spans. In contrast, some cores showed very similar sedimentation throughout time, which also reveals lack of change in the depositional environment. Developing a short-term chronology from the core data can significantly contribute to a better understanding of depositional processes.
- The pilot area is highly variable and there are locations where additional sediment cores would have been useful to determine the character of these areas, especially in boundaries between different types. At several locations, the deepest sediments recovered contained metal levels that were elevated above background levels. This is most notable in the northeastern section of the pilot area, where we were limited to using the hydraulically damped gravity corer due to weather conditions. Interestingly, we also observe metal concentrations that are higher than those in other areas and collecting additional, longer cores at some of these sites as part of later phases could be useful.
- Sediment environments and related information can be presented in various ways. In this report we offer several options that appear the most useful for us. The goal is to provide the results in different ways and with different degrees of interpretation to allow other users to integrate these results into a wide range of applications and decision-making processes.

Benthic Habitats and Ecological Processes: Seafloor & Habitat Characterization

- Acoustic backscatter data derived from several NOAA surveys were effectively used to identify large scale seafloor elements that had specific ranges of acoustic / image properties using image segmentation techniques. These elements are referred to as acoustic patch types, and six specific types were identified.
- The analysis of grab data from sediment sampling cruises in fall 2012 and spring 2013 provided the basis to assess the sedimentary characteristics (percent of gravel, sand, silt, clay) associated with the acoustic patch types comprising the seafloor landscape in the pilot study area. These analyses indicated that each acoustic patch type is associated with a distinct composition of each of these four general sediment types, but that there could be significant spatial variation within acoustics patch types. The six sedimentary compositions were Silt-Clay/Sand, Silt-Sand-Clay, Silty, Clayey Sand, Sand, Gravelly Sand, and Gravel-Sand.
- Several additional variables were used to characterize the acoustic patch types including bathymetry, terrain roughness index (TRI), bottom stress, and slope. These variables were used in addition with percent silt clay to identify and map potential habitat heterogeneity within acoustic patches.
- The analysis of the acoustic data and the identification of the large scale acoustic patch types (on the order of greater several km²) and the meso-scale sub-habitats (on the order

of lesser than km²) within them provides several of the modifiers described in the habitat classification scheme proposed by Auster (2009) that can be incorporated into the classification of LIS. These can be integrated with additional modifiers including anthropogenic processes, chemical processes, and biological processes to further develop the classification scheme.

Benthic Habitats and Ecological Processes: Infaunal Characterization - LISMARC

- Infaunal communities were sampled in fall 2012 and spring 2013, providing the opportunity to assess temporal variation of infaunal communities in the pilot study area relative to sea floor habitat structure. The sampling efforts differed between research cruises and only a subset of the areas sampled in 2012 were also sampled in 2013.
- A total of 101 grab samples and 60 grab samples (0-2 cm) were processed from the October 2012 and May 2013 research cruises, respectively that also provided the sediment grain size data. Photos and video collected were also used.
- The characteristics of benthic infaunal communities (abundance, diversity, community composition) were related to the acoustic patch types identified and varied relative to the habitat heterogeneity within and among acoustic patch types. Thus, acoustic mapping and related characterization can provide information on potential general characteristics of the infauna inhabiting the delineated seafloor habitat patches.
- Abundances in patch types with coarser sediments had higher total abundances than patch types with progressively muddier sediments in both fall and spring. These patches also had higher total abundances in the spring compared to the fall. Other acoustic patch types had relatively similar mean total abundances among fall and spring sampling dates, although seasonal differences in total abundance were spatially variable. Total abundance tended to be highest along the flanks of Stratford Shoal and transitional areas among patch types.
- A high number of infaunal taxa / species were found in the pilot study (242 in October 2012, 171 in May 2013). Mean taxonomic richness per 0.1 m² sample was progressively higher with increasing percentages of sand and gravel in acoustic patch types. This trend was consistent in both fall and spring. Seasonal differences within specific patch types were generally not significant, except in the patch type where sediment composition consisted mainly of coarse sands and gravel. Taxonomic richness was general highest on or along the flanks of Stratford Shoal and in the southeast section of the pilot study area in muddy sand and sand acoustic patch types.
- Taxonomic diversity (a combination of both taxonomic richness and the relative abundance of species) was variable among acoustic patch types and also seasonally with specific patch types. Two different diversity measures (Shannon diversity H' and Fisher's α) were used to assess the consistency of the patterns. In both cases, within-patch diversity was higher in the fall in patches characterized by sandy sediments, and higher in the spring in patches with either coarse or muddy sediments. The variation in these

trends was such that there were few statistical differences in seasonality, but differences among patch types were significant. Infaunal diversity was similar through large portions of the pilot study area, and areas of relatively high diversity found in most acoustic patch types. Thus, the spatial trends in infaunal diversity were complex, with no clear trend that could be associated with general environmental attributes such as depth or sediment type.

- Community structure (taxonomic composition and relative abundances) was relatively distinct among acoustic patches in both fall and spring, with differences in the mix of dominant taxa and the relative variation in community structure. Acoustic patch types with predominantly sandy sediments had the most variable communities, whereas communities in patches with muddy or coarse grained sediments were less variable. The most variability on community structure was found in the acoustic patch type that was located in sandy areas in the southern portions of the pilot area and along the flanks of Stratford Shoal. Community structure also varied depending on whether they were located along transition zones among acoustic patch types or located within the interior of a particular patch types. The transition zones appear to have more diverse / complex communities.
- The overall results of the infaunal analyses indicate that these communities and their characteristics can be closely related to the acoustic patch types identified through the habitat characterization analyses. Furthermore, the level of variation in community characteristics and their patterns of spatial and, to a lesser extent, temporal variability have been identified for these various patch types.
- A comparison of data collected from the mid-1990s with the results of the 2012/13 pilot study revealed that there has potentially been a significant increase in the overall diversity of the infaunal communities within a portion of the pilot study area (specifically the northeast and eastern central section where the 1995/6 sampling was done).

Benthic Habitats and Ecological Processes: Infaunal Characterization - SBU

- Three contrasting areas near Stratford Shoal were identified, each consisting of a homogeneous bottom type and on the basis of backscatter were expected to represent Sand, Mud, and Sandy Mud bottom types. Ten sampling stations were randomly positioned within each area, with sampling stations constrained to be at least 100 meters from the area boundary and any other station. Faunal and sediment sampling was conducted aboard the R/V Pritchard on 6/18/2013 and 9/11/2013. Bottom samples were collected using a modified van Veen grab (0.04 m²).
- A total of 5,640 animals representing 95 taxa were collected in the 30 samples. Average abundance across all 30 samples was 188 individuals per sample. Of the 95 taxa, 42 were polychaetes, 26 were crustaceans, 22 were molluscs, and the remainder (5) was distributed among other groups. Numerical dominants included the polychaetes *Amphitrite artica*, *Paranois gracilis*, and *Polygordius* spp., as well as the amphipods

Ampelisca vadorum and *Leptocheirus pinguis*. These 5 taxa represented about 60% of the total number of individuals collected.

- Average faunal abundances in each area were 442 individuals per sample for Sand, 85 individuals per sample for Mud, and 37 individuals per sample for Sandy Mud. The average number of species per sample was 30 for Sand, 15 for Mud, and 9 for Sandy Mud.
- Largely because of cost, benthic community assessment and monitoring programs rarely collect more than a few replicate grab samples within a habitat. While this standard practice adequately characterizes abundant species, rare species are largely missed. Therefore, a small grab sampling study was designed to determine the number of samples needed to estimate the occurrence of rare species within a habitat (i.e., bottom type.)
- The Chao 2 species richness estimator was used to estimate the number of species present and the fraction of species collected in each bottom type.
- Species accumulation curves, Chao 2 estimates, and the fraction of species collected all fell within the range found for other local studies in the Peconics and in bays along the North Shore of Long Island. Combining all the studies, it is clear that three replicate samples in a habitat, a value often used in benthic studies, would recover only 13-50% of the species present. Even at 10 samples, there is evidence for under sampling in many of the habitats. In the present study, for example, 10 samples recovered only about 60% of the species in Mud bottom types. (Seasonal effects were not part of the study design.)

Benthic Habitats and Ecological Processes: Emergent & Epi-fauna Characterization

- Seafloor imagery was collected during fall 2012 and spring 2013 using three undersea platforms. All acquired digital imagery orthogonal to the seafloor (10-17 October 2012, SEABOSS, 2800 images; 12-13 December 2012, ISIS, 297 images; 13-15 May 2013, Kraken 2, 493 images; 21-24 May 2013, SEABOSS, 1155 images). Images with water turbidity that obscured the seafloor or that were out of focus such that identification of all organisms or biogenic features was impeded were rejected. This step produced a total of 574 processed images for analysis from fall 2012 sampling (SEABOSS = 517 images, ISIS = 57 images) and 630 images for spring 2013 (Kraken2 = 49 images, SEABOSS = 581 images).
- Community structure:
 - Multivariate dispersion indices for both fall and spring confirm that variation in community composition can be explained in part based on differences between groups of samples assigned to Ecognition (acoustic) patch types.
 - Those taxa and features that consistently contributed the greatest to defining unique community compositions include: *Astrangia poculata* (coral), *Crepidula fornicata* (slipper shell limpet), *Mytilus edulis* (blue mussel), barnacle spp., *Corymorpha pendula* (hydrozoan), *Bostrichobranchus pilularis* (solitary ascidian), shell (both intact and broken shell hash), and burrows, among others.

- The overlap observed in the multi-dimensional scaling cluster groupings for both seasons is indicative of the patchy nature of the sedimentary environment and related factors (e.g., slope as it affects small scale erosional and depositional patterns as well as areas where shell and other biological debris accumulate). High spatial variation in assignments of community type by sample unit was common within sample blocks in areas of patchy sedimentary settings
- Diversity Measures – Sampling Effort
 - Species accumulation curves for all species and biogenic features within selected sampling blocks from the initial fall 2012 cruise illustrate adequacy of image sampling. Richness estimators for all fall sampling blocks also suggest effort in most blocks was adequate for mapping purposes. That is, dominant fauna in most blocks were accounted for although greater effort would yield more taxa or features.
- Diversity Measures – Seasonal Variation
 - Examination of diversity maps for richness and summary statistics reveals similar patterns diversity. In general, both measures were higher within each season along the shallower coarse grained regions of the pilot area in contrast to the deeper fine grained region. Further, diversity was higher overall in the spring than during the fall season.
 - Seasonal differences were most pronounced in the deeper fine grain sediments where spring recruitment of species with annual life histories occurred, although spatial patterns of diversity were patchy. Observed richness versus predicted richness based on multiple richness estimators suggests that sample sizes within acoustic patch types were adequate.
 - The greatest differences between observed and estimates of species richness came from the most diverse habitats, those shallow coarse grain features bathed in waters above basin depths. That said, existing samples did differentiate those habitats based on mapping community types.
- Diversity Measures – Species Accounts
 - Three examples are useful in illustrating linkages between species and biogenic feature distributions at small spatial scale. Northern star coral (*Astrangia poculata*) settles and grows on stable hard substratum such as cobble and boulder size rocks. The pilot scale map of coral reflects this distribution but when examined at fine scale, the patchy nature of coral occurrences and variability in cover emerges and is correlated with Ecognition (acoustic) patch types F and E. Blue mussel (*Mytilus edulis*) also exhibits an affinity to stable sediments although the species can settle and grow on a wider range of grain sizes. Dense aggregations of blue mussel were found in the sand wave habitat in the northern region of the study area and occurred in troughs of the sand waves. Lastly, dense

aggregates of shell, an important biogenic feature, are found downslope of the crest of the southern shoal.

- Diversity Measures – Interseasonal Dynamics
 - Diversity measures within sampling blocks exhibited highest levels of diversity on the crests of Stratford Shoal within transition areas for both fall and spring but highest diversity values occurred in the spring. Shallow communities characterized by relatively long-lived species, exhibited a high degree of stability across seasons while deeper fine grain sedimentary settings, characterized by short-lived solitary and colonial species exhibited a high degree of change due to spring recruitment dynamics. Contrasts between fall and spring distributions of *Bostrichobranchus*, *Corymorpha*, and amphipod tubes illustrate some of the most dramatic seasonal differences at the spatial scale of the pilot area. As with small-scale variation of community classification and patterns of cover by taxon or feature, there was a high degree of small-scale variation in diversity both within and between seasons within habitats.
- Diversity Measures – Historical Analysis
 - Long term observational data suggested 20+ years of community stability. However, surveys from the Pilot Mapping Program indicate the loss of *Haliclona oculata* (branching sponge) a previously dominant taxa. However, lack of systematic monitoring and local process studies precludes any understanding of the fine time scale dynamics of change in this community, allowing us to only hypothesize what the drivers of change may be.

Benthic Habitats and Ecological Processes: Integrated Ecological Characterization and Habitat Classification

- Integrating the analyses of spatial and seasonal variation of infaunal and epifaunal communities produced notable results. Of particular interest is the consistent patterns in high diversity of both infaunal and epifaunal taxa along the crest and slopes of Stratford Shoal as well as sloping environments to the southwest and southeast off the north shore of Long Island. This pattern persists using simple species richness (S) and Shannon diversity (H') across seasons and despite sampling at fewer targeted blocks in the spring.
- An integrated habitat map links acoustic patch types to mean bottom tidal stress and the defining ecological characteristics of infauna, epifauna, and biogenic features. Notable is the faunal response to the general gradient in grain size from acoustic patch types A to F (i.e., fine to coarse) along with the concomitant gradient of increasing tidal stress. The trend here is between these characteristics of the physical environment, the shifts in infaunal taxa, the shift from short-lived to long-lived fragile epifaunal species, and the shift from burrowed sediments to high coverage patches of biogenic shell.
- It is important to acknowledge that data to characterize infaunal and epifaunal communities was collected in fundamentally different ways (i.e., grabs versus imagery).

Therefore, comparisons between diversity measures for infauna and epifauna are relative. Future sampling effort should incorporate an element to better integrate epifauna with infauna for statistical comparisons, such as replicate airlift sampling of patch sizes comparable to grabs within each sampling block.

Physical Oceanography

- A high resolution circulation and hydrographic model, an implementation of the Finite Volume Community Ocean Model (FVCOM), was used to predict currents, temperature, salinity and bottom stresses in the study region.
- Six instrumentation platforms were deployed on the bottom of LIS between December 2012 and September 2013 collecting current profiles and water temperature and salinity. These were complimented by two survey cruises in October 2012 and June 2013 collecting temperature and salinity data. Additional information used in the model calibration process were derived from NOAA tidal data, CT DEEP water quality sampling cruises, USGS/Woods Hole climate data, and offshore bouys.
- The model was used to produce spatial data and mapping products of:
 - bottom temperature and salinity distributions throughout the study area for each month;
 - spatial structure of the mean and maximum bottom stress magnitude due to (mainly) tidal currents;
 - spatial structure of the maximum bottom stress magnitude during a simulation of super Storm Sandy
 - spatial structure of the maximum bottom stress magnitude during the entire simulation period excluding those during super Storm Sandy
- The comparison of the model simulations to temperature, salinity, current and bottom stress measurements all show excellent agreement. In the study region, model temperatures were generally within $\pm 1^{\circ}\text{C}$ of measured values, salinities within ± 0.25 ppt, and stresses within $\pm 30\%$. Note, however, that the estimation of stresses through measurements is also imprecise and that discrepancies between predictions and observations in the stresses may arise from the model's underestimation (or inability to represent) higher frequency and finer scale motions. This issue could be improved upon by running a higher resolution model in a particular area of interest.
- The spatial and temporal structures of the temperature, salinity, and stress fields captured by the model show excellent agreement with the field studies and clearly support the model's use as a tool to interpolate spatially between the observations for the purpose of making maps of the characteristics of the bottom environment that are ecologically important.

Data Management

- The data management efforts of the Pilot Project are intended to (1) ensure that partners have access to data during the project to facilitate the creation of final data products, (2) ensure long-term preservation and open access to data generated during the Pilot Project, and (3) establish and refine procedures and protocols for documenting, sharing and archiving data that may be acquired during subsequent efforts.
- In order to meet the needs of all partners with respect to access to data, two parallel data management efforts were undertaken. While these two efforts share some common elements, they provide technical solutions for two different use-cases. The LISMARc data portal provides infrastructure for direct machine access to a subset of data with a focus on data access by numerical models. The LIS Data Portal at LDEO provides a comprehensive metadata catalog and long-term data stewardship solution focused on open access and preservation of all data products (raw and derived) and metadata, ensures compliance with metadata standards, and includes links to related content in distributed data systems.
- Guidelines and workflows have been developed to facilitate data management and integration into the LIS Data Portal @ LDEO, which is responsible for ensuring long-term data curation. The Data Management Efforts undertaken as part of the Pilot Project demonstrate that existing infrastructure can be used to manage data acquired through this effort.

1 Introduction

In 2002 a Connecticut legislative task force found there was a lack of substantial scientific information regarding the seafloor habitats of Long Island Sound (LIS), which hampered the ability to properly respond to and address topics such as the placement of large scale in-water utility infrastructure. A subsequent review by the Connecticut Academy of Science and Engineering identified similar data gaps and deficiencies with respect to benthic species and habitat identification, as well as general mapping and ocean management needs. In 2004, the Connecticut Department of Energy and Environmental Protection (DEEP) resolved two non-compliance issues with LIS electric cable projects involving both Connecticut and New York utility companies. As part of the settlement, a fund seeded with \$6M for research and restoration was created. The Long Island Sound Study, a US EPA National Estuary Program, signed an agreement among members of its policy committee and determined the fund should support new projects that enhance Long Island Sound, promote improved scientific understanding of potential energy infrastructure effects/mitigation of their impacts, and emphasize benthic mapping as a priority need for improved management decisions.

To manage this effort a Steering Committee was formed consisting of representatives from DEEP, US EPA Regions 1 & 2, New York Department of Environmental Conservation, New York Department of State, and the SeaGrant offices of Connecticut and New York. While the committee works in a joint administrative capacity, financial management of the fund is the sole responsibility of DEEP staff. By 2007, the Steering Committee, DEEP, and the University of Connecticut hosted a workshop that tasked regional state, federal, and non-governmental groups to further identify the specific management needs of LIS and how a mapping program could address them. Beginning in 2009 the Steering Committee began to develop the outlines for a benthic mapping program for LIS and formed a collaborative partnership combining national and local expertise and resources. The partners include the National Oceanic and Atmospheric Administration Biogeography Branch and two regional academic consortiums led by the University of Connecticut and Columbia University's Lamont Doherty Earth Observatory.

By 2011, the Steering Committee and partners developed a plan to prioritize areas of LIS by evaluating areas of interest identified by stakeholders based on issues including ecological value, multiple use conflicts, compliance, resource management and potential for further development. Using these high priority areas as a guide, a pilot area was selected. (Figure 1-1) It was expected that by selecting a smaller geographic area to focus on first, the success of completing the larger LIS project area would increase while simultaneously reducing the risk threshold of failure or impact of corrective measures if warranted.

There were two overarching goals for the Pilot Project: 1) define and implement the specific technical components for a mapping program, and 2) assess the overall management of the Pilot Project.

The objectives to achieve the first goal of the pilot included tasks designed to:

- Investigate and evaluate existing data and products that could be incorporated into data products;
- Define the data acquisition approaches and standards for the key data (bathymetry, backscatter, biological/ecological and physical observations) and acquire additional data to fill existing gaps;
- Test technologies and approaches for shallow water mapping;
- Develop, assess and refine data products with a focus on the key derived products (geology, benthic habitat characterization and topography);
- Implement and assess a LIS habitat classification scheme (Auster et al 2009) and;
- Develop a data management strategy (internal and external dissemination & archival).

The contents of this document provide a report on the processes and outcomes of the above objectives.

From the management perspective the pilot will be assessed as to how well the project met the following objectives:

- Establishing a coordinated teaming approach across the participating Consortiums;
- Developing, implementing, and evaluating a technical approach, including logistics and QA/QC protocols;
- Developing procedures that optimize the use of existing data products and data as appropriate;
- Increasing the opportunity of supportive data collection efforts by Federal agencies (i.e. NOAA); and
- Providing metrics on the costs, logistics, and effort needed to produce the desired deliverables.

These elements, along with the material presented in this report, will be reviewed by the LIS Steering Committee to determine the management structure and product parameters required for work plans that can guide future efforts.

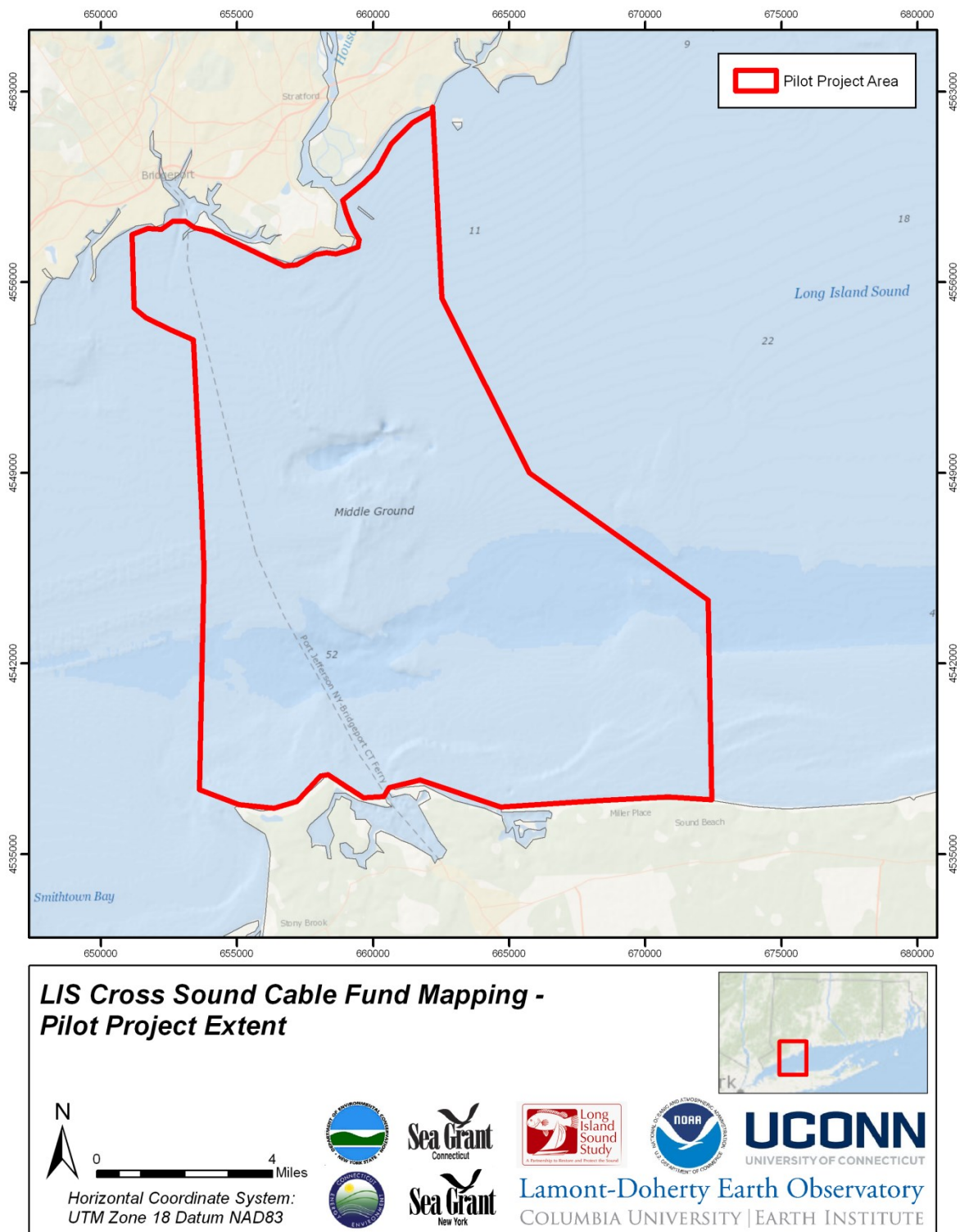


Figure 1-1: Pilot Project Extent

2 Seafloor Topography and Acoustic Intensity

Recommended Citations:

Battista, T. (2015). Objective. Section 2.1, p. 27-28 in: “Seafloor Mapping of Long Island Sound – Final Report: Phase 1 Pilot Project.” (Unpublished project report). U. S. Environmental Protection Agency, Long Island Sound Study, Stamford, CT.

Battista, T. (2015). Historical Context. Section 2.2, p. 28-29 in: “Seafloor Mapping of Long Island Sound – Final Report: Phase 1 Pilot Project.” (Unpublished project report). U. S. Environmental Protection Agency, Long Island Sound Study, Stamford, CT.

Battista, T. and R. Flood. (2015). New Data Acquisition. Section 2.3, p. 29-35 in: “Seafloor Mapping of Long Island Sound – Final Report: Phase 1 Pilot Project.” (Unpublished project report). U. S. Environmental Protection Agency, Long Island Sound Study, Stamford, CT.

Battista, T. (2015). Integrated Products. Section 2.4, p. 35-37 in: “Seafloor Mapping of Long Island Sound – Final Report: Phase 1 Pilot Project.” (Unpublished project report). U. S. Environmental Protection Agency, Long Island Sound Study, Stamford, CT.

Battista, T. (2015). Discussion. Section 2.5, p. 37 in: “Seafloor Mapping of Long Island Sound – Final Report: Phase 1 Pilot Project.” (Unpublished project report). U. S. Environmental Protection Agency, Long Island Sound Study, Stamford, CT.

Battista, T. (2015). Summary/Conclusions. Section 2.6, p. 37-39 in: “Seafloor Mapping of Long Island Sound – Final Report: Phase 1 Pilot Project.” (Unpublished project report). U. S. Environmental Protection Agency, Long Island Sound Study, Stamford, CT.

2.1 *Objective*

Understanding the geophysical composition and relief of the seafloor is a fundamental precursor for explaining the ecological, physical, sedimentary, and oceanographic components of Long Island Sound. This chapter describes activities undertaken to plan for, collect, and process data for two product types – Seafloor Topography and Acoustic Intensity – within the Pilot Project area of LIS. While a number of technical approaches can be used to measure the topography and composition of surficial seafloor habitats, given the range of water depth and water clarity within the Pilot Project area, acoustic systems (i.e. ship-mounted multibeam (MBES) and sidescan sonar systems (SSS)) were implemented to overcome those conditions. Acoustic systems use sonars to actively ensonify the seafloor, providing a valuable means to acquire synoptic, continuous data for a project area. The multibeam and interferometric sidescan sonars (also known as Phase Differencing Bathymetric Sonars -PDBS) used also provide the additional benefit of being able to simultaneously collect coincident depth and intensity (e.g. backscatter) measurements.

There are benefits and weaknesses for each of the acoustic systems (i.e. MBES, SSS, and PDBS) used in Project. All of the sonar systems actively emit and record sound at frequencies determined by the model used. The lower the sound frequency used equates to deeper water penetration, but conversely a larger detection footprint which equates to lower data resolution. Higher frequency systems are optimum for surveying shallow estuaries like LIS since they are able to detect to the maximum depth, but provide the highest resolution of data needed to discern fine-scale topography and feature types. MBES are the most ubiquitous sonar system used for hydrographic and seafloor mapping efforts. These systems have the benefit of being able to collect very dense, highly accurate bathymetry and backscatter data. The drawback of MBES systems is that the swath is a function of water depth, hence their efficiencies are much reduced as water depth decreases. Alternatively, SSS and PDBS broadcast sound at low grazing angles from each side of the sonar, providing much broader bottom coverage. SSS provide very dense backscatter/intensity measurements of the seafloor, but no bathymetry. PDBS are a variant of SSS with the added benefit of being able to also calculate bathymetry. The weakness of PDBS is that depth measurements are generally less accurate further from the sonar, in effect negating the benefit of broad swaths if bathymetric certainty is required.

Acoustic sonars provide highly resolved, accurate measurements of absolute water depth (i.e. bathymetry), but also data collected can be used to depict changes in the seafloor shape (i.e. topography) to highlight seascape changes at a range of spatial scales. Seafloor topography products showing bathymetry and terrain relief are able to depict important features, relief, and seafloor changes to better explain physical, geological, and ecological processes. Additionally, acoustics sonars are able to measure the intensity of sound reflected off the seafloor to better understand the composition and types of benthic habitats. There is a strong relationship between the amount of sound reflected or absorbed by the seafloor based on the hardness, roughness,

grain size, or biological composition of bottom features. Acoustic intensity products provide a valuable means of synoptically measuring and depicting the composition, roughness, and texture of the seafloor to map and identify the distribution of benthic habitats.

The LIS Seafloor Mapping Project also had the additional benefit of bringing together a collaboration of federal, state, and academic partners to identify and fill significant data gaps within the Sound. This chapter describes activities undertaken through the collaborative to maximize coordination, data coverage, product utility, and use/reuse of the data collected for the Pilot Project.

2.2 *Historical Context*

Hydrographic mapping of LIS has provided nautical charts to commercial and recreational mariners for nearly two centuries. Charts provide depth soundings and other details to promote safe navigation, however traditionally these data have been underutilized to support coastal and marine planning purposes. During the LIS seafloor mapping project planning phase, the team recognized the need to explore and identify existing hydrographic charting data within the Pilot project area and to reuse those data to the extent possible. Furthermore the team would evaluate the utility of these existing data, exploit the existing data for strategic planning activities, and reacquire additional data as necessary.

Two bathymetric and sidescan surveys were identified as having been conducted by NOAA covering the northern two-thirds of the study area. These surveys were conducted by the NOAA Ship *Rude* off of Bridgeport, CT from 2001(H11044) and 2003 (H11045). It was determined that the data type and coverage by the *Rude* was sufficient to warrant complete reprocessing. In particular, the bathymetry and sidescan from the *Rude* contained enough valuable information on the depth, composition, and features of the seafloor to create a baseline habitat map in the area of interest for marine spatial planning. In addition, more contemporary data processing techniques would support extracting a more uniform, higher resolution, and continuous digital elevation model than was previously possible.

The two *Rude* surveys were originally collected and processed to support nautical charting updates and for identifying obstructions to safe navigation. Survey H11044 collected bathymetry data using an Odom Echotrac DF3200 MKII Dual Frequency Vertical Beam Sensor (VBES) and a Reson Seabat 9003 Shallow Water Multi Beam EchoSounder (SWMB, MBES). Object detection was done using an EdgeTech 272T/ACI Side Scan Sonar (SSS) system. Survey H1105 used the same VBES system, with the addition of Reson 8125 MBES sonar for bathymetric mapping and a Klein 5000 sidescan sonar for object detection.

The VBES and the MBES data from both sensors were cleaned and reprocessed in CARIS HIPS 8.0 to produce Concurrent Uncertainty Bathymetry Estimator (CUBE) surfaces. The CUBE surfaces were exported as georeferenced XYZ files and imported into ArcGIS, where they were interpolated into 1 m grids and merged into an integrated bathymetry surface. However, after

evaluation of the uncertainty surface of the CARIS derived bathymetric surface, it was determined that additional processing techniques were necessary to better account for the impact of non-continuous source data distribution. In particular, the VBES data had large gaps in data coverage between survey lines and the multibeam data was collected according to sidescan coverage. Hence, while the MBES provided far greater data density than VBES data in locations where it was collected, there were still gaps between survey lines. The final processing approach chosen was to import all the VBES and MBES data into SURFER 11 and interpolate a new elevation model using distance weighted kriging geostatistical technique to 5 m resolution using approximately 5 million data points. Using SURFER, the data interpolation was up-sampled using spline to produce a final 1 m digital elevation model which was then exported as a GeoTiff and ArcGIS raster grid (Figure 2-1).

The standard deviation of depth (m) in the kriging derived bathymetry model varied between 0 m in the data rich multibeam covered areas to as much as 10.3 meter in the regions with the lowest data density. The total seafloor area covered with multibeam sonar was 106 km² and in this area the mean standard deviation of depth was 0.001m. The remaining area of 83.4 km² had significantly lower data density and consisted of a mix of single beam sonar surveys. In this area, the mean standard deviation of depth was 3.19 m. The standard deviation of depth values reported here does not include the uncertainty of the sonar measurements therefore the total uncertainty of the bathymetry model is likely to be higher.

The sidescan data collected by the *Rude* was reprocessed using CARIS 8.0 Geocoder in block segments. These block segments were normalized for uniformity, mosaicked together into one product using ENVI 5.1 and exported as a GeoTiff and ArcGIS raster grid (Figure 2-2).

The reprocessed data from these *Rude* bathymetry and side-scan sonar surveys was available to the project prior to field data collection, and the results were used to help plan ship-based activities during the Pilot Project.

2.3 *New Data Acquisition*

Through the collaborative partnership, a number of new ship-based surveys were conducted within the Pilot Project area (Figure 2-3). These efforts include significant surveys conducted by NOAA's Office of Coastal Survey that includes extensive survey coverage both inside and outside the Pilot Project area. For purposes of this report and effort, only data within the Pilot Project area were included. Additionally, significant collections were conducted by Stony Brook University. The details of both efforts are explained in subsequent sections. Two small surveys conducted by the University of Rhode Island as part of the collaborative mapping effort are not included in this report as details about the collection efforts were not provided to the writing team and sufficient information regarding data referencing was not made available to effectively integrate the URI data with the remaining datasets into a seamless composite.

2.3.1 NOAA Data Acquisition

The Long Island Sound Mapping and Research Collaborative conducted a spatial prioritization in April 2012, and determined a large expanse of the Pilot Project needed to be surveyed off the coast of Port Jefferson, NY in the southern section of the area of interest (Figure 2-3). The OCS planned to survey the remaining area using the NOAA Ship *Thomas Jefferson* and its two 24 foot inshore launch vessels (3101 and 3102). The 4 x 11.5 square mile area was divided into three survey sheets: H12416, H12417, and H12488. The three surveys were carried out from May 19th to August 7th, 2012 using Reson 7125 MBES systems for bathymetry and backscatter.

Backscatter data was planned to be collected simultaneously with the 100% multibeam coverage and recorded using Hypack 2012 MBES acquisition software. Representatives of the Integrated Ocean and Coastal Mapping Team (IOCM) and a Biogeography Branch contractor were brought onboard the *Thomas Jefferson* to perform daily quality control measures to ensure the survey technicians collected calibrated backscatter while they fulfilled their requirements to produce nautical charts. The surveys complied with International Hydrographic Organization (IHO) Order 1 standards for nautical charting, as well as provided high resolution imagery of the seafloor for the benthic habitat assessment.

The *Thomas Jefferson* collected bathymetry for the waters deeper than 30 meters, while the inshore launch vessels 3101 and 3102 surveyed the shallower areas (30 to 0.841 meters). Positioning and attitude for the *Thomas Jefferson* and the launch vessels were determined using a TSS POS MV™ (Position and Orientation System for Marine Vessels) systems and utilizing a Trimble DSM-212L DGPS™ (Differential GPS). Sound velocity profiles were acquired with a Seabird Electronics SeaCat SBE19P CTD profiler and processed using NOAA's Velociwin V8.85 software, then applied directly to the raw data. Data was reduced to Mean Lower-Low Water (MLLW) using verified tides from NOAA's Center for Operational Oceanographic Products and Services (CO-OPS), based on National Water Level Observation Network (NWLON). The sound velocity profiles and the changes in the tides were applied to a 1 m resolution bathymetric surfaces that were generated in CARIS HIPS and SIPs 8.0.

The bathymetry from the *Thomas Jefferson* was submitted to the Atlantic Hydrographic Branch (AHB) for final verification of depths, object detection, and an overall quality assessment. The Combined Uncertainty and Bathymetry Estimator (CUBE) surfaces were carefully reviewed by NOAA hydrographers, and any remaining artifacts in the bathymetry were cleaned.

Acoustic intensity data was logged by the NOAA vessels during multibeam acquisition (i.e backscatter). Representatives of the Integrated Ocean and Coastal Mapping Team (IOCM) and a Biogeography Branch contractor were brought onboard the *Thomas Jefferson* to perform daily quality control measures to ensure the survey technicians collected clean backscatter while they fulfilled their requirements to produce nautical charts. The backscatter data also had to meet the IHO standards for object detection as well. The Reson 7125 collects backscatter in "snippets" that are recorded in .7k files in Hypack. The backscatter snippets were geometrically and

radiometrically corrected using Fledermaus Geocoder Toolbox 7.1 and were mosaicked and exported into a 32-bit floating point GeoTiff.

2.3.2 Stony Brook University Data Acquisition

Two areas were mapped by SoMAS at Stony Brook University. SBU mapping activities started on March 18, 2013 and ended on September 18, 2013; both dates were about 1 year later than anticipated in the project schedule because of delays in the contracting process. Mapping activities started shortly after a contract was in place. The Stony Brook University Kongsberg (Simrad) EM 3000D dual-head multibeam echosounder was installed on both vessels used during this project. In the dual-head mode, the multibeam echosounder can map a swath up to 10 times the water depth although the effective swath width for most of the deep-water area was about 5 or 6 times water depth. Both depth and backscatter data are collected by the EM 3000D. A pole-mounted GeoSwath Plus borrowed from NOAA was also used when mapping with the R/V Pritchard.

The SBU mapping efforts are discussed as being “deep-water” and “shallow-water” mapping projects although the distinction is somewhat artificial as both mapping projects included some work in deeper water and some work in shallower water. The primary distinction is that deep-water surveys were done in the northern portion of the Pilot Project area (the deep-water acoustic area) and primarily used the R/V Seawolf and the shallow-water surveys were done along the southern shore of the Pilot Project area (the shallow-water acoustic area) and primarily used the R/V Donald W Pritchard. Mapping with the R/V Donald W Pritchard along the southern shore of Long Island Sound occurred mostly in water depths less than about 4 m. Mapping with the R/V Seawolf in the northern portion of the Pilot Project area was restricted to water depths greater than about 8 m. Mapping in this deep-water area shallower than about 8 m was done using the R/V Pritchard. The deep-water and shallow-water efforts were also separate tasks in the SBU mapping contract.

The deep-water acoustic area located in the northern portion of the Pilot Project area had been mapped by NOAA in 2001 and in 2003, but products based on 100% multibeam or multibeam backscatter were not available (Figure 2-3). Multibeam mapping in this area provided an opportunity to (1) determine whether any changes in sea-floor morphology could be detected between two mapping efforts about 10 years apart and (2) to collect 100% multibeam bathymetry and backscatter data at about the same time as an extensive suite of benthic samples were to be collected.

Mapped depths in this northern part of the Pilot Project area range from 3.8 m to 58.9 m (NAVD 88), and the areas mapped include Stratford Shoal and Middle Ground, the entrance channel leading to Bridgeport Harbor, a sand-wave field south of Stratford Point, shallow water south of Milford Harbor, and a deep trough between Stratford Shoal and the sand-wave field. The Iroquois Gas pipeline, the AT&T cable area, and the FLAG Atlantic (FA-1) cable exist within

this area. This area was mapped primarily with the R/V Seawolf, although the shoal areas on Stratford Shoals were mapped using the R/V Donald W Pritchard.

One of the two shallow-water acoustic areas mapped during the Pilot Project, lies along the southern shore of Long Island Sound (New York) in water depths less than about 4 m (Figure 2-3). NOAA does not routinely survey less than 4 m, as was the case in LIS. SBU multibeam mapping in this area allowed an opportunity to determine the nature of the sea-bed morphology in this poorly known area.

Mapped depths in this southern shallow-water area ranged from 0.4 m to over 28 m (NAVD 88), and the area includes waters offshore of Crane Neck Point, Flax Pond and Old Field Point in Old Field, the entrance to Port Jefferson Harbor, McAllister County Park, Belle Terre, Port Jefferson, the entrance to Mount Sinai Harbor, Cedar Beach, Mount Sinai, Miller Place and Sound Beach. Numerous rocks are charted in most of these waters and the AT&T cable comes onshore within this area. This area was mapped with the *R/V Pritchard* and no project samples were collected within the area. However, three samples were recovered and described visually to provide some information about the nature of the different backscatter patterns.

2.3.2.1 *Deep Water Acoustics*

We used the Stony Brook EM 3000D multibeam system with two multibeam sonar heads mounted on the hull of the ship to give a swath of up to 256 depths. We used an Applanix WaveMaster motion sensor leased for the project to provide heading and orientation, and we used a Trimble SPS651 GPS receiver to obtain RTK fixes using corrections received by cell phone. Multibeam data was logged with the Simrad "Merlin" program in the .all format. Part of the mapping was done quite far from land in the center of Long Island Sound. In these areas, and in times of poor GPS satellite geometry we were unable to calculate RTK fixes. RTK water-level observations were supplemented by NOAA water-level gauges at Bridgeport and New London, and by a water-level gauge we deployed in Port Jefferson. Sound velocity profiles were obtained at regular intervals (approximately 2 to 6-8 hours) with a sound-velocity probe and/or a CTD. These velocity profiles were entered into the Simrad acquisition computer which corrects the real-time data for sound velocity. Sound velocity was also recorded near the sonar heads throughout the survey.

The multibeam transducers and the electronic equipment were installed on the 80-foot Stony Brook research vessel *R/V Seawolf* over the weekend of March 16 and 17, 2013. The equipment was moved from the *R/V Pritchard* where it had been used in a prior project. While the unit was working on the *R/V Pritchard* prior to the move, the computer would not boot after it was installed on the *R/V Seawolf*. As a result, the computer was swapped out on Monday, March 18, new software licenses were obtained for the replacement computer and mapping started on Tuesday, March 19. Mapping continued for 24 hours/day through Saturday morning, March 23, and resumed from Monday morning, March 25 through Saturday morning, March 30th. This

resulted in 9 24-hour days of mapping activity. During daylight hours we towed a CHIRP subbottom profiler operated by Lamont Doherty Earth Observatory. This R/V Seawolf cruise was the first time we used two EM 3000 transducers on this vessel. We conducted some calibration runs of the multibeam system during the survey, and the Iroquois Gas Pipeline made an ideal feature to use for this calibration. Corrections determined for roll, pitch and heading for each transducer were applied during processing.

2.3.2.2 Shallow Water Acoustics

We used the same multibeam system (EM 3000D, motion sensor and GPS) and operational strategy for the shallow-water acoustic studies as for the deep-water acoustic studies except the transducers were hull-mounted on the 28-foot *R/V Donald W Pritchard*. However, there was no velocity sensor at the transducer head and we used a CTD for the sound velocity profiles. The CTD didn't operate correctly on our last survey day (September 18th) so a velocity profile from an earlier day was used. While the use of an earlier velocity profile had the possible effect of degrading the quality of bathymetric data collected on this day, our later evaluation of the multibeam data suggests that this velocity profile was generally correct since depths agreed quite well with those collected on other. We did a roll calibration of the multibeam system after the multibeam equipment was installed and we confirmed that the pitch and heading orientations were correct.

We borrowed a GeoSwath Plus interferometric side-scan sonar system from NOAA to use during the shallow-water mapping effort. This system was mounted on a pole in the position often occupied by a sidescan sonar during other surveys done at SBU. The footprint of the GeoSwath Plus data is the same as the footprint of the EM-3000D survey except that the GeoSwath Plus was not installed on September 18th. We logged the data from this unit, but we were not able to process the data before this report was due. Subsequent processing of the GeoSwath Plus bathymetry data has occurred using CARIS.

The *R/V Pritchard* can only operate during the day, so the field effort was limited to 12 hours per day and was primarily scheduled for times of high water. Multibeam data was collected on September 3, 4, 5, 6, 9, 10, 11 and 18, 2013. Robert Cerrato (SoMAS, SBU) collected benthic samples in the deep-water acoustic area during the morning of September 11.

2.3.2.3 Multibeam Data Processing

The multibeam data was processed using standard hydrographic software, including CARIS HIPS AND SIPS, Fledermaus and the SwathEd programs created by the University of New Brunswick. Backscatter processing was done using the SwathEd programs and Fledermaus GeoCoder software. The depth data is referenced to NAVD88 (m) and the data is projected in WGS 84 UTM Zone 18N (m). We reported our bathymetry data with respect to NAVD88 rather than to MLLW to facilitate depth comparisons between surveys from different years. The current elevation of MLLW is defined based on the 1983-2001 tidal epoch, and the elevation of

MLLW is likely to be redefined in 2020, 19 years after the 1983-2001 tidal epoch ends. Note that in this part of Long Island Sound water depths referenced to NAVD88 appear to be about 1.15 m deeper than water depths referenced to MLLW. The Trimble SPS651 GPS unit recorded real-time RTK fixes at 1.0 second intervals with elevations referenced to the ellipsoid. These fixes were averaged in six-minute intervals, and the elevation of the geoid at each position was subtracted from the ellipsoidal height to create a water-level curve with respect to NAVD88. The elevation of the geoid was determined using the program Geoid12A Toolkit on the NGS website (http://www.ngs.noaa.gov/cgi-bin/GEOID_STUFF/geoid12A_prompt1.prl). The resulting water-level curve was compared to water-level curves recorded by NOAA at Bridgeport, CT (8467150) and New Haven, CT (8465705) and by a project gauge in Port Jefferson. The gauge data was used to fill any gaps in the RTK water-level curve caused by poor reception of cell-phone signals or poor satellite geometry. Since we used a water-level curve referenced to NAVD88, the depths we report are also referenced to NAVD88.

The multibeam data was processed primarily using the SwathEd software programs from the Ocean Mapping Group at the University of New Brunswick (http://www.omg.unb.ca/omg/research/swath_sonar_analysis_software.html). Water-depth processing included automatic editing using a spike detection filter, manual editing to remove spurious depths, and merging of the water-level record to determine depths relative to NAVD88. The Simrad "Merlin" software corrects the multibeam depth data for the sound velocity profile that has been entered into the program. We entered each sound velocity profile as it was collected, so we did not apply sound-velocity corrections during the processing. However, the sound-velocity structure of the water column can change between the times when sound-velocity profiles are collected. If the sound velocity profile being used is not close enough to the actual profile, the recorded depth swath can show either a "smile" (the outside edges of the depth swath are too shallow) or a "frown" (the outside edges of the depth swath are too deep). A smile generally results if the sound velocity being used is too low whereas a frown results if the sound velocity being used is too high. Wide-swath systems such as the EM 3000D are particularly vulnerable to errors in sound velocity, and a change in velocity of about 3 m/s can change depth at the outer edge of the swath by about 1 m. Fortunately, this kind of systematic velocity error is easy to recognize when the seafloor is generally flat as is the case in Long Island Sound, and one can apply a refraction correction to the depth data to flatten the sea bed when needed. However, because of undocumented changes in the sound-velocity profile, the bathymetric errors at the edges of the bathymetry swath are generally larger than those at the center of the swath. These larger errors at the edges of the wide-swath EM 3000D system can be seen in the striping on several figures (e.g., the map of depth standard deviation in Figure 2.7). Limiting the width of this EM 3000D or other wide-swath bathymetry systems, or collecting more frequent sound velocity profiles using an underway sound-velocity profiling system, would reduce the uncertainty at the edge of the swath.

Bathymetric grids at 5 m and at 1 m were made using SwathEd software and converted to ArcGIS binary grid files (.flt/.hdr). The bathymetric grids were also shaded to produce two "sun-illuminated" geotiff images (.tif/.tfw) for each grid showing the seafloor illuminated from the northwest (si) and northeast (sj). The bathymetry is referenced to NAVD88 (meters) and the grids are projected as WGS-84 UTM Zone 18N (meters).

Bathymetric data collected by the *R/V Seawolf* and *R/V Pritchard* overlaps in the Stratford Shoal/Middle Ground area which allows depths collected during the two field programs to be directly compared. Comparison of 5-m grids in this area show an offset of 0.065 m (*R/V Pritchard* depths are 6.5 cm deeper) with a standard deviation of 0.14 m.

The multibeam bathymetric files were imported into CARIS HIPS AND SIPS using the OMG format, and these data could be gridded to create base maps in HIPS. However, due to the way the data is converted, no subsequent sound velocity correction, other than refraction, could be applied. Initially processing the USB survey data with CARIS HIPS AND SIPS would allow USB survey data to be integrated more easily with NOAA survey data.

Multibeam backscatter was processed both in the SwathEd software and by using the Fledermaus GeoCoder program (Fledermaus version 7.3.6a). SwathEd processing consists of removing across-track variations in signal strength related to beam angle by averaging over 1,000 pings and then using that average to correct the ping-to-ping variation in the data. This method reduces the across-track artifacts, but there can be some artificial variations in backscatter that is introduced by the processing. The Fledermaus GeoCoder program corrects for backscatter angles and bottom slope, and uses the reported dB signal levels to do a more quantitative correction for signal variations due to range and angle. Fledermaus backscatter mosaics at 1 m were created for data collected by both the *R/V Seawolf* and *R/V Pritchard*. Despite being collected with the same equipment and being processed the same way, the backscatter levels on the mosaics differ slightly between the two sets of mosaics. This may be due to higher levels of engine noise on the *R/V Pritchard*. The final Fledermaus backscatter mosaics produced from the SBU data were not stretched to enhance the observed backscatter signals, but were left with the original scaling to allow these data to be merged with NOAA backscatter data collected during this project in the southern portion of the Pilot Project area.

2.4 Integrated Products

The NCCOS Biogeography Branch was tasked with integrating the NOAA OCS surveys from the *Thomas Jefferson* with the data collected by the academic partners in the LISMRM into a seamless 1 x 1m surfaces. The NOAA *Rude* (2001-03) data was not included in the integrated bathymetric products as the SBU surveys resurveyed the majority of the existing survey. Furthermore, the portion of the *Rude* data not resurveyed by SBU (e.g. northern end of the Pilot Project) was deemed to be too sparse to be of benefit as these original surveys were purely single beam echosounder collection. The bathymetry acquired from the NOAA Ship *Thomas Jefferson*

and the SBU *R/V Pritchard* and *R/V Seawolf* were exported as ASCII XYZ files and projected to a common vertical (NAVD88 - North American Vertical Datum 1988) and horizontal (NAD83 - North American Datum 1983) datum using NOAA's Center for Operational Oceanographic Products and Services (COOPS) Vdatum software. The grids were then imported into ArcGIS as 32 bit 1x1m grids. The TJ, Pritchard, and Seawolf datasets were merged using ArcGIS's Raster Calculator to create a seamless 32-bit bathymetric surface for the entire study area of the Long Island Sound Pilot Project (Figure 2-4). The final bathymetric model was comprised of over 48 million soundings with a max standard deviation of 3.64 m calculated from CARIS Cube (SBU max standard deviation 3.64m and NOAA max standard deviation 1.09m).

The backscatter and sidescan mosaic was derived from the acoustic intensity returns collected during the *Thomas Jefferson*, *R/V Pritchard*, and *R/V Seawolf* multibeam acquisitions and the *Rude* sidescan acquisitions. Backscatter imagery can be used to identify soft and hard sediments, depict surficial features of the seafloor, and be used to delineate benthic habitats. The Reson 7125 systems aboard the *Thomas Jefferson* and its inshore launch vessels collected backscatter in "snippets" that are recorded in .7k files in Hypack. The .7k files were merged with the .HSX files to apply bottom intensity data to the positioning, attitude, roll, and heave information of the vessel to create a .GSF file that can be processed in a multibeam geocoder. The backscatter .GSF files were imported into Fledermaus Geocoder Toolbox 7.1 where they were filtered, geometrically and radiometrically corrected, and exported as an 8-bit geotiff with a relative 0-255 value greyscale. SBU also provided an 8-bit backscatter mosaic from the EM3000D multibeam system that was merged with the *Thomas Jefferson* data of the southern section of the Pilot Project Area using ENVI 5.1.

A significantly large and shallow area of the northern section of the Pilot Project was never resurveyed by NOAA and the academic partners, but contained sufficient side scan data from the 2001-2003 *Rude* surveys that were used in the initial spatial prioritization by the LISMR. The *Rude* side scan data was assessed and compared by the Biogeography Branch for quality with the backscatter collected by the *R/V Pritchard* and *R/V Seawolf*, and was deemed suitable to be integrated with acoustic intensity data from the 2012 surveys. The side scan from the *Rude* and the backscatter from the *R/V Pritchard*, *R/V Seawolf*, and *Thomas Jefferson* were merged into an integrated surface by blending the color maps from the overlapping relative intensity values of the three data sets using a georeferenced pixel based mosaicking tool from Envi 5.1 imagery enhancement software (Figure 2-5).

Eight topographic complexity surfaces were derived from the merged 1 x 1 m bathymetric surface. These surfaces specifically included mean depth (Figure 2-6), standard deviation of depth (Figure 2-7), curvature (Figure 2-8), plan curvature (Figure 2-9), profile curvature (Figure 2.10), rugosity (Figure 2-11), slope (Figure 2-12), and slope of slope (Figure 2-13) (Costa et al. 2009). Each of the surfaces was calculated in ArcGIS 10.1 using a 3 x 3 cell neighborhood, where the central pixel in the neighborhood was assigned the calculated value (Figure 2-14). These eight surfaces were included in the classification process because previous studies

demonstrated their utility for characterizing the distribution of hard bottom ecosystems by the biogeography Branch (Pittman, Costa, and Battista 2009). These surfaces were subsequently rendered, stacked, clipped, and exported to create an image with nine different bands (i.e., bathymetry, mean depth, standard deviation of depth, curvature, plan curvature, profile curvature, rugosity, slope, and slope of slope) each band representing a specific topographic complexity metric.

Remote sensing imagery software Envi 5.1 was used to visualize, process, and analyze the stacked topographic complexity surface into its nine principal components (PCs) based on the correlations of the spatial data (Figure 2-15). The backscatter was also used as an ancillary layer further measure the variance in the layered data. The PCA removed information that was highly correlated and thus, redundant across the different bands. The first three PCs were retained in the final image because they contained over 90% of the data variability uniquely describing the complexity and structure of the seafloor and exported into a 3-band 32-bit PCA for habitat delineation (Costa and Battista 2013).

2.5 Discussion

The acoustic products processed for the Pilot Project provided the fundamental spatially organizing information for the analysis conducted in subsequent chapters of the report. The geophysical information contained in the acoustic products conveys important details describing the shape, extent, and composition of surficial features and were used to extract detailed information about benthic habitats, sediment texture, grain size, and sedimentary environments. The acoustic products are used to infer and extract seascape features at a range of spatial scales including fine scale biotopes (Auster et al. 2009) and broader scale geomorphology within Long Island Sound. The following images depict a number of unique and interesting seafloor and man-made features within the Pilot Project area (Figures 2-16 through 19). Further analysis of how the acoustic products were used to inform the analysis of ecological, geological, and physical environments are discussed in subsequent chapters.

2.6 Summary/Conclusions

The Long Island Sound Pilot project was a tremendous success in demonstrating the collaboration of State, Federal, and academic partners to address coastal management needs. The acoustic products produced as a result of those efforts is a clear demonstration of the value of collaboration. The ability of NOAA and SBU to coordinate the collection of contemporary acoustic data to satisfy the requirements of the project, while completing it in a timely and cost-effective method is clear evidence of the success. Acquiring data for the size of the Pilot Project area can be a costly endeavor, but close coordination between groups ensured the maximization of the collection area while minimizing data collection duplication so as to produce a valuable product.

Part of the tasks associated with acoustic data collection included the compilation and evaluation of existing data. While most of the existing data was not used in the final integrated product, it was valuable for planning, determining where field sampling should occur, and identifying locations that would benefit from more contemporary acoustic data collections. To that end, the existing data was a valuable informational source to determine where to target the collection of new acoustic data. Substantial existing data is available for additional areas within LIS and should be explored to their fullest during the planning phases. Reuse of the available existing data in other areas of LIS should be encouraged, but only after those data have been fully evaluated to analysis their actual bottom coverage and integrity. Nonetheless, these existing data will be a valuable tool for planning the scope, cost, and time constraints of subsequent mapping efforts and therefore should be conducted in advance of other scientific activities.

Despite the success of the acoustic mapping efforts, there were some challenges and room for improvement. One difficulty is the separation of activities amongst the partners collecting data and producing products. Typically the acquisition of remote sensing data is driven by the requirements of the end product desired to be produced. In the case of the Pilot Project these tasks were separated between groups, and therefore limited attention was focused on how the data was to be collected so as to best support the creation of end products. For the most part, the explicit details of the end products, the classes intended to be mapped, and production methodology were not finalized till well after the acoustic data had been collected. Hence, techniques to optimize data collection, improve data quality, or evaluate sensors to address those specific requirements were not addressed. This is something that can be addressed during future mapping efforts.

In addition, improvements could be made on the sequence of activities, as mentioned earlier. Future efforts would benefit from being able to fully evaluate existing data before new collection efforts are initiated. Hopefully the contracting issues that led to a nearly one-year delay in the USB survey activities have been resolved which will allow academic surveys to occur sooner in future projects. Additionally, field sampling should be undertaken only when the integrated acoustic products are finalized including the collection of new data. The sampling strategy can then be based on and driven by the underlying information provided from the acoustic data so as best inform, distinguish, and verify the acoustical seafloor classes detected.

And lastly, while having a number of parties independently collect acoustic data had some advantages, there are improvements that could be made to facilitate and ease the data integration. There are also noticeable differences in data quality between the sources of data as no common data quality standard was implemented. It is suggested that minimum common standards be developed and implemented for the collection of new data. This includes not only how the data are explicitly collected, but also the data processing procedures and delivery formats. Standardized procedures should be implemented such that sonar systems are calibrated, verified, and documented at the beginning of survey; data analysis is conducted to measure and report

data quality (i.e. uncertainty). These efforts will better ensure greater uniformity between collection efforts and therefore aide in improving the integration of data from various sources.

2.7 References

- Auster, P.J., Heinonen, K.B., Witharana, C., McKee, M. (2009) A habitat classification for the Long Island Sound region. Long Island Sound Study Technical Report. EPA Long Island Sound Office, Stamford, Connecticut. p. 83.
- Costa, B. M., Battista, T.A. (2013) The Semi-automated Classification of Acoustic Imagery for Characterizing Coral Reef Ecosystems. *Int J Remote Sens* 34(18): 6389-6422.
- Pittman, S. J., Costa, B. M., Battista, T. A. (2009) Using LiDAR Bathymetry and Boosted Regression Trees to Predict the Diversity and Abundance of Fish and Corals. *J Coast Res* 53: 27-38.

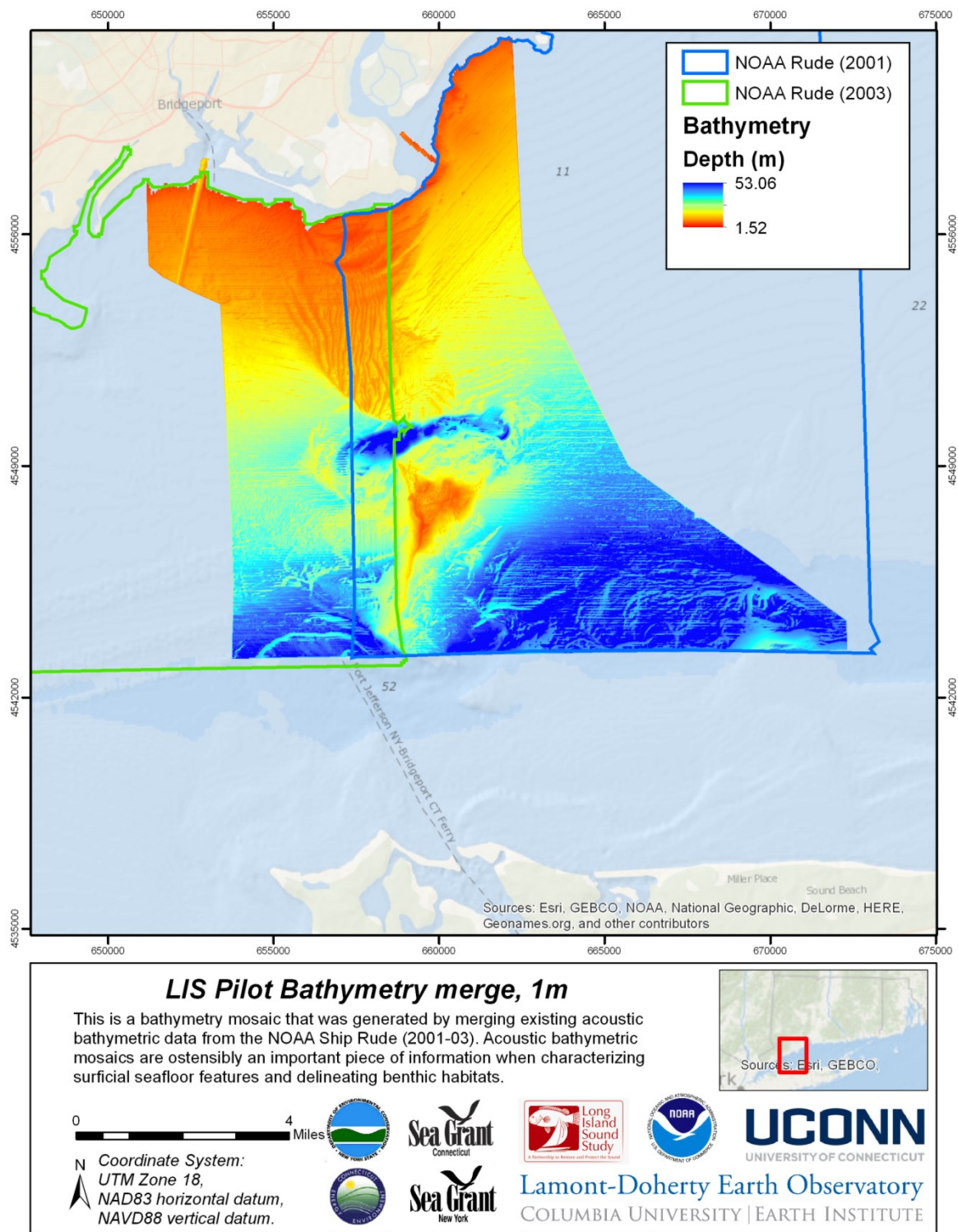


Figure 2-2: Mosaic of bathymetric data produced from existing NOAA surveys.

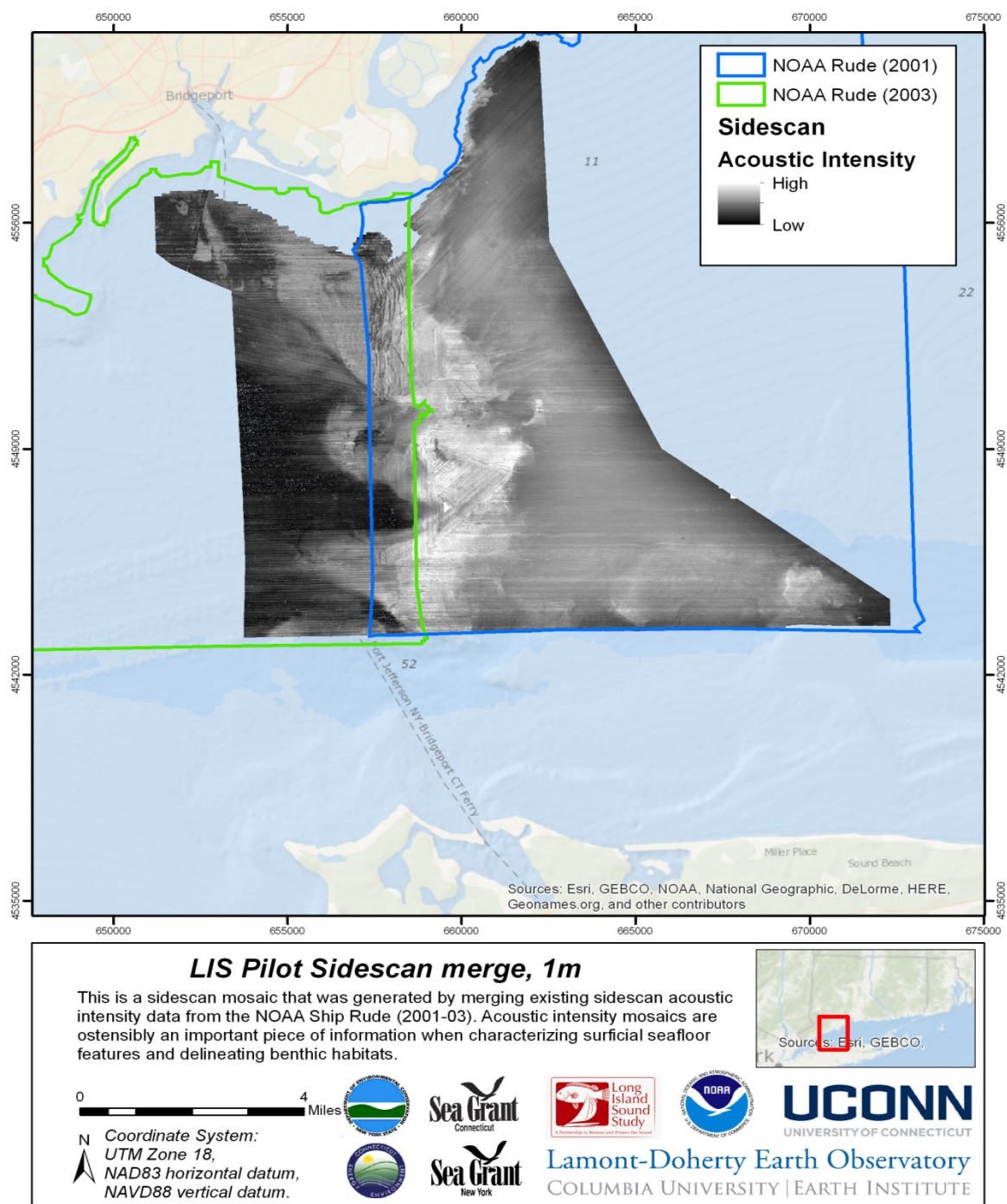


Figure 2-3: Mosaic of sidescan data produced from existing NOAA surveys.

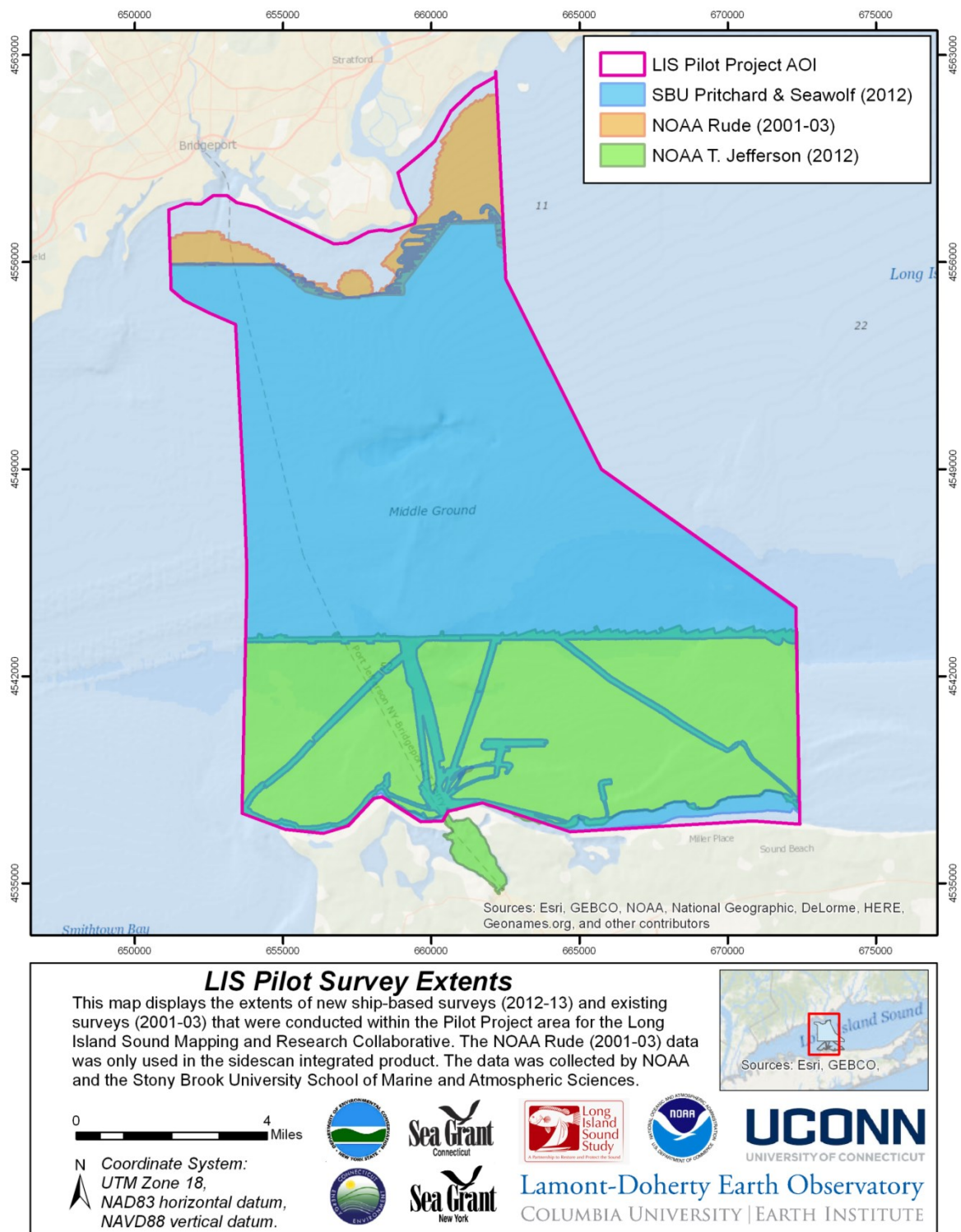


Figure 2-4: Extents of acoustic surveys conducted within the Pilot Project area used to generate the integrated data products.

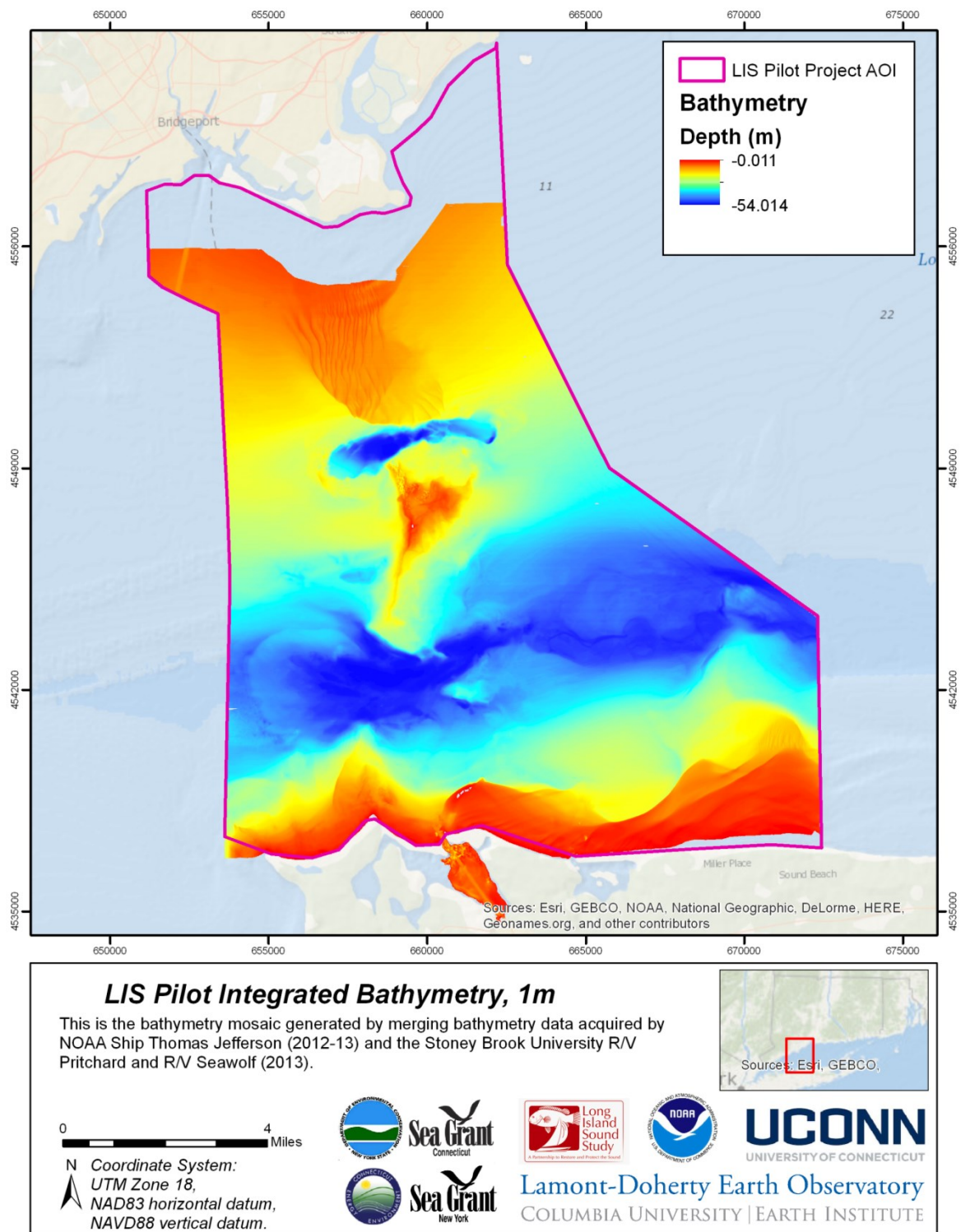


Figure 2-5: Integrated Bathymetry surface for the Pilot Priority area.

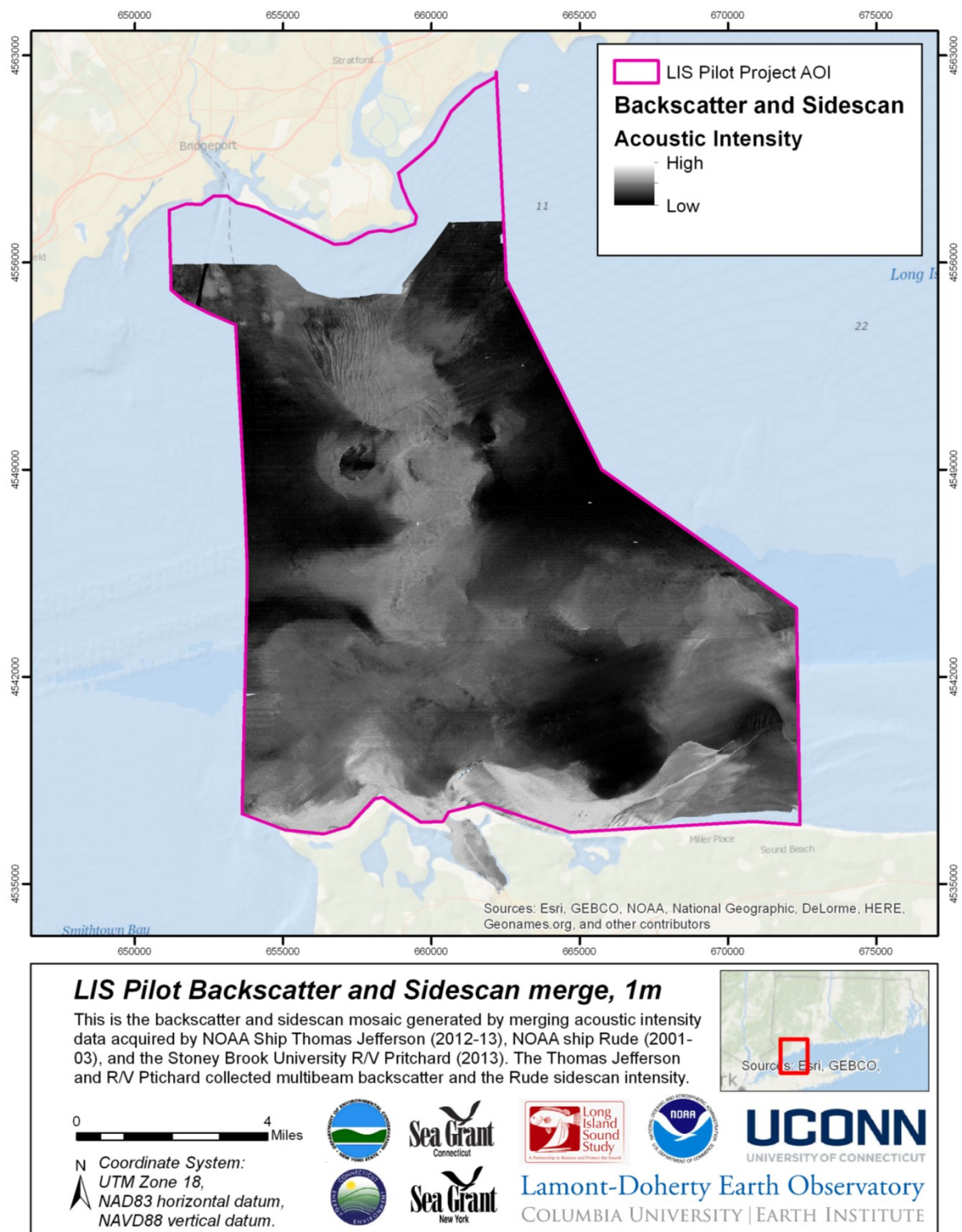


Figure 2-6: Integrated Acoustic Intensity surface for the Pilot Priority area.

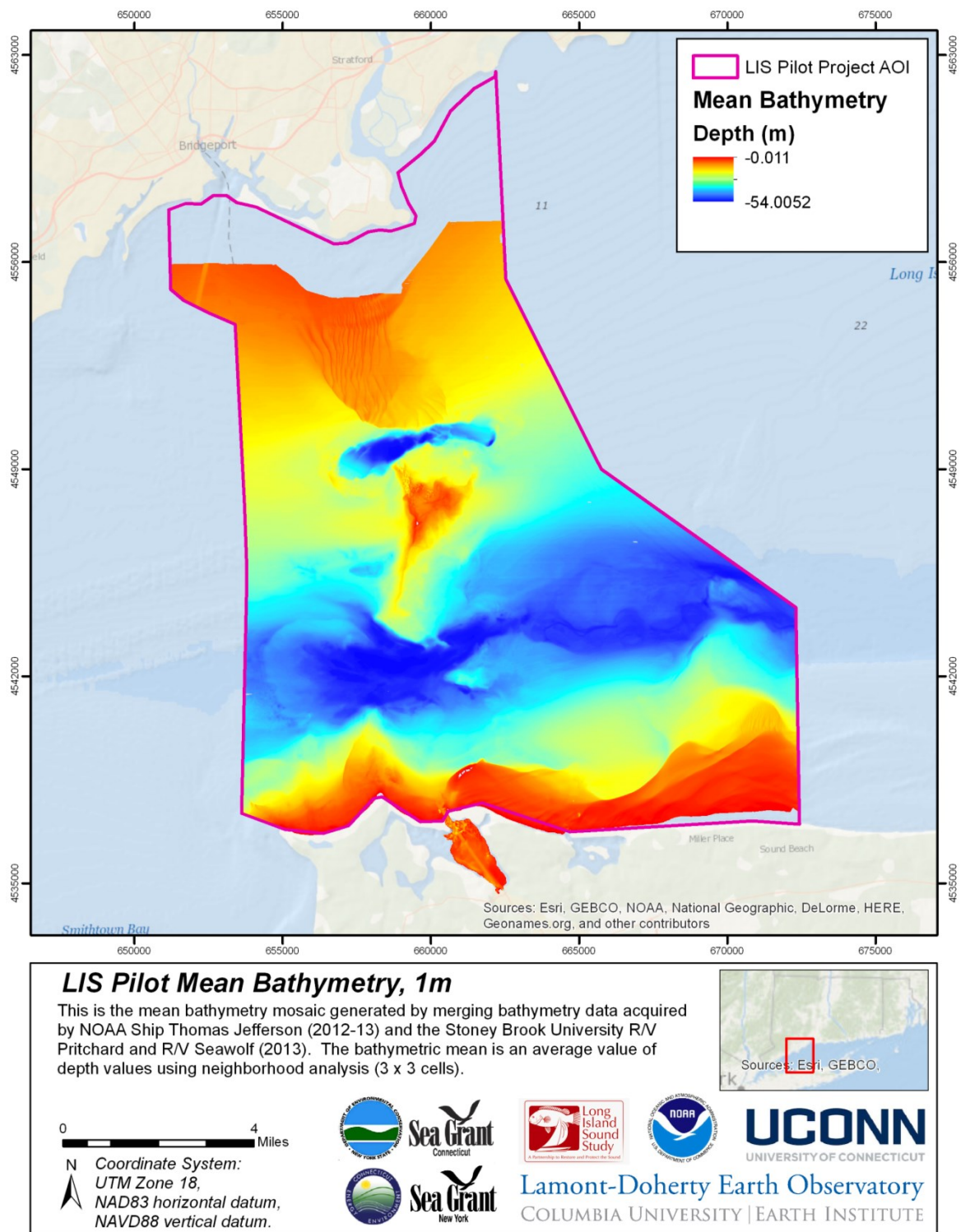


Figure 2-7: Mean bathymetry surface for the Pilot Priority area.

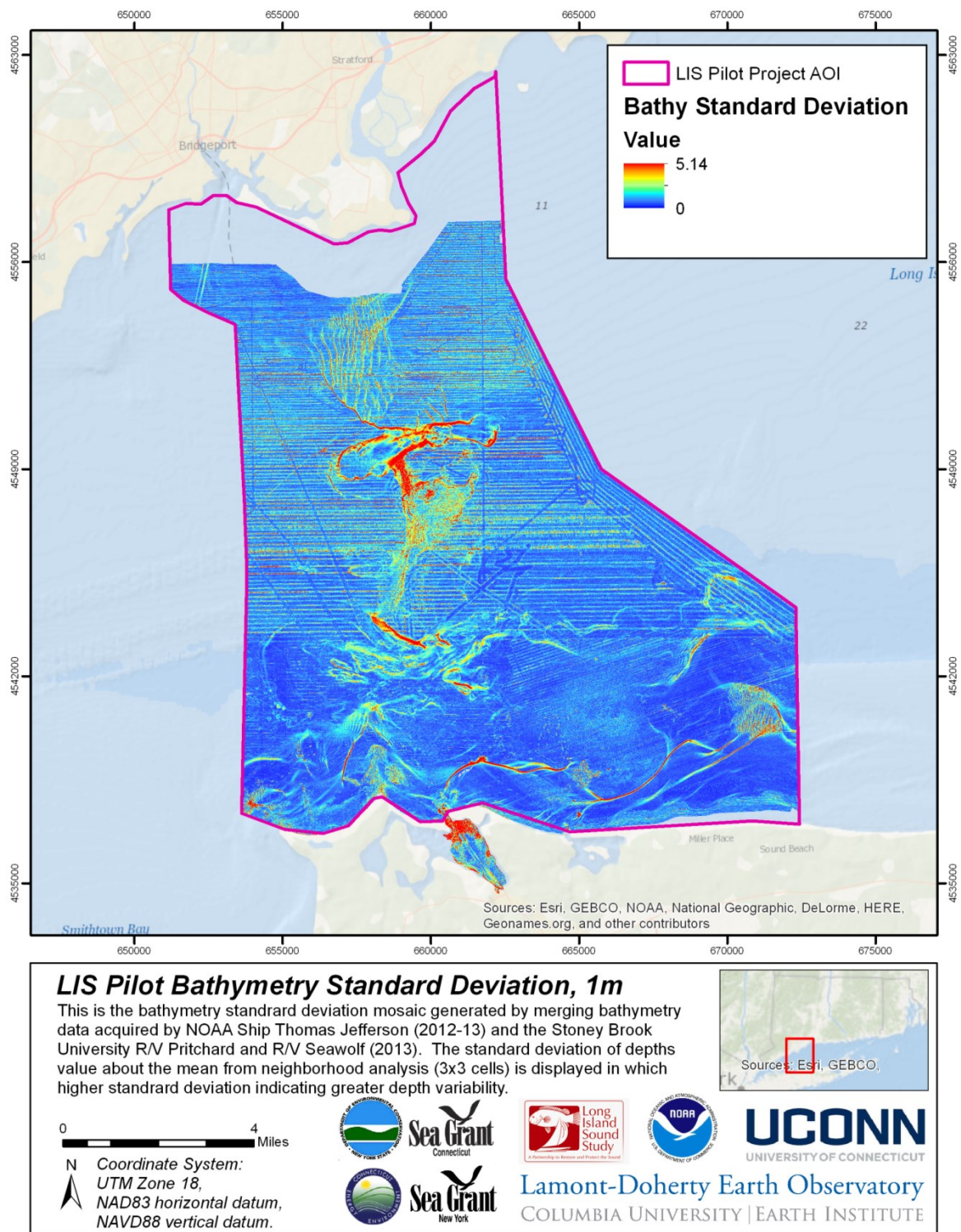


Figure 2-8: Bathymetry standard deviation surface for the Pilot Priority area.

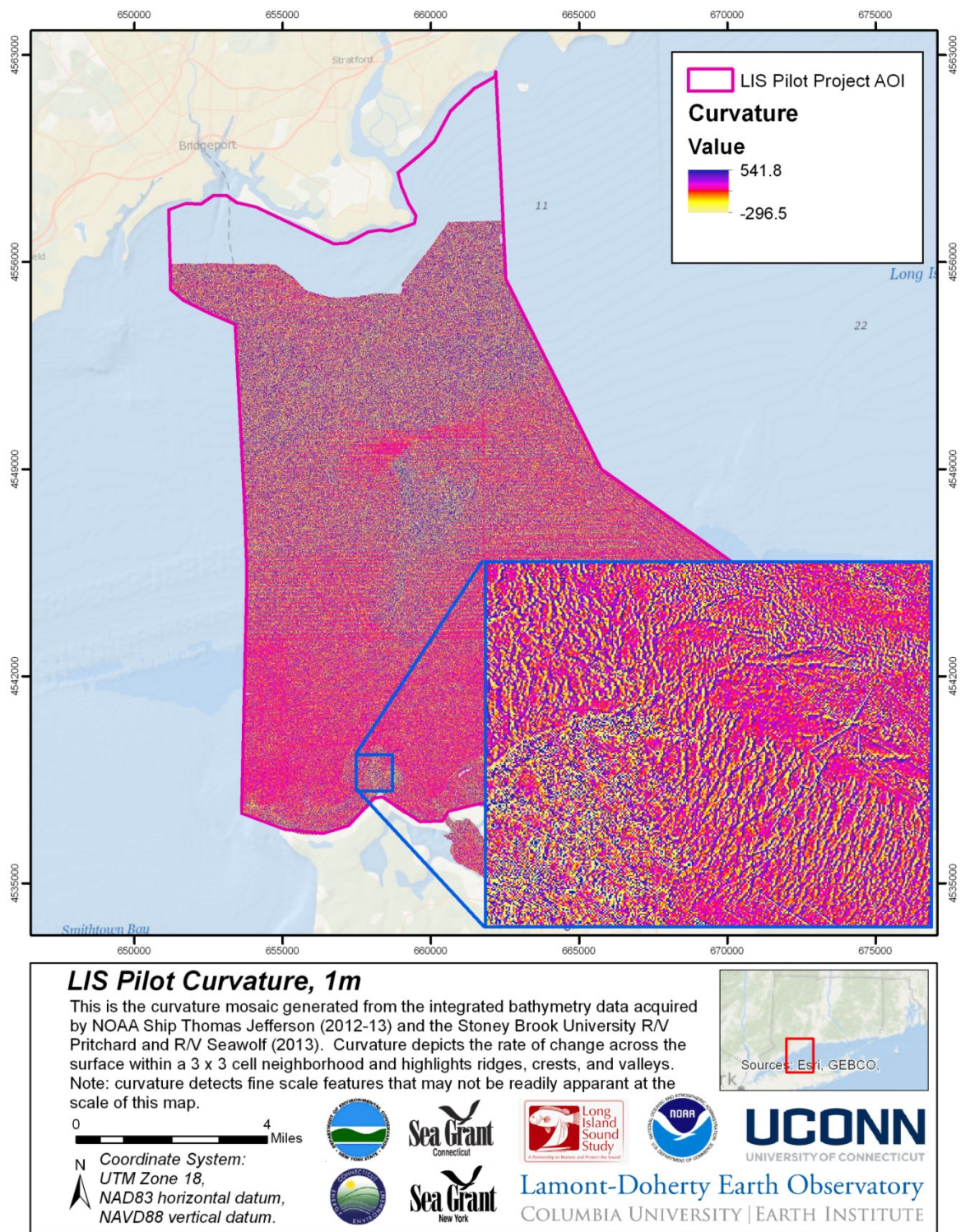


Figure 2-9: Curvature surface for the Pilot Priority area.

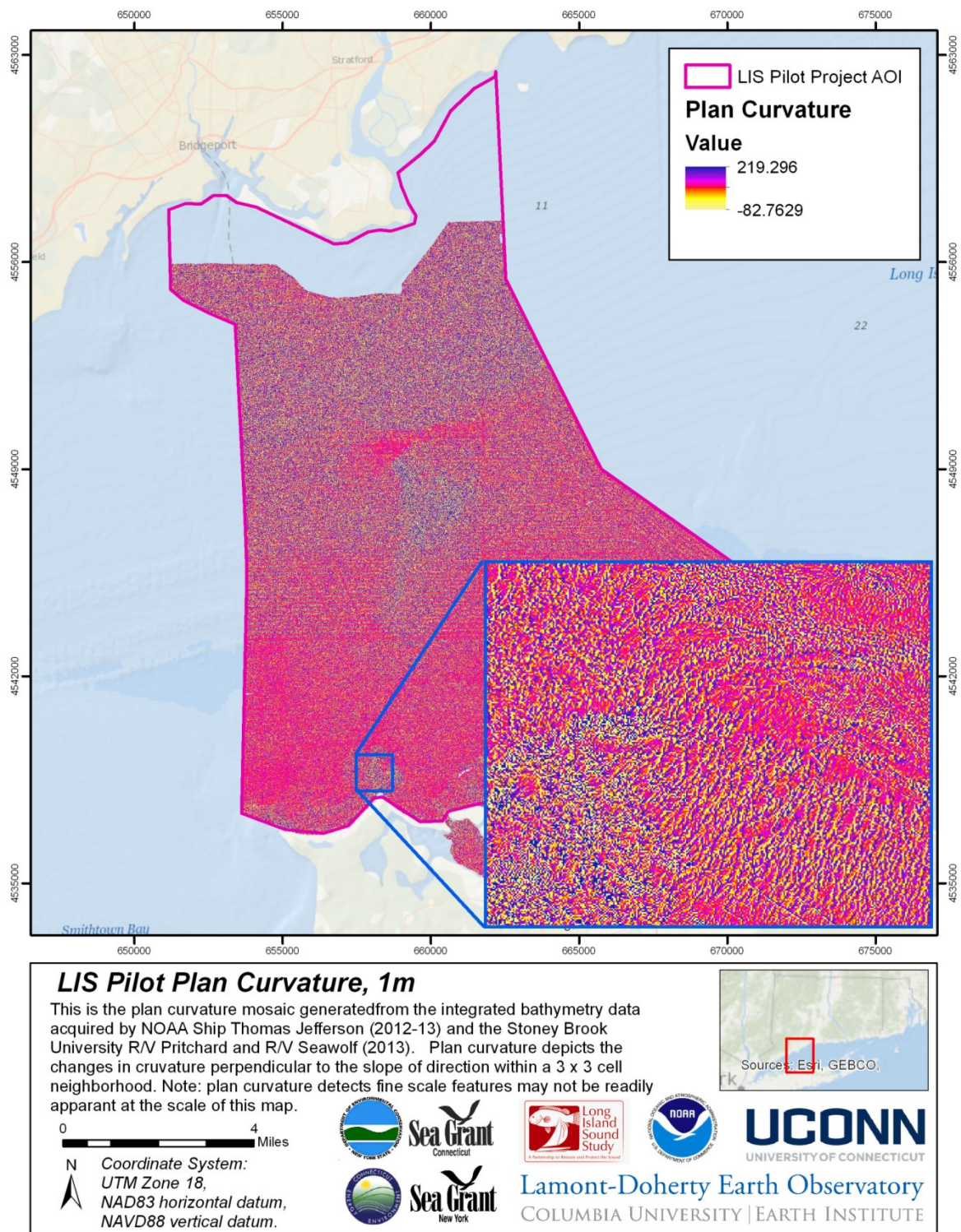


Figure 2-10: Plan curvature surface for the Pilot Priority area.

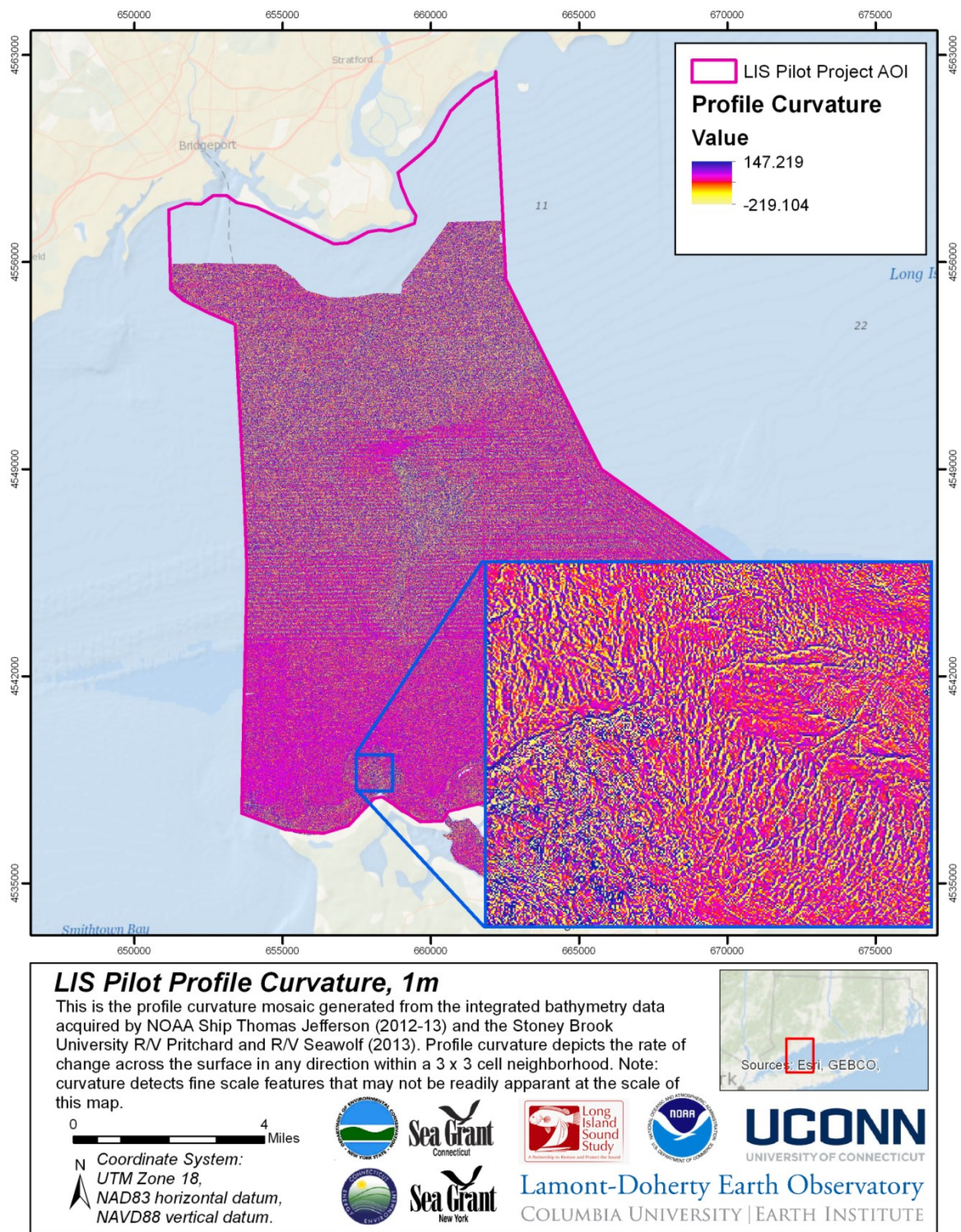


Figure 2-11: Profile curvature surface for the Pilot Priority area.

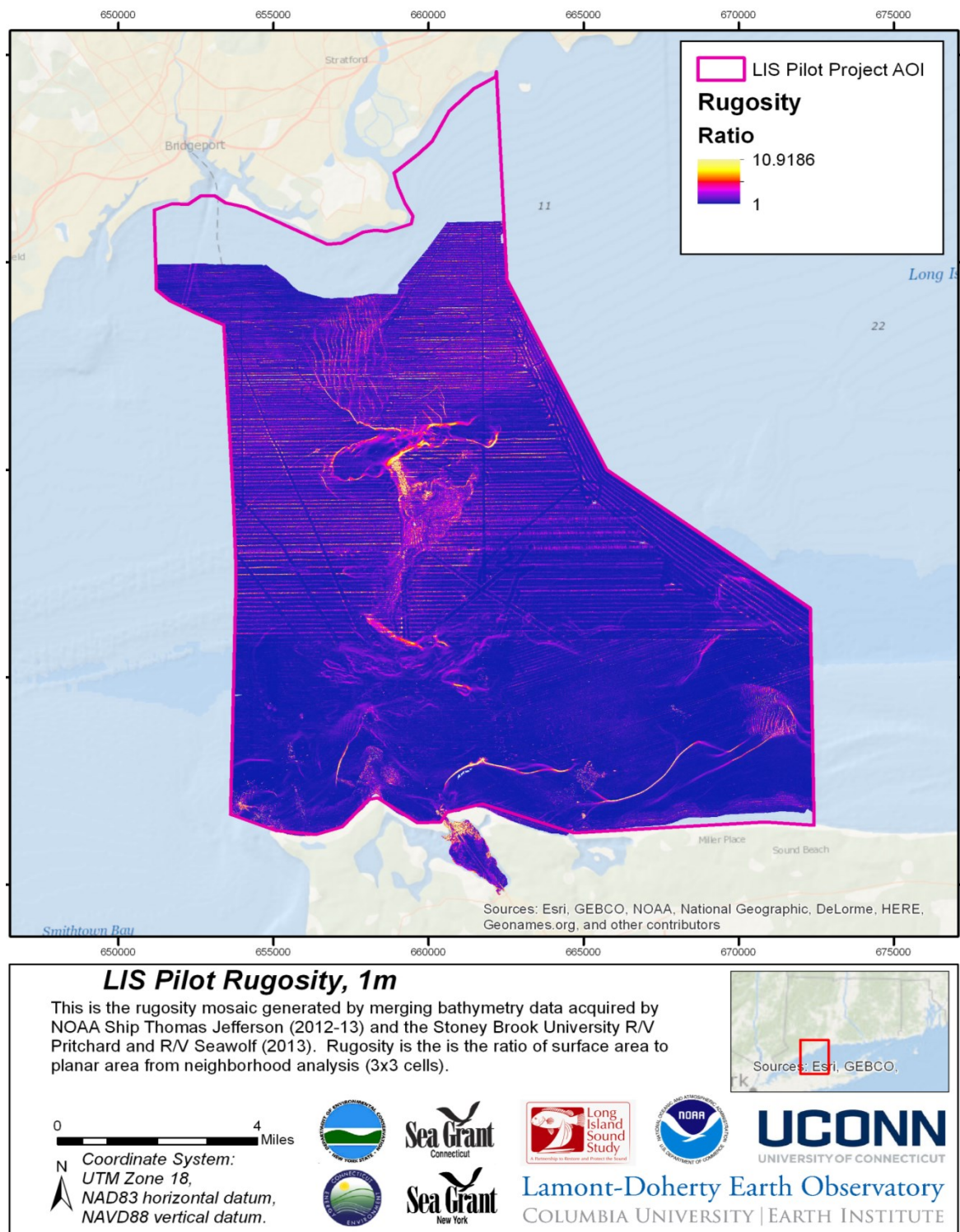


Figure 2-12: Rugosity surface for the Pilot Priority area.

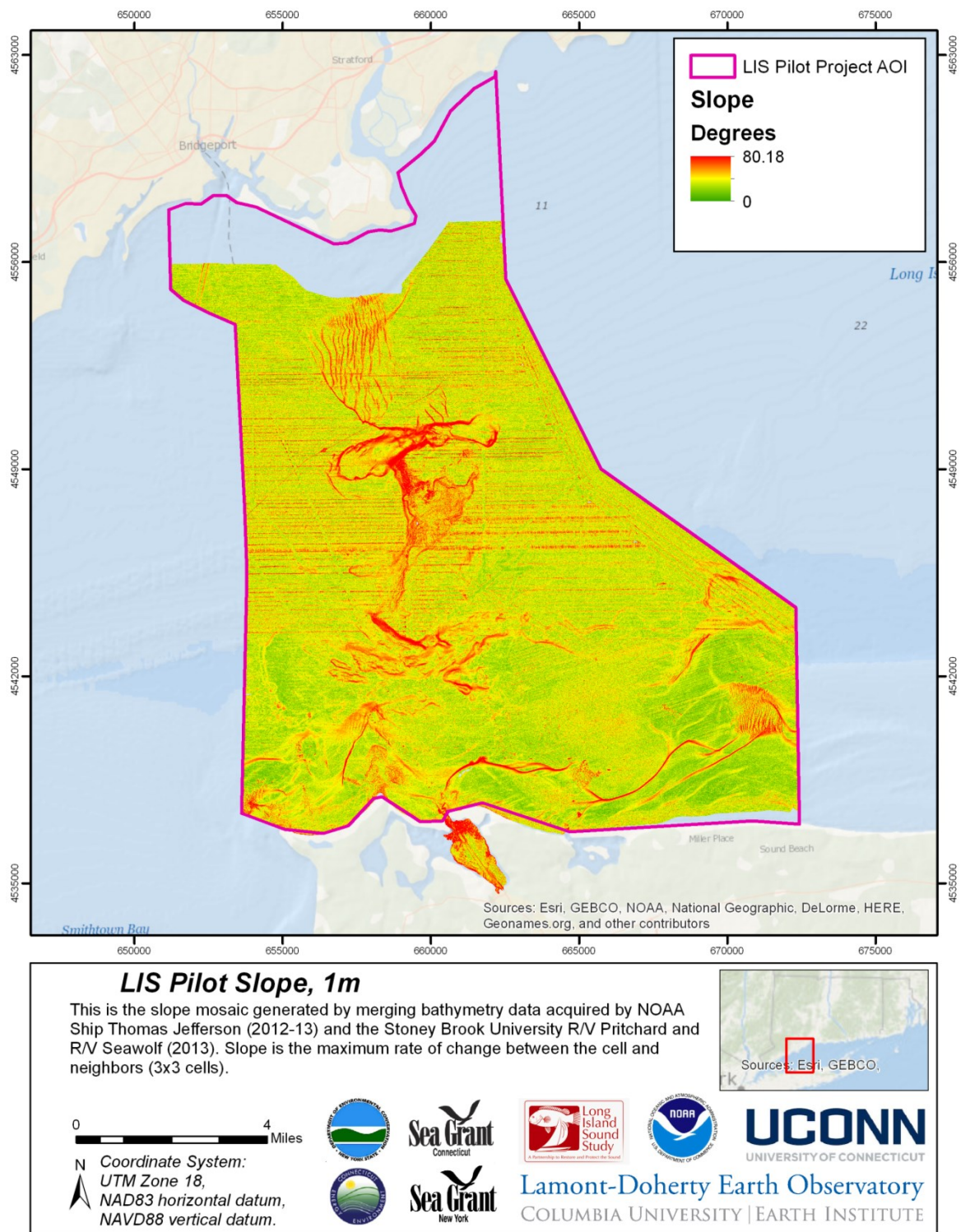


Figure 2-13: Slope surface for the Pilot Priority area.

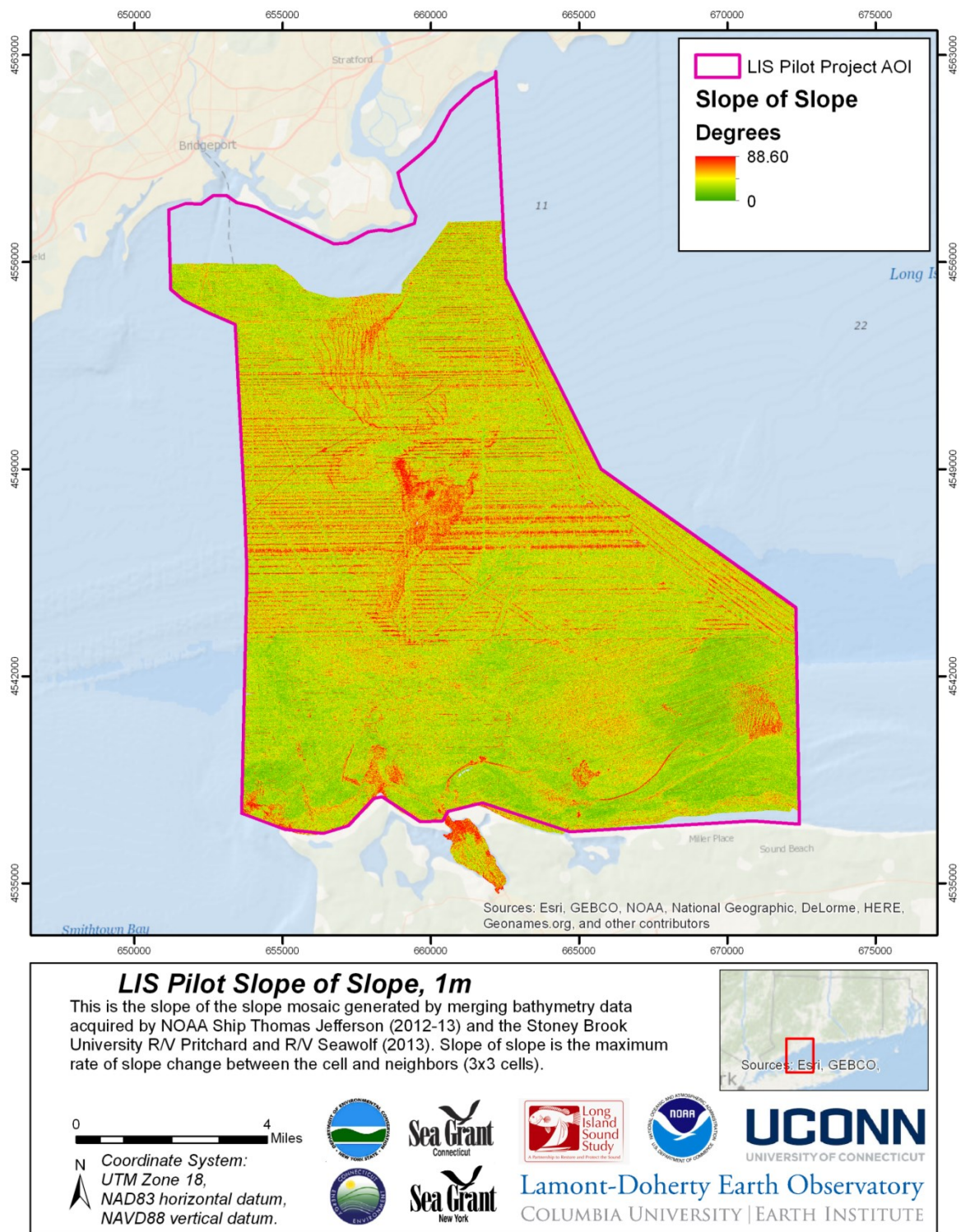


Figure 2-14: Slope of the slope surface for the Pilot Priority area.

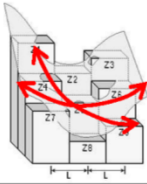
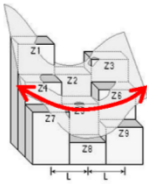
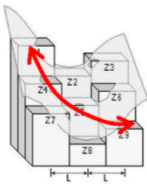
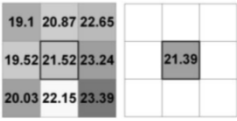
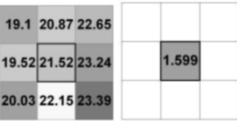
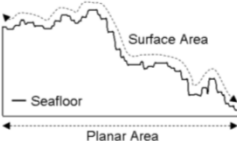
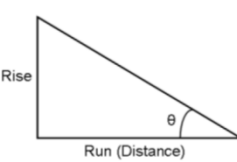
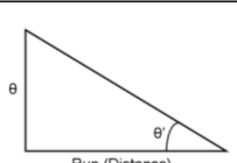
	Dataset	Unit	Description	Tool
Curvature		1/100 z units - = concave + = convex	Rate of change in curvature across the surface highlighting ridges, crests and valleys (3 x 3 cell neighborhood)	Curvature function in ArcGIS 3D Analyst
Plan Curvature		1/100 z units - = concave + = convex	Curvature of the surface perpendicular to the slope direction (3 x 3 cell neighborhood)	Plan curvature function in ArcGIS 3D Analyst
Profile Curvature		1/100 z units - = convex + = concave	Curvature of the surface in the direction (3 x 3 cell neighborhood)	Profile curvature function in ArcGIS 3D Analyst
Depth (Mean)		Meters	Average water depth (3 x 3 cell neighborhood)	Focal statistic in ArcGIS Spatial Analyst
Depth (Standard Deviation)		Meters	Dispersion of water depth values about the mean (3 x 3 cell neighborhood)	Focal statistic in ArcGIS Spatial Analyst
Surface rugosity		Ratio value	Ratio of surface area to planar area (3 x 3 cell neighborhood)	Benthic Terrain Mapper toolbox
Slope		Degrees	Maximum rate of change in slope between cell and 8 neighbors (3 x 3 cell neighborhood)	ArcGIS Spatial Analyst's slope function
Slope of the slope		Degrees of degrees	Maximum rate of maximum slope change between cell and eight neighbors (3 x 3 cell neighborhood)	ArcGIS Spatial Analyst's slope function

Figure 2-15: Descriptions of the eight spatial metrics used to characterize the seafloor complexity in the Pilot Priority area.

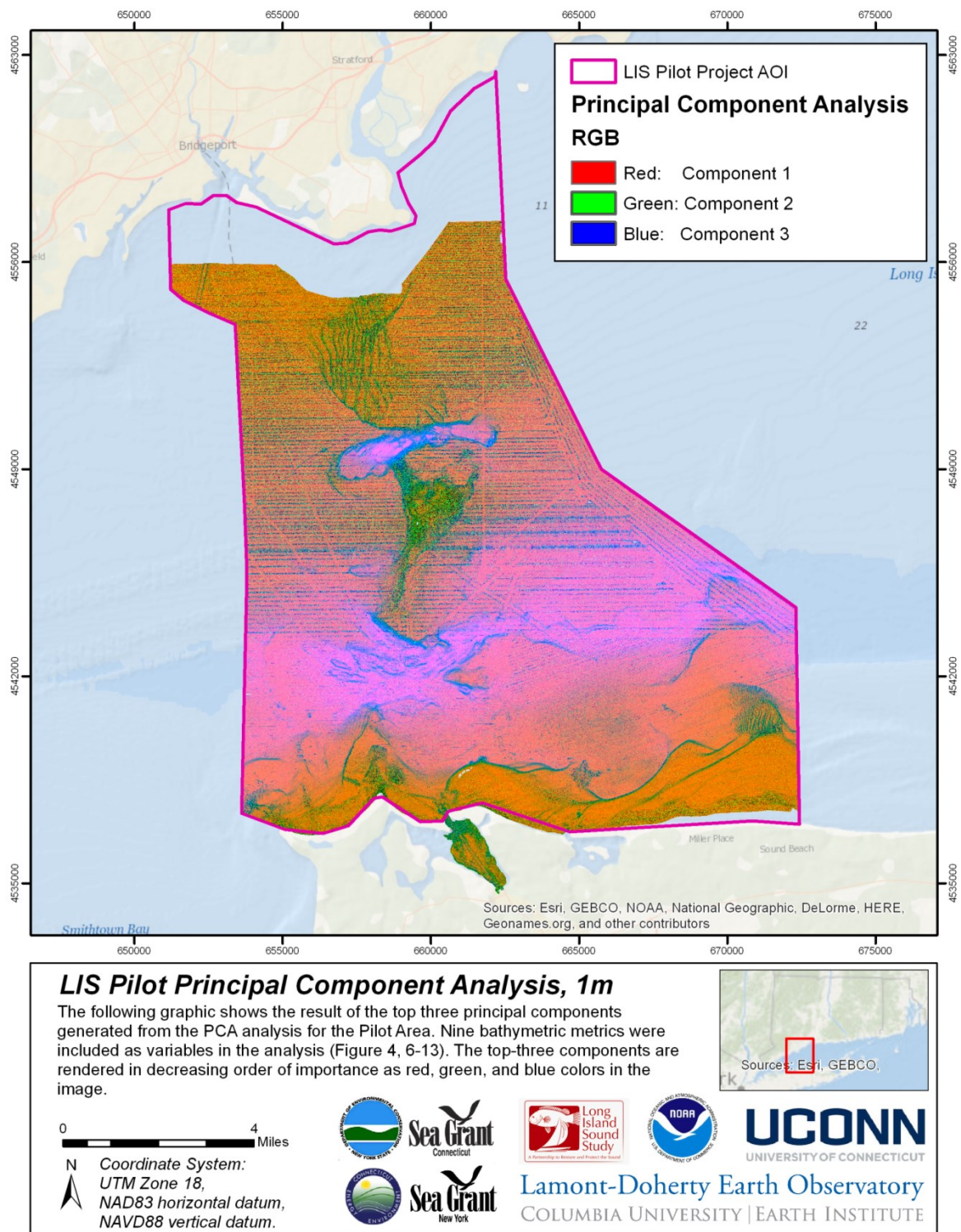


Figure 2-16: Principal component analysis surface for the Pilot Priority area.

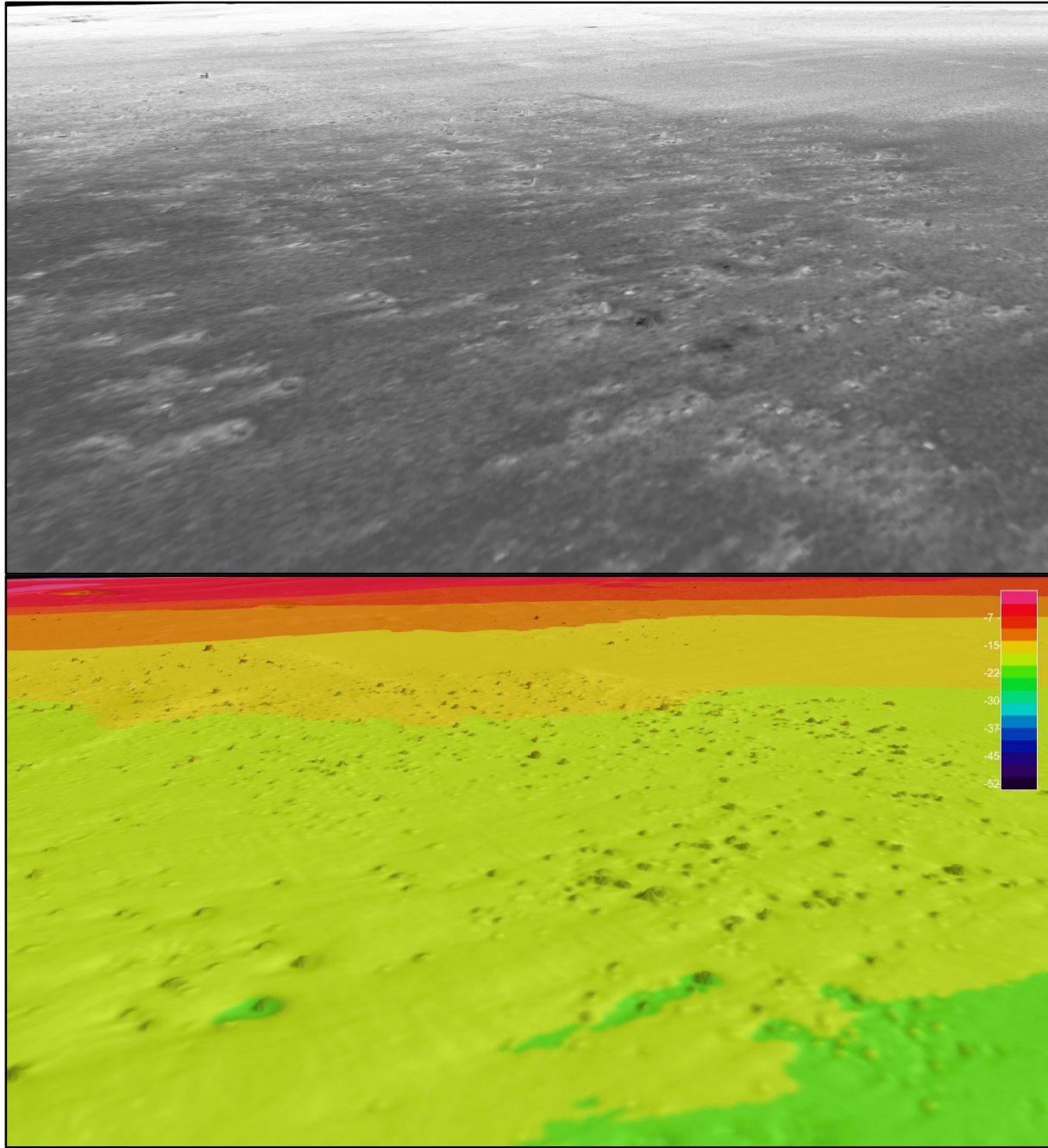


Figure 2-17: Acoustic intensity (top) and bathymetry (bottom) of a boulder field (665034.6 E, 4538735.1 N).

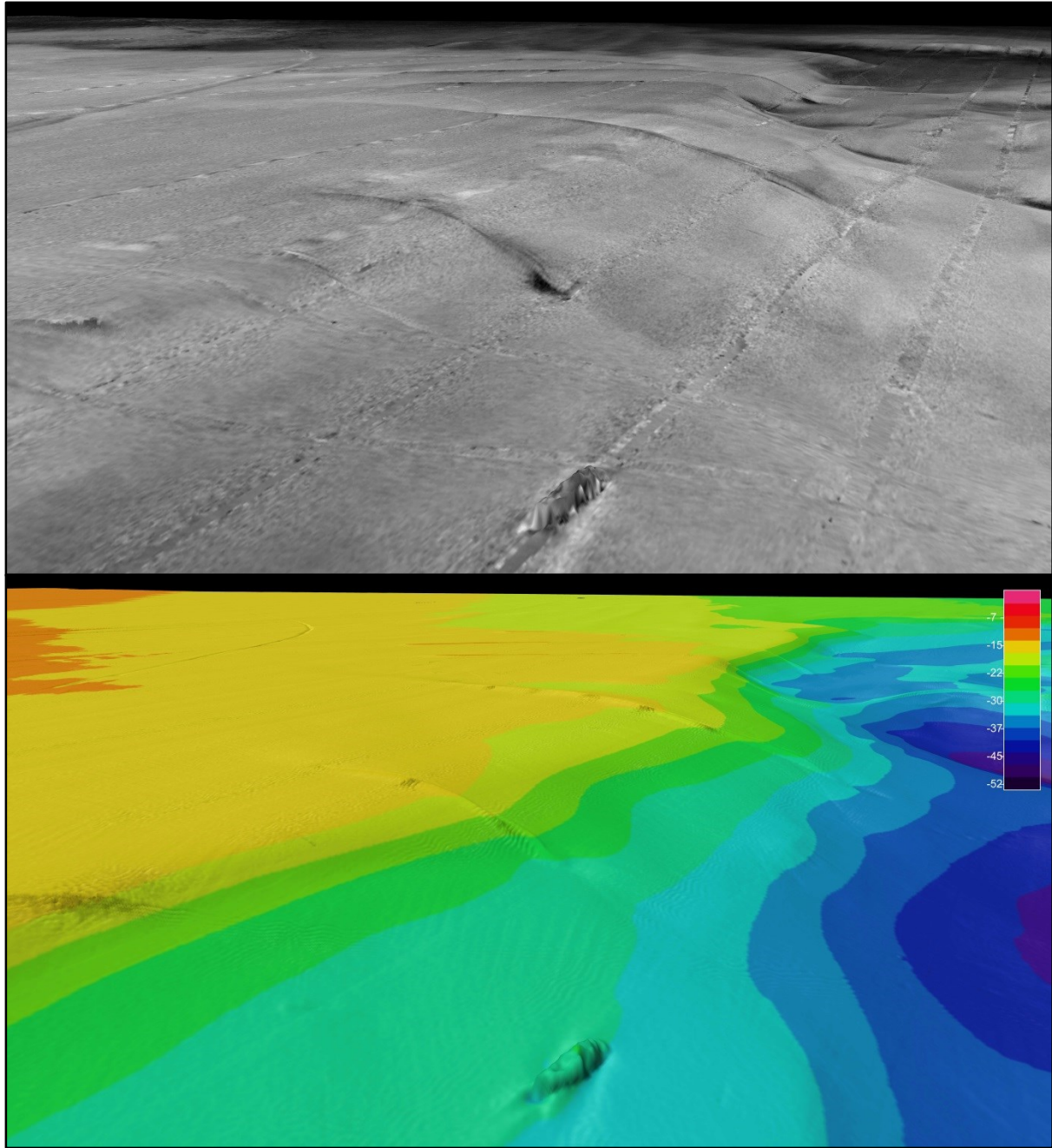


Figure 2-18: Acoustic intensity (top) and bathymetry (bottom) of a shipwreck (center, bottom) and ridge waves (658891.2E, 4550149.5N).

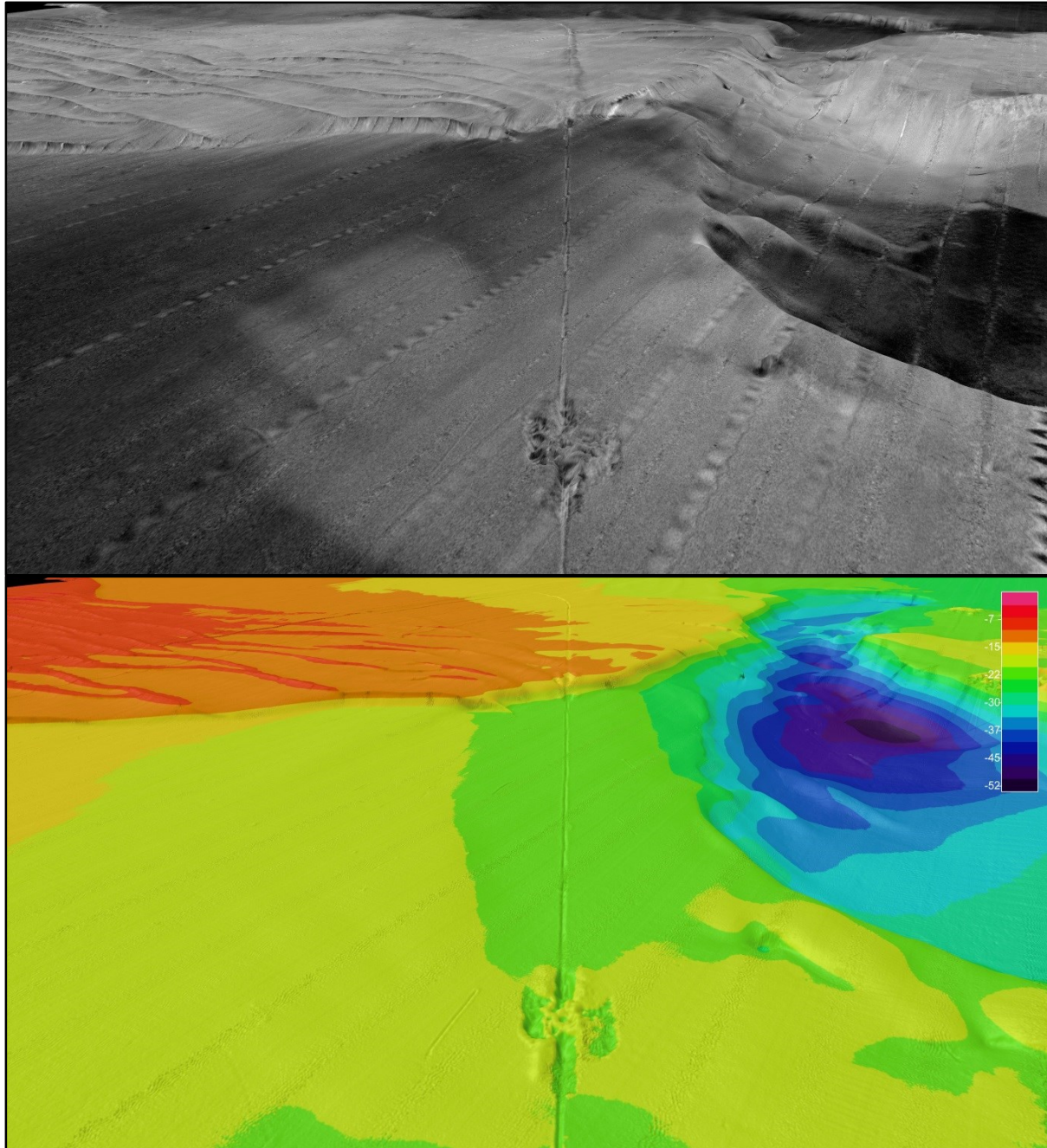


Figure 2-19: Acoustic intensity (top) and bathymetry (bottom) of a pipeline (center, vertical) and ridge-trough (top-right) (656392.5E, 4549627.5N).

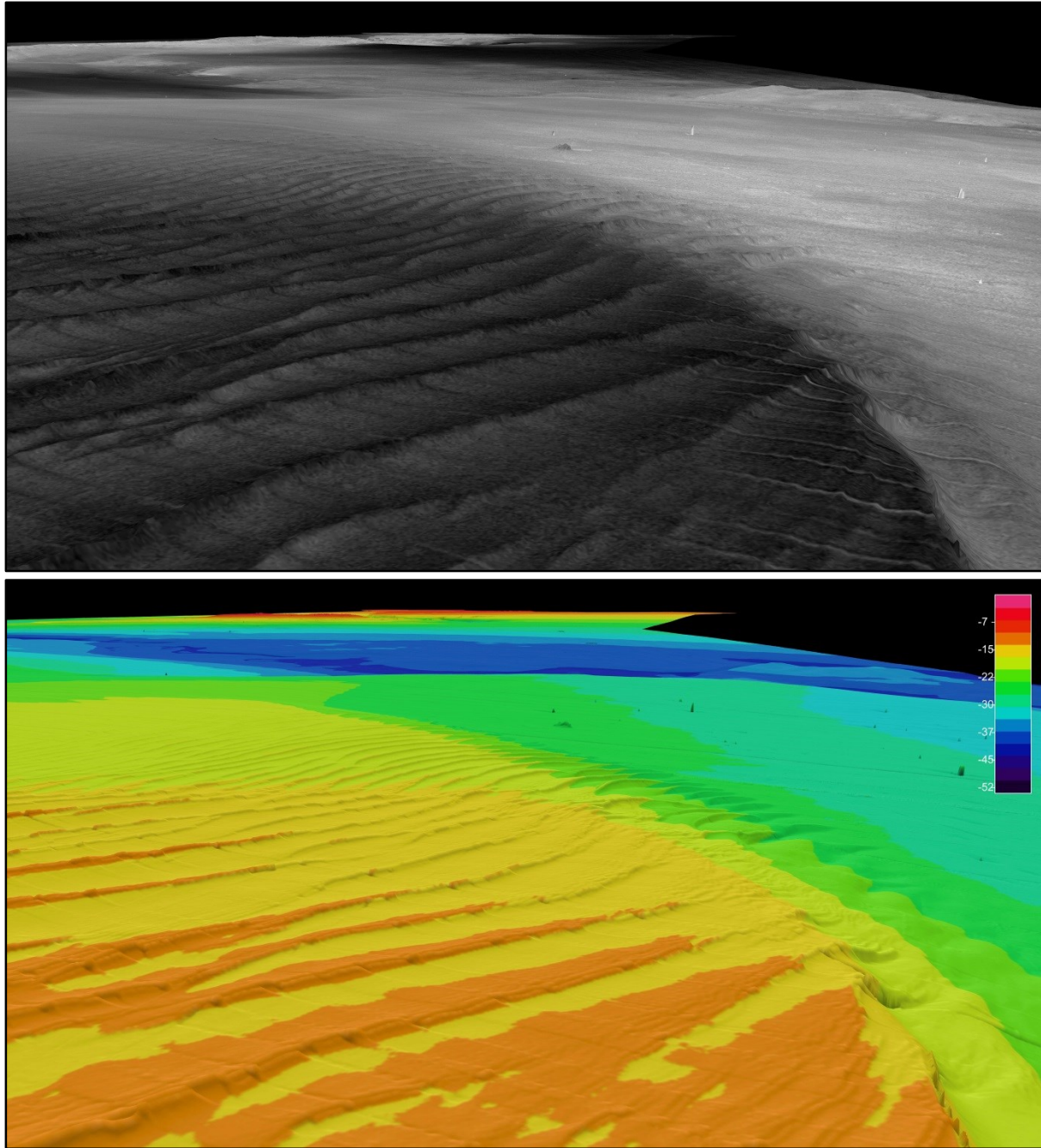


Figure 2-20: Acoustic intensity (top) and bathymetry (bottom) of a sand wave field (671457.4E, 4540851.3N).

3 Sediment Texture and Grain Size Distribution

Recommended Citations:

- Nitsche, F. (2015). Objective. Section 3.1, p. 61 in: “Seafloor Mapping of Long Island Sound – Final Report: Phase 1 Pilot Project.” (Unpublished project report). U. S. Environmental Protection Agency, Long Island Sound Study, Stamford, CT.
- Nitsche, F. (2015). Historical Context. Section 3.2, p. 62-63 in: “Seafloor Mapping of Long Island Sound – Final Report: Phase 1 Pilot Project.” (Unpublished project report). U. S. Environmental Protection Agency, Long Island Sound Study, Stamford, CT.
- Poppe, L.J. (2015). Sediment Sampling and Bottom Photography in Support of Ecological Characterization of Pilot Area. Section 3.3, p.63-65 in: “Seafloor Mapping of Long Island Sound – Final Report: Phase 1 Pilot Project.” (Unpublished project report). U. S. Environmental Protection Agency, Long Island Sound Study, Stamford, CT.
- McHugh, C. and T. Kenna. (2015). Sediment Grab Collection and Analysis. Section 3.4, p. 65-83 in: “Seafloor Mapping of Long Island Sound – Final Report: Phase 1 Pilot Project.” (Unpublished project report). U. S. Environmental Protection Agency, Long Island Sound Study, Stamford, CT.
- Nitsche, F. (2015). Sediment Texture Interpretations and Other Integrated Products. Section 3.5, p. 84-90 in: “Seafloor Mapping of Long Island Sound – Final Report: Phase 1 Pilot Project.” (Unpublished project report). U. S. Environmental Protection Agency, Long Island Sound Study, Stamford, CT.
- Nitsche, F. (2015). Comparison with Older Data. Section 3.6, p. 91 in: “Seafloor Mapping of Long Island Sound – Final Report: Phase 1 Pilot Project.” (Unpublished project report). U. S. Environmental Protection Agency, Long Island Sound Study, Stamford, CT.
- Nitsche F. and C. McHugh. (2015). Summary and Recommendations. Section 3.7, p. 91-92 in: “Seafloor Mapping of Long Island Sound – Final Report: Phase 1 Pilot Project.” (Unpublished project report). U. S. Environmental Protection Agency, Long Island Sound Study, Stamford, CT.

3.1 Objective

Sediment texture, which includes shape, size and three-dimensional arrangement of sediment particles, is an essential element of any habitat classification. Gravel, sand, mud and various mixtures of these major grain size classes provide very different habitats (Galparsoro et al., 2013). Besides its importance for habitats the surface sediment classification is a key element for managing different resources in LIS. In fact, different bottom types can be resources in and of themselves (e.g. sand).

While acoustic data, especially multibeam bathymetry and backscatter can provide information on different grain size composition of the seafloor (coarse sediments usually correspond to high backscatter and finer sediments are smoother and thus correspond to lower backscatter) this acoustic information is not always sufficient to discriminate all differences in grain size that might be relevant for benthic habitats. In some cases, (e.g. in mud-dominated areas) differences in the backscatter can be caused by fine-scale morphology rather than by differences in grain size content (Ferrini and Flood, 2006; Nitsche et al., 2004). Therefore sediment grain size distribution requires analysis of actual samples.

In addition to grain size information the total organic content distribution is of great value for the biological habitat classification since it can be an indicator of biological activity. Basic organic content data can be easily extracted from the same samples as the grain size data and a comparable resolution is desirable. Likewise, information on metal content provides first-order insights on potential contaminant distribution and sediment source areas.

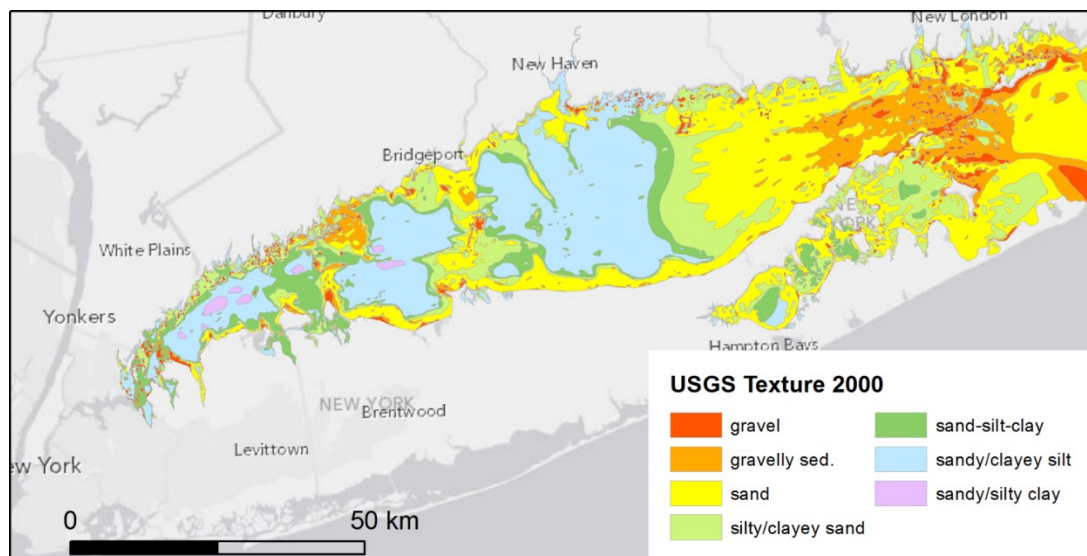


Figure 3-1: USGS grain size map of LIS from 2000 (Poppe et al., 2000).

3.2 Historical Context

Sediment texture has been studied in LIS for many decades because it provides the basis for other studies and management applications. In 2000 USGS compiled existing grain size data and produced a sediment texture map for the entire LIS (Figure. 3.1).

This compilation is based on a large number of grain size data in combination with a limited amount sidescan data where those were available (Poppe et al., 2000). The grain size sample information is compiled in two USGS databases: The LIS Surficial Sediment Sample Database counts >14,000 entries between 1930 and 1998 with a majority ~10,000 from the 1930s (Figure 3.2). The east coast sediment texture database contains ~2420 entries for LIS between 1980 and 2010. The large majority of these data are from sediment grabs and few are from sediment cores and images sources.

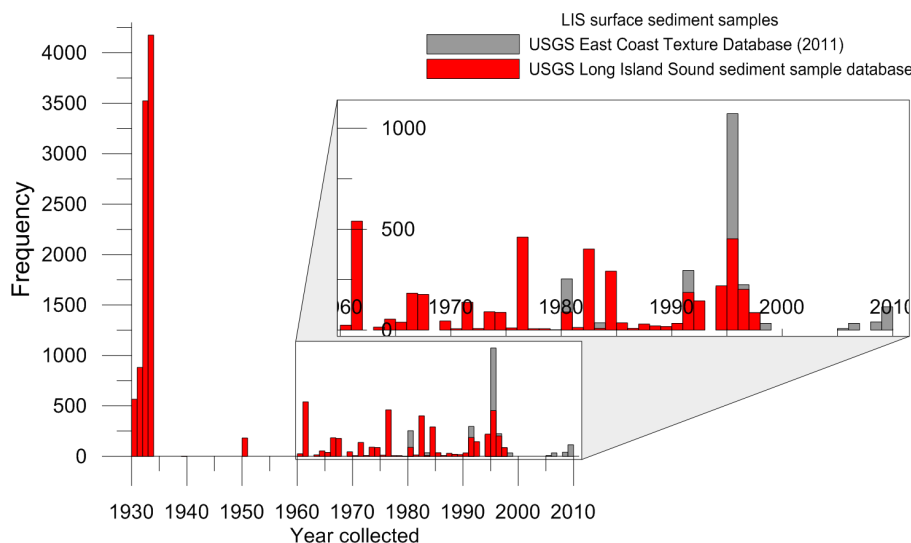


Figure 3-2: Number of existing sediment texture data from the USGS LIS Surficial Sediment Sample Database and the East Coast Sediment Texture Database.

While the density of older grain size data is high, the majority of these samples are older than 20 years. It is unclear to what extent older sediment samples from the 1930s reflect the present condition and if their grain size classification follows the present standards. Samples from the 1930s to 1990s might not represent any changes of the LIS bottom environments during and after this period. On the other hand, grain size data from the 1990s and 2000s might still represent current conditions in some areas that have not changed much. However, the description of biological habitats requires an accurate description of the substrate texture and we cannot be sure beforehand, if the older data still reflect the present state. Even in the case that many of the more recent (10-15 years old) data can be used for this study, the majority of those data is concentrated near Bridgeport and Port Jefferson, whereas there are fewer data in other parts of the pilot study area.

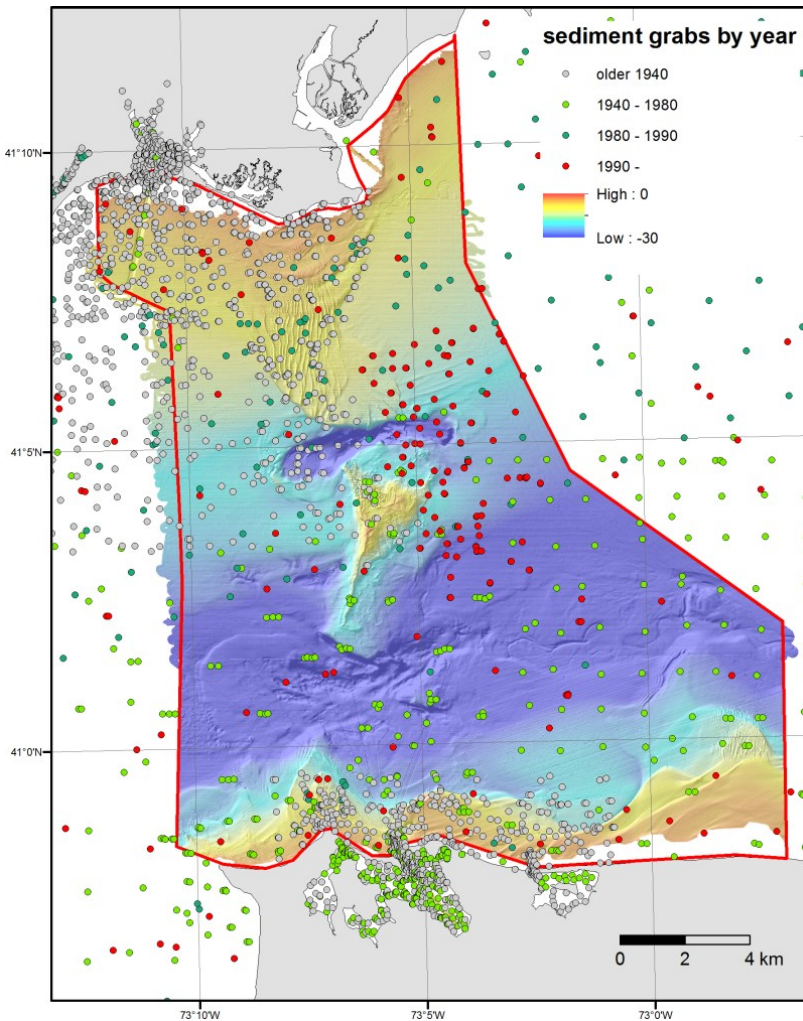


Figure 3-3: Distribution of existing sediment samples in the pilot area. Circles show locations of sediment grab samples colored by collection year: grey circles indicate before 1940, green 1940-1990 and red younger 1990.

3.3 *Sediment Sampling and Bottom Photography in Support of Ecological Characterization of Pilot Area*

3.3.1 *Overview*

Information on surface-sediment characteristics is critical to this component because sediment texture reflects benthic environmental energy and because benthic fauna and flora commonly have strong affinities for specific sediment classes and compositions. The photographic data are needed to appraise intra-station sea floor variability, document mobile fauna and sedimentary structures (indicative of geological and biological processes), and to observe the seabed at stations where samples could not be collected (e.g. boulder fields).

3.3.2 *Sampling*

The Sampling Plan for the sediment texture utilized the design developed for the Ecological Characterization, wherein 40 blocks distributed across sea-floor patches (selection based on depth gradients and geomorphic features; three stations/block) for studies of 1) Epifaunal / Demersal Communities and biogenic habitat characteristics, and 2) Infaunal communities biogenic habitat characteristics. These stations and the resultant data were released to collaborators for incorporation into the LDEO sampling schemes to prevent duplication and assist with the detailed mapping of sediment texture and sedimentary environments.

Data collected included still and video photography and sediment samples for grain-size and total organic carbon (TOC). The data were collected with a van Veen grab sampler equipped with still and video cameras (i.e. SEABOSS system). Video was collected for several minutes while the sampler drifted across the seafloor at 0.5 m above the bottom. During this time, 2-8 still photographs were also collected. Samples were collected from the interval 0-2 cm below the sediment/water interface; sediment sample size depended on the coarseness of the sample (e.g. mud and sand samples were 40-50 g; gravel samples were larger). Duplicate samples were collected for collaborators (e.g. Tim Kenna, LDEO) as requested.

3.3.3 *Data processing*

Grain-size data were generated in the Sedimentation Laboratory at the Woods Hole Coastal and Marine Science Center following methods described by Poppe et al. (2005). Briefly, bulk sediment samples were weighed wet, dried at 60°C, and reweighed to determine water content and correct for salt. The samples were then disaggregated in a sonic bath and wet sieved through a 4-phi sieve to separate the coarse and fine fractions. The coarse fraction (>0.0625 mm) was analyzed by sieving; the fine fraction was disaggregated with a sonic probe and analyzed with a Beckman Counter Multisizer 3. Particle distributions were calculated to whole-phi intervals between -5 and 11 phi, and processed with the program GSSTAT (Poppe et al., 2004). This software extrapolated the distribution to 13 phi and generated the percentages of the major fractions, sediment size classifications, and method of moments statistics. Sediment descriptions are based on the nomenclature proposed by Wentworth (1922) and the size classifications proposed by Shepard (1954) as modified by Schlee and Webster (1967), which is also used by the LDEO group (s. 3.4). Finally, the frequency percents from the 11-, 12-, and 13-phi fractions were combined, and the new 11-phi fraction is defined as 11 phi and finer. Because biogenic carbonate shells commonly form in situ but are not hydraulically equivalent to the host sediments, they usually are not considered to be sedimentologically representative of the depositional environment. Therefore, gravel-sized bivalve shells and other biogenic carbonate debris were manually removed and not included in the sediment grain-size data. Four of the finer grained sediment samples were reanalyzed by pipette, an analytical technique that resolves the entire clay and colloidal clay fractions, to check the results generated by the extrapolated Coulter Counter analyses. The pipette analyses gave results similar to those of the original Coulter

Counter analyses. Silt was still the dominant component and none of the original sediment classifications changed.

Inorganic carbon was removed prior to TOC analysis using vapor acidification; TOC was determined with a PerkinElmer 2400 CHN Analyzer. TOC data were generated in the Chemistry Laboratory at the Woods Hole Coastal and Marine Science Center following methods described by Jablonski et al. (2002).

Still photographs were compiled into both full-resolution archive and reduced-resolution processed galleries. Adobe Creative Suite 3 Photoshop was used adjust image size and to balance brightness and contrast in photographs of the reduced-resolution gallery. Comparisons of time stamps on the digital photographs with the ship's DGPS and latitude and longitudes recorded on the video allowed accurate navigation of the photography.

Spreadsheets of the textural and TOC data and photography stations with identifiers (station ID, navigation, device, etc.) were converted into shapefiles and FGDC-compliant metadata was written.

3.4 *Sediment Grab Collection and Analysis*

3.4.1 *Grab Sampling*

The sampling sites were chosen based on preliminary backscatter data from the area and the location of the USGS samples sites (section 3.3). The goal of the site selection was to achieve a dense, well-distributed coverage of the area while sampling major areas with different backscatter signature and complementing the USGS efforts.

Field work was carried out in June 2013 together with sediment coring (section 4.4). For the grab sampling we used the *R/V Seawolf* (Stony Brook University) for most areas and the *R/V Pritchard* (Stony Brook University) for shallow sites along the southern shore.

In total, we collected 196 grab samples (Table. 3.1). Figure 3.4 shows the location of the sediment grab sites collected by USGS and LDEO/Queens. Together with the new USGS data these samples represent most of the local variations found in the backscatter scatter data except, maybe, few smaller patches.

Table 3-1: Field data details of the sediment collection cruise (LIS1303).

Survey date	Field days	Vessel	Grab samples
June 5-12 2013	6	Seawolf	167
June 13 2013	1	Pritchard	29
Total	7		196

The sediment grabs were collected using a modified van Veen grab. Upon recovery of the grab samples, the following procedure was followed. A surface photo was taken and a brief description about the sediment texture and composition was noted in a table. Each sample was characterized by: whether the surface was oxidized or not, by its stiffness (very soft, soft, stiff, very stiff) and color (gray-green, gray). The grain size (mud, sand, gravel, and pebbles), wood, shell, oyster, mussel, living vegetation and anthropogenic contents were classified as: absent, rare, common and abundant. We also noted if there was hydrogen sulphide odor or not. In the general comments section, we noted particular characteristics of each sample. Upon completion of the visual description, the surface sediments (0-2 cm) were sampled directly into pre-weighed and pre-cleaned polystyrene jars, which were then sealed and placed in a cooler on ice. Sampling tools were cleaned and dried between samples. In addition, we recovered two mini-cores (5 inches long and 2 inches wide) that penetrated into the grab sample, preserving some of the sample stratigraphy. The mini-cores were capped and sealed with electric tape. The mini-cores are presently being curated at the Lamont-Doherty Core Repository under in conditions.

the net sample weight before and after freeze drying. Following this, a representative sub-sample was collected for possible grain size analysis (4-6 g) and the remainder of the sample was homogenized using a mortar and pestle to pass through a 500 micron sieve. Representative sub-samples of the bulk homogenized material were taken for XRF (3-5 g) and CHN (0.5 g). The remaining bulk homogenized material was stored in its original polystyrene jar pending matrix density determination.

3.4.3 *Chemical Assay*

Dried homogenized sediments, SRMs, and blanks consisting of clean SiO₂ powder were analyzed for chemical composition using an Innov-X Alpha series 4000 XRF (Innov-X Systems, Woburn, MA). Approximately 3 g of dried sediments and SRMs selected for dry XRF analysis were packed into sample cups equipped with Mylar polyester supports (Chemplex part Nos. 1330 and 257, respectively). Dry materials were analyzed with the FP-XRF positioned in a sampling test stand supplied by the manufacturer. Analyses and data processing were performed using published protocols which are covered in detail elsewhere (Kenna et al., 2011).

3.4.4 *Matrix Density*

Sediment matrix densities were determined from dry mass and dry volume measurements of homogenized bulk sediments, which were determined after bulk homogenized samples were transferred to 200mL beakers, heated in an oven at $105^{\circ} \pm 5^{\circ}\text{C}$ for at least 24 h, and allowed to cool in a desiccator. Sample mass was determined using an analytical balance and sample volumes were determined using a helium-displacement Penta-pycnometer (Quantachrome Instruments, Boynton Beach, FL). Volume measurements were repeated between 5 and 10 times, until the last five measurements exhibited $<0.01\%$ standard deviation. A reference volume was included within each sample set and rotated sequentially among the cells to check for instrument drift and systematic error. Replicate analysis of several samples indicated a precision of $<0.01\text{ cm}^3$.

3.4.5 *Grain Size Analysis*

The grain size data were generated at Queens College in McHugh's laboratory by using the following procedure: The second set of sediment sample jars were also stored at 4°C , weighed and then frozen. Water content was determined by comparing the net sample weight before and after freeze drying. The dried samples were laid on a paper, flattened and photographed (see Appendix 8-3). The quartering method or 'pie slice' method was used to obtain a representative subsample as follows. The dried sediment sample poured into a conical heap and flattened into a layer. Depending on the size, a $\frac{1}{8}$ to $\frac{1}{4}$ section was sampled vertically with a target weight of 5 to 7 g. The sub-sample was wet sieved through a $63\mu\text{m}$ sieve with deionized water. The fines and water were preserved in jars until the sediment settled. Following this, the water was poured off and the remaining water allowed to evaporate. The fine fraction was then weighed. If the

remaining fine-fraction weighed >1.3 g, it was selected for Sedigraph analysis as follows. Fine fraction samples were soaked in a 60 ml solution of 0.35 percent sodium hexametaphosphate. The matrix density used for the Sedigraph analyses was either obtained from the pycnometer measurements or entered as 2.65 g/cc.

If the weight of the fine fraction was < 1.3 g, the material was analyzed in the LDEO Multisizer II Coulter counting system (Beckman Coulter). In these cases, dried fine fractions were placed in a 1-qt wide-mouth Mason jars and filled to $\frac{3}{4}$ full with Milli-Q water and allowed to soak for at least 24 h. Prior to analysis, samples were disaggregated with a sonic probe for 5 minutes. While stirring vigorously, a representative 100 μ l aliquot was transferred to a 180 beaker containing a filtered electrolyte solution (0.4 percent sodium chloride, 0.02 percent potassium chloride, and 0.1 percent sodium hexametaphosphate). In order to evaluate performance of the Multisizer II, aliquots of certified reference materials (NIST-1021 and NIST-1003C) were routinely analyzed and resulting cumulative mass curves were within the published 95 percent confidence intervals for both CRMs.

The remaining coarse fraction greater than > 63 μ m was sieved through 125 μ m, 250 μ m, 500 μ m, 1000 μ m, 2000 μ m meshes and the mass of each fraction weighted. For the gravel and pebble components (shells, lithic grains), the major axial dimension was measured. The weight data was entered into an excel spread-sheet. Particle distributions were calculated to whole-phi intervals between -5 and >10 phi and processed using a custom Matlab routine, following the Wentworth scale (see section 3.3.3).

3.4.6 *Revision of SediGraph derived grain size data for LIS13-03 sediment grabs*

Comparison with the USGS grain size results revealed a discrepancy between USGS data derived from a Coulter Counter (SB series) and initially reported data based on Sedigraph analysis (LIS-03 series.) The initial suggestion that failure to remove organics prior to analysis as the root cause of problem made sense given the settling tube approach employed by the SediGraph (i.e., the presence of low density material that settled significantly slower than sediments could reasonably explain our results. However, analysis of SB series splits that include the removal of organics clearly indicate that issue remained (Figure 3-5). Additional experiments that examined the effect of cutoff as well as treatment for organics indicate that the cutoff value selected, rather than the presence of organics is a key factor (Figure 3-6). Analysis of samples to a significantly finer cut-off value 0.1 μ m vs 0.8 μ m reveals that the bulk of apparent excess fines fall below 0.1 μ m and are not associated with the clay size fraction.

To treat the samples for organics, we closely followed the Meyer and Fisher (1997) procedure. Approximately 5-7 g of the sample were freeze-dried and weighed (before and after freeze-drying). A solution composed of 100 ml aliquot of 30% hydrogen peroxide and 400 ml aliquot of 4 g sodium hexametaphosphate/l was prepared. Once dried each sample was placed into a 600 ml

Pyrex beaker and the solution added until it completely covered the sample. Digestion was allowed to continue for 12 hours.

Shepard Plot SB Splits 0.8 micron cut-off with H2O2 vs USGS Data

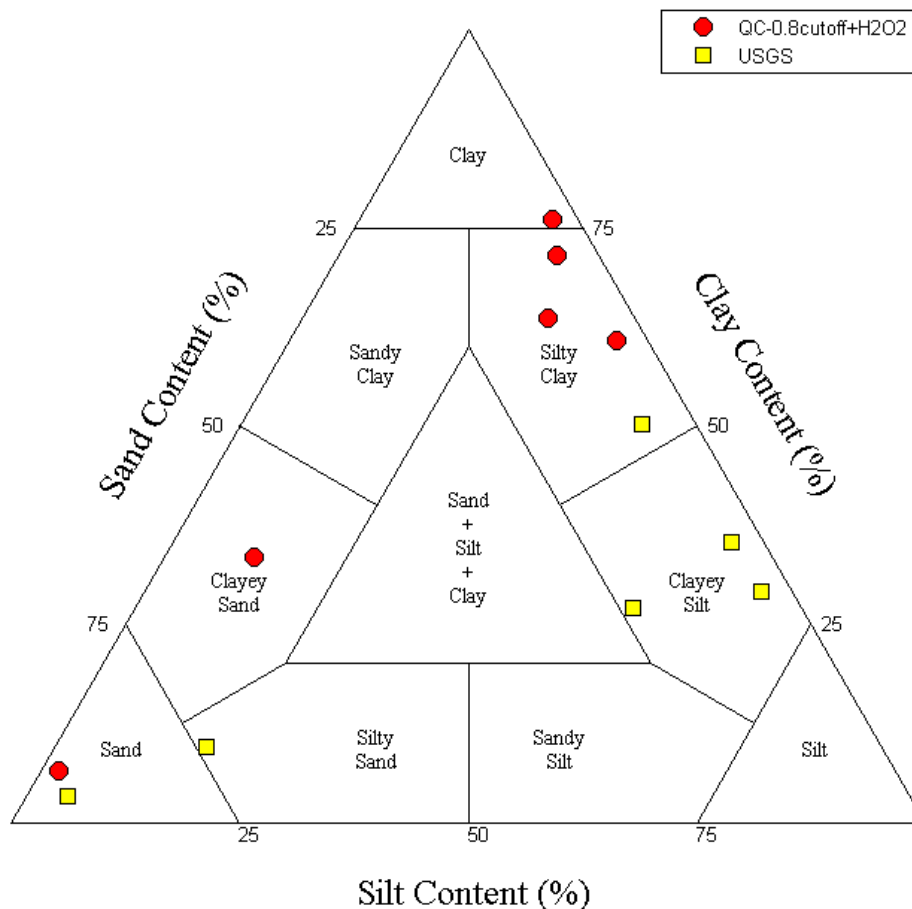


Figure 3-5: SB split results for 6 samples run with treatment for organics down to a 0.8 micron cutoff using LDEO's SediGraph. Results (red circles) indicate significantly higher clay content than USGS results for splits from the same samples. The disagreement between the two datasets suggests that treatment for organics is not the root cause of the elevated clay estimates. Further, the high clay estimates obtained for samples run on the LDEO SediGraph are similar to those generated by Queen's College, suggesting that the issue is not a result of a malfunctioning instrument.

Based on these observations, a procedure was devised to revise the original LIS13-03 series data. The SediGraph data are reported as mass % according to the following equation:

$$\text{mass\%} = (\log(I_m) - \log(I_b)) / (\log(I_f) - \log(I_b)) * 100$$

where:

I_m = the measured x-ray intensity at a given point (mass% being determined)

I_b = the x-ray intensity at baseline (mass% =0)

I_f = the x-ray intensity at full scale (mass % =100)

At the time of analysis, in addition to the calculated mass %, the values of I_b and I_f are also recorded. This allows the raw signal (I_m) to be extracted from the original data. Based on the trend in the I_m data in the lower diameter range, the data can be extrapolated from 0.8 microns to 0.1 microns (Figure 3-7). Once the original and extrapolated I_m data are merged, a revised mass % can be computed based on the recorded I_b and I_f values (Figure 3-8).

Shepard Plot SB Splits 0.1 micron cut-off with and without H2O2 vs USGS Data

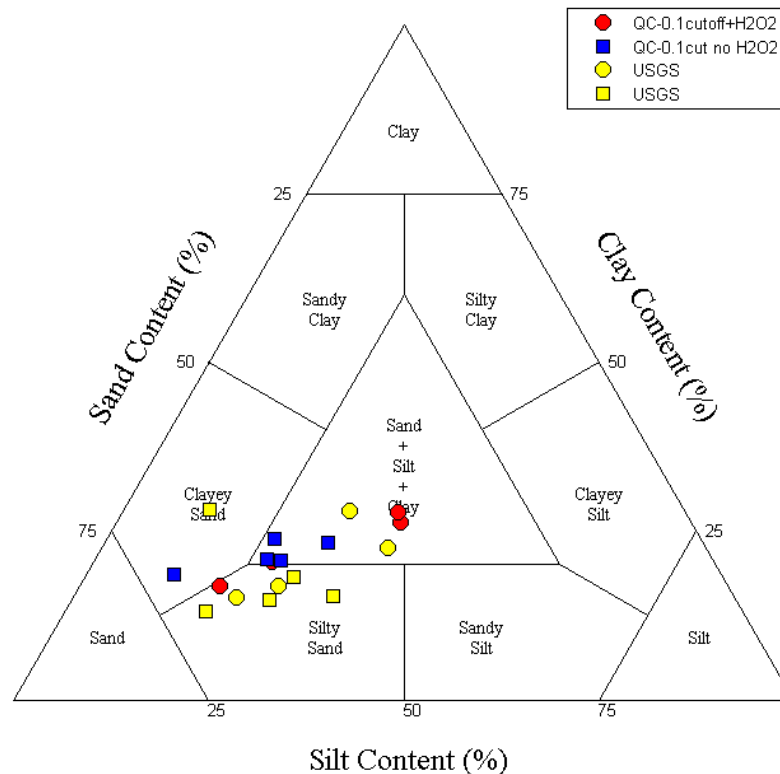


Figure 3-6: SB series split results for 4 samples run with treatment for organics down to a 0.1 micron cutoff (red circles) and 5 samples run without treatment for organics down to a 0.1 micron cutoff (blue squares). Matching yellow circles and squares are corresponding USGS results. Although there is some scatter in the data, there is reasonable agreement between all 3 data sets. This suggests that the organic treatment has minimal effect on the samples tested.

For additional parity, we followed the USGS approach and calculated particle distributions to whole-phi intervals between -5 and 11 phi, and then processed the data with the program GSSTAT (Poppe et al., 2004). Similar to the procedure used for the SB samples, we opted to extrapolate the distribution to 13 phi and generated the percentages of the major fractions, sediment size classifications, and method of moments statistics. When this procedure is performed on the data the results are similar to those obtained for samples treated for organics and run down to a 0.1 micron cutoff (Figure 3-9). Figure 3-10 shows the original and revised

LIS13-03 Series along with USGS SB Series data. In general the revised results are in good agreement with the USGS SB data showing no systematic offset and a similar amount of scatter.

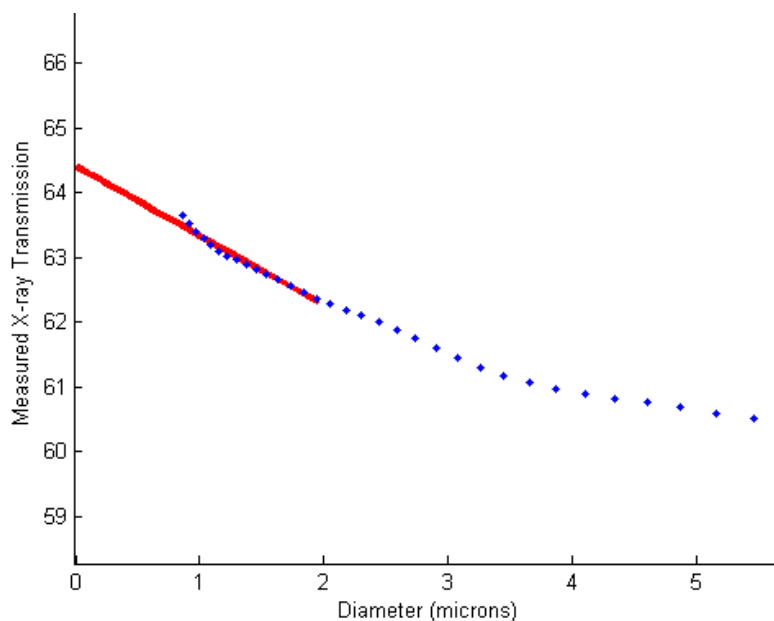


Figure 3-7: Example of extracted Im measured x-ray intensity (blue dots) and extrapolated values (red line).

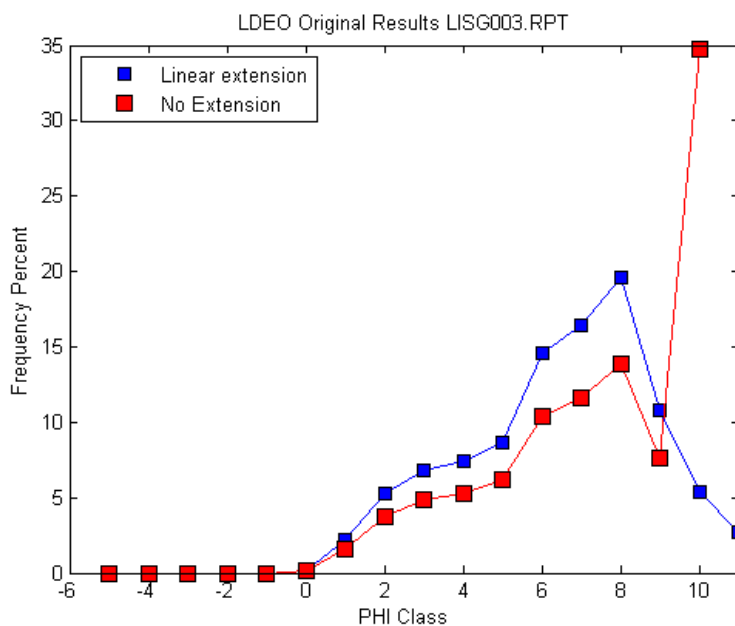


Figure 3-8: Example of extracted Im measured x-ray intensity (blue dots) and extrapolated values (red line).

Shepard Plot LIS Splits 0.1 micron cut-off with H2O2 vs 0.8 micron cut-off original and extended

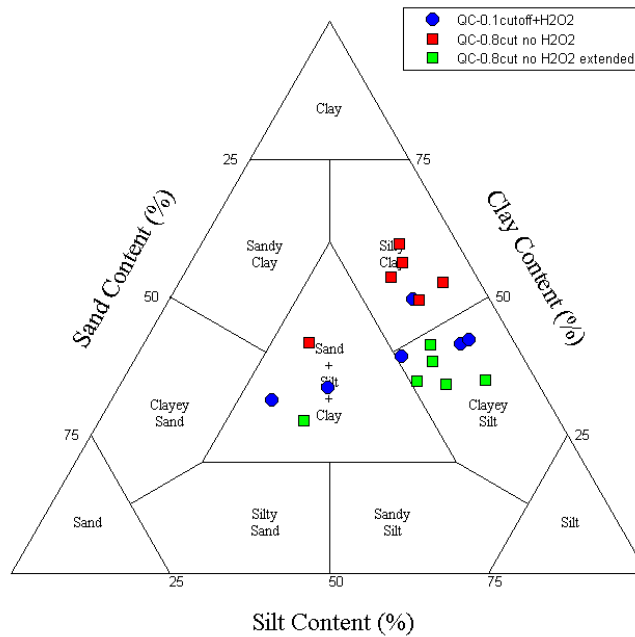


Figure 3-9: LIS13-03 split results for 6 samples run without treatment for organics down to a 0.8 micron cutoff. Initial interpretation (red squares) indicate significantly higher clay content than the revised interpretation (green squares) of the same data, which agree well with data generated from addition sample splits that were treated for organics and run down to a 0.1 micron cutoff (blue circles). The good agreement between the revised data from the first set of analyses (green squares) and data from the second set (blue circles) suggests that the organic treatment has minimal effect on the samples tested and the initially high clay estimates were driven by the Sedigraph cutoff value selected. It further that the correction procedure used to revise the original data is reasonable.

Shepard Plot initial and revised interpretations of LIS13-03 Series data compared to USGS SB Series

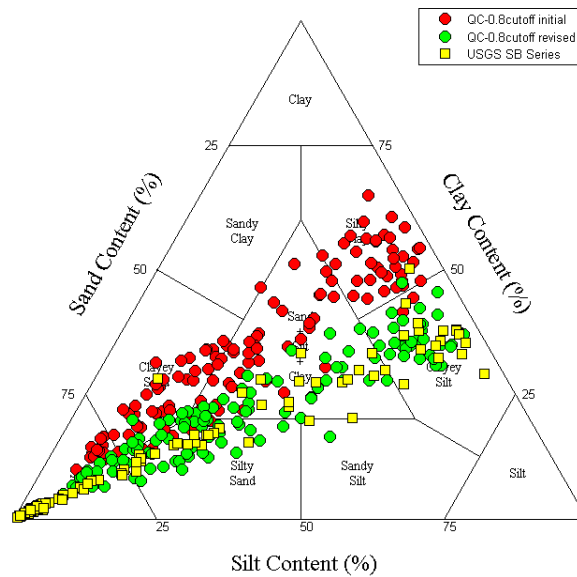
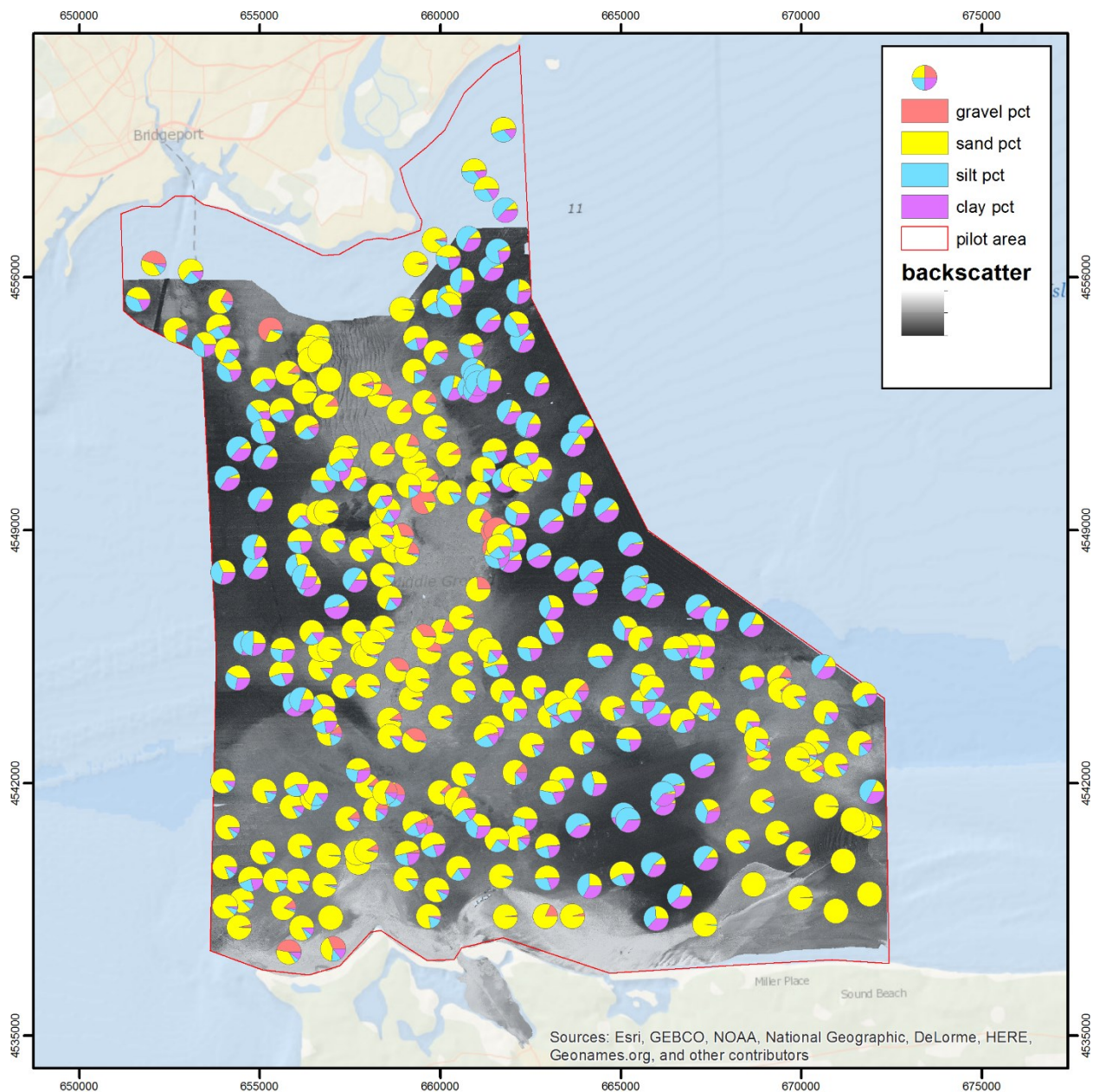


Figure 3-10: Initial (red) and Revised LIS13-03 (green) results compared to USGS SB Series (yellow).

Based on the revision procedure devised, which uses the existing trend in the measured x-ray intensity vs. particle size for each sample, values for the region between 0.8 and 0.1 microns can be estimated. When distributions are re-calculated they are in good agreement with the SB Series data as well as previous data sets, and should be accepted.

Although not definitive and ongoing, our additional experiments with SB Series splits suggest that the impact of non-treatment for organics is negligible. Going forward, rather than dictating a specific procedure or instrument, we recommend that laboratory intercalibration and intercomparison, standard reference materials, as well as some replicate analyses be incorporated into the analytical program and that proficiency be demonstrated prior to commencing additional fieldwork. This approach should in general be adopted where multiple laboratories are making the same measurement.

Figure 3.11 shows the resulting spatial distribution of the corrected grain size analysis results as pie charts in map of the pilot study area.



Sediment Grain Size Composition

Results of grain size analysis of both analysis (USGS and LDEO corrected) are shown as pie charts of gravel, sand, silt, and mud. Grain size data are plotted on top of acoustic backscatter mosaic for comparison.



0 3.6 Miles

Horizontal Coordinate System:
UTM Zone 18 Datum NAD83



Lamont-Doherty Earth Observatory
COLUMBIA UNIVERSITY | EARTH INSTITUTE

Figure 3-11: Grain size distribution (USGS and LDEO combined).

3.4.7 Carbon and Nitrogen (CHN) Analysis

The organic content of the sediment together with grain size are key for understanding the degree of heavy metal contamination and therefore the health of ecosystems. In order to measure the organic carbon content we used the following procedure.

The samples were analyzed with a Costech Carbon-Hydrogen-Nitrogen (CHN) analyzer. Prior to analyses the dried grab samples, that meet a target weight of 27 to 33 mg, were grounded for homogenization to a fine powder with a ball mill for one minute and 30 seconds. The samples were then placed in plastic packets, weighed, folded and placed in a desiccator cabinet with drierite until ready for analyses. Three replicates of each sample were prepared. The mass of carbon for the analyses must fall within 200-1000 μg and for Nitrogen was between 50 – 100 μg . A set of the samples was fumigated. Fumigation took place with a 100 ml of a 12M/N of HCl solution that was placed in a plastic desiccator along with weighed samples that were filled with 50 μl of deionized water in well plates. Acid fumigation occurred for at least 6 hours to eliminate the inorganic carbon/carbonates from the samples. The samples were then removed from the desiccator and placed under a fume hood for ~10 minutes to allow for the remaining condensation from HCl to evaporate. After evaporation of HCl, the samples were stored in a desiccator cabinet with drierite until it was time to dry them. Drying took place in an oven for four hours at 60°C. The samples were then removed and placed in the desiccator cabinet, weighted before folding and weighted after folding. The samples were then placed in micropipette plates and stored again in a desiccator cabinet until it was time for CHN analyses.

After calibration of the instrument with Atropine containing 70.56% carbon and blanks, the samples for both acid-fumigated samples and non-acid-fumigated samples were analyzed in the following order: 12 samples, 1 standard (low organic soil), and 1 blank.. The blanks were not fumigated because they don't contain carbonates. They were only used to find out if the instrument contained leaks. The low organic soil standard was also not fumigated. This was to avoid loss of carbon and because carbon is needed to create the standard curve. The samples were prepared based on the ratio of carbon to nitrogen of 10.775 (Poppe et al., 2000). Estimates of the TOC content of 0.00-3.00% were based on prior work from Long Island Sound (Poppe et al., 2000).

We interpolated the results of carbon and nitrogen percentages using the kriging algorithm in the ArcGIS software package. Figures 3-12 and 3-13 show the resulting distribution of total organic carbon and nitrogen in surface sediments (top 2cm) of the study area, which represents the general trend and overall levels of carbon and nitrogen.

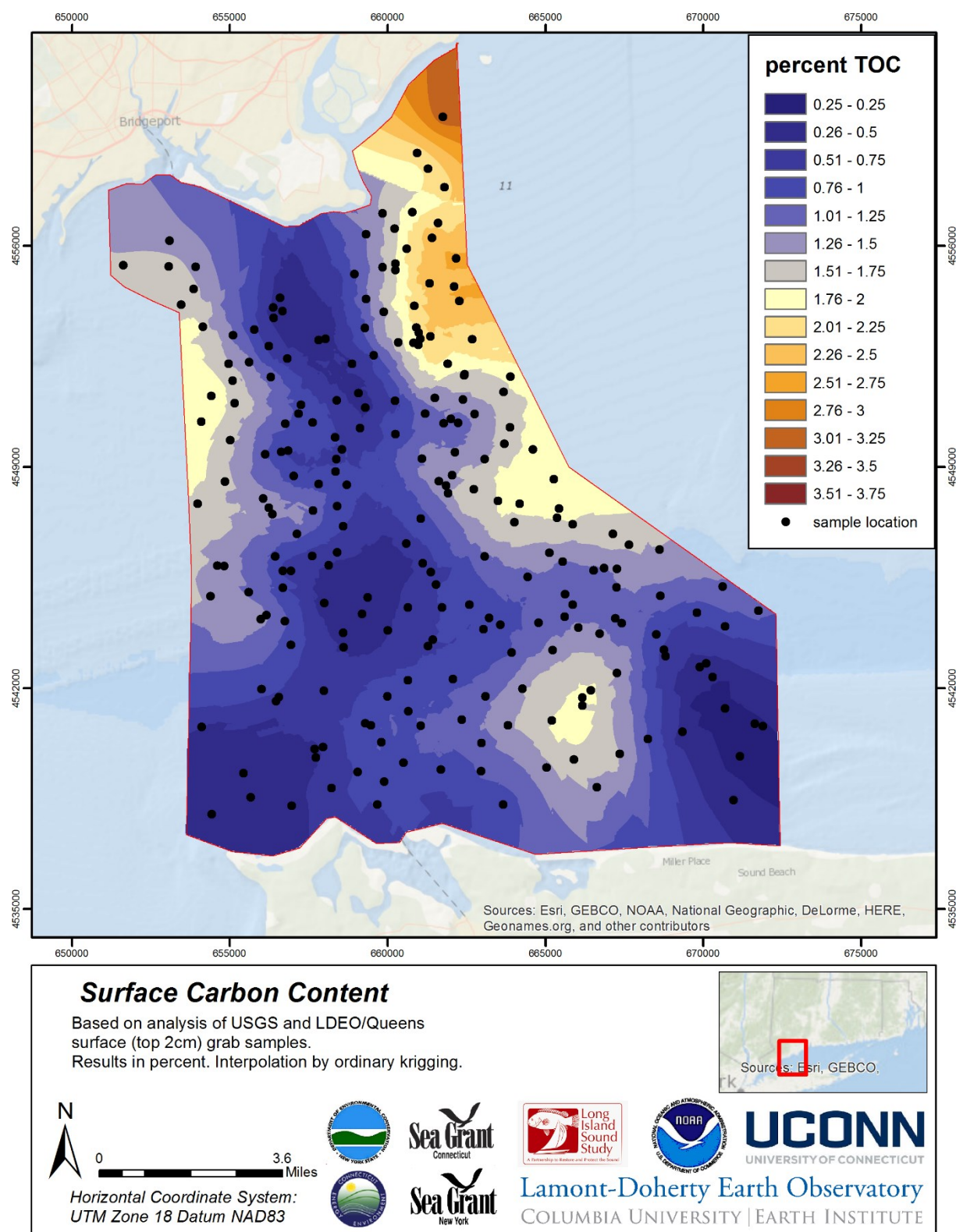


Figure 3-12: Map of interpolated values of surface carbon content based on the described analysis.

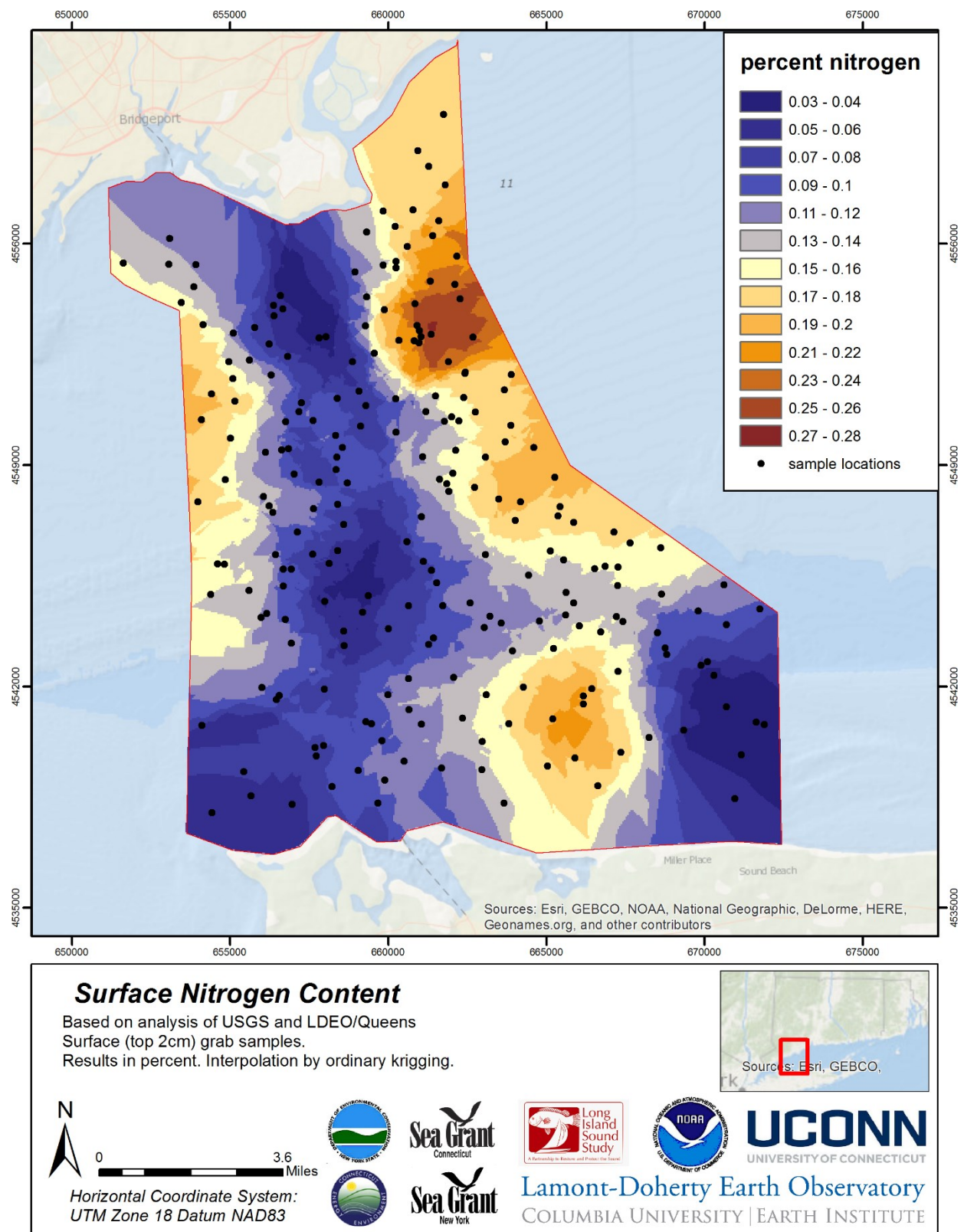


Figure 3-13: Map of interpolated values of surface nitrogen content based on the described analysis.

3.4.8 *Surface Metal Concentrations and Matrix Density*

Metal concentrations and sediment matrix density measured in the surface grab samples were interpolated using the kriging algorithm in ArcGIS and are presented in Figures 3-14 through 3-16 to show the trend in metal distribution across the study area. In general, we observe higher concentration in the northern sections of the study area. Following classification scheme of Long et al. (1995), the majority of measured Pb, Zn, and all Cu levels measured in the surface grab samples fall at or below the minimal effects ranges (ERL) with a small minority of Pb and Zn levels falling in the possible effects ranges (ERL-ERM). (Tab. 3-2). No values fell into the probable effect ranges (i.e. values >ERL-ERM). Although the pattern is not complete, likely sources include fluvial material originating from rivers along the CT coast and industrial activities. Lead and Zn surface distribution patterns are quite similar to each other and largely track areas with the highest clay and silt concentrations. This is consistent with increased surface area and metal sorption sites associated with fine sediment fractions. To a lesser extent Cu is also elevated in the northern sections. Differences between Cu and Pb and Zn may be due to different sources/applications of the metals. Matrix density is indicative of mineral composition and the distribution pattern observed in Figure 3-17 shows low values (2-2.5 g/cm³) in the northwest portion of the study site, while higher values (>2.7 g/cm³) occur in the northwestern portion of the study site. This parameter may be useful for identification and/or evaluation of different sediment sources in Long Island Sound.

Table 3-2: Summary of metal concentration levels after Long et al. (1995)

	Pb (ppm)	No. of samples	%		Zn (ppm)	No. of samples	%		Cu (ppm)	No. of samples	%
ERL	46.7	264	95%		150	226	81%		34	278	100%
ERL-ERM	218	14	5%		410	52	19%		270	0	0%

Total number of samples analyzed = 278

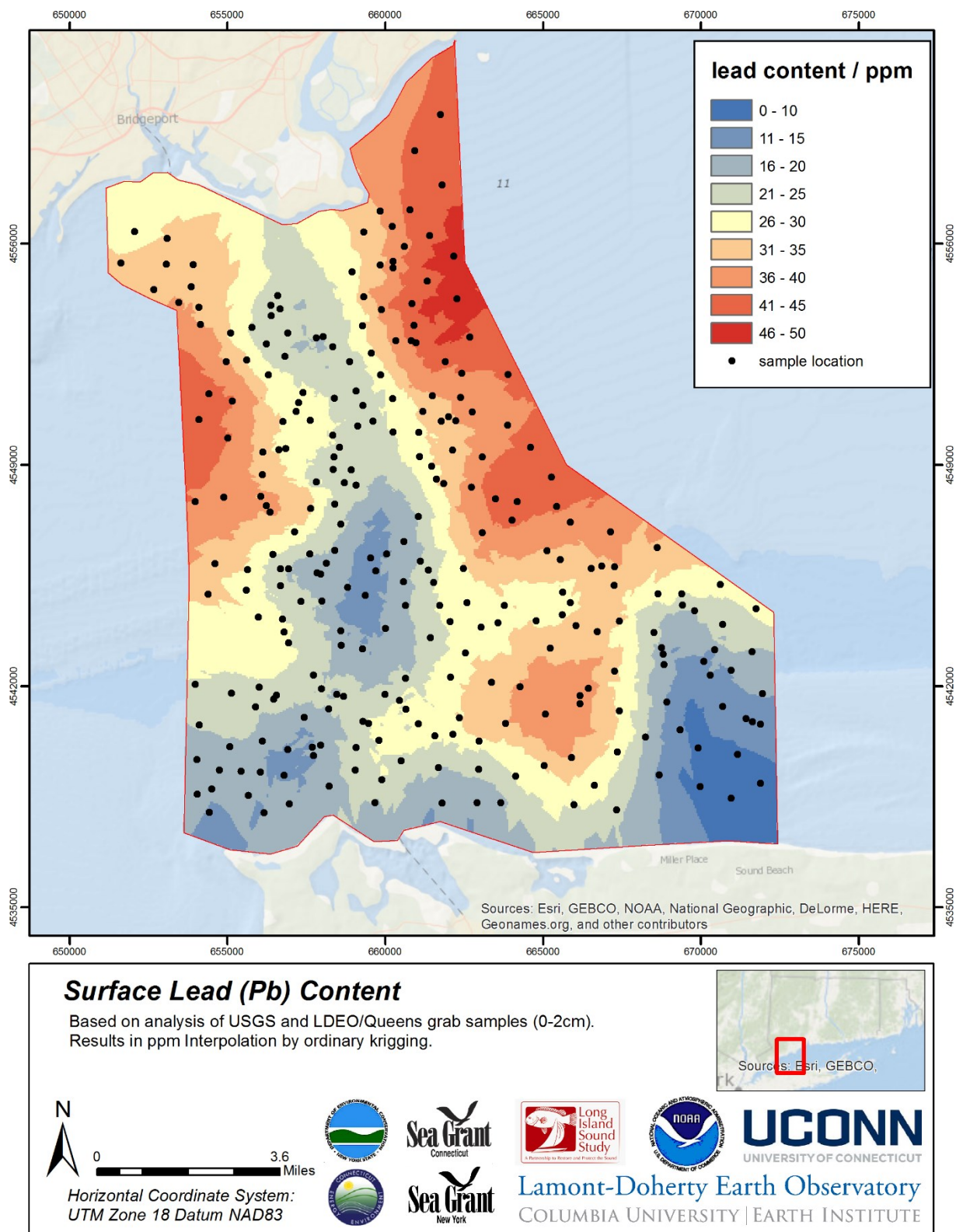


Figure 3-14: Map of interpolated values of surface (0-2cm) Pb concentrations.

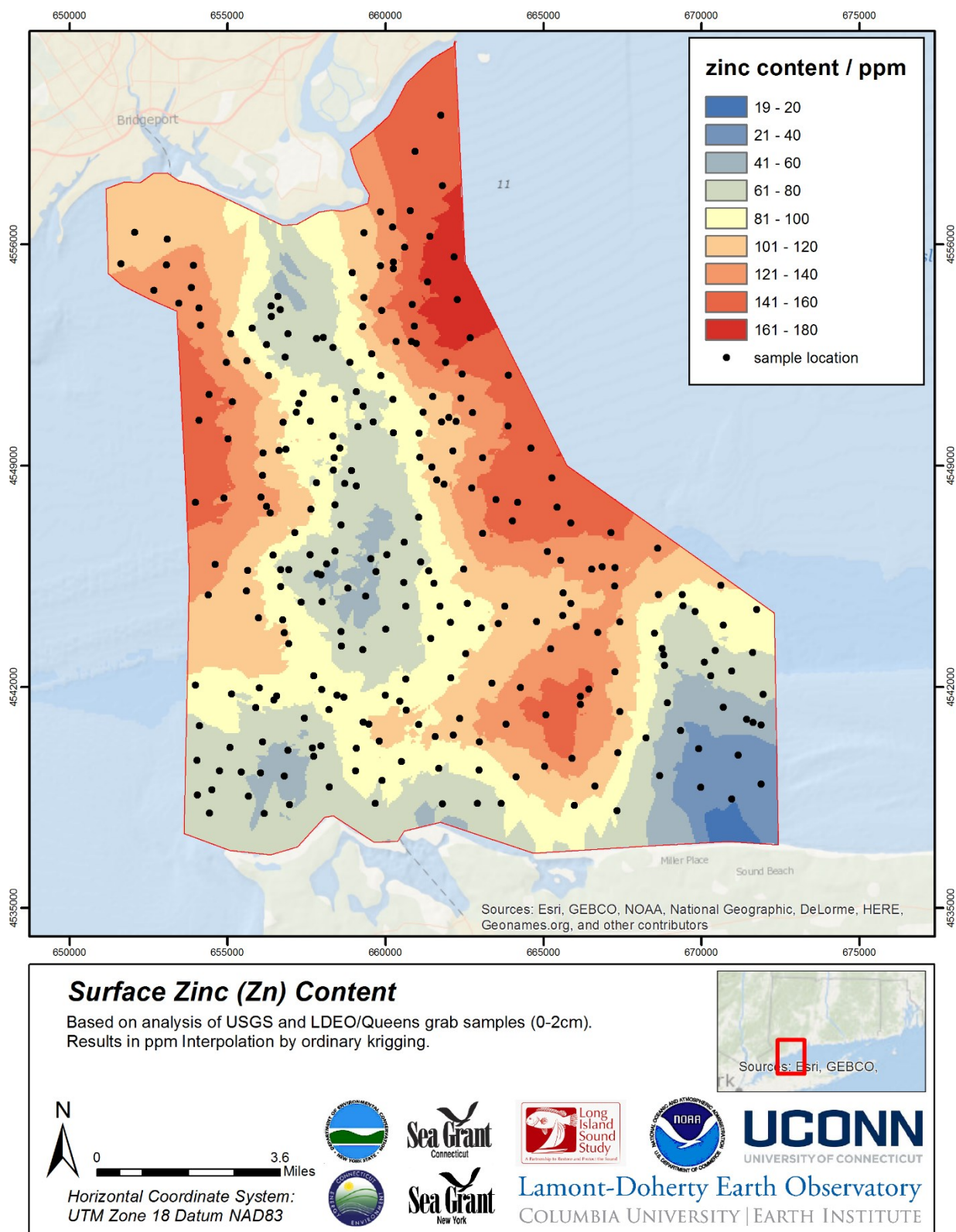


Figure 3-15: Map of interpolated values of surface (0-2cm) Zn concentrations.

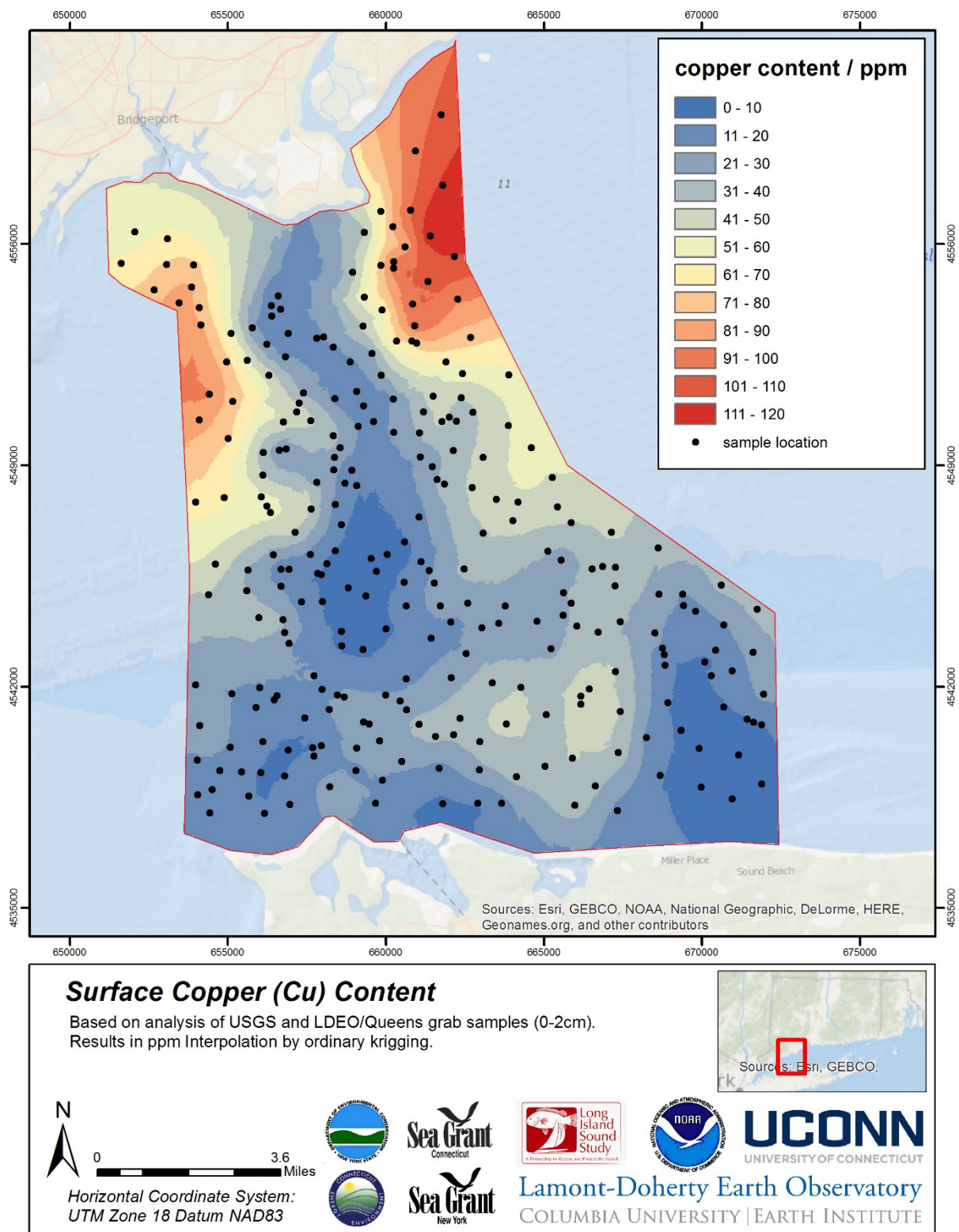


Figure 3-16: Map of interpolated values of surface (0-2cm) Cu concentrations.

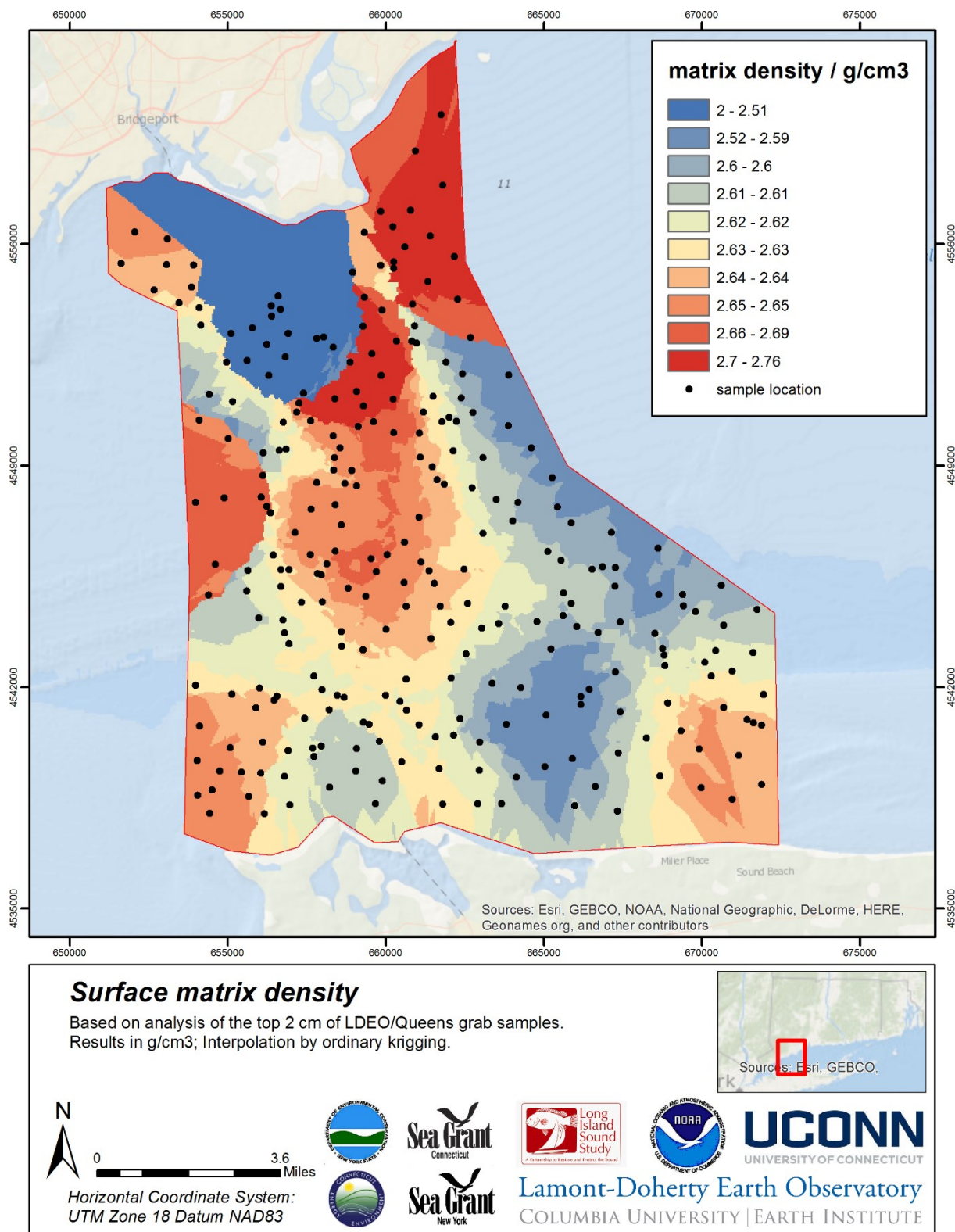


Figure 3-17: Map of interpolated values of surface sediment matrix density.

3.5 Sediment Texture Interpretations and Other Integrated Products

To simplify the interpretation and use of the results we divided the grain size data into distinct classes. The sediment classification scheme traditionally used in the LIS is a modified version of Shepard's (1954) ternary classification system shown in Figure 3-18 (Poppe and Polloni, 2000; Schlee, 1973; Shepard, 1954). This classification scheme provides usable information for determining biological habitat classes and merges with previous interpretations.

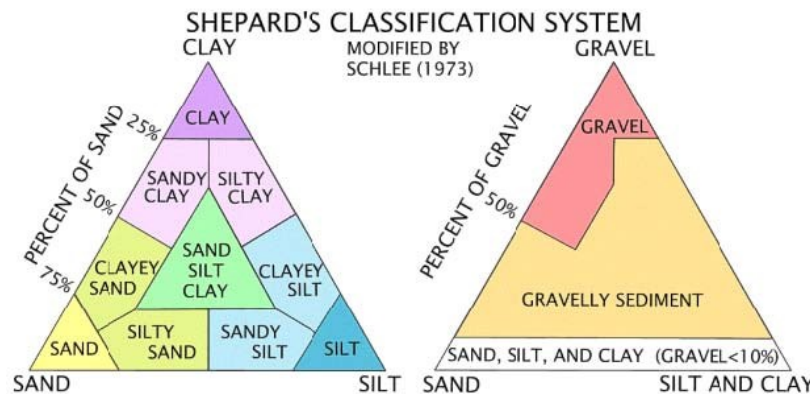


Figure 3-18: Modified sediment grain size classification scheme after (Poppe and Polloni, 2000; Schlee, 1973; Shepard, 1954).

An alternative classification scheme is the classification by Folk (1974) that combines silt and clay into a mud class and has been commonly used in other habitat studies (Figure 3-19). For the sediment texture analysis we combined the samples of the USGS and LDEO/Queens surveys and analysis. For each sample we determined the sediment texture class for both classification systems based on the percentage of gravel, sand, silt, and clay resulting from the grain size analysis. The results of these classifications have been added to the data tables.

For the description of the sediment texture and grain size distribution across the entire study area (excluding some very shallow areas that were not sampled) we combine the results of the grain size analysis with the acoustic data (section 2). For this we loaded these data sets into the ArcGIS geographic information system. We are using the uniformity of backscatter in an area to extrapolate sediment texture from the surrounding samples to this area. In addition, we use the seafloor bathymetry as additional guidance to distinguish boundaries between different morphological features that are likely to correspond to different sediment types. Based on this information we manually delineate polygon features for individual sediment texture areas.

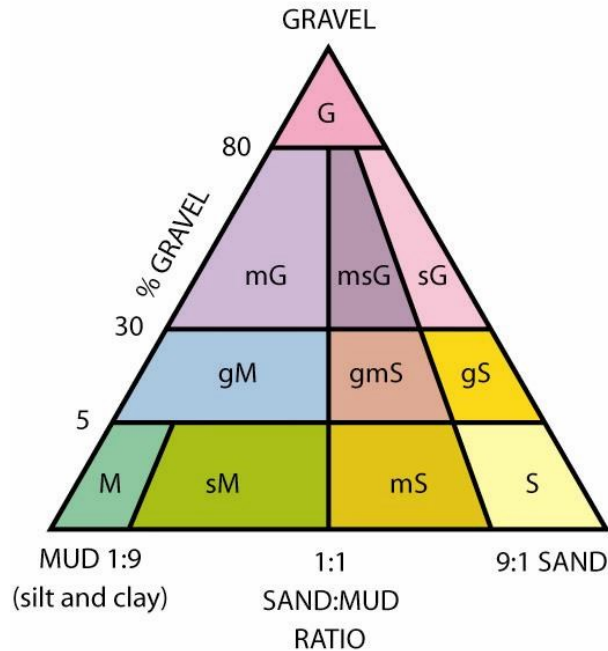


Figure 3-19: Simplified sediment grain size classification scheme after Folk (1974).

Figures 3-20 and 3-21 show the resulting distribution of the interpreted sediment texture for the pilot area.

Although we are providing polygon shapefiles that were manually created those should be used with care. Polygon features have discrete boundaries while in nature these boundaries are often fuzzy and gradual.

Classification schemes can be useful to highlight major trends in the data, but the distinct boundaries could mask real similarities or differences between the data. Samples with compositions directly on either side of boundary could be more similar than samples inside a class. An alternative approach would be to map out the percentage of mud, sand, or gravel over the study area as shown in Figures 3-22 and 3-24. They show the interpolated percentage of mud and sand respectively. Interpolation was done using simple kriging in ArcGIS. This representation of the grain size data reveals trends inside distinct classes and across boundaries. However, it does not reflect distinct boundaries where those actually exist, e.g. as part of morphological features. Also, note, that the approach used here is based on simple interpolation and does not take into account that all types of grain size together need to add up to 100 percent at any location.

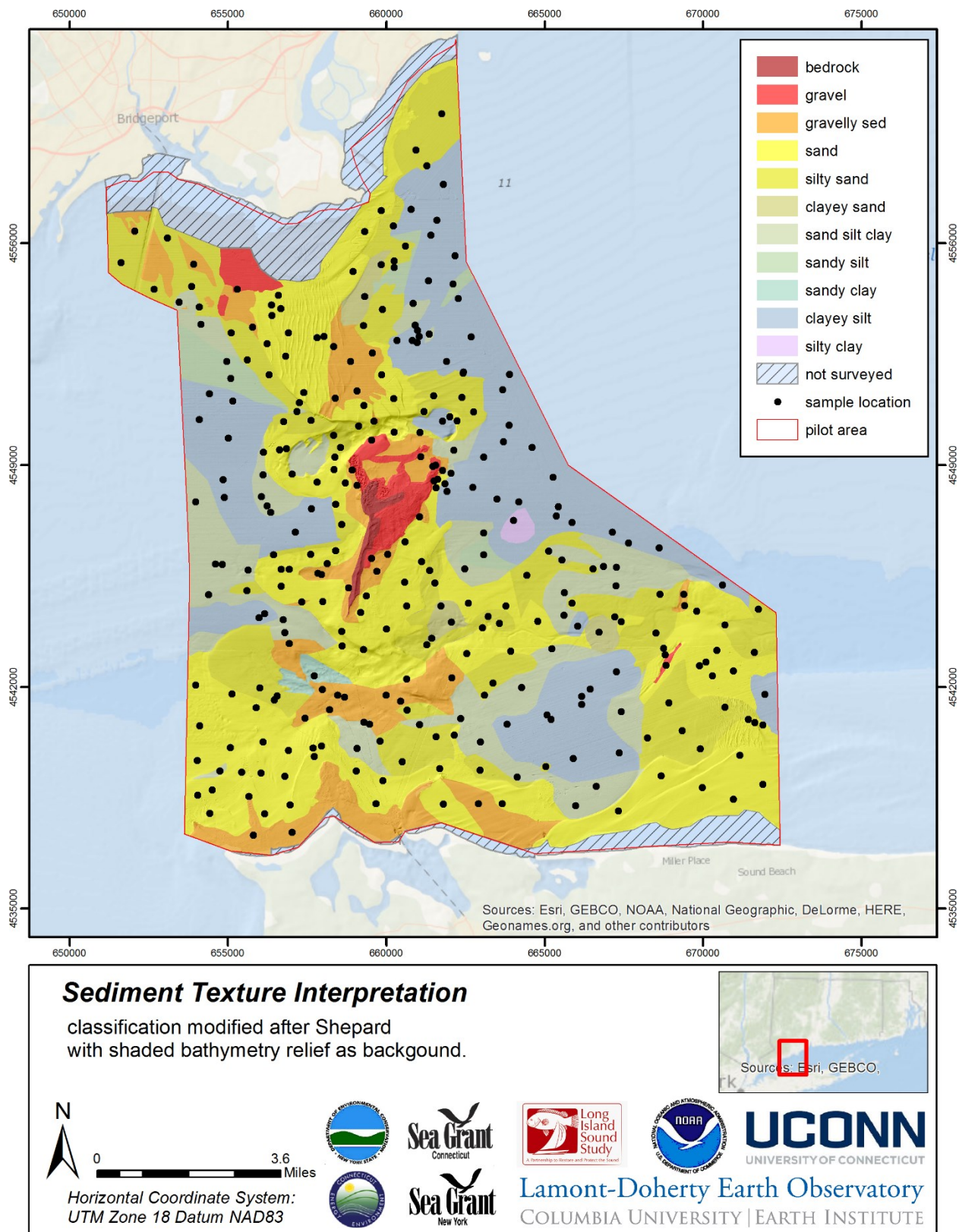


Figure 3-20: Sediment texture interpretation of the pilot area using the modified Shepard classification.

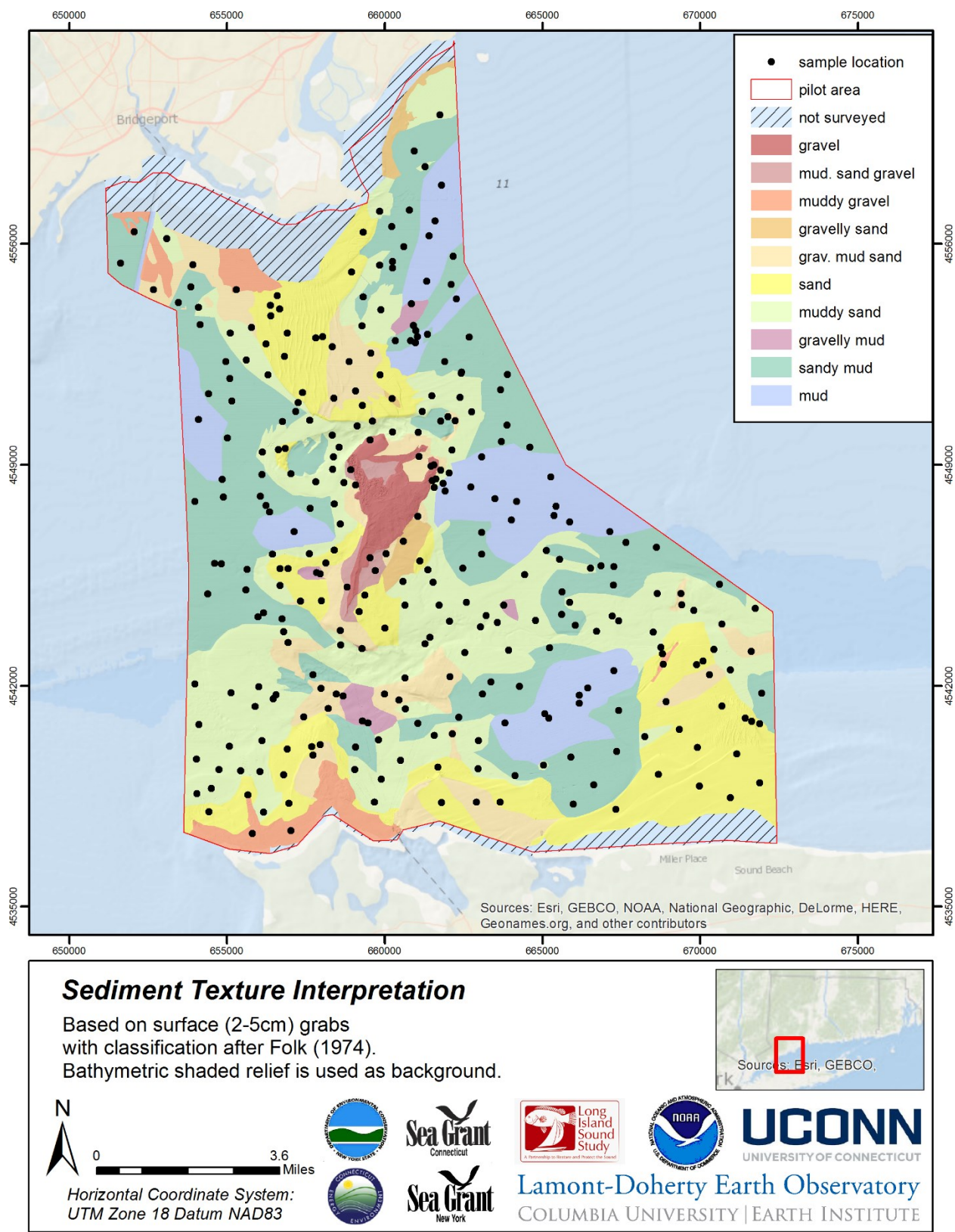


Figure 3-21: Sediment texture interpretation of the pilot area using the classification after Folk (1974).

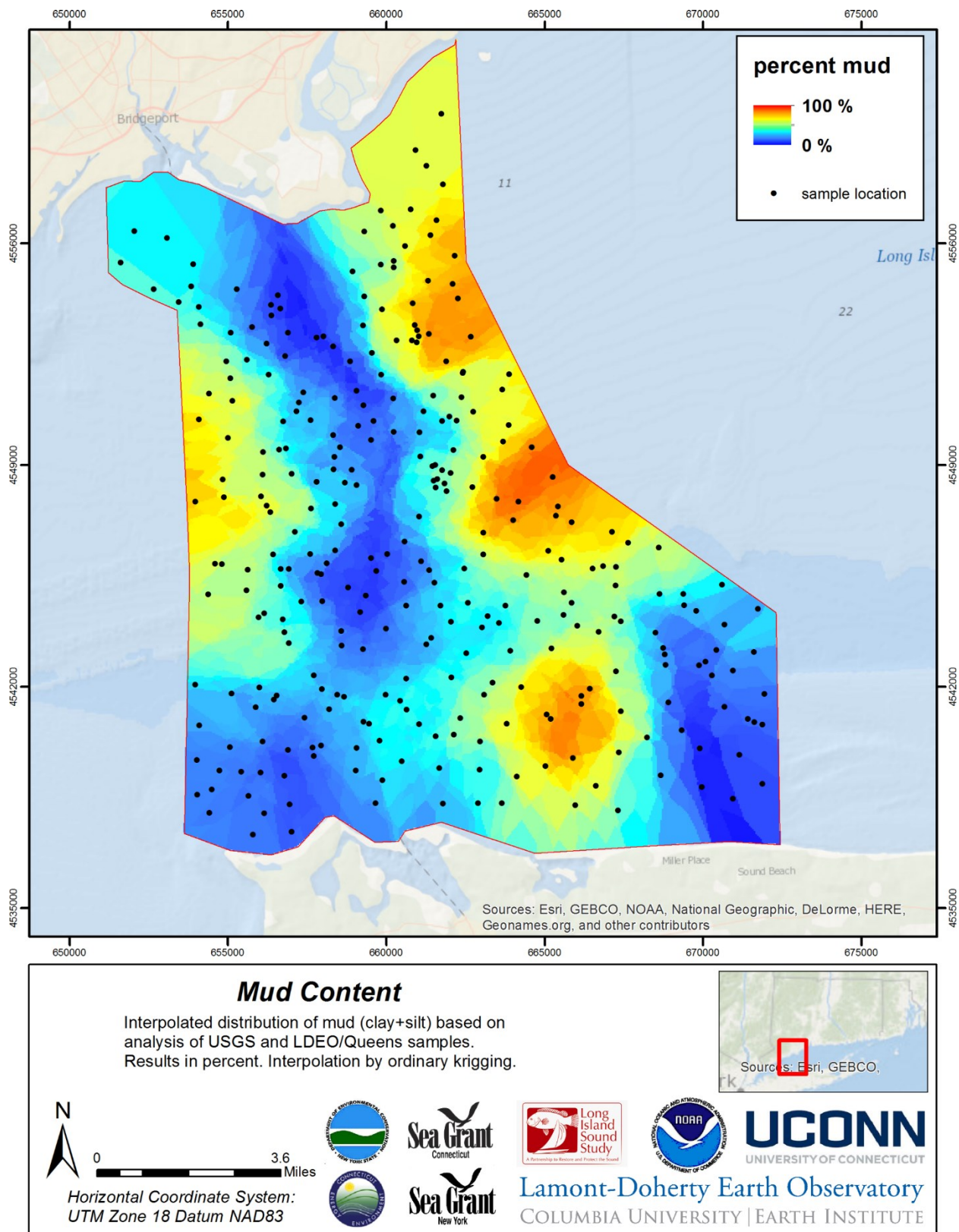


Figure 3-22: Map of interpolated values of mud content based on the grain size results of the combined USGS and LDEO/Queens College data sets.

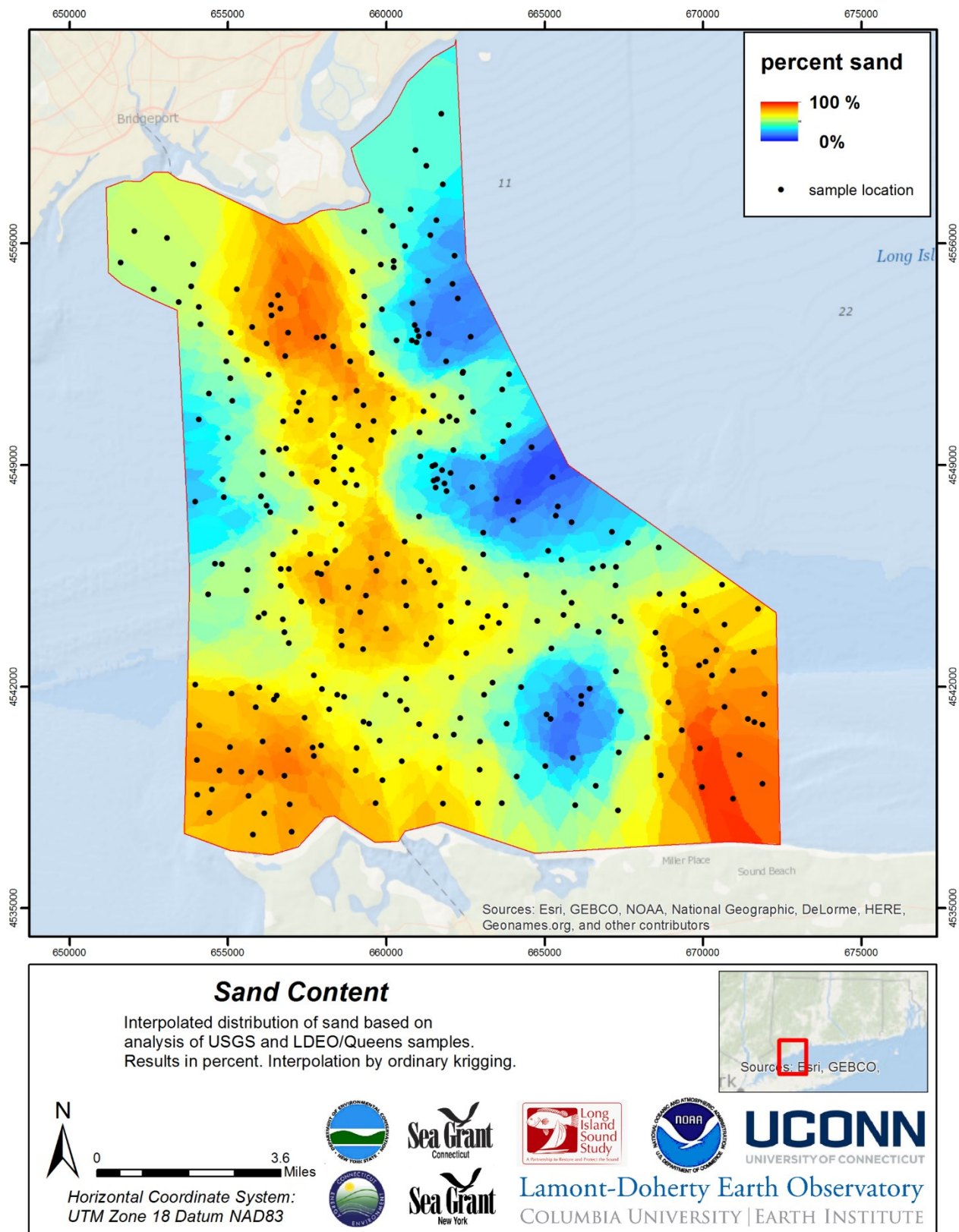


Figure 3-23: Map of interpolated values of mud content based on the grain size results of the combined USGS and LDEO/Queens College data sets.

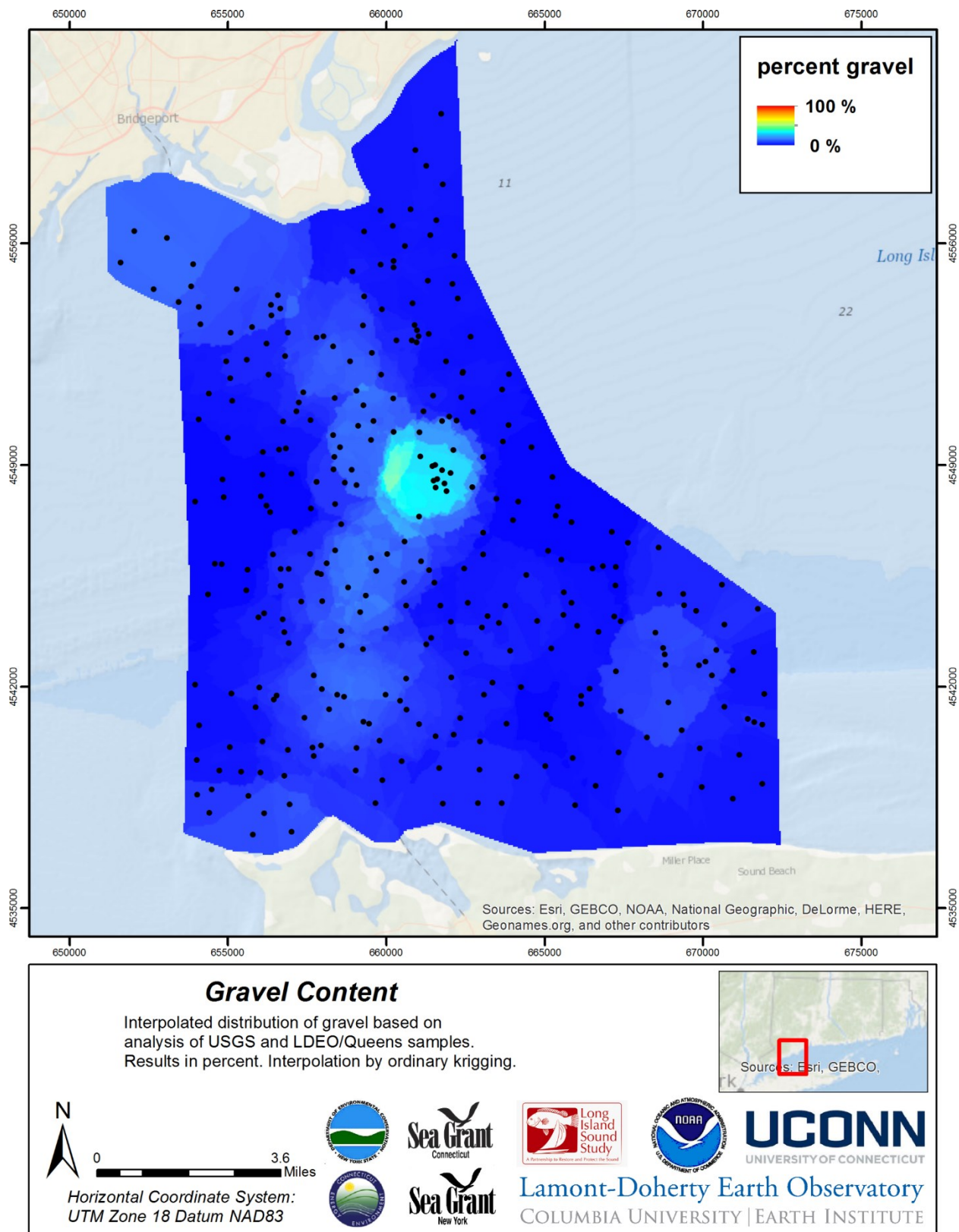


Figure 3-24: Map of interpolated values of gravel content based on the grain size results of the combined USGS and LDEO/Queens College data sets.

3.6 Comparison with Older Data

Detailed, high-resolution backscatter and bathymetry data were only available for small parts of the pilot area (and other sections of Long Island sound) when the Sound-wide sediment texture interpretation was generated. As result, the existing LIS-wide interpretation might not have the required resolution for the detailed habitat maps envisioned by this project. Full coverage of bathymetry and backscatter data allows a more precise and detailed mapping of the boundaries and extent of sediment texture. Since grain size is the basis for many derived habitat products it needs to reflect the environment as accurately as possible. Figure 3-25 compares the earlier with the new sediment texture map for the pilot area.

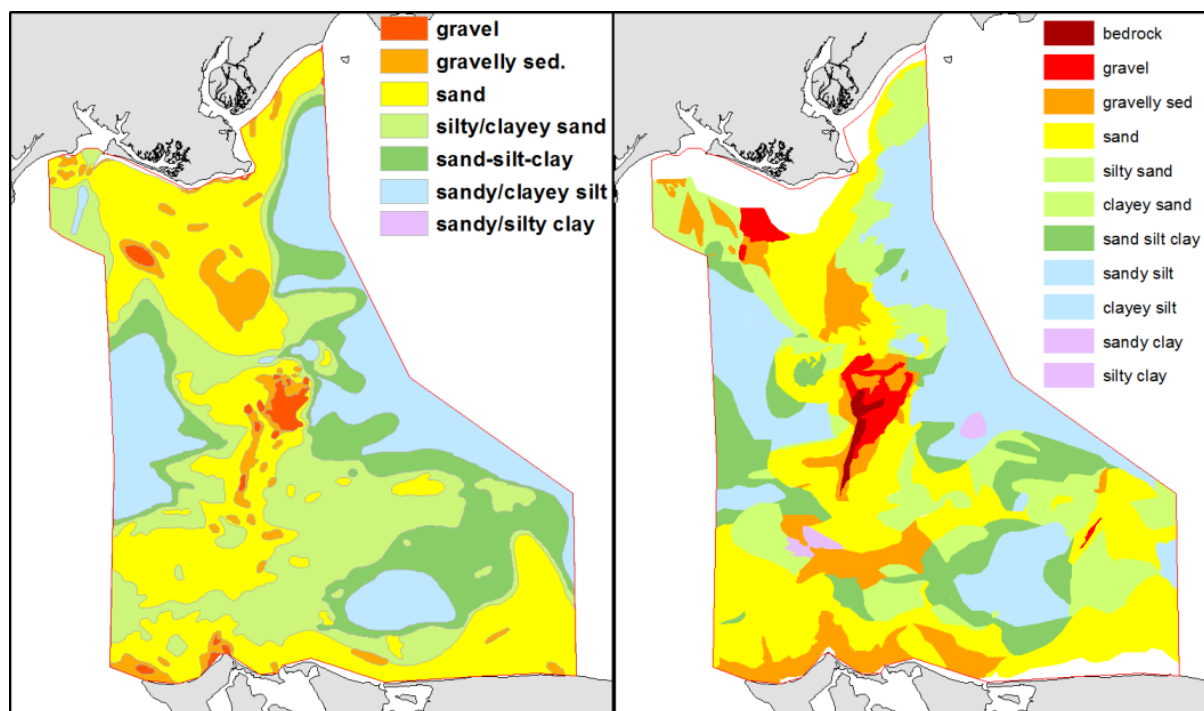


Figure 3-25: Comparison of USGS sediment texture (left) and the new sediment texture interpretation of this study (right). Note that both use the modified Shepard classification and that the new interpretation is based on the grain size results without attempts to reconcile the two data sets.

3.7 Summary and Recommendations

Sediment grain size is an important element for characterizing the seafloor physical environment and a key factor for many habitats. There are abounded old grain size data available, but the seafloor environment is highly variable in places and data several decades old might not reflect the current conditions.

To characterize different environments revealed by the acoustic data, grain size sampling efforts should be planned based on the acoustic, especially backscatter data. Obtaining grain size

samples where the biological samples are taken is encouraged to ensure that both data sets are collocated to minimize effects of spatial variability.

Although the initial grain size measurements conducted by LDEO/Queens systematically differed in the clay content from the USGS measurements, this difference was resolved after reexamining the LDEO/Queens data.

The detailed grain size data reveal a larger pattern of grain size distribution with finer sediment in the center west, the north and center east and a patch of finer grain size in the south. Stratford Shoals are dominated by coarser sediments. Sandy sediments are found in the center north and along the southern shore. Despite this larger pattern there are variations on a smaller scale throughout the study area.

While in most areas the acoustic backscatter data and the grain size data correspond well, there are some locations, e.g. south-east corner, where there sandy sediment do not correspond to high backscatter data. This shows that ground verification is essential for interpreting the acoustic data.

The grain size results can be displayed and visualized in various forms including different classification schemes and interpolated percentages of grain size classes. While for most application it might be useful to use the established, modified Shepard classification scheme some of the additional representations might be useful for other future applications.

Additional analysis on the sediment surface samples including carbon, nitrogen, metals, and matrix density provide valuable, additional information without significant additional cost.

Recommendations

- We recommend that grain size samples should be an integral part of the any future mapping attempt. Sampling locations should be based on acoustic data and be coordinated with biological sampling
- Rather than dictating a specific procedure or instrument, we recommend that laboratory intercalibration and intercomparison, standard reference materials, as well as some replicate analyses be incorporated into the analytical program and that proficiency be demonstrate prior to commencing additional fieldwork. This approach should in general be adopted where multiple laboratories are making the same measurement.
- Maximize the derived information by including additional, value-adding, low-cost analyses including carbon, nitrogen, and metals.
- Integration between surface grain size data and current oceanographic measurements including tides and near bottom shear stress maps.

3.8 References

- Ferrini, V.L. and Flood, R.D., 2006. The effects of fine-scale surface roughness and grain size on 300 kHz multibeam backscatter intensity in sandy marine sedimentary environments. *Marine Geology*, 228(1-4): 153-172.
- Folk, R.L., 1974. *Petrology of sedimentary rocks*. Hemphill Publishing Company, Austin Texas.
- Galparsoro, I., Borja, Á., Kostylev, V.E., Rodríguez, J.G., Pascual, M. and Muxika, I., 2013. A process-driven sedimentary habitat modelling approach, explaining seafloor integrity and biodiversity assessment within the European Marine Strategy Framework Directive. *Estuarine, Coastal and Shelf Science*, 131(0): 194-205.
- Jablonski, S., Mecray, E., Munson, J. and Blackwood, D., 2002. *Geochemical sediment analysis procedures*.
- Kenna, T.C., Nitsche, F.O., Herron, M.M., Mailloux, B.J., Peteet, D., Sritrairat, S., Sands, E. and Baumgarten, J., 2011. Evaluation and calibration of a field portable X-ray fluorescence spectrometer for quantitative analysis of siliciclastic soils and sediments. *Journal of Analytical Atomic Spectrometry*, 26(2): 395-405.
- Long, E.R., MacDonald, D.D., Smith, S.L. and Calder, F.D., 1995. Incidence of Adverse Biological Effects Within Ranges of Chemical Concentrations in Marine and Estuarine Sediments. *Environmental Management*, 19(1): 81-97.
- Meyer A. and A. Fisher, 1997. Data Report: Grain-size analysis of sediments from the Northern Barbados accretionary prisms. In Shipley, T. H, Ogawa, Y, Blum, P, and Bahr, J.M. Editors. *Proceedings of the Ocean Drilling Program Scientific Results*, Vol. 156, 338-341p.
- Nitsche, F.O., Bell, R., Carbotte, S.M., Ryan, W.B.F. and Flood, R., 2004. Process-related classification of acoustic data from the Hudson River Estuary. *Marine Geology*, 209: 131-145.
- Poppe, L., Knebel, H., Mlodzinska, Z., Hastings, M. and Seekins, B., 2000. Distribution of surficial sediment in Long Island Sound and adjacent waters: Texture and total organic carbon. *Journal of Coastal Research*, 16(3): 567-574.
- Poppe, L.J., Eliason, A.H. and Hastings, M.E., 2004. A Visual Basic Program to Generate Sediment Grain-Size Statistics and to Extrapolate Particle Distributions. *Computers & Geosciences*, 30(7): 791-795.
- Poppe, L.J. and Polloni, C.F., 2000. USGS east-coast sediment analysis; procedures, database, and georeferenced displays. U.S. Geological Survey Open-File Report, 2000-358 <http://pubs.usgs.gov/of/2000/of00-358/>.
- Poppe, L.J., Williams, S.J. and Paskevich, V.F., 2005. U.S. Geological Survey East Coast sediment analysis: Procedures, database, and GIS data: U.S. Geological Survey Open-

File Report 2005–1001 DVD-ROM. (Also available at [http://pubs.usgs.gov/of/2005/1001/.](http://pubs.usgs.gov/of/2005/1001/))

Schlee, J., 1973. Atlantic Continental Shelf and Slope of the United States sediment texture of the northeastern part. U.S. Geological Survey Professional Paper, 529-L, 64 pp.

Schlee, J. and Webster, J., 1967. A computer program for grain-size data. *Sedimentology*, 8(1): 45-53.

Shepard, F.P., 1954. Nomenclature based on sand-silt-clay ratios. *Journal of Sedimentary Petrology*, 24: 151-158.

Stein, R., 1985. Rapid train-size analyses of clay and silt fractions by SediGraph 5000D: comparison with Coulter Counter and Atterberg methods. *Journal of Sedimentary Petrology* Vol. 55, 590-593.

Wentworth, C.K., 1922. A scale of grade and class terms of clastic sediments. *Journal of Geology*, 30: 377-392.

4 Sedimentary Environment

Recommended Citations:

Nitsche, F. (2015). Objective. Section 4.1, p. 96 in: “Seafloor Mapping of Long Island Sound – Final Report: Phase 1 Pilot Project.” (Unpublished project report). U. S. Environmental Protection Agency, Long Island Sound Study, Stamford, CT.

Nitsche, F. (2015). Historical Context. Section 4.2, p. 96-98 in: “Seafloor Mapping of Long Island Sound – Final Report: Phase 1 Pilot Project.” (Unpublished project report). U. S. Environmental Protection Agency, Long Island Sound Study, Stamford, CT.

Nitsche, F. (2015). Subbottom Data Collection and Analysis. Section 4.3, p. 98-105 in: “Seafloor Mapping of Long Island Sound – Final Report: Phase 1 Pilot Project.” (Unpublished project report). U. S. Environmental Protection Agency, Long Island Sound Study, Stamford, CT.

Kenna, T. and C. McHugh. (2015). Sediment Cores Collection and Analysis. Section 4.4, p. 106-112 in: “Seafloor Mapping of Long Island Sound – Final Report: Phase 1 Pilot Project.” (Unpublished project report). U. S. Environmental Protection Agency, Long Island Sound Study, Stamford, CT.

Nitsche, F., T. Kenna, and C. McHugh. (2015). Sediment Environment Interpretations and other Integrated Products. Section 4.5, p. 112-121 in: “Seafloor Mapping of Long Island Sound – Final Report: Phase 1 Pilot Project.” (Unpublished project report). U. S. Environmental Protection Agency, Long Island Sound Study, Stamford, CT.

Nitsche, F., T. Kenna, and C. McHugh. (2015). Summary and Recommendations. Section 4.6, p. 122-123 in: “Seafloor Mapping of Long Island Sound – Final Report: Phase 1 Pilot Project.” (Unpublished project report). U. S. Environmental Protection Agency, Long Island Sound Study, Stamford, CT.

4.1 *Objective*

While sediment texture describes the grain size composition, the sedimentary environment describes the processes controlling a certain location such as deposition or erosion. It defines the dynamics of the seafloor in LIS and, therefore, is important for identifying and understanding areas that are stable or changing. Detailed information about the sediment environment provides insights into the physical dynamic of the benthic environment, its stability and evolution. This includes the effect of outside disturbances such as the impact of cables, pipelines, dredging and construction on the bottom of the sound.

The sedimentary temporal and spatial record of these processes can be obtained from combining multibeam bathymetry, backscatter, subbottom, and sediment cores information. The multibeam bathymetry and backscatter data provide the large-scale morphology, dimensions and spatial distribution of features such as bedforms and channels. However, they do not provide any information on the thickness of surface sediment layers or the nature and thickness of subsurface sediments. Thus, what may appear as a sandy bottom in the backscatter data may in fact be only a thin layer of sand atop rock or some other sediment type. This distinction can have significant ramifications for those looking for exploitable sand and aggregate deposits or the potential for seabed erosion or disturbance. Subsurface information from subbottom data and sediment cores are necessary to clearly distinguish depositional and erosional areas or identify a thin layer of sediments covering bedrock outcrop. Subbottom and sediment core data can also reveal if an area has been disturbed by isolated or frequent events in the past that might have changed that environment significantly. While subbottom data provide the spatial coverage necessary for mapping different environments sediment cores provide the temporal evolution and detail needed for the interpretation of the acoustic data.

4.2 *Historical Context*

As an important parameter for understanding the seafloor dynamic sediment environment have been included in most past seafloor studies of the Long Island Sound. Most of these studies were conducted by the USGS and include a LIS-wide interpretation of sediment environments (Figure 4.1; e.g. Knebel and Poppe, 2000; Knebel et al., 1999). Like the sediment texture interpretation (section 3.2) this interpretation was based on previously existing sidescan and seismic data as well as bottom samples and photographs. This classification distinguished deposition, erosion, sorting and transportation environments.

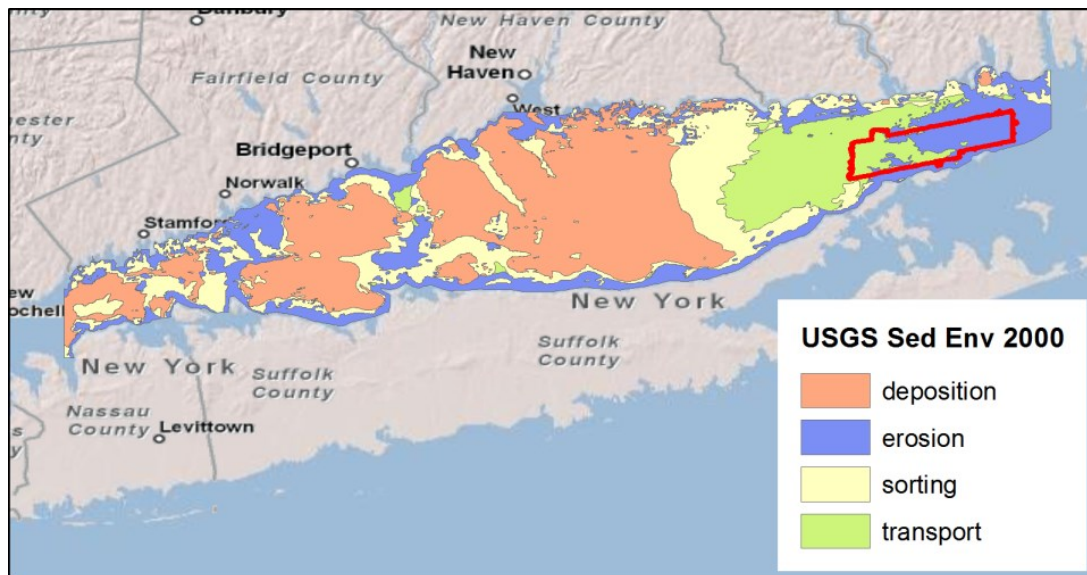


Figure 4.1: LIS sediment environment interpretation (Knebel and Poppe, 2000; Knebel et al., 1999).

This interpretation incorporates subbottom seismic sparker data and sediment core information that have been collected for the entire LIS at a wide grid with 1 - 5 km spacing (Figures 4.2; 4.3) and sediment core information from cores collected between 1967 and 1990s (Figure 4.2).

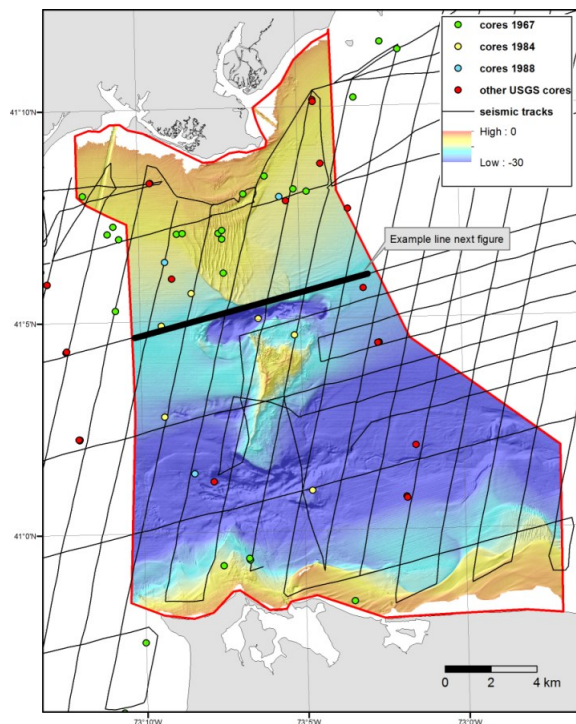


Figure 4.2: Existing USGS seismic lines (thin black) and sediment cores in the pilot area. The subbottom data are from the 1980s and the sediment cores from the 1960s to 1990s. thick black line marks the location of Figure 4.3.

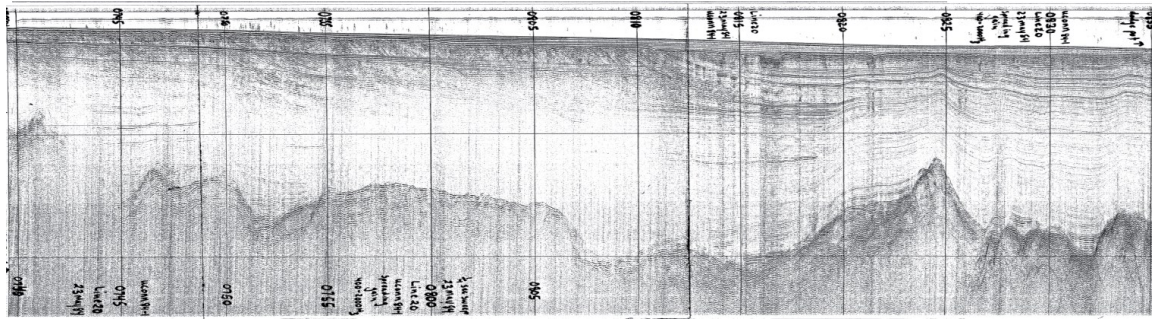


Figure 4.3: Example of a 1984 USGS sparker record of line u84-126 from the pilot area (thick red line in Figure 4.2), which was scanned from analog paper records.

4.3 Subbottom Data Collection and Analysis

4.3.1 Subbottom Principle

Subbottom seismic data provide information on the spatial variation of geological processes such as deposition and erosion as well as insights into ongoing processes and the physical evolution of the benthic environment. They are collected as continuous profiles and show the changes of sediments with depth over a distance.

A sound signal (acoustic energy) is sent from a transmitter source (Figure 4.4). This signal is reflected at the seafloor, but part of the sound energy is passing into the seabed. At each interface where the acoustic parameters are changing a fraction of the sound energy is reflected back. A towed receiver measured the reflected energy and the time that has passed since the signal was transmitted.

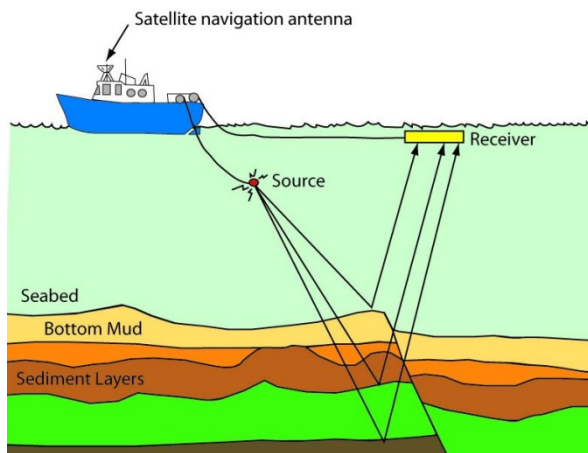


Figure 4.4: Subbottom principle.

4.3.2 Data Acquisition

The subbottom surveys were conducted using a high-resolution Chirp subbottom profiler system consisting of an EdgeTech 424 tow fish and an EdgeTech P3200 acquisition unit with Discovery software (Figure 4.5). This system provides a cleaner signal and higher vertical (0.1m instead of

0.5-1.0m) and lateral (0.5-1m instead of 5-10m) resolution. However, the higher resolution signal does not penetrate the sediments as deeply as the previously used sparker system and therefore only images the upper meters close to the surface. As a result it is complementary to the older data while providing improved details of the near-surface area, which are the main target of this project.

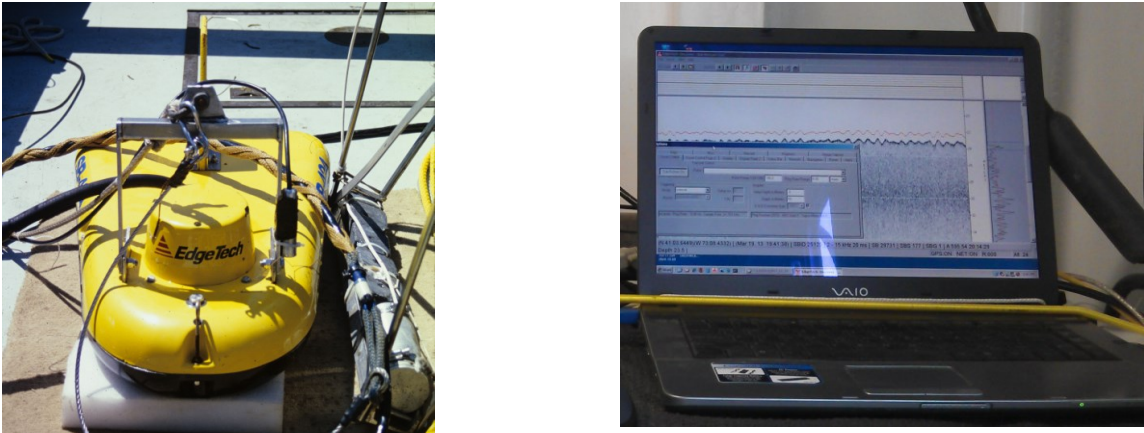


Figure 4.5: Lamont EdgeTech Chirp 424 subbottom profiler system (left) and EdgeTech Discovery software (right).

The system was operated using an acoustic sweep signal between 4-24 kHz that results in a nominal high vertical resolution of 0.1m. The horizontal resolution depends on the survey speed. The system transmits data at a rate of 4-5 pings/second. At survey speeds of 5-6 knots these transmission rates results in an along track spacing of traces between 0.5 and 1m. Data were recorded in EdgeTech's proprietary jsf format as well as in Standard SEG Y format.

The subbottom data are geo-referenced using a differential GPS system, which provides horizontal accuracy <1m. The offset between the ships DGPS antenna and the actual towed fish location was determined for later correction of the positions

Files were recorded continuously along a line and named <survey><orientation><line><part>, for example: LIS1301w100a, with orientation indicated by w (east-west) or n (north-south), line numbers consecutively numbered in the order of acquisition, and different segments marked a, b, c, if these segments are part of a continuous line that was collected into different parts or has been repeated.

The original plan proposed to acquire subbottom data along a grid with a spacing of 500 m in EW direction and 1000 m in NS direction over the entire pilot area except the shallowest areas (<2-3m), but it was modified to cover most of the pilot area while minimizing the efforts and resulting costs. The actual subbottom survey was performed in three stages (Figure 4.6, Table 4.1):

(1) System test (LIS1201): To test the Chirp subbottom system on the Stony Brook vessels and optimize acquisition parameters we conducted a field test in June 2012, which covered mainly the harbor area of Port Jefferson (Figure 4.6; green line).

(2) Measurements in tandem with multibeam collection (LIS1301): For data collection in northern areas (D and E) we towed the subbottom system from the *R/V Seawolf* while the vessel is collecting multibeam data (LIS1301; Figure 4.6 black lines). This resulted in denser (~ 250 m) line spacing in east-west direction and fewer crossing north-south lines.

(3) Survey of the Southern section (LIS1302): The original plan was that the NOAA vessel *Thomas Jefferson* would collect subbottom data in the area C as part of their multibeam survey, but they were unable to do so. Hence we stretched the surveys planned for the A and B areas in a way that they covered most of area C as well (LIS1302; Figure 4.6 blue lines). To combine the different surveys we acquired lines that connect the different surveys.

In total we collected 179 subbottom lines, which represent 1036 km of subbottom data (Table 4.1). While the line density was sufficient to identify and outline most different subbottom facies, additional, crossing north-south lines in the northern section would have been useful to confirm and follow some of the subbottom interpretation from one to another east-west line. In addition there were not enough survey time left to fill the gap between the northern and the southern segments completely. We extended a few of the southern lines to cross the northern section to connect the two.

Table 4.1: Subbottom field data collection details.

Survey	Survey date	Field days	Vessel	# lines	Length/km
LIS1201	June 4 -5 2012	2 days	Pritchard	34	70
LIS1301	March 18-27 2013	8 days	Seawolf	73	550
LIS1302	April 16–25 2013	8 days	Pritchard	72	416
Total		18		179	1036

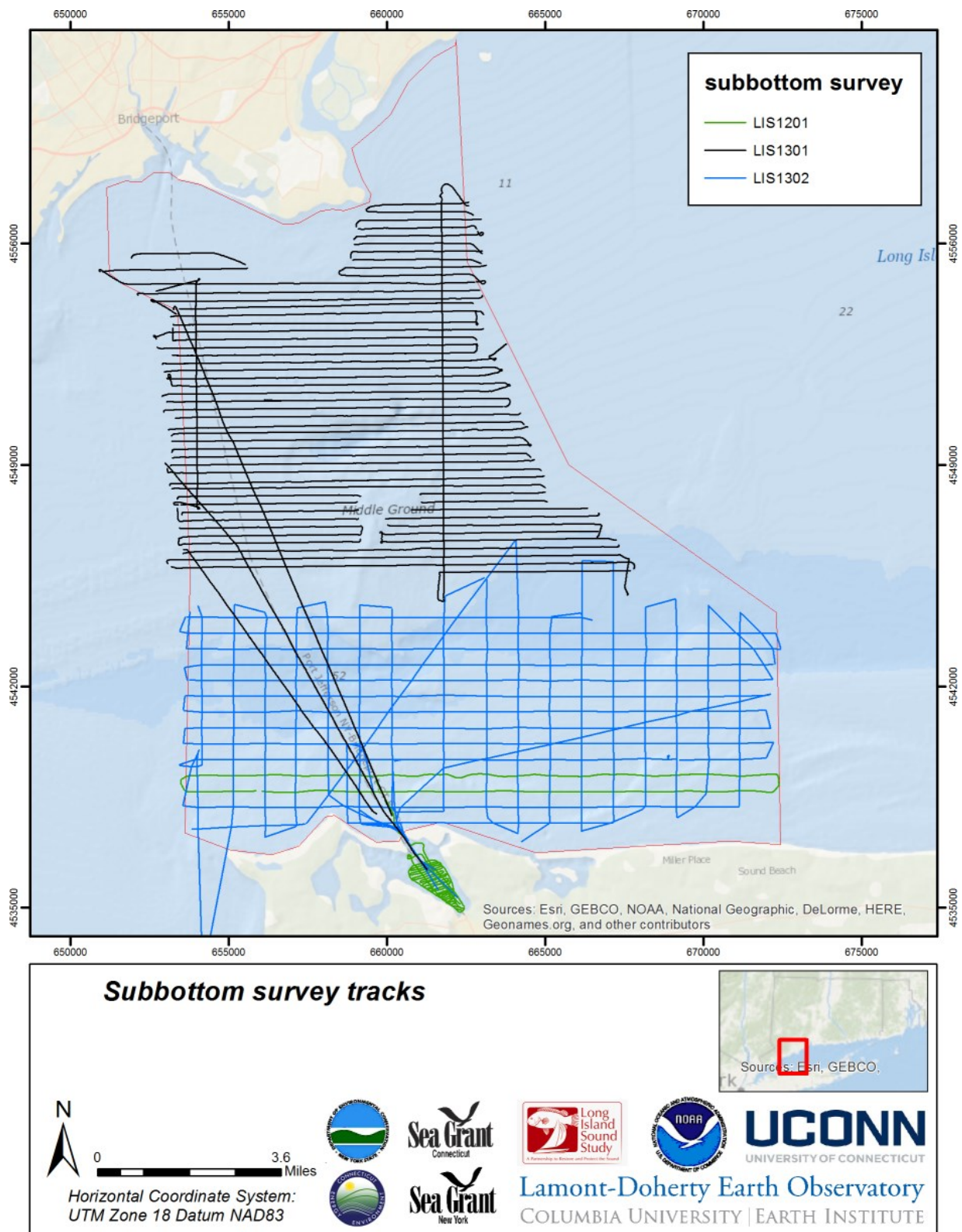


Figure 4.6: Map of the new subbottom profiles collected as part of the pilot project. Different colors indicate the different surveys described in the text.

4.3.3 Data Processing

Data processing was performed using a combination of tools including the EdgeTech Discovery software system, the Seismic Unix processing package, and various in-house scripts. The data were corrected for vertical offset by tides and for horizontal offsets of the tow fish to the GPS antenna (layback correction).

For each subbottom file we generated images in jpeg format. East-west lines are shown with west to the left and north-south lines with south on the left independent of the original orientations. The Discovery software allowed applying a swell filter before image generation to suppress vertical motion effects caused by waves.

The GPS navigation data were converted in text files and linked with shotpoints (number of measurement along a line). These data have been imported in ArcGIS and converted into ESRI shapefiles including point files of individual shotpoints and line files of the track of each seismic line.

For analysis and interpretation of the subbottom data we loaded the processed and corrected SEGY files into the SMT Kingdom Suite software package. This software allows tracing and digitizing individual horizons along one line and from one line to another. It also allows directly overlying locations and results from sediment cores over the subbottom data, which improves interpretation.

4.3.4 Results

The resulting images of all lines together with the SEGY files can be downloaded from the database (<http://www.marine-geo.org/portals/lis/>). The data show a variety of subbottom environments. The maximum depth reflections can be observed in the data varied greatly across the study area. It ranges from no penetration over hard bottom (sand and gravel) to over 20 meters in glacial clay areas. Here we are showing various examples of the data that demonstrate the different bottom environments and features that we observed in the subbottom data.

Multiple sediment layers – deposition: Figure 4.7 shows as subbottom profile with several clear, parallel reflections, in this case, in top 2-3 m below the surface. These layered sediments are often indicative of depositional environments.

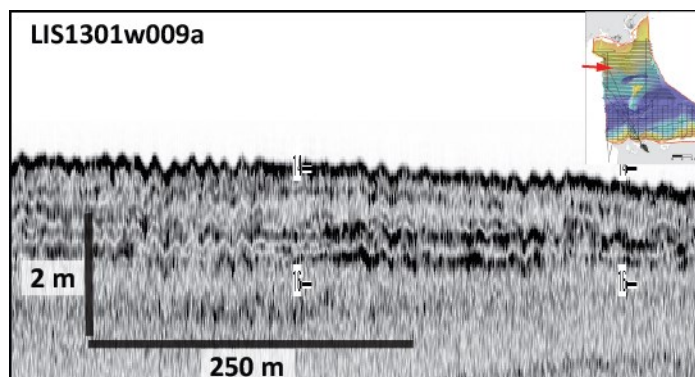


Figure 4.7: Example of depositional environment with multiple layers.

Non-deposition: Figure 4.8 shows a subbottom profile with a strong reflection at the seafloor, but no clear reflection below the seafloor. This could indicate a hard substrate (e.g. sand, gravel, bedrock outcrop) through which the subbottom signal cannot penetrate. The absence of reflections might also indicate that no finer material is deposition here, which can be associated to high-energy environment with current speeds strong enough to move sand.

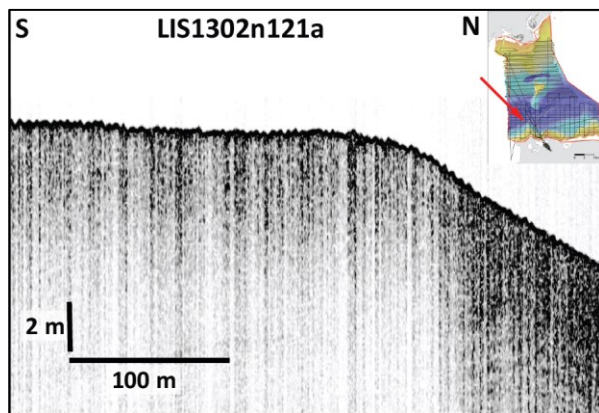


Figure 4.8: Example of sandy, hard bottom with no subbottom penetration in this case indicating a high-energy environment with current speeds strong enough to move sand.

In contrast to Figure 4.8, where we cannot identify any subbottom reflections, Figure 4.9 shows a section, where we can image over 20 m with many parallel reflections. We interpret these reflections as glacial-lacustrine clay layers that formed shortly after the retreat of the ice at the end of the last glaciation when Long Island Sound was a large pro-glacial lake (Uchupi et al., 2001). Many of these reflections are cut off at the seafloor, which suggests that part of the glacial lake layers have been eroded. The absence of any substantial sediment layers above the glacial clay layers indicates that no deposition is occurring here.

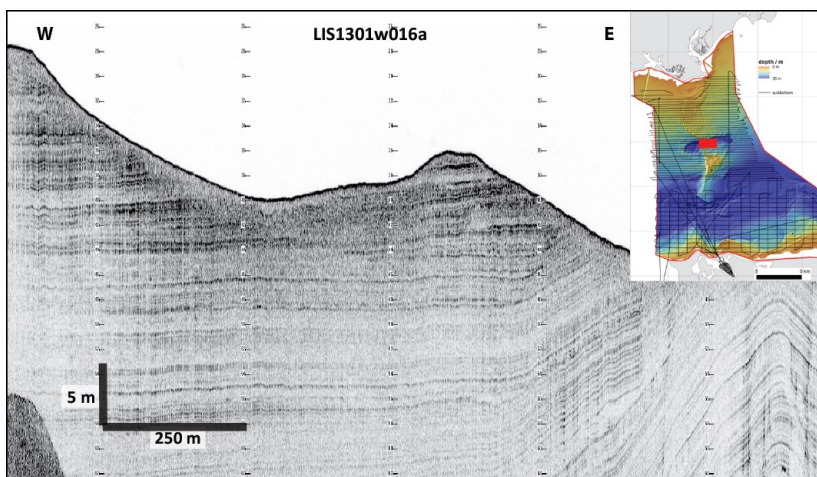


Figure 4.9: Example of subbottom image of over 20m glacio-lacustrine clay layers with clear indication of erosion of older layers on top.

Paleo-channel: In other areas we observe a stronger, slightly diffuse reflection about 6-8 m below the seafloor with occasional depressions (Figure 4.10). Mapping these reflections across the area suggests that they represent the transgression surface, which was formed after the glacial lake drained and before the Long Island Sound was flooded by ocean waters as a result of sea-level rise. The depressions are buried channels of an old river network that drained the area at that time.

That we see this surface in the data suggests that the overlying sediment are softer and probably finer grained, and, thus, don't absorb less of the acoustic energy. This indicates a slow sediment accumulation over time, which is filling the sound at this location. Therefore, such area can be considered depositional.

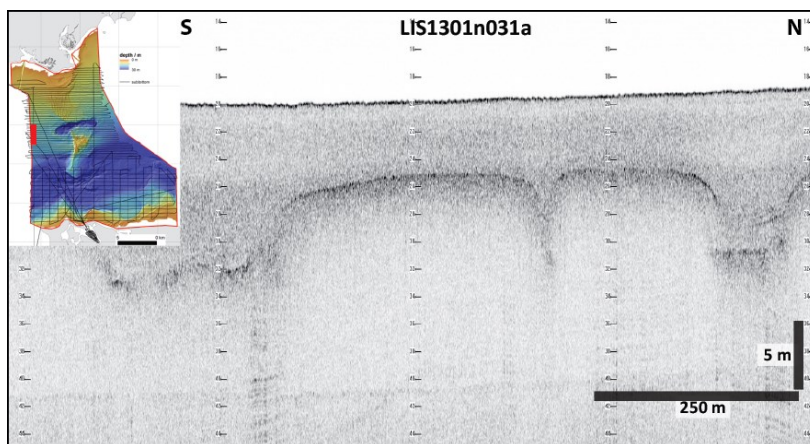


Figure 4.10: Example of subbottom data showing filled paleo channels with several meters of sediment fill above, indicating slow deposition.

Anthropogenic features: Besides natural environments subbottom data provide also a record of human disturbances of the sediments. Figure 4.11 shows two examples of buried pipelines imaged as hyperbolas (top and bottom hyperbola is likely to image the top and bottom of the pipeline). The depth of these hyperbolas also shows if sediment have been accumulating on top of the pipeline or not.

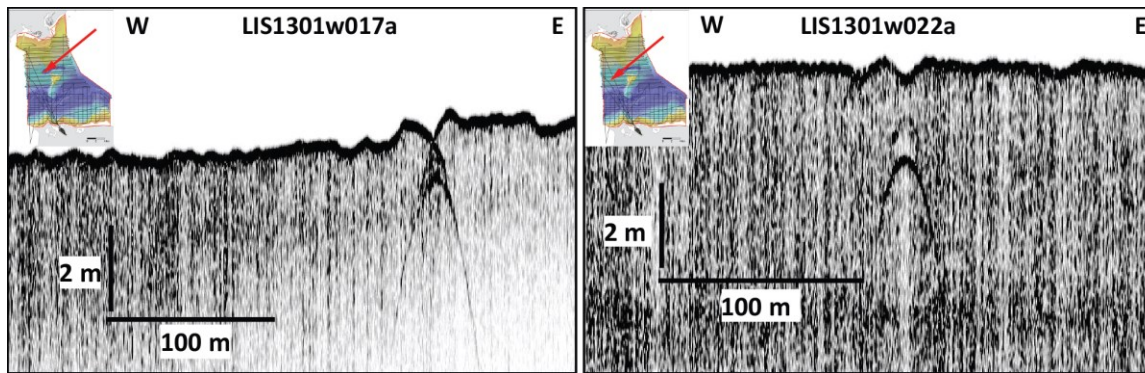


Figure 4.11: Example of the buried pipeline showing up in subbottom data. Top and bottom of the pipeline is at the apex of the hyperbola. Left side show the top of the hyperbola almost at the surface in a non-depositional environment and right examples shows the pipeline buried ~2m below the surface.

Another common example of anthropogenic disturbances of sediments is imaged in Figure 4.12. It shows a dredged channel near Bridgeport. There are clear reflections showing different level of dredging and infill (deposition) of new sediment.

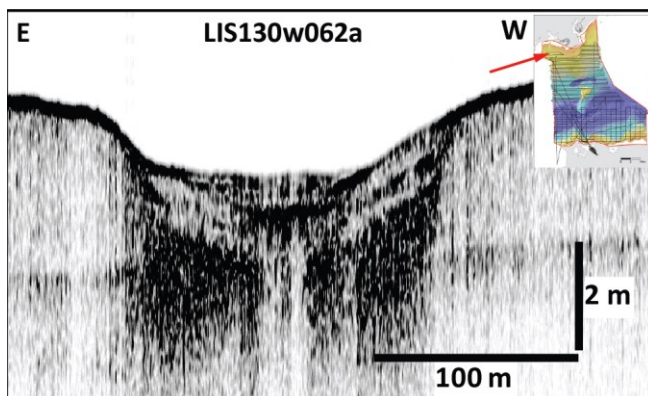


Figure 4.12: Example of dredged channel and different stages of infill of the Bridgeport channel.

The examples described here show the possibilities of the subbottom data, but they also show that in some cases multiple interpretations are possible. To confirm specific interpretations usually requires additional information from sediment cores.

Effect of different survey line layout in northern and southern parts: The denser line spacing in the northern part allowed better mapping of the extent of features and sediment layers, but the small number of cross-lines made it difficult at times to correlate layers from one profile to another, and thus leaving some uncertainty in the interpretation. The wider grid spacing in the southern half of the survey area was sufficient where the sediments are more uniform. Some parts with higher variability would probably have benefited from some additional lines.

4.4 *Sediment Cores Collection and Analysis*

4.4.1 *Sediment Core Collection*

The sampling sites were chosen based on preliminary backscatter data from the area and the location of the USGS samples sites (section 3.3). The goal of the site selection was to achieve a dense, well-distributed coverage of the area while sampling major areas with different backscatter signature and complementing the USGS efforts.

All sediment cores were collected in June 2013 onboard the R/V Seawolf (Stony Brook University – Table 4.2). Two different gravity coring systems were used to collect sediments. GC series cores were collected with the LDEO gravity coring system consists of a core head weighing ~150 kg with an internal check valve and. Clear schedule 40 PVC pipes (2m long x 4” diameter) are connected to the core head via a cam-groove coupling system. HDC series cores were collected with a hydraulically damped gravity corer on loan from USGS. The hydraulically damped gravity corer is a modified gravity corer operated from a quad landing frame that collects 11-cm diameter cores up to 65 cm in length in clear polycarbonate core barrels (Bothner et al., 1997). In both systems, clear liners allow us to visually inspect the length and quality of sediment core as they are collected. This was essential for deciding to retry to take another core at a core location and to determine, if the surface of the sediment core was intact. Once on deck, sediment cores were capped, sealed with tape, and described. The overlying water was retained in the core barrel to reduce disturbance of the sediment during transportation and storage. Cores were stored vertically in a refrigerator at 4°C pending analysis.

In total, we collected 46 sediment cores (Table 4.3 and Figure 4.13). We collected 23 gravity cores and 23 hydraulically damped cores. Gravity core lengths ranged between 45 and 200 cm in length with an average of 125 cm, hydraulically damped cores ranged between 15 and 52 cm in length with an average of 39 cm. While the LDEO system is capable of providing longer cores, it can be limited by weather conditions and bottom currents. In contrast, the USGS system can perform in rough weather and stronger currents, but core length is limited. Our approach of using both systems served us well and provided sampling ability across a range of conditions.

Table 4.2: Field data details of the sediment collection cruise.

Survey date	Field days	Vessel	Core samples
June 5-12 2013	6	Seawolf	46

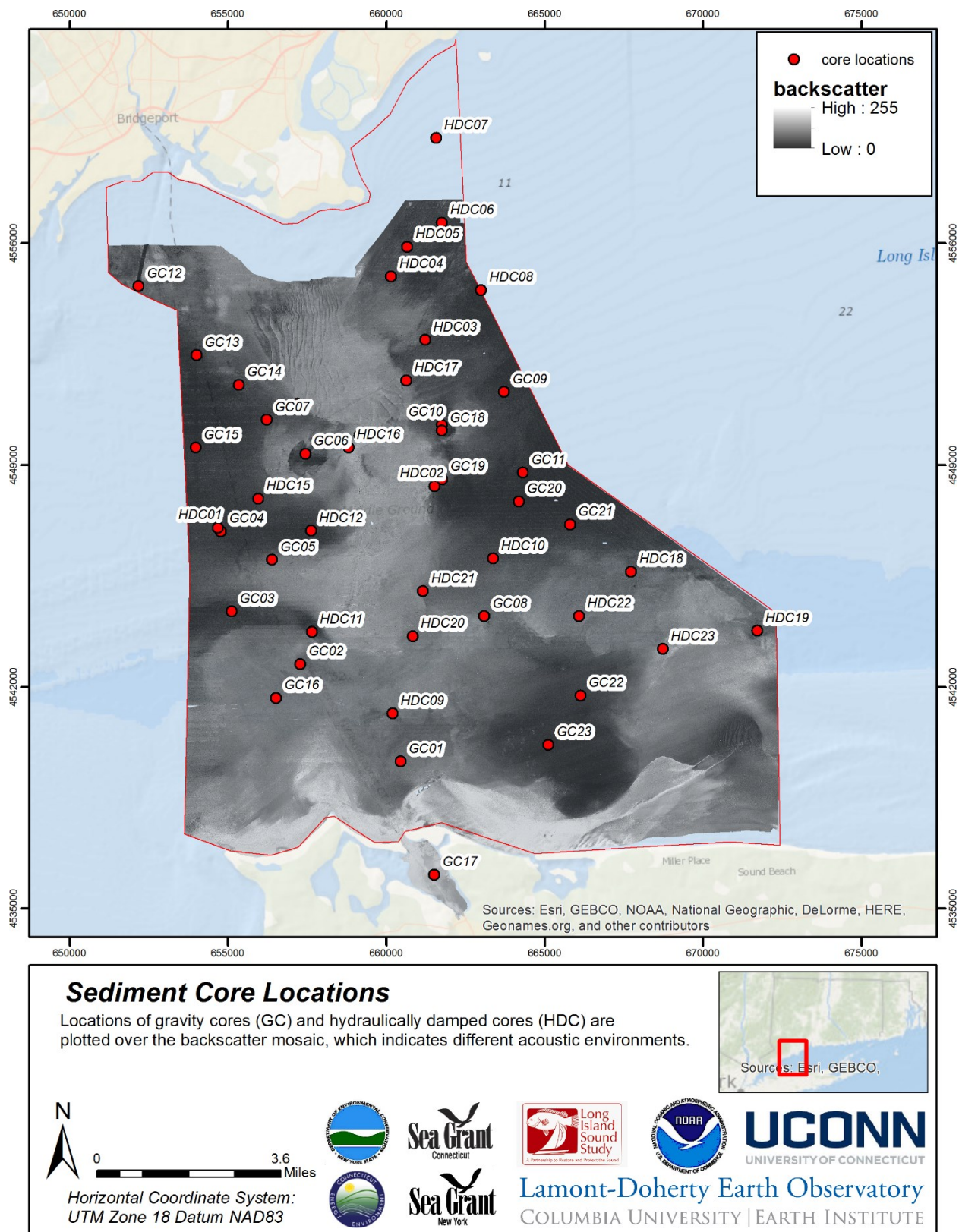


Figure 4.13: Location of the sediment cores over the backscatter mosaic. GCxx are gravity cores and HDCxx are cores taken with the hydraulic-damped corer.

Table 4.3: Sediment Core Sample Information

Core ID	Latitude	Longitude	Water Depth (m)	Sampling Device	Core Length (cm)
GC01	40.992217	-73.0925	28.8	gravity core	92
GC02	41.020517	-73.129367	45.6	gravity core	132
GC03	41.035883	-73.154717	31.6	gravity core	170
GC04	41.058667	-73.15815	23.2	gravity core	175
GC05	41.0503	-73.13915	26.7	gravity core	61
GC06	41.080217	-73.125783	35	gravity core	156
GC07	41.090133	-73.140033	18.7	gravity core	162.5
GC08	41.032917	-73.059917	39.4	gravity core	64.5
GC09	41.096533	-73.050667	23	gravity core	94.5
GC10	41.087617	-73.074233	30	gravity core	163.5
GC11	41.073517	-73.044283	27.4	gravity core	164
GC12	41.12885	-73.1871	12.1	gravity core	61
GC13	41.108883	-73.165883	14.2	gravity core	101
GC14	41.1002	-73.150217	15.5	gravity core	71
GC15	41.082633	-73.166917	19.8	gravity core	59
GC16	41.011017	-73.138733	40.2	gravity core	65.5
GC17	40.9598	-73.080867	7.8	gravity core	44.5
GC18	41.08595	-73.07435	34.1	gravity core	200
GC19	41.072117	-73.074583	25.8	gravity core	162
GC20	41.065333	-73.045983	30.4	gravity core	152
GC21	41.058483	-73.027033	35.4	gravity core	200
GC22	41.009817	-73.024533	29	gravity core	163.8
GC23	40.996033	-73.036967	24.1	gravity core	125.5
HDC01	41.059767	-73.15915	22.7	hydraulic dampened corer	43
HDC02	41.07025	-73.0776	22.5	hydraulic dampened corer	15
HDC03	41.11185	-73.07985	17.2	hydraulic dampened corer	17.2
HDC04	41.130067	-73.0921	13.7	hydraulic dampened corer	51.5
HDC05	41.138383	-73.0858	13.2	hydraulic dampened corer	41.1
HDC06	41.145033	-73.07255	13.2	hydraulic dampened corer	40
HDC07	41.169167	-73.0741	9.2	hydraulic dampened corer	39
HDC08	41.125667	-73.058467	16	hydraulic dampened corer	35.5
HDC09	41.005883	-73.095217	39.6	hydraulic dampened corer	44
HDC10	41.0493	-73.0562	36.4	hydraulic dampened corer	41
HDC11	41.02955	-73.124783	38.5	hydraulic dampened corer	50
HDC12	41.058333	-73.124267	22	hydraulic dampened corer	49
HDC13	41.08505	-73.10535	46.1	hydraulic dampened corer	25
HDC14	41.09445	-73.128317	19.6	hydraulic dampened corer	41.5
HDC15	41.067767	-73.1439	22.4	hydraulic dampened corer	44.5
HDC16	41.081783	-73.109517	54.4	hydraulic dampened corer	23
HDC17	41.100417	-73.087283	18.5	hydraulic dampened corer	48
HDC18	41.044667	-73.004483	40.3	hydraulic dampened corer	38.5
HDC19	41.027033	-72.957633	42.1	hydraulic dampened corer	31.5
HDC20	41.027733	-73.087	39.9	hydraulic dampened corer	44.6
HDC21	41.040433	-73.082767	33.6	hydraulic dampened corer	41.5
HDC22	41.032383	-73.0244	0	hydraulic dampened corer	47
HDC23	41.022483	-72.99325	39.3	hydraulic dampened corer	47.2

4.4.2 *Sediment Core Processing and Archiving*

After cores were collected, they were stored and transported upright in order to preserve the integrity of the core tops. At the end of each day, cores were transported to LDEO's core facility and stored in a walk-in refrigerator at 4°C to before processing. Sediment cores were then carefully de-watered, excess PVC above the core top was removed and a foam plug was securely fitted to stabilized sediments. Sediment cores were split longitudinally and prepared for archive, which includes inserting depth markers, and digitally photographing both core halves. Once split, cores were logged for physical properties, visually described, and analyzed by XRF. In between various processing steps and upon completion of analysis, sediment core samples were placed in D-tubes and stored at 4°C.

4.4.3 *Physical Properties*

Once dewatered and split, sediment cores were logged for physical properties at 1mm intervals using a GEOTEK Multi-Sensor Core Logger. Properties measured included gamma ray attenuation, magnetic susceptibility, as well as p-wave velocity and amplitude. Detailed logs for each core can be found in appendix 8-2. All core data are archived in the database (section 7).

4.4.4 *Determining Metal Content Using X-ray Fluorescence (XRF)*

Split sediment cores were analyzed for lead, zinc, and copper concentrations every 10 cm using an Innov- X Alpha series 4000 handheld X-ray fluorescence (XRF) spectrometer. To prevent contamination of the instrument between measurements, the sediment surface was covered with plastic wrap during analysis. Each measurement was conducted for 120 seconds, which reduced analytical uncertainties to less than a few percent. Metal concentrations made on wet sediments were corrected for water content and are reported on a dry weight basis. Although confirmatory analyses and LIS specific calibrations were not conducted as part of this study, previous studies indicate that the water content corrected XRF data agree well with independent estimates for several contaminant metals and other elements examined. Minor discrepancies between data sets are likely due to inhomogeneity effects between the different techniques – our instrument only measures a small portion of the sediments at a given horizon, whereas the entire sediment horizon is collected, homogenized, and sub samples for independent analyses. Results for Pb, Zr, Sr, Rb, Zn, Cu, Fe, Mn, and Cr were typically within 20% or less of the independent estimate(s).

(Kenna and Nitsche, 2011; Nitsche and Kenna, 2011).

Wet bulk density, derived from gamma ray attenuation was used to calculate water content using the following equation:

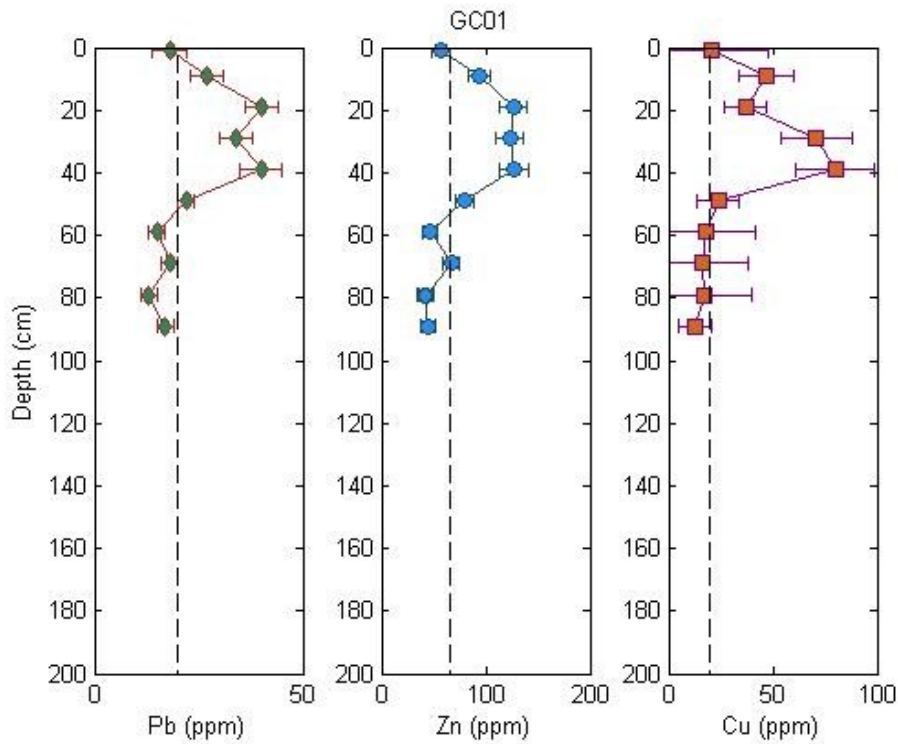
$$Water\ content = \frac{\left(\frac{(\rho_{H_2O} \cdot \rho_{Sed})}{WBD} - \rho_{H_2O} \right)}{(\rho_{Sed} - \rho_{H_2O})} \quad (eq. 1)$$

where :

ρ_{H_2O} = water density

ρ_{Sed} = dry grain density

In this study, we assumed 1g cm^{-3} and 2.6g cm^{-3} , for water and dry grain density, respectively.



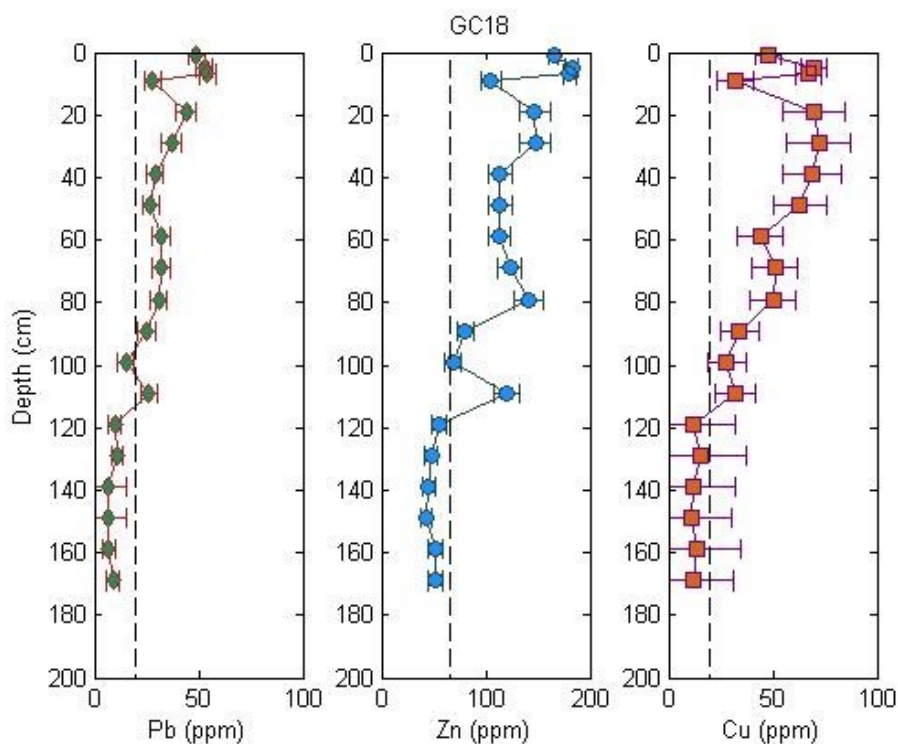


Figure 4.14: Example metal profiles obtained from wet XRF scanned cores

Example profiles are shown in Figure 4.14. We use the presence of metal concentrations in sediments above natural background levels (dashed lines) as a proxy for identifying those sediments impacted by twentieth century activities. Sediments containing elevated metal concentrations will also potentially contain other contaminants of concern, while sediments containing background levels represent sediments deposited prior to the onset of industrial activities and do not pose a significant contamination issue. The penetration depth can vary as a function of not only sediment accumulation rates, but both physical and biological mixing processes as well. Metal profiles for all cores collected appear in Appendix 8-4.

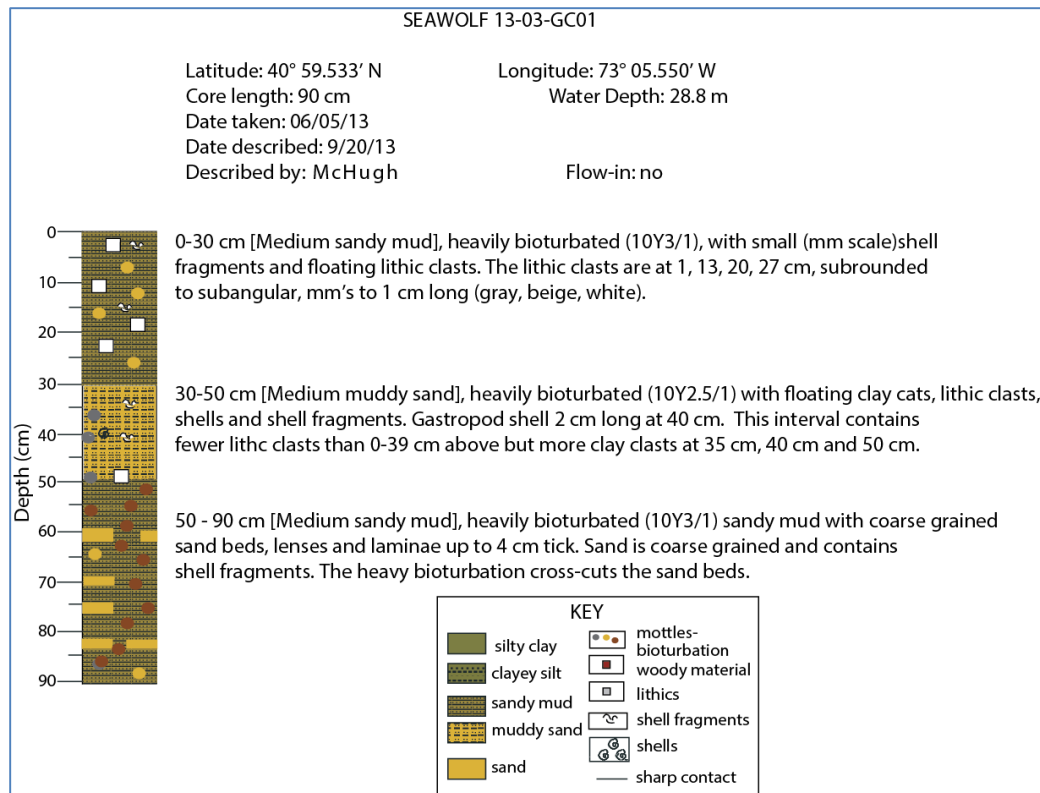


Figure 4.15: Example of a sediment core description.

4.4.5 Sediment Core Descriptions

The gravity and HDC cores were split, photographed and visually described following the Integrated Ocean Drilling Project protocol (e.g., IODP Expedition 317). The observations were entered in core barrel sheets and then in Adobe Illustrator as drawings (Figure. 4.15). The main lithology was determined by using a hand lens and smear slides. The main sedimentary structures include: contacts (sharp, gradual, angular), beds (if greater than 1 cm thick), laminae (if less than 1 cm thick), and lenses (not continuous along the thickness of the core). The grain size was determined by the Wentworth (1922) scale and classified as gravel, pebble, sand, and mud. Bioturbation was characterized as moderate, heavy, very heavy and non-bioturbated. The main accessories are shells and fragments (identified whenever possible), lithic clasts (identified by their size, mineralogy when possible, and their texture as rounded, subrounded and angular), wood, and anthropogenic materials (coal, slag). The degree of sediment disturbance due to the sampling process was also described. Descriptions of all sediment cores are included in Appendix 8-1.

4.5 Sediment Environment Interpretation and other integrated products

The results of the previous sections describe various aspects of the subsurface structure that provide insights in changes with time/depth, spatial changes, the amount of deposition and

amount of metals as proxy for sediment input during industrial times. The integration of this information allows us to distinguish different sediment environments in terms of amounts of depositions, energy regime, disturbances by episodic or occasional events and other aspects.

For this interpretation, we combined and compared the different results using ArcGIS, Kingdom Suite seismic interpretation software and core descriptions. All information from the subbottom data as interpreted in Kingdom Suite, location and results of the sediment core data and analysis, bathymetry and backscatter information (chapter 2) were all loaded into ArcGIS software system. Using our best professional judgment we then manually outlined areas with similar characteristics of the different data sets in form of polygons. The boundaries of the polygons are based on the extent of layers in the subbottom data, changes in backscatter, and distinct morphological features in the bathymetry. Although some of these boundaries are actually well-defined and relative sharp in reality in other cases the boundaries are more gradual. Therefore we advise caution when using the polygons and maps to obtain conditions close to polygon edges.

4.5.1 *Sediment Environment Classification*

The high variability of the pilot study area results in many variations of the sedimentary environments that are influenced by many factors including tidal currents, storms, wave activity, sediment texture, bioturbation, sediment input, pre-existing substrate and several others. However, to achieve quick overviews we distinguish several major groups of sediment environments. The main basic groups are:

Depositional environments: The main indicators for deposition are the presence of anthropogenic levels of metals in significant depth in the sediment cores (more than 0.1 to 0.2 m), absence of signs of disturbed layers in the sediment core descriptions, and/or layers in the subbottom data.

Non-depositional / erosional environments: Usually, we do not know if an area is actively eroding (material is removed) or if had has been eroded in the past and there is just no new material accumulating at present. Even if there are signs of active erosion at present, we can usually not determine how much material has been eroded. Therefore we combine non-depositional and erosional environments into one group.

Areas where the subbottom data show lacustrine glacial clay layers (often truncated) close to the surface are clearly see erosional/non-depositional (Figure 4.9). Most of these are in the deep depression north of Stratford Shoal. It is unclear to what degree the erosion is continuing or if strong current prevent long-term sediment accumulation. To determine this effect would require detailed measurements of currents and repeated observations at this site.

We also categorized areas with gravelly or hard coarse sandy bottom and outcropping bedrock as non-deposition / erosional since it is clear that currents and wave energy do not allow deposition of finer materials here (no new material like gravel/boulders can be transported by the currents)

Dynamic environments: Some environments cannot clearly be classified as depositional or erosional/non-depositional. These are usually dynamic environments where sediment is moved around and therefore temporarily deposited at one location whereas eroding at another. These include areas dominated by sediment waves that usually move and transport material by depositing on one side and eroding on the other side. In other areas we found strong indication of physical mixing and occasional events. For example most of the deep southern channel has sediments with elevated metal levels near the surface, but there are no signs of long-term accumulation. Therefore we assume that strong currents are moving material through these areas and mixing it near the surface, where it may stay temporarily. But eventually the material is moved out of this area.

Based on these main groups we are distinguishing here several main types that reflect the most important categories (Table 4.4). The detailed distribution of the data is shown in Figure 4.16.

Table 4.4: Sediment Environment classes and their definitions.

Classification	Description / Definition
Deposition	Presence of higher metal levels; homogeneous layers, and/or preservation of sedimentary structures in sediment cores and clear layers in the sub bottom; can have bioturbation.
Deposition and erosion	There is one area that seems occasional erosional events (sharp contacts and mixing of sediment above, possibly by storms), but might be depositional otherwise.
Dynamic – sediment waves	Areas that are dominated by sediment waves as seen in the bathymetry and backscatter.
Dynamic - reworked	Contains higher metal concentrations near the surface; indication of mixing, but no signs of long-term deposition (e.g. layers).
Non-deposition / erosion	Areas where elevated metal levels in the sediment cores are absent (no recent material is accumulating); where the subbottom data show erosional features; and/or where backscatter and bathymetry data indicate outcrops, gravel, and boulders that are uncovered by finer sediment.
Unsurveyed	Parts of the pilot study areas where we don't have enough data to assign a category. These are mainly very shallow areas near the shore.

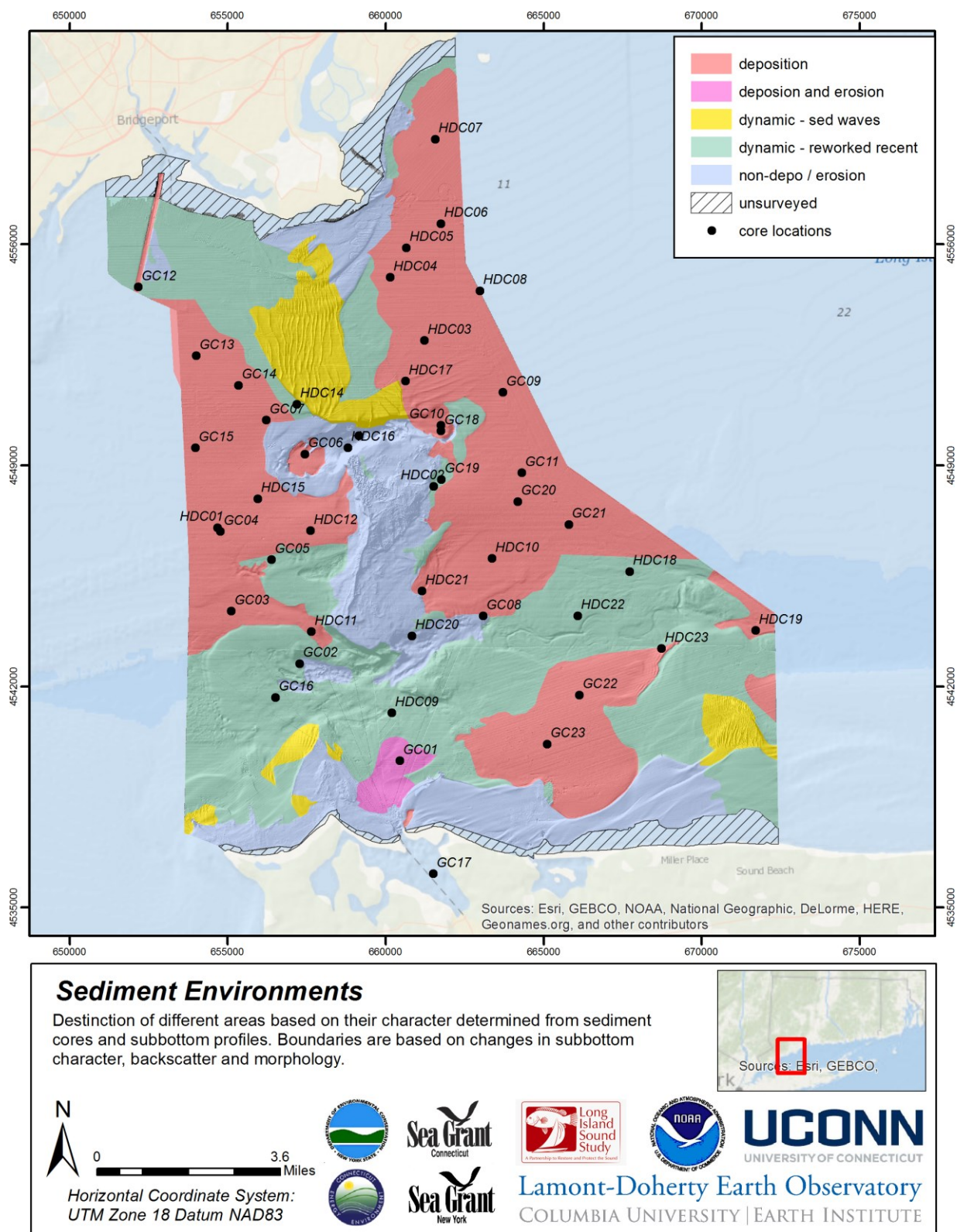


Figure 4.16: Map of sediment environments. See text for description of individual classes.

As mentioned above the combination of the different data sets provide insight into the dominant energy levels of the different areas. High, moderate, or low energy regimes can be caused by tidal currents, other currents, and wave action. They increase mixing and result in sorting, transport and windowing of finer sediments (Table 4.5 and Figure 4.17).

Table 4.5: Interpreted energy regimes of different sediment environments their definition.

Classification	Description / Definition
High energy	Strong signs of current- or wave-related mixing in sediment core, areas of erosion or non-deposition likely to be subject to strong currents.
Moderate/ high energy	Signs of mixing by currents and waves; mix of sand and mud; shell fragments (likely transported).
Moderate energy	Signs of current activity; mix of mud and sand, shells and fragments; some biology; some signs of mixing.
Low / moderate energy	Few signs of current activity; mainly fine grained material, biological activity, layers in sediments and subbottom data. Few sandy layers.
Low energy	No signs of current activity; mainly fine grained material, biological activity, undisturbed layers in sediments and subbottom data.
Unsurveyed	Parts of the pilot study areas where we don't have enough data to assign a category. These are mainly very shallow areas near the shore.

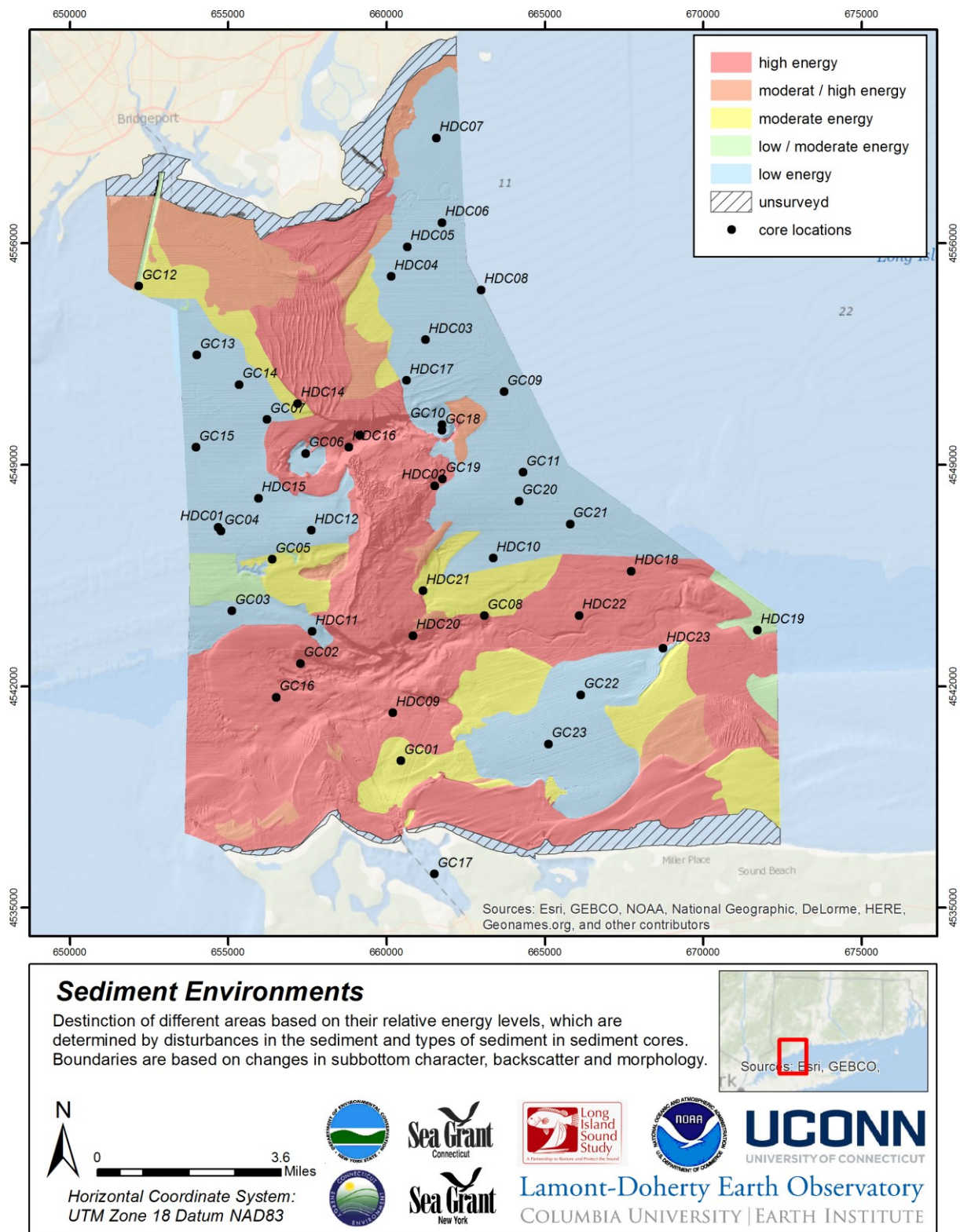


Figure 4.17: Map of interpreted energy regimes of the various sediment environments. See text for description of individual classes.

The different classifications can also be combined to reveal a more complex picture and further distinguish differences in the major categories as shown in Figure 4.18. However, for some applications this may be excessive.

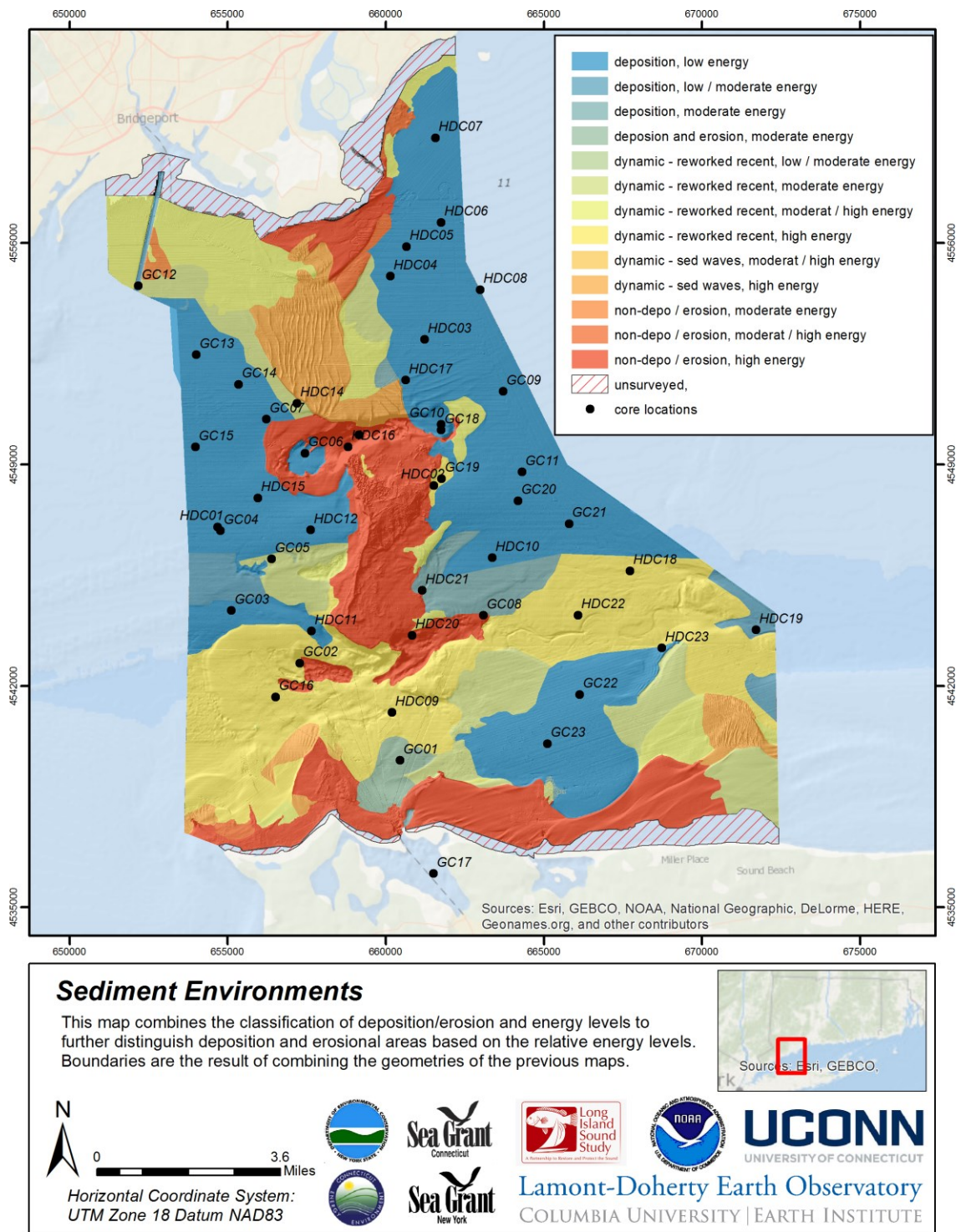


Figure 4.18: Map of interpreted sediment environments and energy regimes combined. See text for description of individual classes.

4.5.2 Interpretation of Different Areas

Classifying different areas based on basic types of process and energy regimes (section 4.5.1) is a useful abstraction for many applications. However, the combination of the different datasets yields much more information about the specifics of different parts of the study area. Much of these details cannot be easily put into categories but might be useful background for science-based management and general understanding of the area. Here we describe briefly the major areas as outlined in figure 4.19. While the outline of some of these areas is similar to the different patches identified based on the acoustic (s. section 5), the history of areas 1, 3, 4 (all patch type A) appears significantly different from each other. A more detailed comparison would be useful.

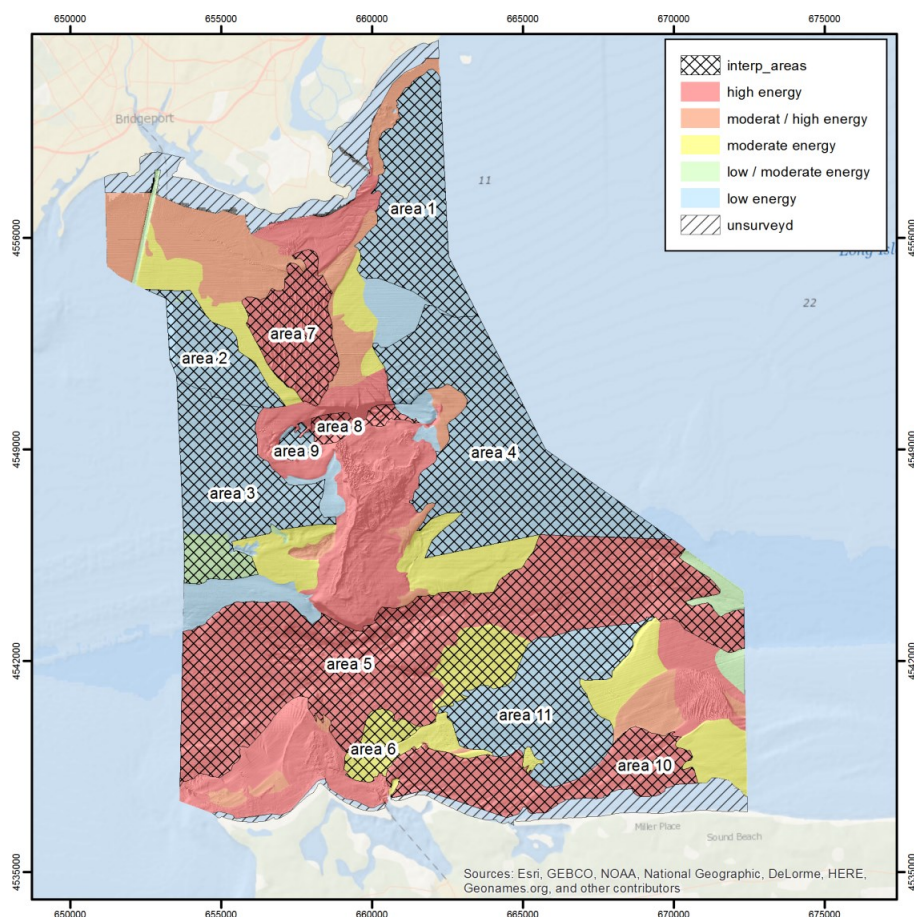


Figure 4.19: Locations of area with more detailed descriptions in the text.

Area 1 – Depositional environment with low energy. It shows frequent shell beds with layers of mud in between. The mud contains very high level of different metals. It is likely that this area receives material from sediment plumes from the rivers leading to the area and thus delivering the mud that contains the metals and is covering the shell beds.

Area 2 – A mainly depositional area. Both subbottom and sediment cores show a major shift in the sedimentation regime from muddy layers to layers with little sand, bioturbation and higher level of metals. Potentially, this represents a shift in sediment source material. This shift could be caused by colonial activities, but also be younger. The higher metal level suggests that the shift occurred more than 100 years ago.

Area 3 – Subbottom layers, sediment core descriptions and metal content clearly show a depositional environment. The soft mud allow subbottom signals to penetrate several (up to 6-8 m) where a stronger reflection with channel-like incisions probably mark the top of the transgression surface (the surface of LIS before it was flooded by rising sea-level). In few places parallel reflections in the subbottom data, which we interpret as glacial layers, are consistent with this interpretation. Layers and internal structure in sediment core data indicate a low energy environment. There seems to be more or less low, but continuous accumulation in this area.

Area 4 – This area is very similar to area 3 with the difference that the transgression surface is not visible in most subbottom data. This could indicate that deposition is thicker here than in area 3 and the surface is below the subbottom penetration. Metals in sediment cores suggest a higher sedimentation rate, but also strong bioturbation, which is probably the reason for the absence of internal reflections. Overall, there seems to be more or less low, but continuous accumulation in this area

Area 5 – The deeper channel in the southern part of the pilot area has sand and sand-mud mixed sediments with occasional gravel. There is no clear subbottom penetration, which also indicated harder surface material. The presence of moderate metal level suggests that some more recent sediment is present. However, the depths of this area and the fact that older, meandering channels, again likely formed pre-transgression, are visible in the bathymetry suggests very little, if any significant deposition. Therefore we conclude that this area is dominated by mixing by strong currents that mix older and younger sediments and bring and move coarser material including sand, little gravel and shell-fragments.

Area 6 – This is a smaller area in the south of the pilot. Sediment core data reveal several episodes of significant sediment input, probably mass flow, but also show unconformities indicative of erosion. Sediments are likely to coming from the shallower areas near the Long Island shore.

Area 7 – Sediment wave field in the north of the pilot area. Sediment waves appear to move towards the west.

Area 8 – Clay layers are exposed and truncated near the surface. The character of the reflections observed in the subbottom data is typical for lacustrine clay deposited in pro-glacial lakes before the Long Island Sound got flooded by the raising sea level. The fact that they are near the surface indicates that erosion might still be ongoing or at least that no deposition is occurring here.

Area 9 – Depositional fan inside the northern deep hole. Fine grained material is transported of the rim of this deep basin and deposited at the western and eastern ends inside the basin. No signs of disturbance suggest that it is a relative quite environment. The presence of elevated metals indicates input of recent material.

Area 10 – There is a band of harder substrate of mainly sand and gravel near the south (and partially also near the north shore. The material and the shallow bathymetry suggest that this area is impacted by waves and not only currents. There are no indications of deposition but erosion and transport of coarser material by wave might be the dominant force here.

Area 11 – This area consists of fine grained sediment (mud or sandy mud) and the sediment cores indicate a low energy regime that is depositional. Variations in elevated metal content in the cores suggest low to moderate sedimentation rates. This area might be sheltered from stronger currents by the surrounding morphology.

4.5.3 *Comparison to Previous Data*

The interpretation of sediment environment provided here differs from previous classifications like the one by USGS described in section 4.2. As result of this LIS mapping pilot study we have much more detailed datasets available that includes full coverage backscatter, multibeam bathymetry, a dense grid of high-resolution subbottom data, and multiple sediment cores. These data allow us to distinguish more details in the environment that was not possible (feasible before).

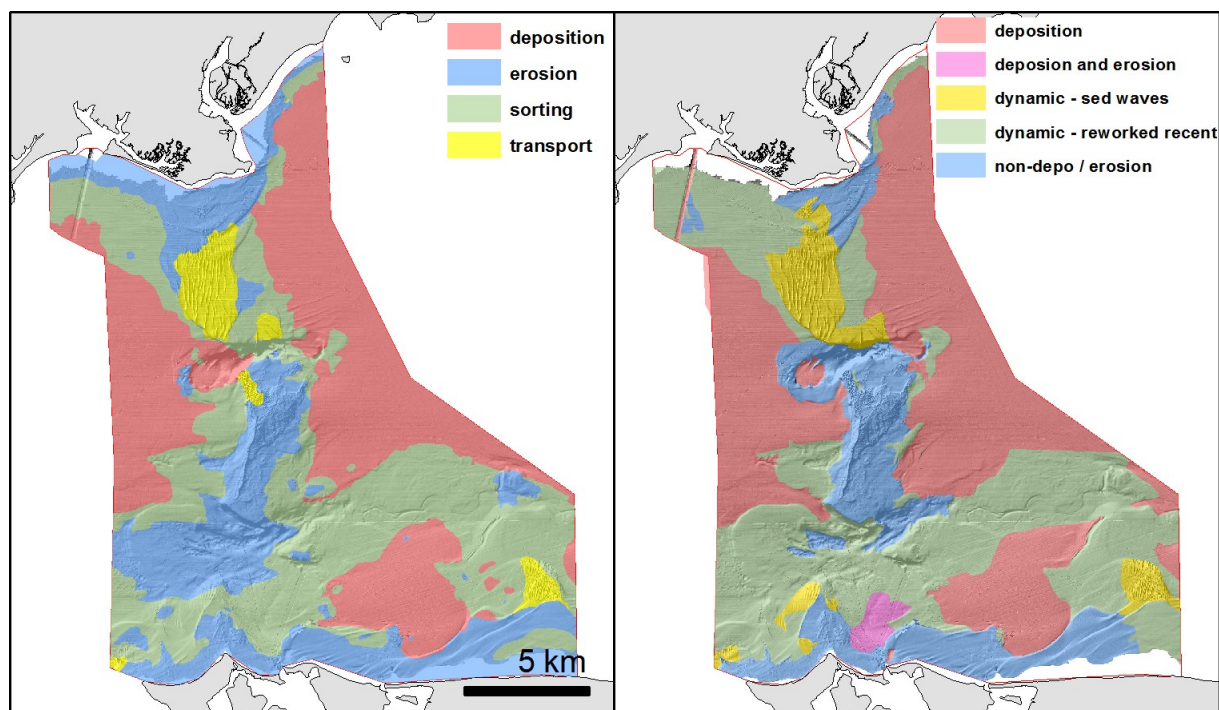


Figure 4.20: Comparison of (left) USGS sedimentary environment (Poppe et al.; 2000) and (right) the new sediment environment interpretation of this study.

4.6 *Summary and Recommendations*

The sediment environment characterizes the dynamic and or stability of an area and how it might be changing. This yields valuable information for understanding the context of the other surface data and habitats.

Subbottom data provide information of the lateral extent of sub-surface layers and changes that enables first order interpretation of the sedimentary environment and allows extrapolation of more detailed information from sediment cores. We collected high-quality data over large areas with over 10m of penetration in some places. In addition, subbottom data can also image details of previous anthropogenic changes such as pipelines, cables and dredge channels, which might yield insights in there effects on the environment.

Sediment cores are critical for identifying changes in environments including the temporal distribution of sediments. We found in many of the cores a dramatic change in the sedimentation within 10 to 20 cm down-core. This also means changes in depositional environments and possibly ecosystems within short-time spans. It is important to take temporal changes into consideration for benthic habitat mapping. In contrast, some cores showed very similar sedimentation throughout time, which also reveals lack of change in the depositional environment. Understanding the time frame on which these changes occurred is very useful. For example, are sediment profile features a result of a single event such as a storm; did they occur at the frequency of tidal current cycles, or at much larger decadal- centennial- or even millennial-time-scales? Developing a short-term chronology from the core data can significantly contribute to a better understanding of depositional processes. This type of information can be useful when considering projects such as the future placement of cables or similar projects.

The pilot area is highly variable and there are locations where additional sediment cores would have been useful to determine the character of these areas, especially in boundaries between different types. At several locations, the deepest sediments recovered contained metal levels that were elevated above background levels. This is most notable in the northeastern section of the pilot area, where we were limited to using the hydraulically damped gravity corer due to weather conditions. Interestingly, we also observe metal concentrations that are higher than those in other areas and collecting additional, longer cores at some of these sites as part of later phases could be useful.

A subset of core sites should be resampled during future phases to allow some assessment of long-term change. The most obvious choice would be to choose from among the sites sampled by USGS in 1996 that we were able to resample in 2013. Cuomo et al. (2014) suggest that long-term coring sites be established in order monitor a variety of constituents including organic carbon content, sediment accumulation and bioturbation.

Sediment environments and related information can be presented in various ways. In this report we offer several options that appear the most useful for us. The goal is to provide the results in different ways and with different degrees of interpretation to allow other users to integrate these results into a wide range of applications and decision-making processes.

Recommendations

- Subbottom data should be included in future phases of the project and should be collected in advance of the sediment core sampling, so that different features observed in the subbottom data can be targeted in the sampling program.
- Sediment cores should be taken in future phases of the project to get a better understanding of the stability of habitats/areas and how it has changed in the past.
- More time and opportunities should be included in future project phases to discuss different environmental settings, past changes, and different ways to describe those with benthic ecologists and managers, so that the results and products are presented in a way that highlight the characteristics most important for benthic habitats as well as for other management purposes.
- A better integration and comparison with other data, especially information on bottom currents and bottom stress could relate some of the interpreted environments to actual current strength for larger areas. Smaller variations, e.g. through local disturbances are probably not represent in the existing models, which have 500-1000 m bin sizes.
- Understanding the long-term sedimentation record from the cores and subbottom profiles will help to better characterize the spatial and temporal distribution of sediments and sedimentation processes to better define depositional environments and how they are being affected by anthropogenic activities. For this purpose more detailed analyses of the cores would be required. For example, calculations of sedimentation rates derived from radioisotope chronology and core X-ray radiograph to better characterize the biological and sedimentary features preserved in the cores.

4.7 References

- Bothner, M.H., Gill, P.W., Boothman, W.S., Baylor, B.B. and Karl, H.A., 1997. Chemical and textural characteristics of sediment at an EPA reference site for dredged material on the continental slope S.W. of the Farallon Islands: U.S. Geological Survey Open-File Report 97-87, 50 p.
- Cuomo, C., Cochran, J.K. and Turekian, K.K., 2014. Geochemistry of the Long Island Sound Estuary. In: J.S.L.e. al. (Editor), Long Island Sound, Springer Series on Environmental Management. Springer Science+Business Media, New York.
- Kenna, T.C. and Nitsche, F.O., 2011. Using X-ray fluorescence spectrometry to rapidly measure metal distributions in Hudson River sediment cores. Final Report of original scope for

- New York State Department of Environmental Conservation Service Contract C006787. pp. 39.
- Knebel, H. and Poppe, L., 2000. Sea-floor environments within Long Island Sound: A regional overview. *Journal of Coastal Research*, 16(3): 533-550.
- Knebel, H.J., Signell, R.P., Rendigs, R.R., Poppe, L.J. and List, J.H., 1999. Seafloor environments in the Long Island Sound estuarine system. *Marine Geology*, 155: 277-318.
- Nitsche, F.O. and Kenna, T.C., 2011. Detailed analysis of deposition in the Hudson River Estuary through integration of geochemical and geophysical data. Final Report of supplemental work for New York State Department of Environmental Conservation Service Contract C006787. pp. 18.
- Uchupi, E., Driscoll, N., Ballard, R.D. and Bolmer, S.T., 2001. Drainage of late Wisconsin glacial lakes and the morphology and late quaternary stratigraphy of the New Jersey - southern New England continental shelf and slope. *Marine Geology*, 172: 117-145.
- Wentworth, C.K., 1922. A scale of grade and class terms of clastic sediments. *Journal of Geology*, 30: 377-392.

5 Benthic Habitats and Ecological Processes

Recommended Citations:

- Zajac, R. (2015). Objectives and Historical Context. Section 5.1, p. 126-129 in: “Seafloor Mapping of Long Island Sound – Final Report: Phase 1 Pilot Project.” (Unpublished project report). U. S. Environmental Protection Agency, Long Island Sound Study, Stamford, CT.
- Penna, S. and R. Zajac. (2015). Seafloor and Habitat Characterization. Section 5.2, p. 131-171 in: “Seafloor Mapping of Long Island Sound – Final Report: Phase 1 Pilot Project.” (Unpublished project report). U. S. Environmental Protection Agency, Long Island Sound Study, Stamford, CT.
- Zajac, R., S. Penna, D. Chadi, J. Frederick, and M. Biegaj. (2015). Infaunal Ecological Characterization - LISMAR. Section 5.3, p. 171-248 in: “Seafloor Mapping of Long Island Sound – Final Report: Phase 1 Pilot Project.” (Unpublished project report). U. S. Environmental Protection Agency, Long Island Sound Study, Stamford, CT.
- Lopez, G. and R. Cerrato. (2015). Infaunal Ecological Characterization - SBU. Section 5.4, p. 249-267 in: “Seafloor Mapping of Long Island Sound – Final Report: Phase 1 Pilot Project.” (Unpublished project report). U. S. Environmental Protection Agency, Long Island Sound Study, Stamford, CT.
- L. M. Stefaniak and P. J. Auster. (2015) Emergent and epi-fauna Characterization. Section 5.5, p. 268-375 in: “Seafloor Mapping of Long Island Sound – Final Report: Phase 1 Pilot Project.” (Unpublished project report). U. S. Environmental Protection Agency, Long Island Sound Study, Stamford, CT.
- Auster, P. J., D. Chadi, S. Penna, L. M. Stefaniak, and R. Zajac. (2015) Integrated Ecological Characterization and Habitat Classification. Section 5.6, p. 376-381 in: “Seafloor Mapping of Long Island Sound – Final Report: Phase 1 Pilot Project.” (Unpublished project report). U. S. Environmental Protection Agency, Long Island Sound Study, Stamford, CT.

5.1 *Objectives and Historical Context*

The main focus of the benthic habitats and ecological processes components of the pilot project was to develop methodologies to best identify and characterize the variety of benthic habitats that comprise the study area and how identify and characterize infaunal and epifaunal communities relative to the sea floor habitats at multiple spatial scales, and to map their spatial distributions relative these habitats. Based on these efforts, information on ecologically significant locations in the pilot study area can be identified as well as how the community characteristics and habitat distributions might shape future impact assessments. Maps depicting sea floor habitats and their ecological communities are critical for many environmental management, conservation, and research activities, and for the growing focus on coastal and marine spatial planning. Such maps depict either separately or in combination the spatial distribution and extent of benthic habitats classified based on physical, geological, geomorphological, and biological attributes and the benthic communities that reside in the mapped habitats. Additionally, maps can be produced that depict ecological process across the sea floor. The field and analytical approaches and results of this portion of the pilot project also provide the framework on which to develop the next phases of the overall Long Island Sound seafloor mapping and ecological characterization project.

5.1.1 *Historical Context*

Maps describing the sedimentary environment, sediment thickness, surficial sediment and total organic carbon had been previously produced that included the pilot area and for Long Island Sound (Figure 5.1-1). These maps have been developed from a combination of acoustic imagery and in situ sampling (Figure 5.1-2). To view these maps dynamically, please see the following URL:http://ccma.nos.noaa.gov/explorer/msp/lis/msp_lis.html. There also existed ecological data (and in some cases related acoustic data) for the pilot area that helped guide the field data collection design for part of the pilot project, and used to assess potential temporal changes in community characteristics. Benthic ecological studies in LIS have a history going back to the mid-1950s (Zajac 1998), however collectively the studies are both spatially and temporally disjointed to various degrees. There were one-time surveys in the mid and late 1970's, providing data that helped establish trends in general community composition, diversity and relationships to habitat features (sediment type, depth, Figure 5.1-3). In some cases the spatial resolution was relatively coarse and in another survey the spatial resolution was high but only CT waters were sampled. In the early 1990s and then in the early 2000s a series of benthic samples were taken in LIS in support of the EPA EMAP and NCA programs, respectively. In addition to benthic community data, data on various pollutants were obtained, as well as toxicity tests performed using sediment samples collected in LIS. In the mid-1990s, Zajac (1998), in conjunction with USGS and the CT DEP, performed a demonstration project on how acoustic imagery/ sea floor mapping and conventional benthic sampling can be coupled to map habitats and understand

benthic communities in LIS; one of the study sites was located in the LIS mapping pilot area (Figure 5.1-4).



Figure 5.1-1: Map of surficial sediment for the pilot area in Long Island Sound.

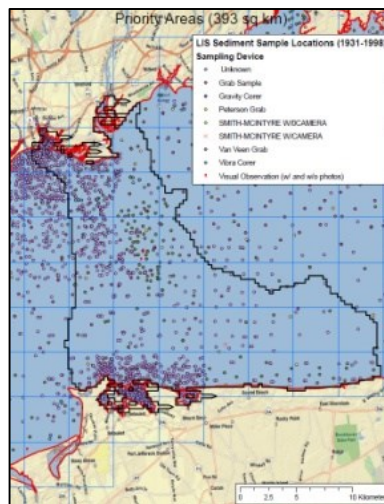


Figure 5.1-2: Map of sediment sample locations in the pilot area in Long Island Sound.

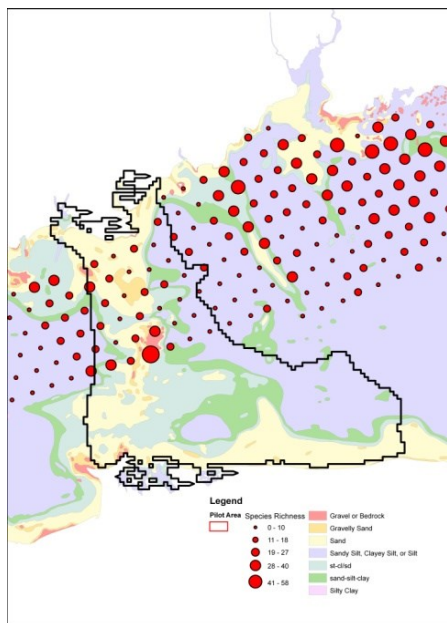


Figure 5.1-3: Spatial pattern of species richness across the northern portion of the pilot study area; data from Pellegrino and Hubbard (1983)



Figure 5.1-4: Side scan mosaic produced by Twichell et al. (1998) located on the eastern flank of the pilot study area; yellow boxes show areas sampled by Zajac (1998) for two years to look at seasonal and yearly changes in benthic community structure in relation to the various seafloor habitat elements found within the mosaic area.

One of the main findings of Zajac's (1998) study was that benthic community structure changes significantly relative to habitat structure both seasonally and yearly. Also, mesoscale habitat variation (on the order of 10's to 100's on m²) is a significant source of community variation, in addition to the large-scale seafloor patch structure that is evident in the side scan mosaic shown in Figure 5.1-4. Using the data set from this study Zajac et al., (2013) showed that infaunal biodiversity varies significantly over different spatial and temporal scales relative to the sea floor structure in a portion of the pilot study area.

Most studies have focused on soft sediment communities. To date, there are no spatially comprehensive assessments of hard substratum community types or states in LIS, and only a limited effort to describe those communities in the pilot project area (Liebman 2007, Poppe et al., 1998, Auster et al. 2009, Heupel and Auster in prep). More recently, Liebman (2007) surveyed selected areas around Stratford Shoal (Figure 5.1-6) using side scan and ROV video. The survey documented critical epibenthic habitat features and communities that can be found in seafloor patches characterized primarily by coarse sediments, rocks, gravel and extensive boulder features. It also documented features that occur in patchy distributions on unconsolidated fine grained cohesive sediments such as lobster burrows. Here lobster burrows exhibited greater spatial scales of patchiness in steeper areas of cohesive sediments. If such patterns could be attributed to fine-scale variation in physical habitat attributes, it may be possible to predict where such aggregations occur and then develop planning tools to avoid such areas or minimize impacts when developing projects offshore.

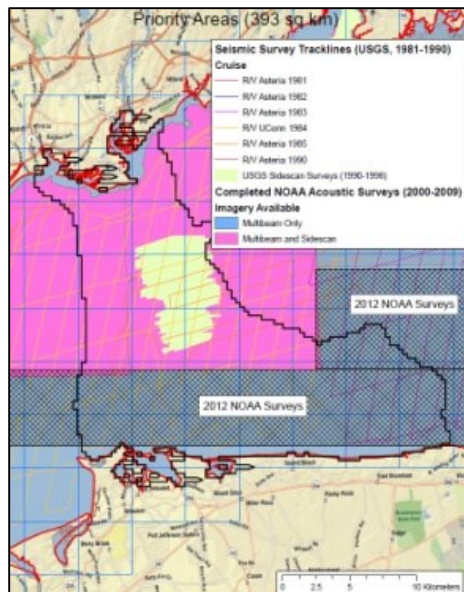


Figure 5.1-5: Map showing the locations of acoustic and video surveys conducted by Liebman and colleagues in 2007.

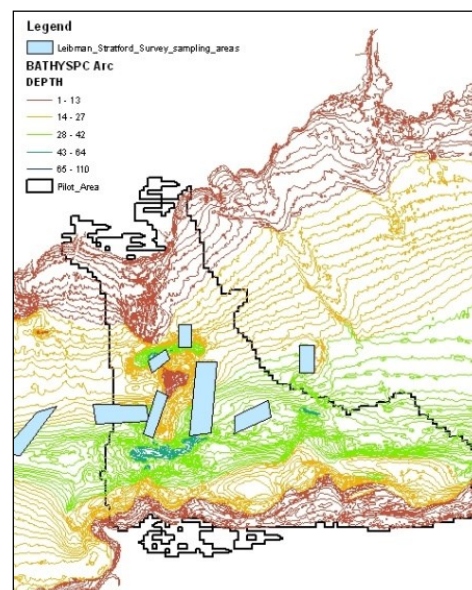


Figure 5.1-6: Map of surveyed areas in Long Island Sound. The maroon areas have been surveyed using acoustic sensors, the hatched areas have not.

While certain geologic and ecological characteristics have been mapped in LIS and more specifically the pilot study area, there remained data gaps that limited the ability to produce contemporary and spatially more comprehensive benthic habitat and ecological maps in the pilot area, and this continues to be the case for the Sound as a whole. These data gaps are spatial, thematic and temporal in nature, and limited the utility of existing products for resource management applications. Spatial data gaps existed because historical information was generally analyzed at coarse spatial scales, limiting its use for the breadth of management applications.

In addition to spatial gaps, there were also thematic and temporal data gaps because existing maps of the seafloor are primarily geologically based (surficial sediment types and sedimentary environments), and do not incorporate geomorphological, bathymetric, and, perhaps most critically, ecological components of habitat, and particularly epifaunal communities and habitats, and habitat forming species (e.g. mussel beds, oyster reefs, sponge communities, tube mats). There were also no maps that show the distribution and variation of both epibenthic and benthic infaunal communities within defined seafloor patches/habitats, except in some areas based on smaller scale studies (see above). In terms of temporal data gaps, many of the data collected that were used to produce geologically themed seafloor maps currently available, were collected over a time span approaching 80 -100 years in the case of the surficial from sediment map, and close to 20 years for spatially coarse side scan data that was used in part to produce the sedimentary environment map. Likewise, no significant ecological sampling of the benthos across the full extent of Long Island Sound, either the epifaunal or infaunal components, nor in shallow or deep waters, over a large spatial scale has been done since the mid-1970s to early 1980s, and no comprehensive sampling in the pilot study area since 1995-1996. Habitat maps produced using contemporary, and generally more accurate data, are more likely to be utilized for many different management applications because they contain added information that may be relevant and scalable to a wider array of issues in the marine environment. Furthermore, new management problems cannot always be anticipated (e.g., with respect to climate change), making extracting the maximum amount of information from acoustic imagery potentially important for being prepared to meet the future needs of the coastal and marine management community.

5.1.2 *References*

- Auster, P.J., Heinonen, K.B., Witharana, C., McKee, M. 2009. A habitat classification scheme for the Long Island Sound region. Long Island Sound Study Technical Report. EPA Long Island Sound Office, Stamford, Connecticut 06904. p.83.
- Leibman, M. 2007. Benthic Habitat Characterization of the Stratford Shoal region of Long Island Sound. OSV Bold survey report. U.S. Environmental Protection Agency New England, Oceans and Coastal Protection Unit, Boston, MA

- Poppe, Lawrence J., Lewis, R.S., Signell, R. P., Knebel, H.J., Persaud, M., Denny, J.F., Kenneth F. Parolsi, K.F., and DiGiacomo-Cohen, M.L. SIDESCAN SONAR IMAGE, SURFICIAL GEOLOGIC INTERPRETATION, AND BATHYMETRY OFF ROANOKE POINT, NEW YORK. 1998, USGS OFR98-502: Chapter 2, No.7
- Zajac, R. 1998. Spatial and temporal characteristics of selected benthic communities in Long Island Sound and management implications, Final Report, Long Island Sound Research Fund Grant CWF-317-R,. Hartford, CT: Connecticut Department of Environmental Protection, Office of Long Island Sound Programs. Available at:
http://www.lisrc.uconn.edu/DataCatalog/DocumentImages/pdf/Zajac_1998.pdf.
- Zajac, R.N., Vozarik, J.M. and Gibbons, B.R. 2013. Spatial and temporal patterns in macrofaunal diversity components relative to sea floor landscape structure. PloS one 8:e65823

5.2 *Seafloor and Habitat Characterization*

5.2.1 *Overview*

Significant advances have been made since the 1950's to characterize the oceans seafloor, and in particular seafloor mapping efforts since the 1990's, however, the detailed spatial distributions and characteristics of seafloor environments and their diverse habitats remain largely poorly known. Sedimentary seafloor environments are comprised of various types and sizes of sedimentary and hard substrate (geologic and biogenic) and geomorphological features (Greene et al. 2005) that provide habitat for diverse benthic communities and ecosystems. Seafloor communities can be classified by general substrate type (e.g. gravel, sand, mud, or clay) reflecting whether fauna reside on the surface, epifauna, or in the sediment, infauna (Kennish, 2001).

Understanding the structure and dynamics of benthic ecosystems and how they respond to disturbances is important for providing policy makers and scientists with the information necessary for coastal marine management. Several research techniques have been developed over the past several decades to study the community structure and diversity of the benthos and provide new types of data that can enhance our understanding of these communities. Specifically these include acoustic seafloor mapping techniques such as multibeam and sidescan sonar that provide the ability to conduct underwater remote sensing (Friedlander et al., 1999; Diaz, 2000; Kostylev et al., 2001; Brown et al., 2002; Greene et al., 2005) and develop base maps for sedimentological and biological observations and associated sampling for accurate interpretation of point measurements (Poppe et al., 1998; Zajac, 1998; Zajac et al., 2000; Hewett et al., 2004).

Data derived from acoustic underwater remote sensing and direct benthic sampling can be combined to create habitat maps. Such maps depict ecological characteristics and provide essential elements for assessments of benthic environments (Cogan et al., 2009). In addition, habitat maps reflect the biological, geographical, and physical environments of the seafloor and can be used for the effective management (Siwabessy et al., 1999) necessary to form policies and designate protected areas for the conservation of ecosystem biodiversity, sustainable fisheries, economic viability, natural and cultural heritage, and education (Airame et al., 2003). Conducting underwater acoustic and direct sampling studies of the seafloor also allows for assessing changes in benthic communities over time (Siwabessy et al. 1999), and to potentially predict responses from future disturbances.

A critical component of the benthic habitats and ecological processes portion of the pilot study was to characterize the sea floor in the study area and identify and map benthic habitats as a framework for assessing infaunal and epifaunal communities. A hierarchical approach (Zhan, 2003; Costa et al., 2012) was used to analyze sidescan and multibeam sonar data of the Stratford Shoal pilot area and to create a series of seafloor maps that depict various aspects of the seafloor structure and, by extension, benthic habitats. These habitat features and their spatial distribution

may be determinants of benthic community structure for both infauna and epifauna. Acoustic data were supplemented with physical and geologic data for the study area including sediment granulometry, bottom stress and geomorphic features. These data were combined with acoustic base maps to create sea floor characteristics maps that can be used for habitat classification. The map products developed can support future habitat map development, habitat classification, and ultimately environmental assessment in LIS. Habitat mapping and classification has become an important component in investigating and assessing seafloor environments; and developing coastal and marine spatial planning scenarios; and for overall regulatory and management efforts (MPA, 2001; Airame et al., 2007). The results and products of this portion of the pilot study addresses the need for establishing a framework for recognizing seafloor habitats in Long Island Sound and providing in-depth information on its ecosystems.

5.2.2 *Study Area*

The study area established for the Seafloor Mapping of Long Island Sound Phase I Pilot Project is a 462 km² portion of the Sound that spans the Stratford Shoal south of Bridgeport and Milford, Connecticut, and north of Setauket and Wildwood on Long Island, New York (Figure 5.2-1). Stratford Shoal (Figure 5.2-2) is a large topographic rise that influences patterns of water flow, sediment erosion and sediment deposition (Knebel & Poppe, 2000; Leibman, 2007). It also includes geological features that formed during the Quaternary Period that includes boulder deposits (Stone et al., 2005), sand waves, and anthropogenic features such as a pipeline, and trawl marks (Poppe et al., 1998). It is also known to support relatively diverse sets of habitats and ecological communities (Zajac, 1999; Zajac et al., 2000; Leibman, 2007).

5.2.3 *General Approach and Methods*

5.2.3.1 *Acoustic Data*

Acoustic backscatter imagery of the study area produced by the National Oceanographic and Atmospheric Association (NOAA; Battista, 2013) was analyzed to identify large-scale seafloor features, or patches, that are related to sediment types and geomorphic features such as sandwaves and transition zones among features (e.g. Knebel and Poppe, 2000; Zajac et al., 2003; Kennish et al., 2004; Brown et al., 2011). The images have a spatial reference of NAD 1983 UTM Zone 18N and were integrated into a single tonally corrected backscatter mosaic with a 1m resolution (Figure 5.2-3; Battista, 2013). The integrated mosaic consisted of composite sidescan and multibeam backscatter sonar imagery from NOAA surveys in west-central Long Island Sound off Milford, CT from 2005 (survey H11044), and along the northern coast of Long Island, New York (surveys H1246_S222, H1247_3101, H124_3102, H1247_S222, and H12416_3101; McMullen et al., 2008). Information on the acoustic imagery can be found on the Marine Geoscience Data System (MGDS) at <http://marine-geo.org>.

A 1m resolution digital bathymetric file produced by Battista (2013) from NOAA charts (Figure 5.2-4) was used in the characterization of the sea floor environments / habitats and also to develop derived data layers including slope and the Topographic Ruggedness Index (TRI) using ArcMap. A digital data file of mean bottom stress (Fake, 2014) was used to include information on potential hydrodynamic forces that may affect seafloor ecology in the habitat characterization process. Bottom stress is determined from the quadratic drag law applied at the point closest to the seafloor where there is a velocity estimate (Signall et al., 2006).

5.2.3.2 Seafloor Sampling and Sediment Data Collection and Processing

Two research cruises were conducted to obtain benthic grab samples and video and photographic imagery to obtain data on sediment characteristics, infaunal communities and epifaunal communities and habitat features. Research cruises were conducted in October 2012 and April 2013. The USGS Seabed Observation and Sampling System (SEABOSS; Figure 5.2-5; Blackwood and Parolski, 2000) was used to collect sediment samples and imagery during these LISMaRC research cruises. Sampling was conducted within thirty 1 km² study blocks that were chosen to represent varied types of sea floor habitats in the pilot study area. In each block 3 to 6 bottom grab samples were collected as well 3 video transects ~1 km in length. During the April 2013 research cruise, 17 additional samples were collected from areas of interest that were not located within sampling blocks (Figure 5.2-1). These blocks and single sample locations were selected throughout the study area to provide information on the range of sediment types, transition zones among them, and ecological communities found throughout the pilot study area based on an initial visual interpretation of the sidescan mosaic and previous studies conducted in the area (see Section 5.1). A small (~ 8 x 5 cm) sample of surficial sediment was collected from each grab and used for particle-size analysis (Poppe et al., 2000) and classified into sediment classes. The remaining sediment was processed on the ship and samples brought back to the lab for further analysis of benthic infauna (see Section 5.3).

Surficial sediment characteristics were determined based on 116 cores taken at the samples sites. The samples were analyzed for percent composition of gravel, sand, silt, and clay in the Wentworth (1922) and Folk (1954) grade scale and classified into a Shepard classification scheme modified by Poppe et al. (2004; Figure 5.2-6) using the sediment grain-size analysis software SEDCLASS (Poppe et al., 2003). The percentages were classified into textural classes gravel, gravelly-sediment, sand, silt, clay, sandy clay, silty clay, clayey silt, sandy silt, silty sand, clayey sand, and sand silt clay (O'Malley, 2007). To supplement data collected during LISMaRC cruises, sediment classification data from past Long Island Sound studies (McMullen, 2005) and sediment composition data from Lamont-Doherty Earth Observatory of Columbia University Collaborative cruises (Nitsche, 2013) was incorporated into the acoustic and habitat classification analysis.

5.2.3.3 Analysis of Acoustic Data and Seafloor Characterization

5.2.3.3.1 Object-oriented Classification

The integrated backscatter mosaic of the seafloor of the pilot area was analyzed using eCognition Developer 64 (Trimble, 2013). This software segments the mosaic into meaningful objects (image-objects) of various sizes based on spectral and spatial characteristics (Lucieer, 2008) to perform a multi-segmentation classification to find regions with similar pixel values based on mean pixel brightness. Based on eCognition terminology, the mean brightness is equivalent to the mean intensity value of the backscatter pixels. The algorithm for multiresolution segmentation works by producing image objects based on pixel intensity to produce discrete objects that are homogeneous with respect to spectral characteristics (Drăguț et al., 2010). The multiresolution segmentation was performed twice with a scale parameter segmentation of 50 and 100 to produce image objects that best represented the backscatter tones. The scale parameter value restricts the objects from becoming too heterogeneous (Trimble, 2012). A low parameter (near 0) would allow for higher heterogeneity and as the scale parameter increases, heterogeneity decreases. In addition, a composition of homogeneity criteria was assigned 0.8 for shape / smoothness and 0.2 for compactness. This criteria controls how the segmentation groups pixels into regions (Trimble, 2012). To determine how these changes affect segmentation, scale parameter segmentations of 50 and 100 were also performed with the default homogeneity criteria assigned 0.1 for shape / smoothness and 0.5 for compactness. The multiresolution segmentation criteria for this study are modeled from previous studies on object-based seafloor image classification conducted by Lucieer (2008). An unsupervised classification was then performed using eCognition by comparing the image objects with the underlying boundaries of pixel tone across the image. This procedure grouped the objects into acoustic classes, acoustic patch types, that were then used as the basis for habitat identification / classification at multiple scales and as the large scale habitat classes that were assessed in conjunction with ecological data and analyses.

5.2.3.3.2 Patch Analysis

A patch metrics analysis was conducted for the acoustic patches that were identified to assess their relative characteristics and composition relative to the overall study area. An analysis of the large- patches was performed using landscape analysis software. Large-scale acoustic patches were analyzed using the Vector-Based Landscape Analysis Tools Extension (V-Late) for ArcGIS (Lang and Tiede, 2003) to evaluate the structure of the landscape- and patch-level metrics. Six variables were calculated for each acoustic class including number of patches (NP), Mean Patch – Area Ratio (MPAR), Proportion (P), Class Area (CA), Total Edge (TE), and Mean Patch Edge (MPE).

5.2.3.3.3 Within-Patch Habitat Classification

The acoustic patch delineation classified / identified large-scale habitat patches across the pilot study area. However, habitat structure and types can vary at smaller-spatial scales within the

acoustic patch types, particularly for large patches. To assess smaller scale, within patch habitat variation, a classification model was developed using ARCGIS Model Builder. Model details are presented below. Briefly, ArcMap Spatial Analyst was used to produce a single raster data file that combined the variables used to define seafloor habitat landscape in this analysis; bathymetry, slope, silt-clay content, TRI and bottom stress. The Combine tool was used to overlay individual raster files for each of these variables and combined all of their pixel values into one file. The sum of these values represents classification criteria for that pixel and the area within the patch it is located. Descriptive statistics for the small-scale subpatches that were identified in the model were calculated using NCSS (Hintze, 2007) to describe pixel characteristics of the five layers that form the subpatches.

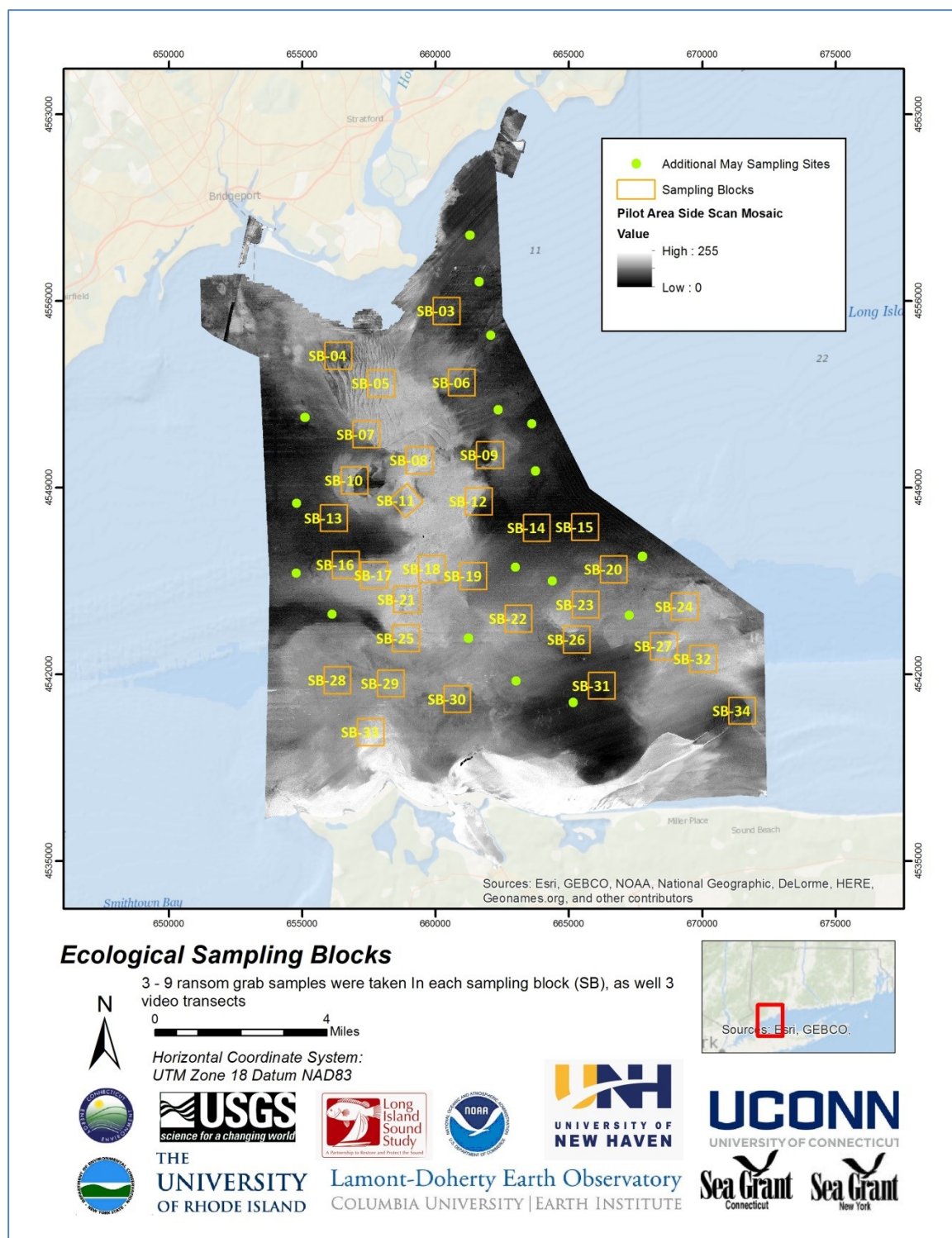


Figure 5.2-1: LISMaRC study area sample blocks (SB). In May 2013, only sampling blocks 3, 5, 6, 11, 12, 13, 15, 16, 19, 24, 25, 28, 31 and 34 were sampled as well as single samples at the additional May 2013 sample sites.

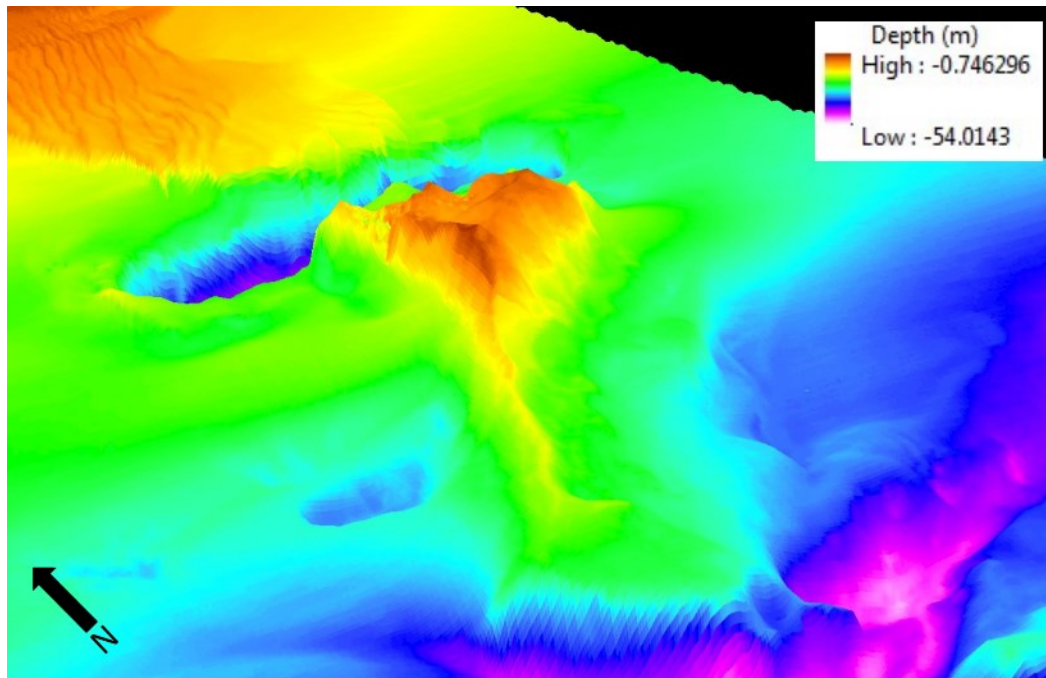


Figure 5.2-2: A 3D screen capture of Stratford Shoal. The red is the highest peak of the shoal and the white is the deepest; depth in meters.

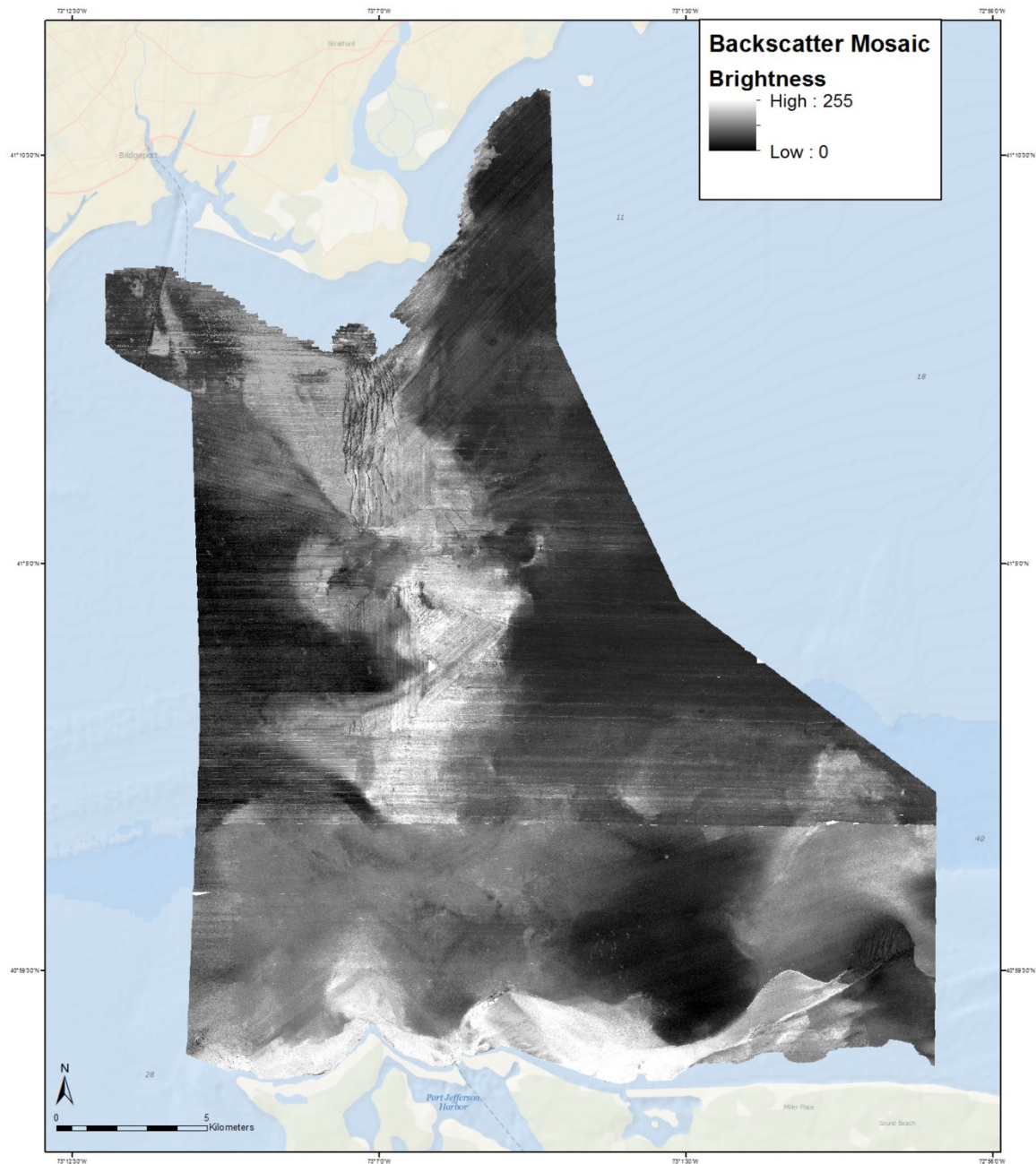


Figure 5.2-3: Integrated 1m² sidescan and multibeam sonar backscatter mosaic (Battista, 2013). Substrate composition can be inferred based on backscatter strength tones; dark tones (high backscatter) generally indicate fine sediment (fine sand, silt, and clay), and light tones (low backscatter) indicate coarse sediment (Goff et al., 2000; Kostylev et al., 2001; Collier and Brown, 2005; Brown and Collier, 2007).

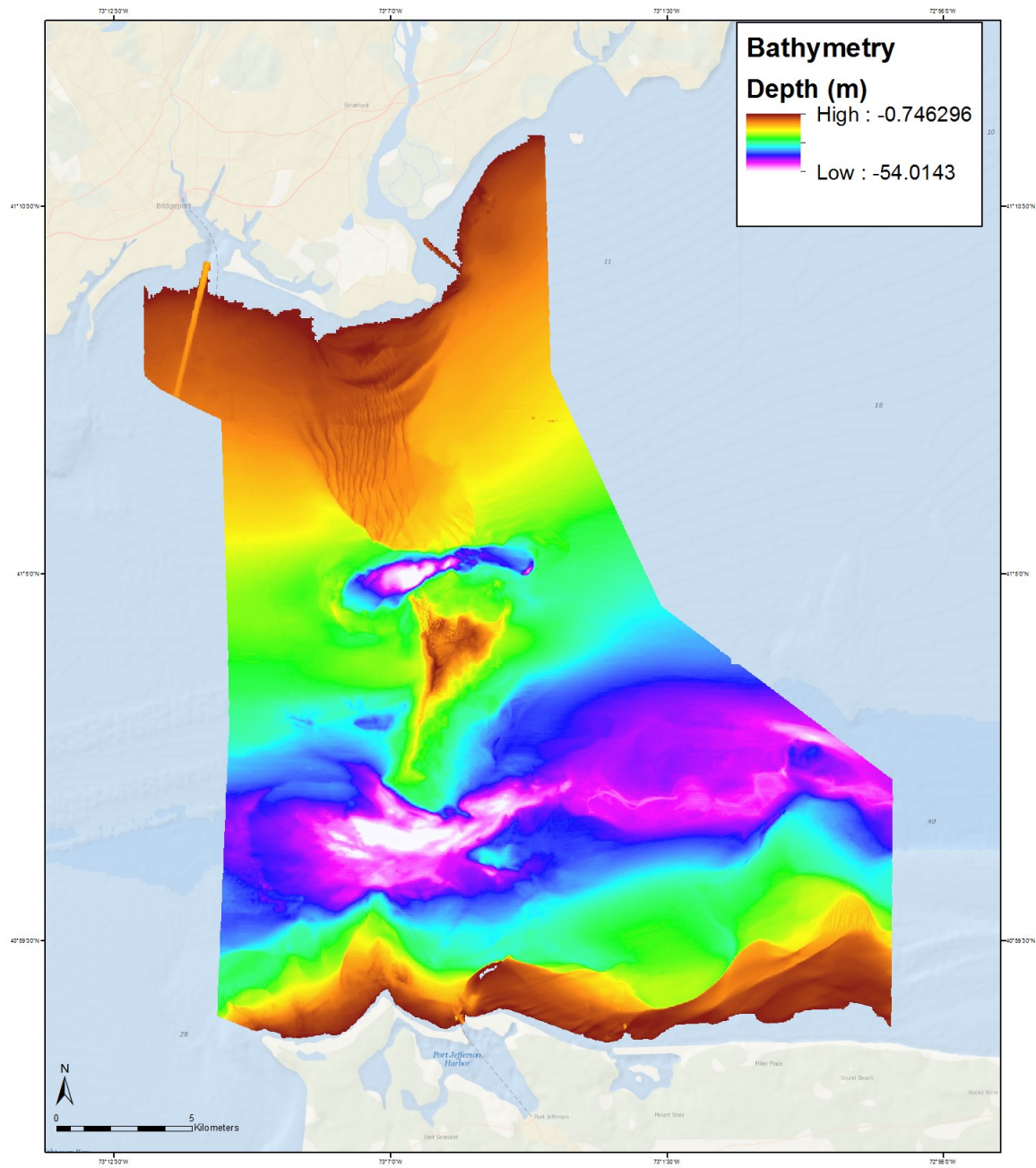


Figure 5.2-4: 1m bathymetry of the study area (Battista, 2013). Depth in meters.



Figure 5.2-5: SEABOSS used to collect sediment samples, photos, and videos of the seafloor. (Photo: Dann Blackwood; Blackwood and Parolski, 2001)

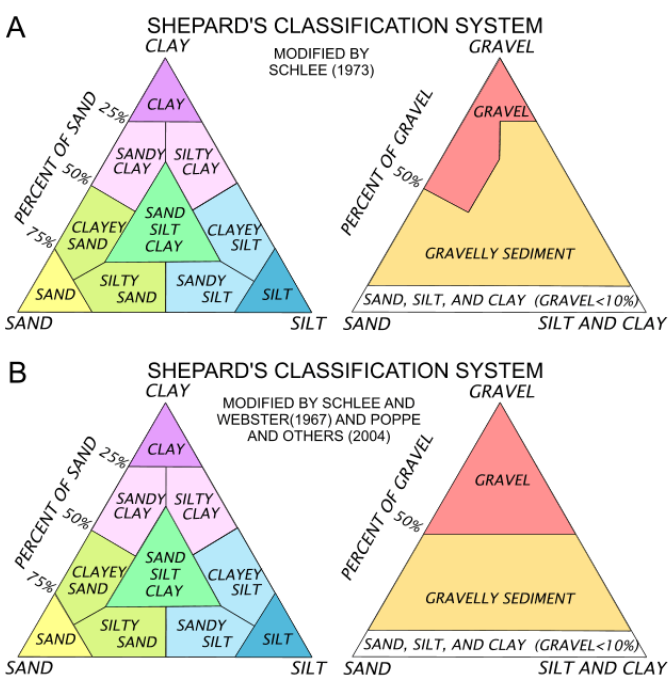


Figure 5.2-6: Shepard's Classification system modified by Schlee and Webster (1967) and Poppe and others (2000ab). Shepard's Classification System (1954) is used to determine the classification of sediment based on percentage of sediment from the grain size analysis of gravel, sand, silt, and clay. The SEDCLASS tool (Poppe et al., 2003) was used by Poppe to determine sediment composition for the LISMaRC cores.

5.2.4 *Acoustic Analysis by Object-oriented Classification*

The integrated backscatter mosaic was processed using four combinations of criteria to compare image-objects that best represented the tonal changes. Using multiresolution segmentation, image-objects (Figure 5.2-7) of the backscatter were constructed such that segments of the sidescan image that had similar tonal characteristics were isolated. These objects were classified into a final six groups based on pixel brightness (Table 5.2-1) using an iterative series of visual interpretations of the tonal changes of the segments and image-object boundaries (unsupervised classification) produced by the segmentation under different criteria. The finalized segmentation criteria optimized the boundaries of tonal change for the image-objects. The visual interpretation of image-objects did not include objects that were due to pixel values associated with swath tones remaining from post-processing or from shadows of anthropogenic or geological features, e.g. sand waves and pipelines (Figure 5.2-8).

During this process, four multiresolution segmentation combinations (Figure 5.2-9) were visually evaluated for the best overall amalgamation of the image-objects that capture the changes that were evident in the sidescan image. The combinations include a scale parameter of 50 or 100 with a default homogeneity criteria assigned 0.1 for shape / smoothness and 0.5 for compactness (Figure 5.2-9A and C) and an adjusted criteria derived from Lucieer (2009) with 0.8 for shape / smoothness and 0.2 for compactness (Figure 5.2-9 B and D). Image-objects produced using the default criteria had characteristics that include high noise such as rough lines and jagged edges. There were also several areas where pixels were grouped into image-objects that were based on the mean brightness of sidescan swath lines and not seafloor backscatter. The adjusted multiresolution segmentation parameters produced objects that had smoother lines and rounder edges. Compared to the default criteria, a larger number of image-objects were formed from swath line mean brightness. These were merged with nearest neighbor image-objects with the most appropriate mean brightness values, eliminating image-objects produced by swath lines. Lastly, each multiresolution segmentation criterion produced a different number of image-objects. The two criteria using a higher scale parameter (100) produced fewer image-objects than the criteria with a lower scale parameter (50). Using these factors, the multiresolution segmentation criteria that produced the best representation of the backscatter tones used a scale parameter of 100 and adjusted criteria. Several areas where image-objects next to lines from digital processing resulted in the miscalculation of mean brightness (Figure 5.2-10). To apply the correct mean brightness for these objects, comparisons were made with the backscatter against image-objects. Additional image-objects that did not match the backscatter were merged with their nearest neighbor that had similar pixel tones (Figure 5.2-11). The final six classes of image-objects were merged with the Convert Image Objects algorithm. This algorithm creates a single image-object per class (Trimble, 2013). The merged objects were exported as GIS thematic shapefiles and imported into ArcMap. These large-scale segments were designated as Acoustic Patches and were assigned class names based on increasing ranges of pixel intensity (see Table 5.2-1; Figure 5.2-12).

5.2.5 *Characteristics of the Acoustic Patches*

Sediment composition was used as the primary factor to characterize the acoustic patches. Sediment composition data determined from samples collected during the October 2012 cruise were sorted in GIS based on their location within each of the initially identified acoustic patches. The mean percent (± 1 SE) content of gravel, sand, silt, and clay was calculated for each acoustic patch (Figure 5.2-13). In addition, the number of occurrences of different sediment classes in the study area identified in a variety of previous studies were tabulated for each patch (Table 5.2-2) to provide additional information about the sediment characteristics of the acoustic patches in order to assess how similar the sediment composition descriptions were to the sediment grain size percentages collected in the LISMaRC research cruises. These data were used to designate an overall sediment classification descriptor for each acoustic patch. However, sediment characteristics can vary across multiple spatial scales within sea floor patches that have general characteristic sediments, e.g., sands or muds. In order to determine how sediment characteristics varied across each acoustic patch the percent composition of silt, muds, sands and gravel were calculated at each sample point and visually assessed (Figure 5.2-14), and the percent composition of each sediment class was spatially interpolated across the entire extent of each acoustic patch type using methods in ArcMap. These efforts yielded an overall more accurate interpretation of the surficial sediment classifications for the acoustic patches. Summaries of the sedimentary characteristics of each patch are presented below.

Acoustic Patch Type A (Silt-Clay/Sand): Acoustic patch type A comprised 32% of the pilot study area (Table 5.2-3) and was found in two main areas (Figure 5.2-12), spanning most of the northeastern border and extending to the bathymetric highs associated with Stratford shoal, and also along the northwest section of the study area. A large area was also found in the southeast section of the study area. There are 53 individual patches of Acoustic patch type A. Based on October 2012 sediment samples, silts comprised the highest percent by weight of the sediments in Acoustic Patch A, followed by clay (Figure 5.2-13). There was a relatively low percentage of sand, and there was no gravel. Sediment classifications were primarily clayey silt (Table 5.2-2). Based on this distribution, Acoustic Patch A is identified as Silt-Clay/Sand. These general sediment characteristics varied across the extent of Acoustic Patch A (Figure 5.2-14). The percent of clay was relatively consistent across all areas of acoustic patch type A, however the amount of silt appear to increase in the central portions of the patches, particularly in the eastern patch (Figure 5.2-15). A higher percentage of sand was present in northeast section of Acoustic Patch A in the large patch that occupied the eastern portion the study area. Interpolations of the sediment components indicate relatively constant percentages of clay, silt, and sand across Acoustic Patch A patches located in the western portion of the study area, whereas there was more spatial variation across Acoustic Patch A in the eastern portion of the study area (Figure 5.2-15). The percentage of clay increased into the deeper water portions of this patch, whereas sand increased toward the northeast corner and along the transition zones to some of the other patches. In the course of this analysis, an area in the southeast portion of the study area as

initially classifies as being Acoustic Patch Type A. However the interpolation analysis indicated the area to be comprised of 100% sand. Inspection of the sidescan mosaic (Figure 5.2-2) indicates that this is an area of large sand waves, indicating that the patch is not silt-clay/sand. This classification may have been the result of tonal changes from integrating several mosaic images and shadow tones from the sand waves and was reclassified as sand and combined into a different acoustic patch type. The topography of Acoustic Patch type A is primarily flat with gentle slopes and covers a wide but mostly intermediate depth range within the study area.

Acoustic Patch Type B (Silt-Sand-Clay): Acoustic Patch B was found on the edges of Acoustic Patch A (Figure 5.2-12) along the bathymetric highs of Stratford Shoal and a main area near the southeastern boundary of the study area. There are also sections near the northern coast that border small sand waves. This patch type comprised 14.5% of the pilot study area and was comprised of 149 individual patches (Table 5.2-3). Based on sediment samples, sands comprised the highest percent by weight of the sediments in Acoustic Patch B, followed by silt, then clay (Figure 5.2-13). A high number of previously collected samples primarily classified the areas comprising this patch type as sand-silt-clay; only one sample that has a gravel classification (Table 5.2-2). Based on this distribution, Acoustic Patch B was characterized as having primarily Silt-Sand-Clay sediments. The sediment characteristic varied between the northern and southern sections of the study area. The northern portions of the patches have consistent percentages of silt, sand, and clay. The sand begins to increase towards the southeastern portion of the study area in a bathymetric low region with high bottom stress. An interpolation analysis of the sediment composition indicates that there is a higher percentage of silt in the north and a higher percentage of sand in the south. The sidescan mosaic shows minimal topography variation throughout Acoustic Patch type B. There are small geomorphic features found within the patch boundaries, such as small, low slope sand waves in the southeast corner of the study area. Parts of the large sand waves in the north are also included in Acoustic Patch B, which were classified as Sand-Silt-Clay based on sidescan mosaic tones. In the northwest corner a shipping channel exists that contributes to tonal irregularities in the sidescan mosaic.

Acoustic Patch Type C (Silty, Clayey Sand): Acoustic Patch type C is found throughout the north to south length of the study area (Figure 5.2-12) primarily along the bathymetric rise of Stratford shoal, along large sand waves in the north, and in a few small of this type the southern portion of the study area. This patch types comprised 6.7 % of the study area primarily as many, 235, small patches (Table 5.2-3). Based on sediment samples, sand comprised the highest percent by weight of the sediments in Acoustic Patch type C followed by silt, then clay (Figure 5.2-13). One sample in the south included a low percentage of gravel. Most previous sediment samples classified the areas comprising patch type C as silty sand, with one site classified as sand and no gravel (Table 5.2-2). Based on this distribution, Acoustic Patch C is classified as being comprised of primarily Silty, Clayey Sand. Although Acoustic Patch C has the most individual patches of the six acoustic patches, it has the second smallest area and smallest mean patch edge (Table 5.2-3). This small overall patch class and the distribution of individual patches

throughout the study area accounts for the wide range of depths these patches are found in. Interpolation analyses of Acoustic Patch C identify high areas of clay and silt in the southern portion of the study area, with an increase of sand in the northern portion. Slope variations occur around small sand waves that exist in the southeastern corner of the study area and along a bathymetric low above the northern portion of the shoal.

Acoustic Patch Type D (Sand): Acoustic Patch type D was one of the two largest sea floor elements in the study area, comprising 33% of the area and having 125 individual patches (Table 5.2-3). These patches were found throughout the center of the study area and extending from the southwest to northwest corners (Figure 5.2-12). A high degree of variation in seafloor characteristics in the study area is associated with habitat variations within this patch type. Based on sediment samples, sand comprised the highest percent by weight of the sediments, followed by low percentages of silt, clay and gravel (Figure 5.2-13). Sediments classifications from previous studies for samples located within areas of patch type D were primarily sand (Table 5.2-2). Based on this distribution, Acoustic Patch D is identified as Sand. The percentage of sand is highest in the north section of the study area and the southeast corner. The percentages of silts and clays are relatively higher in the southwest corner and decrease towards the southeast corner of the study area (Figure 5.2-14). Interpolation of sediment composition indicates a relatively high percentage of clay and silt in the northwest and southwest corners of the patch. Percentage of sand was consistent throughout the patches of this type, but increased in areas with sand waves. In the interpolation, a section in the northwest portion of the study area had a high percentage of clay and silt. Sediment samples from this area indicate that there was a high amount of silt, indicating that this patch is not primarily sand and was combined into a different acoustic patch type. Acoustic Patch D also includes areas of bathymetric highs near the coast and on sand waves; and bathymetric lows at the upper and lower boundaries of the shoal.

Acoustic Patch Type E (Gravelly Sand): Acoustic Patch type E is found in two main areas (Figure 5.2-12), in the center of the study area on the bathymetric high of Stratford shoal and northern sand waves, and along the southern border. There is also a small patch located on the southern western corner of the study area. This patch type comprises 11% of the study area and there are 90 individual patches (Table 5.2-3). Based on sediment samples, sand comprised the highest percent of weight of the sediments in Acoustic Patch type E, followed by gravel (Figure 5.2-13). There was a small amount of silt and clay present. Sediment classifications were primarily sand, but there are also several sites that were classified as gravel and gravel sediment (Table 5.2-2). Based on this distribution, Acoustic Patch E is identified as Gravelly Sand. These sediment characteristics varied throughout the study area (Figure 5.2-14). Areas that were primarily sand were located with sand waves in the northern section of the study area. The percent of gravel was highest at the shoals bathymetric high and at the southeastern corner of Acoustic Patch E. Interpolations of Acoustic Patch E indicates a consistent present of sand throughout the patch with higher levels of gravel in the center of the shoal and northern large sand waves. There are also several small areas that have high silt and clay near the shoal, which

remained after acoustic pixel tone analysis. Inspection of these areas found that the sample in this patch was primarily clay and near the border of an acoustic patch with a similar composition. This patch was reclassified as silty, clayey sand and combined into another acoustic patch. Inspection of the sidescan mosaic indicates that there are several areas of large and small sand waves in patches classified as type E, and in E type patches in the center portion of the shoal, there is part of a boulder outcrop.

Acoustic Patch Type F (Gravel-Sand): Acoustic Patch F was found in two main areas, the center of the study area on the bathymetric high of the shoal and a large area along the southern border (Figure 5.2-12). These patch types comprised only 1.6% of the study area and there are 25 individual patches (Table 5.2-3). Based on sediment samples, sand comprised the highest percentage by weight of the sediments in Acoustic Patch F, followed by gravelly sediment (Figure 5.2-13). There was a very low percentage of silt and clay. Sediment classes designated in previous studies were primarily gravelly sediment, followed by sand (Table 5.2-2). Based on this distribution, Acoustic Patch F is identified as Gravel-Sand. All of the samples that fell in this patch type were located on the bathymetric high of the shoal. The percent of gravel was high in all of these samples. However, one sample was primarily sand with little gravel. This may have been a result of similar tones during acoustic classifications. Interpolations of Acoustic Patch F show a high percentage of gravel and sand and low percentages of clay and silt. The southern patch of this type had consistent sediment classifications from previous work and no samples were collected during research cruises in this area. To determine the predominant sediment type in this patch, data collected from past research studies (McMullen et al., 2005) were incorporated into the analysis of Acoustic Patch F. The average sediment classifications were evaluated since not all of the samples contained percentages for specific sediment fractions (Figure 5.2-16). The upper (northern) patches of Acoustic Patch type F were found to be primarily classified as sandy gravel, gravelly sand, gravelly sediment, and pebbles. The lower (southern) patch of Acoustic Patch type F was classified primarily as mud, sand, and course sand. This indicated that the southern section was not comprised of gravel, but primarily sand and mud. Based on this, this southern patch was reclassified and combined into a different acoustic patch type.

5.2.6 Habitat Analysis by Data Layer Overlay

Digital data files were used to define seafloor habitats and organized as a hierarchical classification system following the classification system proposed by Auster et al. (2009) for Long Island Sound (Figure 5.2-17). The descriptions and terminology used here follow this classification scheme. The pilot study area is between two systems, Western Long Island Sound and Central Long Island Sound within a subtidal subsystem. Acoustic Patches are part of a primary subclass that is impacted by modifiers. The modifiers used in this study include bathymetry, slope, TRI, bottom stress, and silt-clay composition. Each of these modifiers was reclassified into four classes that best represented divisions of the data specific to the modifier (Table 5.2-4). To determine the range within these modifiers, each one was reclassified into 4

quartiles; silt-clay was reclassified into quarter percentiles because the data was previously calculated in percent format. The reclassified layers were combined into one raster layer that portray the overall habitat structure based on pixel values that represent the sum of the values of each of the modifiers at each pixel location.

5.2.7 Digital Data Layer Characteristics

Bathymetry: The depth of the study area ranges from 0.7 m to 54.02 m (Figure 5.2-4). Major features that effect the depth were identified for the entire landscape including a large sand wave field in the north-central section, a small sand field on the shoal and one located near the southeast corner of the study area. On the bathymetric high of the northeast corner of the shoal there is a large boulder field. On the northern and southern boundaries of the shoal are deep canyon features. There are distinct, large-scale, north to south depth gradients and also east to west, away from the shoal.

Slope: The slope layer was derived from the bathymetry layer using ArcMap (Figure 5.2-19). The majority of the study area has primarily very low slopes, especially on the eastern and western sections of the study area. The steepest slopes are found in the boulder field on the shoal, along the boundary of the northern channel, and on sand waves crests found in the northern and southern parts of the study area. Higher slopes are also associated with anthropogenic features such as the channel in the northwest corner and part of the pipeline along the northeast section of the study area.

Terrain Ruggedness Index: The Terrain Ruggedness Index (TRI) layer was also derived from the bathymetry layer using ArcMap (Figure 5.2-18). Areas of high ruggedness are found in the center of the study area at the northern channel, boulder field in the center of the shoal, and northern sand waves. The lower channel also has several areas of high ruggedness in addition to the small sand waves in the southeast corner of the study area.

Silt-Clay: Inverse distance weighting (IDW) interpolation for the entire study area for clay and silt were combined into a single layer (Figure 5.2-20) to show the distribution of silt and clay (Silt-Clay) in the study area. Silt and clay are used because these sediment components are collinear with sand and gravel on the most part and as such can capture the main trends in overall sediment composition. Silt-Clay had the highest distribution on the eastern and western boundaries of the study area. In addition, there is a large patch that is near the southeast corner. The lowest concentrations are on the bathymetric high of the shoal and in areas that are known to have sand waves based on investigation of the sidescan mosaic and bathymetry.

Bottom Stress: Bottom stress of the study area is highest from the center of the northern boundary, down the center to the south, then across from the western to eastern boundary (Figure 5.2-21). There is also a small area to the west of the shoal on the edge of the northern channel. Investigations of the sidescan mosaic and bathymetry shows that the areas of high bottom stress

are associated with sand waves, the bathymetric high of the shoal, and the channel in the south. Areas with the least amount of bottom stress are located nearest to the shore.

5.2.8 *Data Layer Overlay*

The quartile pixel layers for each environmental modifier were overlaid and the values were summed to define the composite characteristics of the seafloor at each pixel location (Figure 5.2-22). The sums of the assigned quartile scores obtained ranged from 5 to 17. For example, a pixel can have the following total classification score of 6 based on individual modifier scores of Bathymetry = 2, Slope = 1, TRI = 1, Silt-Clay = 1, and Bottom Stress = 1. In order to assess variations in habitat structure within the acoustic patch types, and identify potential sub-habitats (referred to here as subpatches), the overlay composite was clipped by each of the acoustic patch type layers and further analyzed. This analysis focused on identifying smaller-scale, within acoustic patch type habitats as they relate to the overall classification of each acoustic patch type and the modifiers. The sum of the modifier scores can be due to many combinations of the individual modifier scores. As such, bathymetry was selected as an overarching modifier, and classified into four depth ranges (Figure 5.2-22) that were related to ranges of average scores for depth that could be obtained for individual total scores. These were 1- <2, 2- <3, 3 - < 4, and 4. As such, the sub-patches are in effect depth related subdivisions of all of the acoustic patches. Depth is an important determinant of ecological structure and dynamics and as such was a logical choice for the overarching modifier. Within each of these depth ranges, composite values for the other modifiers, i.e. TRI, bottom stress, slope, and silt-clay, were averaged thus producing an overall characterization for the depth related sub patches within each acoustic patch type.

Subpatches in Acoustic Patch type A (Figure 5.2-23) were classified to initially test this approach and assess its utility before applying it to all acoustic patch types and to use it as a model for future classifications. Within Acoustic Patch type A, four subpatches based on bathymetry were identified and further classified based on the other modifiers (Table 5.2-5; Figure 5.2-23) that define the multivariate characteristics of these subhabitats. Overall, most subhabitats with high values represent all of the high sums for TRI, bottom stress, and deep depth while the lower sums represent the low values for TRI, bottom stress, and shallow depth. This is not a continuous upward trend because the location of the patches in relation to the shoal will reflect different strengths on the subhabitat classifications due to changes in topography. The final classification of Acoustic Patch A results in four subhabitats classified into depth classes: shallow, shallow / intermediate, intermediate/deep, and deep (Tables 5.2-5 & 6). Throughout Acoustic Patch type A, the slopes are minimal. The shallow subhabitat is located on the northeast and northwest corners of the study area, along the edge of the bathymetric rise of the shoal, and a small section on the southern boundary of this portion of Acoustic Patch type A. These areas also have minimal bottom stress and TRI. The shallow / intermediate subhabitats are primarily located in the western section of the patch, with a smaller portion on the eastern boundary and southern tip of the area. The Intermediate / deep section is located primarily on the eastern

portion of the study area, with a small section on the western portion. This subhabitat type also has the largest area. The influence from bottom stress is low as the TRI increases to moderate. The deep class is the smallest subhabitat is Acoustic Patch A and is only located on the eastern portion of the patch. This subhabitat has a moderate influence from bottom stress and a high influence from TRI.

This model is structured so that the classification of subhabitats can be repeated for patches B-F. Although this model divides the bathymetry into four ranges, the resulting subpatches may have different characteristics when assessed for the other patch types. Each subpatch is subject to different conditions such as the presence or absence of geomorphic features that would adjust topographic values for slope, TRI, or bottom stress. Ground-truth images of the study area show examples of the different acoustic patch type A subhabitats that lay within this large-scale habitat designation (Figure 23A - D).

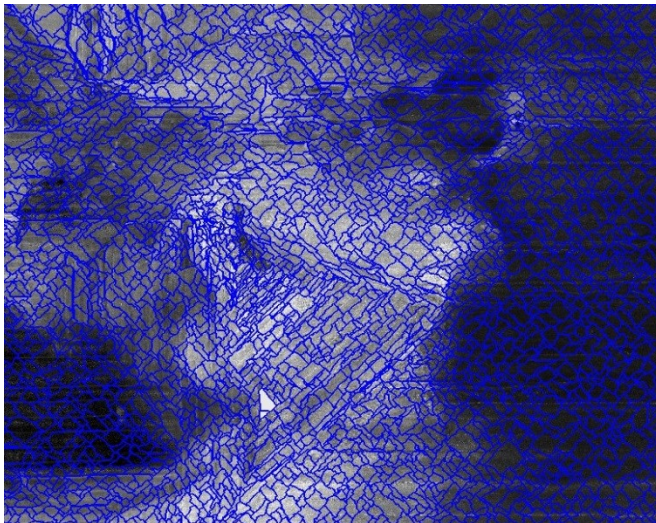


Figure 5.2-7: A screenshot of image objects produced in eCognition of the integrated backscatter image.

Table 5.2-1: Sediment classes (i.e. acoustic patch class) developed in eCognition based on mean brightness of objects.

Sediment Class	Starting Mean Brightness	Ending Mean Brightness
A	0	54.99
B	55	76.99
C	77	87.99
D	88	129.99
E	130	172.99
F	173	254
No Data	254.1	255

A



B

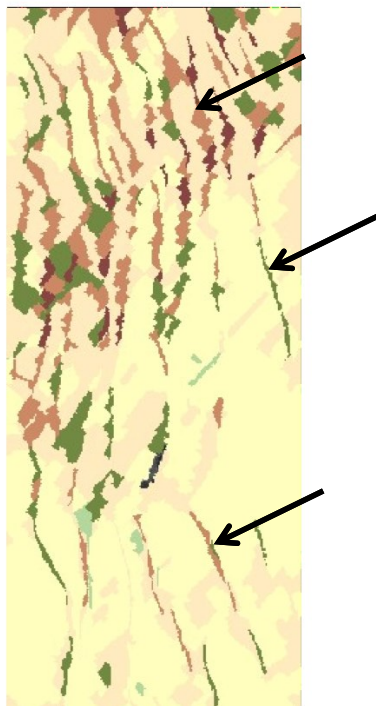


Figure 5.2-8: A) Example of image objects produced from swath lines (linear stripping due to edges of acoustic swaths). The arrows identify lines in green (colors vary).

Figure 5.2-8: B) Example of image objects produced by sand wave shadows. The arrows identify some of the image objects that were produced and can also be identified with brown and green colors.

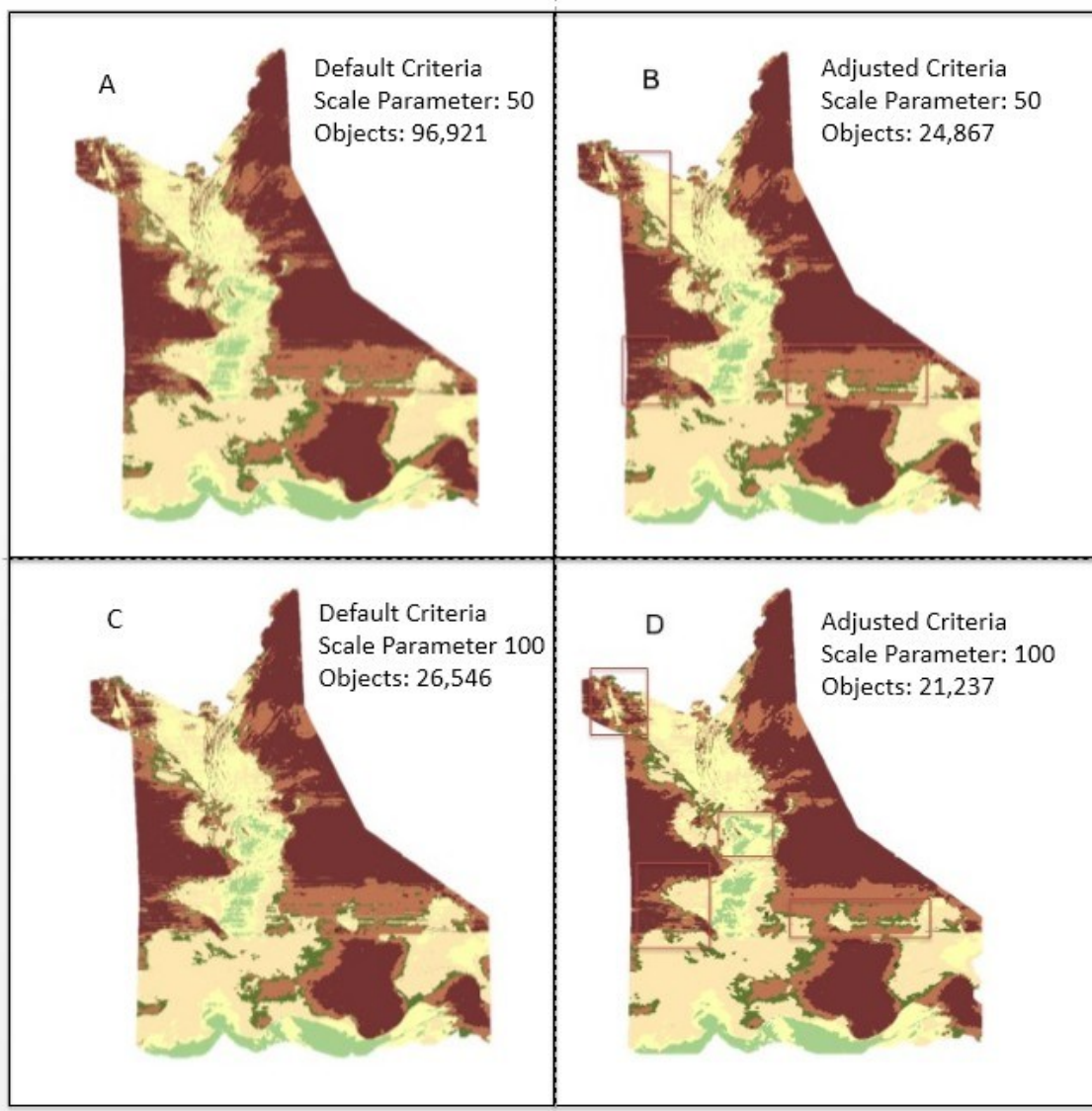


Figure 5.2-9: A comparison of multiresolution segmentation results. A) Image objects produced using the default variable with a scale parameter of 50. B) Image objects produced using the adjusted variable with a scale parameter of 50. C) Image objects produced using the default variable with a scale parameter of 100. D) Image objects produced using the adjusted variable with a scale parameter of 100. Areas that exhibited noticeable differences in image object shape and compactness are outlined as boxes in (B) & (D)

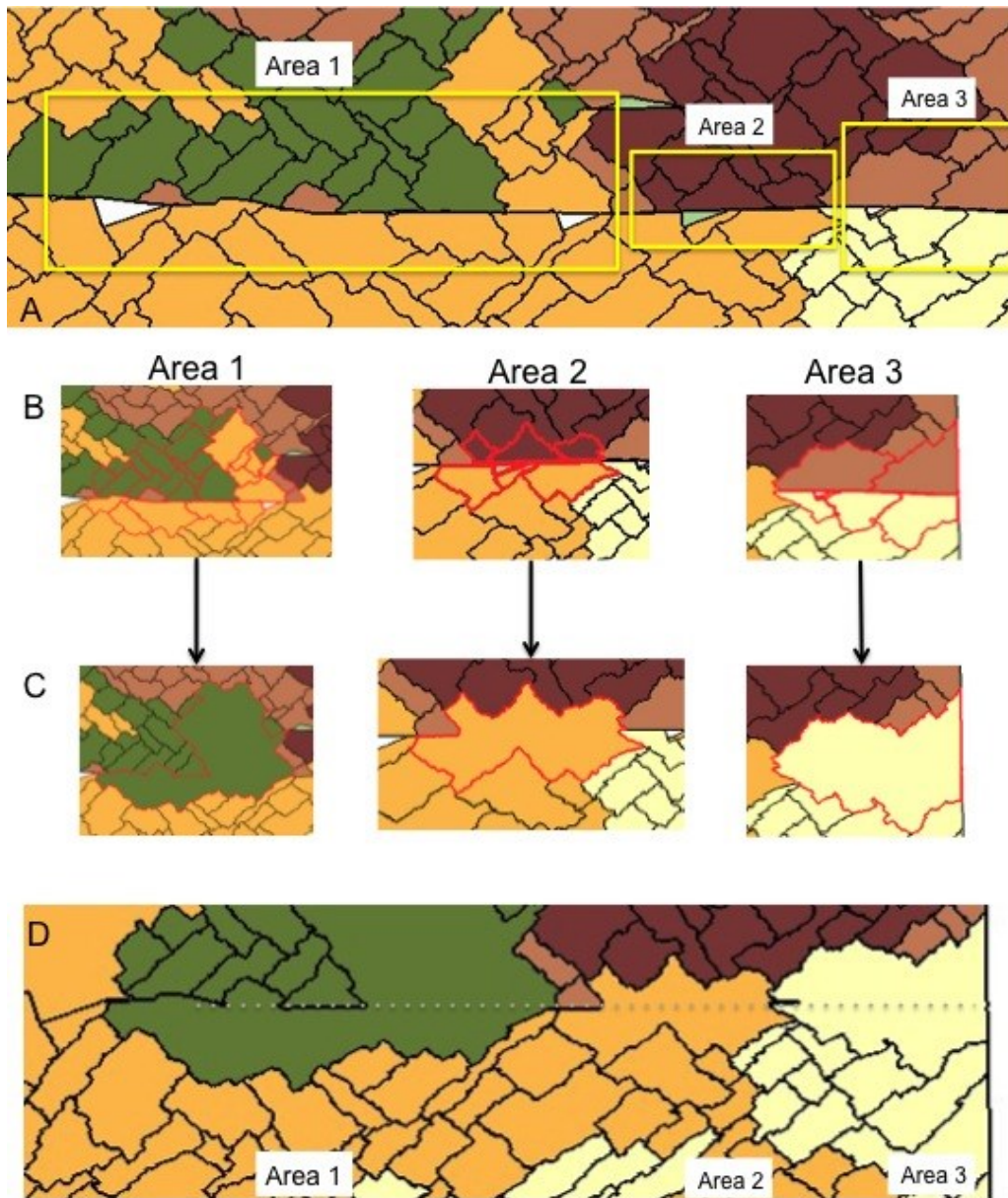


Figure 5.2-10: Image object editing. A) A line remained after the digital stitching of two mosaics. The pixels from each mosaic were not able to group properly, giving the appearance of different backscatter strengths on each side of the line. B) Objects were grouped according to the object classes that matched the sidescan backscatter mosaic. C) Objects were merged. D) The new objects match the tones of the sidescan backscatter.

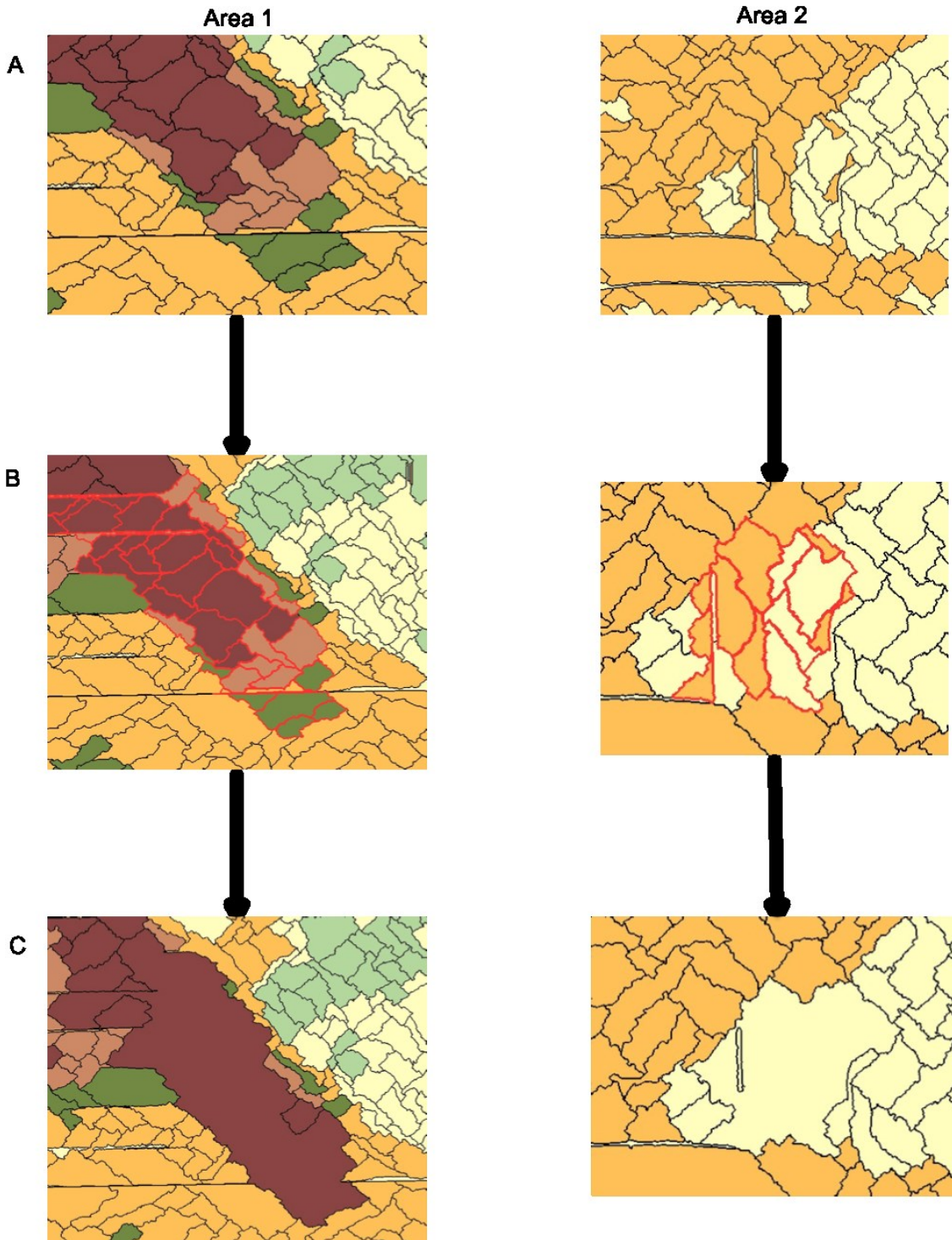


Figure 5.2-11: Examples of image objects that were miscalculated during the multiresolution segmentation. (A) Areas of miscalculation identified. (B) Objects that did not match the backscatter tones were identified. (C) Objects were merged with their nearest neighbor with similar pixel tones.

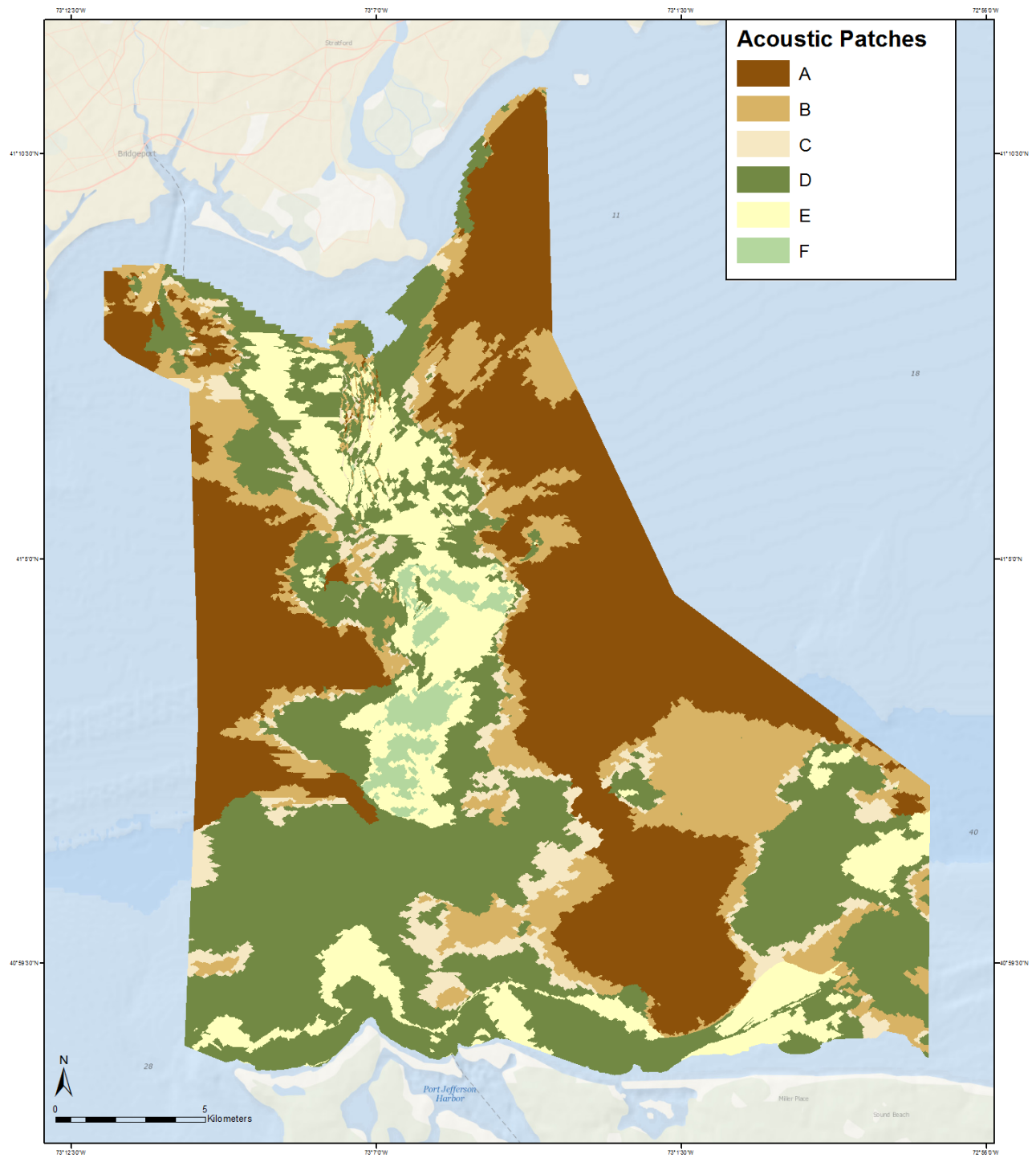


Figure 5.2-12: Acoustic Patches produced using eCognition.

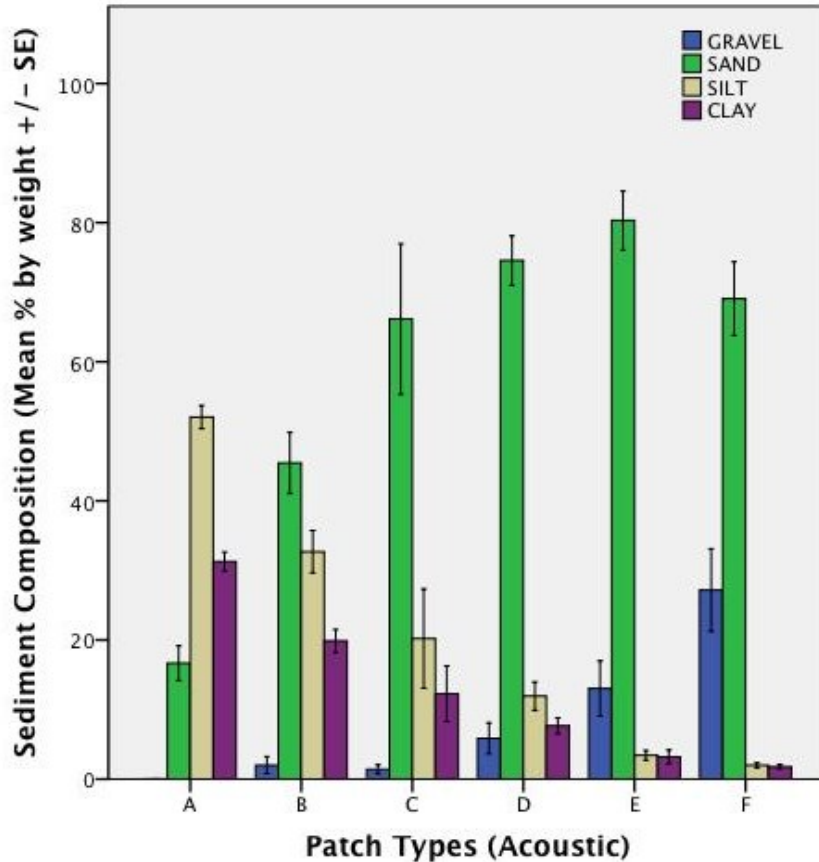


Figure 5.2-13: Mean sediment composition of the acoustic patches derived from eCognition.

Table 5.2-2: Number of occurrences of different sediment classes assigned to sampled points located in each acoustic patch in previously assembled sediment class databases for Long Island Sound.

	A	B	C	D	E	F
CLAYEY SILT	22	2	0	0	0	0
GRAVEL	0	0	0	1	1	0
GRAVELLY SEDIMENT	0	1	0	5	8	5
SAND	0	2	1	16	13	1
SAND SILT CLAY	6	7	0	1	0	0
SANDY SILT	1	2	0	1	0	0
SILTY CLAY	1	0	0	0	0	0
SILTY SAND	3	5	3	8	0	0
TOTAL	33	19	4	32	22	6

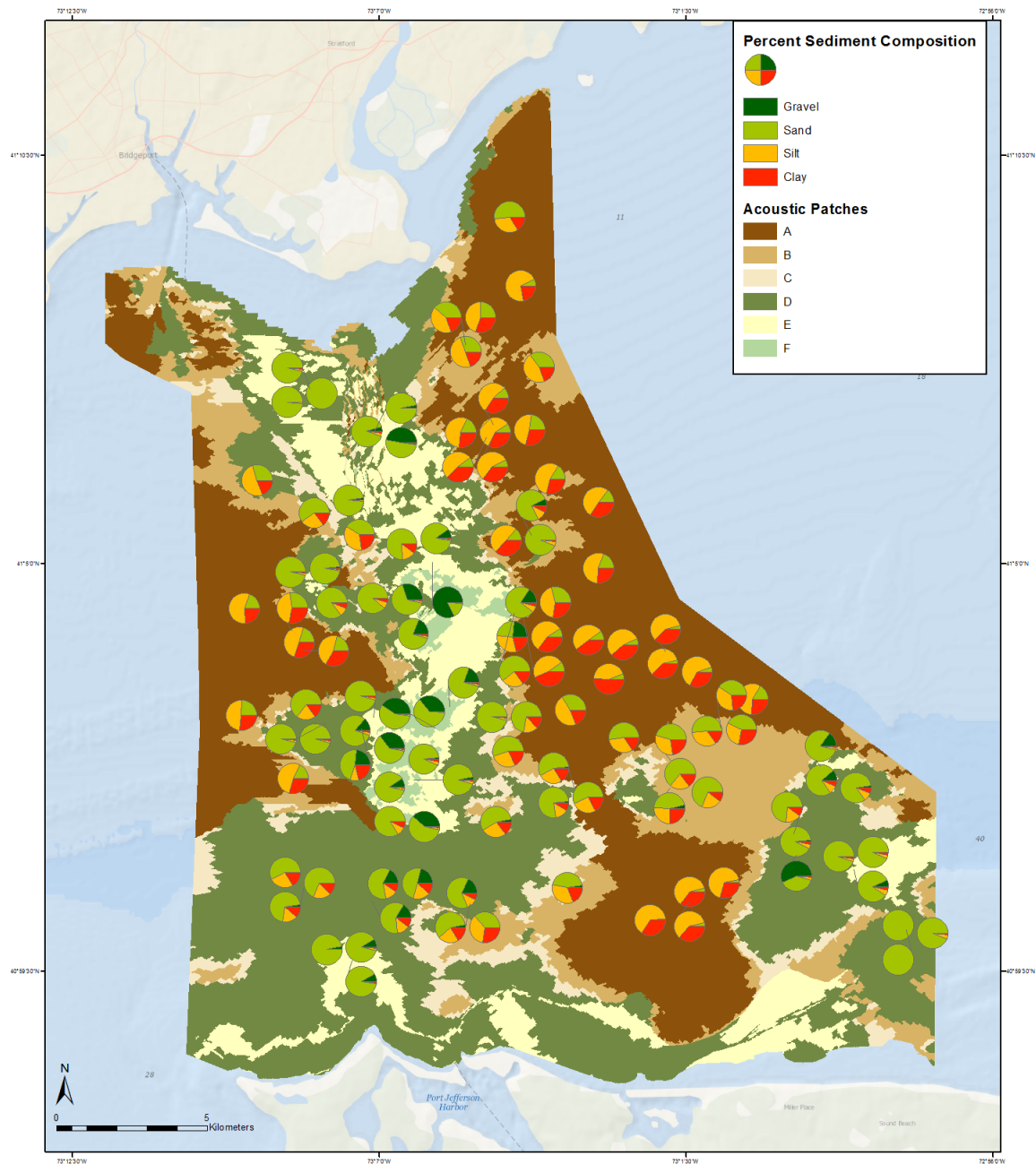


Figure 5.2-14: Acoustic map with percent sediment composition pie charts. Pie charts were used to represent the percent composition of sand, silt, clay, and gravel in the cores. This illustrates the distribution of composition and their relationships with acoustic patches.

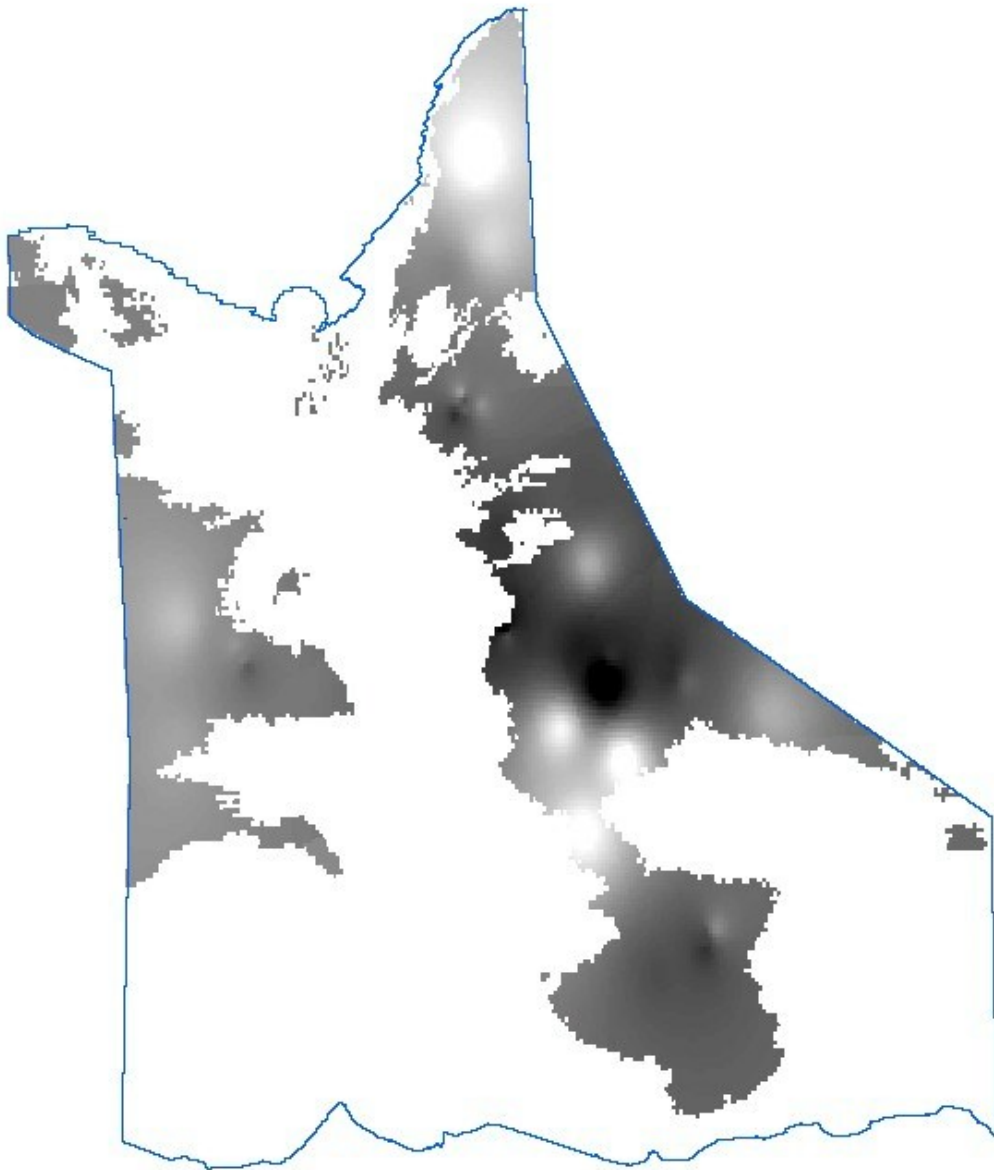


Figure 5.2-15: Example of sediment percent composition interpolation showing the interpolated percent composition of clay sediments for Acoustic Patch A. Darker areas indicated a higher percentage of clay in the overall sediment composition.

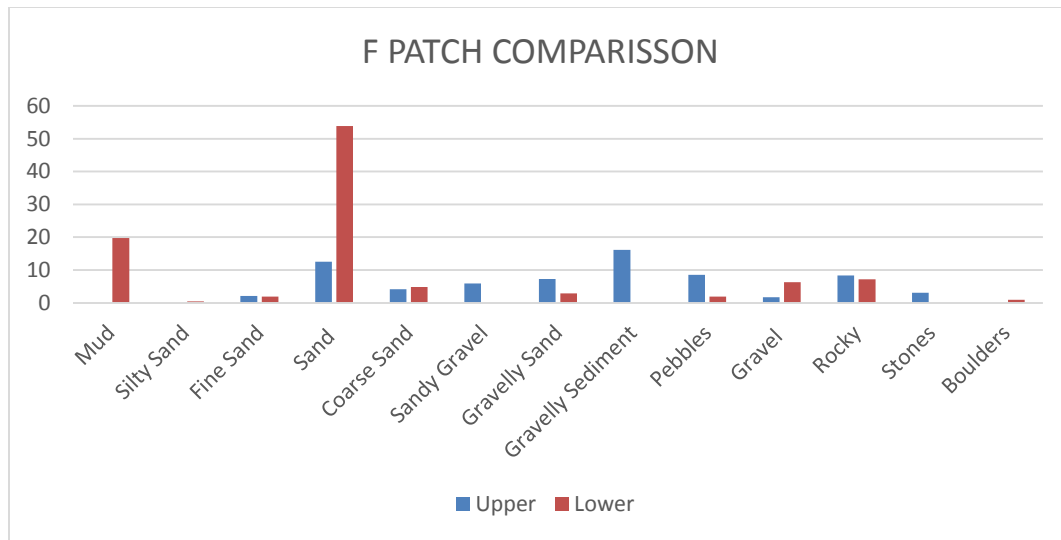


Figure 5.2-16: Average sediment classifications of the lower and upper sections of Patch F. Sediment classes are based on individual projects included in McMullen et al. (2005).

Table 5.2-3: Acoustic patch analysis of area, edge, and form. Number of Patches (NP), Mean Patch – Area Ratio (MPAR), Proportion (P), Class Area (CA), Total Edge (TE), Mean Patch Edge (MPE). Total Patches: 677, Total Area: $2.9 \times 10^8 \text{ m}^2$

Class	NP	MPAR	P	CA	TE	MPE
A: SILT-CLAY/SAND	53	0.176	32.74	97115534	377380	7120.38
B: SAND-SILT-CLAY	149	0.112	14.53	43092533	669078	4490.46
C: SILTY, CLAYEY SAND	235	0.081	6.69	19854594.14	526852.59	2241.93
D: SAND	125	0.122	33.04	97985913	892916	7143.33
E: GRAVELLY SAND	90	0.26	11.39	33788404	504748	5608.31
F: GRAVEL-SAND	25	0.124	1.61	4768327	96130	3845.2

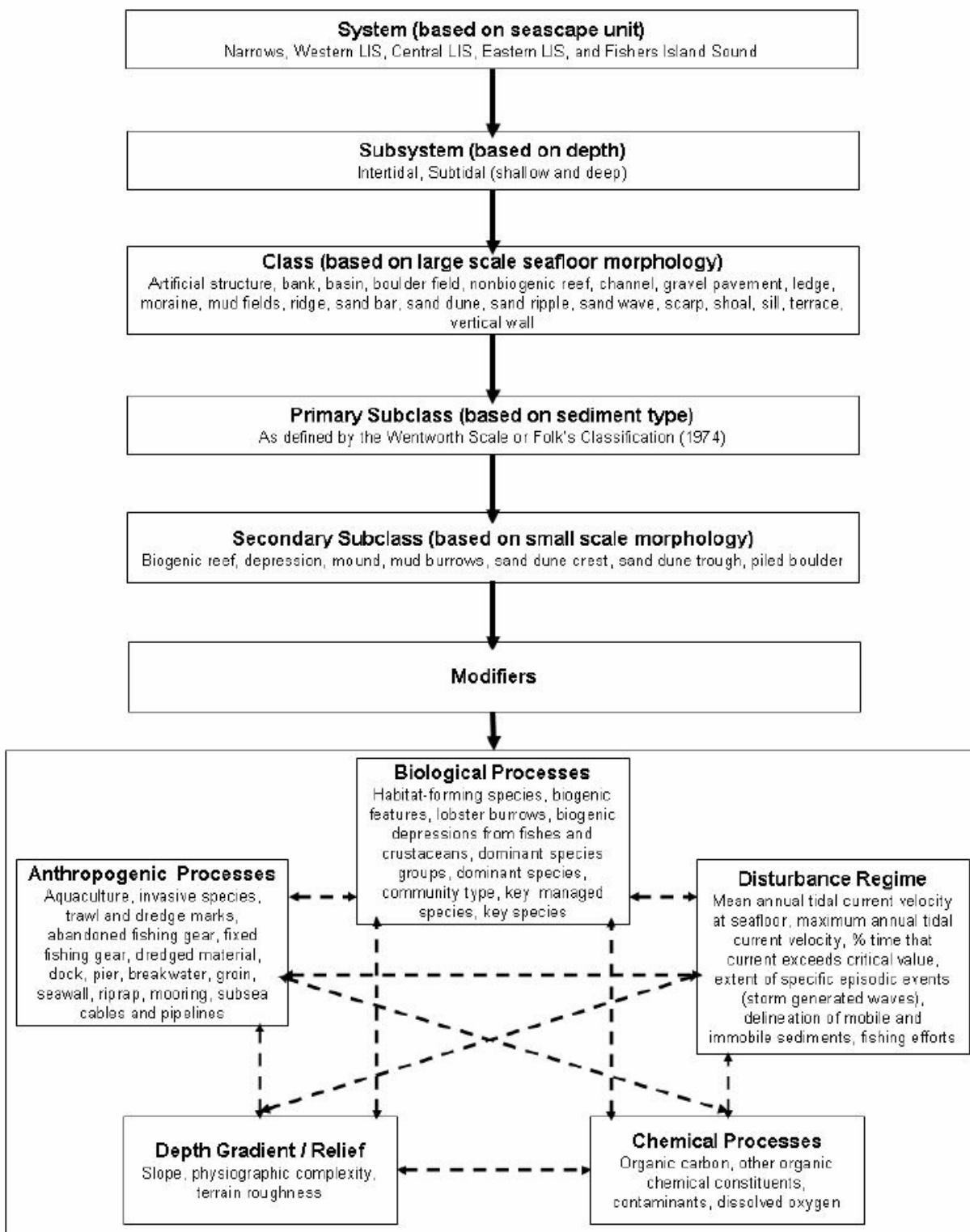


Figure 5.2-17. Habitat classification scheme developed by Auster et al. 2009 for Long Island Sound.

Table 5.2-4. Quartile ranges for environmental variables used as modifiers for within acoustic patch type habitat modeling and scores assigned to each quartile.

Layer	Range	Value
Bottom Stress (Pascal's)	0.002381 – 0.048761	1
	0.048761 – 0.059674	2
	0.059674 – 0.7468	3
	0.7468 – 0.118332	4
Slope (degrees)	0.000027 – 5.97319	1
	5.97319 – 6.0	2
	6.0 – 8.627929	3
	8.627929 – 84.619835	4
Bathymetry (meters)	-54.014286 - -32.498196	4
	-32.498196 - -22.47128	3
	-22.47128 - -11.817682	2
	-11.817682 - -0.95519	1
TRI (values stretched)	0 – 0.57646	1
	0.57646 – 1.056843	2
	1.056843 – 1.537226	3
	1.537226 – 24.499544	4
Silt-Clay (percent)	0 – 25	1
	25 - 50	2
	50 – 75	3
	75 – 100	4

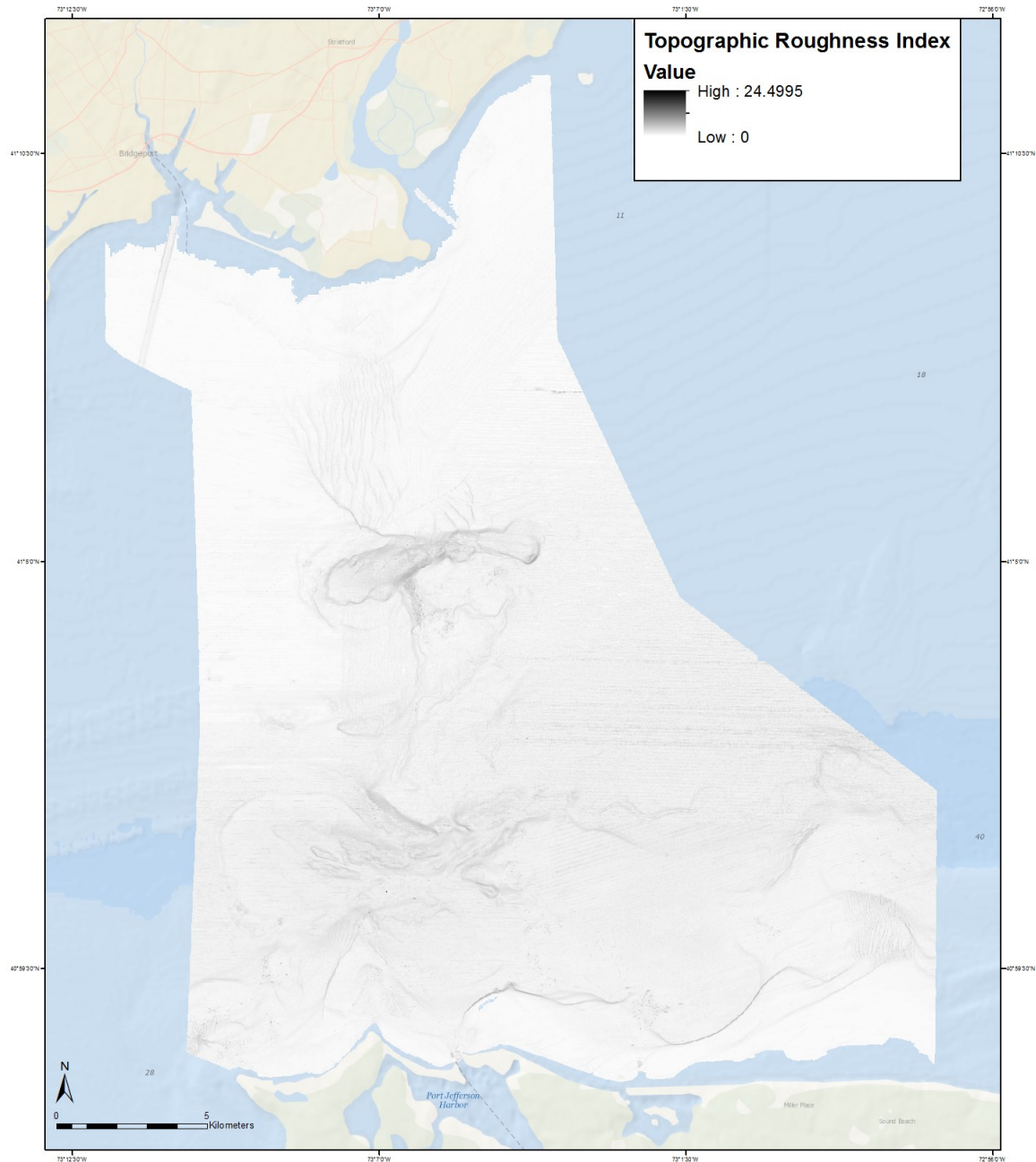


Figure 5.2-18: Terrain Ruggedness Index derived from the bathymetry image (Battista, 2013) using a quantitative measure of topographic heterogeneity introduced by Riley et al. (1999) and calculated in ArcMap using instructions outlined by Colley (2010).

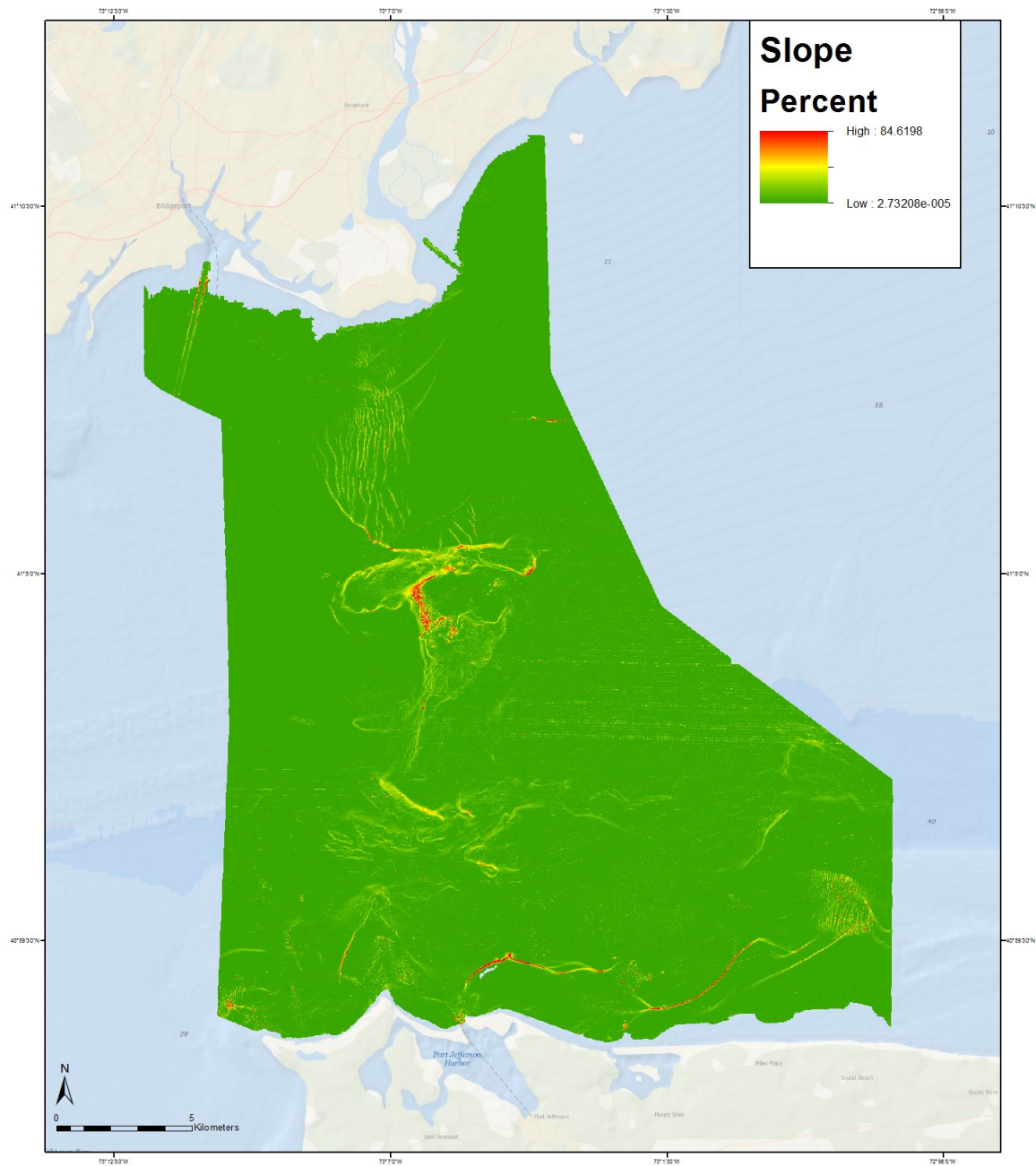


Figure 5.2-19. Slope layer of the study area generated from the bathymetry image in ArcMap.

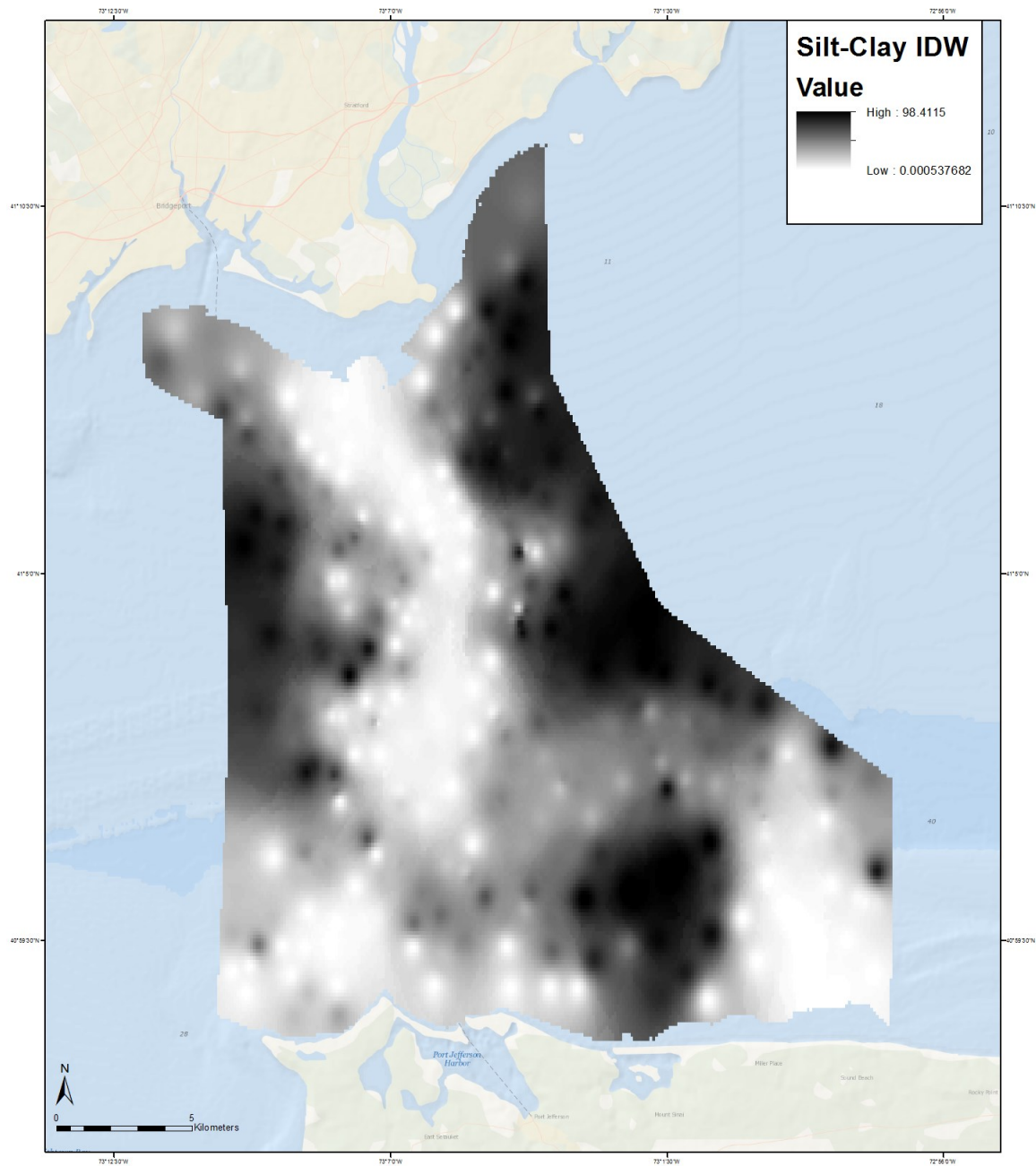


Figure 5.2-20: Inverse distance weighted (IDW) interpolation of the percent composition of silt and clay in cores taken during LISMaRC Collaborative cruises and Lamont-Doherty Earth Observatory of Columbia University Collaborative cruises.

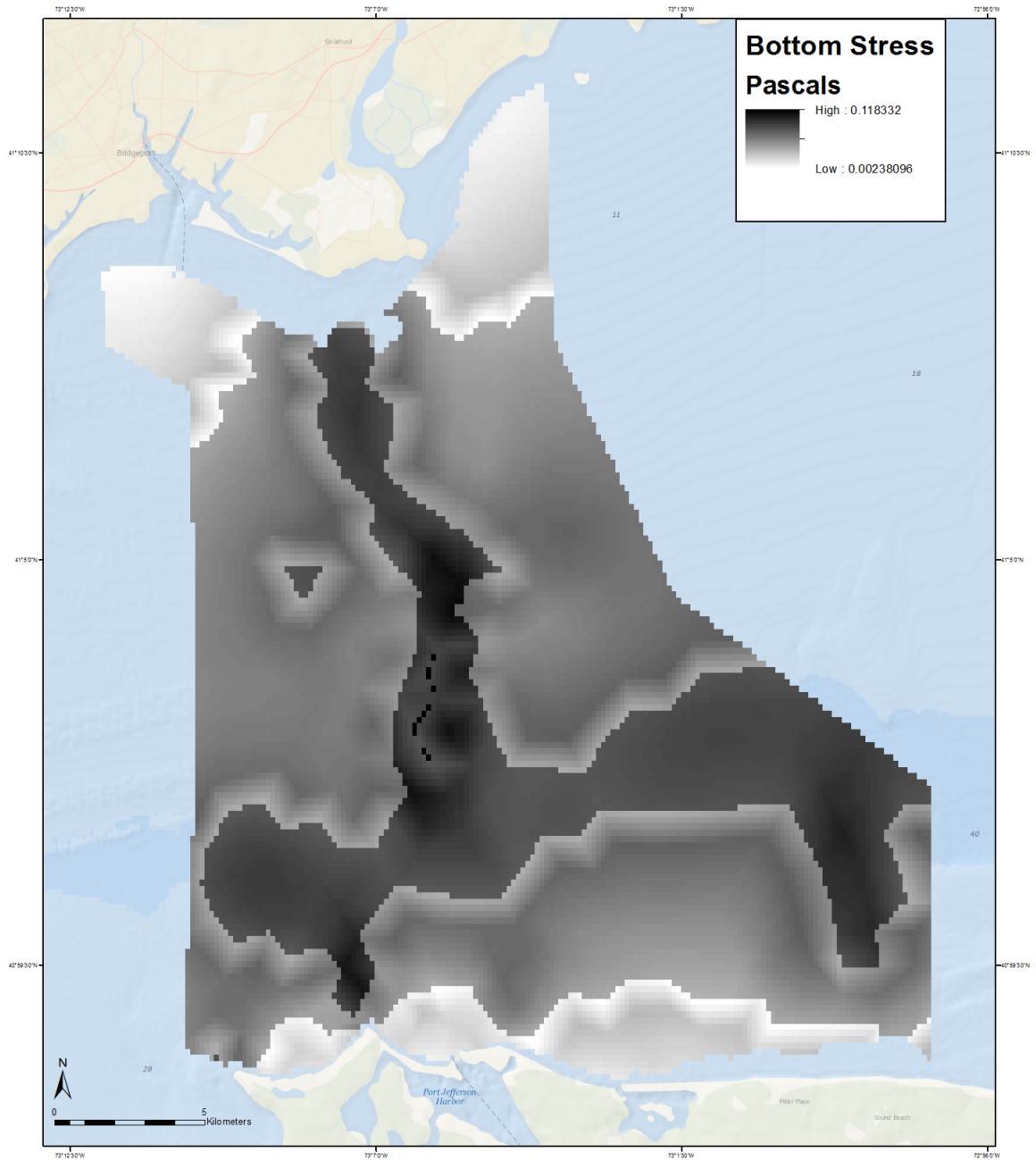


Figure 5.2-21: Bottom Stress of the study area. 1 Pascal is equal to 1 Newton of force over a square meter.

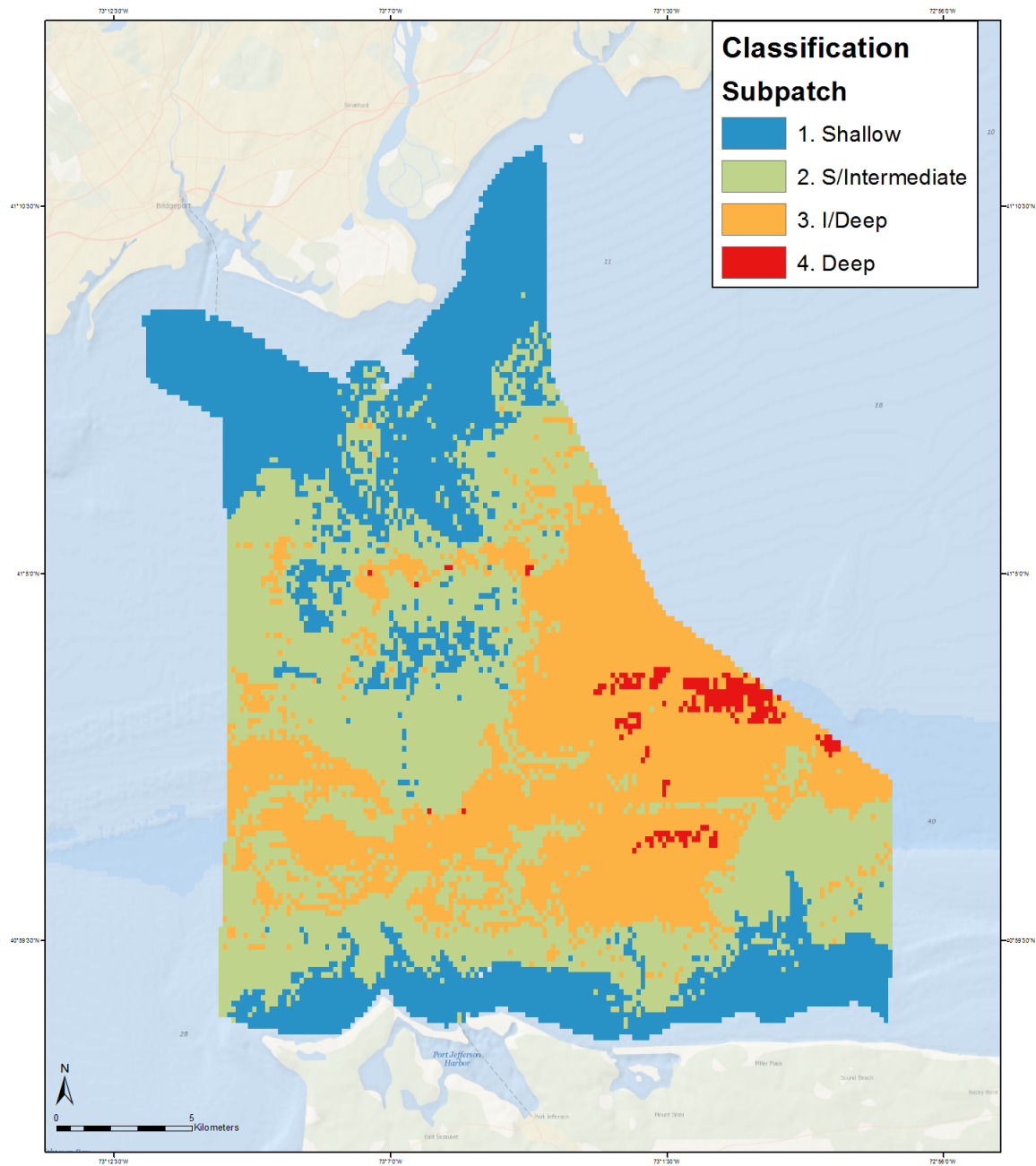


Figure 5.2-22: Overlay of pixel layers to represent the subpatches found throughout the study area based on the modifier of depth.

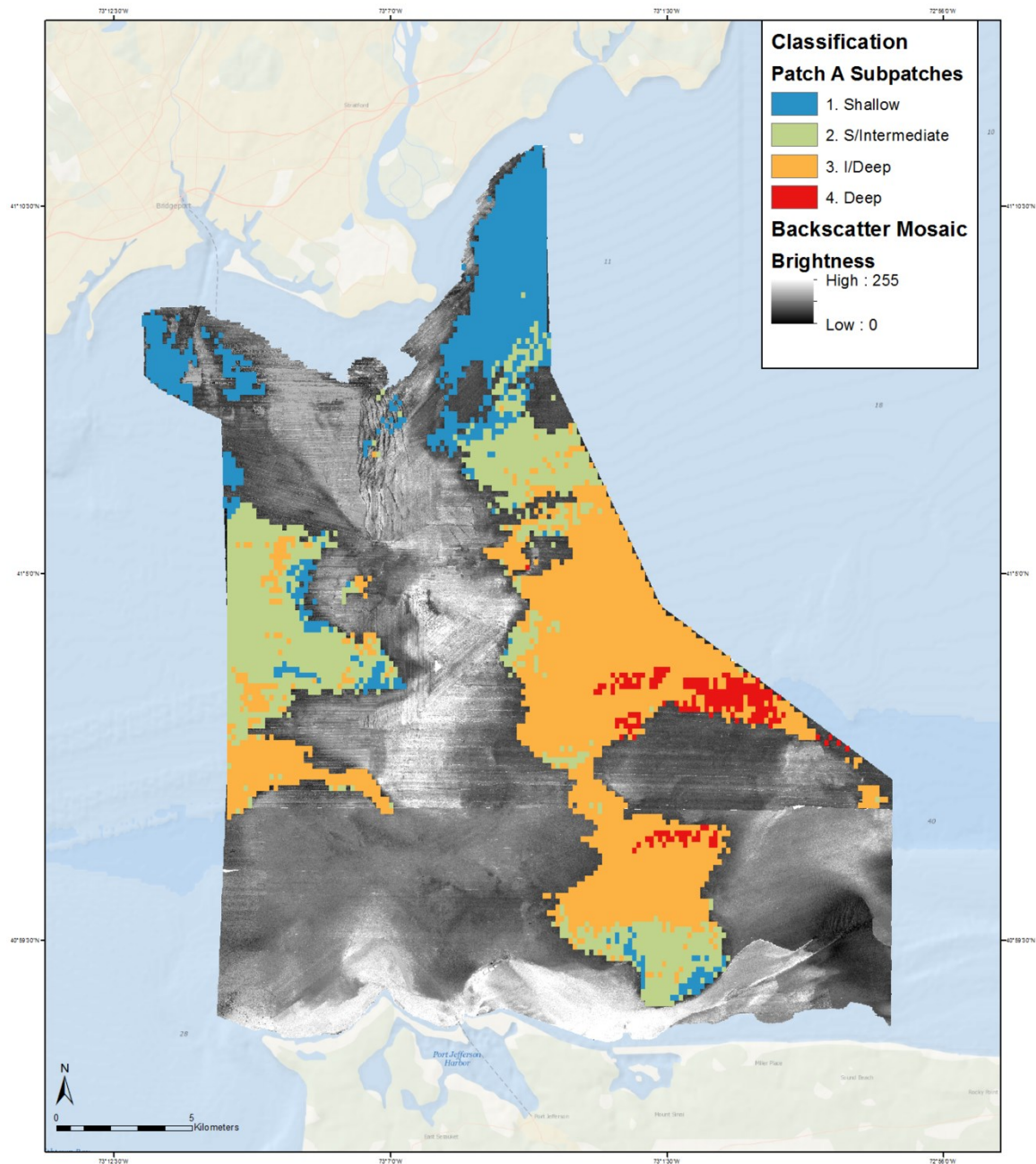


Figure. 5.2-23: Subpatch map of acoustic patch type A.

Table 5.2-5: Value range, mean and standard deviation for habitat modifiers form the analysis of subpatches for Acoustic patch type A.

Subpatch	Layer	Pixel Count	Mean	Standard Deviation	Standard Error	Minimum	Maximum	Range
1	Bathymetry	1071	-10.5061 m	4.501268	0.137544	-28.00	-4	24
	Silt-Clay	1088	57.5083 %	21.38898	0.648449	5	92	87

Subpatch	Layer	Pixel Count	Mean	Standard Deviation	Standard Error	Minimum	Maximum	Range
	Bottom Stress	1088	0.0161 P	0.0161		0	0.0884	
	TRI	1071	0.0924	0.35893	1.10E-02	0	6	6
	Slope	1066	0.1060°	0.575739	1.76E-02	0	11	11
2	Bathymetry	1490	-19.4302 m	4.44557	0.115169	-44	-6	38
	Silt-Clay	1494	64.6165 %	15.76709	0.407921	5	91	86
	Bottom Stress	1494	0.0531 P	0.0108		0	0.0882	
	TRI	1490	0.2691	0.467248	1.21E-02	0	3	3
	Slope	1490	0.0906°	0.431133	1.12E-02	0	8	8
3	Bathymetry	2461	-28.9655 m	5.822093	0.117361	-46	-6	40
	Silt-Clay	2487	67.8717 %	19.20083	0.385019	5	98	93
	Bottom Stress	2487	0.0617 P	0.008		0	0.088	
	TRI	2461	0.9041	0.601951	1.21E-02	0	4	4
	Slope	2461	0.3218°	0.676889	1.36E-02	0	9	9
4	Bathymetry	200	-35.7600 m	2.402344	0.169871	-46	-32	14
	Silt-Clay	200	64.4850 %	18.57755	1.313631	9	94	85
	Bottom Stress	200	0.0752 P	0.0058		0	0.0857	
	TRI	200	1.1650	0.599644	4.24E-02	0	5	5
	Slope	200	0.44°	0.7934405	0.05610471	0	7	7

Table 5.2-6: Subhabitat classifications of Patch A located in between Western and Central LIS. Modifiers are ranged from lowest to highest influence on the Subhabitat (Minimal – Low – Moderate – High).

	Modifiers			
Depth Subhabitat	Silt-Clay	Bottom Stress	TRI	Slope
1. Shallow	Moderate	Minimal	Minimal	Minimal
2. Shallow/Intermediate	Moderate	Low	Low	Minimal
3. Intermediate/Deep	Moderate - high	Low	Moderate	Minimal
4. Deep	Moderate	Moderate	High	Minimal

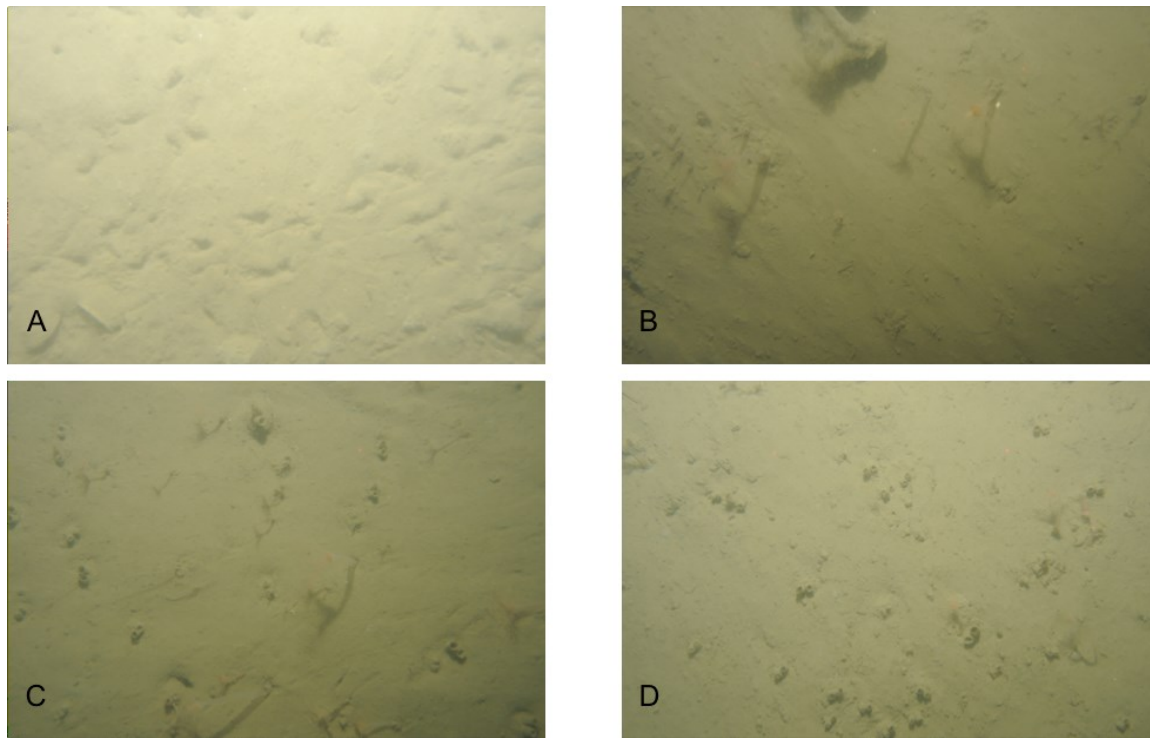


Figure 5.2-24: Photo of each subpatch classification from cruise photos. A. NB 2-5 B. SBM 15-1 C. NB 6-1 D. NB 7-1

5.2.9 Concluding Overview

The incorporation of sediment cores and percent composition of gravel, sand, silt, and clay is an important component to determine the sediment classes associated with the elements / patches comprising a seafloor landscape. These were used to provide an overall understanding of the composition of each acoustic patch and can be further used to define habitats with large scale patches at varying levels of detail. Using individual patches as the extent for interpolating the sediment surface helped to identify areas of interest. The overall evaluation of the Acoustic Patches and the sediment composition of cores and backscatter mosaic resulted in a re-evaluation of the classification of several patches. Assessing variation within the acoustic patches was important in this evaluation and found to be essential to interpret patch and core relationships. Patches that were identified as reflecting relationships with different sediment classifications were reclassified to further reflect the sediment distribution of the study area. Habitat patches include several components that contribute to the hierarchical classification of small- and large-scale habitats. This model represents only a few of the modifiers described in the habitat classification scheme proposed by Auster (2009) that can be incorporated into the classification of the pilot study area and other portions of LIS. Additional modifiers include anthropogenic processes (e.g. channels, trawl marks, debris), chemical processes (e.g. dissolved oxygen, organic carbon), and biological processes (e.g. habitat forming species, dominant species, burrows, depressions). The overlay of quartile maps (bathymetry, TRI, silt-clay, bottom stress,

and slope) produced a highly detailed model of the characteristics of the seafloor. The addition of factors will only improve the strength of the map and act as a common reference framework for management and conservation discussions and decision-making (Harris, 2012).

5.2.10 *References*

- Airamé, S.; Dugan, J.; Lafferty, D.; Leslie, H.; McArdle, A.; Warner, R. 2007. Applying Ecological Criteria to Marine Reserve Design: A Case Study from the California Channel Islands. *Ecological Applications*. Vol. 13, No. 1, Supplement: The Science of Marine Reserves, pp. S170-S184.
- Auster, P.J., Lindholm, J., Schaub, S., Funnell, G., Kaufman, L.S., Valentine, P.C. 2003. Use of sand wave habitats by silver hake. *Journal of Fish Biology*. Vol. 62, pp. 143-152.
- Auster, P.J., Heinonen, K.B., Witharana, C., McKee, M. 2009. A habitat classification scheme for the Long Island Sound region. Long Island Sound Study Technical Report. EPA Long Island Sound Office, Stamford, Connecticut 06904. p.83.
- Battista, T. 2013. LIS: NOAA_Acoustics. Marine Geoscience Data System. www.marine-geo.org
- Benn, A.R.; Weaver, P.P.; Billet, D.S.M.; van den Hove, S.; Murdock, A.P., et al. 2010. Human activities on the deep seafloor in the North East Atlantic: an assessment of spatial extent. *PloS ONE* 5(9): e12730
- Blackwood, D. and K. Parolski. 2001. Seabed observation and sampling system. *Sea Technology*. Vol. 4, pp.39–40.
- Brown, C.J.; Cooper, K.M.; Meadows, W.J.; Limpenny, D.S.; Rees, H.L. 2002. Small-scale mapping of sea-bed assemblages in the Eastern English Channel using sidescan sonar and remote sampling techniques. *Estuarine, Coastal and Shelf Science*. Vol. 54, pp 263-278.
- Brown, C.J. and Collier, J. 2007. Mapping benthic habitat in regions of gradational substrata: An automated approach utilizing geophysical, geological, and biological relationships. *Estuarine, Coastal, and Shelf Science*. Vol. 78, pp. 203- 214.
- Brown, C.J.; Todd, B.J.; Kostylev, V.E.; Pickrill, R.A. 2011. Image-based classification of multibeam sonar backscatter data for objective surficial sediment mapping of Georges Bank, Canada. *Continental Shelf Research*. Vol. 31, pp. s110-s119.
- Childs, C. 2004. Interpolating surfaces in ArcGIS Spatial Analyst. *ArcUser*. July- September, pp. 32-35.
- Cogan, C., Todd, B., Lawton, P., Noji, T. 2009. The role of marine habitat mapping in ecosystem-based management. *ICES Journal of Marine Science*, 66: 2033–2042.

- Collier, J. and Brown, C. 2005. Correlation of sidescan backscatter with grain size distribution of surficial seabed sediments. *Marine Geology*. Vol. 214, pp. 431–449
- Cooley, S.W. 2010. Terrain Roughness – 12 Ways. In www.GIS4Geomorphology.com. Retrieved November 1, 2013, from <http://gis4geomorphology.com/roughness-topographic-position/>
- Copeland, A.; Edinger, E.; Bell, T.; LeBlanc, P.; Wroblewski, J.; Devillers, R. 2011. Chapter 19. Geomorphic features and benthic habitats of a sub-arctic fjord: Gilbert Bay, Southern Labrador, Canada. *Seafloor Geomorphology as Benthic Habitat*. GeoHab atlas of seafloor geomorphic features and benthic habitats. Elsevier. London.
- Costa, B.M.; Tormey, S.; and Battista, T.A. 2012. Benthic habitats of Buck Island Reef National Monument. NOAA Technical Memorandum NOS NCCOS 142. Prepared by the NCCOS Center for Coastal Monitoring and Assessment biogeography Branch. Silver Spring, MD. 64 pp.
- Dartnell, P. and J.V. Gardner. 2004. Predicting seafloor facies from multibeam bathymetry and backscatter data. *Photogrammetric Engineering & Remote Sensing*. Vol. 70, No.9, pp. 1081-1091.
- Diaz, J.V. 2000. Analysis of Multibeam Sonar Data for the Characterization of Seafloor Habitats. The University of New Brunswick. 153 p.
- Drăguț, L.; Tiede, D.; Levick, S. 2010. ESP: a tool to estimate scale parameter for multiresolution image segmentation of remotely sensed data, *International Journal of Geographical Information Science*. Vol. 24:6, pp. 859-871
- ESRI. 2013. ArcGIS. WWW.esri.com/software/arcgis March 31, 2013
- Fake, T. 2013. Stratford mean bottom stress (Tides). UCONN LIS Mapping. http://lismapping2.dms.uconn.edu/layers/geonode:stratford_bstress_mean
- [FGDC] – Federal Geographic Data Committee. 2012. FGDC-STD-018-2012. Coastal and Marine Ecological Classification Standard. Reston, VA: Federal Geographic Data Committee.
- Folk, R.L. 1974. *The Petrology of Sedimentary Rocks*. Austin: Hemphill Publishing Co., 182p.
- Friedlander, A., Boehlert, G., Field, M., Mason, J., Gardner, J., Dartnell, P. 1999. Sidescan-sonar mapping of benthic trawl marks on the shelf and slope off Eureka, California. *Fishery Bulletin*. Vol 97. pp. 786-801

- Goff, J. A.; Olson, H. C.; Duncan C. S. 2000. Correlation of side-scan backscatter intensity with grain-size distribution of shelf sediments, New Jersey margin. *Geo-Marine Letters*. Vol. 20, pp. 43-49
- Greene HG, Yoklavich MM, Sullivan D, Cailliet GM. 1995. A geophysical approach to classifying marine benthic habitats: Monterey Bay as a model. Applications of side-scan sonar and laser-line systems in fisheries research. Alaska Fish and Game Special Publication No. 9, Juneau, p 15–30
- Greene, H. G., Yoklavich, M. M., Starr, R., O’Connell, V. M., Wakefield, W. W., Sullivan, D. L., MacRea, J. E., and Cailliet, G. M., 1999. A classification scheme for deep-water seafloor habitats. *Oceanologica Acta*. Vol. 22(6), pp. 663-78
- Greene, G., Bizzarro, J., Tilden, J., Lopez, H., Erdey, M. 2005. The benefits and pitfalls of geographic information systems in marine benthic habitat mapping. *Place Matters*. Chapter 3 pp. 33-56
- Harris, P.T. 2012. Chapter 4: Biogeography, benthic ecology, and habitat classification schemes. Seafloor geomorphology as benthic habitats. *GeoHab atlas of seafloor geomorphic features and benthic habitats*. Elsevier. London.
- Hewitt, J.E.; Thrush, S.F.; Legendre, P.; Funnell, G.A.; Ellis, J.; Morrison, M. 2004. Mapping of marine soft-sediment communities: integrated sampling for ecological interpretation. *Ecological Applications*. Vol. 14(4), pp. 1203-1216.
- Hintze, J. 2007. NCSS and GESS. NCSS, LLC. Kaysville, Utah. www.ncss.com.
- Kennish, M. 2001. Benthic communities of the Barnegat Bay – Little Egg Harbor estuary. *Journal of Coastal Research*. SI 32, pp. 167-177
- Kennish, M.; Haag, S.; Sakowicz, G.; Tidd, R. 2004. Side-scan sonar imaging of subtidal benthic habitats in the Mullica River – Great Bay Estuarine System. *Journal of Coastal Research*. Special issue No. 45. NERRS Research and monitoring: A Nationally Integrated Program. Pp. 227-240
- Knebel, K. and Poppe, L. 2000. Sea-Floor Environments within Long Island Sound: A Regional Overview. *Journal of Coastal Research*. Vol. 16, No. 3, pp. 533-550
- Kostylev, V., Todd, B., Frader, G., Courtney, R.C., Cameron, G., Pickrill, R. 2001. Benthic habitat mapping on the Scotian Shelf based on multibeam bathymetry, surficial geology and sea floor photographs. *Marine Ecology Progress Series*. Vol. 219: 121–137.
- Lang, S., and Tiede, D. 2003. [vLATE Extension für ArcGIS - vektorbasiertes Tool zur quantitativen Landschaftsstrukturanalyse](#), ESRI Anwenderkonferenz 2003 Innsbruck. CDROM

- Leibman, M. 2007. Benthic Habitat Characterization of the Stratford Shoal region of Long Island Sound. OSV bold survey report. U.S. Environmental Protection Agency New England, Oceans and Coastal Protection Unit, Boston, MA
- Lucieer, V.L. 2008. Object-oriented classification of sidescan sonar data for mapping benthic marine habitats. *International Journal of Remote Sensing*. Vol. 29, No. 3, pp. 905-921
- Lund, K and Wilbur, A.R. 2007. Habitat classification feasibility study for coastal and marine environments in Massachusetts. Massachusetts Office of Coastal Zone Management. Boston, MA. 31 pages + appendices
- Lundblad, E.R., Wright, D.J., Miller, J., Larkin, E.M., Rinehart, R., Naar, D.F., Donahue, B.T., Anderson, S.M., Battista, T. 2006. A benthic terrain classification scheme for American Samoa. *Marine Geodesy*. Vol. 29, pp. 89-111.
- [MPA] - Marine Protected Areas: Tools for Sustaining Ocean Ecosystems. 2001. Committee on the Evaluation, Design, and Monitoring of Marine reserves and Protected Areas in the United States, Ocean Studies Board, Commission on Geosciences, Environment, and Resources, National Research council. National Academy Press, Washington, D.C., U.S.
- McMullen, K.; Poppe, L.J.; Paskevich, V.; Doran, E.; Moser, M.; Chirstman, E., and Beaver, A. 2005. Surficial geological interpretation and sidescan sonar imagery of the sea floor in west-central Long Island Sound. U.S.G.S. Open-File report 2005- 1018.
- McMullen, K.Y.; Poppe, L.J.; Schattgen, P.T.; Doran, E.F. 2008. Enhanced sidescan-sonar imagery, north-central Long Island Sound. U.S. Geological Survey Open-File Report 2008-1174
- Nitsche, F. 2013. Sediment grain size data. Lamont-Doherty Earth Observatory of Columbia University.
- Nybakken, J., Bertness, M. 2004. *Marine biology: an ecological approach*, sixth edition. Pearson, San Francisco, California, U.S.
- O'Malley, J. 2007. U.S. Geological Survey ArcMap Sediment Classification Tool: Installation and User Guide. Open-File Report 2007-1186. U.S. Geological Survey, Reston, Virginia.

5.3 *Infaunal Ecological Characterization - LISMARC*

The main focus of this portion of the pilot project was to characterize the infaunal communities across the different sea floor environments found in the pilot study area, and more specifically to assess differences among the large-scale acoustic patch types identified through our analyses of the backscatter data (see Section 5.2) and also ecological variability with these patch types.

Infaunal communities comprise those organisms that live in seafloor sediments and/or just at the sediment water interface. The acoustic patch types can be viewed as large-scale (on the order of 10-100s of km²), general habitat types based on their sediment composition and associated physical dynamics and characteristics. These characteristics vary on a relative basis within each acoustic patch type, creating smaller scale habitats with specific sets of characteristics that may support different sets of ecological communities. Based on these efforts, information on ecologically significant locations in the pilot study area can be identified as well as how the infaunal community characteristics and habitat distributions might shape future impact assessments and management efforts.

5.3.1 *Field Data Acquisition*

Samples for ecological characterization were collected during two sampling periods, October 2012 and May 2013. The sampling design comprised a series of sampling blocks (SB) that were distributed across the pilot study area based on acoustic backscatter and bathymetric data that was available prior to the October 2012 sampling period. The spatial distribution and locations of the SBs were selected with the overall objective to sample as many of the different seafloor habitats that were evident in the side scan mosaic that had been previously developed for the study area (Figures 5.2-1, 5.2-3). These included both areas that were well within large-scale seafloor features (large-scale patches) and areas where there were transitions among large scale features. Initial identification of seafloor features was based on previous work conducted in the pilot study area (Zajac 1998, Zajac et al. 2000, Poppe et al. 2000, Kneble and Poppe, Liebman 2007, Zajac et al. 2013), visual interpretations of the available side scan mosaic and general information from the literature on seafloor mapping and ecological characterization using acoustic data for habitat identification characterization (e.g. Brown, 2012 Kostylev et al. 2001). This planning phase resulted in the selection of 34 SBs. Two of these, SB1 and SB2 were shallow water sites were not sampled either in October 2012 nor May 2013. In October 2012, all blocks were sampled except SB26. Several other SBs were not sampled completely for infaunal grab samples and/or epifaunal video transects during the research cruises due to weather conditions, poor bottom visibility, bottom hazards for the sampling equipment, and related lost ship time.

Within each SB, both infaunal grab and epifauna video / photographic samples were collected using the USGS SEABOSS system (Figure 5.2-5). Details on the capabilities and equipment deployed on this sampling device are given in Section 5.2. The sampling design included at least three randomly located grab samples (generated using ArcGIS) and three video transects in each SB. In several SBs, more than three grab samples were obtained in order to sample specific seafloor features or conditions present in an SB. Infaunal samples were collected with a 0.1 m² modified Van Veen grab. The SEABOSS was lowered to just above the sea floor and then was allowed to drift for several minutes to collect video and still images (used for the epifaunal analyses, see Section 5.5), after which a grab sample was collected. Video data was collected

along 300 m long transects that were equally spaced apart in the SB and oriented along any evident gradients of sea floor and bathymetric change that could be established from the side scan and bathymetry data used to develop the sampling design. Position along the transect and constant ship speed were maintained by the research vessel's (R/V Connecticut) dynamic positioning system.

5.3.2 Infaunal Sample Processing and General Analytical Approaches

In the field, the entire contents of the grab sample obtained at each sampling site was washed on a 500 µm using filtered seawater, after a small portion of surficial sediment, approximately 10 cm² by 2 cm deep, was removed for sediment analyses. The sieved sample was preserved with 70% ethanol and stained with Rose Bengal. In the lab, samples were sorted under a dissecting microscope and individuals were identified to the lowest possible taxon. A total of 101 samples and 60 samples were processed from the October 2012 and May 2013 research cruises, respectively.

After the data sets were assembled, several sets of statistical and GIS-based analyses were conducted to assess the characteristics of infaunal communities (total abundance, taxonomic/species richness [species richness and taxonomic richness are use interchangeably here and represent the number of taxa that were differentiated to the lowest possible taxonomic level], species diversity, community composition and related metrics) among and within the large-scale acoustic patches that were identified, and to map the spatial trends in community structure and biodiversity relative to sea floor habitat structure. Community composition and related metrics were analysed using multivariate analyses, including classification analysis (clustering), non-metric multidimensional scaling (MDS) and canonical analysis of principal coordinates (CAP). These analyses determine community similarities and trends among and within SBs and among large-scale acoustic patches. Species contributions to community similarities within acoustic patches and dissimilarities among patches were assessed using similarity percentage analysis (SIMPER). Statistical differences in community structure were assessed using an analysis of similarities (ANOSIM) procedure. All these procedures were carried out using PRIMER+ PERMOVA software (Clarke and Gorley 2006; Anderson et al. 2008). Calculation of several diversity indices were also carried out in PRIMER. Shannon diversity was calculated as:

$$H' = - \sum_{i=1}^S (p_i \times \log_{10} p_i)$$

where, S is the total number of species/taxa, p_i is the proportion of individuals belonging to the i th species. Higher values of H' indicate greater species diversity. Fisher's diversity index, α , was also calculated using the formula:

$$S = a \times \ln(1+N/a)$$

where S is number of taxa, N is number of individuals and a is the Fisher's alpha. Higher values of α indicate great species diversity. Fisher's alpha is considered to be a robust measure of taxonomic diversity as it is relatively insensitive to rare species, and as such was used in addition to the more commonly used H' . Using two diversity indices provides the opportunity to assess species diversity more fully, and potentially compare to other studies that use these two common indices. Differences in total abundance, taxonomic richness, and Shannon and Fisher's diversity were tested using nested analysis of variance (ANOVA) in the NCSS statistical software package (Hintze 2012). Differences were tested among the acoustic patches using both a one way ANOVA by grouping all samples in an acoustic patch irrespective of their SB location, and also using a nested ANOVA with replicate samples within sampling blocks as the nested factor. This analysis allowed for assessing the variation at small spatial scales, i.e. at the SB level, and taking that into account for the larger scale analysis among acoustic patches. The results of the statistical analyses were used to develop GIS data layers that depicted the spatial distribution of community types and biodiversity across the pilot study area. Details of analytical steps and conditions are provided below as needed.

5.3.3 *Infaunal Community Characterization and Mapping – October 2012*

5.3.3.1 General infaunal community characteristics

A total of 242 infaunal taxa were identified in the October 2012 samples. 95% of these were identified to the species level. There were significant differences among the acoustic patches (i.e. the large-scale sea floor environments identified for analysis if the acoustic imagery) for several overall community attributes including total abundance, taxonomic richness and taxonomic diversity. Two sets of analyses were conducted, one using the entire data set, and another with oligochaetes and archiannelids excluded. The latter set of analyses were done because these two groups of small annelid worms had extremely high abundances in only a few samples, and despite data transformations that would reduce their relative impact on the statistical analyses, their high abundances likely masked more general patterns of community structure across the pilot study area. The highest infaunal total abundances were found in acoustic patches E and F, (both with, ~425 to 550 individuals per 0.1 m², and without excluded taxa), although total abundance in these acoustic patches was highly variable (Figure 5.3-1). Total abundance was relatively similar among acoustic patches A, B, C and D, with mean of ~100 to 150 individuals per 0.1 m² sample. For both the full data set and without oligochaetes and archiannelids, there was no significant difference in total abundance among the acoustic patches, because of this high local variation (Table 5.3-1). The nested factor sampling block was highly significant, indicating strong differences among sampling blocks within acoustic patches. This suggests that total abundances at this time were sufficiently variable within acoustic patches to mask differences among patches. A one way ANOVA was conducted not including SBs as a nested factor to determine differences among acoustic patches, and in this case Total abundance differences among acoustic patches was statistically significant ($F_{5,95} = 5.35$, $p < 0.001$).

To visualize how total abundance varied spatially in more detail, total abundances were mapped at each sample site (Figure 5.3-2). This indicated the high variability within and among acoustic patches, and in some cases within a sampling block, reflecting the statistical test results given above. Although variable there were some distinct spatial patterns. Total abundance was generally low across all portions of acoustic patch type A, although there were some areas where relatively high abundances were found in this patch type. Very high abundances were found along the southern spine of Stratford Shoal in acoustic patch types E and F, with the highest abundances were found to be highly localized in certain areas. Acoustic patch type D also had spatially variable total abundance. Note that in some cases such as in the northwest corner of the study area and along some of the transition areas among acoustic patch types, that total abundance was extremely variable even on a local scale as represented by the markers (points) that are right next to each other representing the three samples that were taken within an SB.

Several measures were used to assess infaunal diversity, including taxonomic (species) richness (i.e. the number of distinct taxa found) and several measures of biotic diversity (which take into account both the variety of taxa /species, i.e. richness, and the relative abundances among the species, i.e. evenness). Taxonomic richness varied considerably among the acoustic patches. The lowest mean richness was in acoustic patches A and B, ~15 to 20 taxa 0.1 m^{-2} , and the highest in E and F, ~30–40 taxa 0.1 m^{-2} ; richness was intermediate acoustic patches C and D, ~25 taxa 0.1 m^{-2} (Figure 5.3-3). These differences in taxonomic richness were significant both at the scale of sampling blocks and also among the acoustic patches (Table 5.3-1), indicating variable richness patterns across several spatial scales. This pattern is clearly evident when taxonomic richness at each sampling site is mapped across the pilot study area (Figure 5.3-4). Moderate to high species richness is found along the transitional areas from acoustic patch type A and B onto the coarser sediments associated with Stratford Shoal and acoustic patches D, E and F.

Shannon diversity calculated using the full data was highest in acoustic patch C with somewhat lower values in the other acoustic patches, and the lowest in acoustic patch A (Figure 5.3-5). When oligochaetes and archiannelids were excluded, Shannon diversity was similar in acoustic patches C, D, E, and F, and lower in A and B than in the other patches. This reflects the large effect a few very abundant taxa can have on evenness and as such the overall diversity measure. These differences were statistically significant (Table 5.3-1). Spatial variation for Shannon diversity was not as great as for species richness, with many locations in acoustic patches D, E and F having similar levels of Shannon diversity, 1.01 to 1.25 (Figure 5.3-6). Locations with the highest Shannon diversity were distributed across the pilot study area. However, the southwest section of the study area had a relatively high number of high diversity sites.

Fishers's diversity is measured using a different scale, but indicated an overall similar pattern to Shannon diversity in terms of lower mean diversity in acoustic patches A and B relative to the other acoustic patches (Figure 5.3-7). When oligochaetes and archiannelids were excluded, the differences among acoustic patches C and D and E and F were somewhat accentuated, with

slightly higher mean Fisher's diversity in patches E and F. Interestingly, there were no statistically significant differences in Fisher's diversity at the local, SB level, but differences among acoustic patches were significant (Table 5.3-1). Fisher's alpha is less sensitive to rare species than Shannon diversity and as such may provide a more robust assessment of local versus larger spatial scale diversity across the study area. The spatial patterns of Fisher's diversity reveal patterns similar to that for species richness and Shannon diversity, such as higher diversity in the southwest section of the study area, less variable diversity patterns in acoustic patch A and generally lower diversity in the northern portion of the study area (Figure 5.3-8).

The acoustic patches are characterized by specific combinations and amounts of different sediment classes (See section 5.2), and sediment characteristics are critical habitat factors for infauna with species often being found in specific ranges of sediment sizes (e.g. sands vs. muds on a general basis). Mean total abundance of infauna (with oligochaetes and archiannelids excluded) was similar across sediment-classes of the point locations where samples were taken, except for one sandy silt sample (Figure 5.3-9). Mean species richness, Shannon diversity and Fisher's diversity increased as sediment-size increased with low values in silty-clay, clayey-silt and sand-silt-clay, and higher values in silty-sand, sand, gravelly-sediment and gravel. The trends also suggest a steady increase in diversity as grain size increases across the broad sediment classes used here. This trend has been previously reported when comparing benthic species richness across the whole of LIS (Zajac 1998), and agrees with previous studies and hypotheses that indicate increasing diversity with increasing sediment grain-size / variability (e.g. Whitlatch 1981, Etter and Grassle 1992, Gray 2002, Thrush et al. 2003). The interesting aspect here is that this trend is occurring over the small and meso-scale spatial patterns of sediment variation within and among the large-scale acoustic patch types.

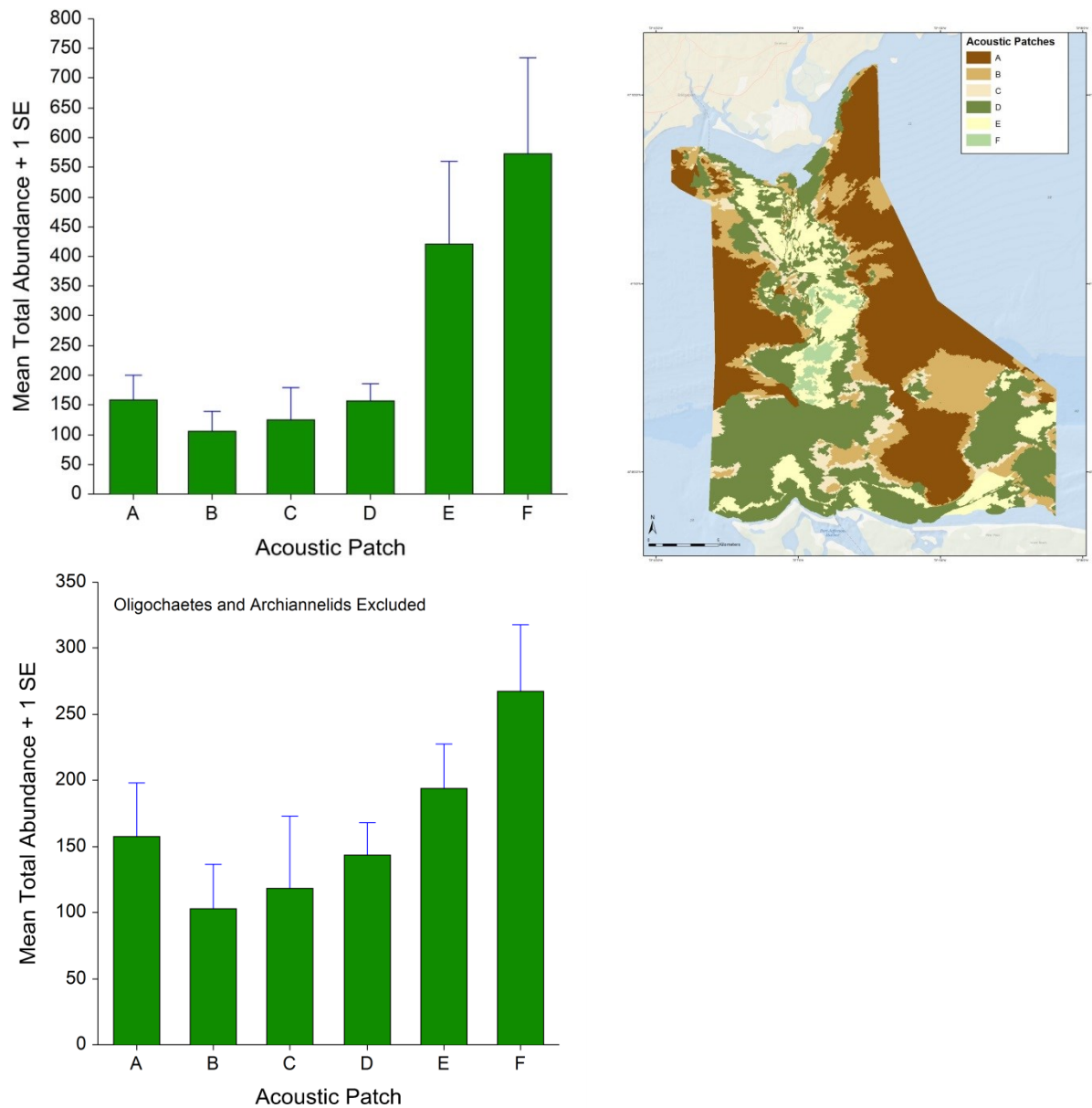


Figure 5.3-1. Mean total infaunal abundance (+1 standard error) 0.1 m⁻² in acoustic patch types in the LIS Mapping and Ecological Characterization pilot study area. Means are shown for all data (top) and with oligochaetes and archiannelids excluded (as noted). Map of pilot study areas depicts the acoustic patches.

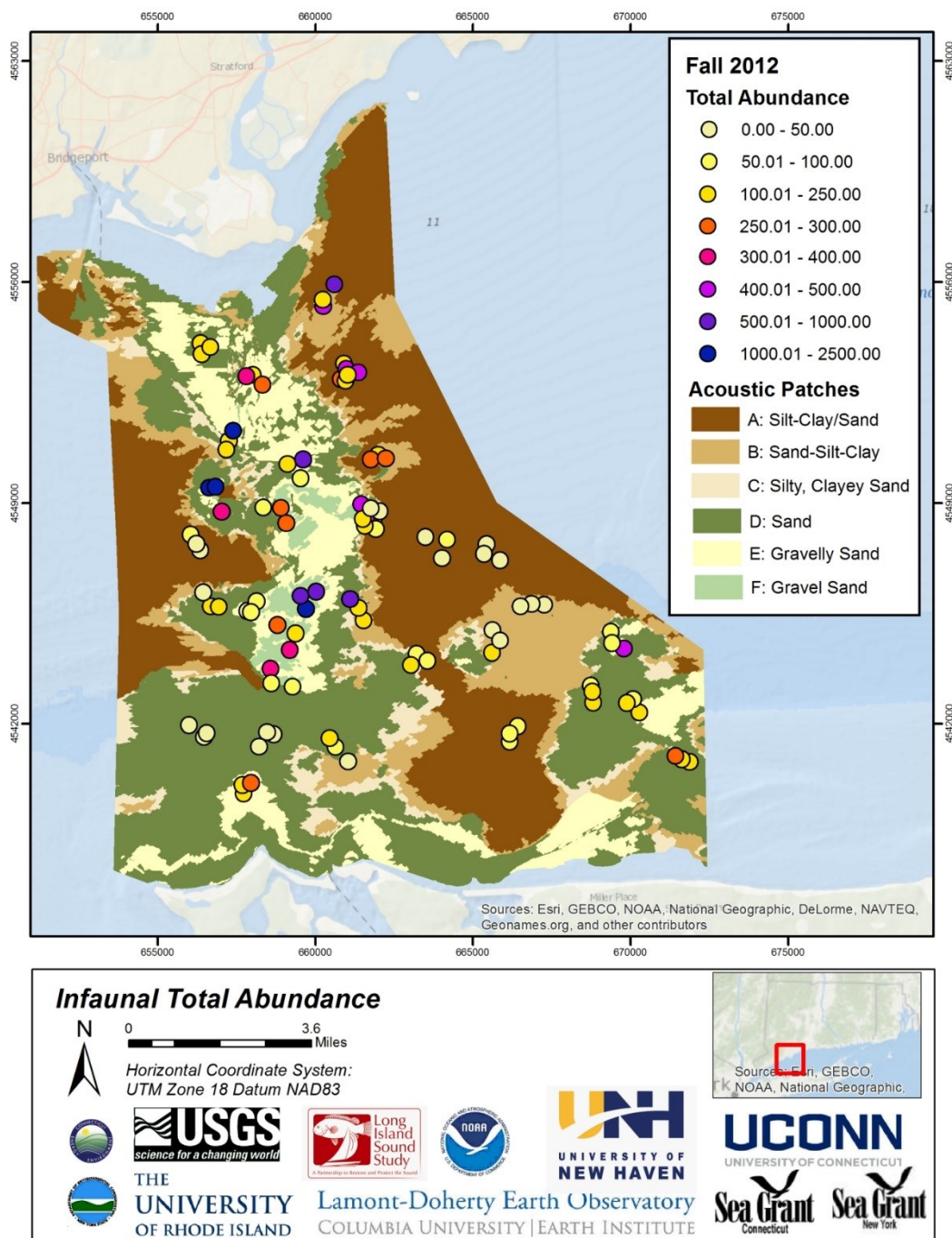


Figure 5.3-2. Spatial distribution of infaunal total abundances (per 0.1 m²) across the Stratford Shoal pilot study area (full data set).

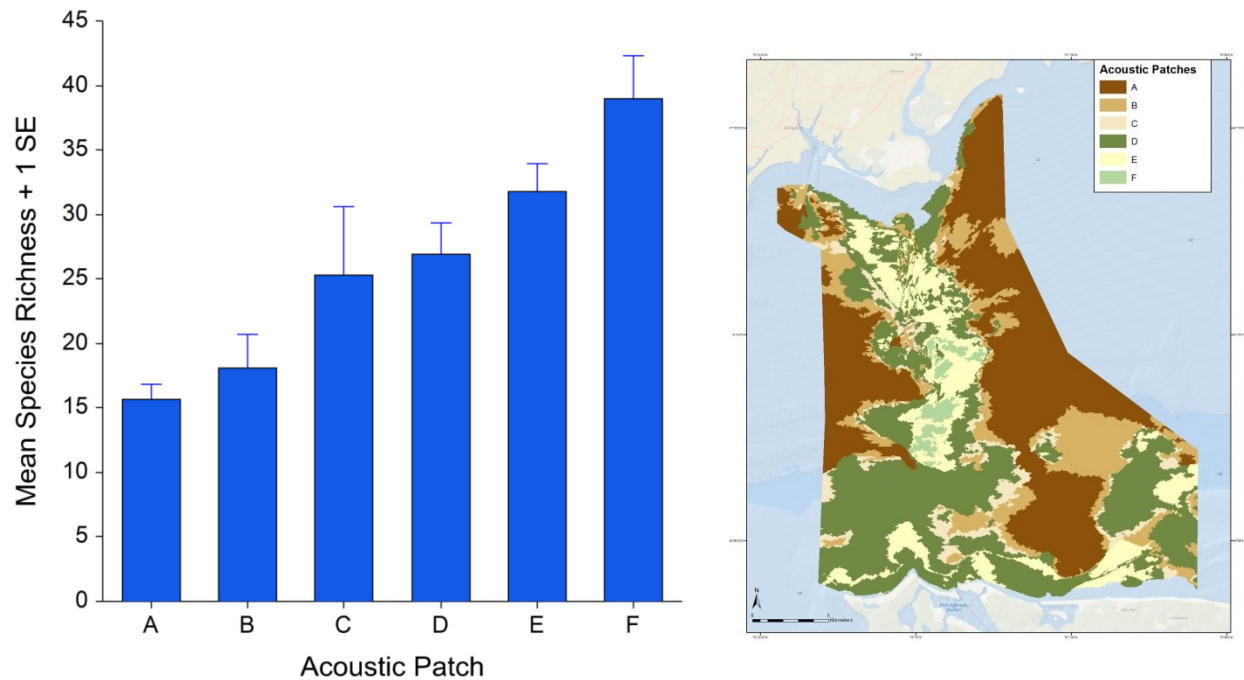


Figure 5.3-3. Mean infaunal species/taxonomic richness (+1 standard error) 0.1 m⁻² in acoustic patch types in the LIS Mapping and Ecological Characterization pilot study area. Means are shown for all data. No plot is given for oligochaetes and archiannelids excluded as the plot would show a slightly lower mean for certain acoustic patches. Map of pilot study areas depicts the acoustic patches.

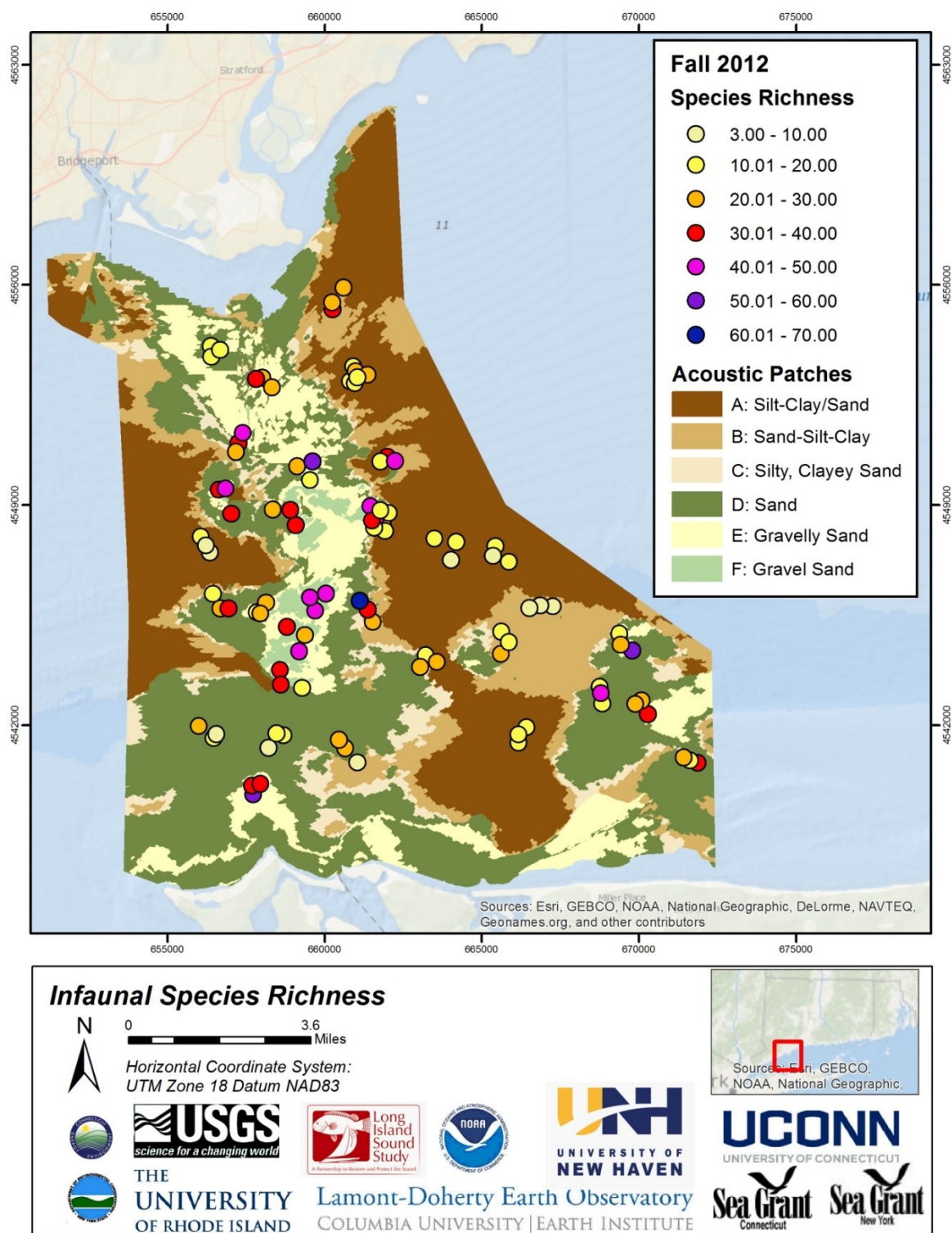


Figure 5.3-4. Spatial distribution of infaunal species/ taxonomic richness (per 0.1 m²) across the Stratford Shoal pilot study area using the full data set.

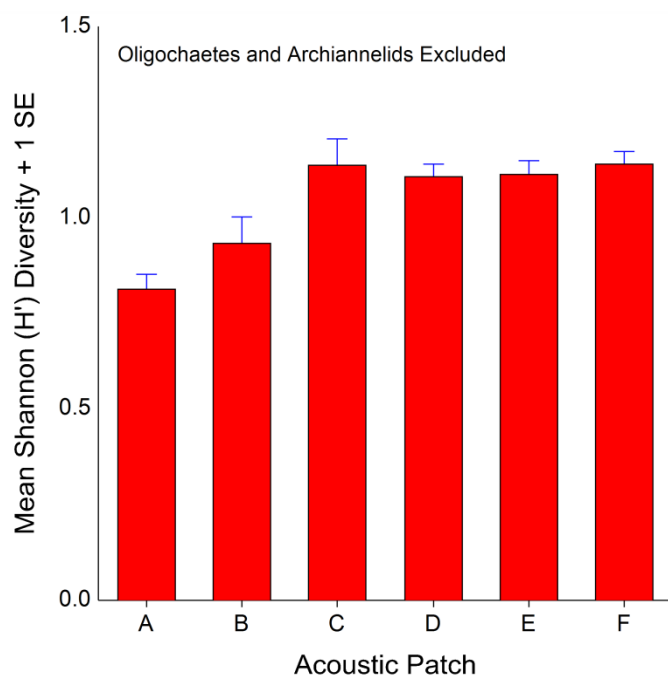
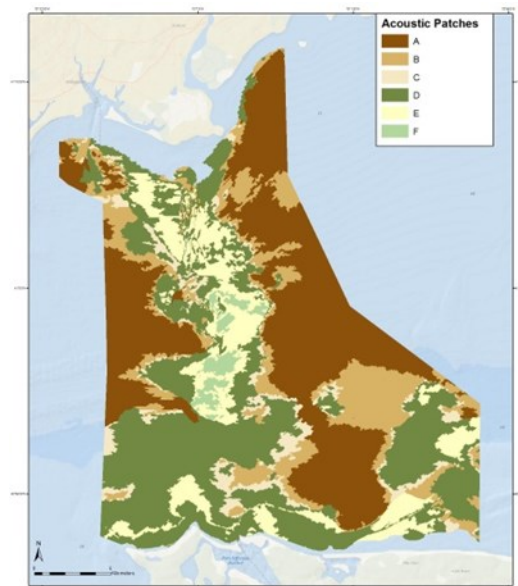
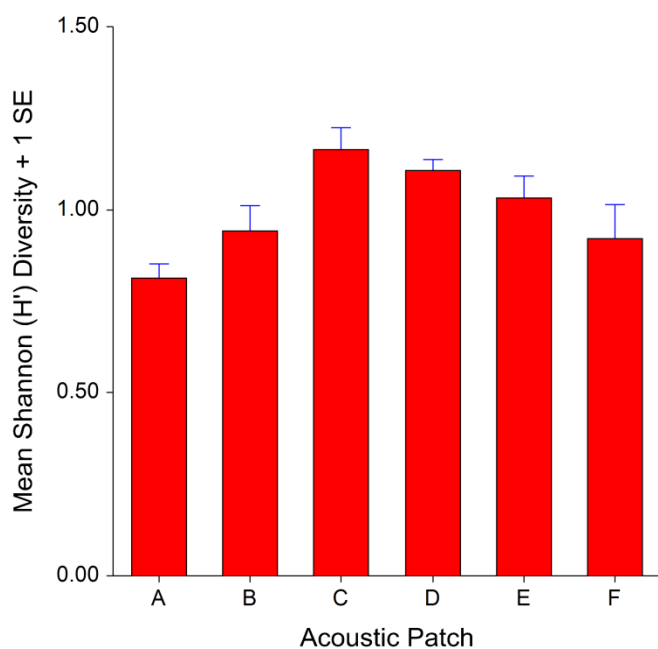


Figure 5.3-5. Mean infaunal Shannon (H') diversity (+1 standard error) in acoustic patch types in the LIS Mapping and Ecological Characterization pilot study area. Means are shown for all data (top) and with oligochaetes and archiannelids excluded (as noted). Map of pilot study areas depicts the acoustic patches.

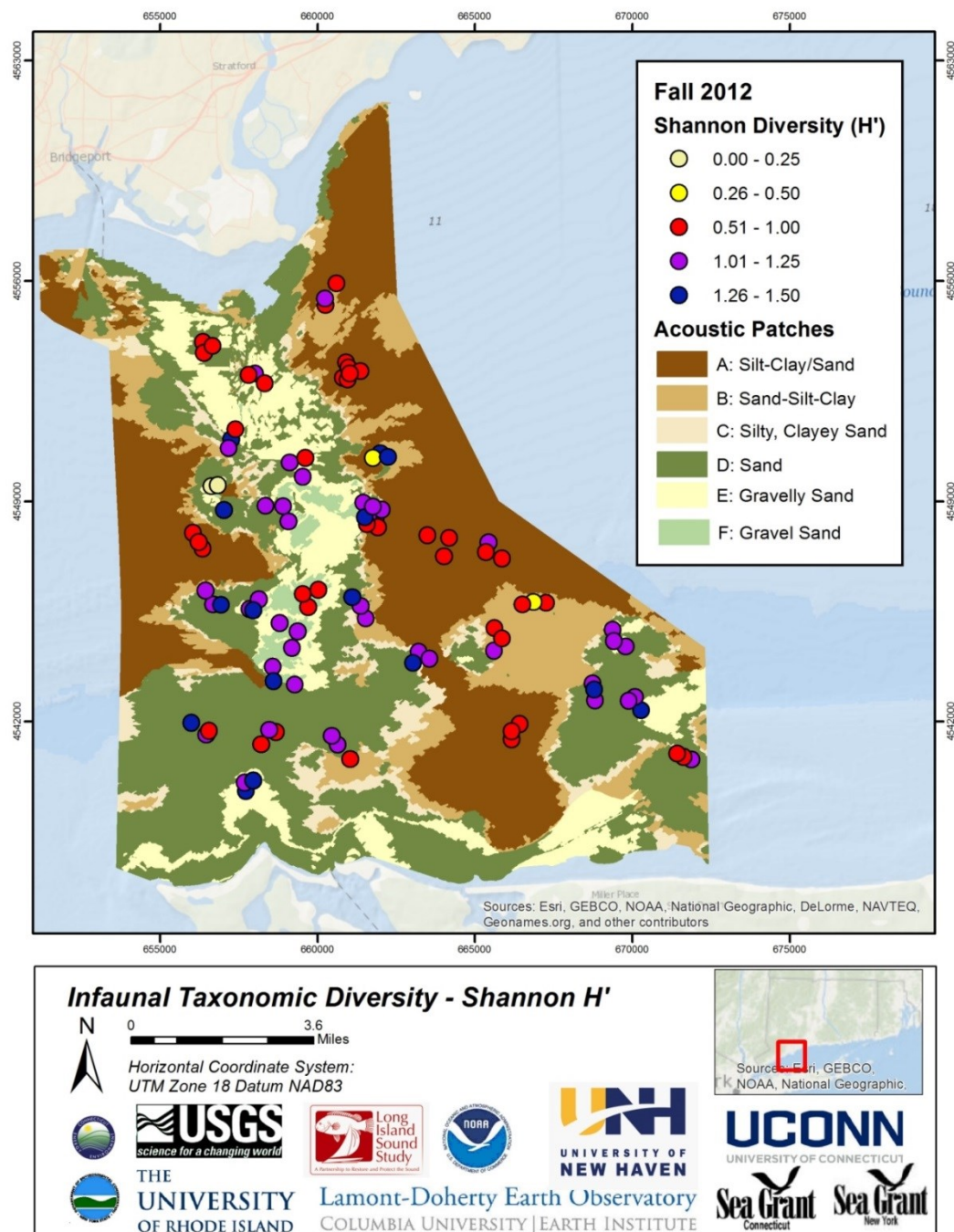


Figure 5.3-6. Spatial distribution of Shannon diversity for infaunal taxa across the Stratford Shoal pilot study area using the full data set. This metric measures diversity by incorporating the number of taxa and their relative abundance. Increasing values indicate higher diversity.

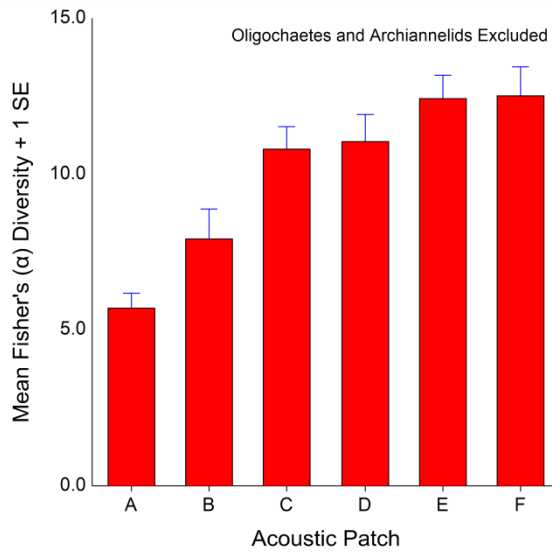
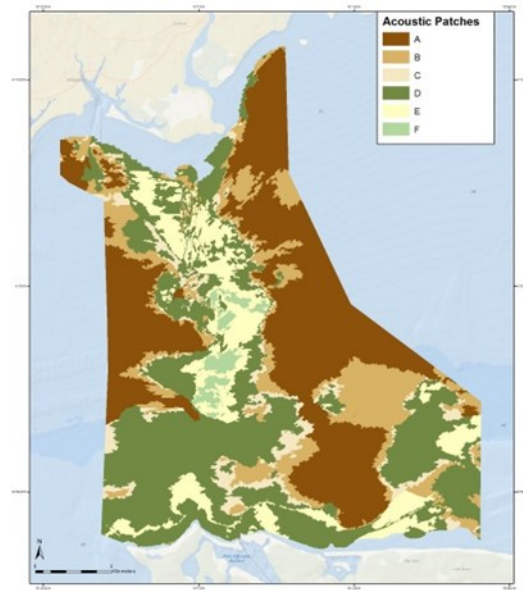
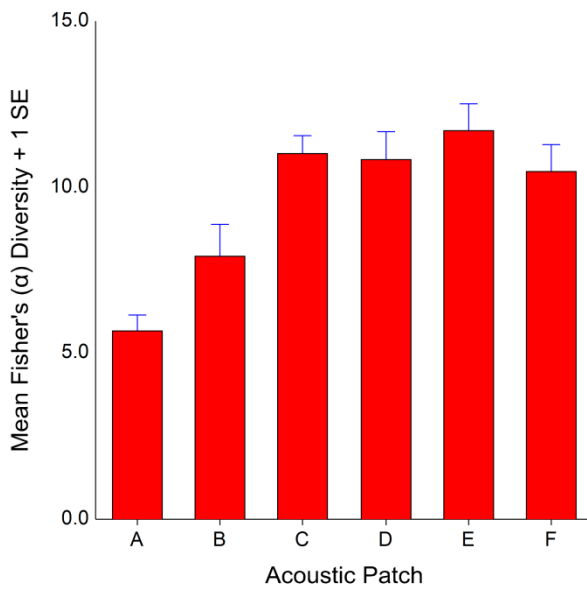


Figure 5.3-7. Mean infaunal Fisher's (α) diversity (+1 standard error) in acoustic patch types in the LIS Mapping and Ecological Characterization pilot study area. Means are shown for all data (top) and with oligochaetes and archiannelids excluded (as noted). Map of pilot study areas depicts the acoustic patches.

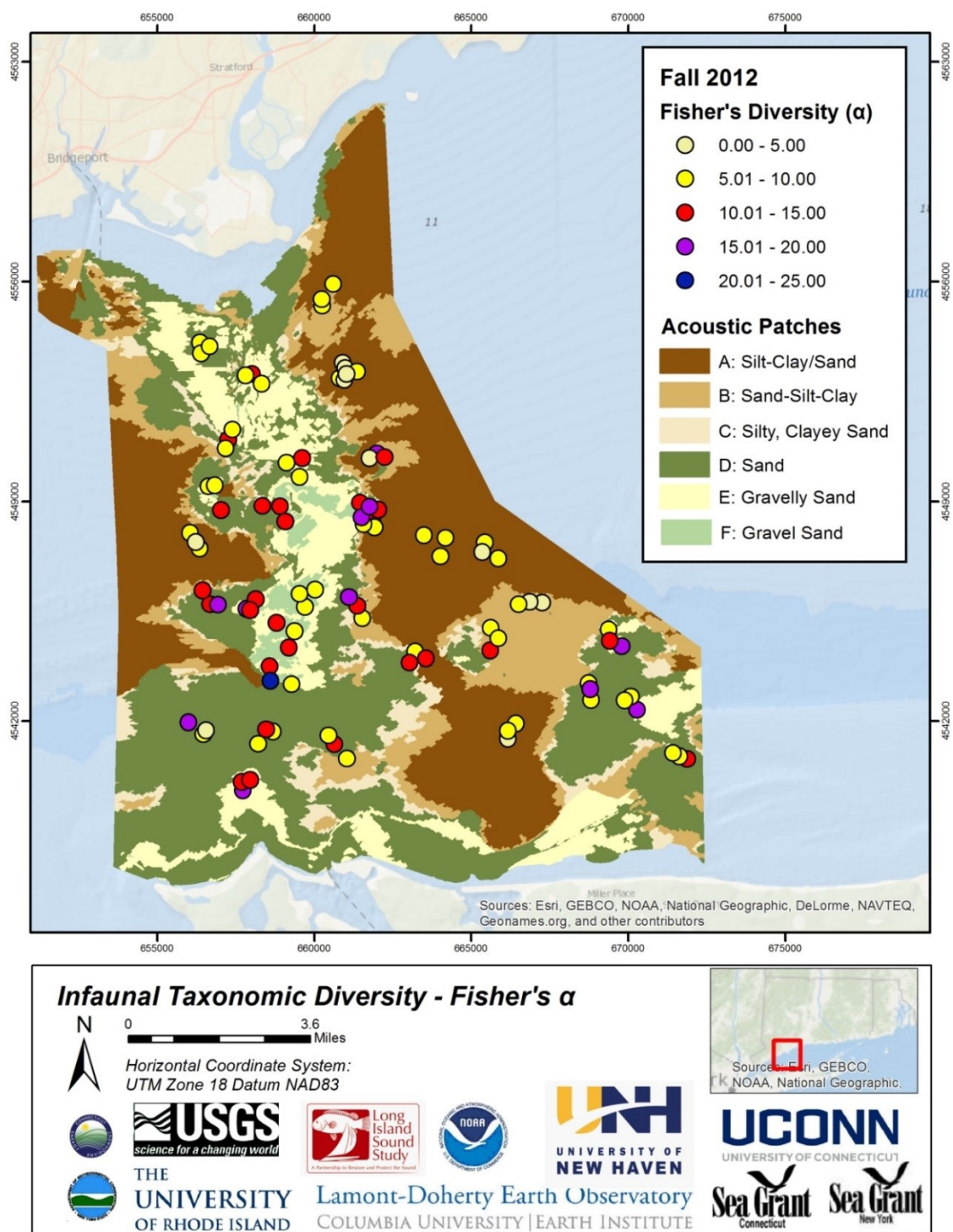


Figure 5.3-8. Spatial distribution of Fisher's diversity for infaunal taxa across the Stratford Shoal pilot study area using the full data set. Fisher's α predicts the number of species at different levels of abundance and higher values indicate higher diversity.

Table 5.3.1. Results of statistical analyses of community attributes among acoustic patch types. Differences in total abundance, species richness and two measures ecological diversity, the Shannon diversity index H' and the Fisher diversity index α , were tested using nested analysis of variance with sampling blocks nested within acoustic patches. This was done in order to assess statistical difference in these community attributes both at the smaller spatial scale of the sampling blocks and the larger-scale scale of the acoustic patches. Two sets of analyses were performed; one set with all taxa, and another set with the oligochaetes and archiannelids removed due to their very high abundances in a small number of samples, which could potentially mask community patterns in the overall data set. If significant differences were found among acoustic patch a Tukey-Kramer multiple-comparison test was used to assess statistical difference among specific acoustic patches. Total abundance and species richness were log transformed to meet ANOVA assumptions. * Term significant at $\alpha = 0.05$

Total Abundance

All data

Term	DF	Sum of Squares	Mean Square	F-Ratio	Prob Level	Power (Alpha=0.05)
Acoustic Patch	5	4.921146	0.9842293	1.95	0.121179	0.557513
Nested: Sampling Block	25	12.60392	0.5041569	5.18	0.000000*	
S	70	6.81493	0.09735615			
Total (Adjusted)	100	24.34				
Total	101					

Oligochaetes and archiannelids excluded

Term	DF	Sum of Squares	Mean Square	F-Ratio	Prob Level	Power (Alpha=0.05)
Acoustic Patch	5	2.420962	0.4841924	1.17	0.353174	0.343160
Nested: Sampling Block	25	10.37854	0.4151415	5.27	0.000000*	
S	70	5.517893	0.07882704			
Total (Adjusted)	100	18.31739				
Total	101					

Species Richness

All data

Term	DF	Sum of Squares	Mean Square	F-Ratio	Prob Level	Power (Alpha=0.05)
Acoustic Patch	5	1.780485	0.356097	5.15	0.002219*	0.958554
Nested: Sampling Block	25	1.730251	0.06921003	2.59	0.000940*	
S	70	1.867136	0.02667337			
Total (Adjusted)	100	5.377872				
Total	101					

Multiple-Comparison Test

Group	Count	Mean	Different From Groups
A	23	1.192419	E, F
B	14	1.211569	E, F
C	3	1.399918	
D	31	1.396559	
E	23	1.493088	A, B
F	7	1.59069	A, B

Oligochaetes and archiannelids excluded

Term	DF	Sum of Squares	Mean Square	F-Ratio	Prob Level	Power (Alpha=0.05)
-------------	-----------	-----------------------	--------------------	----------------	-------------------	---------------------------

Acoustic Patch	5	1.714445	0.3428889	4.70	0.003679*	0.938975
Nested: Sampling Block	25	1.82505	0.07300198	2.78	0.000425*	
S	70	1.840286	0.0262898			
Total (Adjusted)	100	5.37978				
Total	101					

Multiple-Comparison Test			Different From
Group	Count	Mean	Groups
A	23	1.190052	E, F
B	14	1.198387	E
C	3	1.381213	
D	31	1.386521	
E	23	1.480702	A, B
F	7	1.578986	A

Shannon Diversity

All Data						
Term	DF	Sum of Squares	Mean Square	F-Ratio	Prob Level	Power (Alpha=0.05)
Acoustic Patch	5	1.319203	0.2638406	3.16	0.023870*	0.797006
Nested: Sampling Block	25	2.08443	0.08337721	2.24	0.004386*	
S	70	2.603919	0.03719883			
Total (Adjusted)	100	6.007552				
Total	101					

Multiple-Comparison Test			Different From
Group	Count	Mean	Groups
A	23	0.814202	D
B	14	0.9432946	
C	3	1.16298	
D	31	1.105864	A
E	23	1.030938	
F	7	0.9207749	

Oligochaetes and archiannelids excluded

Term	DF	Sum of Squares	Mean Square	F-Ratio	Prob Level	Power (Alpha=0.05)
A: Acoustic_Patch	5	1.676996	0.3353991	6.69	0.000442*	0.990062
B(A): Sampling_Block	25	1.253744	0.05014977	1.75	0.034742*	
S	70	2.001797	0.0285971			
Total (Adjusted)	100	4.932537				
Total	101					

Multiple-Comparison Test			Different From
Group	Count	Mean	Groups
A	23	0.8132108	D, E, F
B	14	0.9319767	
C	3	1.137032	
D	31	1.10749	A
E	23	1.11404	A
F	7	1.141478	A

Fishers Diversity

All data	Sum of	Mean	Prob	Power
----------	--------	------	------	-------

Term	DF	Squares	Square	F-Ratio	Level	(Alpha=0.05)
Acoustic Patch	5	549.8969	109.9794	7.38	0.000228*	0.994972
Nested: Sampling Block	25	372.5784	14.90313	1.13	0.335228	
S	70	922.8755	13.18394			
Total (Adjusted)	100	1845.351				
Total	101					

Multiple-Comparison Test			Different from
Group	Count	Mean	Groups
A	23	5.68464	D, E
B	14	7.914653	
C	3	11.00083	
D	31	10.83018	A
E	23	11.70824	A
F	7	10.46893	

Oligochaetes and archiannelids excluded

Term	DF	Sum of Squares	Mean Square	F-Ratio	Prob Level	Power (Alpha=0.05)
Acoustic Patch	5	695.4396	139.0879	10.12	0.000022*	0.999722
Nested: Sampling Block	25	343.462	13.73848	0.97	0.516567	
S	70	992.1244	14.17321			
Total (Adjusted)	100	2031.026				
Total	101					

Multiple-Comparison Test			Different From
Group	Count	Mean	Groups
A	23	5.703842	D, E, F
B	14	7.911818	E
C	3	10.79307	
D	31	11.02574	A
E	23	12.42584	A, B
F	7	12.51246	A

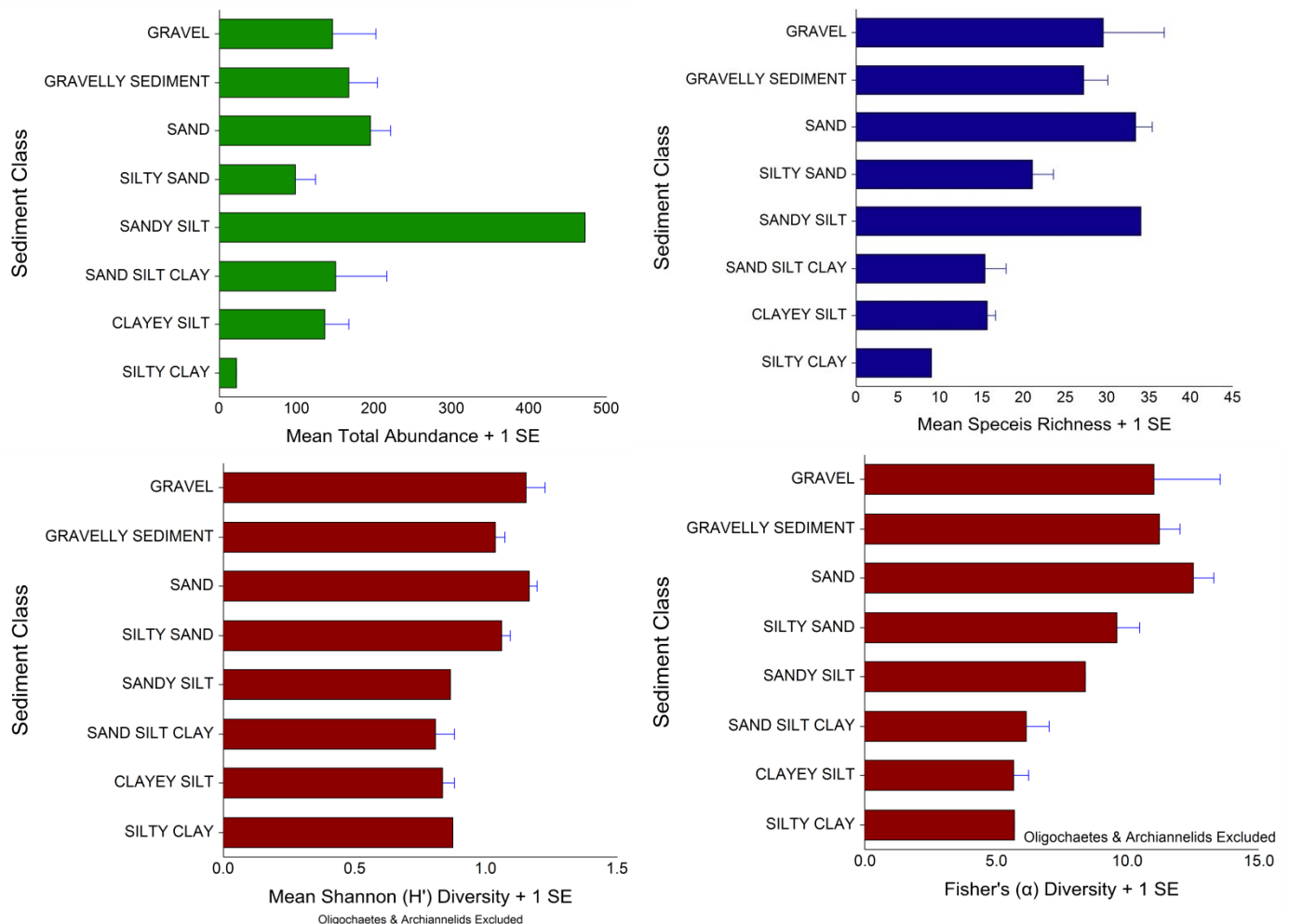


Figure 5.3-9. Mean total abundance, species richness, Shannon diversity and Fisher's diversity in sediment classes found in the acoustic patches (using the full data set). See Section 5.2 for which sediment classes are found in which acoustic patches. Values are per 0.1 m².

5.3.3.2 Infaunal Community Structure Differences among Acoustic Patch Types October 2012

A series of analyses were conducted to assess community structure (i.e. taxonomic composition and relative abundances of taxa found) across the pilot study area and how infaunal communities vary within and among the acoustic patches designated, and other habitat features in the pilot study area. Based on the results of classification analysis and MDS ordination, communities found at each sample site generally sorted out by acoustic patch, although communities in certain acoustic patch types were more variable than in others (Figure 5.3-10, Table 5.3-2). Infaunal communities in acoustic patches A and B were generally clustered together, as were communities in acoustic patches E and F. Communities at sample sites located in acoustic patches C and D were much more spread apart in the MDS ordination and were included in many more different clusters in the classification, indicating high variation in infaunal community structure across these acoustic patch types. Global dispersion and the Index of

Multivariate Dispersion (IMD) assesses the relative variability within and among groups, respectively, and acoustic patches B, D and C had the highest overall dispersion, and the variability of community structure in these acoustic patches was generally greater than in the other acoustic patches, A, E and F (Table 5.3-2). A multivariate analysis similarity (ANOSIM) indicated that there were significant differences in community structure among the acoustic patch types on an overall basis, and that the only pairs of acoustic patch types where infaunal community structure was not significantly different were B and C, D and F, and E and F (Table 5.3-3). In order to assess relative differences community structure at the local, sampling block, level relative to larger-scale, among acoustic patches variation, a permutational multivariate analysis of variance was conducted (Table 5.3-4). In this case, infaunal community structure was significantly different at both the sampling block and acoustic patch levels. As such, even after accounting for the significant variation in community structure at the sampling block level, differences among acoustic patch types in terms of infaunal community structure were statistically significant. The pairwise comparisons of acoustic patch types based on the PERMANOVA analysis suggested that community structure among pairs of patch types were more similar than indicated by the ANOSIM test. Of note were fewer differences among pairwise comparisons of acoustic patch types A, B and C, and among D, E and F.

The results of the multivariate analyses presented above indicate that community structure varies significantly at both small and large spatial scales. There are statistically significant differences in infaunal community structure among the acoustic patch types, and there was high variation within acoustic patch types at the sampling block level. In order to assess just how distinct are the sets of communities found within specific acoustic patch types a canonical analysis of principal coordinates (CAP) was performed. The CAP analysis supplements the other multivariate analyses with respect to characterizing the differences among groups that have been designated *a priori*, in this case the acoustic patch types. The CAP analysis on the October 2012 infaunal data yielded a more distinct separation of communities at sample sites within specific acoustic patch types (Figure 5.3-11). The correlations for the first two ordination axes were high, 0.8784 for CAP1 and 0.6584 for CAP2. This suggests that although there is a fair level of variation in community structure across the pilot study area, acoustic patches do have distinguishable sets of communities and as such can be analyzed in more detail to assess the range and characteristics of communities within each acoustic patch type. These analyses are presented below in the section on characterizing communities within acoustic patches.

The multivariate analyses also indicated that there was significant variation at the sampling block level. Several community characteristics were found to be quite variable within a number of blocks (e.g. Figures 5.3-2 and 5.3-4), and some sampling points within a SB were located in transition areas among acoustic patch types, and thus different sedimentary environments. This spatial distribution of samples and sampling blocks was specifically developed to assess how community structure varied among the large-scale seafloor environments that were evident in the side scan mosaics that were used to initially develop the sampling design. Such transition zones

among different habitats may be areas of increased diversity and unique community structure, representing ecotones among habitats at different spatial scales (Zajac et al. 2003, and references therein). To assess any such differences, each sampling block was characterized whether it was located within the interior of an acoustic patch or along a transition zone among different acoustic patch types. For those that were located along transition zones, they were classified according to the acoustic patches that were spanned by the sampling block. The abundances of taxa in each sampling block were averaged and several multivariate analyses were conducted to assess whether there were differences in community structure among interior and transition zone sampling blocks. MDS analysis indicates that infaunal communities found in the interior acoustic patches versus those along transition zones were somewhat distinct, but with some interior SBs characterized by sand and gravel-sand sediments being more similar to transitional patches with similar sediment types (Figure 5.3-12). An ANOSIM test indicated a marginally significant difference ($R=0.065$, $p = 0.088$) among interior and transition zone sampling blocks.

5.3.3.3 Characterizing Communities within Acoustic Patches Based on October 2012 Samples

In order to characterize the variety of infaunal communities within each acoustic patch type, samples located within each acoustic patch type were analyzed separately using cluster analysis and MDS. These analyses assess the relative level of infaunal community variation within acoustic patch types. MDS ordinations were used to identify community types [i.e., groupings of samples that had similar taxonomic composition and relative abundances of the taxa and relatively distinct from other samples taken in that acoustic patch type], supplemented by cluster analyses that use permutations tests to identify clusters that differed significantly from a random set of cluster groupings (Figure 5.3-13). Four community types were identified in acoustic patch A and their locations differed across the study area (Figure 5.3-14). Community types A1 and A2 were found in the central and southern portions of acoustic patch type A, in the eastern portion of the study area. Community type A3 was found in the northern portion of the study area, whereas community type A4 was located in acoustic patch type A which comprised the western-central portion of the study area, west of Stratford Shoal. Four infaunal communities were distinguished in acoustic patch type B, which had a varying spatial distribution. Community types B1 and B3 were found in a large B patch in the southeast corner study area; B3 was found in the northeast portion of the study area, whereas B4 in the transition area between acoustic patch type B and C along the eastern flank of Stratford Shoal (Figure 5.3-14). There were only two sampling blocks located in acoustic patch type C, and these differentiated into two community types, C1 found in the transition sound between acoustic patch type C and D on the western flank of Stratford Shoal and C2 found in the northern portion of the study area in an area of large sand waves. As was noted above, community structure in acoustic patch type D was highly variable, and 8 community types were distinguished for this acoustic patch type (Figure 5.3-13), with each community type generally found within specific type D patches (Figure 5.3-14). Community type D1 was found in the far southeastern section of the study area in an area of large sand waves; D3 was found in the large acoustic patch type D in the southwest

section of the study area; D4 was found along the eastern flank of Stratford Shoal; and community types D5 to D8 were primarily located along the east and west flanks of Stratford Shoal and the northern portion of the study area. Community type D2 was primarily found along the south and west flanks of Stratford Shoal, however it was also found in the sand and sandwaves areas in acoustic patch type D located in the southeast portion of the study area. The five community types found in acoustic patch type E were primarily located either along the central portion of Stratford Shoal running from north to south (E1, E2, and E3), or in transition areas in the southeastern portions of the study area (E4, E5). The four community types in acoustic patch type F were the most spatially consistent occurring primarily along the southern spine of Stratford Shoal (F1, F2, F3). Community type F4 was found in one location in a transition zone along the eastern-central flank of Stratford Shoal (Figure 5.3-14).

5.3.3.4 Community Composition and Characteristics

Analyses of community composition and the characteristics of the species that are found in different communities, can provide important ecological insights into the potential dynamics of the communities and how these may vary among different habitats at varying spatial scales. Similarity of percentages analysis (SIMPER) was conducted to assess the dominant species comprising the collection of communities found in each acoustic patch (Tables 5.3-5 to 5.3-10). Overall, the similarity levels within the community types designated ranged from approximately 30% to 55%. These similarity levels reflect that the SIMPER analyses were performed using the full data set and no transformations (e.g. square root or log) to down weight taxa that had very high abundances. This was done so that the average abundances of the dominant species and their contributions to community structure/similarity were expressed in untransformed units. Using the full data set incorporates all the less abundant and rare species (e.g. having only few occurrences and generally low abundance), and as such drive similarity levels among specific sample pairs down as well as the overall average similarity between sample pairs among samples found in a particular community type. However, the MDS community analyses (Figure 5.3-13) were based on transformed data and they indicated relatively distinct groupings of samples that can be designated as community types for the purposes of characterizing how infaunal communities vary within and among acoustic patches.

Four community types were designated for acoustic patch A (Table 5.3-5). Species common to most of the community types included the polychaetes *Nephtys incisa*, *Sigambra tentaculata* and *Amphitrite ornata*, the small nut clam *Nucula proxima*, and the pinnotherid crab, *Pinnixa sayana*. Several other species of note found in acoustic patch type A communities include the burrowing callinassid shrimp *Gilvossius setimanus*, the burrowing anemone *Ceriantheopsis americanus*, and the polychaetes *Levinsenia gracilis* and *Owenia fuisformis*. Several of these species (*Ceriantheopsis*, *Nucula*) were key in separating out acoustic patch A communities from communities in the other acoustic patches (Figure 5.3-11). The composition of these communities is similar to the mud communities identified by previous researchers in studies of the large central basin of LIS and the muddy areas of the western basin (Zajac 1998). The

presence of large burrowing and tube-building species (e.g. *Amphitrite*, *Owenia*) indicates well-developed communities that both bioturbate and bind sediments, leading to complex habitat surface features.

Acoustic Patch B was comprised of four community types as well, although community B4 was represented at one sample site (Table 5.3-6). The general taxonomic composition of acoustic patch B communities was similar to that found in acoustic patch A, but with several additional species that occurred in moderately high relative abundances, including the gastropods *Acteocina canaliculata* and *Turbonilla* spp., and the maldanid polychaete *Sabaco elongates*. Community B4 was particularly diverse within this acoustic patch type, with 17 taxa contributing to 90% of the overall similarity within the community. The communities are comprised of a variety of functional groups including tube builders (e.g. *Sabaco*, *Clymenella*, *Owenia*, *Polydora*, *Amphitrite*); deep dwellers (*Gilvossius*), subsurface and near surface burrowers (e.g. *Nephtys*, *Levinsenia*) and surface dwellers (e.g. *Pinnixia*, *Acteocina*, *Turbonilla*). This indicates ecologically dynamic communities not dominated by a small set of species of functional groups. Community B4 comprises only one sample site that had very low abundances of a few species, underscoring the potential high degree of variability that can occur among areas at small and large spatial scales.

Only two communities types were designated for acoustic patch type C (Table 5.3-7), likely, in part, the result of only three sampling sites falling within this acoustic patch type. Community C1 had a similar composition to several of the communities designated for acoustic patches A and B. Community C2, represented by a single sample site is unique its taxonomic composition. The dominant taxa were the mussel *Mytilus edulis*, oligochaetes, phoronids, as well as slipper shell mollusc *Crepidula* and a relatively high density of the bivalve *Andara transversa*. This site was located within a large sand wave field in the northern portion of the pilot study area, and as represent a distinct community inhabiting a distinct type of habitat.

As was presented above, communities in acoustic patch D were quite variable (Figure 5.3-10), and eight community types were designated, two of which were represented by a single sample site (Table 5.3-8). Many of the community types in this acoustic patch were dominated by the polychaetes *Nephtys incisa* and *Spiophanes bombyx*, oligochaetes, the bivalves *Tellina agilis* and *Anadara transversa*, and the pinnotherid crab *Pinnixa sayana*. The communities differed on the basis of relatively high abundances of specific species that were not found in the other community types in acoustic patch type D. For example, several of the communities, D2, D4 and D5, had high abundances of amphipods; D2 and D6 had relatively high abundances of the callinassid shrimp *Gilvossius setimanus*; community type D1 had a relatively high abundance of caprellid amphipods suggesting that there were also patches of hydrozoans that these types of amphipods normally inhabit. Community type D4 had a relatively high abundance of the gastropod genus *Turbonilla*. Of the two community types that were comprised of single sample sites, community D7 was comprised of only a few species at very low abundances, whereas community type D8 was dominated by the polychaete *Levinsenia gracilis*, the gastropod

Acteocina canaliculata, and the bivalves *Nucula proxima* and *Pitar morrhuanus*. Overall the communities found in acoustic patch D were relatively diverse with respect to how many species accounted for 90% of the cumulative similarity within each community type.

Acoustic patch E was comprised of five community types (Table 5.3-9). The dominant taxonomic group in two of the communities, E1 and E2 was oligochaetes; for E3 it was the bivalve *Anadara transversa*; and for E4 and E5 it was the pinnithred crab *Pinnixa sayana*. These species were also abundant in other community types in addition to the ones they were the numerical dominant in. For example, *Anadara transversa* was found in very high abundances in community type E1 and E2. Taxa comprising community types E4 and E5 had relatively low average abundances relative to the other the type communities. All the acoustic patch E communities have a diverse mix of functional types, and the relative composition amongst the community types were more diverse than found in other acoustic patch types. Also a relatively large number of species/taxa accounted for 90% of the overall average similarity found for each community type.

Four community types were found in acoustic patch F, two of which are represented by single sample sites (Table 5.3-10). Community type F1 at a very high degree of average similarity and was dominated by oligochaetes and the amphipod *Ampelisca abdita*, and also had high abundances of the polychaetes *Levinsenia gracilis* and *Nephtys incise*. Community type F2 also had a relatively high average abundance of oligochaetes but also high abundances of the bivalves *Anadara transversa*, and *Astarte undata*, spionid polychaetes in the genus *Polydora* and the crab *Pinnixa sayana*. Community type F3 had high abundances of oligochaetes and also the amphipod *Ampelisca abdita*. Several species of spionid polychaetes, *Polydora cornuta* and *Spiophanes bombyx* were also abundant and as *Owenia fusiformis*, *Pinnixa sayana* and a set of unidentified molluscs. Community type F4 was dominated by the polychaete *Tharyx acutus*, but also had high densities of *Crepidula fornicate* and *Crepidula plana*.

Table 5.3-2. Multivariate dispersion of infaunal communities within acoustic patch types and the Index of Multivariate Dispersion (IMD) among acoustic patches in the LIS pilot study area for October 2012. Dispersion is a measure of the variation among communities and IMD contrasts the average rank of similarities among samples of a certain acoustic patch class with the average rank of other classes (Clarke and Warwick, 2001). The greater the relative variability among acoustic patches, the closer the IMD is to -1. Similarities calculated using the Bray-Curtis resemblance function on square root transformed data.

Acoustic Patch	Dispersion
F	0.619
A	0.694
E	0.866
B	1.191
D	1.216
C	1.546

Pairwise Comparisons	
Acoustic Patch pairs	IMD
A, D	-0.522
A, E	-0.184
A, C	-0.787
A, F	0.083
B, A	0.473
B, D	-0.009
B, E	0.322
B, C	-0.363
B, F	0.542
C, F	0.81
D, E	0.359
D, C	-0.378
D, F	0.583
E, C	-0.665
E, F	0.278

Table 5.3-3. Results of ANOSIM analysis testing infaunal community differences among acoustic patches. Similarities calculated using the Bray-Curtis resemblance function on square root transformed data. Global test based on 1000 random permutations of the data; most pairwise tests were also based on 1000 permutations, but some were less depending on number of samples in the acoustic class patches being compared.

Global R: 0.322; $p = 0.001$

Pairwise Tests

Groups	R	Significance Level %
A, D	0.316	0.001
A, E	0.819	0.001
A, C	0.464	0.011
A, F	0.885	0.001
B, A	0.162	0.013
B, D	0.112	0.034
B, E	0.526	0.001
B, C	0.145	0.232
B, F	0.373	0.001
C, F	0.567	0.008
D, E	0.105	0.006
D, F	0.005	0.511
E, C	0.436	0.015
E, F	0.008	0.439

Table 5.3-4. Results of permutational multivariate analysis of variance (PERMANOVA) for differences among acoustic patches with sampling blocks (SB) nested with acoustic patches. The analysis tests “the simultaneous response of one or more variables to one or more factors in an ANOVA experimental design on the basis of any distance measure, using permutation methods” (Anderson 2005). The analysis was based on a Type III (partial) sums of squares and 1000 permutations of residuals under a reduced model. Ac = Acoustic Patch; Sa = Sampling Block.

PERMANOVA table of results

Source	df	SS	MS	Pseudo-F	P - permutation
Ac	5	44125	8825.0	2.6307	0.001
Sa(Ac)	47	1.8172E5	3866.5	2.2745	0.001
Res	48	81595	1699.9		
Total	100	3.1942E5			

Pair-wise tests- Acoustic Patches

Groups	t	P - permutation
A, D	1.9298	0.001
A, E	2.8286	0.001
A, C	1.3114	0.063
A, F	2.0977	0.002
B, A	0.9338	0.575
B, D	1.2092	0.079
B, E	2.0327	0.001
B, C	1.0103	0.406
B, F	1.5571	0.004
C, F	1.1683	0.138
D, E	1.5271	0.002
D, C	0.9296	0.615
D, F	1.1606	0.142
E, C	1.2423	0.069
E, F	0.8884	0.731

Table 5.3-5. Results of similarity percentage analysis (SIMPER) for acoustic patch A communities in October 2012. Table shows the percent contribution of each species to the total similarity within each community type. Av.Abund = average abundance per 0.1 m²; Av.Sim = average similarity among replicates at the site; Sim/SD = Similarity standard deviation; Contrib% = percent contribution to within site similarity; Cum.% = cumulative similarity.

Community A1: Average similarity: 40.60

Species	Av.Abund	Av.Sim	Sim/SD	Contrib%	Cum.%
<i>Polydora cornuta</i>	17.67	13.37	1.05	32.94	32.94
<i>Sigambra tentaculata</i>	10.67	6.79	1.15	16.72	49.66
<i>Pinnixa rectinens</i>	5.17	4.01	2.31	9.88	59.54
<i>Amphitrite ornata</i>	4.50	3.60	1.73	8.87	68.41
<i>Pinnixa sayana</i>	5.17	3.53	0.92	8.69	77.10
<i>Levinsenia gracilis</i>	4.00	3.18	1.20	7.82	84.92
<i>Gilvossius setimanus</i>	2.33	1.18	0.72	2.90	87.82
<i>Hutchinsoniella macracantha</i>	1.33	0.89	1.19	2.19	90.01

Community A2: Average similarity: 43.88

Species	Av.Abund	Av.Sim	Sim/SD	Contrib%	Cum.%
<i>Nephtys incisa</i>	8.00	12.85	1.80	29.28	29.28
<i>Sigambra tentaculata</i>	5.67	9.59	0.95	21.86	51.14
<i>Amphitrite ornata</i>	4.50	7.44	1.30	16.95	68.09
<i>Pinnixa sayana</i>	3.50	6.09	2.47	13.87	81.95
<i>Ceriantheopsis americanus</i>	1.67	2.81	1.22	6.41	88.37
<i>Sabaco elongatus</i>	1.33	2.16	1.11	4.92	93.29

Community A3: Average similarity: 58.64

Species	Av.Abund	Av.Sim	Sim/SD	Contrib%	Cum.%
<i>Nucula proxima</i>	230.25	41.38	3.25	70.58	70.58
<i>Nephtys incisa</i>	21.75	5.29	2.95	9.02	79.60
<i>Sigambra tentaculata</i>	17.50	3.01	1.23	5.14	84.74
<i>Owenia fusiformis</i>	7.38	1.45	1.16	2.48	87.21
<i>Yoldia limatula</i>	7.50	1.36	1.07	2.31	89.53
<i>Levinsenia gracilis</i>	8.63	1.34	0.84	2.28	91.81

Community A4: Average similarity: 27.21

Species	Av.Abund	Av.Sim	Sim/SD	Contrib%	Cum.%
<i>Nephtys incisa</i>	4.00	10.38	2.38	38.13	38.13
<i>Nucula proxima</i>	14.33	9.88	0.58	36.30	74.43
<i>Amphitrite ornata</i>	1.67	3.46	2.38	12.71	87.14
<i>Pinnixa sayana</i>	2.67	1.65	0.58	6.05	93.19

Table 5.3-6. Results of similarity percentage analysis (SIMPER) for acoustic patch B communities. Table shows the percent contribution of each species to the total similarity within each community type. Av.Abund = average abundance per 0.1 m² sample; Av.Sim = average similarity among replicates at the site; Sim/SD = Similarity standard deviation; Contrib% = percent contribution to within site similarity; Cum.% = cumulative similarity.

Community Type B1: Average similarity: 20.28

Species	Av.Abund	Av.Sim	Sim/SD	Contrib%	Cum.%
<i>Amphitrite ornata</i>	3.25	7.96	0.54	39.25	39.25
<i>Pinnixa sayana</i>	2.75	4.83	0.49	23.83	63.09
<i>Gilvossius setimanus</i>	1.5	1.88	0.82	9.25	72.33
<i>Oligochaeta</i>	2.5	1.82	0.83	8.99	81.33
<i>Sabaco elongatus</i>	1	1.04	0.41	5.14	86.46
<i>Nephtys incisa</i>	1.75	0.7	0.41	3.46	89.92
<i>Pitar morrhuanus</i>	2	0.7	0.41	3.46	93.38

Community Type B2: Average similarity: 24.59

Species	Av.Abund	Av.Sim	Sim/SD	Contrib%	Cum.%
<i>Nephtys incisa</i>	16.2	4.24	1.65	17.26	17.26
<i>Sigambra tentaculata</i>	13.6	3.91	1.51	15.92	33.18
<i>Polydora cornuta</i>	20.4	2.47	1.31	10.05	43.24
<i>Pinnixa sayana</i>	6.6	2.35	1.96	9.57	52.81
<i>Nucula proxima</i>	65.4	1.89	0.33	7.67	60.48
<i>Amphitrite ornata</i>	6.4	1.82	1.14	7.4	67.89
<i>Owenia fusiformis</i>	11.4	1.44	0.59	5.84	73.73
<i>Acteocina canaliculata</i>	6.8	0.98	0.69	3.98	77.71
<i>Pinnixa rectinens</i>	2	0.74	0.58	3	80.71
<i>Prionospio steenstrupi</i>	5	0.56	0.8	2.27	82.98
<i>Levinsenia gracilis</i>	1.8	0.53	0.37	2.17	85.15
<i>Clymenella mucosa</i>	3.8	0.48	0.56	1.94	87.08
<i>Nemertea</i>	5	0.33	0.32	1.35	88.44
<i>Hutchinsoniella macracantha</i>	0.6	0.31	0.61	1.26	89.7
<i>Mediomastus ambiseta</i>	7.2	0.31	0.44	1.25	90.95

Community type B3: Average similarity: 29.41

Species	Av.Abund	Av.Sim	Sim/SD	Contrib%	Cum.%
<i>Amphitrite ornata</i>	9.25	10.59	1.8	36	36
<i>Nephtys incisa</i>	5.5	4.09	3.44	13.9	49.9
<i>Turbonilla spp.</i>	6.5	4.04	1.96	13.74	63.64
<i>Sabaco elongatus</i>	4	2.85	1.19	9.68	73.33

<i>Owenia fusiformis</i>	1.75	1.66	1.98	5.65	78.98
<i>Corophium spp.</i>	2.75	1.31	0.8	4.46	83.44
<i>Levinsenia gracilis</i>	3.5	1.27	0.66	4.32	87.77
<i>Ampharete acutifrons</i>	0.75	0.89	0.82	3.02	90.79

Community type B4: only 1 sample

Species	Abundance
<i>Acteocina canaliculata</i>	5
<i>Nephtys spp.</i>	1
<i>Yoldia limatula</i>	1

Table 5.3-7. Results of similarity percentage analysis (SIMPER) for acoustic patch C communities. Table shows the percent contribution of each species to the total similarity within each community type. Av.Abund = average abundance per 0.1 m² sample; Av.Sim = average similarity among replicates at the site; Sim/SD = Similarity standard deviation; Contrib% = percent contribution to within site similarity; Cum.% = cumulative similarity.

Group C1

Average similarity: 16.60 (only two samples so no Sim/SD)

Species	Av.Abund	Av.Sim	Sim/SD	Contrib%	Cum.%
<i>Nephtys incisa</i>	16	7.11		42.86	42.86
<i>Amphitrite ornata</i>	3.5	2.37		14.29	57.14
<i>Oligochaeta</i>	3	2.37		14.29	71.43
<i>Nucula proxima</i>	4.5	1.58		9.52	80.95
<i>Acteocina canaliculata</i>	4.5	0.79		4.76	85.71
<i>Cossura longicirrata</i>	1	0.79		4.76	90.48

Community Type C2; one sample only

Species	Abundance
<i>Mytilus edulis</i>	33
<i>Oligochaeta</i>	13
<i>Phoronida</i>	8
<i>Stenopleustes inermis</i>	8
<i>Polydora spp.</i>	6
<i>Rithropanope harrisi</i>	6
<i>Anadara transversa</i>	5
<i>Crepidula plana</i>	5
<i>Tellina agilis</i>	5
<i>Erichthonius brasiliensis</i>	4
<i>Parapionosyllis longicirrata</i>	4
<i>Pinnixa sayana</i>	3

Table 5.3-8. Results of similarity percentage analysis (SIMPER) for acoustic patch D communities. Table shows the percent contribution of each species to the total similarity within each community type. Av.Abund = average abundance per 0.1 m² sample; Av.Sim = average similarity among replicates at the site; Sim/SD = Similarity standard deviation; Contrib% = percent contribution to within site similarity; Cum.% = cumulative similarity.

Community Type D1: Average similarity: 35.47

Species	Av.Abund	Av.Sim	Sim/SD	Contrib%	Cum.%
<i>Tellina agilis</i>	44.25	16.07	1.46	45.31	45.31
<i>Oligochaeta</i>	18.75	4.91	0.58	13.85	59.17
<i>Spiophanes bombyx</i>	9.25	3.79	2.3	10.69	69.86
<i>Nephtys picta</i>	13.25	2.42	0.49	6.82	76.68
<i>Spiochaetopterus oculatus</i>	3.75	2.03	4.84	5.73	82.4

<i>Caprellidae</i>	11.25	1.79	0.41	5.03	87.44
<i>Ilyanassa trivittata</i>	4	1.51	1.48	4.25	91.69

Community Type D2: Average similarity: 30.69

Species	Av.Abund	Av.Sim	Sim/SD	Contrib%	Cum.%
<i>Spiophanes bombyx</i>	13	5.75	1.07	18.74	18.74
<i>Pinnixa sayana</i>	7.33	3.76	1.25	12.24	30.99
<i>Oligochaeta</i>	9.67	3.75	0.99	12.21	43.2
<i>Anadara transversa</i>	5.5	2.52	1.01	8.2	51.39
<i>Mulinia lateralis</i>	3.83	1.98	1.03	6.46	57.86
<i>Gilvossius setimanus</i>	3	1.51	0.81	4.91	62.77
<i>Ampelisca vadorum</i>	5.5	1.43	0.56	4.66	67.43
<i>Ampelisca macrocephala</i>	4.83	1.31	0.43	4.26	71.68
<i>Levinsenia gracilis</i>	2.5	1.05	0.68	3.43	75.11
<i>Nephtys incisa</i>	2	1.03	0.82	3.35	78.46
<i>Polydora spp.</i>	2.67	0.97	0.75	3.16	81.62
<i>Ancistrosyllis groenlandica</i>	1.5	0.84	1.3	2.73	84.35
<i>Pitar morrhuanus</i>	1	0.69	1.34	2.24	86.58
<i>Rithropanope harrisi</i>	1.33	0.47	0.47	1.54	88.12
<i>Astarte undata</i>	1.17	0.43	0.37	1.4	89.53
<i>Leptocheirus pinguis</i>	2	0.26	0.44	0.84	90.37

Community Type D3: Average similarity: 32.78

Species	Av.Abund	Av.Sim	Sim/SD	Contrib%	Cum.%
<i>Nephtys incisa</i>	4.8	9.58	1.9	29.21	29.21
<i>Tellina agilis</i>	3.4	5.7	1.2	17.39	46.6
<i>Pinnixa sayana</i>	3.8	4.78	0.78	14.58	61.18
<i>Sigambra tentaculata</i>	1.4	1.98	0.95	6.03	67.21
<i>Amphitrite ornata</i>	1.8	1.54	0.49	4.7	71.91
<i>Yoldia limatula</i>	1.2	1.53	1.16	4.66	76.56
<i>Paraonis fulgens</i>	1	1.29	0.57	3.95	80.51
<i>Pitar morrhuanus</i>	2	1.23	0.32	3.77	84.27
<i>Nucula proxima</i>	1.2	1.08	0.6	3.3	87.57
<i>Clymenella mucosa</i>	1.4	1.04	0.56	3.17	90.74

Community Type D4: Average similarity: 30.66

Species	Av.Abund	Av.Sim	Sim/SD	Contrib%	Cum.%
<i>Turbonilla spp.</i>	20.6	9.1	1.45	29.69	29.69
<i>Nephtys incisa</i>	7.8	3.04	0.86	9.92	39.61
<i>Sabaco elongatus</i>	8.6	2.96	0.95	9.66	49.27
<i>Pinnixa sayana</i>	4.2	2.88	1.4	9.4	58.67
<i>Ampelisca abdita</i>	6.6	2.57	1.23	8.38	67.04
<i>Maldane sarsi</i>	2.6	1.21	1.12	3.94	70.98
<i>Pinnixa rectinens</i>	4	1.21	0.36	3.93	74.91
<i>Amphitrite ornata</i>	4	1.05	0.59	3.42	78.34
<i>Sigambra tentaculata</i>	3	0.82	0.93	2.67	81.01
<i>Corophium spp.</i>	2.6	0.79	0.57	2.56	83.57
<i>Anadara transversa</i>	2	0.72	0.59	2.35	85.92
<i>Turbellaria</i>	1.8	0.71	0.98	2.3	88.23
<i>Mollusca</i>	9.4	0.62	0.4	2.02	90.24

Community Type D5: Average similarity: 26.51

Species	Av.Abund	Av.Sim	Sim/SD	Contrib%	Cum.%
<i>Nephtys incisa</i>	21	6.35	55.74	23.94	23.94
<i>Macoma tenta</i>	20	5.78	1.67	21.81	45.75
<i>Ampharete acutifrons</i>	7.67	2.43	6.74	9.17	54.91

<i>Amphitrite ornata</i>	5.33	1.82	1.08	6.87	61.78
<i>Spiophanes bombyx</i>	11.33	1.34	0.58	5.07	66.85
<i>Ampelisca abdita</i>	19.33	1.12	0.58	4.23	71.08
<i>Clymenella mucosa</i>	8.67	1.12	0.58	4.23	75.31
<i>Levinsenia gracilis</i>	7	0.69	0.58	2.61	77.91
<i>Mediomastus ambiseta</i>	6	0.67	0.58	2.54	80.45
<i>Prionospio steenstrupi</i>	6.33	0.67	0.58	2.54	82.98
<i>Oligochaeta</i>	28.67	0.58	6.83	2.17	85.16
<i>Sigambra tentaculata</i>	4	0.56	0.58	2.11	87.27
<i>Corophium spp.</i>	1.33	0.46	4.19	1.75	89.02
<i>Sabaco elongatus</i>	3.67	0.46	4.19	1.75	90.77

Community Type D6: Average similarity: 23.69

Species	Av.Abund	Av.Sim	Sim/SD	Contrib%	Cum.%
<i>Oligochaeta</i>	34.83	5.48	0.95	23.16	23.16
<i>Mollusca</i>	10.33	2.04	0.9	8.59	31.75
<i>Anadara transversa</i>	16	1.85	1.19	7.81	39.56
<i>Spiophanes bombyx</i>	20	1.56	0.82	6.58	46.14
<i>Nephtys incisa</i>	10.17	1.27	1.19	5.34	51.48
<i>Owenia fusiformis</i>	5.67	0.85	1.31	3.6	55.08
<i>Gilvossius setimanus</i>	4.83	0.62	0.65	2.62	57.7
<i>Leptocheirus pinguis</i>	39.17	0.62	0.27	2.62	60.32
<i>Polychaeta spp.</i>	4.83	0.61	0.85	2.57	62.88
<i>Pinnixa sayana</i>	2.5	0.52	1.05	2.18	65.07
<i>Ampelisca abdita</i>	31.33	0.51	0.67	2.15	67.22
<i>Ampharete acutifrons</i>	5.83	0.51	0.67	2.15	69.37
<i>Aglaophamus verrilli</i>	4.17	0.48	0.98	2.04	71.41
<i>Ampelisca vadorum</i>	11.5	0.43	0.48	1.81	73.22
<i>Amphipoda spp</i>	7.83	0.37	0.54	1.56	74.78
<i>Clymenella torquata</i>	1.67	0.36	0.56	1.52	76.3
<i>Cirratulus grandis</i>	2.5	0.36	2.28	1.5	77.8
<i>Scalibregma inflatum</i>	1.67	0.32	1.01	1.34	79.14
<i>Tellina agilis</i>	4.33	0.3	0.73	1.27	80.41
<i>Pinnixa rectinens</i>	6.83	0.28	0.71	1.2	81.61
<i>Ampharete spp.</i>	2.67	0.25	0.72	1.08	82.68
<i>Polydora cornuta</i>	31.5	0.25	0.29	1.06	83.74
<i>Aricidea spp.</i>	5	0.25	0.55	1.04	84.78
<i>Spionidae</i>	1.83	0.23	0.68	0.99	85.77
<i>Spiochaetopterus oculatus</i>	1.5	0.21	1.1	0.88	86.65
<i>Pitar morrhuanus</i>	2.33	0.21	0.4	0.88	87.53
<i>Turbellaria</i>	1.17	0.2	0.61	0.85	88.38
<i>Diopatra cuprea</i>	1.17	0.2	0.34	0.84	89.22
<i>Sabaco elongatus</i>	4.67	0.2	0.3	0.83	90.05

Community Type D7: single sample

Species	Abundance
<i>Sabaco elongatus</i>	3
<i>Anadara transversa</i>	2
<i>Gilvossius setimanus</i>	2
<i>Pinnixa sayana</i>	2
<i>Owenia fusiformis</i>	1

Community Type D8; single sample

Species	Abundance
<i>Levinsenia gracilis</i>	26
<i>Acteocina canaliculata</i>	22

<i>Nucula proxima</i>	14
<i>Pitar morrhuanus</i>	11
<i>Owenia fusiformis</i>	10
<i>Sigambra tentaculata</i>	8
<i>Polychaeta spp.</i>	7
<i>Spio setosa</i>	5
<i>Harmothoe imbricata</i>	4

Table 5.3-9. Results of similarity percentage analysis (SIMPER) for acoustic patch E communities. Table shows the percent contribution of each species to the total similarity within each community type. Av.Abund = average abundance per 0.1 m² sample; Av.Sim = average similarity among replicates at the site; Sim/SD = Similarity standard deviation; Contrib% = percent contribution to within site similarity; Cum.% = cumulative similarity.

Community Type E1: Average similarity: 49.53

Species	Av.Abund	Av.Sim	Sim/SD	Contrib%	Cum.%
Oligochaeta	1597.33	45.25	1.18	91.36	91.36
<i>Spiophanes bombyx</i>	49.33	1.74	2.83	3.52	94.87
<i>Tellina agilis</i>	24.67	0.49	1.45	0.99	95.86
<i>Ampelisca abdita</i>	16.33	0.27	0.73	0.55	96.41
<i>Anadara transversa</i>	47.33	0.25	1.41	0.51	96.92
<i>Ampharete acutifrons</i>	5.67	0.24	21.85	0.48	97.4
<i>Crepidula plana</i>	9	0.18	3.23	0.36	97.76
<i>Levinsenia gracilis</i>	10	0.15	0.94	0.3	98.06
<i>Ampelisca vadorum</i>	5	0.1	0.58	0.2	98.25
<i>Owenia fusiformis</i>	2.33	0.07	1.81	0.14	98.4
<i>Glycera americana</i>	2.33	0.07	1.88	0.14	98.54
<i>Orbinia ornata</i>	5.33	0.07	0.58	0.14	98.68
<i>Tharyx acutus</i>	3.33	0.07	4.52	0.13	98.82
<i>Nephtys spp.</i>	10	0.06	0.58	0.12	98.93
<i>Pitar morrhuanus</i>	3.33	0.06	0.58	0.12	99.05

Community Type E2: Average similarity: 32.51

Species	Av.Abund	Av.Sim	Sim/SD	Contrib%	Cum.%
Oligochaeta	41.4	9.65	2.11	29.67	29.67
<i>Ampelisca vadorum</i>	47.2	6.45	0.98	19.84	49.51
<i>Anadara transversa</i>	22.5	3.81	1.13	11.71	61.22
<i>Spiophanes bombyx</i>	11.4	1.68	0.97	5.17	66.39
<i>Ancistrosyllis groenlandica</i>	6.3	1.11	1.28	3.4	69.79
<i>Nephtys incisa</i>	4.2	1.1	1.86	3.37	73.16
<i>Tellina agilis</i>	8.4	1.05	0.58	3.23	76.4
<i>Astarte undata</i>	3.9	0.65	0.67	1.99	78.39
<i>Ampharete americana</i>	5.1	0.64	0.64	1.96	80.34
<i>Nephtys picta</i>	3.4	0.61	0.98	1.89	82.23
<i>Crepidula plana</i>	4.9	0.6	0.6	1.84	84.07
<i>Pinnixa sayana</i>	14.9	0.49	0.42	1.49	85.56
<i>Tharyx acutus</i>	3.5	0.47	0.7	1.46	87.02
<i>Rithropanope harrisi</i>	3.1	0.43	0.74	1.34	88.36
<i>Ampelisca abdita</i>	4	0.38	0.41	1.18	89.54
<i>Levinsenia gracilis</i>	1.9	0.29	1.06	0.88	90.42

Community Type E3: Average similarity: 16.73

Species	Av.Abund	Av.Sim	Sim/SD	Contrib%	Cum.%
<i>Anadara transversa</i>	11.33	4.47	0.58	26.69	26.69
<i>Epitonium spp</i>	2	2.93	2.31	17.49	44.18
<i>Mulinia lateralis</i>	7.67	2.1	0.58	12.53	56.71

<i>Rithropanope harrisi</i>	3.33	1.78	3.77	10.65	67.37
<i>Crepidula fornicata</i>	3.67	0.96	0.58	5.72	73.09
<i>Ampelisca spp.</i>	0.67	0.72	0.58	4.33	77.42
<i>Levinsenia gracilis</i>	2	0.72	0.58	4.33	81.75
<i>Ensis directus</i>	0.67	0.42	0.58	2.51	84.25
<i>Nephtys incisa</i>	0.67	0.42	0.58	2.51	86.76
<i>Pherusa affinis</i>	2.33	0.42	0.58	2.51	89.27
<i>Pitar morrhuanus</i>	1.33	0.42	0.58	2.51	91.77

Community Type E4: Average similarity: 28.72

Species	Av.Abund	Av.Sim	Sim/SD	Contrib%	Cum.%
<i>Pinnixa sayana</i>	6.6	3.78	1.04	13.18	13.18
<i>Ampelisca vadorum</i>	5.6	3.55	1.11	12.37	25.55
<i>Gilvossius setimanus</i>	5	2.91	1.12	10.15	35.69
<i>Ancistrosyllis groenlandica</i>	3.8	2.9	1.4	10.09	45.78
<i>Anadara transversa</i>	7.6	2.47	0.56	8.61	54.39
<i>Oligochaeta</i>	3.2	2.02	1.01	7.05	61.44
<i>Nephtys incisa</i>	3.2	1.64	1.98	5.7	67.14
<i>Spiophanes bombyx</i>	2.4	0.97	0.76	3.37	70.51
<i>Nephtys spp.</i>	1.2	0.86	0.89	3.01	73.52
<i>Ampelisca macrocephala</i>	9.6	0.86	0.32	2.98	76.5
<i>Sabaco elongatus</i>	3.6	0.64	0.48	2.24	78.74
<i>Levinsenia gracilis</i>	1.8	0.59	0.48	2.05	80.79
<i>Epitonium spp</i>	3.2	0.56	0.32	1.93	82.73
<i>Rithropanope harrisi</i>	1.4	0.47	0.52	1.65	84.38
<i>Tellina agilis</i>	1.2	0.47	0.59	1.63	86.01
<i>Crepidula plana</i>	1	0.37	0.6	1.28	87.29
<i>Ilyanassa trivittata</i>	0.8	0.37	0.6	1.28	88.57
<i>Owenia fusiformis</i>	0.8	0.36	0.62	1.26	89.84
<i>Ampharete americana</i>	0.8	0.29	0.62	1.01	90.84

Community Type E5: Average similarity: 31.95

Species	Av.Abund	Av.Sim	Sim/SD	Contrib%	Cum.%
<i>Pinnixa sayana</i>	6	5.92		18.52	18.52
<i>Pinnixa rectinens</i>	7	4.73		14.81	33.33
<i>Amphitrite ornata</i>	3	3.55		11.11	44.44
<i>Nephtys incisa</i>	8	3.55		11.11	55.56
<i>Polydora cornuta</i>	14.5	2.37		7.41	62.96
<i>Ampharete acutifrons</i>	1.5	1.18		3.7	66.67
<i>Aricidea spp.</i>	1.5	1.18		3.7	70.37
<i>Cancer borealis</i>	1	1.18		3.7	74.07
<i>Exogene spp.</i>	1.5	1.18		3.7	77.78
<i>Gilvossius setimanus</i>	1.5	1.18		3.7	81.48
<i>Glycera americana</i>	1	1.18		3.7	85.19
<i>Oligochaeta</i>	2.5	1.18		3.7	88.89
<i>Sabaco elongatus</i>	1	1.18		3.7	92.59

Table 5.3-10. Results of similarity percentage analysis (SIMPER) for acoustic patch F communities. Table shows the percent contribution of each species to the total similarity within each community type. Av.Abund = average abundance per 0.1 m² sample; Av.Sim = average similarity among replicates at the site; Sim/SD = Similarity standard deviation; Contrib% = percent contribution to within site similarity; Cum.% = cumulative similarity.

Community Type F1: Average similarity: 71.94

Species	Av.Abund	Av.Sim	Sim/SD	Contrib%	Cum.%
<i>Oligochaeta</i>	621.33	53.82	7.03	74.82	74.82

<i>Ampelisca abdita</i>	117	7.62	5.28	10.59	85.41
<i>Levinsenia gracilis</i>	38.67	2.19	0.98	3.05	88.46
<i>Nephtys incisa</i>	13.67	1.21	5.8	1.69	90.15

Community Type F2: Average similarity: 43.96

<u>Species</u>	<u>Av.Abund</u>	<u>Av.Sim</u>	<u>Sim/SD</u>	<u>Contrib%</u>	<u>Cum.%</u>
<i>Polydora spp.</i>	16	7.69		17.5	17.5
<i>Anadara transversa</i>	38	6.59		15	32.5
<i>Oligochaeta</i>	32	6.59		15	47.5
<i>Astarte undata</i>	11	4.95		11.25	58.75
<i>Pinnixa sayana</i>	11	4.95		11.25	70
<i>Ampelisca vadorum</i>	10	2.75		6.25	76.25
<i>Nephtys incisa</i>	5	2.2		5	81.25
<i>Spiophanes bombyx</i>	7.5	1.65		3.75	85
<i>Ampharete americana</i>	2	1.1		2.5	87.5
<i>Ancistrosyllis groenlandica</i>	3.5	1.1		2.5	90

Community Type F3: single site

<u>Species</u>	<u>Av.Abund</u>
<i>Oligochaeta</i>	191
<i>Ampelisca abdita</i>	112
<i>Polydora cornuta</i>	24
<i>Pinnixa sayana</i>	14
<i>Owenia fusiformis</i>	14
<i>Mollusca</i>	12
<i>Spiophanes bombyx</i>	11
<i>Aricidea spp.</i>	8
<i>Amphitrite ornata</i>	7
<i>Maldane sarsi</i>	7

Community Type F4: single site

<u>Species</u>	<u>Av.Abund</u>
<i>Oligochaeta</i>	20
<i>Tharyx acutus</i>	88
<i>Crepidula fornicata</i>	52
<i>Crepidula plana</i>	24
<i>Rithropanope harrisi</i>	9
<i>Tellina agilis</i>	7
<i>Trichophoxus epistomus</i>	6
<i>Spiophanes bombyx</i>	5

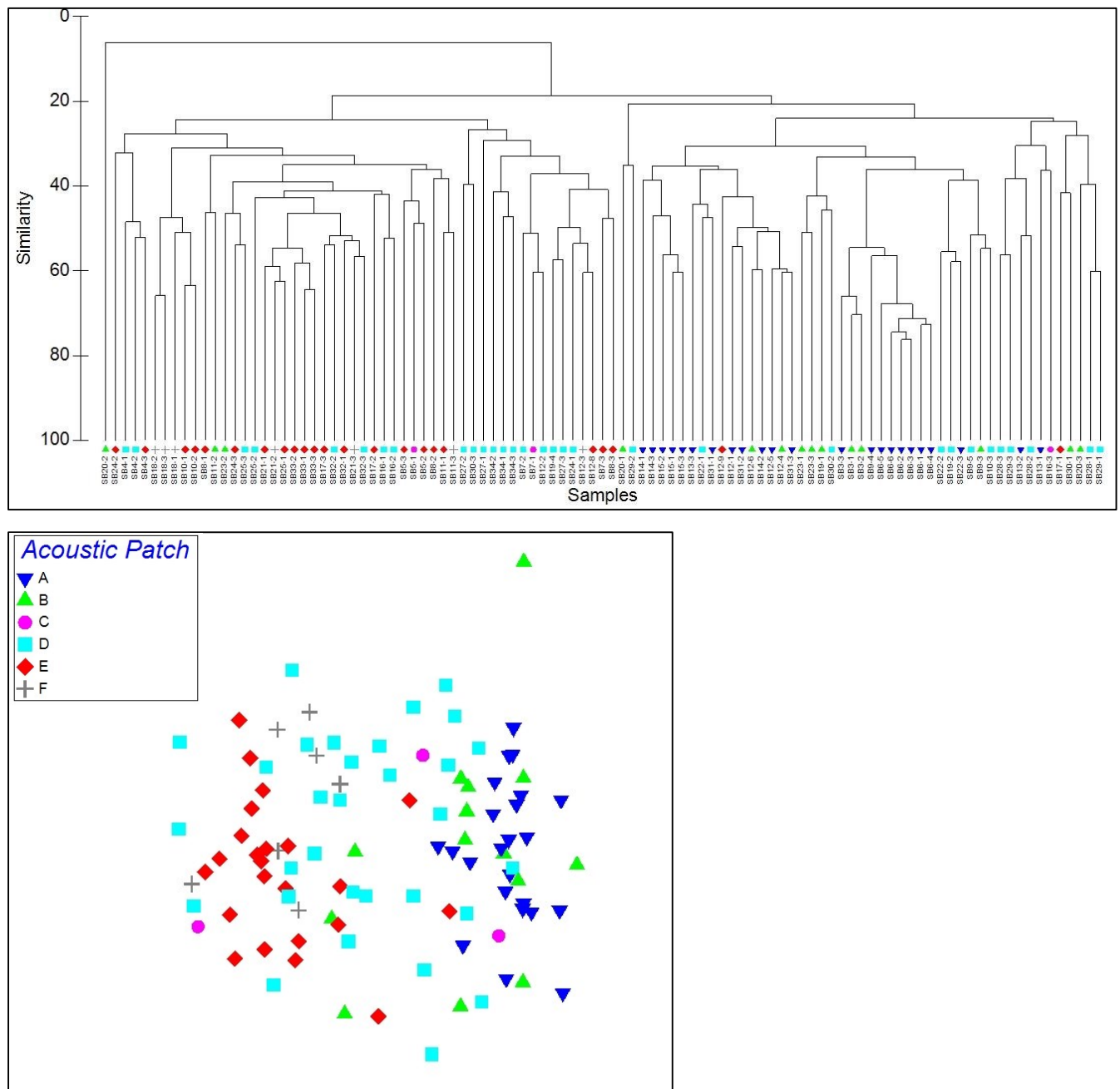


Figure 5.3-10. Results of multivariate classification (top) and MDS (bottom) analysis of similarities in infaunal community structure across the pilot study area in October 2012. The classification (cluster) analysis links sample site that have similar community structure; the similarity axis is interpreted as percent similarity based on taxonomic composition and relative abundances of taxa in the samples. In the nMDS ordination, the closer sample points are to each other the more similar they are. For both analyses, the full October 2012 data set was used, data were square root transformed (to reduce the influence of very abundant species), and sample similarities were computed using the Bray-Curtis resemblance function.

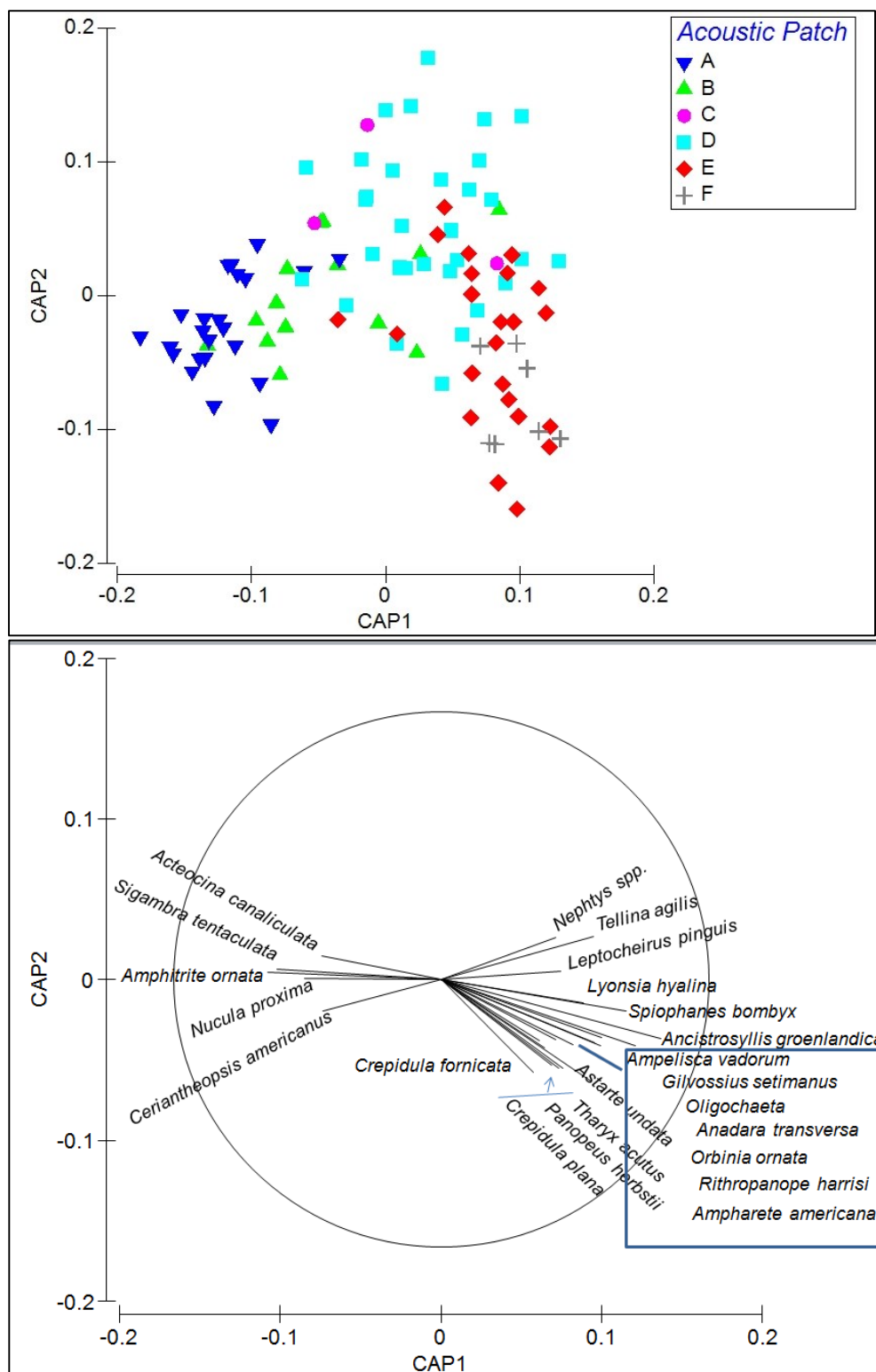


Figure 5.3-11. Top- Results of CAP ordination on infaunal community based on October 2012 samples. Bottom - Species correlations with ordination axes; only species that have correlations >0.40 are shown. Species in blue box are related to the short vectors indicated by blue line.

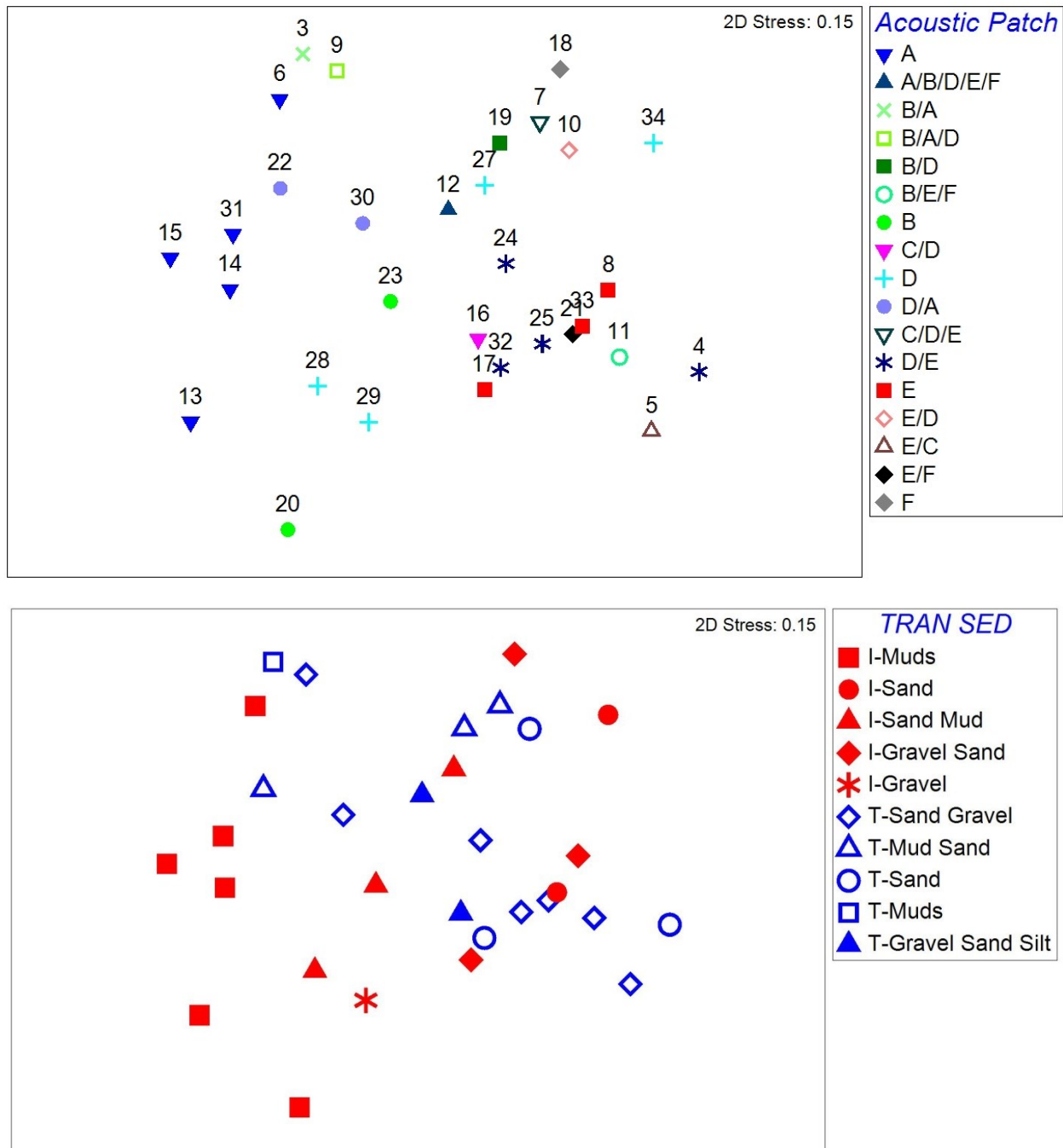


Figure 5.3-12. Results of MDS ordination of community structure among sampling blocks (averaged data). Top graph shows ordination of sampling blocks designated by which acoustic patch they were totally within (single patch designations) or spanning (multiple patch designations). Lower graph shows the same ordination with the sampling blocks identified by whether they are interior (I) were transitional (T) and by the sediment type(s) found in the sampling block.

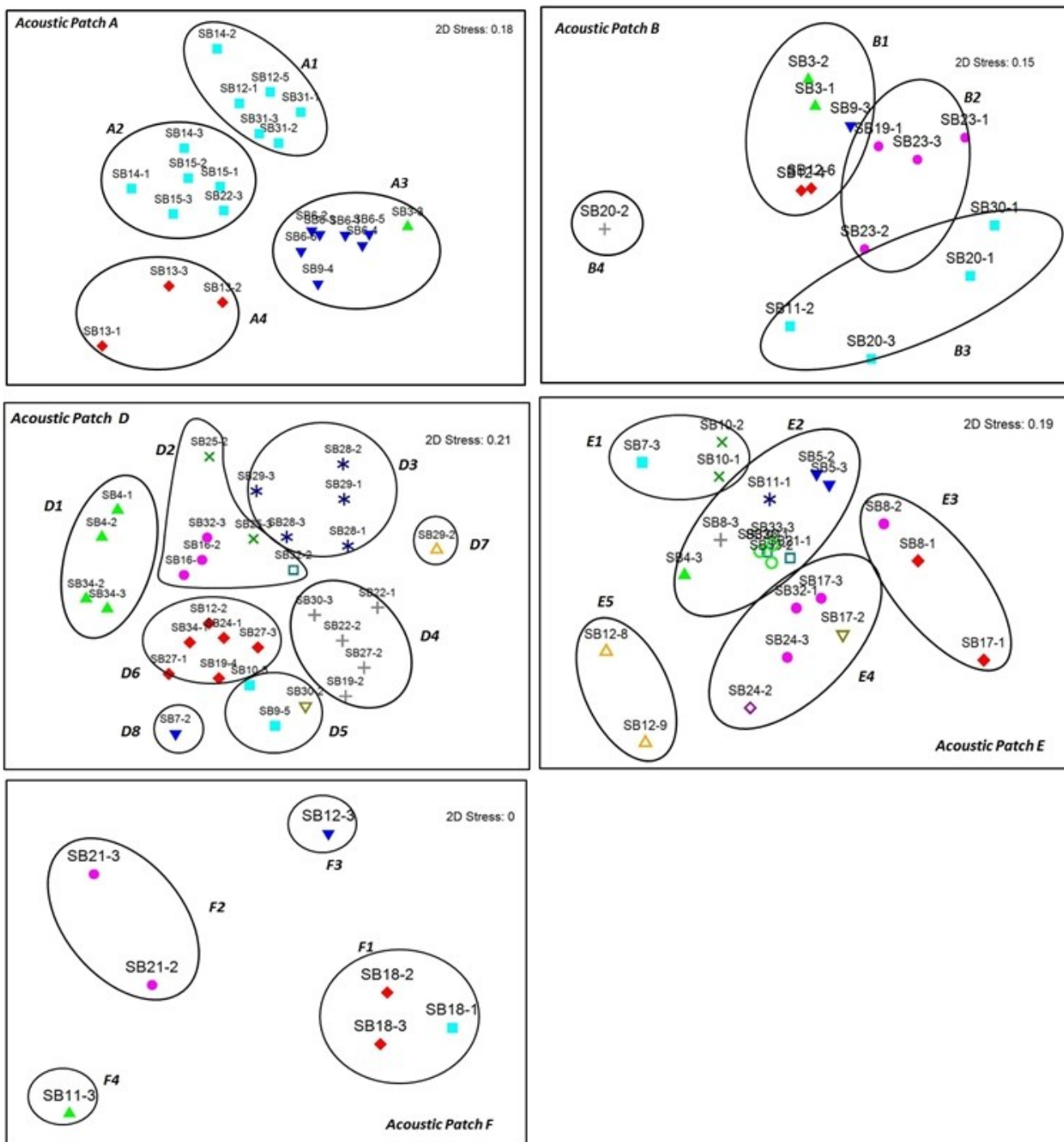


Figure 5.3-13. Results of within acoustic patch MDS analyses and sub-patch communities identified for October 2012 samples. Cluster analyses were also used to help identify within patch community types.

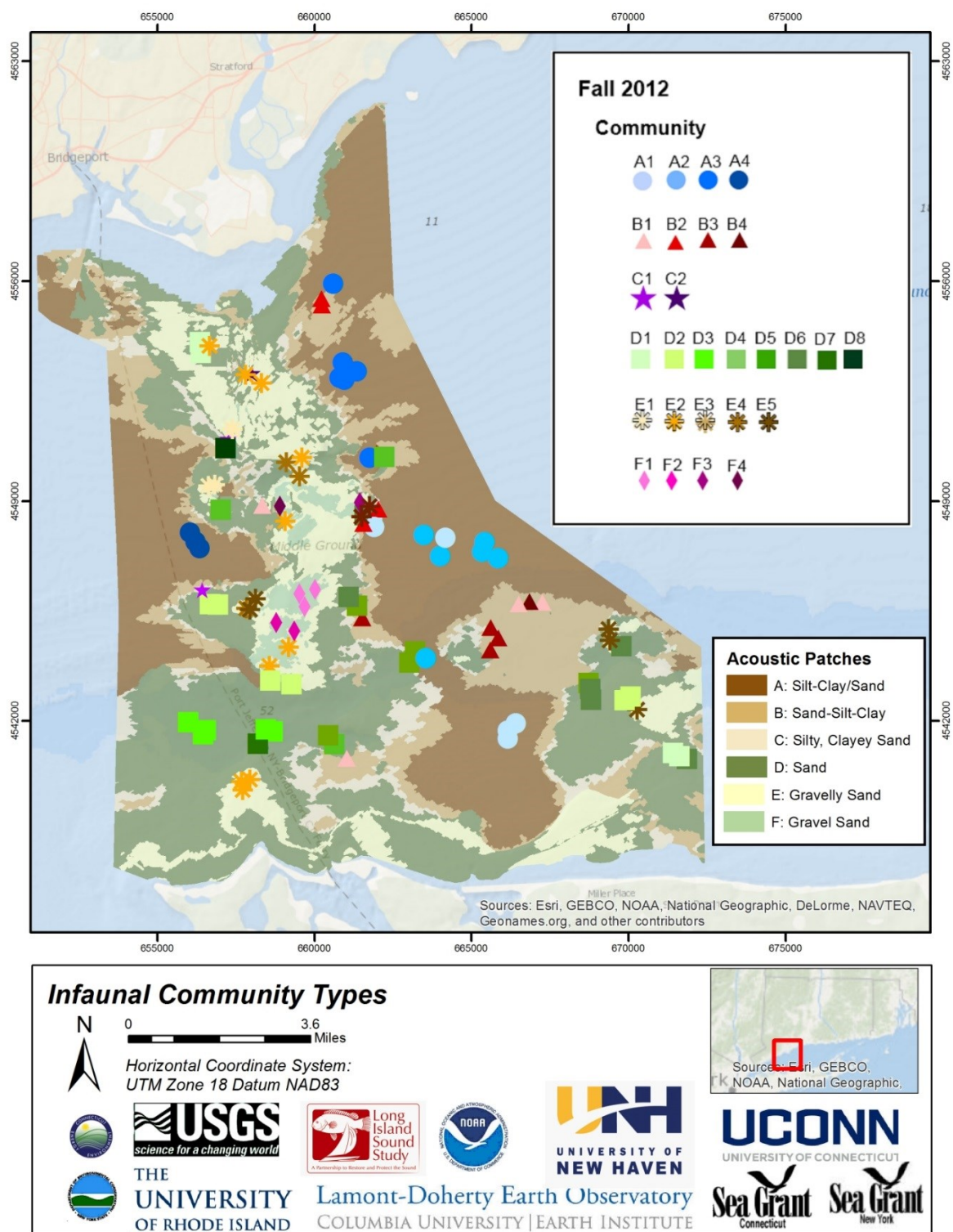


Figure 5.3-14. Spatial distribution of infaunal community types designated within acoustic patch types in the study area.

5.3.4 *Infaunal Community Characterization and Mapping – May 2013*

5.3.4.1 General Community Characteristics May 2013

In May 2013, infaunal total abundances varied considerably among the acoustic patch types, with significantly higher abundances in patch types E and F compared to A, B and C (Table 5.3-11, Figure 5.3-15). Very high abundances of oligochaetes and archiannelids were found in several samples in acoustic patch types E and F. When these taxa were excluded, abundances remained highly variable in these patches, and patch type F had the highest mean abundance across the study area. May 2013 total abundances at each sample site varied spatially across the pilot study area (Figure 5.3-16). Highest total abundance was along the transitions from one acoustic patch type to another primarily along the flanks of Stratford Shoal, and in the southeast section of the study area in an area of transition across acoustic patch types B, C and D. Moderate abundances (~ 100 -200 individuals 0.1 m^{-2}) were found across most areas of the study area in several acoustic patch types, and the lowest abundances in deeper water sections of acoustic patch types A.

Taxonomic richness exhibited a trend similar to total abundance with respect to acoustic patch types, with significantly higher mean taxonomic richness among patch type F and types A, and B (Table 5.3-11, Figure 5.3-15). There were several locations with high infaunal taxonomic richness (> 30 taxa 0.1 m^{-2}) along the flanks of, or directly on Stratford Shoal, in the southwest in a large patch of acoustic patch type D, and also in the southeast across a transition among patch types C and D (Figure 5.3-17). Moderate taxonomic richness (20-30 taxa 0.1 m^{-2}) was found in many areas of the study area and in different acoustic patch types, but many of these locations were in transition areas among acoustic patch types.

Mean Shannon diversity was similar among acoustic patch types (Figure 5.3-18), and there was no statistically significant difference among patch types (Table 5.3-11). Spatial variation across the study area was low, although there was a weak north to south gradient of lower to higher Shannon diversity across acoustic patch types (Figure 5.3-19). Likewise, there was no significant difference in Fishers diversity among the acoustic patch types, although higher levels were found in patch types C, D and F for both diversity indices, with similar levels among acoustic patch types A, B and E. Spatial variation in Fisher's diversity was somewhat more pronounced, although a weak north to south gradient was evident as well using this measure of sample diversity (Figure 5.3-20). Most high diversity locations were located along transitions among patch types.

Nested ANOVA was used to assess the relative variation in these community characteristics at different spatial scales by assessing differences at the SB level and at the acoustic patch level (Table 5.3-12). For total abundance there was a significant difference at the SB level when the full data set was used, but no significant differences at the SB level and a significant difference among acoustic patch types when oligochaetes and archiannelids were excluded. This difference

underscores the affect that extremely high abundant taxa can have on statistical comparisons when spatial differences are not taken into account. When these taxa were included the high variability at specific sampling blocks masked potential differences at this scale, and concurrently accentuated differences among acoustic patch types. When excluded differences at the SB were revealed and when taking into account variation at this scale, any differences among acoustic patch types were not statistically significant. Differences at the SB level were significant for taxonomic richness, Shannon diversity and Fisher's diversity, whereas differences among acoustic patch types were not statistically significant. This indicates a high level of smaller-scale, within acoustic patch type spatial variation at this time of the year. Such variation may be due to local differences in processes such as recruitment and population growth.

Table 5.3-11. Results of one way analysis of variance testing differences in community parameters among acoustic patch types for the May 2013 data set. Taxonomic richness and total abundance were logX +1 transformed to meet test assumptions. * Term significant at $\alpha = 0.05$. If significant, a Tukey-Kramer Multiple-Comparison Test was conducted to test differences among individual group means. These analyses were conducted in order to incorporate the additional samples that were taken in May 2013 that were not located in specific sampling blocks.

Total Abundance

Source Term	DF	Sum of Squares	Mean Square	F-Ratio	Prob Level	Power (Alpha=0.05)
Acoustic Patch	5	4.569542	0.9139085	6.75	0.000059*	0.996061
S(A)	54	7.310445	0.1353786			
Total (Adjusted)	59	11.87999				
Total	60					

Multiple Comparison Test

Group	Count	Mean	Different From Groups
A	27	2.057245	E, F
B	9	1.980079	E, F
C	3	1.886326	E, F
D	13	2.376223	
E	6	2.743997	A, B, C
F	2	2.945238	A, B, C

Species Richness

Source Term	DF	Sum of Squares	Mean Square	F-Ratio	Prob Level	Power (Alpha=0.05)
A: Acoustic Patch	5	0.8474497	0.1694899	4.40	0.001973*	0.950783
S(A)	54	2.081135	0.03853954			
Total (Adjusted)	59	2.928585				
Total	60					

Multiple Comparison Test

Group	Count	Mean	Different From Groups
A	27	1.28568	F
B	9	1.243214	F
C	3	1.312171	
D	13	1.447819	
E	6	1.510802	

F 2 1.768595 A, B

Shannon Diversity

Term	DF	Sum of Squares	Mean Square	F-Ratio	Prob Level	Power (Alpha=0.05)
A: Acoustic Patch	5	0.2738206	0.05476413	0.81	0.548660	0.267794
S(A)	54	3.65732	0.06772815			
Total (Adjusted)	59	3.931141				
Total	60					

Fisher's Diversity

Source	DF	Sum of Squares	Mean Square	F-Ratio	Prob Level	Power (Alpha=0.05)
A: Acoustic Patch	5	116.2201	23.24401	1.77	0.133907	0.565612
S(A)	54	707.715	13.10583			
Total (Adjusted)	59	823.9351				
Total	60					

Table 5.3-12. Results of nested one way analysis of variance testing differences in community parameters within sampling blocks and among acoustic patch types for the May 2013 data set. Taxonomic richness and total abundance were logX +1 transformed to meet test assumptions. All community metrics were tested using the full data set and after removing oligochaetes and archannelids from the data. In all cases except total abundance the results were the same only the ANOVA results excluding these taxa are presented for these metrics. Only data located within sampling blocks were used for these analyses. * Term significant at $\alpha = 0.05$. Tukey-Kramer multiple-comparison test assessed statistical differences among specific acoustic patches if ANOVA was significant.

Term	DF	Sum of Squares	Mean Square	F-Ratio	Prob Level	Power (Alpha=0.05)
Acoustic Patch	5	4.510557	0.9021114	9.76	0.002970*	0.982139
Nested: Sampling Block	8	0.7395155	0.09243944	0.70	0.690418	
S	29	3.840496	0.1324309			
Total (Adjusted)	42	9.090569				
Total	43					

Multiple Comparison Test – Acoustic Patch Type

Group	Count	Mean (log)	Different From Groups
A	17	2.159771	E
B	4	1.591956	D, E, F
C	1	2.004321	
D	13	2.376223	B
E	6	2.743997	A, B
F	2	2.945238	B

Total Abundance – archiannelids and oligochaetes excluded

Source	DF	Sum of Squares	Mean Square	F-Ratio	Prob Level	Power (Alpha=0.05)
Acoustic Patch	5	2.404786	0.4809572	1.88	0.204601	0.370149
Nested: Sampling Block	8	2.051793	0.2564741	2.69	0.024206*	
S	29	2.768126	0.09545263			
Total (Adjusted)	42	7.224705				
Total	43					

Taxonomic Richness	Sum of	Mean	Prob	Power
--------------------	--------	------	------	-------

Term	DF	Squares	Square	F-Ratio	Level	(Alpha=0.05)
Acoustic Patch	5	0.8726965	0.1745393	1.75	0.228996	0.347161
Nested: Sampling Block	8	0.7970166	0.09962708	3.76	0.003962*	
S	29	0.7693064	0.02652781			
Total (Adjusted)	42	2.439019				
Total	43					

Shannon Diversity		Sum of	Mean		Prob	Power
Term	DF	Squares	Square	F-Ratio	Level	(Alpha=0.05)
Acoustic Patch	5	0.7767351	0.155347	1.26	0.367670	0.254442
Nested: Sampling Block	8	0.9887249	0.1235906	2.36	0.042847*	
S	29	1.515715	0.05226604			
Total (Adjusted)	42	3.281175				
Total	43					

Fisher's Diversity		Sum of	Mean		Prob	Power
Term	DF	Squares	Square	F-Ratio	Level	(Alpha=0.05)
Acoustic Patch	5	221.0948	44.21895	1.65	0.251270	0.328462
Nested: Sampling Block	8	214.1235	26.76544	2.38	0.041878*	
S	29	326.4796	11.25792			
Total (Adjusted)	42	761.6979				
Total	43					

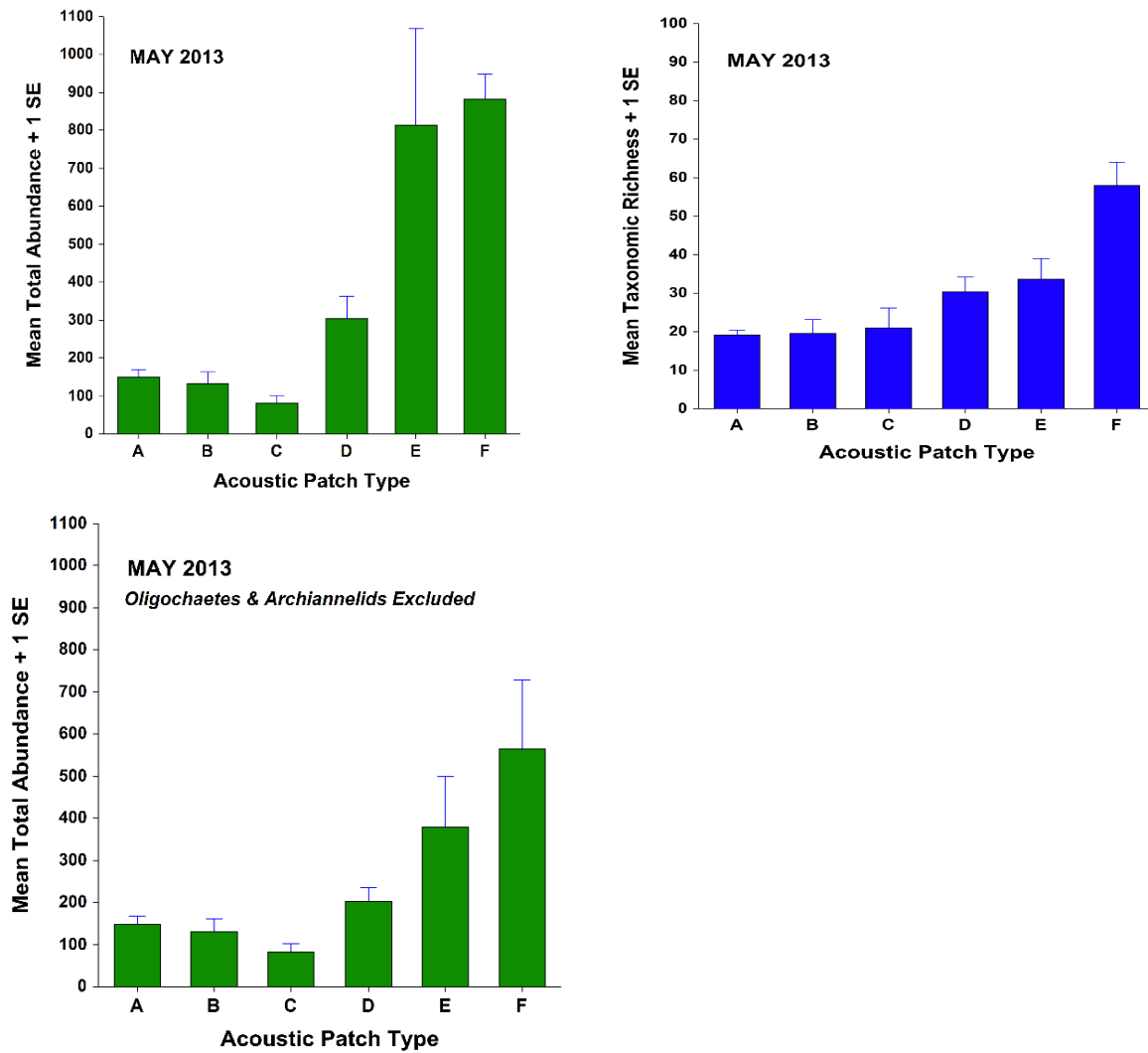


Figure 5.3-15. Mean total abundance and taxonomic richness (+1 standard error) per 0.1 m² in the acoustic patch types designated in the pilot study area. See text for details.

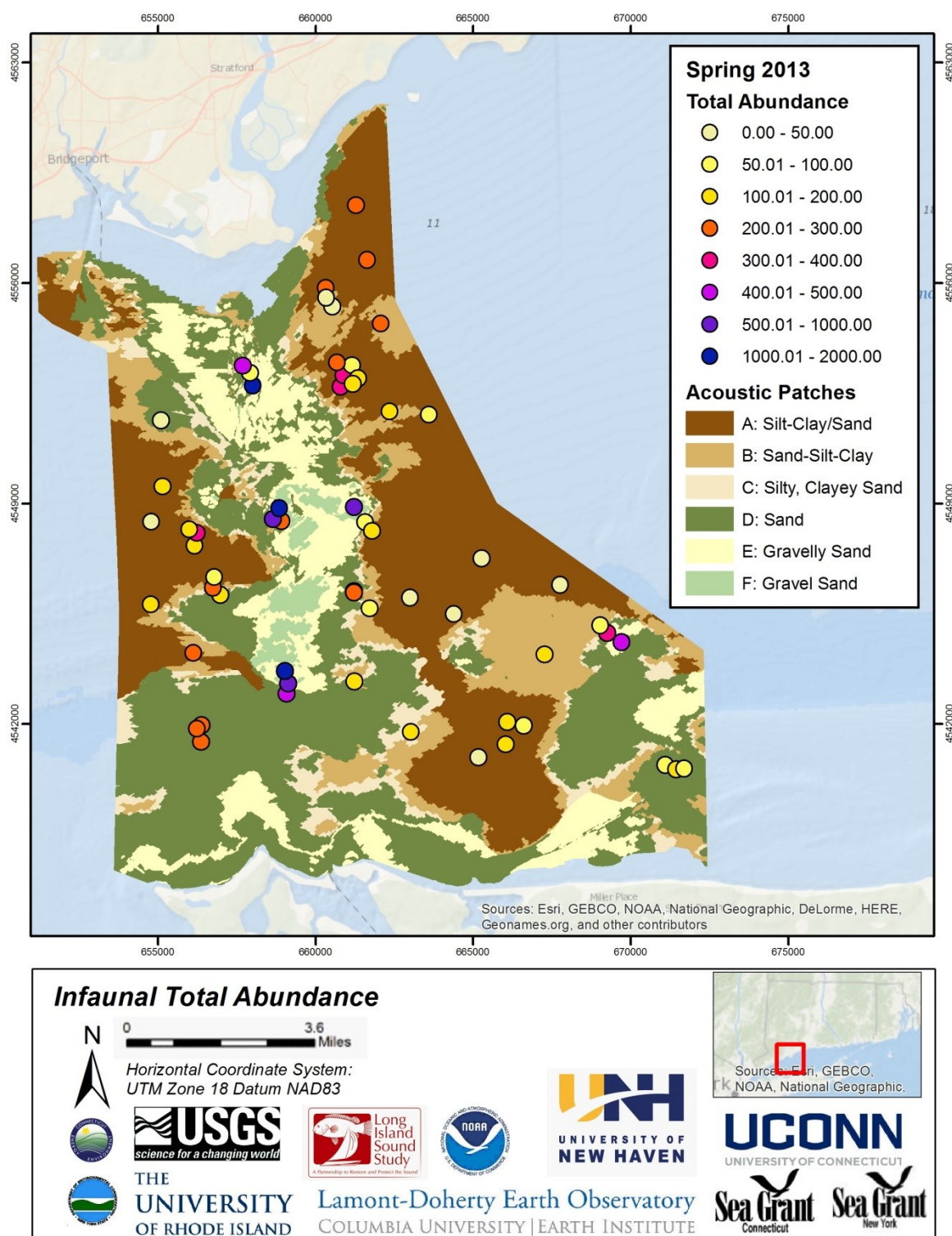


Figure 5.3-16. Total infaunal abundance per 0.1 m² in spring (May) 2013 samples in the pilot study area, all taxa included.

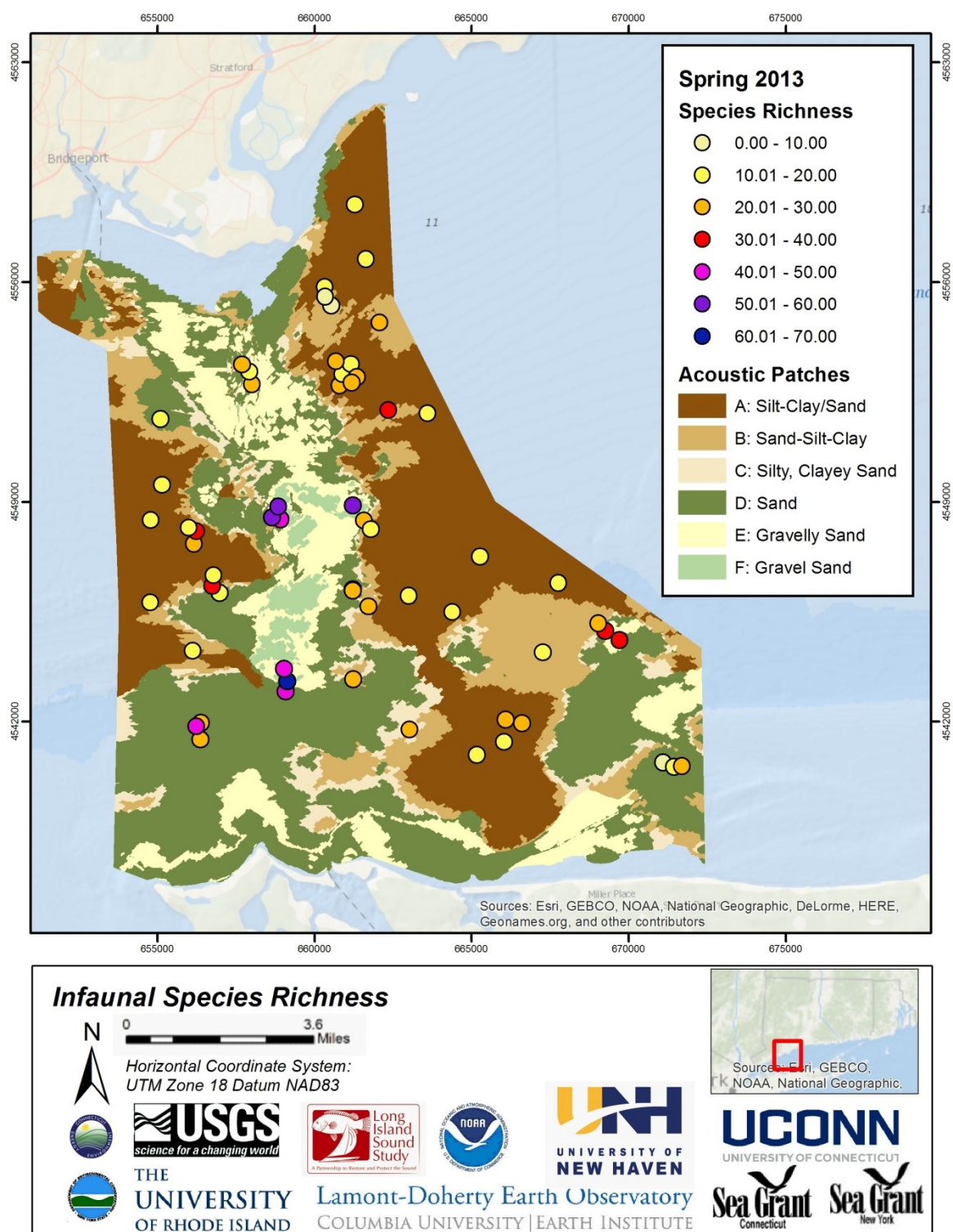


Figure 5.3-17 Infaunal species (taxonomic) richness in spring (May) 2013 samples in the pilot study area, all taxa included.

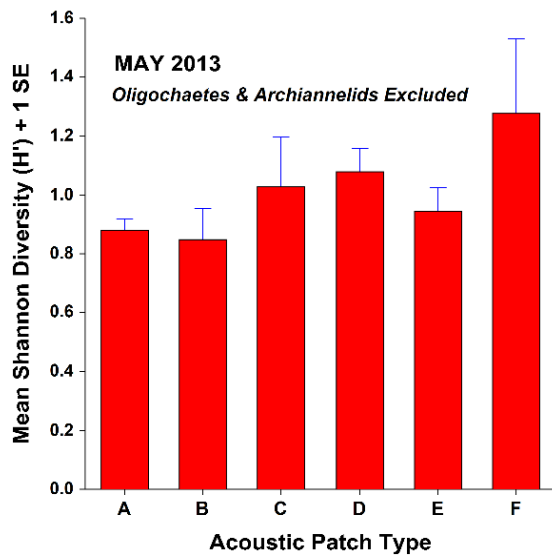
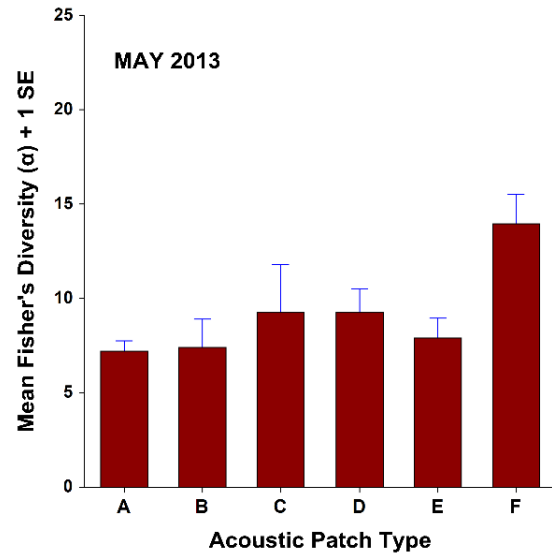
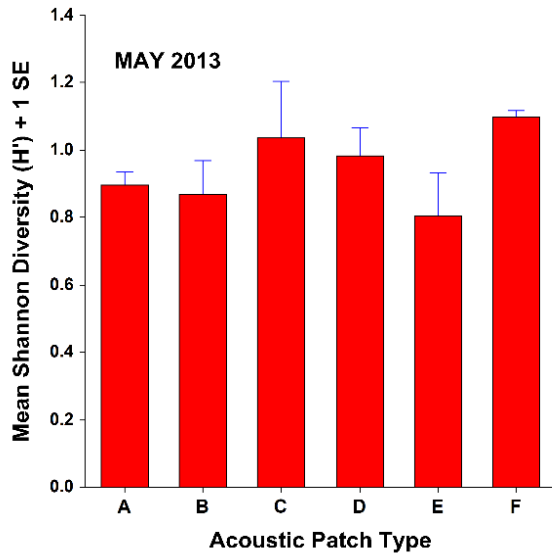


Figure 5.3-18. Differences in mean Shannon (left, top and bottom) and Fisher's (right) diversity (+1 standard error) among acoustic patch types in the pilot study area.

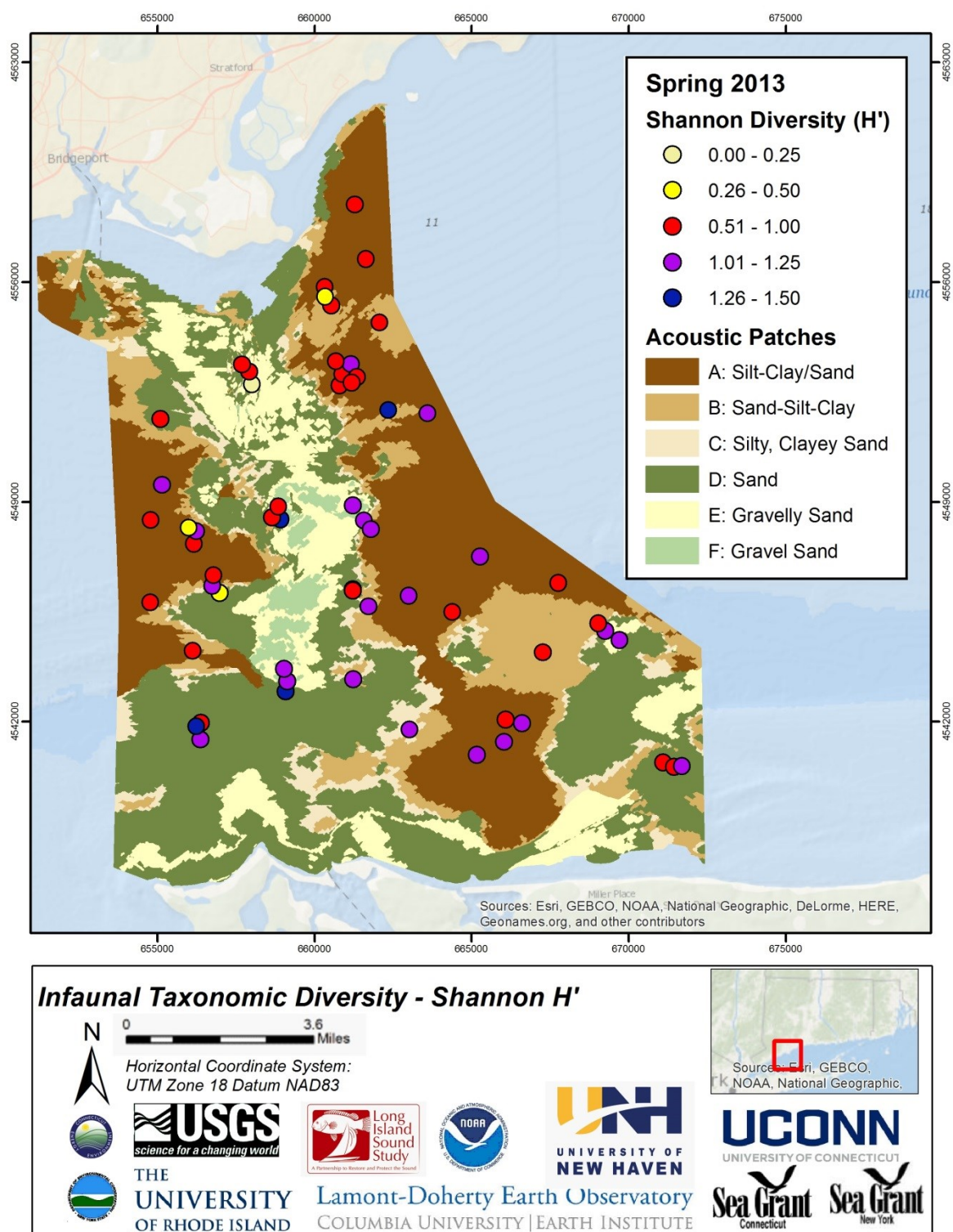


Figure 5.3-19. Infaunal Shannon species (taxonomic) diversity in spring (May) 2013 samples in the pilot study area. All taxa included.

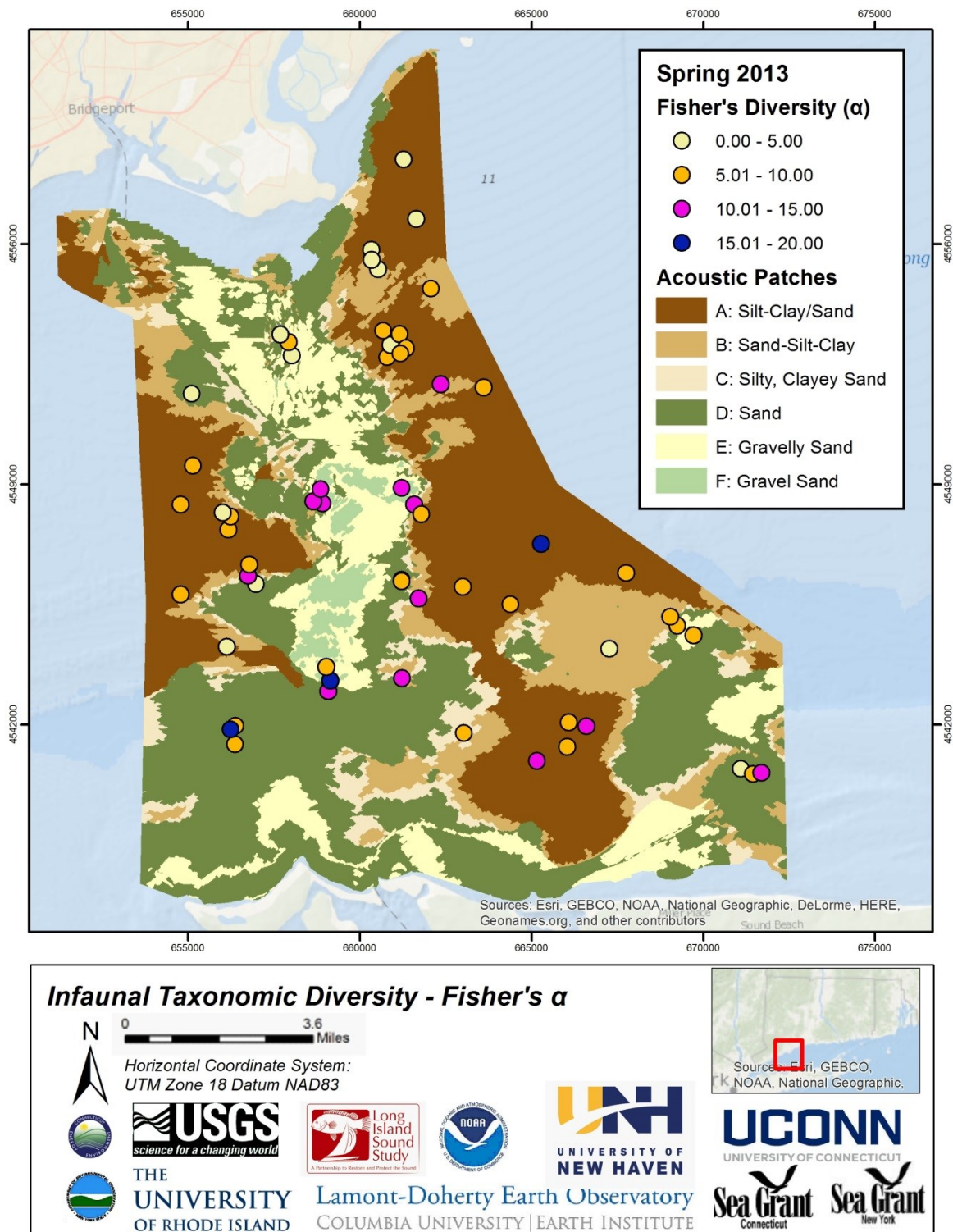


Figure 5.3-20. Infaunal Fisher's species (taxonomic) diversity in spring (May) 2013 samples in the pilot study area, all taxa included.

5.3.4.2: Community composition and characteristics, May 2013

Based on the results of classification analysis and MDS ordination (Figure 5.3-21), community structure at the sample locations in May 2013 was generally related to acoustic patch type, although communities in certain acoustic patch types were more variable than in others. Samples collected in acoustic patch types A and B were generally tightly clustered indicating relatively higher similarity in community structure. Communities in acoustic patch type C also were similar to patch types A and B. There was a clear separation among these acoustic patch types and patch types D, E and F. Within the latter group, samples taken in types D and E showed less relative community similarity than the A, B and C group (less distinct clustering and more separated in the ordination). Samples from acoustic patch type F were closely grouped. Dispersion measures indicate that acoustic patch types A and F had less variable community structure with increasing community variability in acoustic patch types C, B, E and D, respectively (Table 5.3-13). A CAP analysis indicates that community structure at sampling sites were strongly identified with acoustic patch types (Figure 5.3-22), with CAP1 and CAP2 axes correlations of 0.915 and 0.734, respectively.

Differences in community structure among acoustic patches in May 2013 were statistically significant based on multivariate permutation tests (Tables 5.3- 14 & 15). An ANOSIM test assessing differences among acoustic patch types and pairs of patch types indicated a highly significant difference among acoustic patch types and also among many of the pairs of patch types. A PERMANOVA test was conducted to take into account variation at the sampling block level in conjunction with testing among patch type differences. This test indicates that community differences were statistically significant at the smaller spatial scale of sampling blocks as well as at the patch scale. The pairwise tests reflect the results of the MDS and CAP ordinations, with significant differences between the A, B and C group of patch types and the D, E and F group.

Community structure also varied at the sampling block (SB) level, with a relatively wide separation of SBs in the ordination space (Figure 5.3-23). The SBs were grouped based on whether they found wholly within a patch, i.e. interiors, versus spanning several acoustic patch types (transitional). The variation found can be related to this difference, and an ANOSIM test indicated that there was a statistically significant difference in community structure among SBs located in the interior versus edges (transition zones) of patches ($R=0.246$; $p = 0.013$).

5.3.4.3 Characterizing Communities within Acoustic Patches May 2013

Community composition within each acoustic patch type for the May 2013 samples was assessed using a SIMPER analysis (Table 5.3-16). Community composition and relative numerical dominants were similar in acoustic patch types A, B and C, reflecting the multivariate analyses presented for the May 2013 samples. Acoustic patch type A communities were dominated by the bivalves *Nucula proxima* and *Yolida limatula*, the polychaetes *Nephtys incisa*, *Levinsonia gracilis* and *Sigambra tentaculata*. The tunicate *Bostrichobranchus pilularis* was also found in

moderate abundance. Acoustic patch type B communities had a similar mix of numerically dominant species although *Bostrichobranhus* had a much higher abundance whereas *Nucula* was found at lower abundances. More species accounted for the overall similarity among individual samples in patch type B than in A. Communities in acoustic patch type C were dominated by *Nephtys incisa*. *Sigambra tentaculata* and *Bostrichobranhus pilularis* were also found at relatively high abundances. In general, the community composition and dominants found in acoustic patch types A, B and C are typical for muddy, sandy-mud habitats of central and western Long Island Sound (Zajac 1998). The tunicate *Bostrichobranhus* was a seasonal dominant as well as several of the amphipod taxa.

Communities in acoustic patch type D were dominated by high abundances of archiannelids and oligochaetes, and relatively moderate abundances of *Bostrichobranhus pilularis*, amphipods including *Ampelisca abdita*, and *Leptocheirus pinguis*, and the polychaete *Nephtys incisa*. Several bivalves were also abundant including *Anadara transversa*, *Pitar morhuanna* and *Tellina agilis*. The large number of taxa contributing to overall similarity indicates a more complex set of communities in this acoustic patch type. Acoustic patch type E communities were similar to patch type D in terms of composition, but Archiannelids were very abundant as well as *Leptocheirus pinguis*. *Andara* and oligochaeteas were also found in high abundance. Moderate abundances were found of other amphipods as well as *Nephtys* and the ampharetid polychaete *Ampharete americana*. Acoustic patch type F communities were also similar in composition types D and E, but in this case amphipod taxa dominated, in particular *Ampelisca abdita* and the corophid *Leptocheirus pinguis*. The dominant polychaetes were *Ampharete* and the polynoid *Harmothoe extenuate*. The composition and abundances indicate that the communities in patch types D, E and F were dominated at this time by small tubicolous taxa, that often can form dense mats on the sea floor (e.g. amphipods), and by seasonal dominants such as the tunicate.

Only a limited analysis of community structure within acoustic patch types was possible since just a subset of sampling blocks were sampled in May 2013. There were only two samples taken in acoustic patch type C and only three in acoustic patch type F, and as such community types were not analyzed in these patch types. However, the analyses for the other acoustic patch types (Figure 5.3-24) do provide some measure of the variation of community structure within acoustic patch types at this time of the year (Figure 5.3-25), and how such variation may have changed seasonally with respect to the spatial distribution of communities across the patches comprising a specific acoustic patch type. Three community types were recognized in acoustic patch type A. Community type spA1 was distributed along the southeast portion of the study area in this patch type. Community type spA3 was found primarily in the northeast section of the pilot study area, although this community type was also found in the area just west of Stratford Shoal. Community type spA2 was found primarily on the western portion of the study area although a few sites were also found in on the eastern side of Stratford Shoal. Although fewer community types were found in this patch type in the spring, the general locations and spatial patterns of community groups are similar to that found October 2012 (Figure 5.3-14), suggesting relatively

consistent within-patch type variability among fall and spring in this acoustic patch type. Three community types were also found for acoustic patch type B, although two of these were comprised of single samples. The most samples were found to be of the type spB1 and these were distributed throughout the study area, indicating that community structure in acoustic patch type B was fairly consistent at this time across the individual areas making up acoustic patch type B. The two differing communities, spB2 and spB3 were found next to each other in an area in the north section of the study area, indicating relatively high variation in community structure over a short distance at least in this acoustic type B patch. For acoustic patch type D, three separate communities were recognized, and these were fairly consistent spatially. Community type spD1 was found only in the southeast corner of study area, type spD2 was found in the southwest section the study area, whereas samples comprising community type spD3 were found distributed across all of Stratford Shoal from its northern to southern extent. Communities in acoustic patch type E were also fairly spatially consistent with type spE3 primarily in the southeast section of this study area and at the southern limit of Stratford Shoal, whereas the other spE type communities were found on Stratford Shoal itself. Overall, although limited, a comparison to the distribution of community types within acoustic patch types for the October 2012 (fall) data suggest that spatial differences in community types within the various acoustic patches may remain relatively consistent from fall to spring in the pilot study area. (Figure 5.3-30).

Table 5.3-13. Multivariate dispersion of infaunal communities within acoustic patch types and the Index of Multivariate Dispersion (IMD) among acoustic patches in the LIS pilot study area for May 2013. Dispersion is a measure of the variation among communities and IMD contrasts the average rank of similarities among samples of a certain acoustic patch class with the average rank of other classes (Clarke and Warwick, 2001). The greater the relative variability among acoustic patches, the closer the IMD is to -1. Similarities calculated using the Bray-Curtis resemblance function on square root transformed data.

Global Analysis

<u>Factor value</u>	<u>Dispersion</u>
F	0.412
A	0.907
C	1.088
B	1.238
E	1.317
D	1.334

Pairwise Comparisons

<u>Factor values</u>	<u>IMD</u>
B, A	0.316
B, E	-0.052
B, D	-0.016
B, F	0.611
B, C	0.185

A, E	-0.399
A, D	-0.437
A, F	0.519
A, C	-0.217
E, D	0.067
E, F	0.867
E, C	0.289
D, F	0.909
D, C	0.424
F, C	-1

Table 5.3-14. Results of ANOSIM analysis testing infaunal community differences among acoustic patches in May 2013 samples. Similarities calculated using the Bray-Curtis resemblance function on square root transformed data. Global test based on 999 random permutations of the data; most pairwise tests were also based on 999 permutations, but some were less depending on number of samples in the acoustic class patches being compared.

Global Test

Sample statistic (Global R): 0.369

Significance level of sample statistic: 0.001%

Pairwise Tests

Groups	R Statistic	Significance Level %
B, A	0.131	0.1
B, E	0.328	0.004
B, D	0.199	0.01
B, F	0.237	0.255
B, C	-0.194	0.777
A, E	0.718	0.001
A, D	0.534	0.001
A, F	0.721	0.007
A, C	-0.054	0.542
E, D	0.015	0.397
E, F	-0.344	0.964
E, C	0.321	0.083
D, F	-0.185	0.681
D, C	0.206	0.174
F, C	1	0.1

Table 5.3-15. Results of permutational multivariate analysis of variance (PERMANOVA) for differences among acoustic patches with sampling blocks (SB) nested with acoustic patches for May 2013 samples. The analysis tests “the simultaneous response of one or more variables to one or more factors in an ANOVA experimental design on the basis of any distance measure, using permutation methods” (Anderson 2005). The analysis was based on a Type III (partial) sums of squares and 999 permutations of residuals under a reduced model. Ac = Acoustic Patch; Sa = Sampling Block.

PERMANOVA Table

Source	df	SS	MS	Pseudo-F	P(perm)
Ac	5	29556	5911.2	2.0734	0.003
Sa(Ac)	21	69694	3318.8	1.7036	0.001
Res	33	64288	1948.1		
Total	59	1.6985E5			

Pair wise tests for Acoustic Patches

Groups	t	P- permutational
B, A	1.0527	0.353
B, E	1.4443	0.057
B, D	1.2626	0.097
B, F	1.3673	0.068
B, C	0.7607	0.838
A, E	2.15	0.002
A, D	2.0938	0.001
A, F	1.8663	0.025
A, C	0.77247	0.759
E, D	0.78708	0.836
E, F	0.75231	0.937
E, C	1.3978	0.061
D, F	0.92138	0.552
D, C	1.2488	0.132
F, C	1.7024	0.362

Table 5.3-16. Results of similarity percentage analysis (SIMPER) for acoustic patch type communities for MAY 2013 samples. Table shows the percent contribution of each species to the total similarity within each community type. Av.Abund = average abundance per 0.1 m² sample; Av.Sim = average similarity among replicates at the site; Sim/SD = Similarity standard deviation; Contrib% = percent contribution to within site similarity; Cum.% = cumulative similarity.

Acoustic Patch Type A; Average similarity: 29.04

Species	Av.Abund	Av.Sim	Sim/SD	Contrib%	Cum.%
<i>Nucula proxima</i>	62.63	9.85	0.57	33.93	33.93
<i>Nephtys incisa</i>	13.93	5.99	1.13	20.63	54.56
<i>Sigambra tentaculata</i>	6.85	1.92	0.79	6.61	61.16
<i>Levinsenia gracilis</i>	8.26	1.78	0.54	6.12	67.29
<i>Yoldia limatula</i>	10.37	1.43	0.59	4.94	72.23
<i>Acteocina canaliculata</i>	4.74	1.27	0.93	4.39	76.61
<i>Bostrichobranchus pilularis</i>	4.22	1.06	0.44	3.65	80.27
<i>Phoronis</i> spp.	2.96	0.76	0.68	2.62	82.88
<i>Pitar morhuanna</i>	3.44	0.74	0.57	2.55	85.44
<i>Nephtys</i> spp.	2.48	0.63	0.47	2.16	87.6
<i>Amphitrite</i> spp.	1.37	0.56	0.69	1.92	89.52
<i>Pinnixia sayanna</i>	1.67	0.46	0.35	1.59	91.12

Acoustic Patch Type B: Average similarity: 16.81

Species	Av.Abund	Av.Sim	Sim/SD	Contrib%	Cum.%
<i>Nephtys incisa</i>	12.78	2.85	0.89	16.96	16.96
<i>Nucula proxima</i>	30.11	2.56	0.35	15.25	32.21

<i>Bostrichobranchnus pilularis</i>	18.11	2.3	0.32	13.66	45.87
<i>Sigambra tentaculata</i>	8.56	1.12	0.54	6.67	52.54
<i>Acteocina canaliculata</i>	3.67	0.99	0.69	5.92	58.46
<i>Levinsenia gracilis</i>	10.11	0.91	0.45	5.39	63.85
<i>Mulinia lateralis</i>	3	0.75	0.81	4.45	68.29
<i>Amphitrite</i> spp	2.11	0.68	0.63	4.04	72.33
<i>Ampelisca abdita</i>	1.44	0.58	0.96	3.44	75.77
<i>Turbonilla elegantula</i>	2.56	0.45	0.42	2.66	78.42
<i>Yoldia limatula</i>	4.33	0.41	0.49	2.47	80.89
<i>Unciola irroata</i>	2.22	0.41	0.37	2.45	83.34
<i>Pitar morhuanna</i>	3.11	0.33	0.34	1.94	85.28
Oligochaeta	1.44	0.26	0.49	1.52	86.8
<i>Asychis elongata</i>	1.44	0.23	0.58	1.39	88.19
<i>Nephtys</i> spp.	1.11	0.23	0.38	1.36	89.54
<i>Owenia fusiformis</i>	1	0.2	0.36	1.17	90.72

Acoustic Patch Type C: Average similarity: 21.67

Species	Av.Abund	Av.Sim	Sim/SD	Contrib%	Cum.%
<i>Nephtys incisa</i>	14.33	8.33	1.15	38.46	38.46
<i>Sigambra tentaculata</i>	6	1.96	0.58	9.05	47.51
<i>Owenia fusiformis</i>	1.67	1.58	4.78	7.29	54.81
<i>Nucula proxima</i>	8.33	1.37	0.58	6.32	61.13
<i>Bostrichobranchnus pilularis</i>	5.33	1.31	0.58	6.03	67.16
<i>Amphitrite</i> spp	1.67	1.25	5.29	5.78	72.94
<i>Yoldia limatula</i>	2	1.25	5.29	5.78	78.73
<i>Acteocina canaliculata</i>	4.33	0.65	0.58	3.02	81.74
Nemertea	1.67	0.65	0.58	3.02	84.76
<i>Gilvossius setimanus</i>	1	0.47	0.58	2.17	86.93
<i>Mulinia lateralis</i>	1	0.47	0.58	2.17	89.09
<i>Nephtys</i> spp.	2	0.47	0.58	2.17	91.26

Acoustic Patch Type D: Average similarity: 15.94

Species	Av.Abund	Av.Sim	Sim/SD	Contrib%	Cum.%
Archiannelida	75.15	2.78	0.34	17.44	17.44
Oligochaeta	27	2.1	0.53	13.19	30.64
<i>Nephtys incisa</i>	12.08	1.73	0.83	10.85	41.49
<i>Bostrichobranchnus pilularis</i>	22.15	1.38	0.25	8.68	50.17
<i>Tellina agilis</i>	14.31	1.18	0.41	7.41	57.58
<i>Leptocheirus pinguis</i>	12.77	0.9	0.55	5.63	63.21
<i>Ampharete americana</i>	7.15	0.46	0.41	2.9	66.11
<i>Pitar morhuanna</i>	5.92	0.45	0.4	2.8	68.91
<i>Ampelisca</i> spp.	7	0.39	0.47	2.43	71.34
<i>Ampelisca abdita</i>	11.85	0.34	0.25	2.14	73.48
<i>Paradoneis lyra</i>	6.08	0.32	0.3	1.98	75.46
<i>Spiophanes bombyx</i>	3.54	0.25	0.49	1.57	77.03
<i>Anadara transversa</i>	6.77	0.25	0.36	1.55	78.58
<i>Unciola irroata</i>	4.85	0.23	0.33	1.41	79.99
<i>Amphitrite</i> spp	1.62	0.2	0.39	1.25	81.24
Mollusca	1.62	0.2	0.39	1.23	82.47
<i>Naissarius trivitattus</i>	3	0.19	0.43	1.22	83.69
<i>Pinnixia sayanna</i>	2.15	0.19	0.37	1.21	84.9

<i>Levinsenia gracilis</i>	2.38	0.17	0.27	1.05	85.95
<i>Sigambra tentaculata</i>	1.92	0.17	0.39	1.04	86.99
<i>Nephtys picta</i>	4.38	0.16	0.24	1.01	88
<i>Lyonsia hyalina</i>	1.38	0.14	0.65	0.9	88.9
<i>Nephtys</i> spp.	3.54	0.14	0.27	0.88	89.78
<i>Aricidia</i> spp.	1.46	0.12	0.53	0.76	90.54

Acoustic Patch Type E Average similarity: 16.04

Species	Av.Abund	Av.Sim	Sim/SD	Contrib%	Cum.%
Archiannelida	375.83	4.99	0.44	31.08	31.08
<i>Leptocheirus pinguis</i>	67.33	4.11	0.45	25.6	56.68
Oligochaeta	59.5	2.04	0.86	12.73	69.4
<i>Ampelisca abdita</i>	45.83	1.12	0.44	6.98	76.39
<i>Tellina agilis</i>	9.67	0.56	0.61	3.47	79.86
<i>Nephtys incisa</i>	6.5	0.42	0.49	2.62	82.48
<i>Anadara transversa</i>	40.17	0.33	0.51	2.08	84.56
<i>Pinnixia sayanna</i>	4	0.27	0.81	1.66	86.22
<i>Ampharete americana</i>	6.17	0.22	0.71	1.38	87.6
<i>Paradoneis lyra</i>	6.33	0.21	0.39	1.33	88.94
<i>Panopeus herbstii</i>	2.67	0.15	0.62	0.94	89.88
<i>Owenia fusiformis</i>	3	0.14	0.35	0.89	90.77

Acoustic Patch Type F - Average similarity: 29.33

Species	Av.Abund	Av.Sim	Contrib%	Cum.%
Archiannelida	152.5	8.61	29.34	29.34
<i>Ampelisca abdita</i>	145.5	3.74	12.74	42.08
<i>Anadara transversa</i>	36.5	2.83	9.65	51.74
<i>Nephtys picta</i>	16.5	1.81	6.18	57.92
Oligochaeta	164.5	1.47	5.02	62.93
<i>Paradoneis lyra</i>	14	1.36	4.63	67.57
<i>Spiophanes bombyx</i>	12	1.13	3.86	71.43
<i>Ampharete americana</i>	11.5	1.02	3.47	74.9
<i>Harmothoe extenuata</i>	15.5	0.91	3.09	77.99
<i>Lyonsia hyalina</i>	11	0.91	3.09	81.08
<i>Nephtys incisa</i>	6.5	0.68	2.32	83.4
<i>Leptocherius pinguis</i>	94.5	0.57	1.93	85.33
<i>Pitar morhuanna</i>	7.5	0.57	1.93	87.26
<i>Mytilus edulis</i>	10	0.45	1.54	88.8
<i>Acmira catherinae</i>	4.5	0.34	1.16	89.96
<i>Ampelisca</i> spp.	4	0.23	0.77	90.73

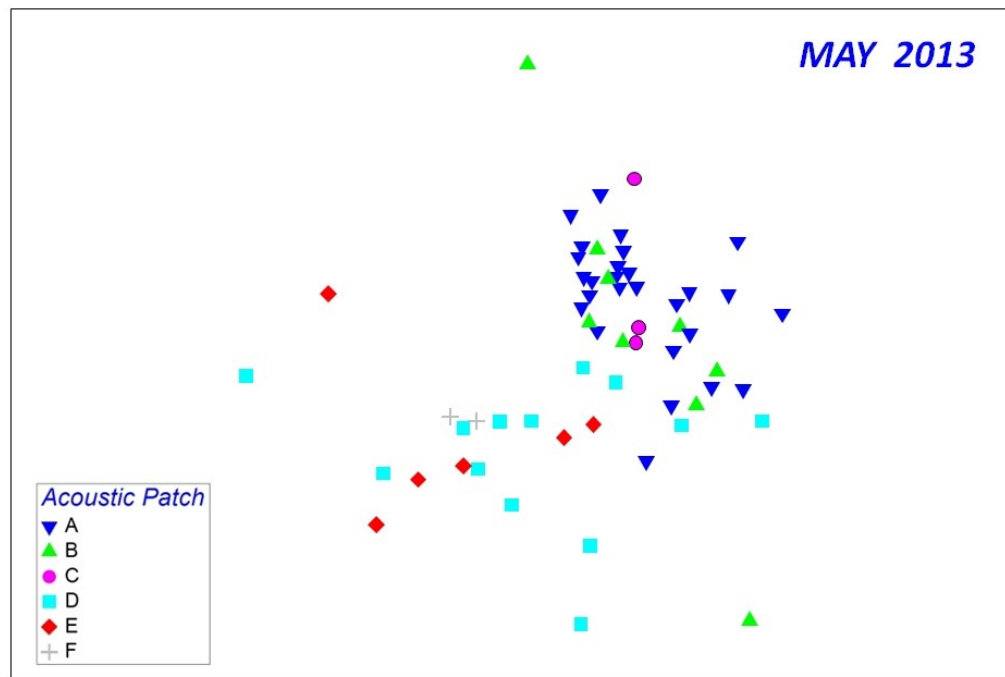
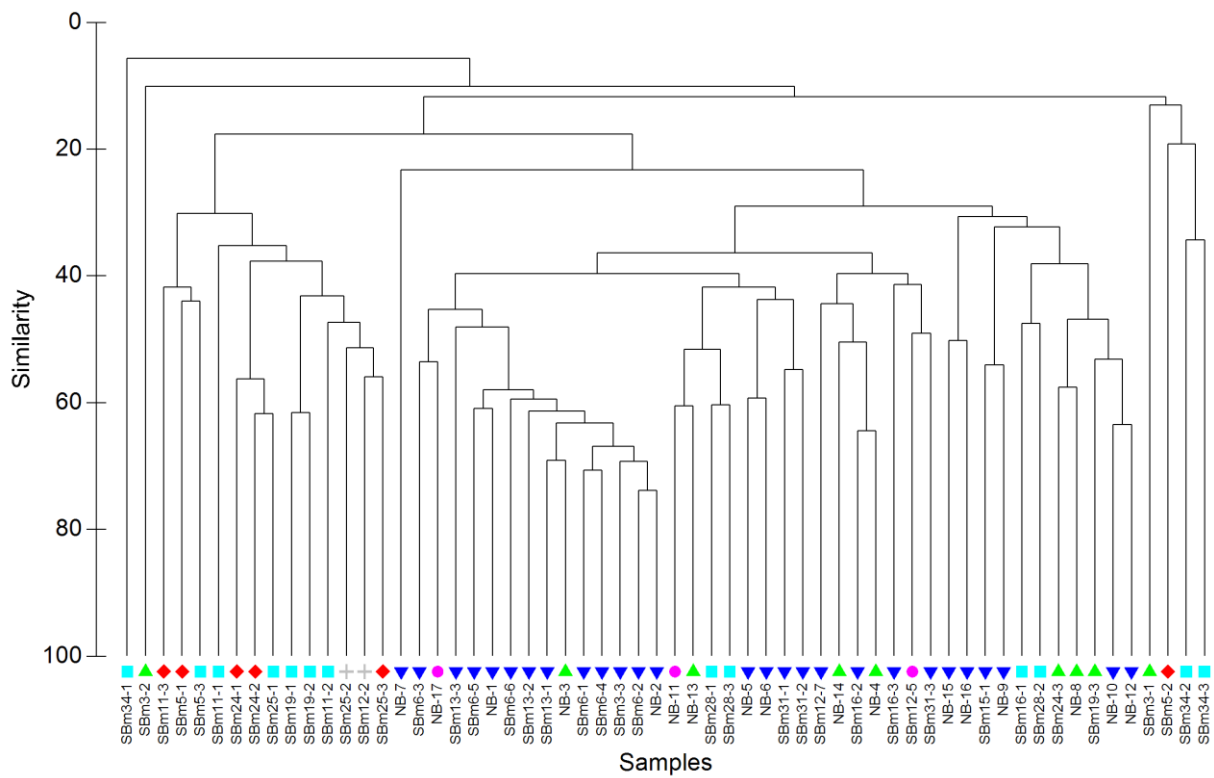


Figure 5.3-21. Classification (top) and MDS ordination (bottom) of benthic infaunal samples from spring (May) 2013 samples from the pilot study area, using the full data set. Acoustic Patch key is same for both plots.

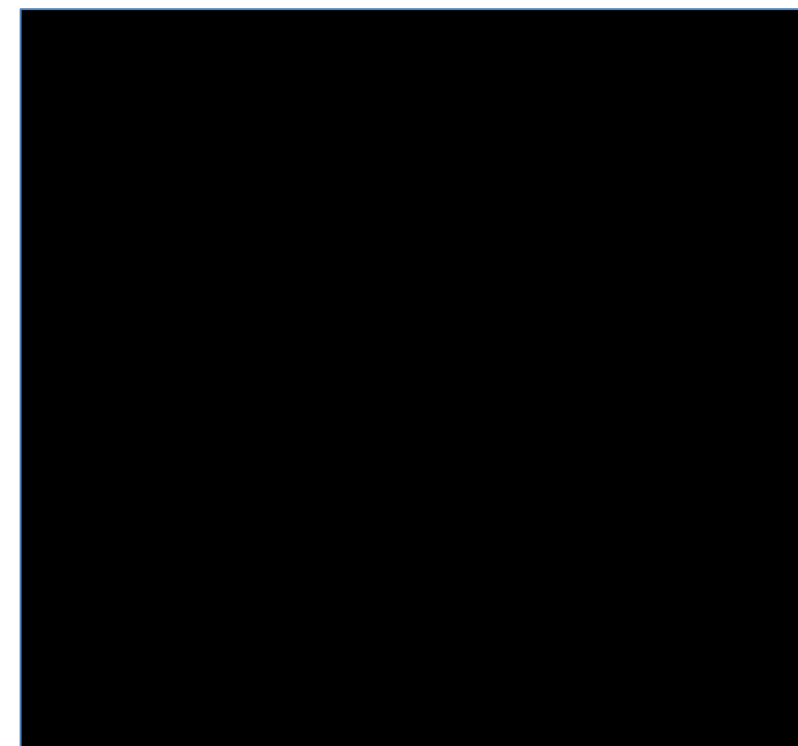
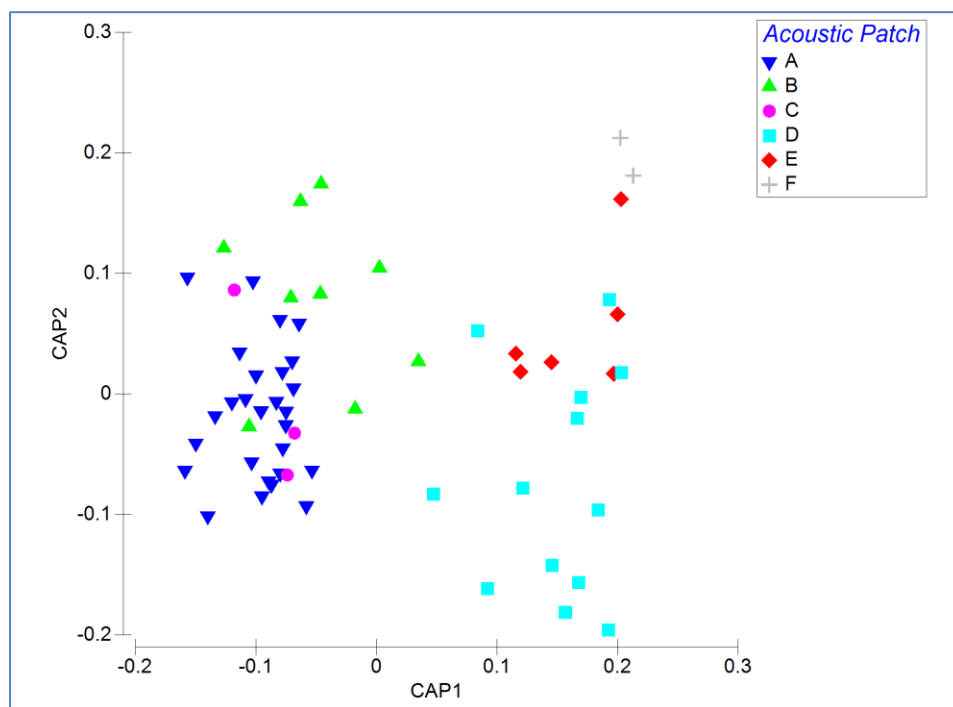


Figure 5.3-22. Top- Results of CAP ordination on infaunal community based on May 2013 samples. Bottom - Species correlations with ordination axes; species selected by dominance and functional type. These correlations indicate which species are most most related to the sample separation in the ordination.

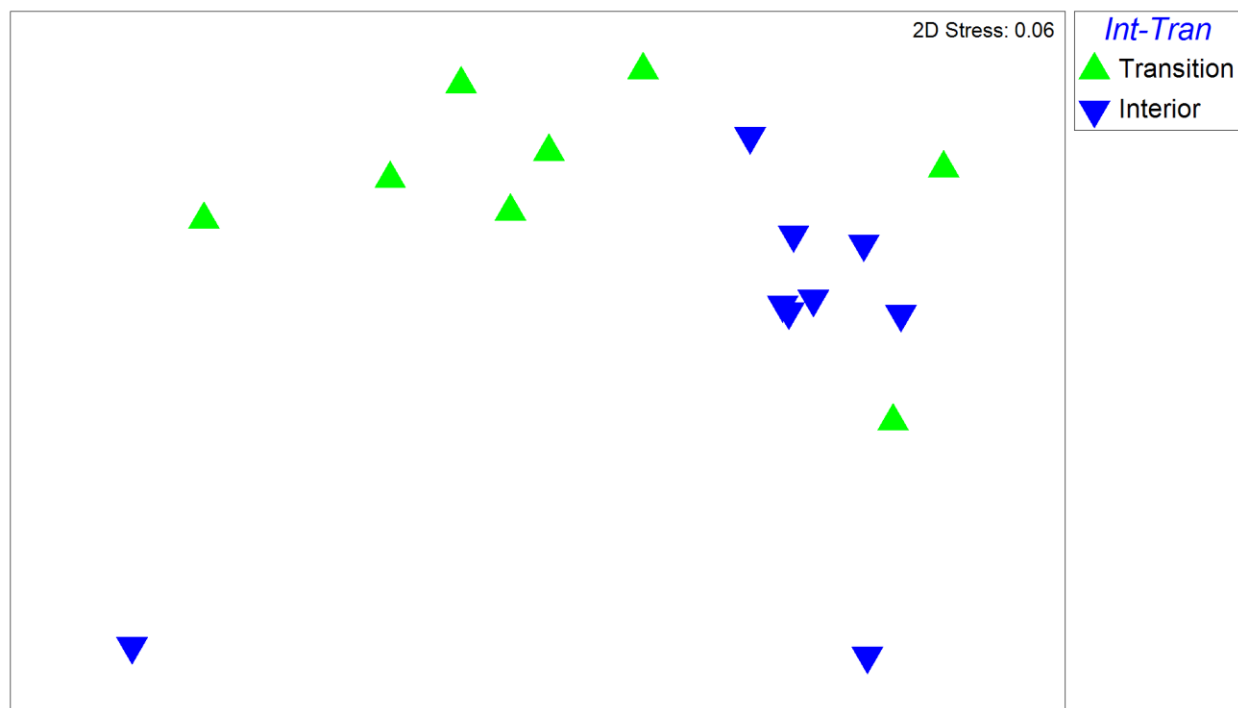


Figure 5.3-23. Results of MDS ordination of community structure based on averaging at the sampling block (SB) level. SBs are differentiated whether they were located wholly within a specific acoustic patch type (Interior) or spanned several acoustic patch types (Transition). Additional May 2013 samples were included in this analysis; these were all interior samples and designated by general blocks depending on location in the study area.

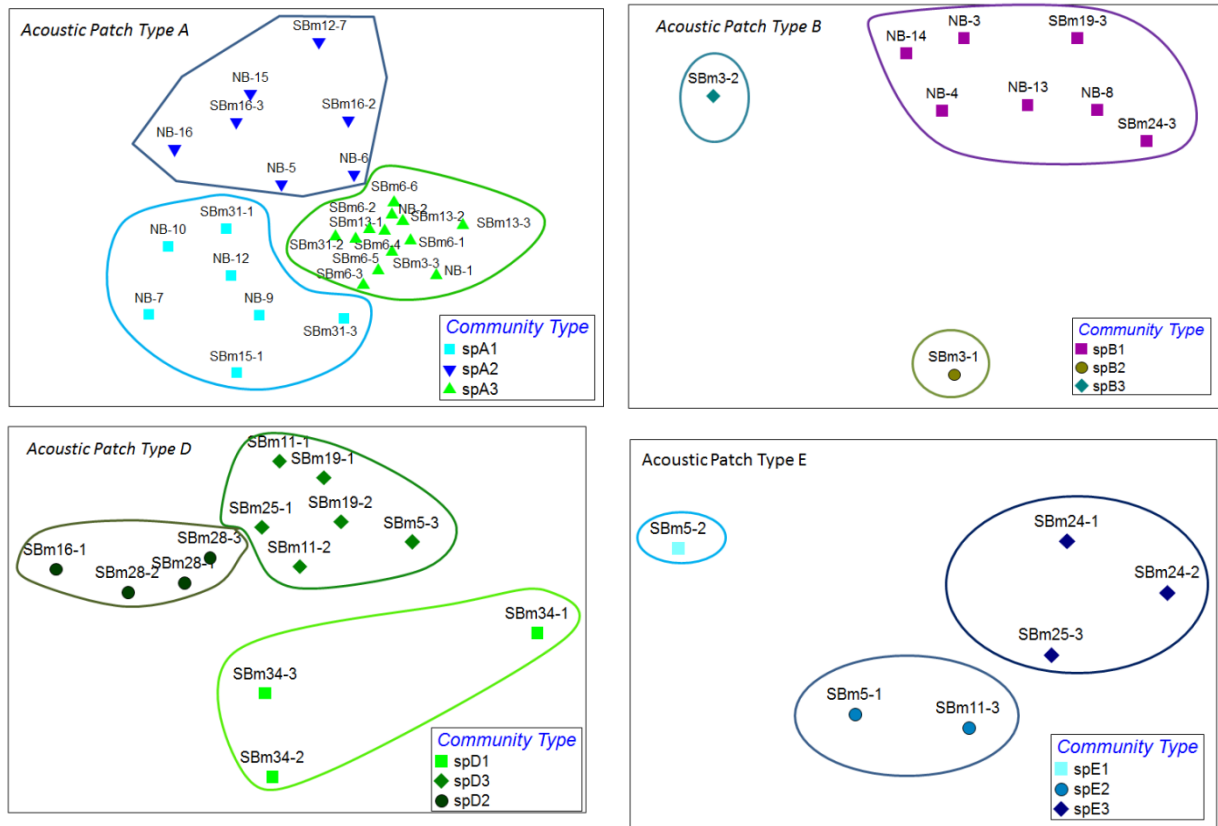


Figure 5.3-24. Results of within acoustic patch MDS analyses and sub-patch communities identified for the May 2013 data set. Cluster analyses were also used to help identify within patch community types.

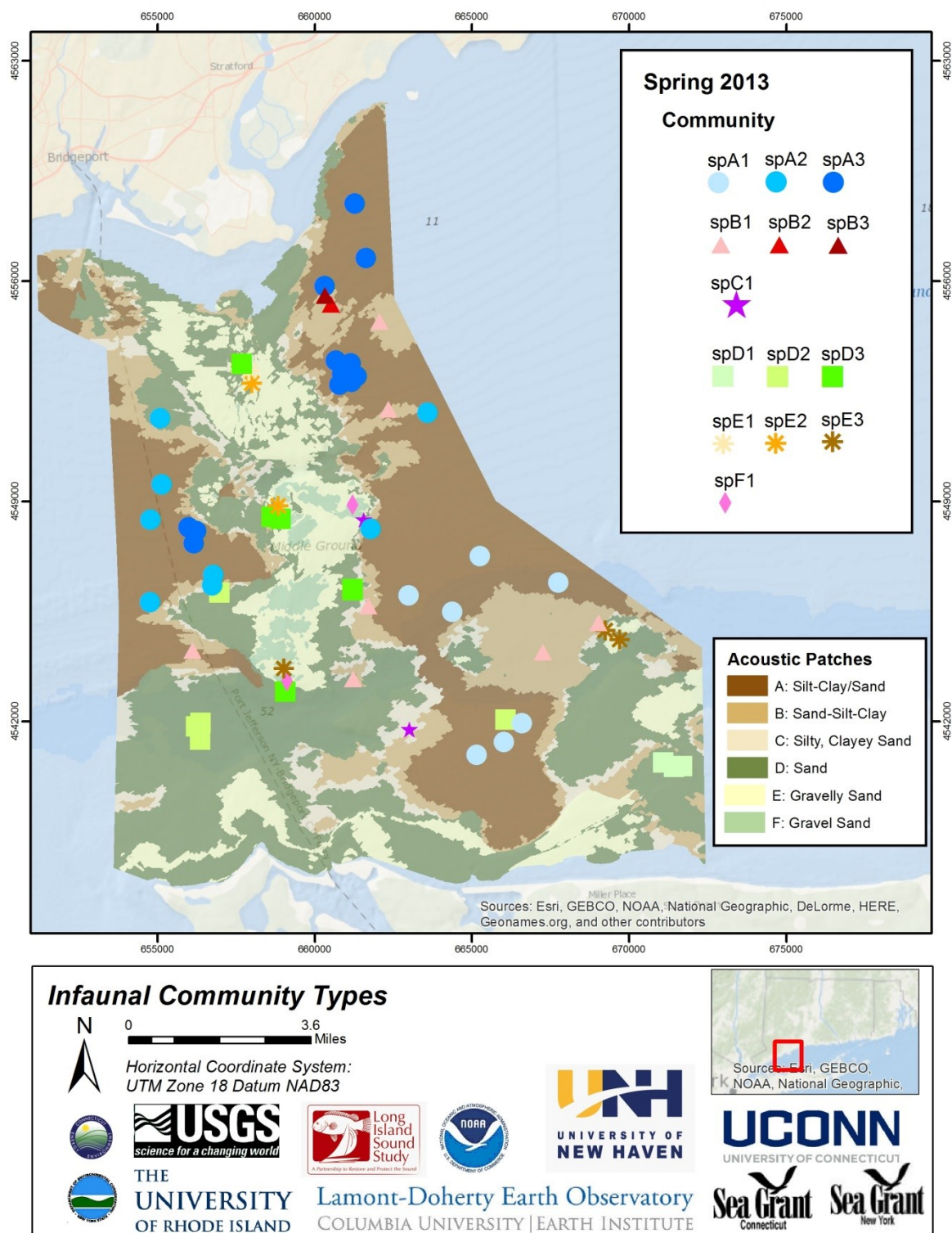


Figure 5.3-25. Spatial distribution of infaunal community types designated within acoustic patch types in the study area in May 2013. The community designations (A1, A2, etc.) do not correspond to the community types shown for the October 2012 (Fall)

5.3.5 *Seasonal Changes in Infaunal Communities – Fall 2012 and Spring 2013*

The fall 2012 and spring 2013 data sets provide the opportunity to assess temporal variation of infaunal communities in the pilot study area relative to sea floor habitat structure, at least on a seasonal fall to spring cycle. The sampling efforts differed between research cruises and only a subset of the SBs sampled in October 2012 were also sampled in May 2013. Also, a set of single samples were taken in additional areas of acoustic patch types A and B in May 2013 to provide broader spatial coverage in the sampling of these patch types given the large overall area several individual patches of these types occupy (Figure 5.2-1). This also allows some assessment of how sampling effort may affect trends in community characteristics.

Total abundance was significantly different among fall 2012 and spring 2013 when the full data sets from both sampling periods were used (Table 15.3–17), however there was no significant difference among dates when just SBs sampled in both periods were used in the analysis. In this case there was also a significant interaction between date and acoustic patch, indicating that date differences were significant for some set of SBs. In both analyses differences among acoustic patch types were statistically significant. The difference in the statistical results with respect to date may be due to the sampling effort in different acoustic patch types during each sampling period. In May 2013, many more samples were taken in acoustic patch types A and B than in the other patch types. As such, differences among dates in acoustic patch type A were may have been less variable due to sampling effort. Overall, there were much higher abundances in acoustic patch types D, E and F in May 2013, whereas the temporal differences in acoustic patch types A, B and C differed depending on the data set used (Figure 5.3-26). When SBs sampled only in both seasons were used in the analysis, the difference for acoustic patch type B was much greater as well as for patch types E and F. When individual sampling blocks were compared it is apparent that seasonal differences were quite varied among the individual sampling blocks, with some showing much higher abundances in May 2013, some higher in October 2012, while others showed little change (Figure 5.3-26). Of note also is the high variability associated with many of the means indicating large, local/small-scale differences in abundance, particularly for the May 2013 data. This suggests spring / early summer population dynamics for different sets of species are operating at smaller and varying spatial scales, such as localized recruitment, and in turn may be a cause of the high level of variation in total abundance in May relative to October.

Mean taxonomic richness was slightly higher in most acoustic patch types in May than in October, although there was a large difference in patch type F (Figure 5.3-27). However, overall these was no significant difference in taxonomic richness with respect to date, but differences among acoustic patches were significant across all the sampling dates (Table 5.3–17). There was a marginally significant interaction between acoustic patch and date for taxonomic richness indicating date effects for some acoustic patch types, likely primarily acoustic patch type F. There were no statistically significant differences due to sampling period (date) for Shannon diversity, although in many cases the October 2012 values were higher than in May 2013 (Figure

5.3-27, Table 5.3-17). Differences in Shannon diversity among acoustic patches were statistically significant. There was also no significant difference in Fisher's diversity among sampling dates, but differences among acoustic patch types.

To assess how community characteristics changed spatially between the fall 2012 and spring 2013 sampling dates, the data were averaged by sampling block for each date in order to focus on broader scale changes that may be occurring across the pilot study area. These values were then compared at the SB level using a GIS overlay approach. Infaunal abundances were generally much higher in areas along Stratford Shoal in May 2013 than in fall, October, 2012 sampling (Figure 5.3-28). In contrast many of the areas that had relatively high abundances in the fall, along the eastern flank of Stratford Shoal and the shallow water areas in the northern portion of the pilot study area at much lower abundances in the spring that were found in the fall. Areas samples in the southern portion of the study area generally had lower total infaunal abundance in both fall and spring in varied acoustic patch types. Temporal spatial variation in taxonomic (species) richness was generally low on or along the edges of Stratford Shoal, with many of the blocks that were sampled in each season having consistently high species richness (Figure 5.3-29). Several sampling blocks that were found in the northeast and southeast portions of the study area as well as on the western flank of Stratford Shoal had lower taxonomic richness in the spring than found in the fall. As such, it appears that taxonomic richness may be fairly consistent season to season in areas on and around Stratford Shoal, whereas community characteristics is more variable in areas of acoustic patches that are further away from the Shoal.

Shannon diversity exhibited an increasing northeast to a south-southwest trend in fall 2012, and to some extent this was evident also in the spring 2013 samples although not as strongly (Figure 5.3-30). Many of the sites had similar Shannon diversity levels, reflecting the statistical results noted above. Seasonal differences in Fisher's diversity were more spatially variable (Figure 5.3-31), although several of the areas that had high diversity in the fall also have high diversity in the spring. These are mostly associated with sample sites along or on Stratford Shoal, however an SB in the southeast portion of the study area and also in the northeastern section had consistently high Fisher's diversity in both seasons. Overall these results suggest that there are sections of specific acoustic patch types that have relatively consistent levels of taxonomic diversity in the study area.

Table 5.3-17. Results of two way ANOVA testing differences in infaunal community characteristics due to sampling date (seasons) and acoustic patch type, and their interaction. Tests were based on all samples and only including data from sampling blocks (SBs) for which samples were obtained in both fall 2012 and spring 2013 are given. * Term significant at $\alpha = 0.05$. Total abundance and taxonomic richness were $\log(x+1)$ transformed. Shannon and Fisher's diversity indices were based on data that excluded archiannelids and oligochaetes.

Total Abundance						
Source		Sum of	Mean		Prob	Power
Term	DF	Squares	Square	F-Ratio	Level	(Alpha=0.05)

A: DATE	1	0.870289	0.870289	4.85	0.029161*	0.590350
B: Acoustic_Patch	5	8.162025	1.632405	9.10	0.000000*	0.999898
AB	5	0.716615	0.143323	0.80	0.552077	0.281218
S	149	26.7293	0.1793913			
Total (Adjusted)	160	36.75682				
Total	161					

Total Abundance SBs only

Source		Sum of	Mean		Prob	Power
Term	DF	Squares	Square	F-Ratio	Level	(Alpha=0.05)
A: DATE	1	0.325146	0.325146	2.05	0.155737	0.293574
B: Acoustic_Patch	5	3.960401	0.7920802	5.00	0.000483*	0.977646
AB	5	1.910691	0.3821382	2.41	0.043128*	0.738111
S	81	12.82734	0.1583622			
Total (Adjusted)	92	19.11843				
Total	93					

Taxonomic Richness

Source		Sum of	Mean		Prob	Power
Term	DF	Squares	Square	F-Ratio	Level	(Alpha=0.05)
A: DATE	1	0.04264355	0.04264355	1.12	0.291860	0.182983
B: Acoustic_Patch	5	2.245332	0.4490664	11.78	0.000000*	0.999998
AB	5	0.08161253	0.01632251	0.43	0.828382	0.161013
S	149	5.678522	0.03811089			
Total (Adjusted)	160	8.307633				
Total	161					

Taxonomic Richness SBs only

Source		Sum of	Mean		Prob	Power
Term	DF	Squares	Square	F-Ratio	Level	(Alpha=0.05)
A: DATE	1	0.008533965	0.008533965	0.24	0.627433	0.076950
B: Acoustic_Patch	5	1.38853	0.2777061	7.72	0.000006*	0.999104
AB	5	0.4041723	0.08083446	2.25	0.057258	0.702598
S	81	2.912202	0.03595312			
Total (Adjusted)	92	4.67225				
Total	93					

Shannon Diversity

Source		Sum of	Mean		Prob	Power
Term	DF	Squares	Square	F-Ratio	Level	(Alpha=0.05)
A: DATE	1	0.01926378	0.01926378	0.43	0.513284	0.099801
B: Acoustic_Patch	5	1.936783	0.3873566	8.63	0.000000*	0.999807
AB	5	0.2752784	0.05505569	1.23	0.299133	0.426944
S	149	6.684142	0.04486001			
Total (Adjusted)	160	9.239756				
Total	161					

Shannon Diversity, SBs only

Source		Sum of	Mean		Prob	Power
Term	DF	Squares	Square	F-Ratio	Level	(Alpha=0.05)
A: DATE	1	0.0005007323	0.0005007323	0.01	0.916825	0.051229
B: Acoustic_Patch	5	1.419902	0.2839804	6.22	0.000062*	0.994396
AB	5	0.3548387	0.07096773	1.56	0.182116	0.518240
S	81	3.69574	0.04562642			
Total (Adjusted)	92	5.437531				
Total	93					

Fisher's Diversity

Source		Sum of	Mean		Prob	Power
Term	DF	Squares	Square	F-Ratio	Level	(Alpha=0.05)
A: DATE	1	0.6183584	0.6183584	0.04	0.832412	0.055097
B: Acoustic_Patch	5	766.7474	153.3495	11.14	0.000000*	0.999995
AB	5	88.8456	17.76912	1.29	0.270669	0.448225
S	149	2050.391	13.76101			
Total (Adjusted)	160	3078.635				
Total	161					

Fisher's Diversity SBs only

Source		Sum of	Mean		Prob	Power
Term	DF	Squares	Square	F-Ratio	Level	(Alpha=0.05)
A: DATE	1	0.6702397	0.6702397	0.05	0.830514	0.055174
B: Acoustic_Patch	5	643.0096	128.6019	8.85	0.000001*	0.999790
AB	5	108.1366	21.62732	1.49	0.202881	0.497580
S	81	1177.36	14.53531			
Total (Adjusted)	92	1939.241				
Total	93					

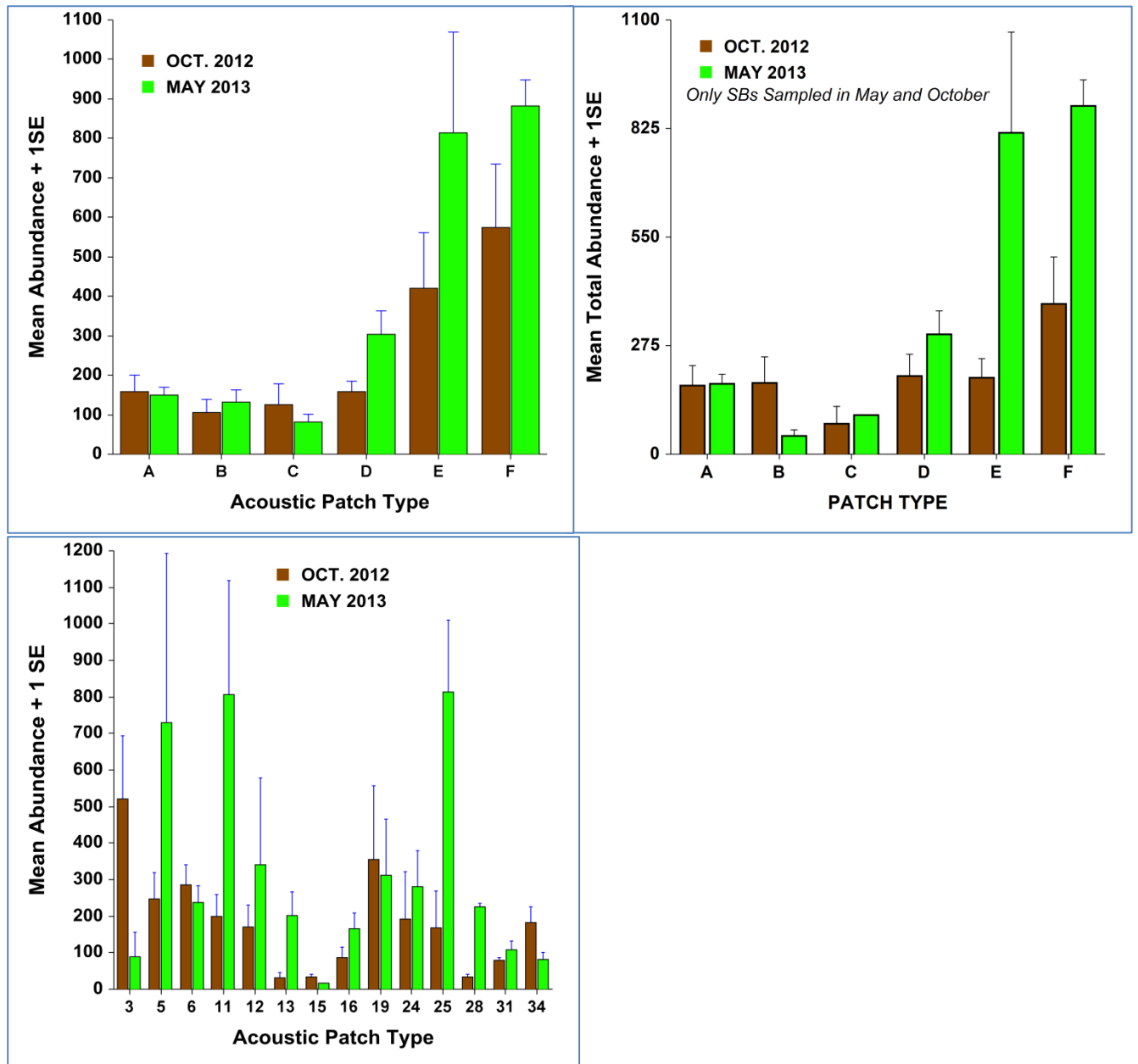


Figure 5.3-26. Comparison of mean total abundance per 0.1 m² among acoustic patches and sampling dates for the full data set (top left) and based on SBs samples only at both times (top right). Also shown are differences among fall and spring for individual SBs

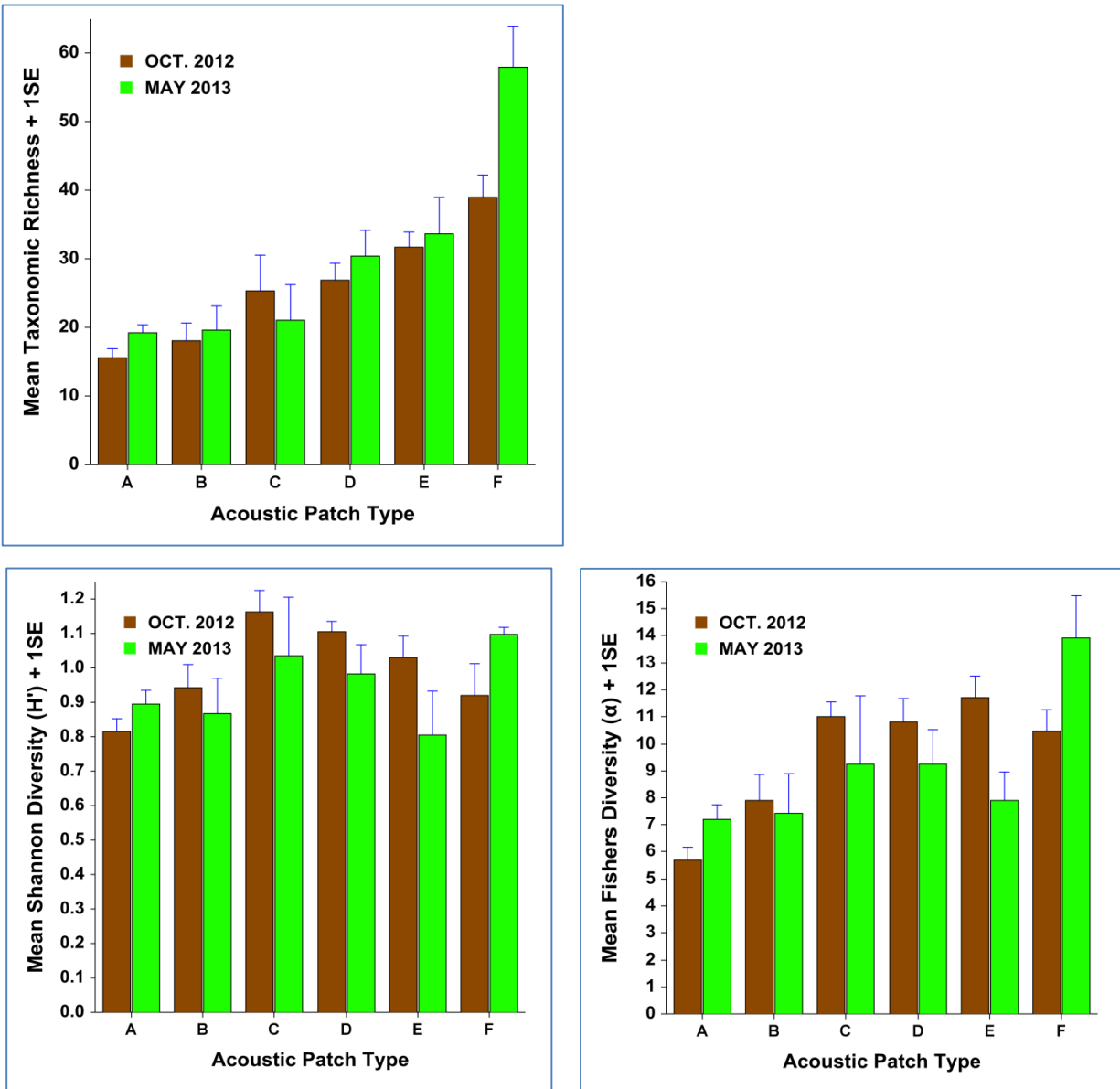


Figure 5.3-27. Comparisons of mean taxonomic richness per 0.1 m²(top), Shannon diversity, and Fisher's diversity (bottom) among October 2012 in May 2013 sampling dates and acoustic patch types based on the full data sets.

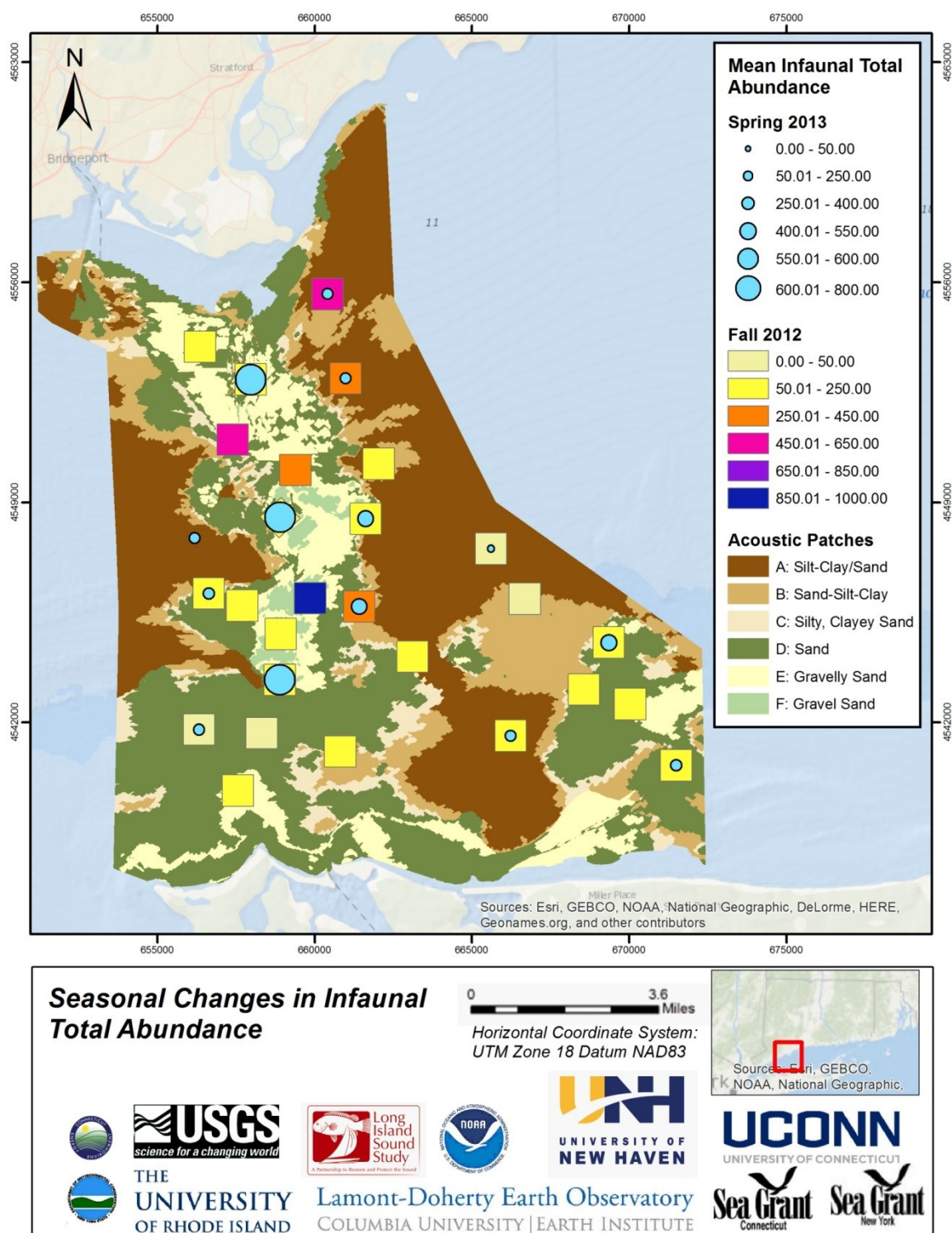


Figure 5.3-28. Seasonal comparisons of changes in infaunal total abundance in the pilot study area.

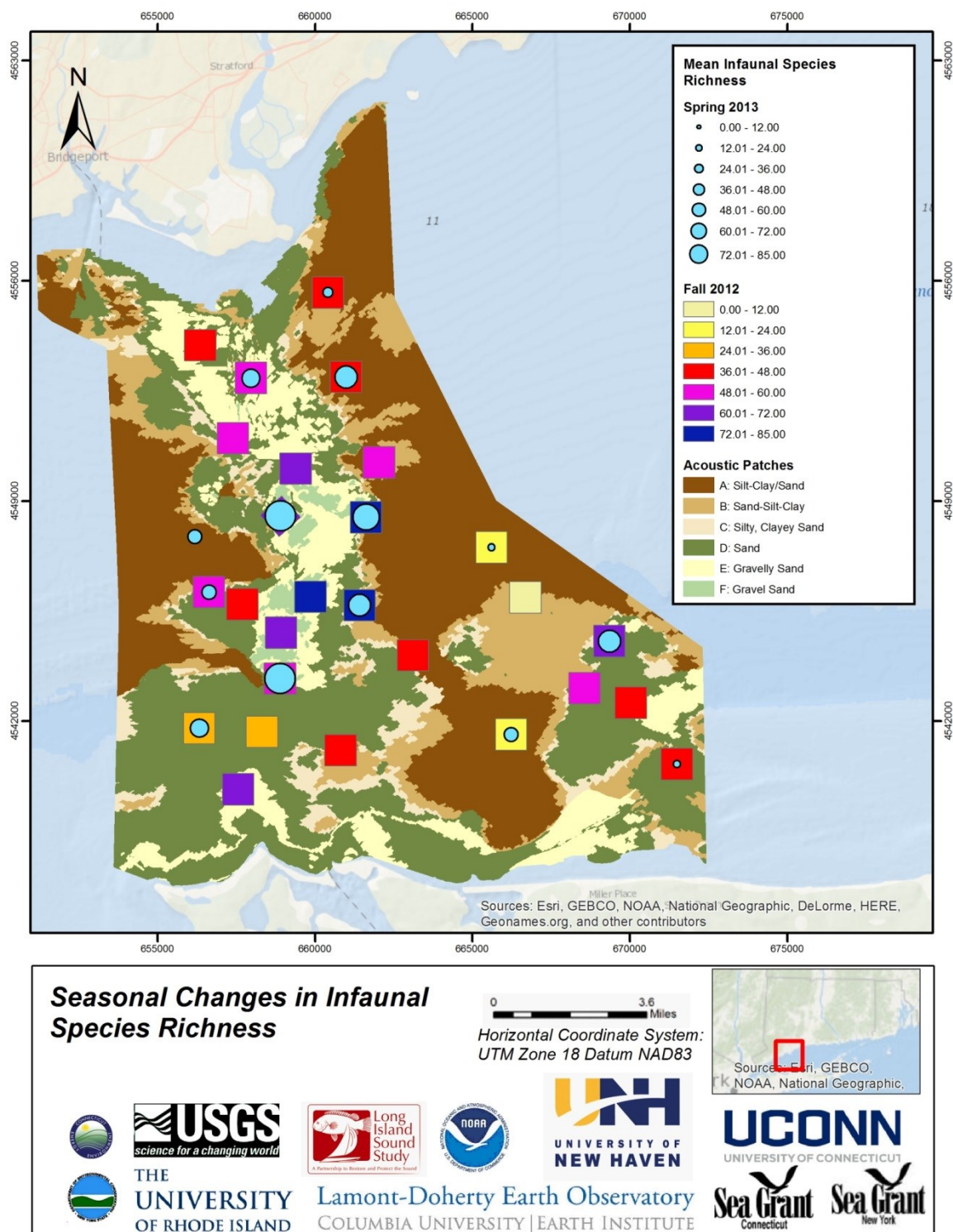


Figure 5.3-29. Comparison of seasonal changes in infaunal taxonomic (species) richness in the pilot study area.

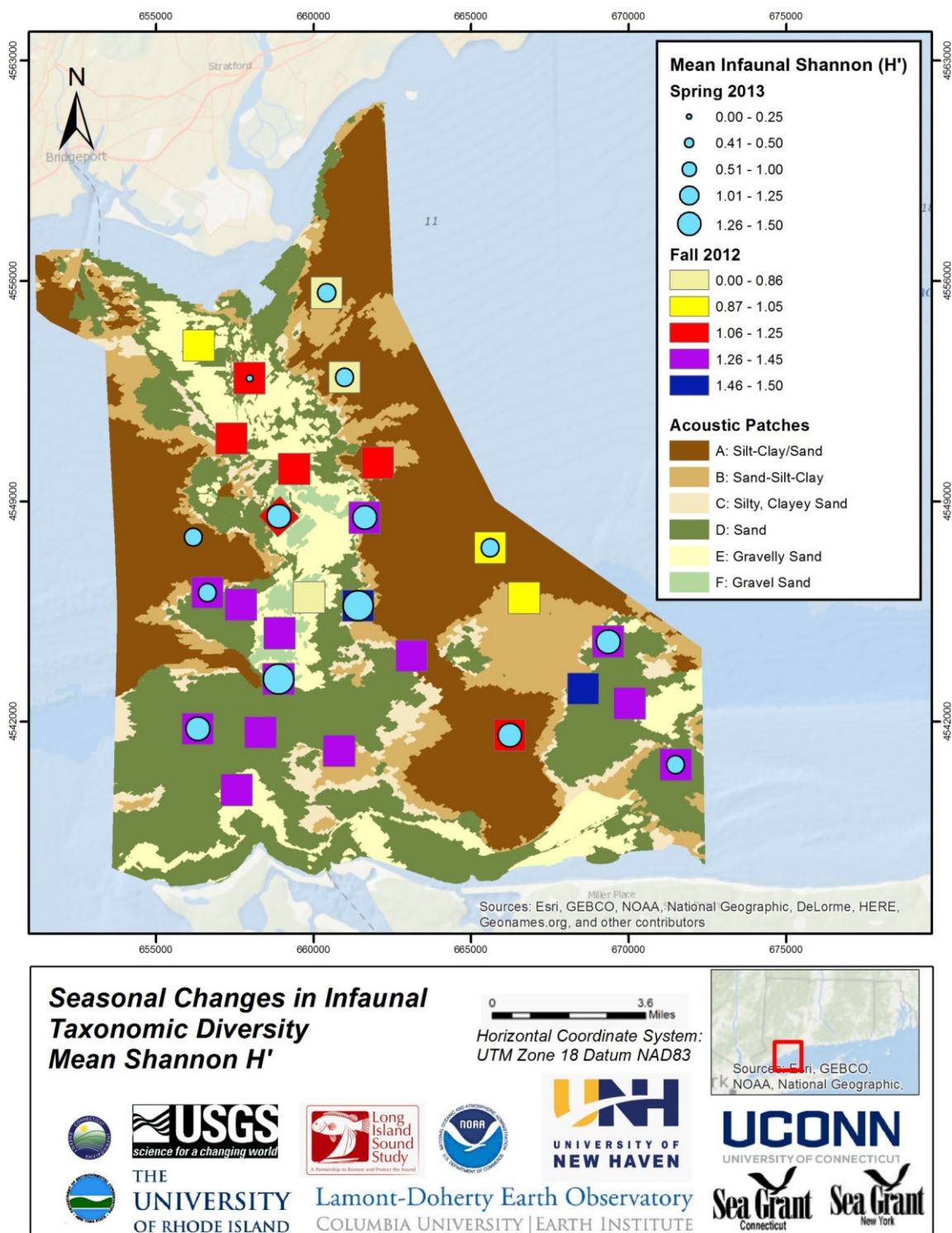


Figure 5.3-30. Comparison of seasonal changes in infaunal Shannon diversity in the pilot study area.

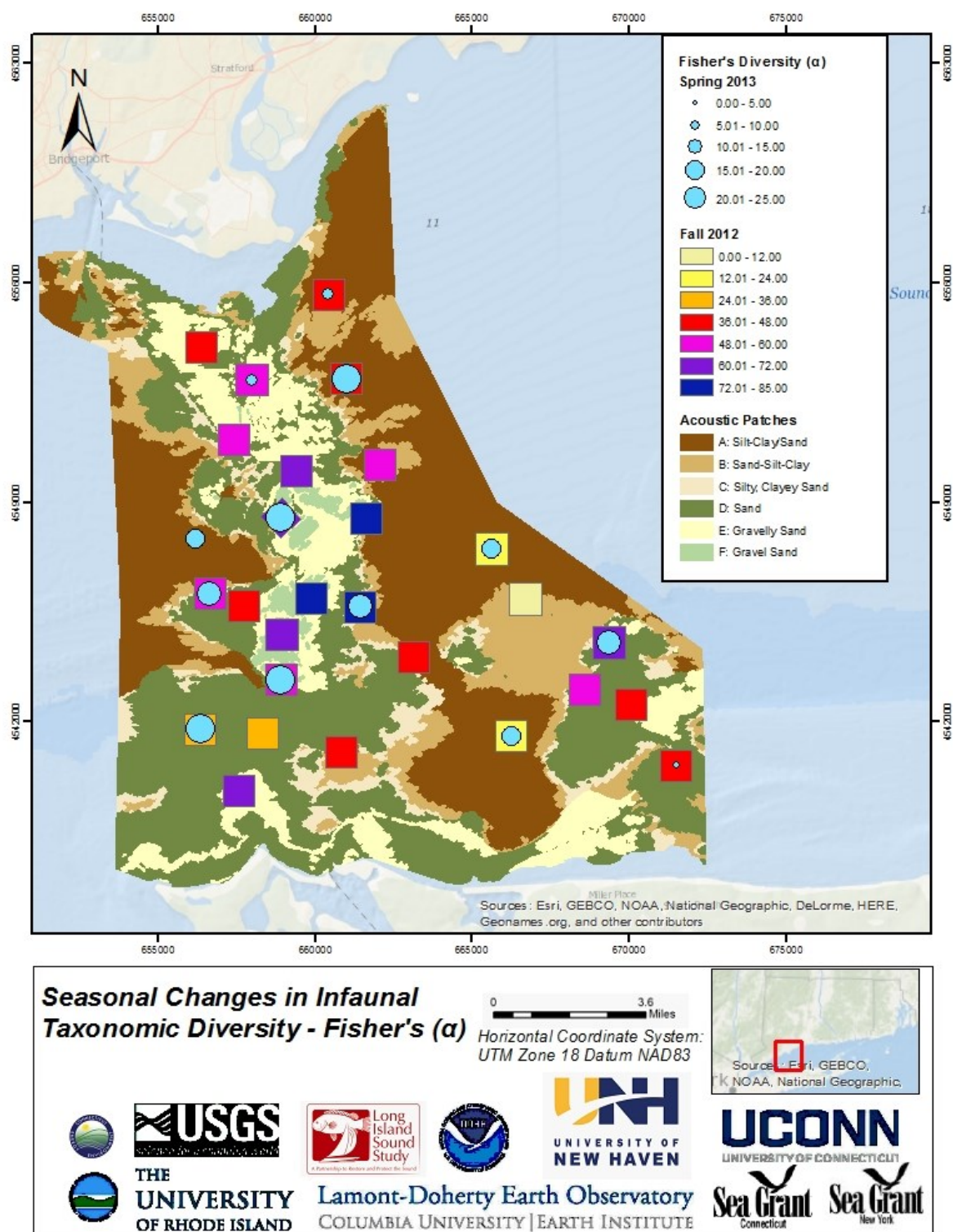


Figure 5.3-31. Comparison of seasonal changes in Fisher's diversity in the pilot study area.

5.3.6 *Historical Comparisons of Infaunal Taxonomic Diversity and Community Composition*

In 1995 and 1996, Zajac (1998) conducted a study in an area including the eastern flank of Stratford Shoal and the sea floor east of that (Figure 5.3-32) to assess infaunal community characteristics across a variety of sea floor habitats that were identified based on analyses of side scan mosaics developed by Twichel et al. (1998). As such, the approach of that study was similar to that of this pilot study in terms of utilizing sea floor mapping to identify sea floor environments / habitats and sample specific known patch types to assess the infaunal communities associated with each habitat type. Zajac's (1998) study provides an opportunity to assess long-term changes in infaunal community structure in a portion of the pilot study area, and thus may provide insights as to the temporal stability of the communities in a portion of the large-scale, sea floor environments (acoustic patch types) identified.

The comparisons were made using the 1995-1996 data collected in a series of sampling sites that were located primarily in acoustic patch types A, B and D (Figure 5.3-32) and data from 2012 and 2013 sampling blocks that were located in these acoustic patch types closest to the 1995-1996 sampling sites. These included SB-6, SB-8, SB-12, SB 19 and SB 14. In order to control to the extent possible for seasonal changes, only samples from April 1995, Jun 1996, and October 1995 and 1996 were used in order to correspond with the same seasonal time frame as the October 2012 and May 2013 samples taken during the pilot study. The data sets from the two studies differ with respect to the area sampled and how the samples were processed. The 1995-1996 data are based on 6 cm diameter x 15 cm deep cores taken from a grab sample (either a 0.1 m² or 0.05 m² Van Veen grab sampler) and processed on a 212 µm sieve. The samples for the pilot study presented in this report consisted of the whole 0.1 m² grab sample processed on a 0.5 mm sieve. In both cases species were sorted under a dissecting microscope and identified to lowest possible taxonomic level, with the identifications being primarily done by the same two persons in both studies. Given these differences in sampling, diversity data from the two studies were compared using species accumulation curves, as comparisons using taxonomic diversity measures such as Shannon's or Fisher's diversity indices would not be appropriate given their use of abundances of taxa found in a sample. Potential changes in community structure among the two studies were assessed by calculating community similarity within 1995-1996 sampling locations and then comparing these to the results of the community structure analyses presented above for the October 2012 and May 2013 sampling periods.

5.3.6.1 Historical Diversity Comparisons

For these comparisons, samples in the sampling blocks were pooled to get a composite assessment of changes in taxonomic richness between the 1995/1996 and 2012/ 2013 time periods. Although data from several different smaller-scale habitat types were combined, the pooling was relatively consistent in terms of the types of large-scale habitats (e.g., acoustic patch types) which were sampled, the proportion in each habitat type, and their general location in the pilot study area. To assess the potential (predicted) number of species for each set samples we

used the Chao2 estimator (Chao 1987; Colwell and Coddington 1994), which uses presence-absence data from multiple samples in aggregate to estimate the species diversity of the whole. This estimator is defined as:

$$S_2 = S_{obs} + \frac{Q_1^2}{2Q_2}$$

where S_2 is the predicted number of species, S_{obs} is the number of observed species, Q_1 is the number of singleton species occurring in only one sample (i.e., the number of species with only a single occurrence in the sample) and Q_2 is the number of doubletons occurring in two samples (the number of species with exactly two occurrences in the sample). The estimate can be recalculated as more samples are progressively added to the overall pool of samples producing a species accumulation curve in relationship to the number of samples. The variance of the Chao2 estimate can be also be calculated (Colwell and Coddington, 1994), and it has been shown to be a relatively robust and accurate technique for extrapolating the number of species under various sampling conditions and for small sample sizes (e.g. Foggo et al. 2003, Walther and Moore, 2005).

Species accumulation curves indicate that taxonomic diversity differed considerable both within and among the 1995/1996 and 2102/2013 study periods (Figure 5.3-33). In the 1990's taxonomic diversity was relatively low except in the April 1995 samples. The April 1995 species accumulation curve falls below both the October 2012 and the May 2013 accumulation curves, although the standard deviation envelope overlaps with the May 2013 curves. The highest taxonomic diversity was found in October 2012, greatly surpassing all of the other sampling periods, with maxima at approximately 200 taxa compared to approximately 125 taxa for April 1995. In addition to this analysis, species accumulation curves for a wider area of LIS, including the 1995/96 sites shown in Figure 5.3-32 and an additional set of samples obtained south of the Norwalk Islands (taken in April 1995 and October 1996), were compared with May 2012 species accumulation curve (Figure 5.3-34). The difference in species richness / biodiversity is striking, with substantively more species found in 2012, suggesting an intriguing possible long-term trend of increasing diversity in this portion of Long Island Sound, even with sampling differences taken into account. The most species were found in October 2012, suggesting that perhaps warming bottom water temperatures are increasing the active season for groups of benthic taxa and/or that species that normally were not be able to establish themselves in LIS due to sharper seasonal differences in physical conditions may be increasingly doing so.

Species composition in the 1995 / 1996 samples indicates that the overall suite of species found in those years continued to be present in the 2012/2013 samples (compare Tables 5.3-5 through 5.3-10 and 5.3-15 to Table 5.3-18). However, the species that were dominant in April 1995 were not the same ones that were dominant in May 2013. For example, the polychaetes *Cossura longocirrata* and *Mediomastus ambiseta* and the bivalve *Mulinia lateralis*, the dominants in April 1995, were not found as frequently nor at the same density levels as in 2012/ 2013. In

October 1996, only a few species comprised the infaunal communities, and as in the April 1995 samples, the dominant was *Mediomastus ambiseta* which was not found in high abundances in the 2012/2013 samples. Although abundances are not directly comparable due to differences in sampling and processing, the April 1995 abundances suggest that dominant species found at that time greatly exceed that found for the same species in 2012/2013. For example, by extrapolation (taking into account sample size and the sieve size used) the abundance of *Cossura longocirrata* was ~ 500 individuals per 0.1m² in April 1995, whereas in the 2012/2013 samples it was generally found at less than 5 individuals per 0.1m². *Sigambra tentaculata* was found in similar densities (~ 10- 20 individuals per 0.1m²), and *Nephtys incisa* was found at somewhat lower abundances in 2012/2013 (~ 6 - 20 individuals per 0.1m² compared to about 20 -30 in the 1995/96 samples).

Overall, these decadal comparisons suggest that infaunal diversity has increased, perhaps significantly, in the pilot study area between 1995/96 and 2012/13, and that community composition has shifted from being dominated by species that are considered to be responsive to disturbed / impaired conditions, such as *Mediomastus ambiseta* and *Mulinia lateralis*, to a more even mix of a variety of dominants depending on location in the pilot area. The causes for these trends are not known but may include changes in the physical characteristics of near bottom waters such as higher temperatures extending into the fall, changes in productivity patterns, improvement in environmental conditions relative to the habitat and ecological requirements of the overall species pool in this region of LIS, and influx and establishment of species that were not commonly found in LIS over this period of time. They also underscore the need for assessing / monitoring benthic community structure over regular periods of time so that directional changes can be identified, as these provide a potentially important context within which to interpret findings of more current studies and also to inform marine spatial planning and environmental management of LIS.

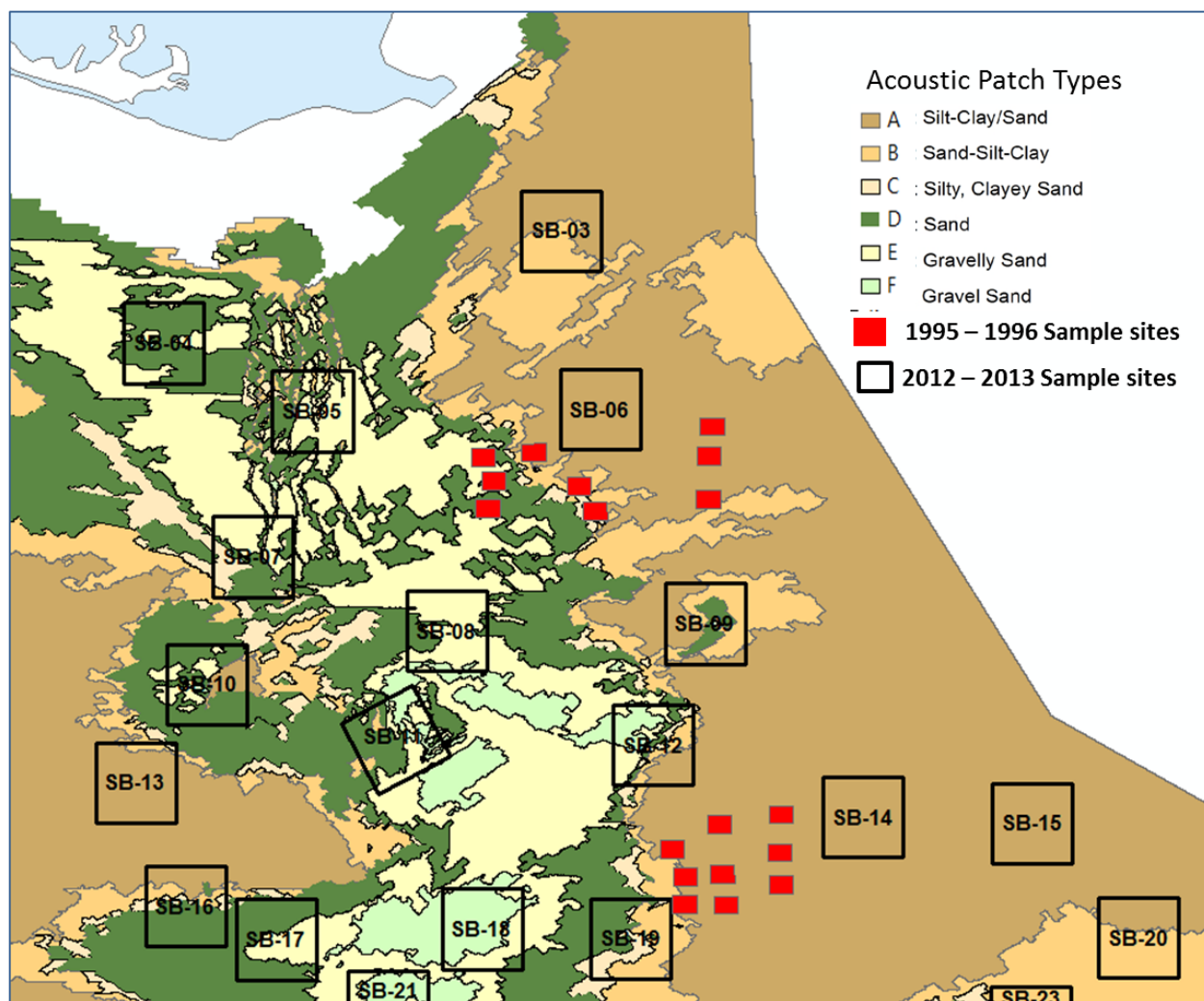


Figure 5.3-32. Locations of 1995-1996 sampling areas relative to benthic sampling areas in the pilot area taken in 2012-2013. The 1995-1996 data were compared to data collected in SB-6, SB-8, SB-12, SB 19 and SB 14 for the pilot study.

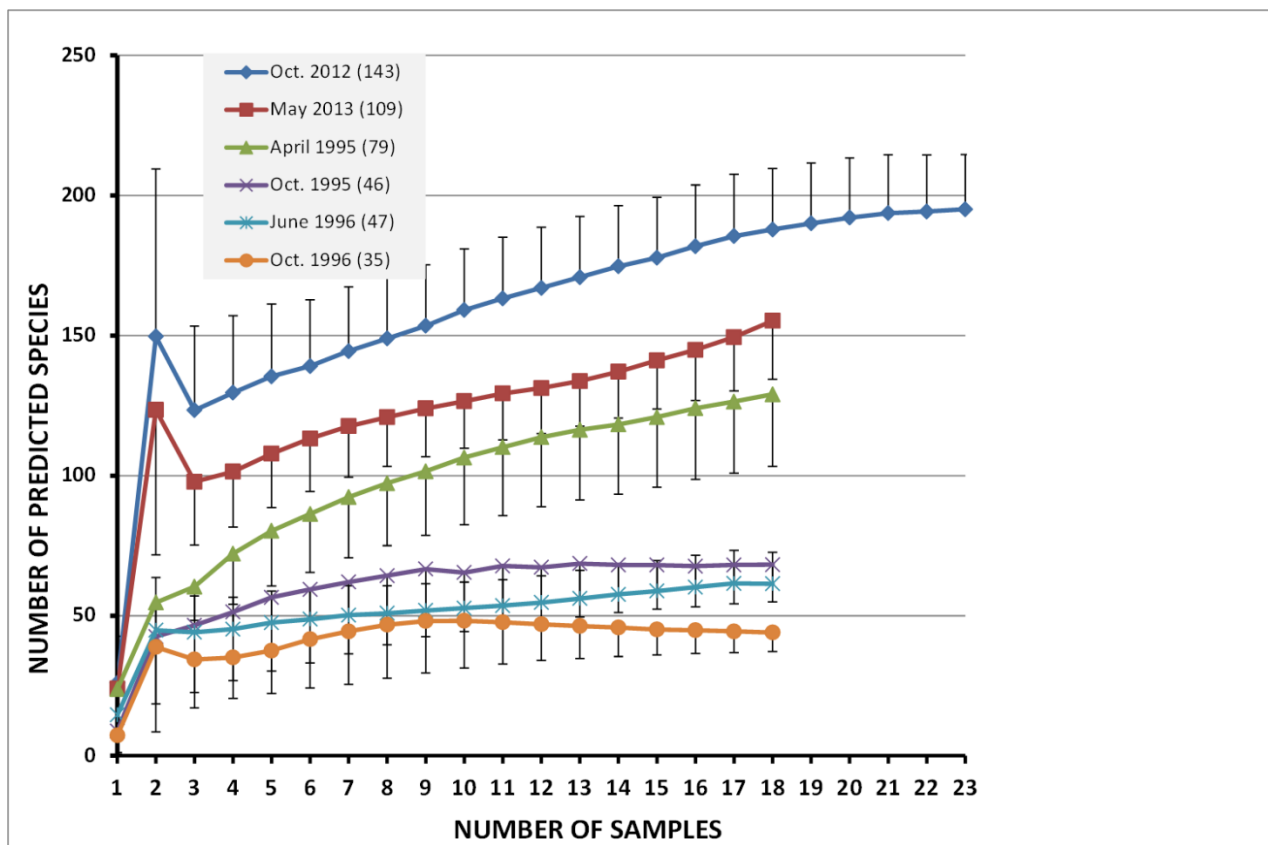


Figure 5.3-33. Species accumulation curves for combined benthic samples taken at 1995/1996 and 2012/2013 sites noted in Figure 5.3-32. Error bars are standard deviations.

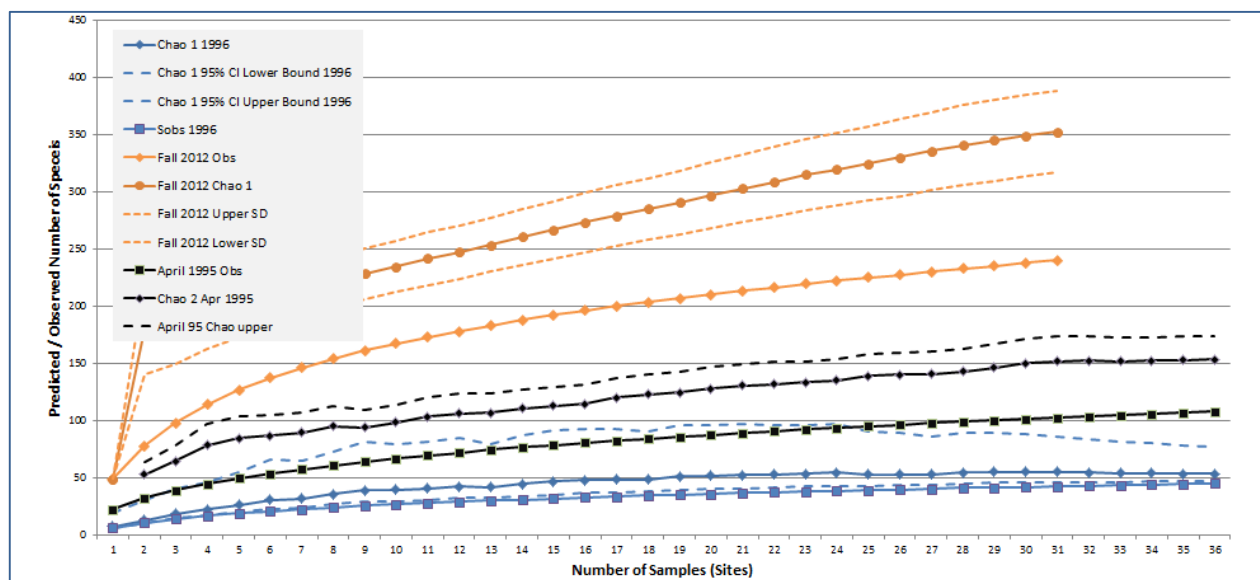


Figure 5.3-34. Species accumulation curves for combined benthic samples taken in April 1995 and October 1996 from western Long Island Sound including the sampling sites shown in Fig. 5.3-32

within the pilot area and also sites south of the Norwalk Islands. These are compared to the Fall 2012 samples (combined for each sampling block) obtained in the pilot study area.

Obs = taxa observed; the Chao values are the predicted number of species in the samples.

Table 5.3-18. Results of similarity percentage analysis (SIMPER) for benthic communities sampled in the pilot study area in April 1995 and October 1996. The general composition shown can be compared to Tables 5.3-5 through 5.3-10 and 5.3-15. Table shows the percent contribution of each species to the total similarity within each community type. Av.Abund = average abundance per 28.3 cm² sample; Av.Sim = average similarity among replicates at the site; Sim/SD = Similarity standard deviation; Contrib% = percent contribution to within site similarity; Cum.% = cumulative similarity. Data across all sampling blocks were combined for each sampling period.

April 1995 (Average similarity: 58.73)

Species	Av.Abund	Av.Sim	Sim/SD	Contrib%	Cum.%
<i>Cossura longocirrata</i>	44.33	16.26	1.26	27.68	27.68
<i>Mulinia lateralis</i>	40.17	7.62	0.94	12.97	40.65
<i>Mediomastus ambiseta</i>	21.56	7.38	1.57	12.56	53.22
<i>Nucula proxima</i>	28.44	4.98	1.51	8.49	61.70
<i>Yoldia limatula</i>	14.17	3.59	1.22	6.11	67.81
<i>Paraonis lyra</i>	7.22	3.46	0.79	5.89	73.70
<i>Oligochate a</i>	16.50	2.86	0.94	4.87	78.58
<i>Ampharete americana</i>	10.50	2.44	0.48	4.15	82.73
<i>Rhynchocoela a</i>	4.28	1.19	1.18	2.02	84.75
<i>Nephtys incisa</i>	3.11	1.17	1.10	1.99	86.74
<i>Telina agilis</i>	5.39	0.98	0.81	1.68	88.41
<i>Streblospio benedicti</i>	4.11	0.90	0.89	1.54	89.95
<i>Sigambra tentaculata</i>	2.56	0.68	0.92	1.16	91.12

Group Oct-96 (Average similarity: 37.44)

Species	Av.Abund	Av.Sim	Sim/SD	Contrib%	Cum.%
<i>Mediomastus ambiseta</i>	17.67	13.44	0.70	35.90	35.90
<i>Paraonis lyra</i>	1.39	10.13	0.58	27.06	62.97
<i>Oligochate a</i>	3.78	3.38	0.60	9.04	72.01
<i>Streblospio benedicti</i>	3.44	2.65	0.45	7.07	79.08
<i>Nephtys incisa</i>	1.17	1.85	0.48	4.94	84.01
<i>Nucula proxima</i>	1.89	1.44	0.56	3.85	87.86
<i>Rhynchocoela_A</i>	1.17	1.24	0.70	3.31	91.17

5.3.7 Summary

Infaunal communities were sampled in fall 2012 and spring 2013, providing the opportunity to assess temporal variation of infaunal communities in the pilot study area relative to sea floor habitat structure. The sampling efforts differed between research cruises and only a subset of the areas sampled in October 2012 were also sampled in May 2013.

The characteristics of benthic infaunal communities (abundance, diversity, community composition) were related to the acoustic patch types identified and varied relative to the habitat heterogeneity within and among acoustic patch types. Thus, acoustic mapping and related characterization can provide information as to the potential general characteristics of the infauna inhabiting the delineated seafloor habitat patches.

Abundances in patch types with coarser sediments had higher total abundances than patch types with progressively muddier sediments in both fall and spring. These patches also had higher total abundances in the spring compared to the fall. Other acoustic patch types had relatively similar mean total abundances among fall and spring sampling dates, although seasonal differences in total abundance were spatially variable. Total abundance tended to be highest along the flanks of Stratford Shoal and transitional areas among patch types.

A heretofore unquantified high number of infaunal taxa / species were found in the pilot study (242 in October 2012, 171 in May 2013). Mean taxonomic richness per 0.1 m² sample was progressively higher with increasing percentages of sand and gravel in acoustic patch types. This trend was consistent in both fall and spring. Seasonal differences within specific patch types were generally not significant, except in the patch type where sediment composition consisted mainly of coarse sands and gravel. Taxonomic richness was general highest on or along the flanks of Stratford Shoal and also in the southeast section of the pilot study area in muddy sand and sand acoustic patch types.

Taxonomic diversity (which combine both taxonomic richness and the relative abundance of species) was variable among acoustic patch types and also seasonally with specific patch types. Two different diversity measures (Shannon diversity H' and Fisher's α) were used to assess the consistency of the patterns. In both cases, within patch diversity was higher in the fall in patches characterized by sandy sediments, and higher in the spring in patches with either coarse or muddy sediments. The variation in these trends was such that there few statistical differences in seasonality, but differences among patch types were significant. Infaunal diversity was similar through large portions of the pilot study area, and areas of relatively high diversity found in most acoustic patch types. Thus, the spatial trends in infaunal diversity were complex, with no clear trend that could be associated with general environmental attributes such as depth or sediment type.

Community structure (taxonomic composition and relative abundances) was relatively distinct among acoustic patches in both fall and spring, with differences in the mix of dominant taxa and the relative variation in community structure. Acoustic patch types with predominantly sandy sediments had the most variable communities, whereas communities in patches with muddy or coarse grained sediments were less variable. The most variability on community structure was found in the acoustic patch type that was located in sandy areas in the southern portions of the pilot area and along the flanks of Stratford Shoal. Community structure also varied depending on whether they were located along transition zones among acoustic patch types or located within the interior of a particular patch types. The transition zones appear to have more diverse / complex communities.

The overall results of the infaunal analyses indicate that these communities and their characteristics can be closely related to the acoustic patch types identified through the habitat characterization analyses. Furthermore, the level of variation in community characteristics and

their patterns of spatial and, to a lesser extent, temporal variability have been identified for these various patch types, and that such this information can be used to guide future assessment and management with respect to various types of projects that may necessitate sampling of infaunal communities or their consideration within the scope of coastal marine spatial planning. For example, acoustic patch type D was characterized by primarily sand sediments, with low levels of silt, clay and gravel, and patches of this type were located across the pilot study area. Communities in this acoustic patch type were highly variable on a relative basis, had high diversity, and showed variation among seasons. As such it would be recommended that any necessary sampling of these types of environments include high replication in order to account for this variation.

5.3.8 References

- Anderson, M.J. 2005. PERMANOVA: a FORTRAN computer program for permutational multivariate analysis of variance. Department of Statistics, University of Auckland, New Zealand.
- Anderson, M., Gorley, R. and Clarke, K. 2008. Permanova+ for PRIMER. Plymouth, UK: Primer-E.
- Brown, C.J., Sameoto, J.A. and Smith, S.J. 2012. Multiple methods, maps, and management applications: Purpose made seafloor maps in support of ocean management. *Journal of Sea Research* 72:1-13.
- Chao, A. 1987. Estimating the population size for capture–recapture data with unequal catchability. *Biometrics* 43:783–791.
- Clarke, K.R. and Warwick, R.M. 2001. Change in marine communities: an approach to statistical analysis and interpretation. Natural Environment Research Council, Plymouth Marine Lab Plymouth (United Kingdom).
- Clarke, K. and Gorley, R. 2006. User manual/tutorial. PRIMER-E Ltd., Plymouth.
- Colwell RK, Coddington JA. 1994. Estimating terrestrial biodiversity through extrapolation. *Philosophical Transactions of the Royal Society of London Series B: Biological Sciences* 345: 101-118.
- Etter, R.J. and Grassle, J.F. 1992. Patterns of species diversity in the deep sea as a function of sediment particle size diversity. *Nature* 360:576-578.
- Foggo A, Attrill MJ, Frost MT, Rowden AA (2003) Estimating marine species richness: an evaluation of six extrapolative techniques. *Marine Ecology Progress Series* 248: 15-26.
- Hintze, J. 2012. NCSS 8. NCSS, LLC. Kaysville, Utah, USA. www.ncss.com
- Gray, J.S. 2002. Species richness of marine soft sediments. *Marine Ecology Progress Series* 244:285-297.

- Knebel, H.J. and Poppe, L.J. 2000. Sea-floor environments within Long Island Sound: a regional overview. *Journal of Coastal Research*: 533-550.
- Kostylev, V.E., Todd, B.J., Fader, G.B., Courtney, R., Cameron, G.D. and Pickrill, R.A. 2001. Benthic habitat mapping on the Scotian Shelf based on multibeam bathymetry, surficial geology and sea floor photographs. *Marine Ecology Progress Series* 219:121-137.
- Leibman, M. 2007. Benthic Habitat Characterization of the Stratford Shoal region of Long Island Sound. OSV Bold Survey Report. U.S. Environmental Protection Agency, New England Oceans and Coastal Protection Unit, Boston, MA.
- Poppe, L.J., Knebel, H.J., Mlodzinska, Z.J., Hastings, M.E. and Seekins, B.A. 2000. Distribution of surficial sediment in Long Island Sound and adjacent waters: texture and total organic carbon. *Journal of Coastal Research*: 567-574.
- Thrush, S.F., Hewitt, J.E., Norkko, A., Nicholls, P.E., Funnell, G.A. and Ellis, J.I. 2003. Habitat change in estuaries: predicting broad-scale responses of intertidal macrofauna to sediment mud content. *Marine Ecology Progress Series* 263:e112.
- Twichell DC, Zajac RN, Poppe LJ, Lewis RS, et al. 1998. Sidescan sonar mosaic of Long Island Sound off Milford, Connecticut, United States Geological Survey, Geologic Investigations Series Map I-2632. 2 sheets.
- Walther BA, Moore JL. 2005. The concepts of bias, precision and accuracy, and their use in testing the performance of species richness estimators, with a literature review of estimator performance. *Ecography* 28: 815-829.
- Whitlatch, R.B. 1981. Animal-sediment relationships in intertidal marine benthic habitats: some determinants of deposit-feeding species diversity. *Journal of Experimental Marine Biology and Ecology* 53:31-45.
- Zajac, R. 1998. Spatial and temporal characteristics of selected benthic communities in Long Island Sound and management implications, Final Report, Long Island Sound Research Fund Grant CWF-317-R,. Hartford, CT: Connecticut Department of Environmental Protection, Office of Long Island Sound Programs. Available at: <http://pubs.usgs.gov/of/1998/of98-502/chapt4/rz1cont.htm>
- Zajac, R.N., Lewis, R.S., Poppe, L.J., Twichell, D.C., Vozarik, J. and DiGiacomo-Cohen, M.L. 2000. Relationships among sea-floor structure and benthic communities in Long Island Sound at regional and benthoscape scales. *Journal of Coastal Research*: 627-640.
- Zajac, R.N., Lewis, R.S., Poppe, L.J., Twichell, D.C., Vozarik, J. and DiGiacomo-Cohen, M.L. 2003. Responses of infaunal populations to benthoscape structure and the potential importance of transition zones. *Limnology and Oceanography* 48: 829-842.
- Zajac, R.N., Vozarik, J.M. and Gibbons, B.R. 2013. Spatial and temporal patterns in macrofaunal diversity components relative to sea floor landscape structure. *PloS one* 8:e65823

5.4 *Infaunal Ecological Characterization - SBU*

Largely because of cost, benthic community assessment and monitoring programs rarely collect more than a few replicate grab samples within a habitat. While this standard practice adequately characterizes abundant species, rare species are largely missed, sacrificed for cost-efficiency (Cao et al., 1998). Unfortunately, this practical consideration has consequences that are antithetical to the goals of an assessment or monitoring program. For example, rare species are often more sensitive to disturbances than abundant species, and the presence/absence of rare species can serve as reliable indicators of environmental health (Cao et al., 1998; Gaston, 1998). Rare taxa may also include functionally important “keystone” species, critical to energy and material flows (Hooper et al., 2005), and their loss could go undetected by sampling but have a significant impact on a system.

Given that a full characterization of benthic community structure in well-defined habitats may be a potentially important long term goal of the Long Island Sound mapping program, a small grab sampling study was designed to determine the number of samples needed to estimate the occurrence of rare species within a habitat (i.e., bottom type). Based on prior studies in the Peconic Bays ecosystem and bays on the North Shore of Long Island (Cerrato et al., 2007; Cerrato et al., 2008), it was anticipated that 10 or more samples would be required to collect approximately 70% of the benthic species present in a bottom type. The results of the current study verify this result and extend it to habitats in Long Island Sound.

5.4.1 *Infaunal Sample Acquisition*

Sampling areas were selected on the basis of a visual examination of the backscatter in the 3m multibeam mosaic produced by Roger Flood for the LIS mapping program. Backscatter was taken as a proxy for bottom type, and 3 contrasting areas near Stratford Shoal were identified, each consisting of a homogeneous bottom type (Figure 5.4-1). The areas ranged from 1.4 to 2.1 km² and on the basis of backscatter were expected to represent sand, mud, and sandy mud bottom types. Ten sampling stations were randomly positioned within each area, with sampling stations constrained to be at least 100 meters from the area boundary and any other station.

Faunal and sediment sampling was conducted aboard the R/V Pritchard operated by Stony Brook University. Samples in the sand and mud areas were collected on 6/18/2013 and the sandy mud area was sampled on 9/11/2013. Bottom samples were collected using a modified van Veen grab (0.04 m²). Subsamples of sediments for grain size and organic content were drawn from each grab sample and turned over to colleagues in the Lamont group. The remaining sediment was washed through a 0.5 mm sieve for fauna. All material left on the sieve was preserved in 10% buffered formalin and stained with rose bengal.

5.4.2 Infaunal Sample Processing

Faunal samples were rewashed in the lab and transferred to 70% ethanol before sorting and identification. Individual organisms were identified to species level whenever possible and the total for each taxon enumerated. All abundances in this report are expressed as the number of individuals per sample (i.e., per 0.04 m²). A geodatabase was created in ArcGIS version 10.1 (ESRI, 380 New York Street, Redlands, CA) to display the data. Data were imported into the geodatabase from Excel spreadsheets.

Calculations for species accumulation curves and species richness estimates were carried out using the `specpool()` and `poolaccum()` functions in the `vegan` package of R. Species accumulation curves were obtained by generating 100 random permutations of sample order in a data set and then tabulating the cumulative number of species observed vs. number of samples.

The Chao 2 species richness estimator (Chao, 1987) was used to estimate the number of species present and the fraction of species collected in each bottom type. A comparison of species richness estimators by Colwell and Coddington (Cowell et al., 1994) suggested that the Chao 2 estimator worked extremely well to predict species richness. It was also particularly well suited for small sample sizes (< 25). The Chao 2 estimator was calculated as

$$S_2^* = S_{obs} + (L^2 / 2M)$$

where S_2^* was the estimated species richness, S_{obs} was the observed number of species in the samples, L was the number of species that occurred in only one sample, and M was the number of species that occurred in exactly two samples. The variance of S_2^* was estimated as

$$\text{var}(S_2^*) = M \left[\left(\frac{L/M}{4} \right)^4 + (L/M)^3 + \left(\frac{L/M}{2} \right)^2 \right]$$

S_2^* can be used in a sequential manner as each sample is added to a pooled set. As in the case of generating species accumulation curves, the order that samples are added affects the shape of the curve of S_2^* vs. the number of pooled samples. The analysis thus required generating an ensemble by randomly permuting sample order 100-200 times and calculating the mean S_2^* for the ensemble. The curve of S_2^* vs. the number of pooled samples increases initially with sample size until about the square root of twice the total fauna is observed (Cowell et al., 1994). At that point the estimator should level off and become independent of sample size (Cowell et al., 1994). Evidence that the estimator has leveled off and become stable is necessary before it can be used with confidence. Assuming that the Chao 2 estimator is stable, an estimate of the fraction of species collected with sampling effort can be obtained by dividing the species accumulation curve by the Chao 2 value.

It is very important to note that both species accumulation curves and the Chao 2 estimator are within-habitat estimators that assume constant probability of species collection across all samples. This restricts their application to a single habitat or bottom type. To see why this is so, imagine sampling in two distinct habitats, designated as habitat A and B, where the probability of collecting various species differs and where some species are, for example, unique to one of the two habitats. If 75% of the samples were collected in habitat A and samples from both A and B were pooled to calculate species accumulation curves and the Chao 2 estimator, the results would reflect more of the A habitat species assemblage. These results would be very different if 75% of the samples were collected in habitat B. Outcomes and interpretations, therefore, are highly dependent on the allocation of samples to habitats by an investigator.

This constant probability of species collection across samples was explicitly assumed in the derivation of the Chao 2 estimator (Chao, 1987). This restriction in its use would also hold for pooling samples across seasons within a habitat, since the probability of collecting a species would be expected to change in time.

5.4.3 Resulting Infaunal Data

Visual examination of the samples prior to sieving qualitatively confirmed the bottom type of each area and henceforth these areas will be designated as the Sand, Mud, and Sandy Mud sites. Water depths ranged from 20.7 to 26.4 m at the Sand site, 20.3 to 21.9 m at the Mud site, 32.4 to 33.3 m at the Sandy Mud site. Sample locations, water depths, and grab penetration depths are listed in Table 5.4-1.

A total of 5,640 animals representing 95 taxa were collected in the 30 samples. Average abundance across all 30 samples was 188 individuals per sample. Of the 95 taxa, 42 were polychaetes, 26 were crustaceans, 22 were molluscs, and the remainder (5) was distributed among other groups (Table 5.4-2). Numerical dominants included the polychaetes *Amphitrite artica* (10 per sample), *Paranois gracilis* (11 per sample), and *Polygordius* spp. (56 per sample), and the amphipods *Ampelisca vadorum* (17 per sample) and *Leptocheirus pinguis* (19 per sample) (Table 5.4-3). These 5 taxa represented about 60% of the total number of individuals collected. A total of 81 of the 95 taxa had abundances that were less than 1% of the individuals collected and together represented about 17% of the individuals collected.

Average faunal abundances in each area were 442 individuals per sample for Sand, 85 individuals per sample for Mud, and 37 individuals per sample for Sandy Mud. The average number of species per sample was 30 for Sand, 15 for Mud, and 9 for Sandy Mud.

- a) Sand: Abundances ranged from 179 to 712 individuals per sample and the number of species varied from 24 to 35 species per sample. A total of 72 taxa were collected. The most abundant taxa was the polychaete *Polygordius* spp., and it represented 38.4% of the total number of individuals in the sand samples. Other abundant species included the polychaete *Amphitrite artica* (6.8%), and the amphipods *Ampelisca vadorum* (11.3%) and *Leptocheirus*

pinguis (12.6%). A total of 60 of the 72 taxa had abundances that were less than 1% of the individuals collected in Sand (Table 5.4-3).

- b) Mud: Faunal abundances varied from 54 to 129 individuals per sample. The number of species varied from 10 to 21 species per sample. A total of 36 taxa were collected. Numerically abundant taxa included the polychaetes *Nephtys incisa* (13.3%), *Paranois gracilis* (27.9%), and *Sigambra* sp. (12.3%), and the bivalve *Nucula annulata* (16.8%). A total of 22 of the 36 taxa had abundances that were less than 1% of the individuals collected in Mud (Table 5.4-3).
- c) Sandy Mud: Abundances varied from 8 to 87 individuals per sample, and the number of species ranged from 5 to 13 species per sample. A total of 31 species were collected. The polychaetes *Amphitrite cirrata* (6.2%), *Nephtys incisa* (21.8%), *Paranois gracilis* (24.7%), and *Sigambra* sp. (24.5%) were the dominant species. A total of 17 of the 31 taxa had abundances that were less than 1% of the individuals collected in Sandy Mud (Table 5.4-3).

5.4.4 Infaunal Data Analysis

Sample sizes within each area were large enough to successfully determine an estimate of Chao 2 (Table 5.4-4), yielding 94 species for Sand, 60 for Mud, and 41 for Sandy Mud. About 1-2 new species per sample were still being added to each area after 10 samples, based on the slope at the end of the species accumulation curves, suggesting that rare species were still being detected (Figure 5.4-2a). Dividing the species accumulation curve results by the Chao 2 values, 10 samples recovered about 76% of the fauna in the Sand, 60% in the Mud, and 75% in the Sandy Mud areas (Figure 5.4-2b).

Species accumulation curves (Figure 5.4-3a), Chao 2 estimates (Figure 5.4-4), and the fraction of species collected (Figure 5.4-3b) all fell within the range found for other local studies in the Peconics and in bays along the North Shore of Long Island. Combining all the studies, it is clear that three replicate samples in a habitat, a value often used in benthic studies, would recover only 13-50% of the species present (Figure 5.4-3b). Even at 10 samples, there is evidence for under sampling in many of the habitats. In the present study, for example, 10 samples recovered only about 60% of the species in the Mud area.

One component not addressed in the present study was the effect of season on species richness. Seasonal effects were not part of the study design because of limited resources. The Sandy Mud area had the fewest species but it is not clear whether this result was related to sediment differences or seasonal changes in the composition of the fauna. The other two areas were sampled in the spring, so comparisons should be treated with caution.

Cao et al., 1998 found that small sample sizes effectively removed rare species from an analysis and underestimated differences among sites. They found that because rare species are undersampled in greater numbers at unimpacted sites relative to impacted sites, limiting the

sample size in a study tends to reduce the sensitivity of multivariate approaches to detect change. This is an important consideration moving forward if a monitoring structure for detecting change is a priority.

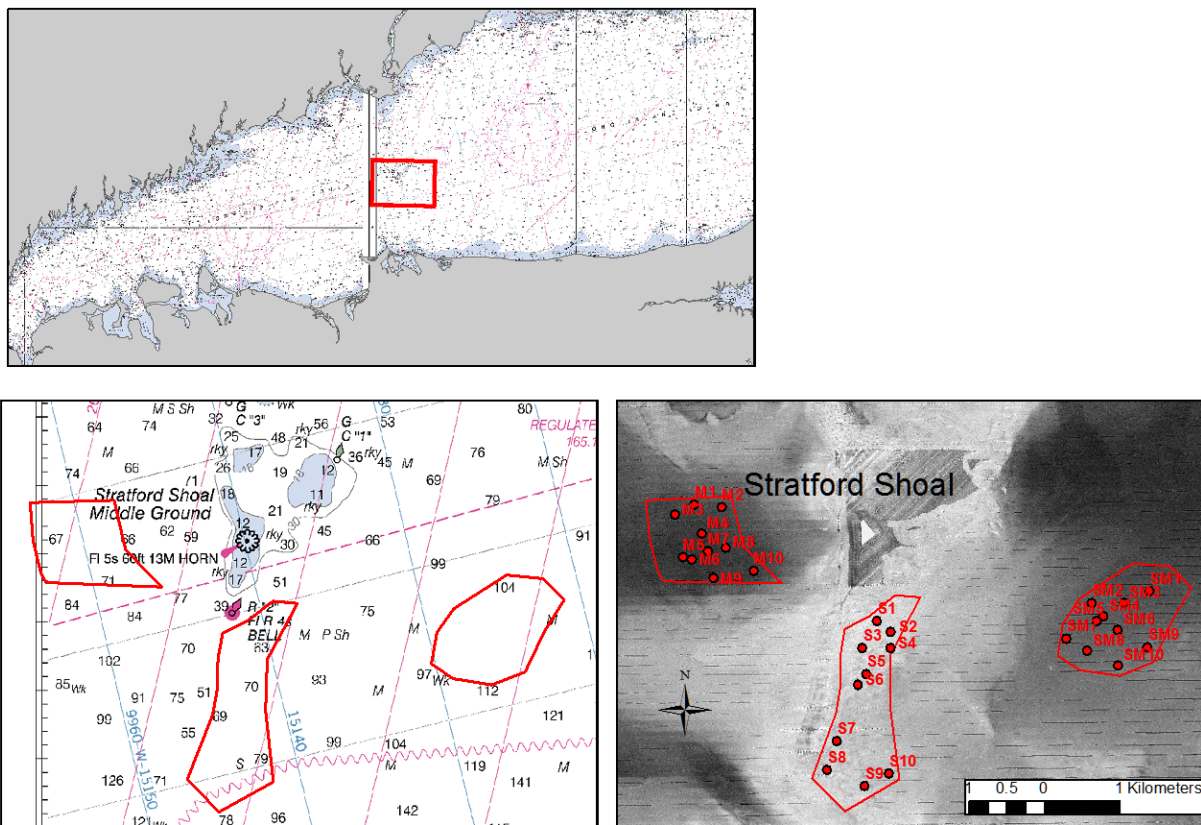


Figure 5.4-1 Station locations. S = Sand, M = Mud, and SM = sandy mud areas.

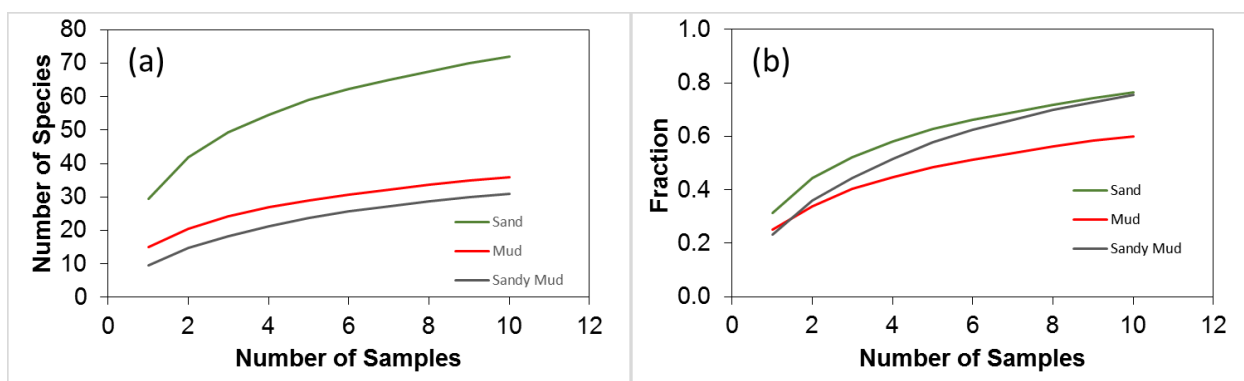


Figure 5.4-2 Species accumulation curves (a) and the fraction of species sampled (b) determined by dividing the species accumulation results by the Chao 2 estimate.

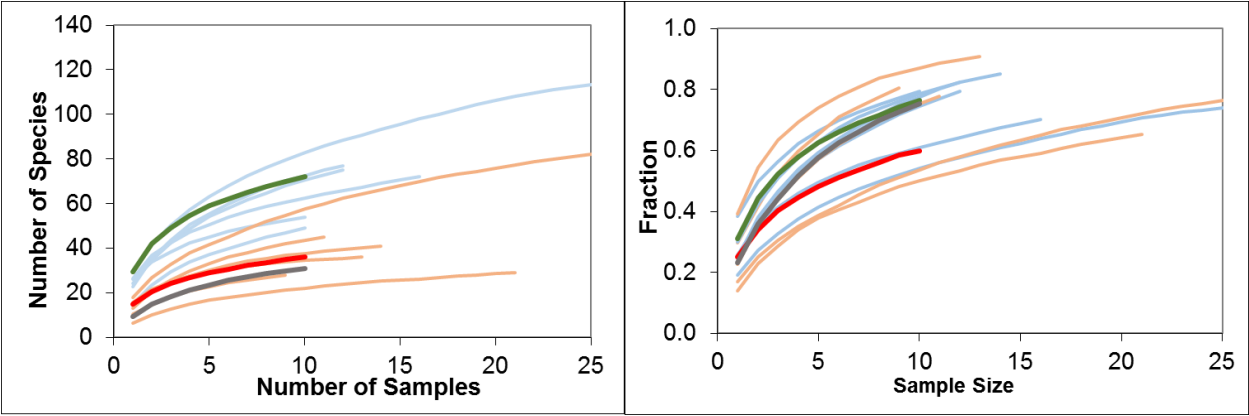


Figure 5.4-3 Species accumulation curves (a) and the fraction of species sampled (b) compared to prior studies in the Peconic Bays system [5.4-4] and bays on the North Shore of Long Island [5.4-5]. Data sets are Sand (green), Mud (red), Sandy Mud (grey), North Shore bays (orange), and Peconics (blue).

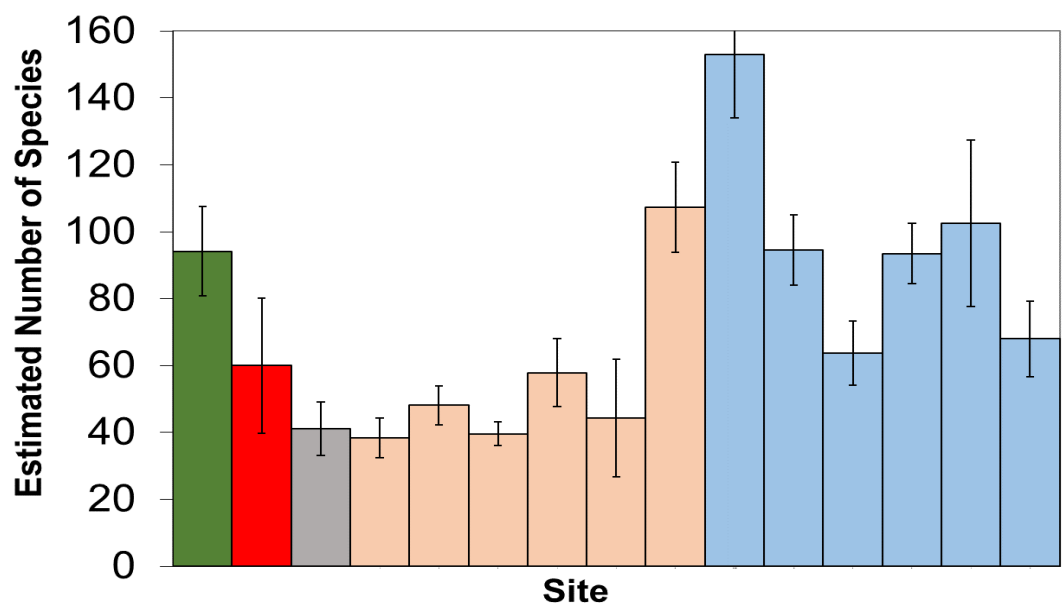


Figure 5.4-4. Comparison of the Chao 2 estimates to prior studies in the Peconic Bays system [5.4-4] and bays on the North Shore of Long Island [5.4-5]. Data sets are Sand (green), Mud (red), Sandy Mud (grey), North Shore bays (orange), and Peconics (blue).

Table 5.4-1 Field data for each sampling location.

Station ID	Sample ID	Latitude	Longitude	Date	Water Depth (m)	Grab Depth (cm)
M1	L010	41.0640333	-73.1282833	6/18/2013	21.4	9.5

Station ID	Sample ID	Latitude	Longitude	Date	Water Depth (m)	Grab Depth (cm)
M2	L009	41.0636167	-73.1239667	6/18/2013	20.7	9.5
M3	L011	41.0628500	-73.1313833	6/18/2013	21	9.5
M4	L012	41.0605167	-73.1272000	6/18/2013	20.3	9.5
M5	L013	41.0577500	-73.1302500	6/18/2013	21.3	9.5
M6	L014	41.0574500	-73.1288833	6/18/2013	21.3	9.5
M7	L015	41.0583833	-73.1262833	6/18/2013	20.9	9.5
M8	L008	41.0587500	-73.1234500	6/18/2013	20.9	8.5
M9	L016	41.0551667	-73.1255000	6/18/2013	21.9	9.5
M10	L007	41.0559333	-73.1191000	6/18/2013	21.4	9.5
S1	L006	41.0496167	-73.0998000	6/18/2013	20.7	6
S2	L005	41.0482833	-73.0976500	6/18/2013	22.6	6.5
S3	L003	41.0464167	-73.1022333	6/18/2013	21.6	7
S4	L004	41.0463450	-73.0978410	6/18/2013	22.9	6
S5	L017	41.0433000	-73.1016833	6/18/2013	21.6	6.5
S6	L002	41.0420500	-73.1030167	6/18/2013	22.9	6
S7	L018	41.0353667	-73.1065833	6/18/2013	22.3	5
S8	L001	41.0319333	-73.1082167	6/18/2013	21.2	5
S9	L020	41.0299333	-73.1023167	6/18/2013	24	5
S10	L019	41.0313667	-73.0984500	6/18/2013	26.4	5
SM1	L029	41.0524833	-73.0565500	9/11/2013	32.7	10
SM2	L027	41.0512000	-73.0657833	9/11/2013	32.4	10
SM3	L028	41.0511500	-73.0607000	9/11/2013	32.6	10
SM4	L026	41.0495833	-73.0640000	9/11/2013	32.7	10
SM5	L025	41.0490333	-73.0650500	9/11/2013	32.7	10
SM6	L030	41.0479167	-73.0617667	9/11/2013	33.3	10
SM7	L024	41.0470167	-73.0699333	9/11/2013	32.7	10
SM8	L023	41.0455167	-73.0666667	9/11/2013	32.9	10
SM9	L022	41.0457667	-73.0571333	9/11/2013	33	10
SM10	L021	41.0436667	-73.0618333	9/11/2013	33	10

Table 5.4-2 Faunal data tabulated by sample and by species. Values are the number of individuals per sample.

	1	2	3	4	5	6	17	18	19	20	7	8	9	10	11	12	13	14	15	16	21	22	23	24	25	26	27	28	29	30
	S	S	S	S	S	S	S	S	S	S	M	M	M	M	M	M	M	M	M	M	SM	SM	SM	SM	SM	SM	SM	SM	SM	SM
Sample ID	L001	L002	L003	L004	L005	L006	L017	L018	L019	L020	L007	L008	L009	L010	L011	L012	L013	L014	L015	L016	L021	L022	L023	L024	L025	L026	L027	L028	L029	L030
ANNELIDA																														
Oligochaeta																														
Oligochaeta spp.													1				1			1										
Polychaeta																														
<i>Ampharete arctica</i>	27	21	26	23	52	29	21	24	29	47																				
<i>Amphitrite cirrata</i>													1								2	6		2	3	2	2	4	2	
<i>Ancistrosyllis groenlandica</i>	2		1	3		4	3	1	9	2																				
<i>Aricidea catherinensis</i>	14	8	24	31	58	38	16		26	1											1									
<i>Asabellides oculata</i>	1		1		4				3	5						2														
<i>Asychis elongata</i>							1														1	3		1			1			
<i>Brada</i> sp.									5	1																				
<i>Brania wellfleetensis</i>								2	3		1																			
Capitellidae spp.				1	1								2		1		4			5					1		3			
<i>Clymenella zonalis</i>					1				3	1												1			1	1		1	1	
<i>Cossura longocirrata</i>																	1													
<i>Drilonereis longa</i>					1	1	1	1																						
<i>Eteone heteropoda</i>										1																				
<i>Exogone dispar</i>	1								5	3																				
<i>Glycera americana</i>			2		1				1																					

	1	2	3	4	5	6	17	18	19	20	7	8	9	10	11	12	13	14	15	16	21	22	23	24	25	26	27	28	29	30
	S	S	S	S	S	S	S	S	S	S	M	M	M	M	M	M	M	M	M	M	SM	SM	SM	SM	SM	SM	SM	SM	SM	SM
Sample ID	L001	L002	L003	L004	L005	L006	L017	L018	L019	L020	L007	L008	L009	L010	L011	L012	L013	L014	L015	L016	L021	L022	L023	L024	L025	L026	L027	L028	L029	L030
<i>Gyptis vittata</i>													1		1			3												
<i>Harmothoe</i> sp.	2	8	19	9	16	13	17		1	1																				
<i>Lumbrineris fragilis</i>		1				1		1																						
Maldanidae sp. (juveniles)																	3													
<i>Melinna cristata</i>																								1	1			3	1	
<i>Minuspio</i> sp.											9	3	1			2	2	1	3	3					2		6			1
<i>Nephtys incisa</i>							1		3		10	13	15	16	12	11	10	10	8	8	5	6	4	5	11	8	18	10	10	4
<i>Nephtys picta</i>	2	1	3	5	4	1	6	3	6	5																				
<i>Nereis grayi</i>																					1					1				
<i>Orbinia swani</i>				1					3																					
<i>Paranaitis speciosa</i>	1		1		2	2																								
<i>Paraonis gracilis</i>								1			12	5	13	16	23	19	32	34	42	42				10	2	13	16	25	15	11
<i>Parapionosyllis longicirrata</i>	14	1		1		1		1																						
<i>Phyllodoce arenae</i>		1	1	1				1																						
<i>Polydora</i> spp.	3			1			2		1	5	1		23	1		1														
<i>Polygordius</i> spp.	204	88	92	240	280	120	142	108	192	228																				
<i>Potamilla reniformis</i>	3	3	6	3	3	1	3																							
<i>Sabellaria vulgaris</i>				1																										
<i>Scalibregma inflatum</i>		3				1	1		5																					
<i>Schistomeringos caecus</i>					1	1																								
<i>Scolecipis squamata</i>											3	1	1					1	2	3										
<i>Sigambra</i> sp.											3	8	3	11	9	5	12	10	5	39	2	1	3	13	16	16	25	8	7	

	1	2	3	4	5	6	17	18	19	20	7	8	9	10	11	12	13	14	15	16	21	22	23	24	25	26	27	28	29	30
	S	S	S	S	S	S	S	S	S	S	M	M	M	M	M	M	M	M	M	M	SM	SM	SM	SM	SM	SM	SM	SM	SM	SM
Sample ID	L001	L002	L003	L004	L005	L006	L017	L018	L019	L020	L007	L008	L009	L010	L011	L012	L013	L014	L015	L016	L021	L022	L023	L024	L025	L026	L027	L028	L029	L030
<i>Sphaerosyllis erinaceus</i>						1																								
<i>Spiochaetopterus oculatus</i>																						1								
<i>Spiophanes bombyx</i>	5	7	1	4		6	5	1	19	7																				
Terebellidae spp.	1																													
<i>Tharyx</i> sp.			12	19	23	11	9		1			1		1	2		1			1				1			1	1		
ARTHROPODA																														
Amphipoda																														
<i>Ampelisca vadorum</i>	9	96	81	102	26	59	62		53	11	1		1	4		1		3	1							1				
<i>Corophium</i> sp.		1							12	5																				
<i>Dulichia</i> sp.			1															1												
<i>Erichthonius brasiliensis</i>			1	4		3	1																							
<i>Leptocheirus pinguis</i>	9	69	2	67	21	18	41	5	259	65																				
<i>Luconacia incerta</i> (Caprellid)				10	1	4	2																							
<i>Metopella</i> sp.					1																									
<i>Parametopella cypri</i>				1						1																				
<i>Paraphoxus spinosus</i>						2																								
<i>Phoxocephalus holbolli</i>	6	4	4	20	8	4	9																							
<i>Stenothoe minuta</i>	1	3	3	5			1																							
<i>Unciola irrorata</i>	4	11	4	4	3	5	2	2	25	5						1														

	1	2	3	4	5	6	17	18	19	20	7	8	9	10	11	12	13	14	15	16	21	22	23	24	25	26	27	28	29	30
	S	S	S	S	S	S	S	S	S	S	M	M	M	M	M	M	M	M	M	M	SM	SM	SM	SM	SM	SM	SM	SM	SM	SM
Sample ID	L001	L002	L003	L004	L005	L006	L017	L018	L019	L020	L007	L008	L009	L010	L011	L012	L013	L014	L015	L016	L021	L022	L023	L024	L025	L026	L027	L028	L029	L030
Cephalocarida																														
Cephalocarida sp. (possibly <i>H. macracantha</i>)																									2			1	2	
Cirripedia																														
<i>Balanus amphitrite</i>	10	3			110	25	7			1																				
Cumacea																														
<i>Oxyurostylis smithi</i>														1				2						1						
Decapoda																														
Brachyuran (true crabs)																														
<i>Panopeus herbstii</i>	1	1	6	4	2	4	3		1	1			1																	
<i>Pinnixa</i> sp.		5		1		2		1	4	4	1		5			1					1	2					1			
<i>Portunidae</i> sp. (juv: <i>C. maenas</i> / <i>O. cellatus</i>)	1																													
crab megalops																									1				1	
Caridean (shrimp)																														
<i>Crangon septemspinosa</i>			1					1	1																					
Ghost Shrimp																														
<i>Gilvossius setimanus</i>							1																	1						

	1	2	3	4	5	6	17	18	19	20	7	8	9	10	11	12	13	14	15	16	21	22	23	24	25	26	27	28	29	30
	S	S	S	S	S	S	S	S	S	S	M	M	M	M	M	M	M	M	M	M	SM	SM	SM	SM	SM	SM	SM	SM	SM	SM
Sample ID	L001	L002	L003	L004	L005	L006	L017	L018	L019	L020	L007	L008	L009	L010	L011	L012	L013	L014	L015	L016	L021	L022	L023	L024	L025	L026	L027	L028	L029	L030
Shrimp (juvenile)								1																						
Isopoda																														
Cyathura polita																					1							1		
Mysidacea																														
Heteromysis formosa					1																									
Neomysis americana																												1		
Tanaidacea																														
Leptochelia savignyi								4																						
CHORDATA																														
Ascidacea																														
Molgula sp. (probably M. manhattensis)		2							7			1					1	1												
CNIDARIA																														
Actinaria spp.												1	1	1		1					2							1	1	
MOLLUSCA																														

	1	2	3	4	5	6	17	18	19	20	7	8	9	10	11	12	13	14	15	16	21	22	23	24	25	26	27	28	29	30
	S	S	S	S	S	S	S	S	S	S	M	M	M	M	M	M	M	M	M	M	SM	SM	SM	SM	SM	SM	SM	SM	SM	SM
Sample ID	L001	L002	L003	L004	L005	L006	L017	L018	L019	L020	L007	L008	L009	L010	L011	L012	L013	L014	L015	L016	L021	L022	L023	L024	L025	L026	L027	L028	L029	L030
Bivalvia																														
<i>Anadara transversa</i>	2	3	2	4	1	2	3	2	6																					
<i>Astarte undata</i>		4	2	2	2	2	7	1	1	3																				
Bivalvia juvenile (possibly <i>Crassinella</i> sp)	1										1																			
<i>Ensis directus</i>		1	1				1																							
<i>Lyonsia hyalina</i>		6	1	3	2	1	1	5	8	1																				
<i>Macoma tenta</i>								2						1																
<i>Mulinia lateralis</i>								2			4		2	1	1					1			1							
<i>Mytilus edulis</i>	1	3	2	6	3	18	7			3																				
<i>Nucula annulata</i>											14	34	44	36	2	2	1	2	2	6							1			
<i>Pandora gouldiana</i>						1				1																				
<i>Pitar morrhuanus</i>		4					3	1	8	3	7	3	3	1	1	1				3	3		3	1	2			1		1
<i>Tellina agilis</i>	2	2						5		2																				
<i>Yoldia limulata</i>											10	3	5	2	1	1	1	2	1	6		1				1				
Gastropoda																														
<i>Acteocina canaliculata</i>											5		4	1	6	4	2	4	5	6					1			1		
<i>Anachis avara</i>						1					1	1																		
<i>Crepidula fornicata</i>			1																											
<i>Crepidula plana</i>	1																													
<i>Gastropoda juveniles</i>	118				12	8		5					1																	

	1	2	3	4	5	6	17	18	19	20	7	8	9	10	11	12	13	14	15	16	21	22	23	24	25	26	27	28	29	30
	S	S	S	S	S	S	S	S	S	S	M	M	M	M	M	M	M	M	M	M	SM	SM	SM	SM	SM	SM	SM	SM	SM	SM
Sample ID	L001	L002	L003	L004	L005	L006	L017	L018	L019	L020	L007	L008	L009	L010	L011	L012	L013	L014	L015	L016	L021	L022	L023	L024	L025	L026	L027	L028	L029	L030
<i>Ilyanassa trivittata</i>		1		1					2			4	1	1		3		1	4	3			1				4	2		
Naticidae spp.		1		2		1						3		1	1															1
<i>Turbonilla</i> sp.																					1									
<i>Urosalpinx cinerea</i>												1																		
PLATYHELMINTHES																														
<i>Stylochus ellipticus</i>																									1					
ECHIUROIDEA/SIPUNCULA				5		6	2		8	1	1				1															
Number of Species	28	30	28	32	28	35	31	24	33	28	17	14	21	16	14	14	14	14	10	14	7	11	7	10	13	8	11	13	9	5
Notes:																														
1. sp. = single species																														
2. spp. = multiple species																														
3. S=Sand, M=Mud, SM=Sandy Mud																														

Table 5.4-3 Average abundance and composition of the fauna in each area.

		Average Abundance (per sample)					Percent of Fauna			
Major	Taxa	Sand	Mud	Sandy	Overall		Sand	Mud	Sandy	Overall
Oligochaete	Oligochaeta spp.	0	0.3	0	0.10		-	0.35	-	0.05

		Average Abundance (per sample)					Percent of Fauna			
Major	Taxa	Sand	Mud	Sandy	Overall		Sand	Mud	Sandy	Overall
Polychaete	<i>Ampharete arctica</i>	29.9	0	0	9.97		6.77	-	-	5.30
Polychaete	<i>Amphitrite cirrata</i>	0	0.1	2.3	0.80		-	0.12	6.18	0.43
Polychaete	<i>Ancistrosyllis groenlandica</i>	2.5	0	0	0.83		0.57	-	-	0.44
Polychaete	<i>Aricidea catherinensis</i>	21.6	0	0.1	7.23		4.89	-	0.27	3.85
Polychaete	<i>Asabellides oculata</i>	1.4	0.2	0	0.53		0.32	0.23	-	0.28
Polychaete	<i>Asychis elongata</i>	0.1	0	0.6	0.23		0.02	-	1.61	0.12
Polychaete	<i>Brada</i> sp.	0.6	0	0	0.20		0.14	-	-	0.11
Polychaete	<i>Brania wellfleetensis</i>	0.5	0.1	0	0.20		0.11	0.12	-	0.11
Polychaete	Capitellidae spp.	0.2	1.2	0.4	0.60		0.05	1.41	1.08	0.32
Polychaete	<i>Clymenella zonalis</i>	0.5	0	0.5	0.33		0.11	-	1.34	0.18
Polychaete	<i>Cossura longocirrata</i>	0	0.1	0	0.03		-	0.12	-	0.02
Polychaete	<i>Drilonereis longa</i>	0.4	0	0	0.13		0.09	-	-	0.07
Polychaete	<i>Eteone heteropoda</i>	0.1	0	0	0.03		0.02	-	-	0.02
Polychaete	<i>Exogone dispar</i>	0.9	0	0	0.30		0.20	-	-	0.16
Polychaete	<i>Glycera americana</i>	0.4	0	0	0.13		0.09	-	-	0.07
Polychaete	<i>Gyptis vittata</i>	0	0.5	0	0.17		-	0.59	-	0.09
Polychaete	<i>Harmothoe</i> sp.	8.6	0	0	2.87		1.95	-	-	1.52
Polychaete	<i>Lumbrineris fragilis</i>	0.3	0	0	0.10		0.07	-	-	0.05
Polychaete	Maldanidae sp. (juveniles)	0	0.3	0	0.10		-	0.35	-	0.05
Polychaete	<i>Melinna cristata</i>	0	0	0.6	0.20		-	-	1.61	0.11
Polychaete	<i>Minuspio</i> sp.	0	2.4	0.9	1.10		-	2.82	2.42	0.59
Polychaete	<i>Nephtys incisa</i>	0.4	11.3	8.1	6.60		0.09	13.26	21.77	3.51
Polychaete	<i>Nephtys picta</i>	3.6	0	0	1.20		0.82	-	-	0.64
Polychaete	<i>Nereis grayi</i>	0	0	0.2	0.07		-	-	0.54	0.04
Polychaete	<i>Orbinia swani</i>	0.4	0	0	0.13		0.09	-	-	0.07
Polychaete	<i>Paranaitis speciosa</i>	0.6	0	0	0.20		0.14	-	-	0.11
Polychaete	<i>Paraonis gracilis</i>	0.1	23.8	9.2	11.03		0.02	27.93	24.73	5.87
Polychaete	<i>Parapionosyllis longicirrata</i>	1.8	0	0	0.60		0.41	-	-	0.32
Polychaete	<i>Phyllodoce arenae</i>	0.4	0	0	0.13		0.09	-	-	0.07

		Average Abundance (per sample)					Percent of Fauna			
Major	Taxa	Sand	Mud	Sandy	Overall		Sand	Mud	Sandy	Overall
Polychaete	<i>Polydora</i> spp.	1.2	2.6	0	1.27		0.27	3.05	-	0.67
Polychaete	<i>Polygordius</i> spp.	169.4	0	0	56.47		38.36	-	-	30.04
Polychaete	<i>Potamilla reniformis</i>	2.2	0	0	0.73		0.50	-	-	0.39
Polychaete	<i>Sabellaria vulgaris</i>	0.1	0	0	0.03		0.02	-	-	0.02
Polychaete	<i>Scalibregma inflatum</i>	1	0	0	0.33		0.23	-	-	0.18
Polychaete	<i>Schistomeringos caecus</i>	0.2	0	0	0.07		0.05	-	-	0.04
Polychaete	<i>Scolecopsis squamata</i>	0	1.1	0	0.37		-	1.29	-	0.20
Polychaete	<i>Sigambra</i> sp.	0	10.5	9.1	6.53		-	12.32	24.46	3.48
Polychaete	<i>Sphaerosyllis erinaceous</i>	0.1	0	0	0.03		0.02	-	-	0.02
Polychaete	<i>Spiochaetopterus oculatus</i>	0	0	0.1	0.03		-	-	0.27	0.02
Polychaete	<i>Spiophanes bombyx</i>	5.5	0	0	1.83		1.25	-	-	0.98
Polychaete	Terebellidae spp.	0.1	0	0	0.03		0.02	-	-	0.02
Polychaete	<i>Tharyx</i> sp.	7.5	0.6	0.3	2.80		1.70	0.70	0.81	1.49
Amphipod	<i>Ampelisca vadorum</i>	49.9	1.1	0.1	17.03		11.30	1.29	0.27	9.06
Amphipod	<i>Corophium</i> sp.	1.8	0	0	0.60		0.41	-	-	0.32
Amphipod	<i>Dulichia</i> sp.	0.1	0.1	0	0.07		0.02	0.12	-	0.04
Amphipod	<i>Erichthonius brasiliensis</i>	0.9	0	0	0.30		0.20	-	-	0.16
Amphipod	<i>Leptocheirus pinguis</i>	55.6	0	0	18.53		12.59	-	-	9.86
Amphipod	<i>Luconacia incerta</i> (Caprellid)	1.7	0	0	0.57		0.38	-	-	0.30
Amphipod	<i>Metopella</i> sp.	0.1	0	0	0.03		0.02	-	-	0.02
Amphipod	<i>Parametopella cypris</i>	0.2	0	0	0.07		0.05	-	-	0.04
Amphipod	<i>Paraphoxus spinosus</i>	0.2	0	0	0.07		0.05	-	-	0.04
Amphipod	<i>Phoxocephalus holbolli</i>	5.5	0	0	1.83		1.25	-	-	0.98
Amphipod	<i>Stenothoe minuta</i>	1.3	0	0	0.43		0.29	-	-	0.23
Amphipod	<i>Unciola irrorata</i>	6.5	0.1	0	2.20		1.47	0.12	-	1.17
Cephalocarid	Cephalocarida sp. (possibly H.	0	0	0.5	0.17		-	-	1.34	0.09
Barnacle	<i>Balanus amphitrite</i>	15.6	0	0	5.20		3.53	-	-	2.77
Cumacean	<i>Oxyurostylis smithi</i>	0	0.3	0.1	0.13		-	0.35	0.27	0.07
Brachyuran	<i>Panopeus herbstii</i>	2.3	0.1	0	0.80		0.52	0.12	-	0.43

		Average Abundance (per sample)					Percent of Fauna			
Major	Taxa	Sand	Mud	Sandy	Overall		Sand	Mud	Sandy	Overall
Brachyuran	<i>Pinnixa</i> sp.	1.7	0.7	0.4	0.93		0.38	0.82	1.08	0.50
Brachyuran	<i>Portunidae</i> sp. (juv: <i>C. maenas</i> / <i>O.</i>	0.1	0	0	0.03		0.02	-	-	0.02
Brachyuran	crab megalops	0	0	0.2	0.07		-	-	0.54	0.04
Caridean	<i>Crangon septemspinosa</i>	0.3	0	0	0.10		0.07	-	-	0.05
Ghost shrimp	<i>Gilvossius setimanus</i>	0.1	0	0.1	0.07		0.02	-	0.27	0.04
Shrimp	Shrimp (juvenile)	0.1	0	0	0.03		0.02	-	-	0.02
Isopod	<i>Cyathura polita</i>	0	0	0.2	0.07		-	-	0.54	0.04
Mysid	<i>Heteromysis formosa</i>	0.1	0	0	0.03		0.02	-	-	0.02
Mysid	<i>Neomysis americana</i>	0	0	0.1	0.03		-	-	0.27	0.02
Tanaid	<i>Leptochelia savignyi</i>	0.4	0	0	0.13		0.09	-	-	0.07
Ascidian	<i>Molgula</i> sp. (probably <i>M.</i>	0.9	0.3	0	0.40		0.20	0.35	-	0.21
Cnidarian	<i>Actinaria</i> spp.	0	0.4	0.4	0.27		-	0.47	1.08	0.14
Bivalve	<i>Anadara transversa</i>	2.5	0	0	0.83		0.57	-	-	0.44
Bivalve	<i>Astarte undata</i>	2.4	0	0	0.80		0.54	-	-	0.43
Bivalve	<i>Bivalvia</i> juvenile (<i>Crassinella</i> sp.?)	0.1	0.1	0	0.07		0.02	0.12	-	0.04
Bivalve	<i>Ensis directus</i>	0.3	0	0	0.10		0.07	-	-	0.05
Bivalve	<i>Lyonsia hyalina</i>	2.8	0	0	0.93		0.63	-	-	0.50
Bivalve	<i>Macoma tenta</i>	0.2	0.1	0	0.10		0.05	0.12	-	0.05
Bivalve	<i>Mulinia lateralis</i>	0.2	0.9	0.1	0.40		0.05	1.06	0.27	0.21
Bivalve	<i>Mytilus edulis</i>	4.3	0	0	1.43		0.97	-	-	0.76
Bivalve	<i>Nucula annulata</i>	0	14.3	0.1	4.80		-	16.78	0.27	2.55
Bivalve	<i>Pandora gouldiana</i>	0.2	0	0	0.07		0.05	-	-	0.04
Bivalve	<i>Pitar morrhuanus</i>	1.9	1.9	1.1	1.63		0.43	2.23	2.96	0.87
Bivalve	<i>Tellina agilis</i>	1.1	0	0	0.37		0.25	-	-	0.20
Bivalve	<i>Yoldia limulata</i>	0	3.2	0.2	1.13		-	3.76	0.54	0.60
Gastropod	<i>Acteocina canaliculata</i>	0	3.7	0.2	1.30		-	4.34	0.54	0.69
Gastropod	<i>Anachis avara</i>	0.1	0.2	0	0.10		0.02	0.23	-	0.05
Gastropod	<i>Crepidula fornicata</i>	0.1	0	0	0.03		0.02	-	-	0.02
Gastropod	<i>Crepidula plana</i>	0.1	0	0	0.03		0.02	-	-	0.02

		Average Abundance (per sample)					Percent of Fauna			
Major	Taxa	Sand	Mud	Sandy	Overall		Sand	Mud	Sandy	Overall
Gastropod	<i>Gastropoda</i> juveniles	14.3	0.1	0	4.80		3.24	0.12	-	2.55
Gastropod	<i>Ilyanassa trivittata</i>	0.4	1.7	0.7	0.93		0.09	2.00	1.88	0.50
Gastropod	Naticidae spp.	0.4	0.5	0.1	0.33		0.09	0.59	0.27	0.18
Gastropod	<i>Turbonilla</i> sp.	0	0	0.1	0.03		-	-	0.27	0.02
Gastropod	<i>Urosalpinx cinerea</i>	0	0.1	0	0.03		-	0.12	-	0.02
Flat Worm	<i>Stylochus ellipticus</i>	0	0	0.1	0.03		-	-	0.27	0.02
Sipunculid	Sipunculid	2.2	0.2	0	0.80		0.50	0.23	-	0.43
	Total Number of Species	72.0	36	31	95					
	Species per Sample	29.7	14.8	9.4	18.0					
	Abundance per Sample	441.6	85.2	37.2	188.0					
	Percent of Fauna						100.0	100.0	100.0	100.0
	Rare fauna (< 1%)						60	22	17	81
	Common (>= 1%)						12	14	14	14

Table 5.4-4 Species per sample, total number of species, and species richness based on the Chao 2 estimator for each bottom type. Values in parentheses are standard errors.

	Sample Size	Species per Sample	Total Number of Species	Chao 2 Number of Species
Sand	10	29.7 (1.0)	72	94.2 (13.3)
Mud	10	14.8 (0.9)	36	60.0 (20.2)
Sandy Mud	10	9.4 (0.9)	31	41.1 (8.0)

5.4.5 References

- Cao Y, Williams DD, Williams NE (1998). How important are rare species in aquatic community ecology and bioassessment? *Limnol Oceanogr* 43: 1403-1409.
- Gaston KK (1998). Ecology: Rarity as double jeopardy. *Nature* 394: 229-230.
- Hooper DU, Chapin, III FS, Ewel JJ, Hector A, Inchausti P, Lavorel S, Lawton JH, Lodge DM, Loreau M, Naeem S, Schmid B, Setälä H, Symstad AJ, Vandermeer J, Wardle DA (2005) Effects of Biodiversity on Ecosystem Functioning: A Consensus of Current Knowledge. *Ecol Monogr* 75: 3-35.
- Cerrato RM, Maher NP (2007) Benthic Mapping for Habitat Classification in the Peconic Estuary: Phase I Groundtruth Studies. Marine Sciences Research Center Special Report No. 134. State University of New York, Stony Brook, New York. 276 pp.
- Cerrato RM, Holt L (2008) North Shore Bays Benthic Mapping: Groundtruth Studies. Final Report to the NYS Department of Environmental Conservation. Marine Sciences Research Center Special Report No. 135. Stony Brook University, Stony Brook, NY. 184 pp.
- Chao A (1987) Estimating the population size for capture-recapture data with unequal catchability. *Biometrics* 43: 783-791.
- Colwell RK, Coddington JA (1994). Estimating terrestrial biodiversity through extrapolation. *Phil Trans Roy Soc Lon B* 345: 101-118.

5.5 *Emergent and Epi-Fauna Characterization*

5.5.1 *Background and Objectives*

This element of the project is the first to our knowledge to develop spatially comprehensive maps and interpretive products for Long Island Sound based on (and inclusive of) emergent- and epi-faunal elements of seafloor communities. In large part, this is due to the difficulties inherent in sampling the hard substratum habitats upon which epi-faunal organisms depend, as well as the fragility of those emergent taxa and biogenic structures that occur on the surface of fine-grained sediments. Hard substratum habitats are spatially rare in Long Island Sound, especially in deep waters (>10 m) of the central and western basins (Kenebel & Poppe, 2000, Poppe et al., 2000). These seafloor communities contribute uniquely to the rich biological diversity of Long Island Sound as well as functioning as physical habitat features and prey for a wide range of vagile species including fish, crustaceans, and molluscs of economic importance (e.g., Auster et al. 1995, 1997, 1998; Langton et al. 1995; Malatesta and Auster 1999). Further, a number of these species or species groups could serve as sentinels of climate change based on morphologies that include calcium carbonate structures (e.g., northern star coral *Astrangea poculata*; bivalve molluscs) and for assessing direct and indirect responses to natural and human-caused events due to structural fragility and environmental thresholds (e.g., turbidity, temperature, salinity, wave energy).

The objectives of this project element were to produce: (1) maps of defined community types based on emergent- and epi-fauna data collected during both fall 2012 and spring 2013, (2) maps of emergent- and epi-fauna species diversity based on both fall 2012 and spring 2013 data, (3) an analytic report of epifaunal and emergent community types based on detailed processing of sample data and, where historic data exists, comparisons with historic community state, (4) in collaboration with other project elements, a map integrating infaunal and epifaunal/emergent species diversity, (5) an inter-annual diversity map of epifauna/emergent fauna based on both fall 2012 and spring 2013 data, (6) a map of inter-annual spatial variations of epifauna/emergent fauna based on both fall 2012 and spring 2013 data, and (7) in collaboration with other project elements, a report on inter-annual/decadal variability.

5.5.2 *Image Acquisition & Methods*

Seafloor imagery was collected to assess seasonal composition and spatial variation of epi- and emergent faunal communities and associated habitat features during fall 2012 and spring 2013 (see Figure 5.5-1 for general workflow plan) in sampling blocks identified *a priori* based on multibeam bathymetry and backscatter data (Figure 5.5-2). Three undersea platforms were used (Figure 5.5-3) but all acquired digital imagery orthogonal to the seafloor (Figure 5.5-4; 10-17 October 2012, SEABOSS, 2800 images; 12-13 December 2012, ISIS, 297 images; 13-15 May 2013, Kraken 2, 493 images; 21-24 May 2013, SEABOSS, 1155 images). The December 2012

cruise using ISIS (Instrumented Seafloor Imaging System) and May 2013 cruise using the Kraken2 ROV were conducted primarily to acquire imagery in topographically complex and spatially constrained habitats where maneuverability of the camera platform is required to collect adequate image samples. Such areas were difficult to access using SEABOSS (e.g., the boulder reef feature along the southern spine of Stratford Shoal, the steep walls of the cut between north and south shoal regions, troughs between sand waves that support mussel dominated communities). All images were taken using artificial lighting (electronic flash or daylight color temperature lighting using HMI or LED sources) to enhance color saturation, edge sharpness, and depth of field. Paired parallel lasers were mounted adjacent to cameras and projected points into each image at 20 cm spacing to facilitate image calibration. All imagery was batch processed using the automated color correction routine in Irfanview software (version 4.35) in order to enhance color saturation and delineate color boundaries to facilitate identification of taxa.

Each image was subsequently examined for clarity and focus. Images with water turbidity that obscured the seafloor or that were out of focus such that identification of all organisms or biogenic features was impeded were rejected. This step produced a total of 574 processed images for analysis from fall 2012 sampling (SEABOSS = 517 images, ISIS = 57 images) and 630 images for spring 2013 (Kraken2 = 49 images, SEABOSS = 581 images).

Each color corrected image was analyzed for percent cover of all living organisms and biogenic features (e.g., shell, mud tubes, burrows). Each image was quantified using ImageJ software (version 1.45s; Abramoff et al. 2004) and was overlaid with a square grid (Figure 5.5-5). The grids did not extend to the edges of the images, but as the edges were sometimes out of focus due to air-water optical distortions caused by the flat port and open aperture of the underwater camera, this was considered acceptable. Because of variation in aspect ratios of the different cameras used across vehicles, the grid cells used for analysis were not consistent, (192 grid squares for all images except those from May 2013 SEABOSS with 216 grid squares) but cover was subsequently normalized based on calculations for percent cover (details below).

Within each grid square, organisms and biogenic features were identified to lowest possible taxonomic level and marked using the "cell counter" tool in ImageJ. This function displays a mark on each object as selected in the image and, in a separate window, displays counts of each object type. ImageJ only classifies objectives and related numerical counts as a series of undefined "Types" (e.g., Type 1, Type 2, etc.) and does not have a custom naming feature. Therefore, workflow processing of images required a separate record of the identity of "types" for each image and subsequently rectifying counts with actual taxonomic and feature classifications post-processing.

Several counting conventions (i.e., decision rules) were required to address variability in the cover of organisms and biogenic habitat features on the seafloor. Some colonial organisms (e.g., coral, sponge) and biogenic features occupied multiple grid squares. In addition, some solitary

organism (e.g. mussel, crab, gastropod) also were present in multiple squares. Such individuals were counted in each square to account for the area of coverage in each image. Conversely, more than one organism or biogenic feature could be in a single square and were each counted in order to account for all biological elements within an image. Therefore, the total grid count could be greater than the total number of squares in the grid (but then normalized across images by calculating percent cover, as described below). Total counts for each taxa or type of biogenic feature from each image were entered into a spreadsheet. All taxa, including fish fauna captured in images, and biogenic features were counted from imagery (a complete list of taxa and features is in Table 5.5-7). Taxa and features from the full matrix were parsed for analyses (Table 5.5-1) as invertebrates (i.e., both sessile and mobile invertebrates), biogenic features (i.e., those structures produced by biota such shell, worm tubes, burrows), and habitat forming species (i.e., those sessile invertebrate species that are structure forming such as hydroids, branching sponges). A screen shot of the processed image with the grid and counter window was archived. Using the scaling lasers in each image to calibrate length, the width and height of both the image and the grid was measured using the "measure" tool in ImageJ and area of coverage was calculated. Counts were converted to percent cover by dividing the count for each type of organism or feature by the total number of squares for the image. Percent cover was then arcsine transformed ($\arcsine(\sqrt{\%cover})$) to equalize variance in proportion data. These data were subsequently used in analyses to address objectives regarding characterization of communities, variation in patterns of diversity, distribution of habitat features, and seasonality of patterns (Fig. 5.5-6).

Maps, shapefiles, and layer files were created for the % cover of each habitat forming species, biogenic feature, and diversity measures in ArcMap (v10.1). Based on geospatial location, extracted from navigation files, each image was assigned to a sedimentary habitat based on analysis of backscatter data using Ecognition (see section 5.2). Color schemes for visualization of percent cover in maps of taxa or features are based on data binned as quintiles, species richness (S) maps are based on data binned by whole number richness (simply, the number of species or biological "types" in a sample), Shannon diversity maps ($H' \log 10$; a measure integrating species richness and the abundance of each species or type) are based on data binned as deciles, and community types based on number of categories from cluster groupings.

5.5.3 *Community Structure*

Fall 2012 and spring 2013 data sets were analyzed separately to assess seasonal differences in community composition across the seafloor landscape. All multivariate analyses were implemented using Primer v6.1.13 software (Clarke and Warwick 2001). The data set was reduced to include only habitat forming species and biogenic features, and all species of mollusk shell (i.e., clapper, unarticulated valves and partial identifiable valves) were combined as an aggregate category.

Jaccard's index was used to create a resemblance matrix. Non-metric multi-dimensional scaling (MDS) and cluster analyses (group average, complete linkage) were implemented to assess similarities between samples with each image serving as the sample unit (Figure 5.5-7). Stress values for each plot indicate that two-dimensional representation of the distance between samples is adequate. Community types were defined via the cluster analysis with thresholds based on distance measures of 32% for Fall 2012 and 10% for Spring 2013, resulting in 5 and 6 clusters, respectively (Figure 5.5-8). Sample units in the MDS plot were assigned to Ecognition patch types to facilitate assessment of correlation with variability in the sedimentary environment across the larger landscape. Multivariate dispersion indices for both fall and spring (Table 5.5-2) confirm that variation in community composition can be explained in part based on differences between groups of samples assigned to Ecognition patch types. R values for an ANOSIM using Ecognition acoustic patch type as a factor were significant for both fall and spring for $p=0.10$. It is notable that neither sample block or transect when used as a factor in these analyses produced significant results, or ecologically useful patterns when visualized. Paired comparisons based on community composition assigned to Ecognition patch types were implemented for both fall and spring using the SIMPER procedure. The top 90% of taxa contributing to dissimilarity between pairs of patch types are summarized in Table 5.5-8. Those taxa and features that consistently contributed the greatest to defining unique community compositions include: *Astrangia poculata* (coral), *Crepidula fornicata* (slipper shell limpet), *Mytilus edulis* (blue mussel), barnacle spp., *Corymorpha pendula* (hydrozoan), *Bostrichobranchus pilularis* (solitary ascidian), shell (both intact and broken shell hash), and burrows, among others.

The overlap observed in the MDS cluster groupings for both seasons is indicative of the patchy nature of the sedimentary environment and related factors (e.g., slope as it affects small scale erosional and depositional patterns as well as areas where shell and other biological debris accumulate). High spatial variation in assignments of community type by sample unit was common within sample blocks in areas of patchy sedimentary settings (Figure 5.5-9).

5.5.4 Diversity Measures

The pilot area exhibited a remarkable diversity of emergent, epifaunal, and vagile invertebrate taxa and biogenic habitat features. All habitat-forming species and biogenic features demonstrably have been shown to function as habitat based on variable levels of association with vagile species (e.g., Langton et al. 1995; Malatesta and Auster 1999) so here all biological structures have been included in initial assessments of the adequacy of sampling. There are a wide range of measures used to quantify diversity and many have been controversial in terms of their utility (Gray 2000). Here we used simple and widely utilized measures that are easily interpretable and useful for comparisons within a study area.

5.5.4.1 Sampling effort for characterization

One of the objectives of this pilot project was to develop and test the efficacy of methods for ecological mapping and characterization of seafloor habitats in Long Island Sound. Species richness (S) of seafloor communities, simply the number of species or unique taxa within a sample, is a useful measure for assessing the adequacy of sampling within a particular area. Species accumulation curves for all species and biogenic features within selected sampling blocks from the initial fall 2012 cruise illustrate adequacy of image sampling (Figure 5.5-10). Note that all curves are beyond the inflection point and approaching an asymptote. Notable is the greater number of taxa and biogenic features in sampling blocks on the shoal and hard substratum. While not all of the selected sampling blocks have reached an asymptote, all of the curves are beyond the inflection point and approaching an asymptote and can be considered to be adequately sampled. Interestingly, the richness curves show that there are a greater number of taxa and biogenic features in sampling blocks on the shoal and harder substrates.

Richness estimators (calculated using Primer v6.1.13) for all fall sampling blocks also suggest effort in most blocks was adequate for mapping purposes (Table 5.5-3). That is, dominant fauna in most blocks were accounted for although greater effort would yield more taxa or features. Note there were several sample blocks, mostly those in the deeper basins east and west of Stratford Shoal, where usable imagery was extremely limited. This is due to problems with storm induced suspended sediments. While adequate imagery was limited in particular sampling blocks, sample size based on occurrence in Ecognition patch types increases effort and spatial extent of samples (see details in the following section). Notable too is that even when all imagery across the pilot area for the fall surveys was considered (n=574 images, S=63), the Chao 2 estimator predicts 91 species although this is the highest estimate across all of the estimation approaches.

5.5.4.2 Seasonal Variation in Diversity

Species richness (S) and Shannon Diversity ($H' \log 10$) were calculated using Primer (v6.1.13) for each season on the following groups: invertebrates, habitat forming species, biogenic features, invertebrates and biogenic features combined, and habitat forming species and biogenic features combined. The final two measures incorporate the two classes of species as well as structural evidence of their presence. The final measure incorporates all elements of biogenic habitat diversity.

Examination of diversity maps (Figures 5.5-11 – 5.5-20 for richness, 5.5-21 - 5.5-30 for H' index) and summary statistics (Table 5.5-4) based on each of these species and feature configurations reveals similar patterns diversity. In general, both measures were higher within each season along the shallower coarse grained regions of the pilot area (Ecognition patch types F, E and D) in contrast to the deeper fine grained regions (patch types C, B and A). Further, diversity was higher overall in the spring than during the fall season. Seasonal differences were most pronounced in the deeper fine grain sediments where spring recruitment of species with annual life histories occurred, although spatial patterns of diversity were patchy (Figure 5.5-31).

Observed richness versus predicted richness based on multiple richness estimators suggests that sample sizes within Ecognition patch types were adequate (Table 5.5-5). The greatest differences between observed and estimates of species richness came from the most diverse habitats, those shallow coarse grain features bathed in waters above basin depths. That said, existing samples did differentiate those habitats based on mapping community types.

5.5.5 *Species Accounts*

Cover details for each habitat forming taxon and biogenic feature found in each Ecognition patch type were calculated using Sigmaplot v11 (i.e., mean, standard deviation, standard error, range, maximum and minimum values, median) and summarized in Table 5.5-6. Maps of each taxon and feature for each season illustrate spatial variability within sampling blocks and associations with Ecognition patch types (Figures 5.5-32 – 5.5-61). For most detail in regards to spatial variation, viewing in GIS and zoom to transect scale is recommended. Three examples are useful in illustrating linkages between species and biogenic feature distributions at small spatial scale. Northern star coral (*Astrangia poculata*) settles and grows on stable hard substratum such as cobble and boulder size rocks. The pilot scale map of coral reflects this distribution but when examined at fine scale, the patchy nature of coral occurrences and variability in cover emerges and is correlated with Ecognition patch types F and E (Figure 5.5-62). Variation in percent cover reflects both variations in the cover of hard substratum nested within a matrix of finer grain sediments as well as competition for space with other epifaunal taxa. Next, blue mussel (*Mytilus edulis*) also exhibits an affinity to stable sediments although the species can settle and grow on a wider range of grain sizes. Notably, blue mussel attains a degree of stability by interweaving byssus threads of multiple individuals. Dense aggregations of blue mussel were found in the sand wave habitat in the northern region of the study area and occurred in troughs of the sand waves evident from the BPI (bathymetric position index) map coverage (Figure 5.5-63). Based on visual observations it appears that sediments in troughs are finer grain and more stable than those coarse grained sediments found on the crests of the sand waves, and fine grained sediments may drape gravel in the troughs of sand waves. Finally, dense aggregates of shell, an important biogenic feature, are found downslope of the crest of the southern shoal. Examination of blue mussel cover on transects from deep to shallow water over the BPI coverage in this region illustrate how shell cover values at the bottom of slopes (Figure 5.5-64).

5.5.6 *Inter-seasonal Dynamics*

Different habitats exhibited varying degrees of change across the seasonal sampling. Diversity measures within sampling blocks exhibited highest levels of diversity on the crests of Stratford Shoal within transition areas for both fall and spring but highest diversity values occurred in the spring (Figures 5.5-65 and 5.5-66). Shallow communities characterized by coral and mussel, relatively long-lived species, exhibited a high degree of stability across seasons (Figure 5.5-67) while deeper fine grain sedimentary settings, characterized by short-lived solitary and colonial hydroids, solitary ascidians, and amphipods (based on emergent tubes), exhibited a high degree

of change due to spring recruitment dynamics (Figure 5.5-68). Contrasts between fall and spring distributions of *Bostrichobranthus* (Figures 5.5-40 and 5.5-41), *Corymorpha* (Figures 5.5-42 and 5.5-43), and amphipod tubes (Figures 5.5-32 and 5.5-33) illustrate some of the most dramatic seasonal differences at the spatial scale of the pilot area. As with small-scale variation of community classification and patterns of cover by taxon or feature, there was a high degree of small-scale variation in diversity both within and between seasons within habitats (Figure 5.5-69).

5.5.7 Historical Analysis: Loss of an Erect Sponge on a Rock Reef at Stratford Shoal

(This section is based on a manuscript currently in review at Marine Biodiversity Records. The current citation is: Stefaniak, L.M., P.J. Auster and I. Babb. In press. Loss of erect sponges on an offshore rock reef in Long Island Sound (NW Atlantic). Marine Biodiversity Records.)

Stratford Shoal is a topographic high running north-south across Long Island Sound, separating the western and central basins of this large estuary in the northwest Atlantic (Figure 5.5-70A; Knebel & Poppe, 2000). Currents over the shoal are primarily tidally-generated and run in an east-west direction, with accelerated flows occurring over the shoal (Knebel & Poppe, 2000). The southern portion of the shoal has a linear, north-south trending gravel reef, dominated by boulders on the topographic high along the crest (10 – 25 m in depth; Figure 5.5-70B; also see Figure 3-34) that descends to depths of 30 – 35 m with sediments composed of cobble to coarse sands and shell debris. While there had not been a systematic biological monitoring program focused on Stratford Shoal, this area had been visited multiple times from 1991 to 2012 using remotely operated vehicles, camera sleds, and divers to acquire imagery of the seafloor for various projects (Figure 5.5-70B). We used this archived imagery to produce a time series of presence-absence data for epifaunal organisms, allowing a coarse resolution assessment of community changes over time.

Initial observations in 1991 revealed a community on the boulder reef dominated by suspension-feeding, epifaunal invertebrates (>80% cover of rock surfaces; on average > 2 *H. oculata* colonies per m² unpublished data). Dominant taxa in the community included *Haliclona oculata* (Linnaeus, 1759; branching sponge), *Astrangia poculata* (Ellis & Solander, 1786; northern star coral), *Mytilus edulis* (Linnaeus, 1758; blue mussel), and erect bryozoans occurring at high densities. The same community was identified from 2007 and 2010 image records (Figure 5.5-71A - F). While we did not return to the same locations each year, all observations were consistent with this community type being distributed throughout the reef. These observations suggest a nearly 20-year period of community stability.

In October 2012, seafloor images of Stratford Shoal were collected as part of a systematic biological survey to produce an ecological map of Long Island Sound. These images include five transects perpendicular to the boulder reef (total transect length: 1500 m; Figure 5.5-70B). While *A. poculata* was still abundant, *H. oculata* was entirely absent in this imagery (Figure 5.5-

72A-B). Current, weather, and visibility constrained the area of the reef we were able to observe, so we returned in early December 2012 to search a larger area (total transect length: ~2000 m) and confirm our initial assessment (Figure 1B). While the resolution of the imagery taken makes it impossible to rule out the presence of microscopic resting stages (gemmules; Fell, 1974), no adult sponges were found (Figure 5.5-72C-D). *Haliclona oculata*, with its characteristic branching morphology, was absent in 2012, but other sponges exhibiting massive [*Cliona celata*, (Grant, 1826)] and encrusting (*Microciona* sp.) growth forms were present in very low abundance (≤ 1 colonies/m²). Whether the observed change reflects a short-term disturbance from which the community will recover or a shift in long-term community state remains unclear. Subsequently, detailed video surveys of the reef in May 2013, only eight months after our first indication that *H. oculata* was gone, revealed continued absence of this species. Because of the *ad hoc* and aperiodic nature of previous, simple presence-absence surveys, the driver of such change remains unknown.

There are a number of mechanisms that may have contributed, individually or synergistically, to the die-off of *H. oculata* at Stratford Shoal. The first possibility, that our survey in October 2012 was late enough in the year for adult sponges to have regressed into an overwintering stage, is unlikely. Though the shallow water sponge *Haliclona loosanoffi* (Hartman, 1958) exhibits an annual growth, reproduction, and regression cycle in New England, such cycles are rare in marine sponges (Fell, 1978). Koopman and Wijffels (2008) found reduced growth rates in adult *H. oculata* during winter months, but no overall die-off. Dredge sampling in Fishers Island Sound (an extension of the eastern end of Long Island Sound) found active adult *H. oculata* throughout the year for three years (1971-1974; Fell, 1974). Additionally, full-sized adult sponges were observed on Stratford Shoal in April 2010, which would not be expected if sponges regressed during colder months (Figure 5.5-71E-F).

If the Stratford Shoal population of *H. oculata* in Long Island Sound was the result of a one-time pulse recruitment event, subsequent senescence of adult sponges could lead to the sudden disappearance of the entire population. Given that the recruitment dynamics of isolated, mid-Sound populations and the typical life span of *H. oculata* are unknown, recruitment failure and adult senescence as mechanisms for population loss are speculation. However, *H. oculata* populations in Fishers Island Sound were found to be reproductively active on an annual basis (reproductive structures present March – June) over a three-year (1971-1974) sampling period (Fell, 1974). This suggests that the Stratford Shoal *H. oculata* population would have been reproductively active during at least some years between 1991 and 2010. In addition, examination of images across the time series reveals sponges across a range of sizes, suggesting but not confirming the presence of multiple cohorts, as size variation could simply be due to variable growth rates (Kaandorp, 1999).

Interspecific interactions such as predation or competition could impact sponge populations but are not likely to be the sole driver of community change in this case. Numerous predators are known to prey on *H. oculata*, including echinoderms (*Henricia sanguinolenta* (O.F. Müller,

1776); Dijkstra *et al.*, 2012), nudibranchs (Koopmans *et al.*, 2009), and fish (Chase, 2002). However, predation events for sponges tend to be sublethal (Wulff, 2006). The branching growth form of *H. oculata* with a small area of attachment even for large individuals gives *H. oculata* the potential to be a strong competitor on hard substrates where the primary limiting resource is space (e.g., Bell, 2007). If *H. oculata* had been competitively excluded, its replacement was not obvious in the October 2012 survey. *Crepidula fornicata* (Linnaeus, 1758) stacks found growing on boulders could have undercut *H. oculata*, either weakening the sponges' attachment or dislodging the sponges altogether. However, *H. oculata* was found to be associated with *C. fornicata* communities in southern England (Barnes *et al.*, 1973). But while no strong evidence suggests that interspecific interaction was a primary driver, we cannot discard the possibility that predation and competition played roles in the disappearance of *H. oculata* at Stratford Shoal. Generally, there is limited field evidence for competition or predation in sponges because dead sponges rapidly disintegrate and damaged areas quickly repair (Wulff, 2006). The 2.5-year lapse between the 2010 and 2012 observations makes it impossible to determine if there was a temporary pulse of predators or competitors that could have resulted in the total loss of adult sponges.

Unlike annual regression or recruitment failure followed by senescence of the adult population, thermal stress induced by increasing temperatures as a result of climate change may be more likely to have been involved in the loss of *H. oculata* from benthic habitats on Stratford Shoal. Long Island Sound has warmed over the last 40 years (Howell & Auster, 2012). The summer of 2011 was particularly warm, with surface temperatures in the central and western sound reaching 26.3 to 27.3 °C, respectively, in August (unpublished data – My Sound Oceanographic Observation Buoy; www.mysound.uconn.edu). The thermal tolerances of *H. oculata* have never been directly tested, but some evidence exists. A shallow water branching sponge identified only as *Haliclona* sp. from Long Island Sound was reproductively active in water as warm as 25 °C (Fell *et al.*, 1984). In the western Atlantic, *H. oculata* is found from the Gulf of St. Lawrence in the north to North Carolina in the south, but is often found in deeper waters (Hartman, 1958). Historically, bottom temperatures from these areas have ranged from 1 to 20 °C, annually (Hartman, 1958). A mass mortality of *H. oculata* in the Netherlands in 2006 was hypothesized to be the result of an unusually warm summer (~23 °C; Koopmans & Wijffels, 2008), but this was not tested. Perhaps the most relevant evidence in favor of thermal stress as a strong driver is the continued conspicuous presence of both *A. poculata* and *C. celata*, on Stratford Shoal. *Astrangia poculata* can tolerate summer temperatures up to 27 °C (Jaques *et al.*, 1983). Members of the *C. celata* species complex share *H. oculata*'s Atlantic distribution (and therefore, its Atlantic temperature distribution), but are also found in the Gulf of Mexico (Hartman, 1958; Xavier *et al.*, 2010) in areas where water temperatures can exceed 30 °C (Miller *et al.*, 2010). Higher thermal tolerances for these two species would allow them to persist even at temperatures that would negatively affect *H. oculata*.

Increased temperatures may also work synergistically with disease, which could have caused a die-off. Increased water temperatures are linked to increased virulence of sponge disease, and environmental stress may reduce innate immune systems in sponges (Webster, 2007).

Theoretically, the branching morphology should be the most effective at battling disease because of the relative ease of compartmentalizing diseased areas (Webster, 2007), but Shield and Witman (1993) found that diseased areas were often found at the base of the sponge, potentially weakening the sponge and increasing the chance of dislodgement. Rapid disintegration of dead tissue makes detection of sponge disease difficult (Webster, 2007). Disease was attributed as the cause of a *H. oculata* die-off in northern Wales in 1988-89, but no testing was undertaken to determine the presence of a pathogen (Webster, 2007).

A major event that could have affected mid-Sound populations of *H. oculata* in Long Island Sound between 2010 and 2012 was Hurricane Irene. Heavy rainfall in the Housatonic, Connecticut, and Thames River watersheds resulted in freshwater and terrigenous sediment inputs into Long Island Sound up to two orders of magnitude greater than before the storm (USGS 2013). Surface salinities in the sound were reduced to as low as 21.5 ppt (unpublished data – My Sound Oceanographic Observation Buoy; www.mysound.uconn.edu; 1991 to 2007 average: 26.21 – 30.05 psu; Whitney, 2010), and the Connecticut River was visibly discolored with sediment (NASA, 2013). Reduced salinities could have affected sponge populations. While *H. oculata* has decreased growth rates at lower salinities (Koopmans & Wijffels, 2008), *A. poculata* also may have reduced abundances at low salinities (Patrizzi, 2010) and salinities below 20 ppt would also negatively affect *C. celata* populations (Hartman, 1958). Since *A. poculata* and *C. celata* were apparently not affected, low salinity due to Hurricane Irene was likely not the primary driver of the *H. oculata* die-off at Stratford Shoal.

Increased sedimentation due to Hurricane Irene is unlikely to have had strong negative effects on *H. oculata*. Populations of *H. oculata* in waters off New Brunswick are usually found in areas with silt and sedimentation (Ginn, 1997). In Lough Hyne, Ireland, sponge richness is greatest at the site with the most sedimentation (Bell, 2007). Even some encrusting sponges can live under sediment (Bell, 2007), but tubular sponges are able to actively avoid sedimentation by deflecting settling sediment with their exhalant water jet (Bell, 2004). Multi-tube sponges such as *H. oculata* may be less suited to avoid sedimentation in that manner; however, they still may be able to withstand occasional increased sediment loads (Bell, 2004). Additionally, while the *H. oculata* population is no longer present at Stratford Shoal, large, healthy-looking *C. celata* sponges, which presumably would also have been negatively affected by increased sediment loading, were found during our surveys.

Along with freshwater and sediment input, Hurricane Irene also caused strong wind-driven water movement in Long Island Sound with a maximum wave height of 5.27 m and maximum wind speed of 32.1 ms⁻¹ in the central sound (unpublished data– My Sound Oceanographic Observation Buoy; www.mysound.uconn.edu). These surface conditions can translate to significant increases in shear stress at the seafloor during storms based on wave-current

interactions. A previous study at a 20 m deep site in the central sound measured maximum daily tidal flows at 20-40 cm s⁻¹ with average peak shear stress of 3 dyn cm⁻² during calm conditions (Wang et al. 2000). During a storm event that produced significant wave heights up to approximately 1.7 m, shear stress increased to a peak value of 36 dyn cm⁻², a factor of 10 from nominal tidal induced stresses (Wang et al. 2000). Wave height during the period of maximum impact of Hurricane Irene, approximately 3 times that of the smaller storm, would have produced greatly increased bottom stresses along the entire reef. Because of their small point of attachment, arborescent sponges such as *H. oculata* are more likely to be dislodged during storms than massive sponges such as *C. celata*. *Haliclona oculata* is one of a number of sponge species that produces gemmules: encapsulated masses of cells thought to be resting stages to wait out unfavorable environmental conditions (Fell, 1974). Unlike the shallow water sponge *Haliclona loosanoffi*, gemmules in *H. oculata* do not appear to be winter resting stages but may assist with asexually reestablishing populations after adult sponges are dislodged (Fell, 1974). An average of 76% of *Haliclona oculata* individuals collected year-round in Fishers Island Sound had gemmules located at the base of the sponge, where they may survive even if the sponge is dislodged (Fell, 1974). Because of the proximity of Hurricane Irene to the imaging of Stratford Shoal in 2012, even if gemmules were able to persist through the storms, *H. oculata* communities may not have yet had time to recover to the point of detection by remote imaging.

In addition to the effects of extreme events, western Long Island Sound is subject to seasonal summer hypoxia (defined as dissolved oxygen as less than or equal to 3.0 mg l⁻¹). The southern shoal region is classified in the fourth decile (i.e., 30-40%) in terms of years that the area has experienced seasonal hypoxia from 1991 -2011, with a seasonal low dissolved oxygen level between 2.0-2.99 mg l⁻¹ at the end of August 2011 just prior to Hurricane Irene (CT DEEP, 2011). Clearly, the sponge population at Stratford Shoal persisted despite multiple hypoxic events over most of the time period of our observations. However, the periods of exposure and magnitude of hypoxia are unresolved, so the roles of acute or chronic exposure to reduced oxygen remain unclear as an explanation for their local extirpation.

In locations where *H. oculata* are found, populations tend to be stable over many years (e.g., Kluijver & Leewis, 1994; Ginn, 1997; Bell *et al.*, 2006; Koopmans & Wijffels, 2008). In addition to the current observations, only two other mass die-offs of *H. oculata* have been recorded: one in Wales that was attributed to disease and one in the Netherlands that was potentially the result of high temperatures (Webster, 2007; Koopmans & Wijffels, 2008). The analysis presented here suggests that increased temperatures in Long Island Sound combined with the effects of water movement driven by Hurricane Irene are likely the primary drivers of the *H. oculata* die-off at Stratford Shoal, with interspecific interactions and disease as potential, but untestable, synergistic drivers. However, in the absence of an intensive monitoring program, determining the causes of sponge die-offs in the field is extremely difficult because dead sponges rapidly disintegrate, taking evidence of mechanisms with them (Wulff, 2006).

This case study highlights the need for additional monitoring of important habitats such as Stratford Shoal and increased understanding of the biology and ecology of the species found there. Hard substratum reefs are spatially rare in Long Island Sound, especially in the central and western basins and in deep (>10 m) water (Kenebel & Poppe, 2000, Poppe *et al.*, 2000). Isolated, mid-Sound hard substrate communities in Long Island Sound also have few or no conspicuous non-native species, unlike nearshore habitats, where non-native species are abundant (unpublished data). The boulder reef at Stratford Shoal had, prior to this study, been sampled three times in the last two decades, and *H. oculata* is a highly conspicuous sponge with some biological data available from previous studies (e.g., Hartman, 1958; Fell, 1974; Kluijver & Leewis, 1994; Ginn, 1997; Bell *et al.*, 2006; Koopmans & Wijffels, 2008). However, lack of systematic monitoring and local process studies precludes any understanding of the fine time scale dynamics of change in this community, allowing us to only hypothesize what the drivers of change may be. Understanding of the dynamics of isolated, mid-Sound reef communities and the functional roles of component species (e.g., *H. oculata* can be important habitat for fishes, Houziaux *et al.*, 2007) is needed in order to assess the role of natural variation versus human-caused drivers and to link management actions to goals for conservation and sustainable use.

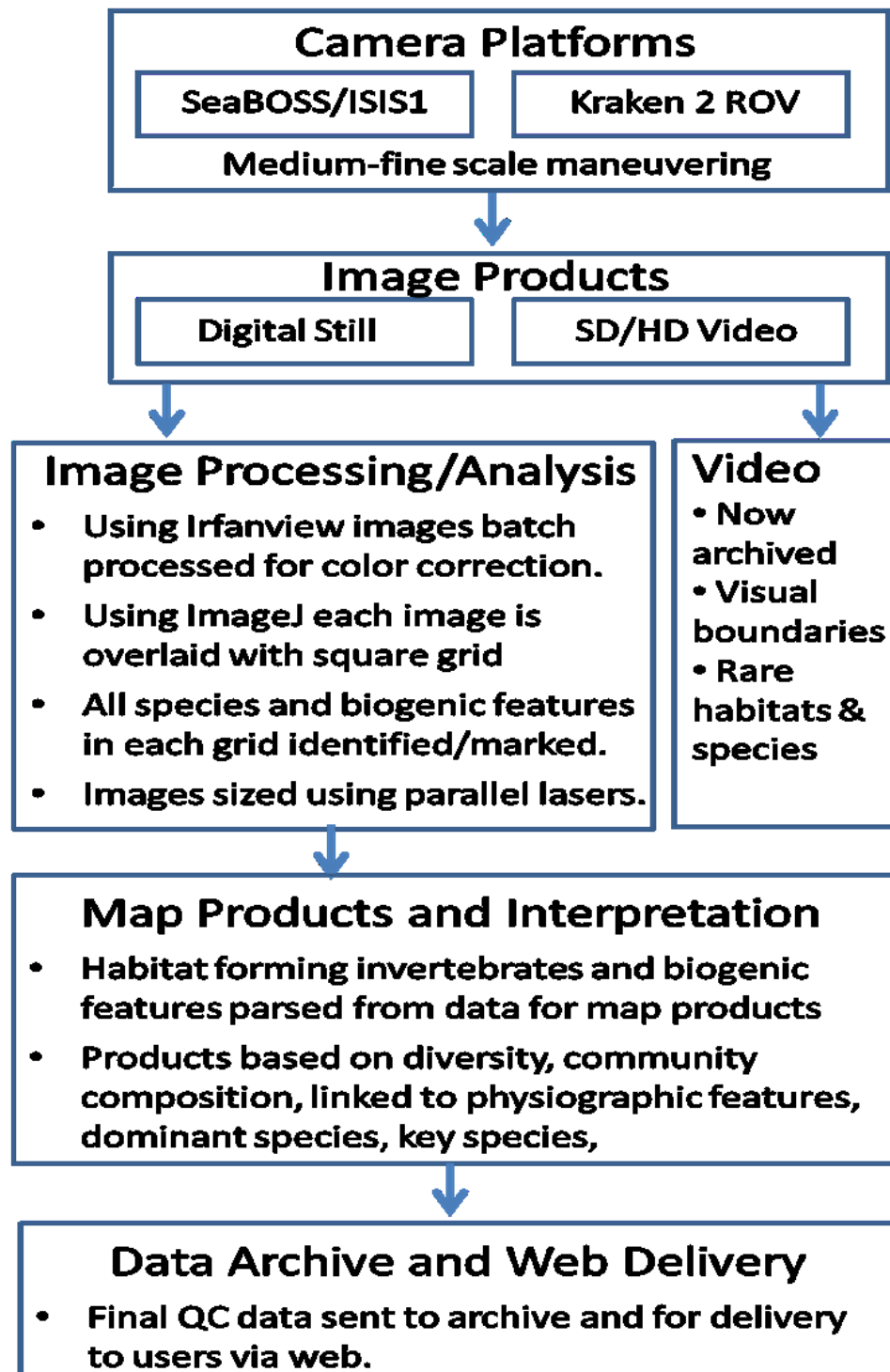
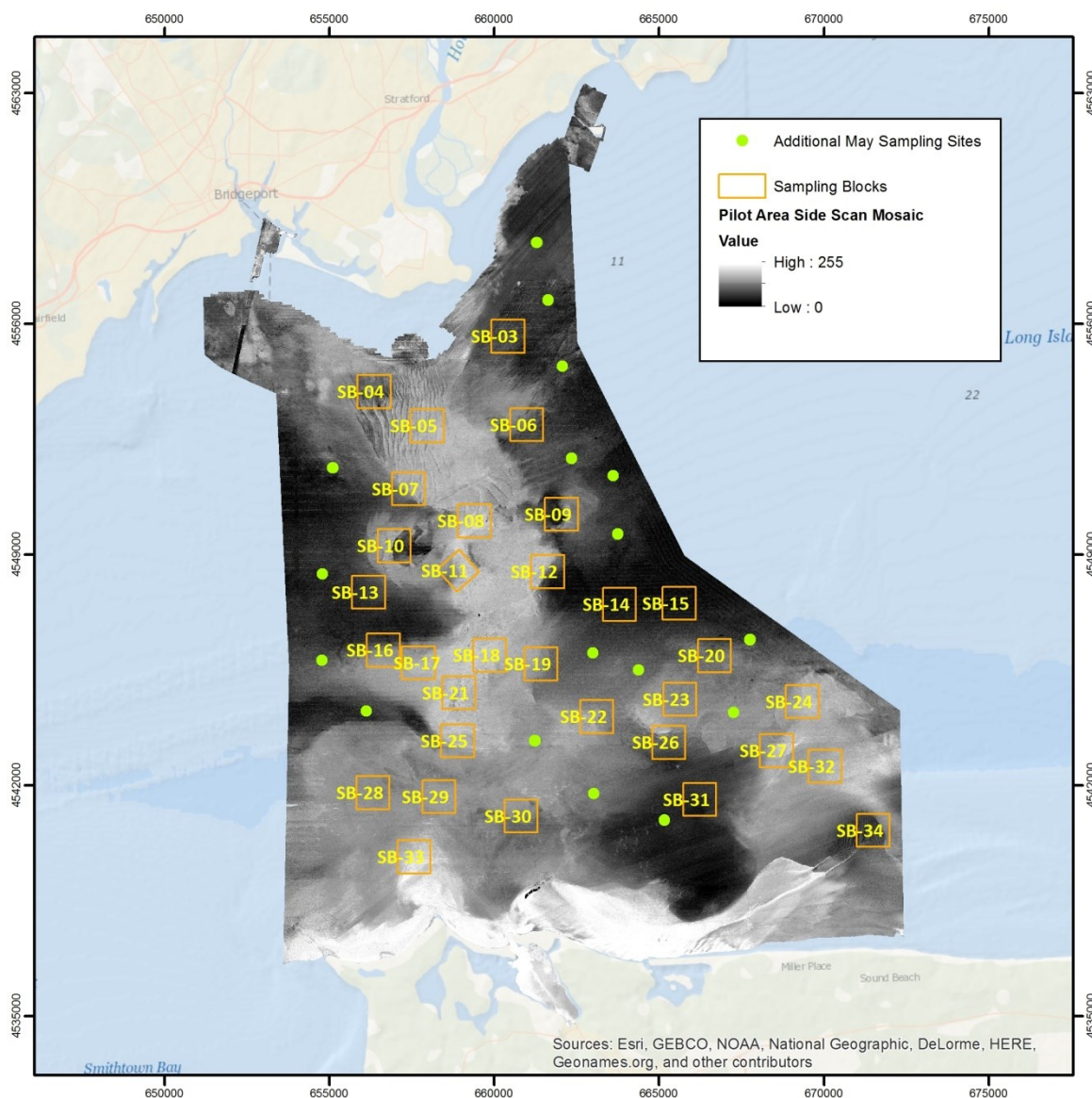


Figure 5.5-1. Workflow for acquisition and analysis of georeferenced imagery of emergent and epifaunal communities



Ecological Sampling Blocks

Imaging transects for census of emergent- and epi-faunal taxa were conducted within each sampling block (SB) across two seasons.



0 4 Miles

Horizontal Coordinate System:
UTM Zone 18 Datum NAD83



THE
UNIVERSITY
OF RHODE ISLAND

Lamont-Doherty Earth Observatory
COLUMBIA UNIVERSITY | EARTH INSTITUTE



Figure 5.5-2.

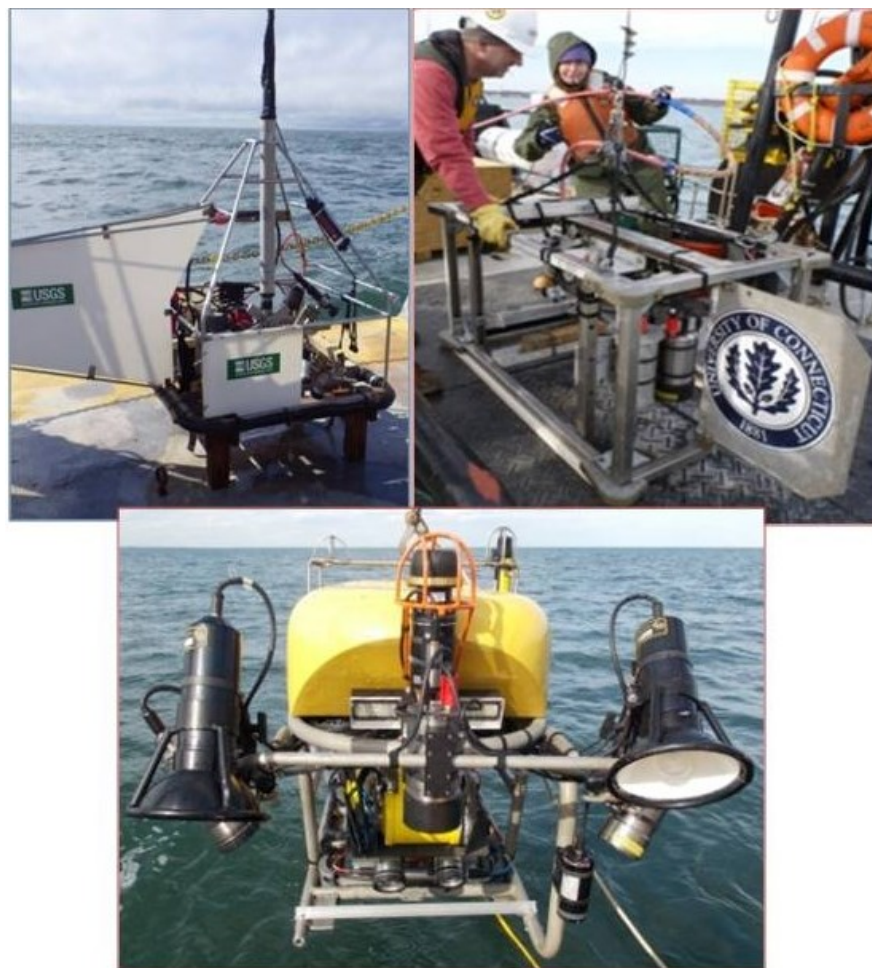


Figure 5.5-3. Underwater vehicles used to acquire seafloor imagery: ISIS - Instrumented Seafloor Imaging System (top left), SeaBOSS - Seabed Observation and Sampling System (top right), and the Kraken 2 remotely operated vehicle (bottom).

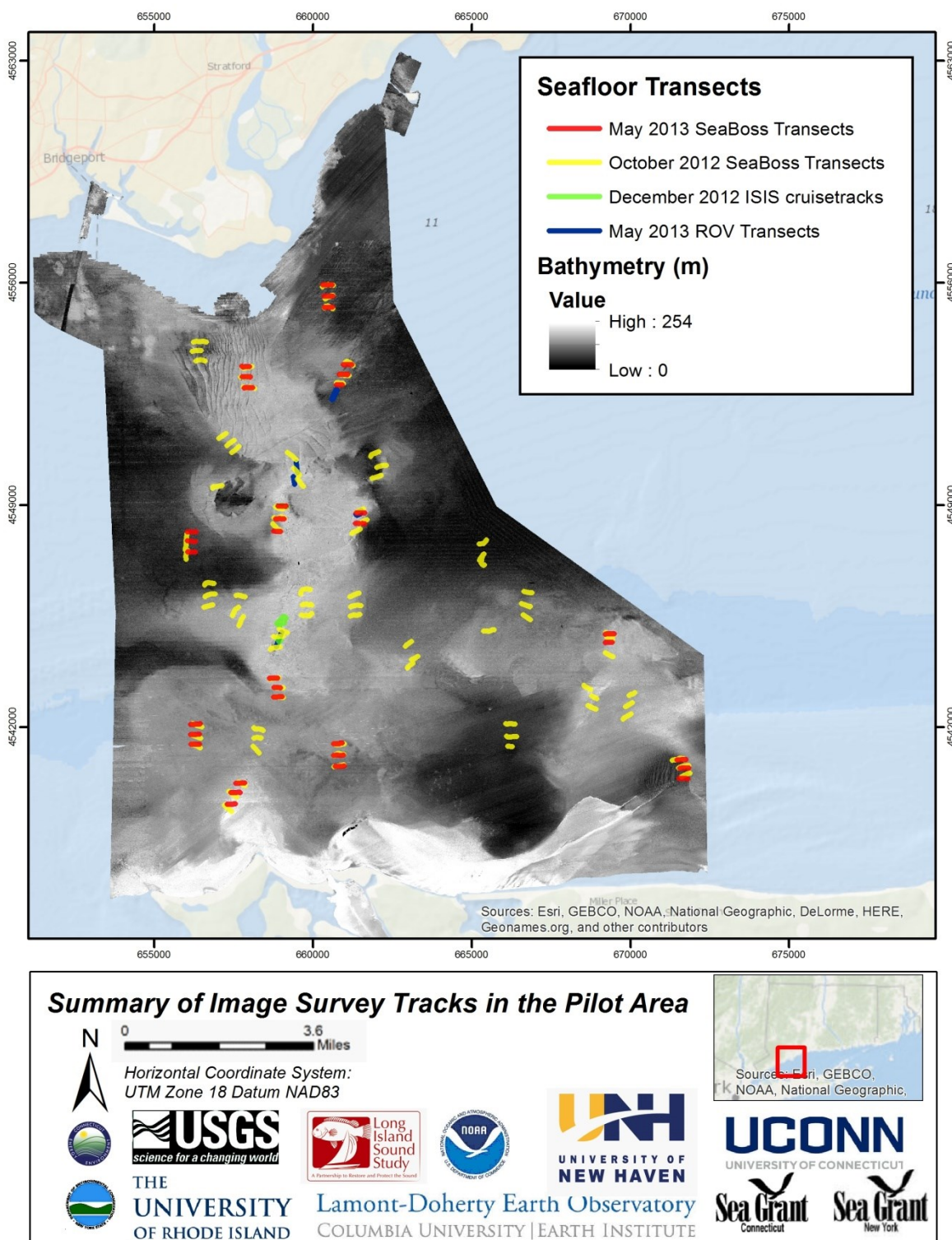


Figure 5.5-4.

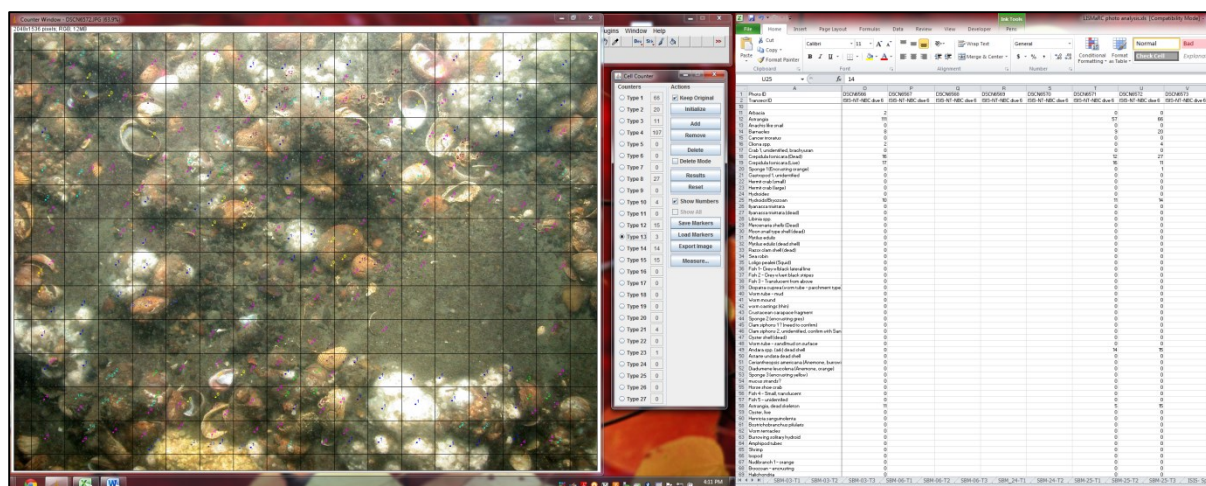


Figure 5.5-5. Example of grid over a seafloor image in ImageJ software. Window to the right of image automatically tallies cumulative counts of object types as described in text. These counts are manually translated to a spreadsheet (samples as columns) with actual taxonomic or biogenic feature identifications (rows).

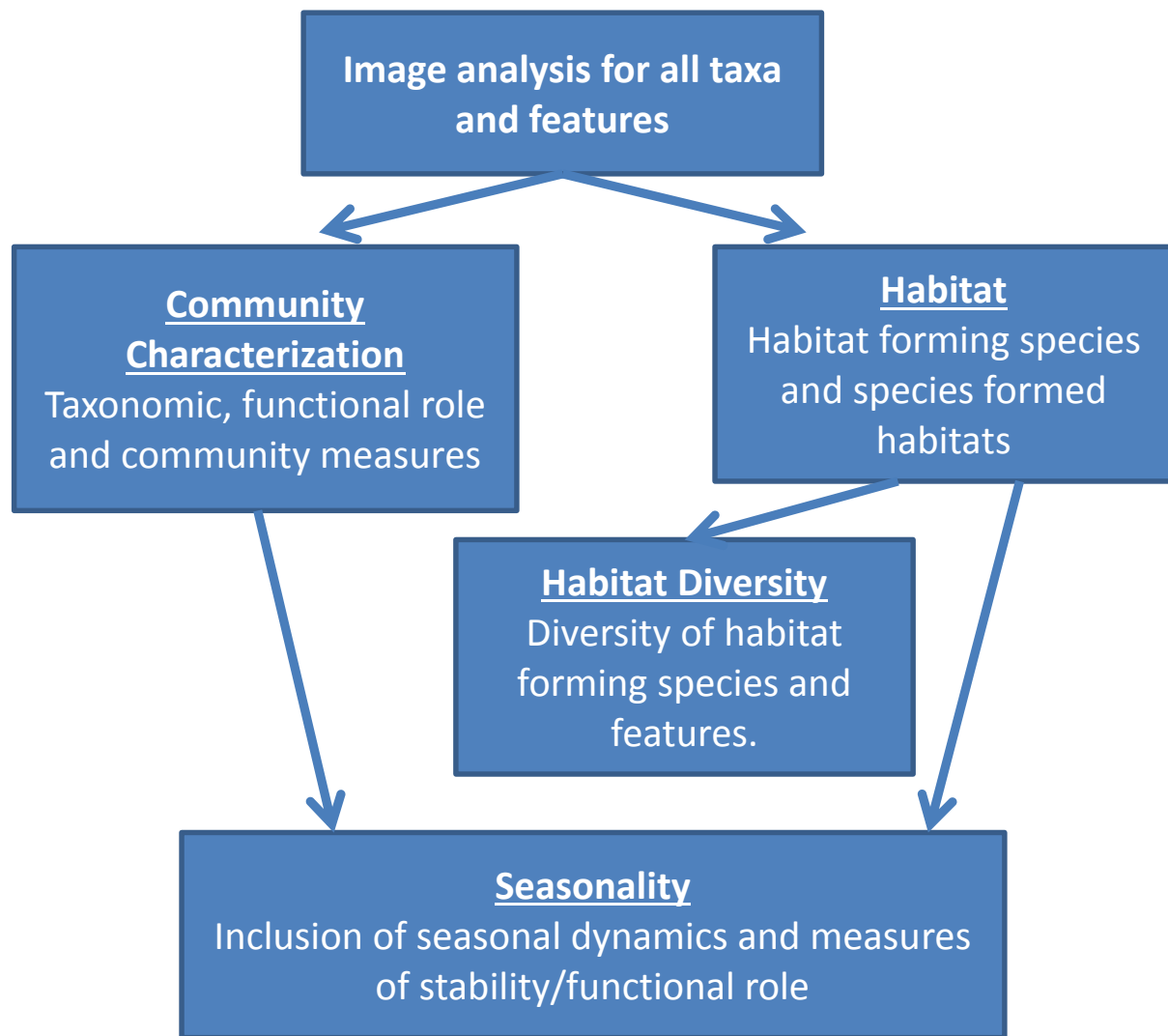
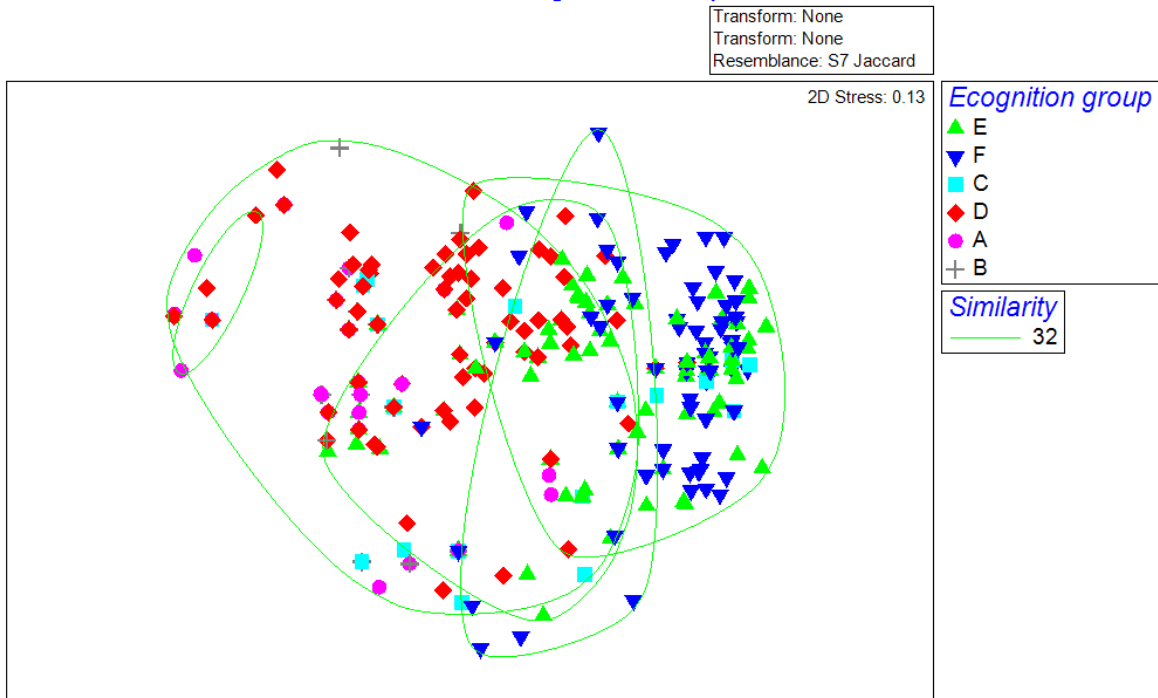


Figure 5.5-6. Generalized flow diagram for use of analytic results to produce map products for ecologic attributes as identified in the Long Island Sound Habitat Classification Scheme (Auster et al. 2009; i.e., habitat forming species, biogenic features, dominant taxa, dominant taxonomic groups, community type, key managed species key ecologic species, diversity).

Fall 2012 emergent- and epi-fauna



Spring 2012 emergent- and epi-fauna

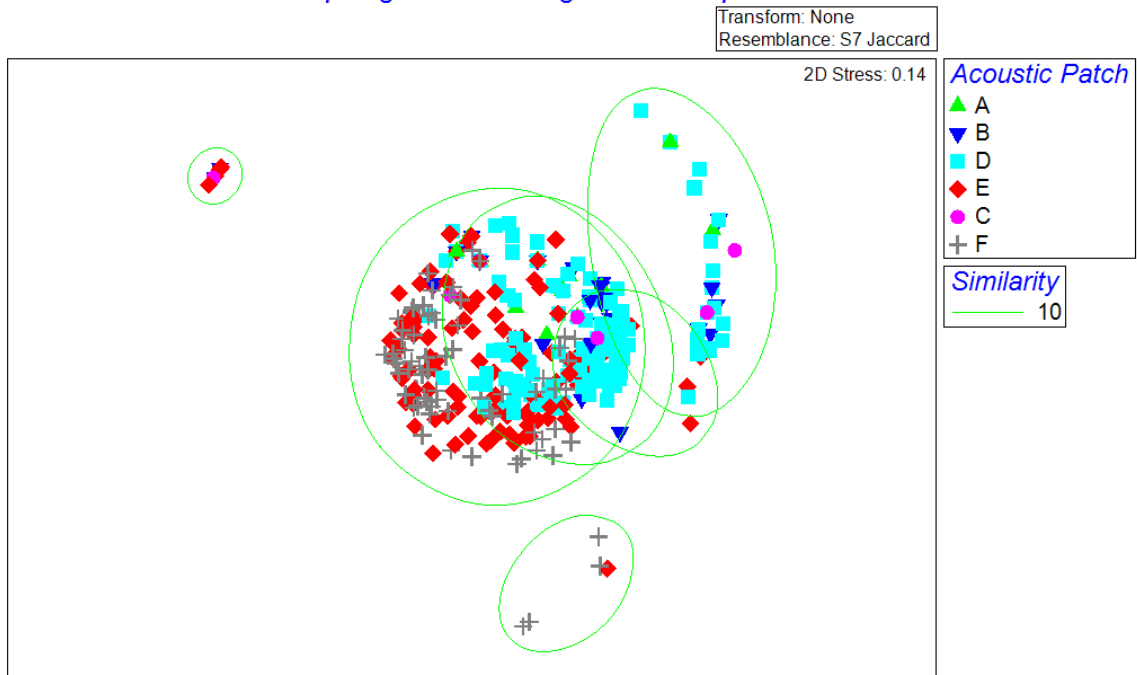


Figure 5.5-7. MDS plots of community composition for fall 2012 and spring 2013 periods. See text for detailed explanation.

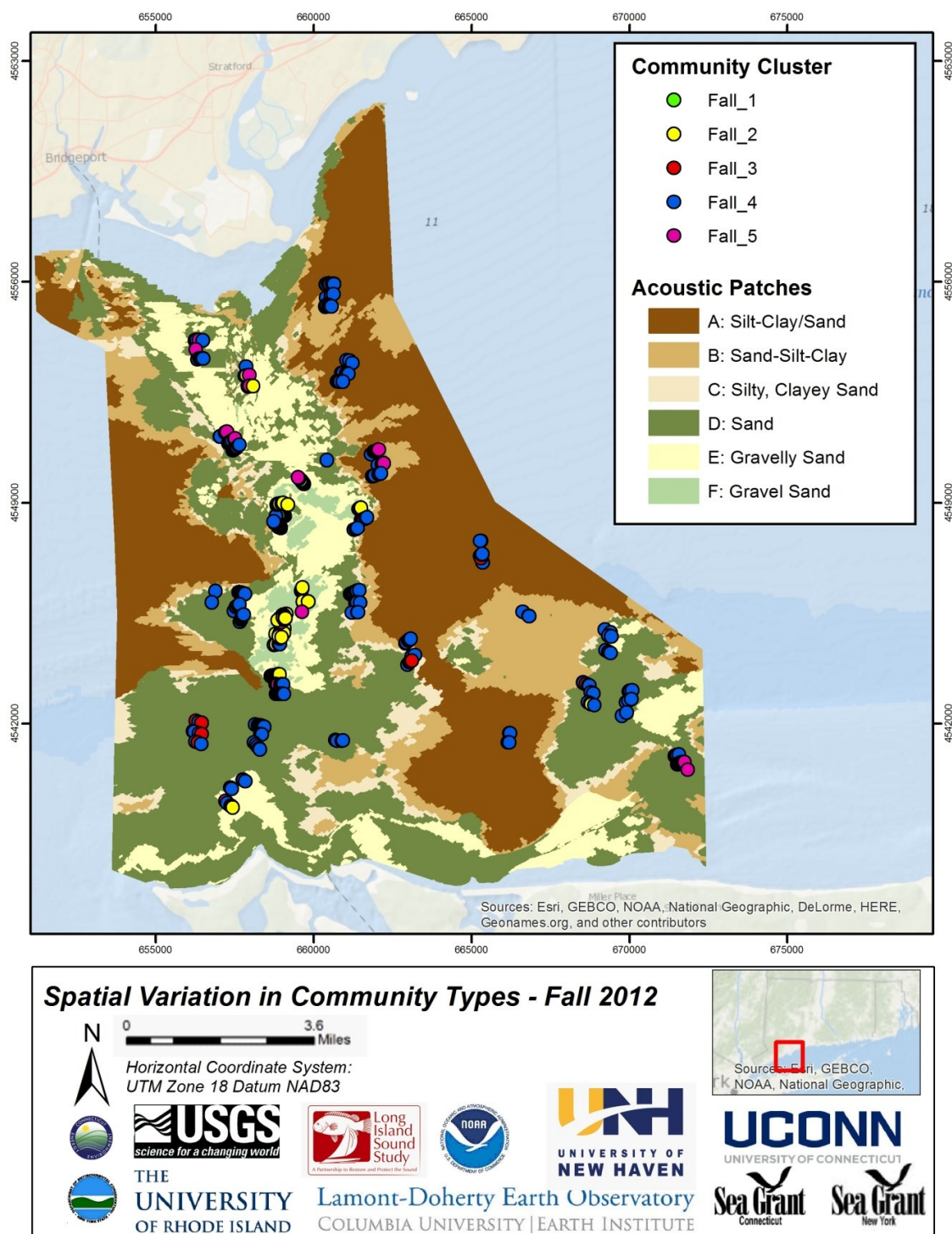


Figure 5.5-8a. Large scale spatial variation in community types based on multivariate analyses for fall (above) and for spring time periods (next page). Small scale variation within sampling blocks is evident when viewed at such smaller spatial scales.

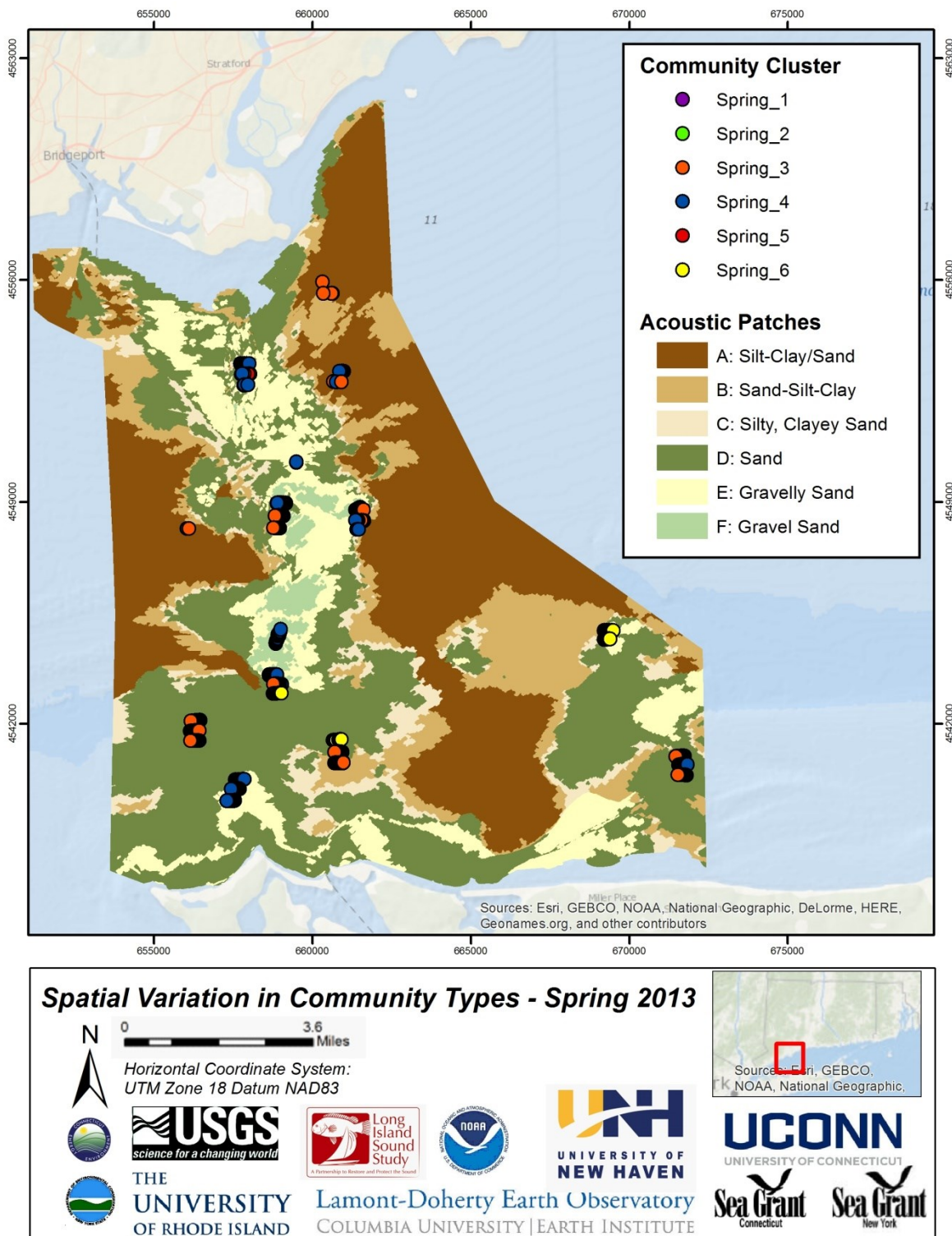


Figure 5.5-8b (continued).

SB-11

SB-34

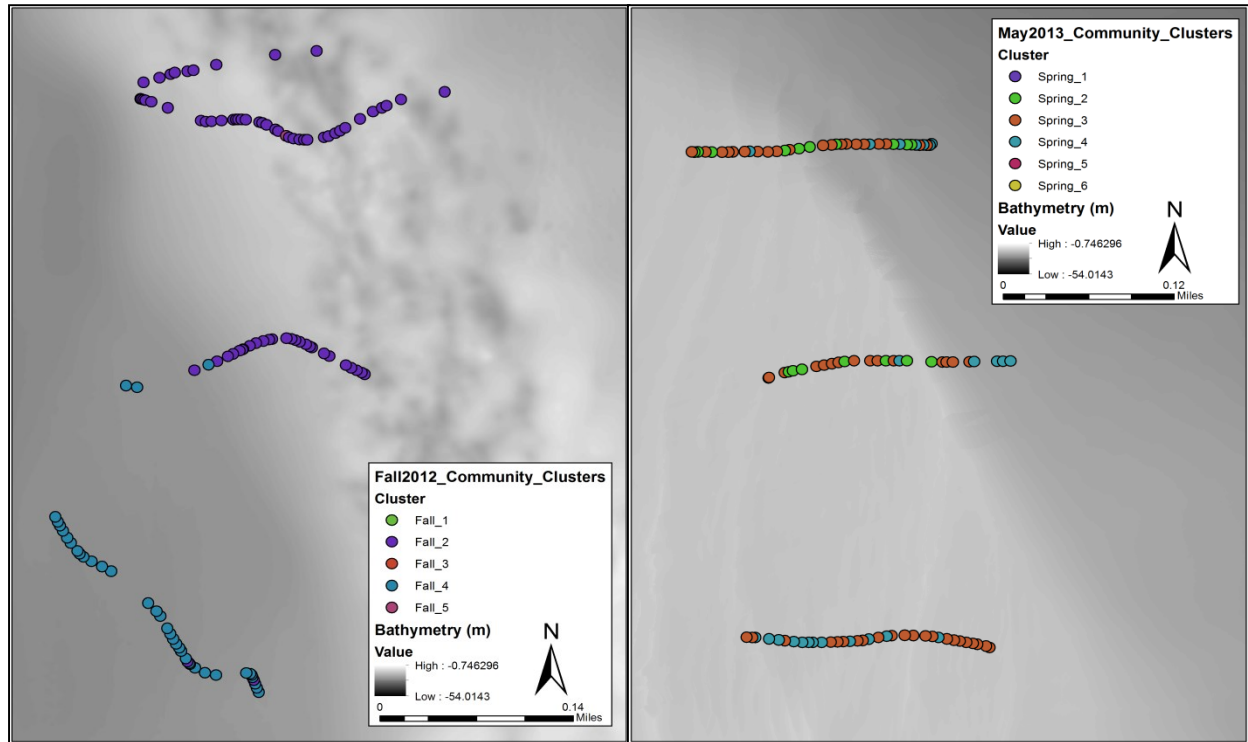


Figure 5.5-9. Examples of variability in seafloor community type observed within transects and within sample blocks.

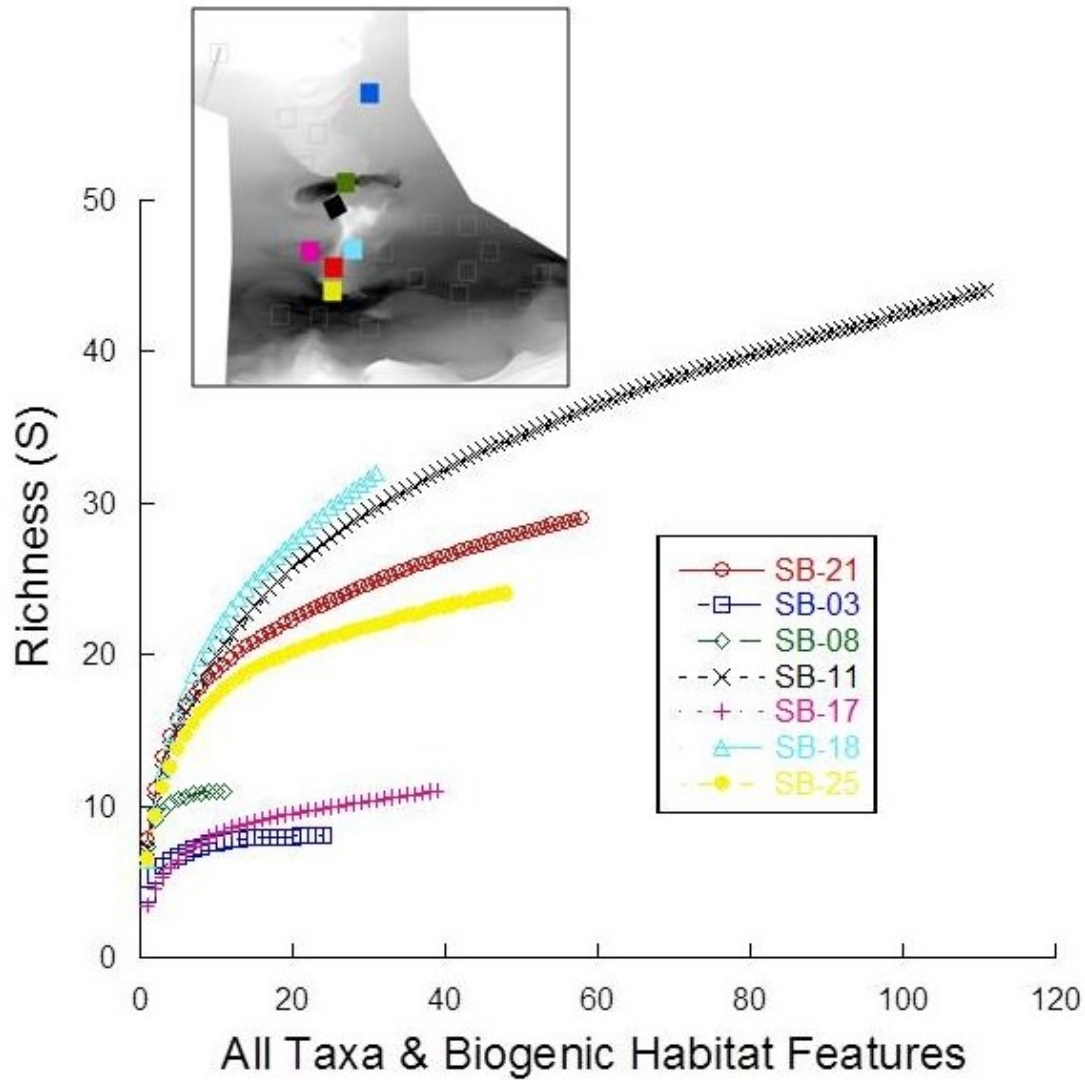


Figure 5.5-10. Species accumulation curves for all invertebrate taxa and biogenic features in selected sample blocks from fall 2012 survey. Note that all curves are beyond an inflection point and approaching asymptote.

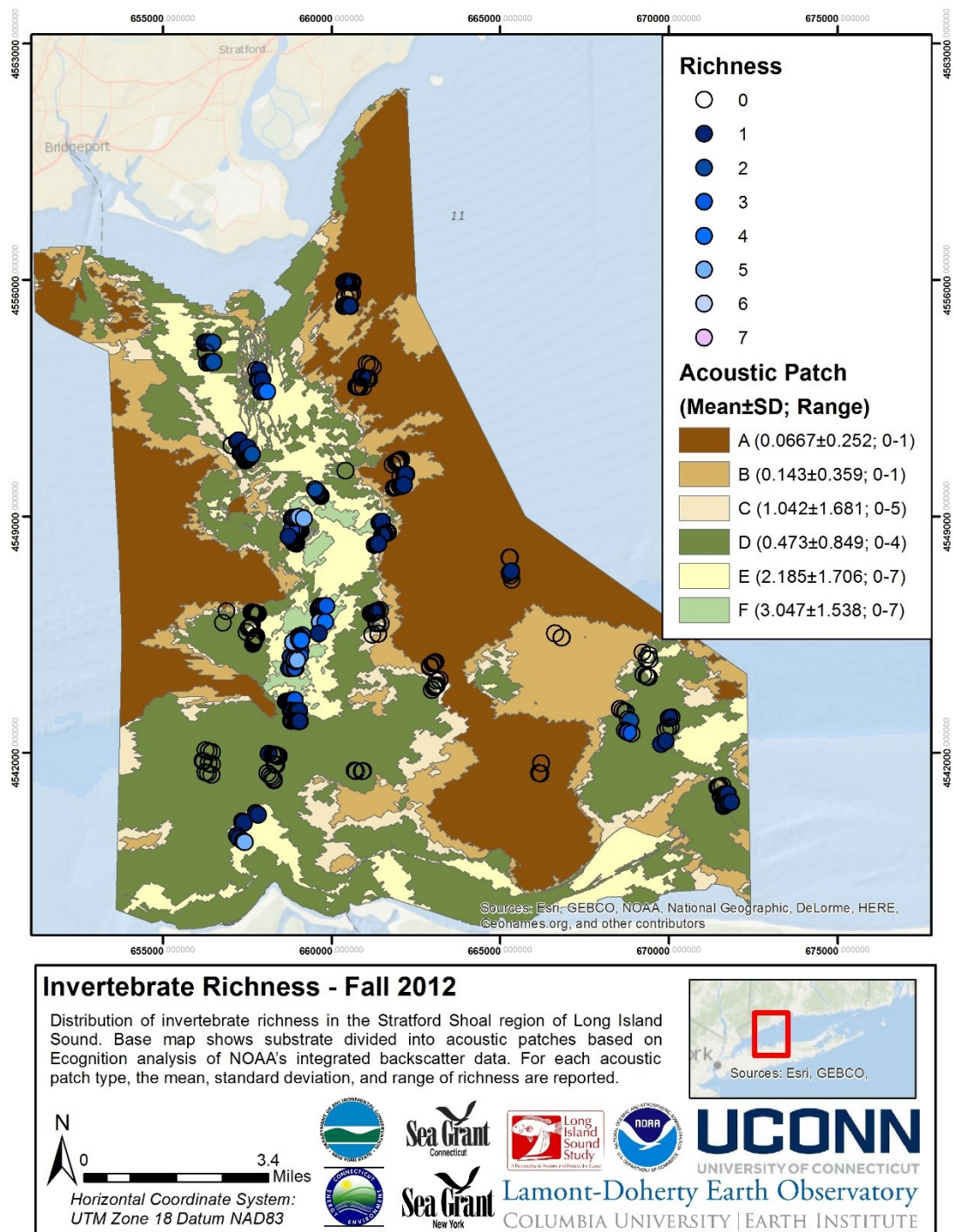


Figure 5.5-11

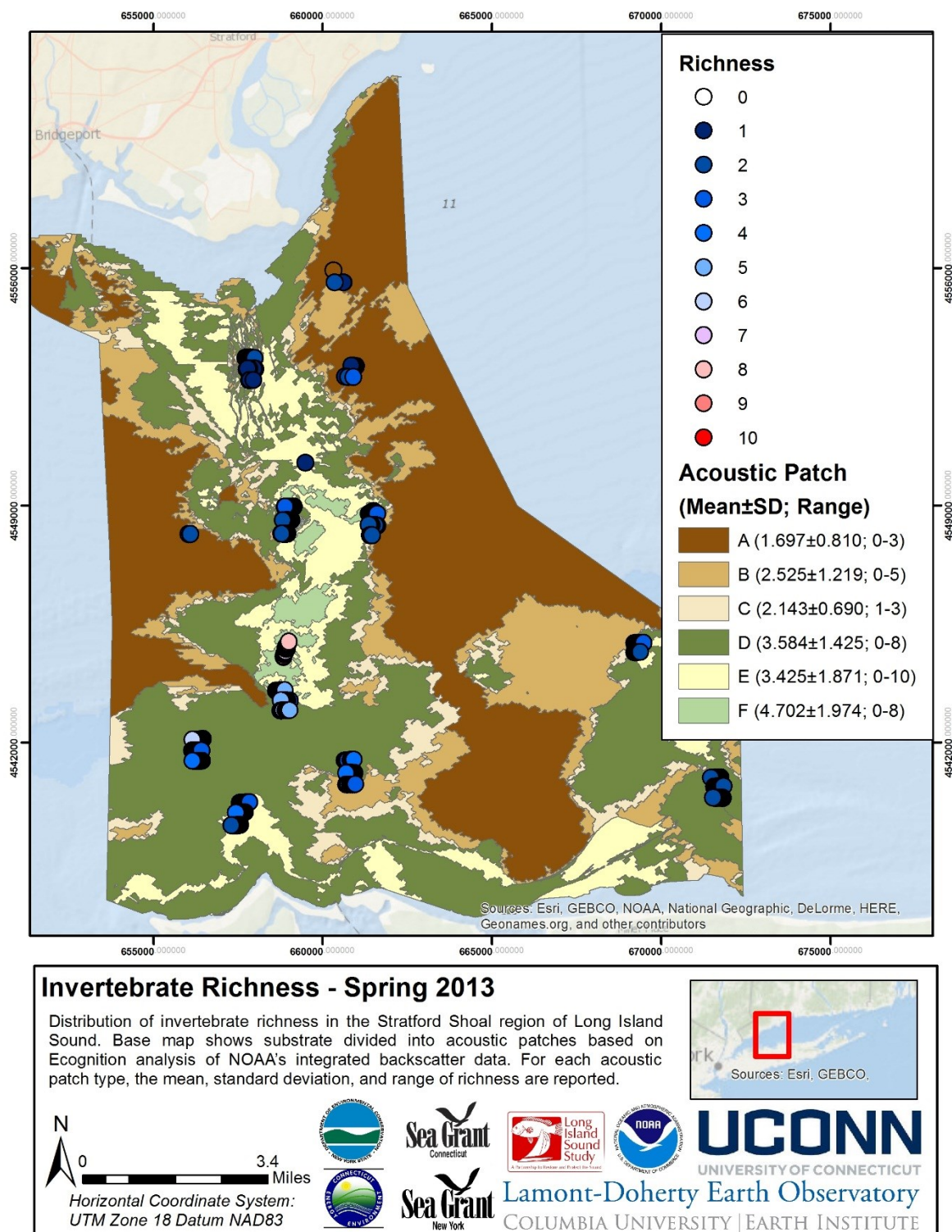


Figure 5.5-12.

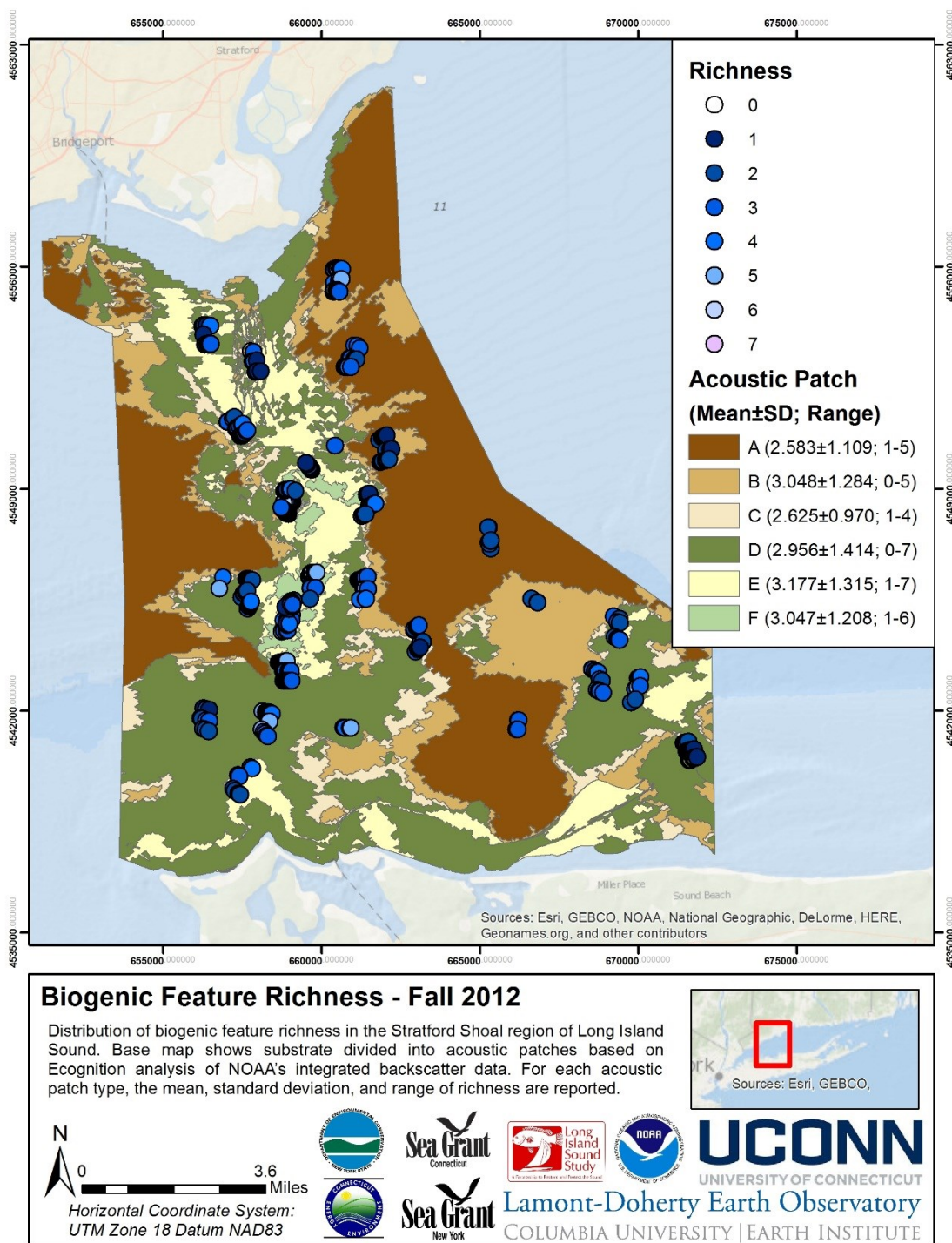


Figure 5.5-13.

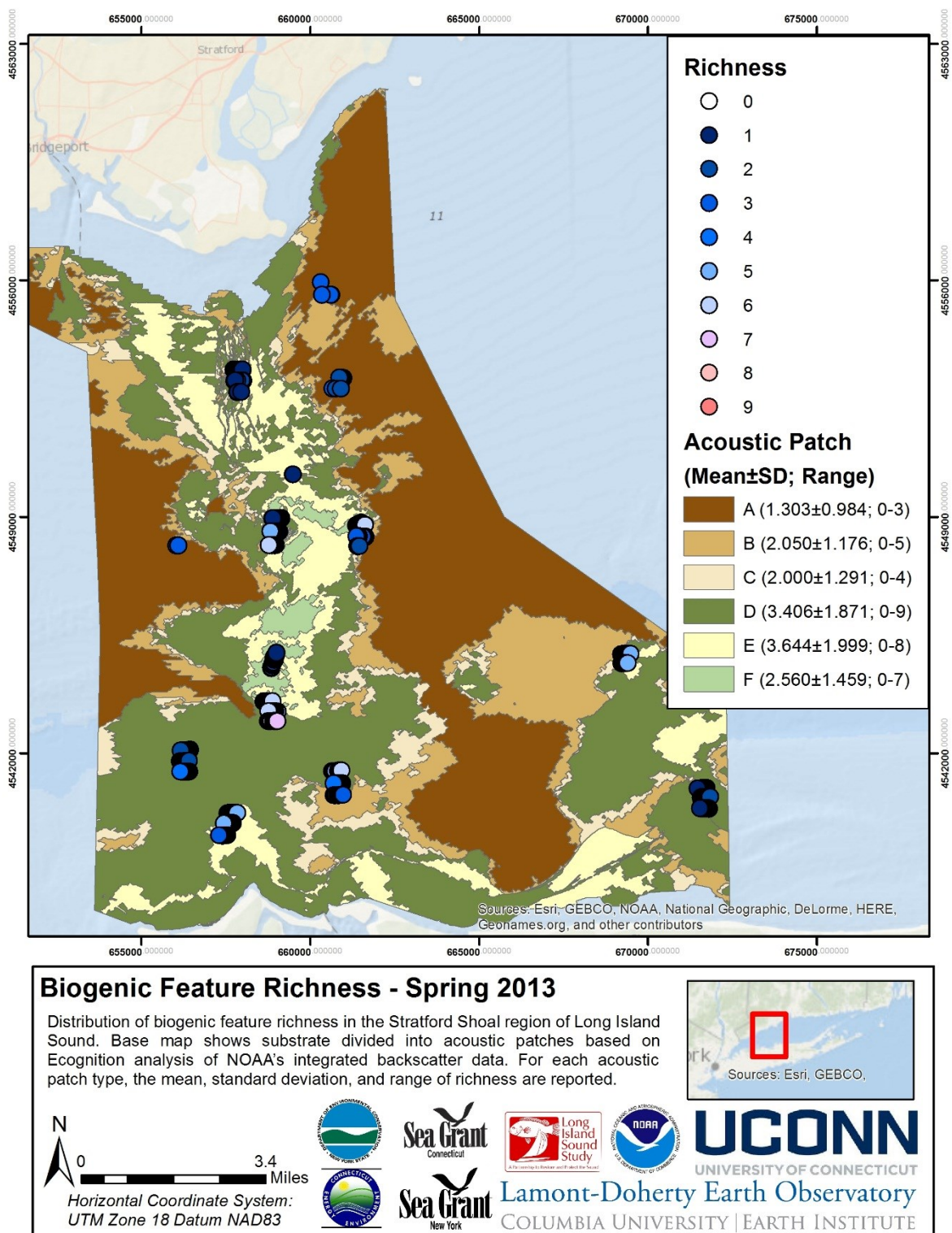


Figure 5.5-14.

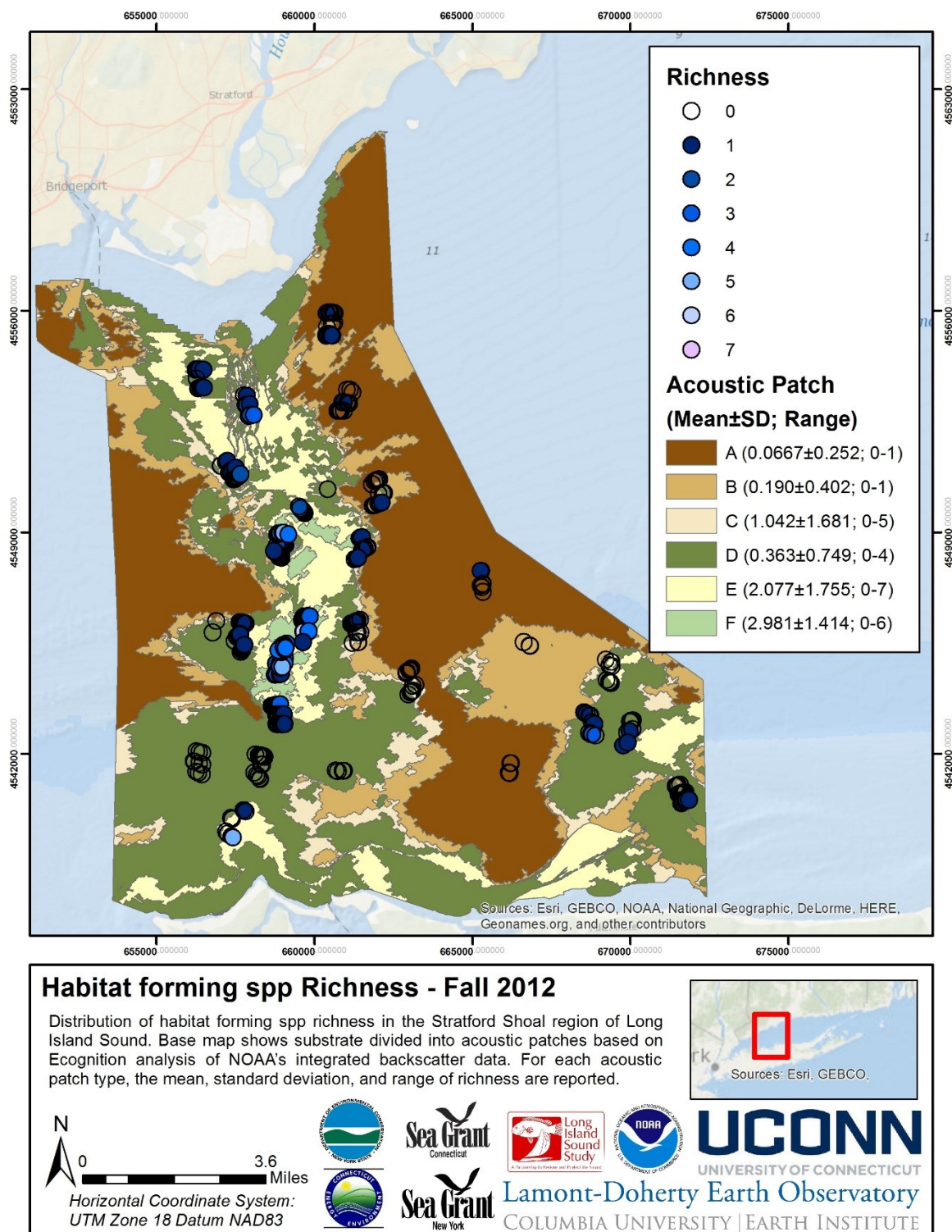


Figure 5.5-15.

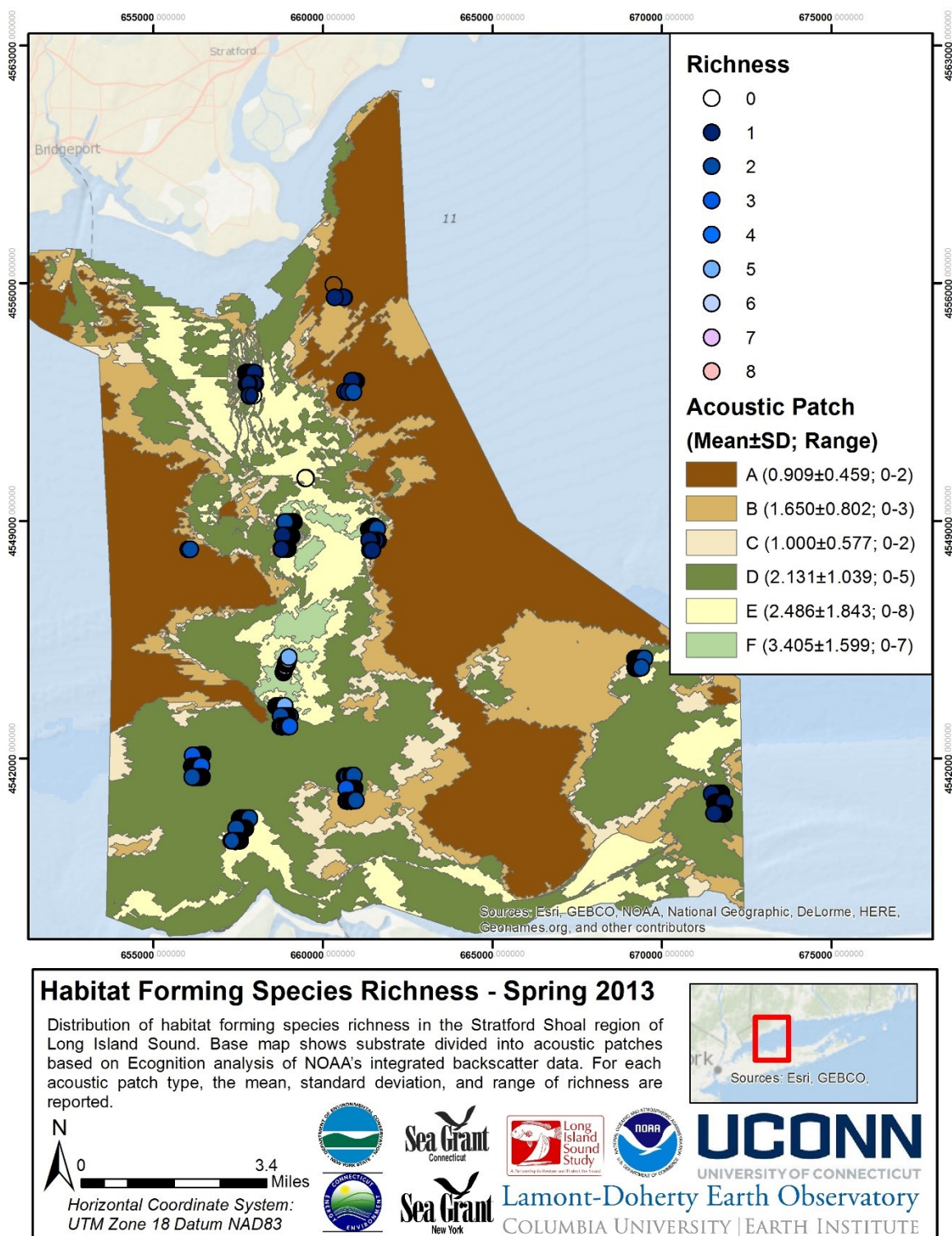


Figure 5.5-16

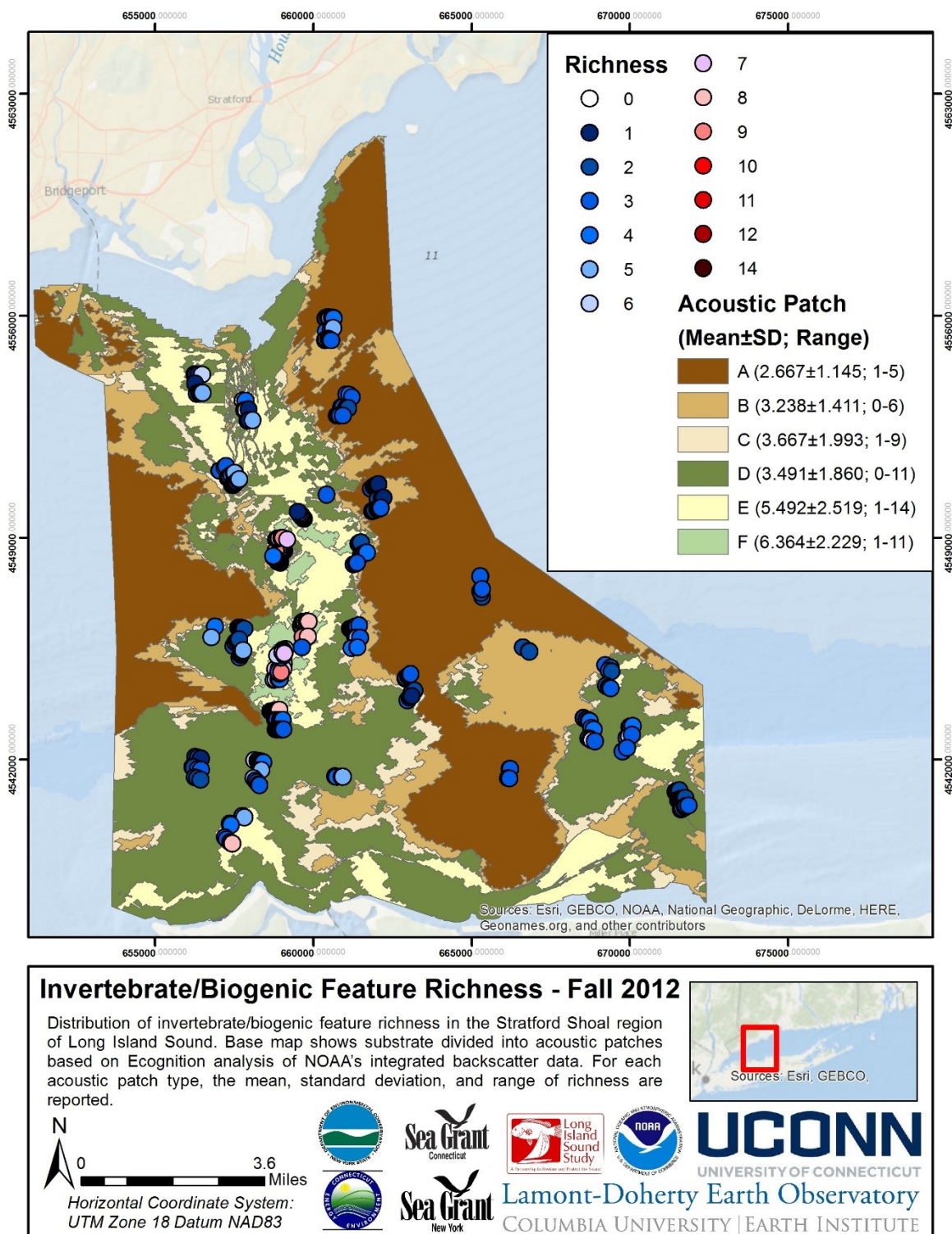


Figure 5.5-17

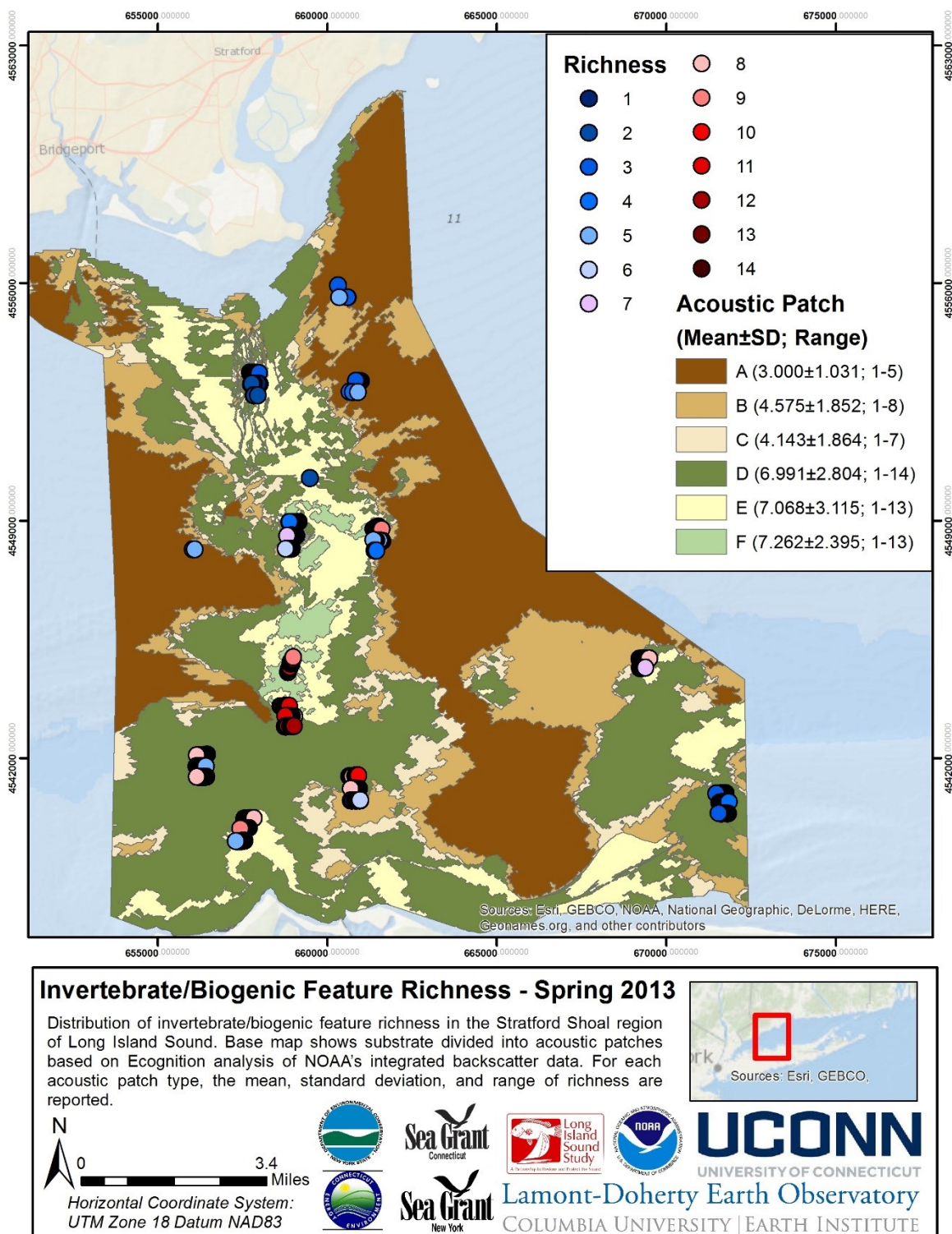


Figure 5.5-18

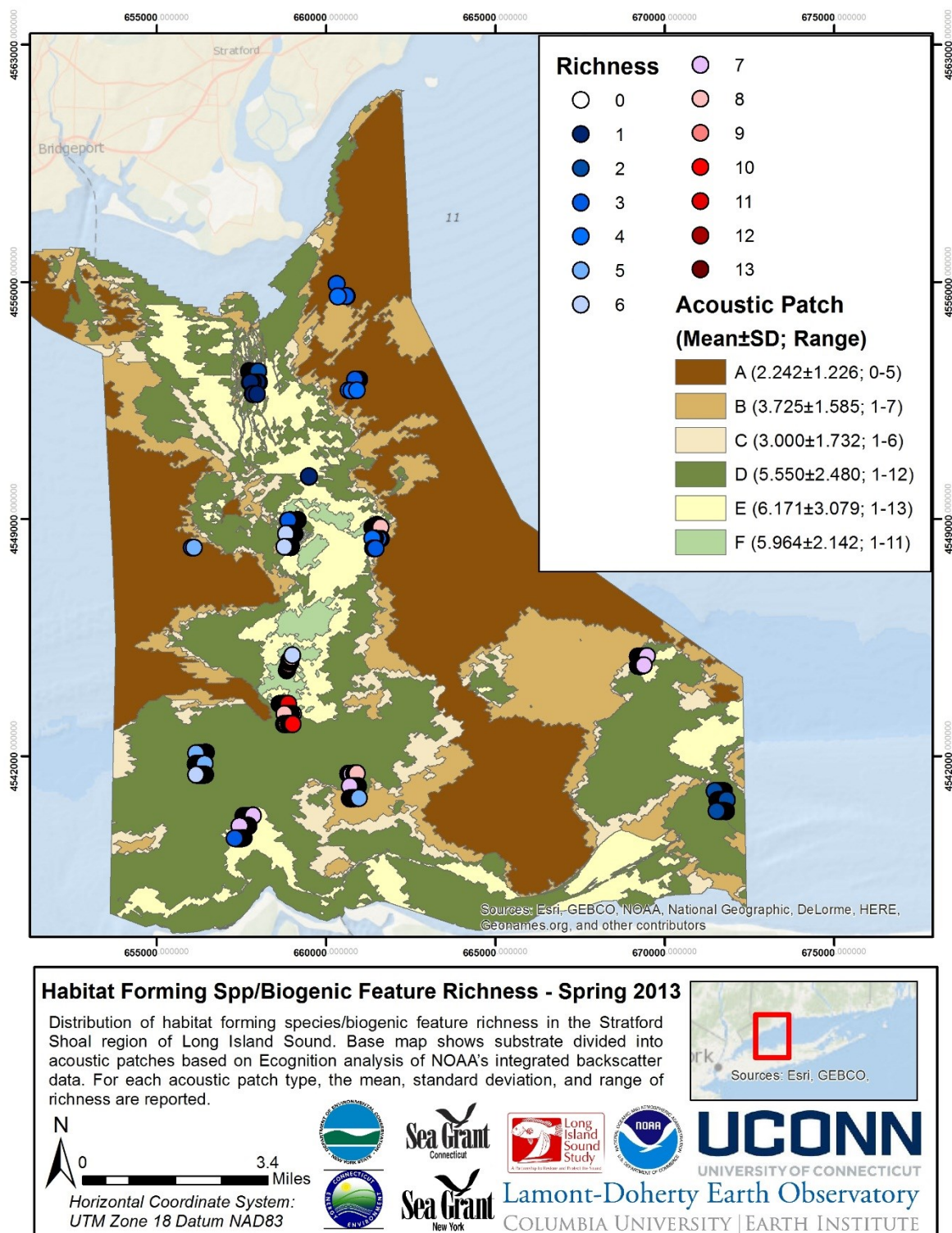


Figure 5.5-19. Figure 5.5-20.

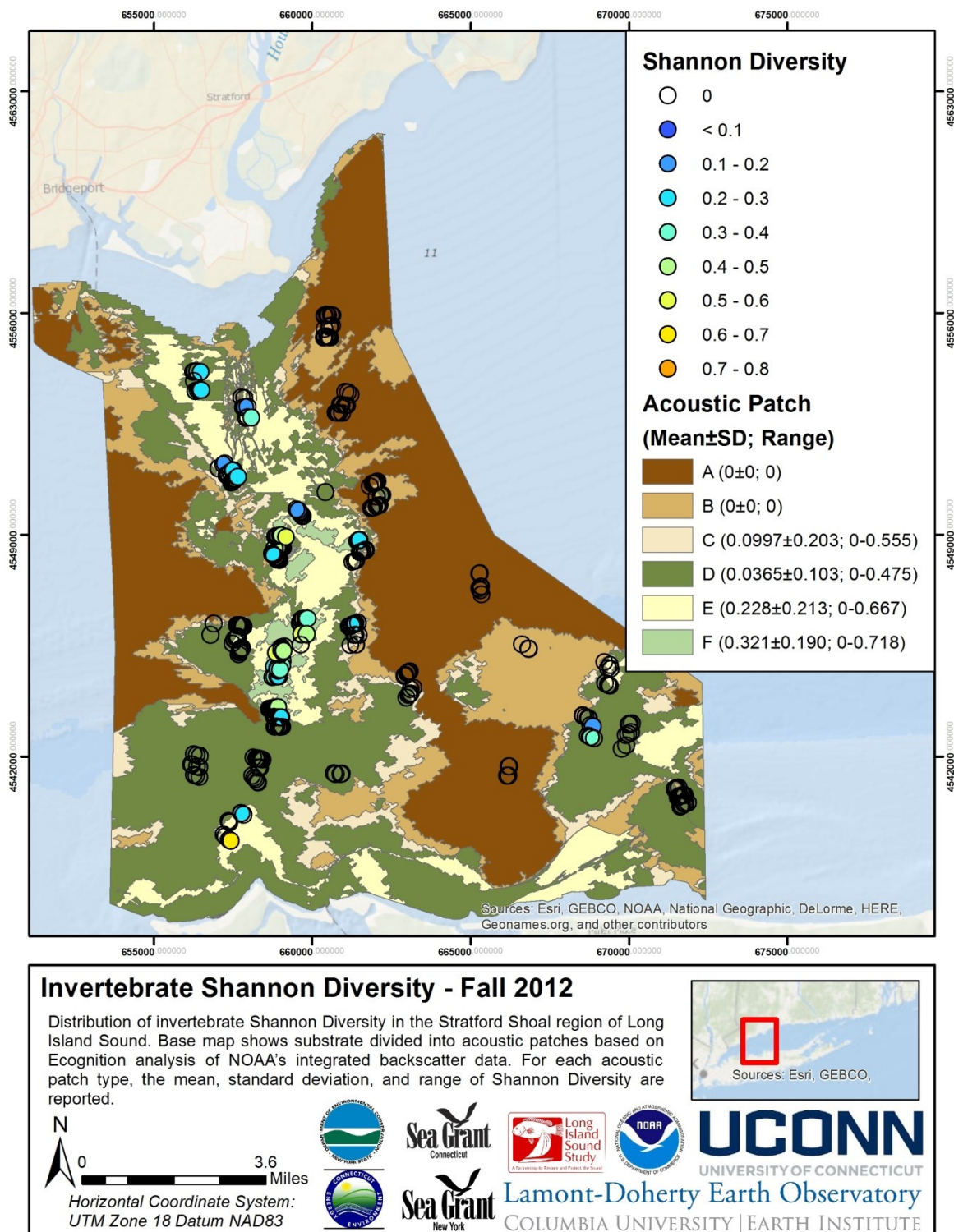


Figure 5.5-21.

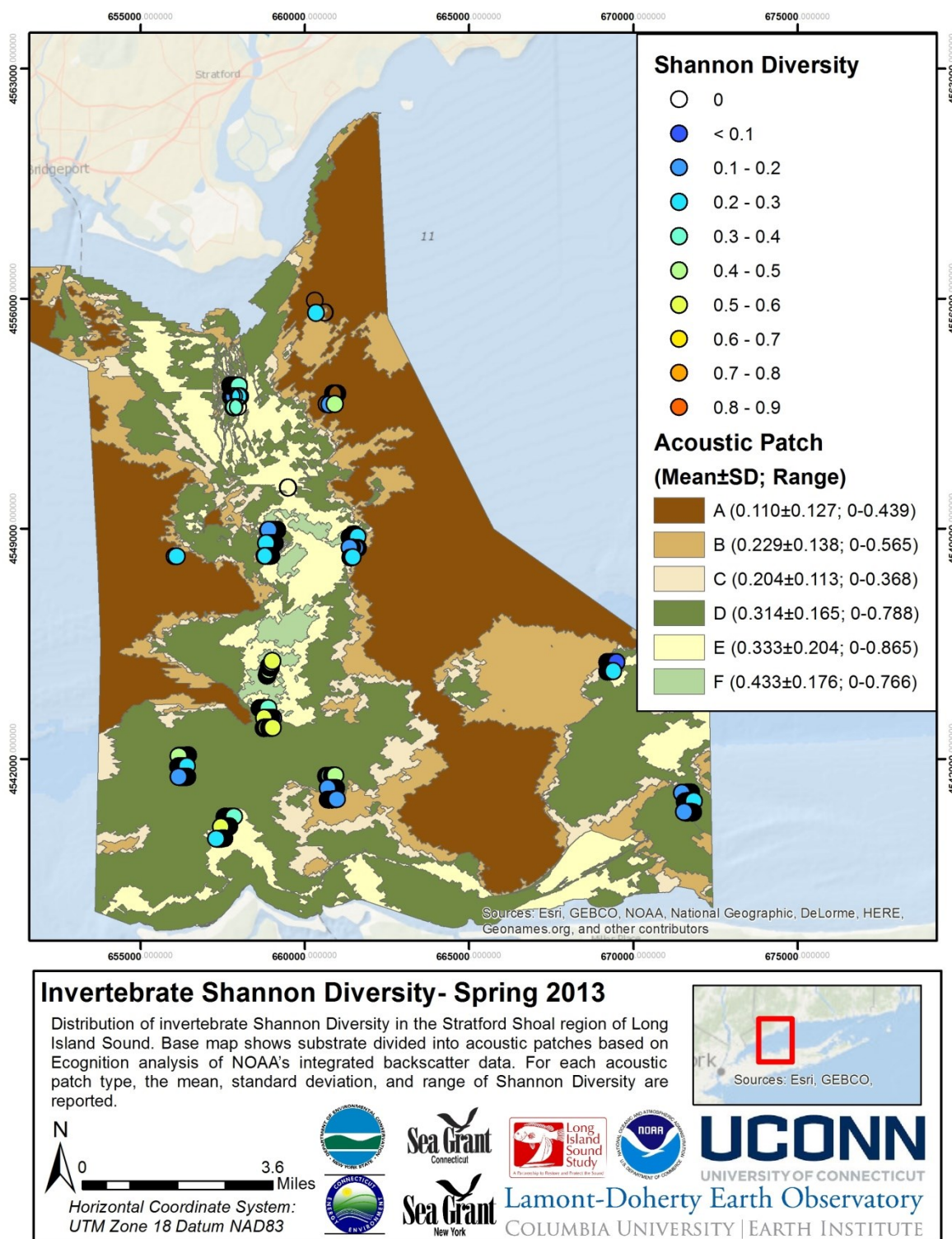


Figure 5.5-22.

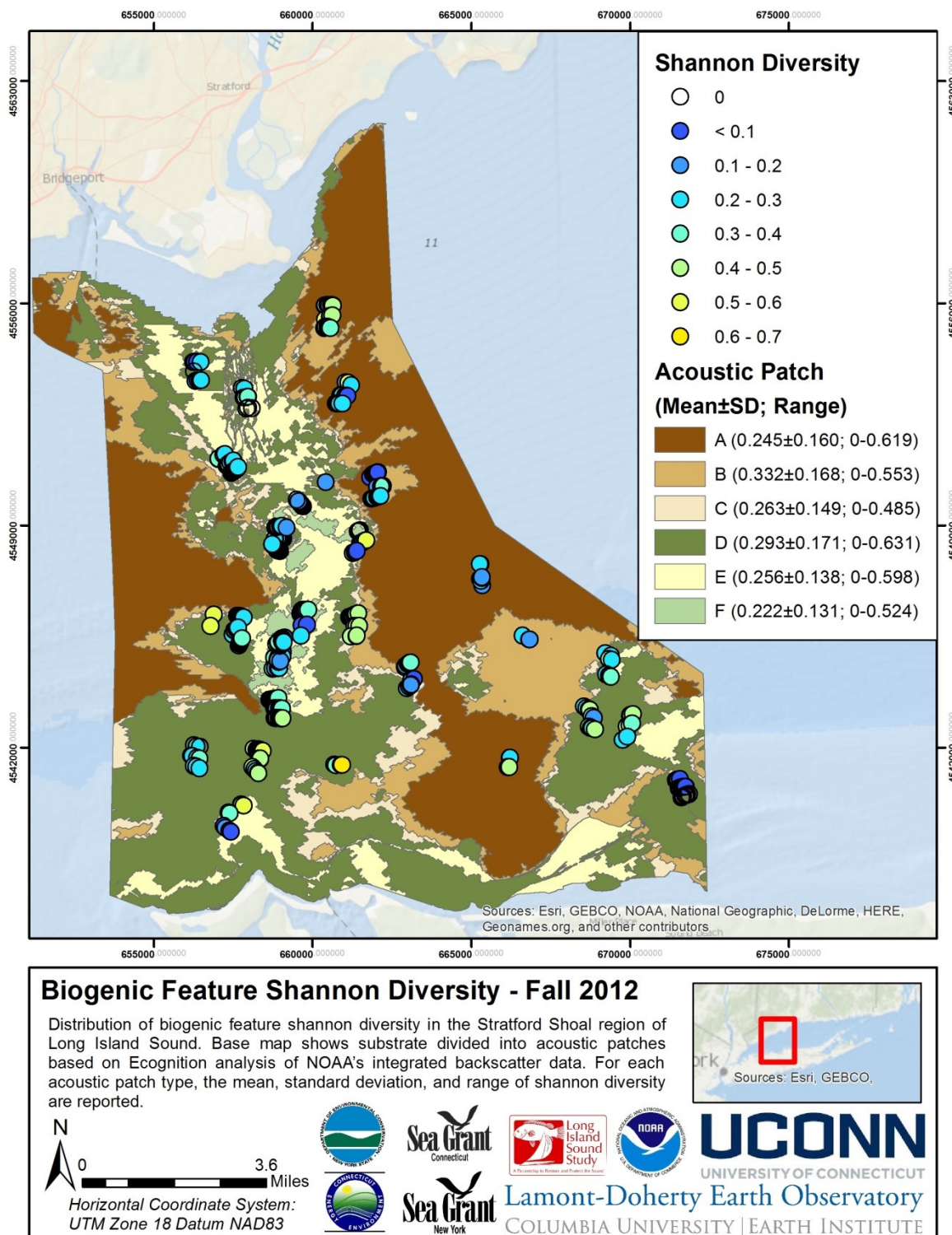


Figure 5.5-23

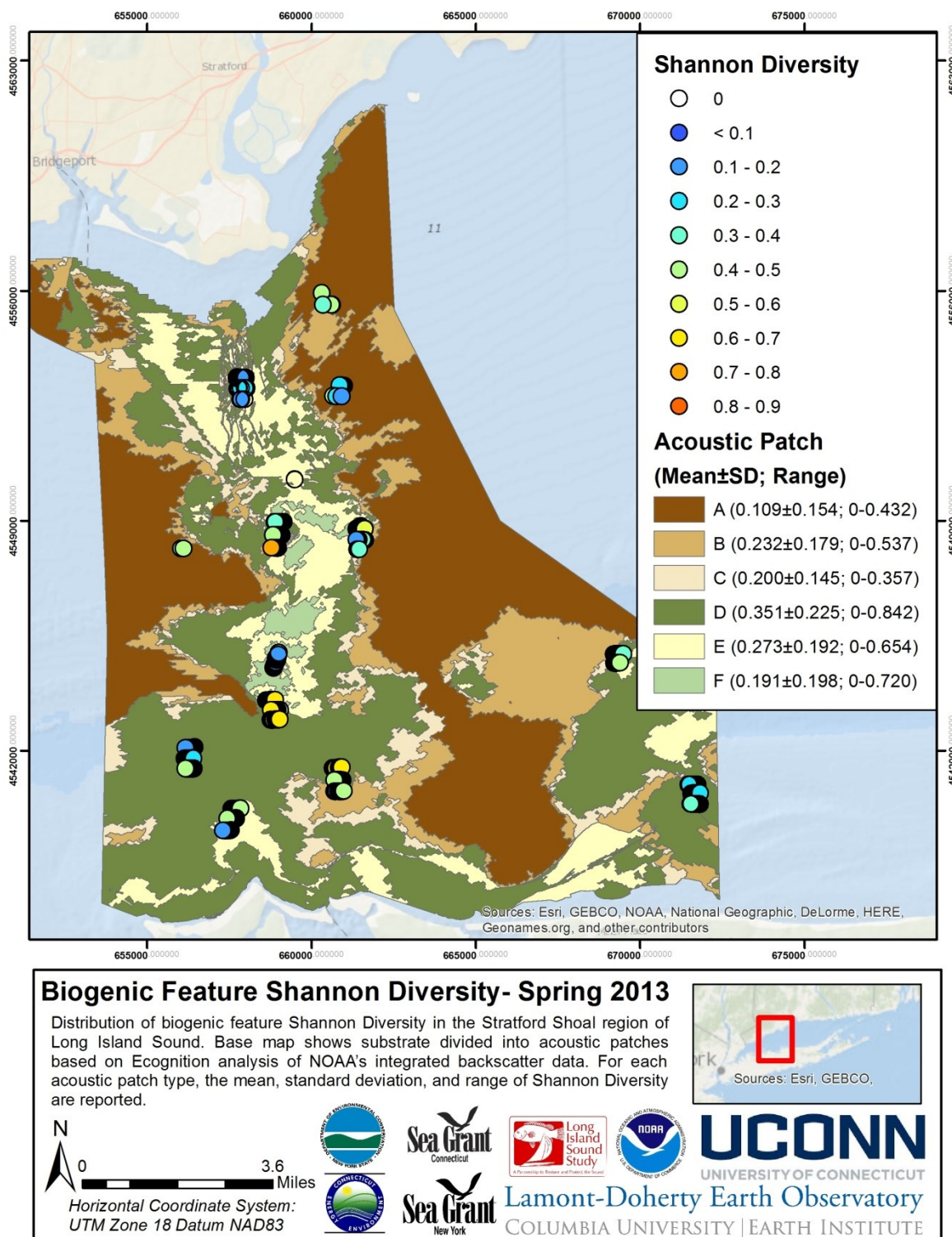


Figure 5.5-24

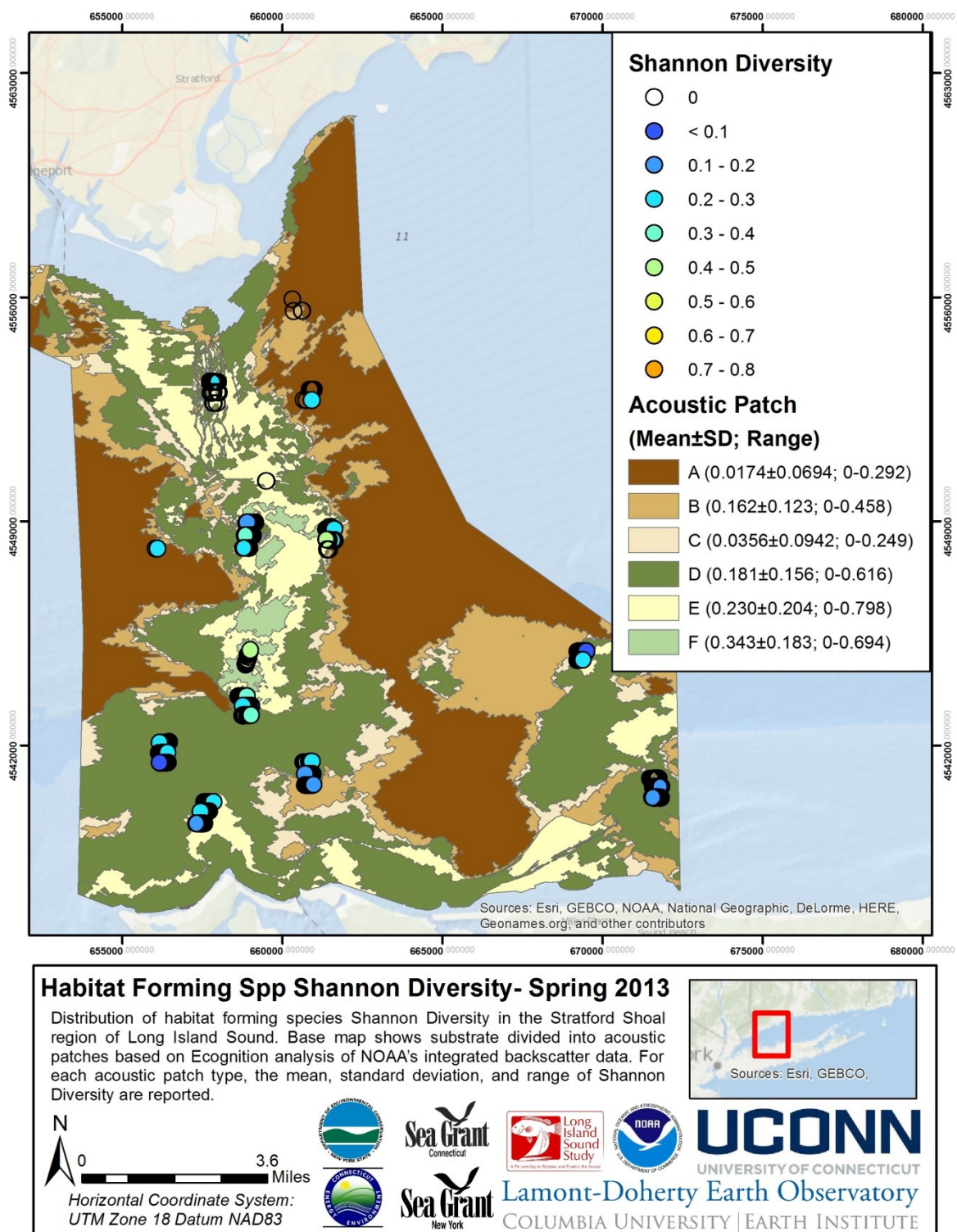


Figure 5.5-26

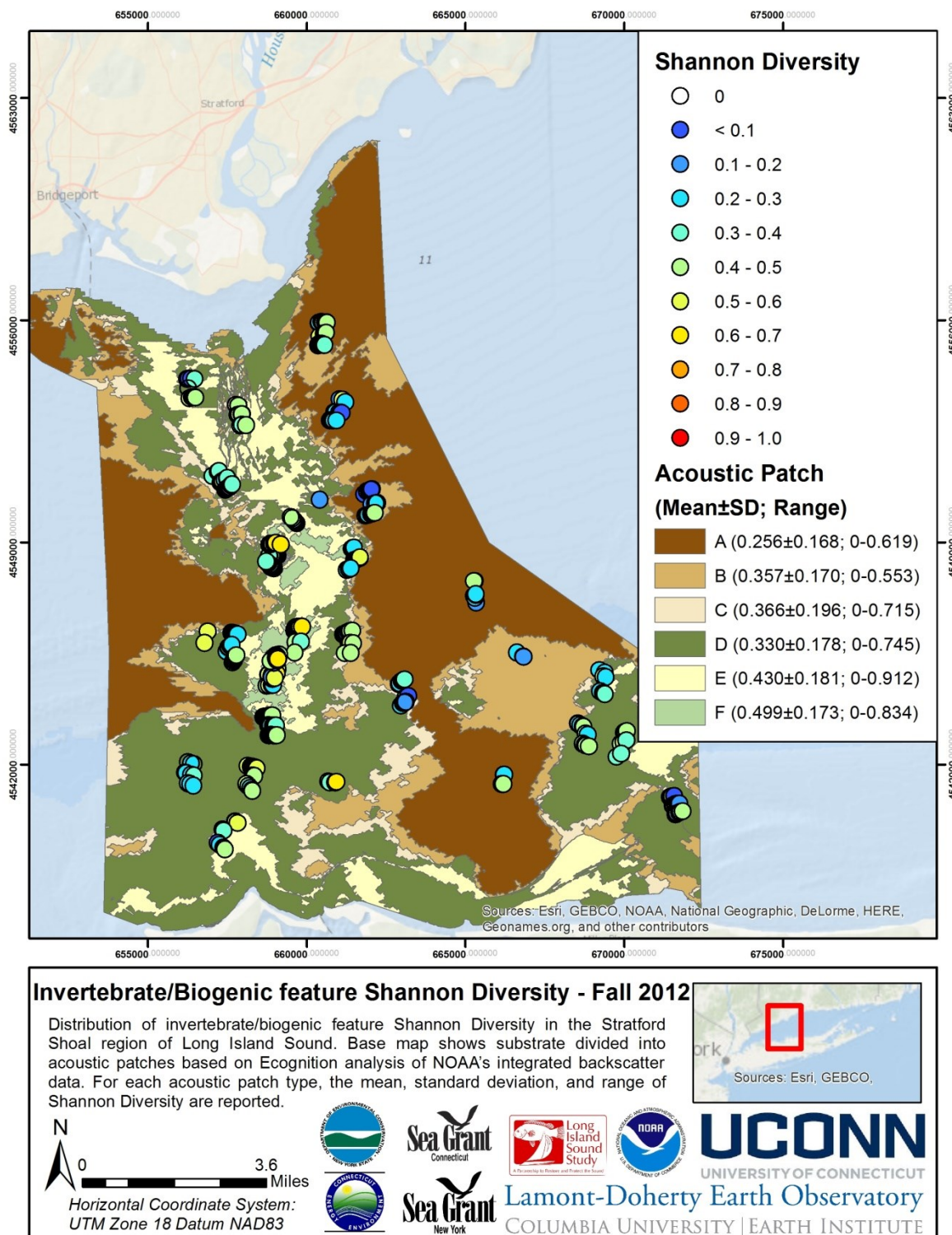


Figure 5.5-27

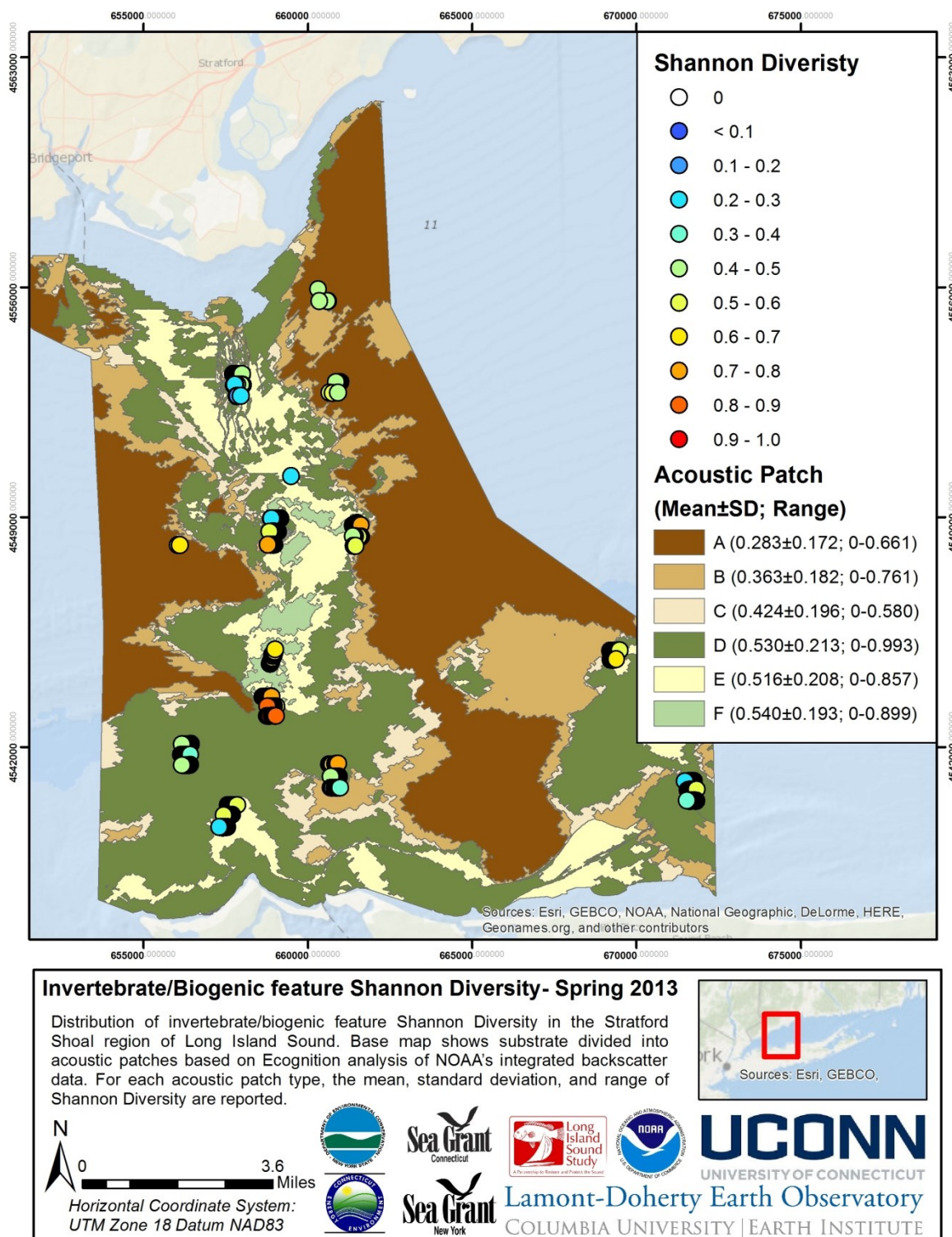


Figure 5.5-28.

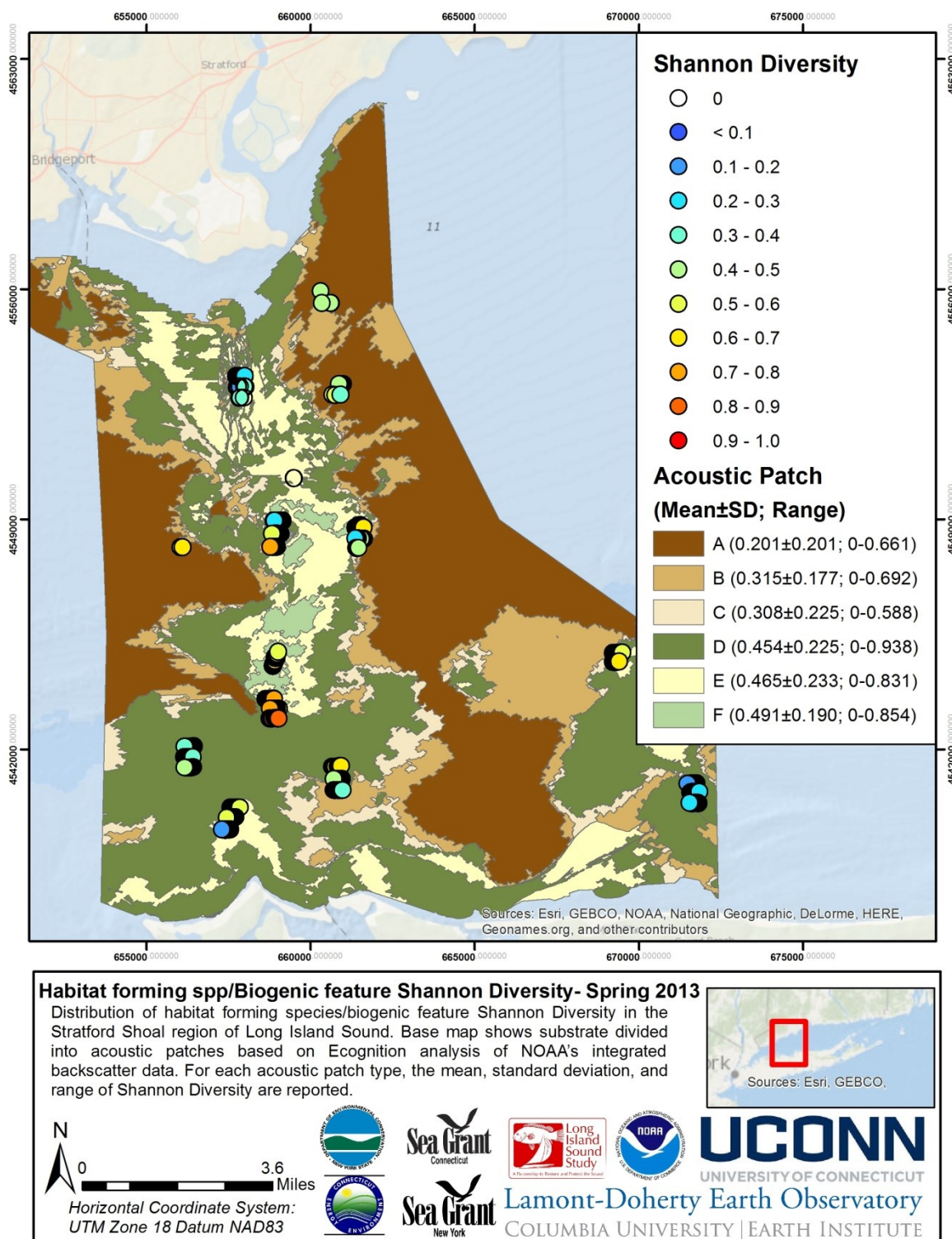


Figure 5.5-30.

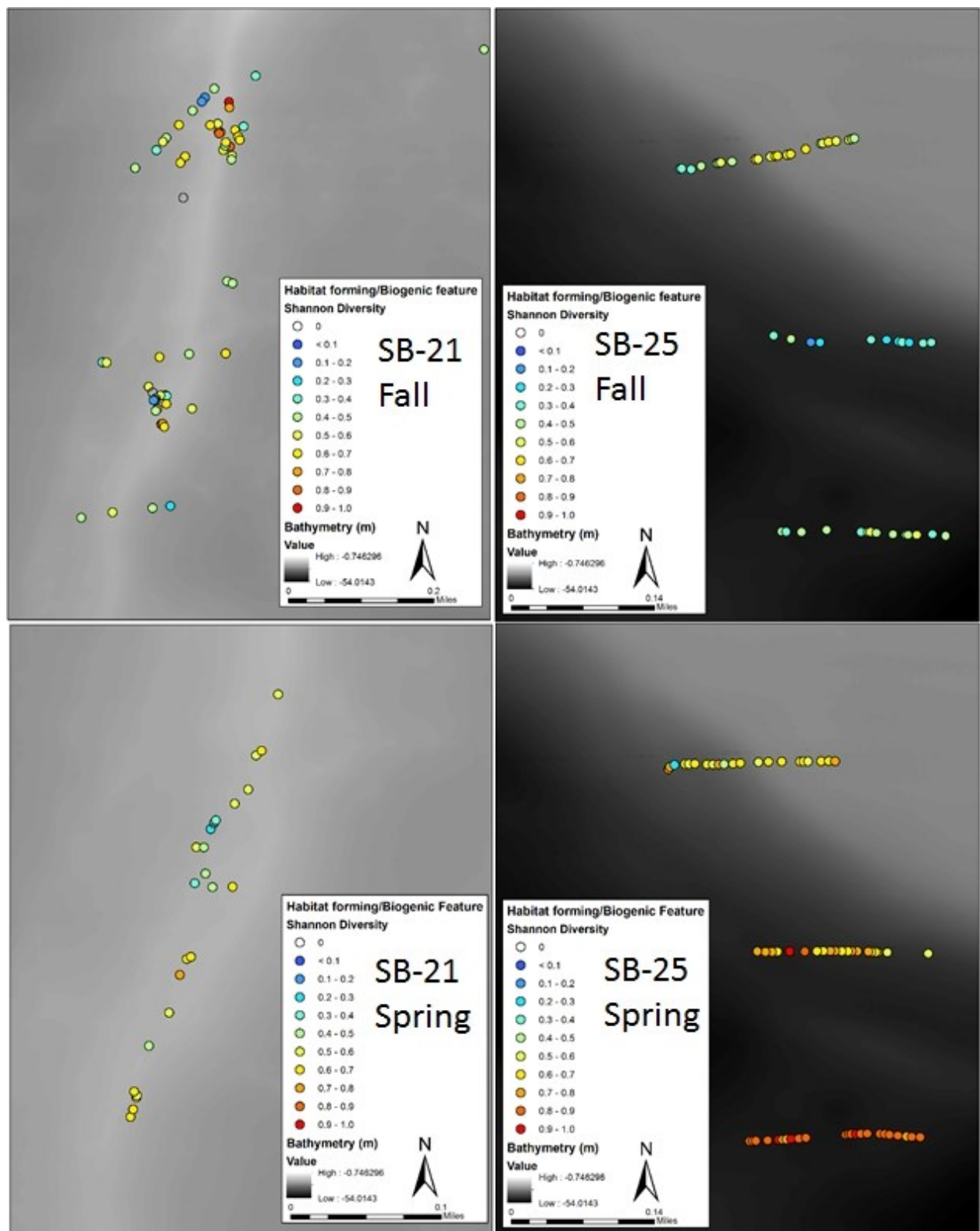


Figure 5.5-31. Example of patchiness in diversity across images.

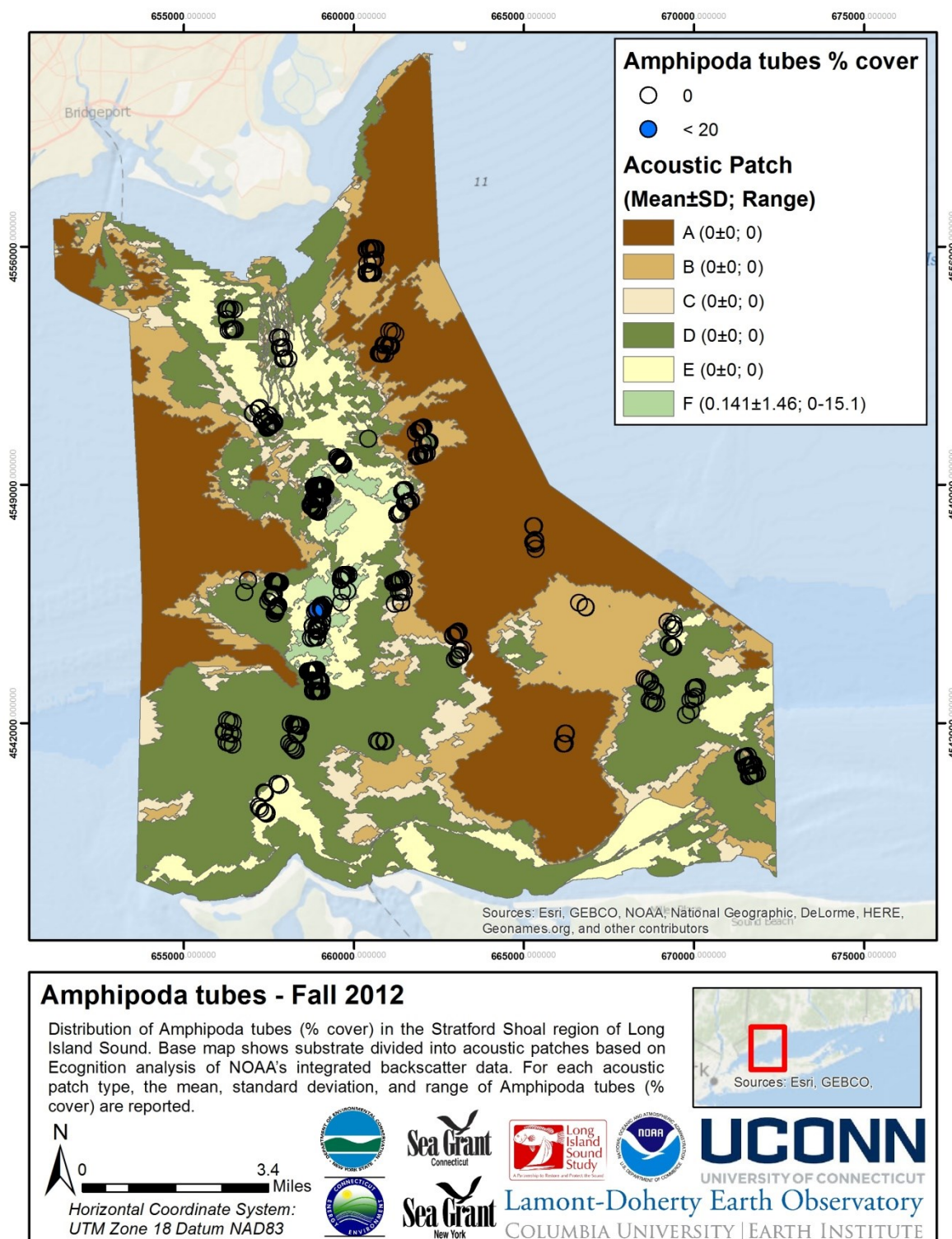


Figure 5.5-32.

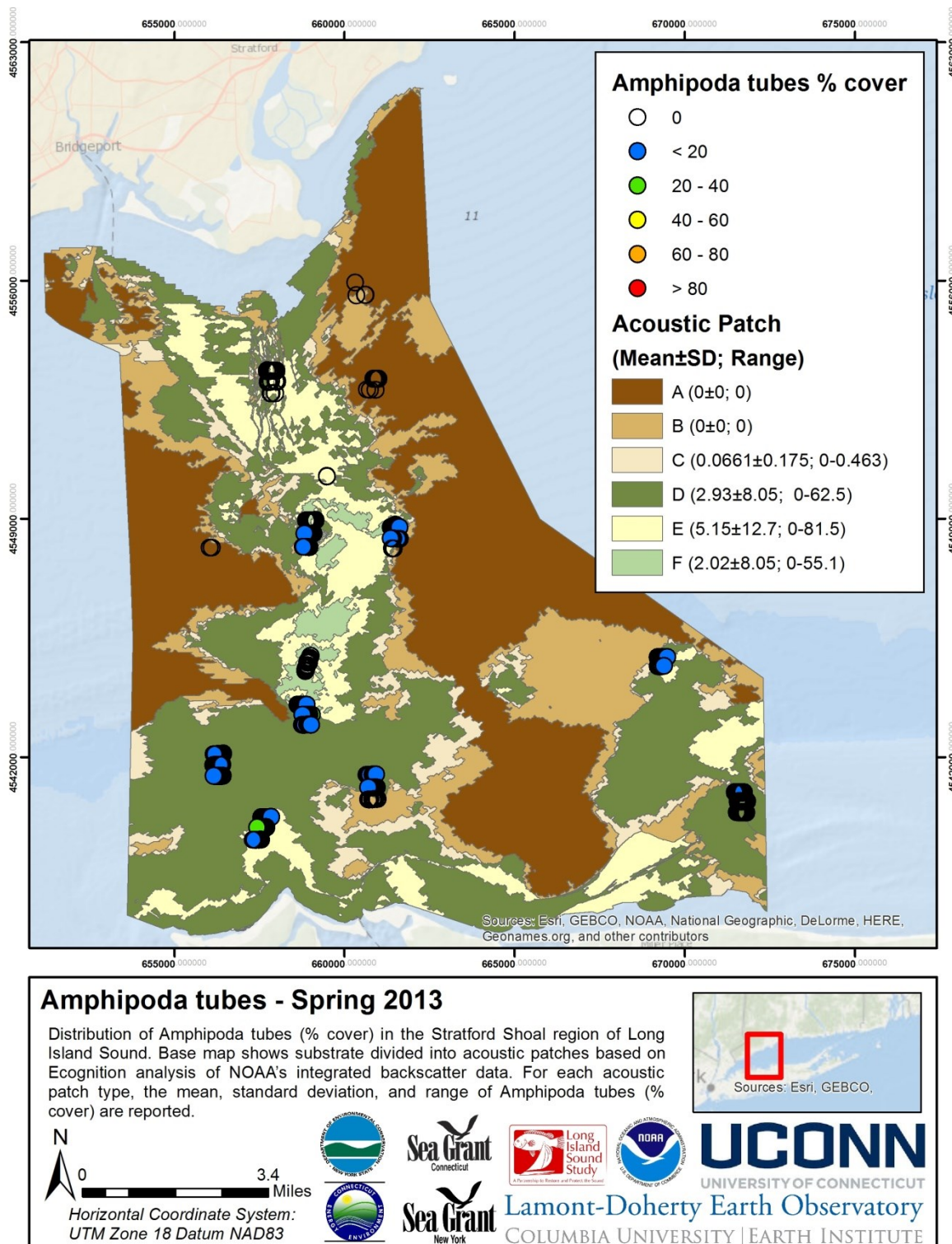


Figure 5.5-33.

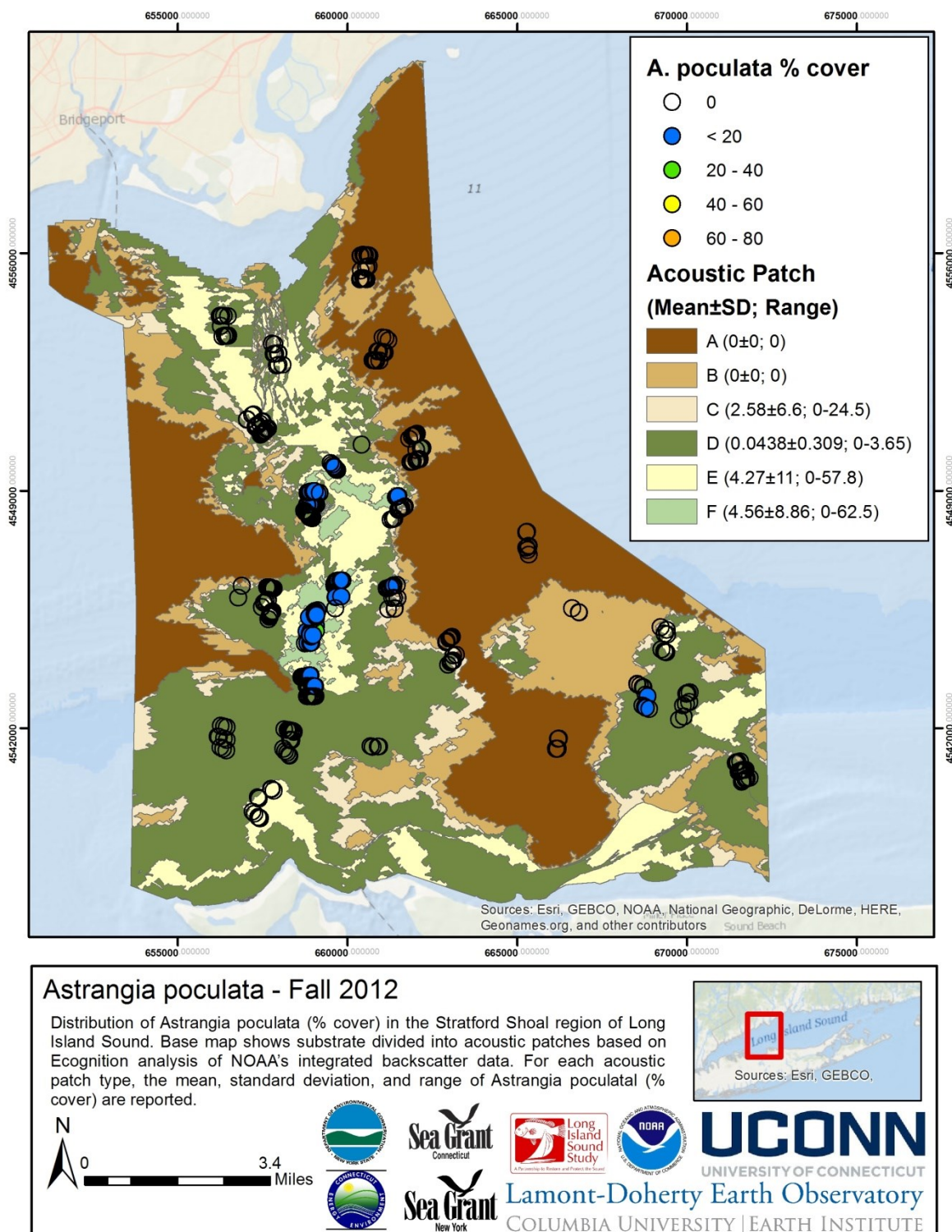


Figure 5.5-34.

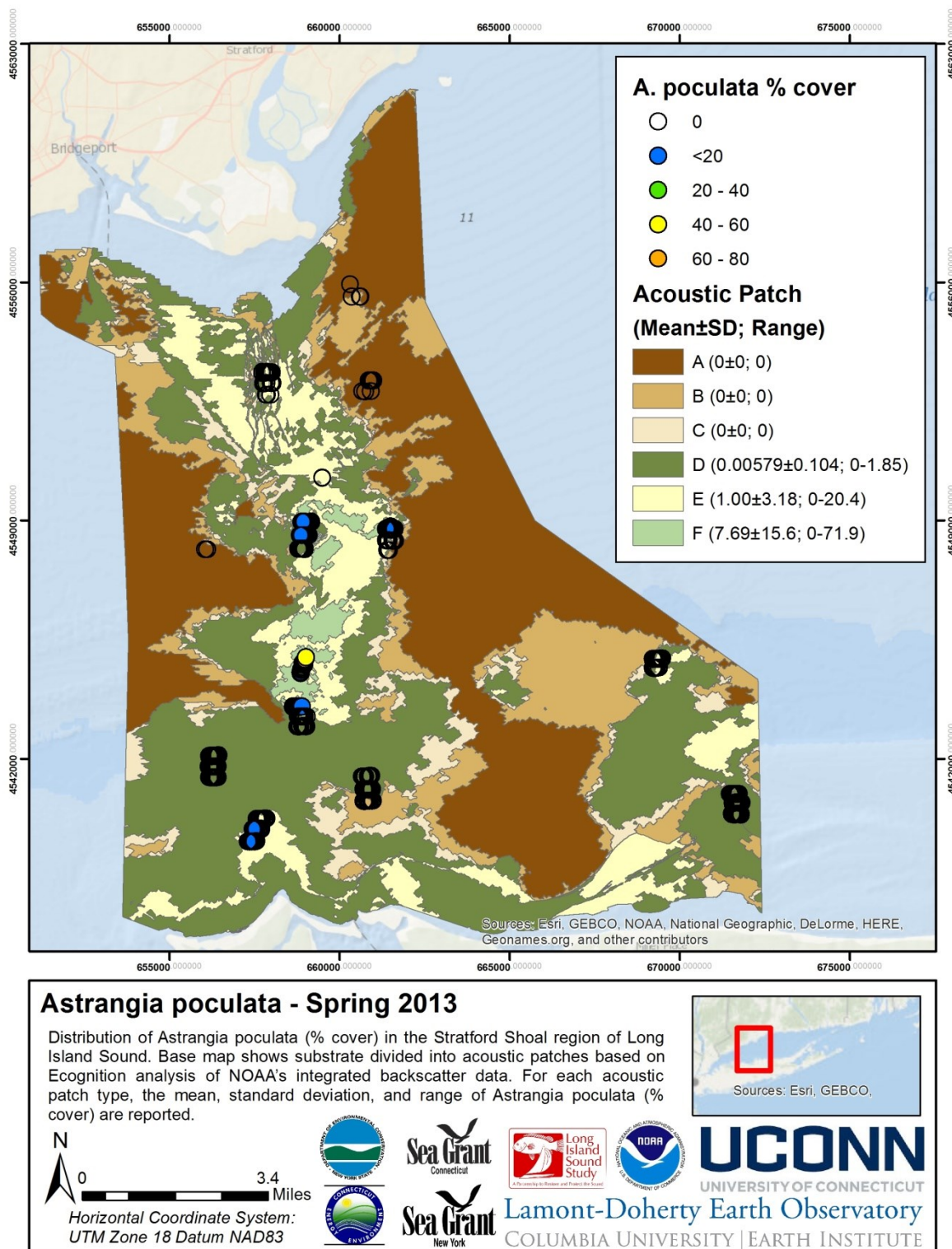


Figure 5.5-35.

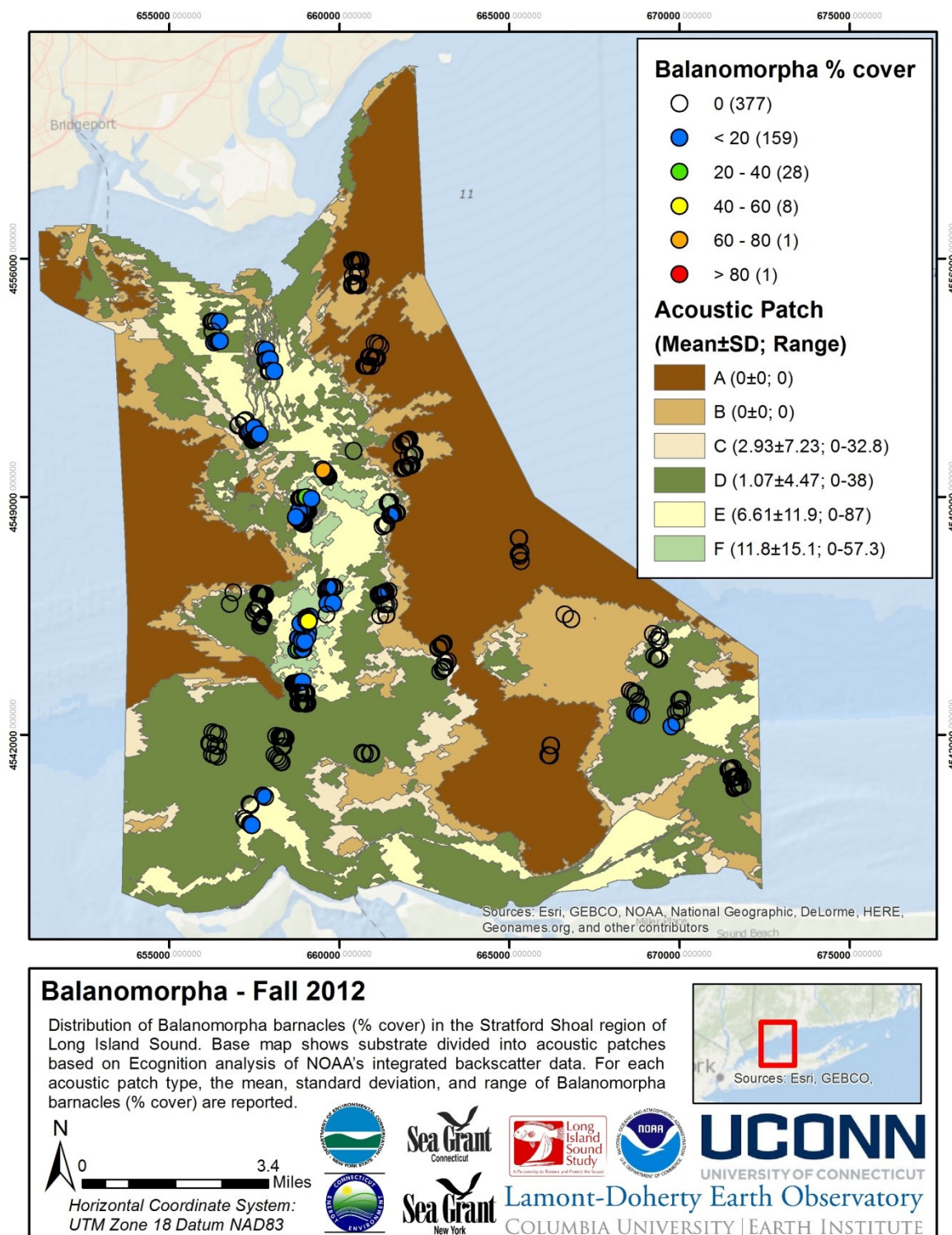


Figure 5.5-36.

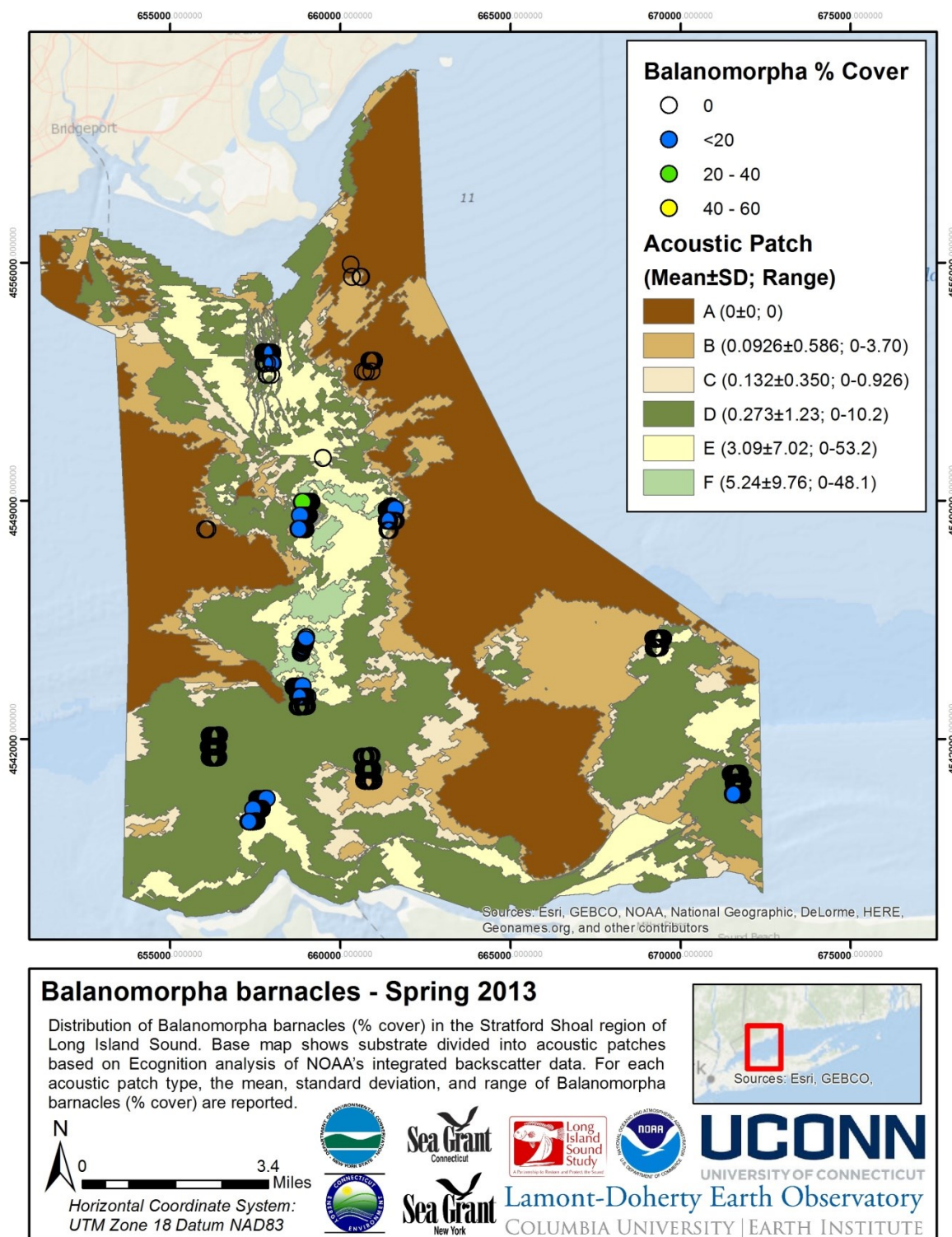


Figure 5.5-37.

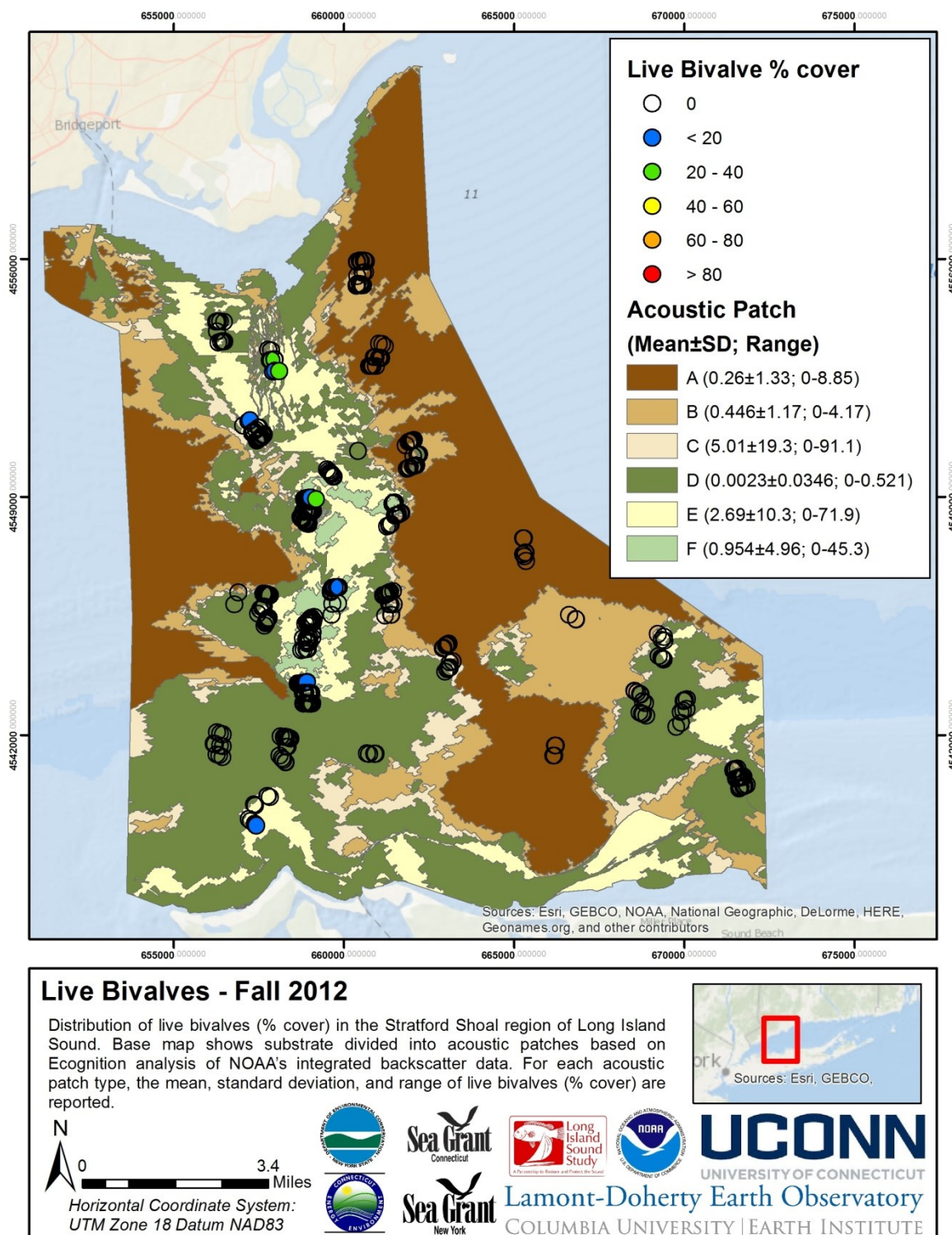


Figure 5.5-38.

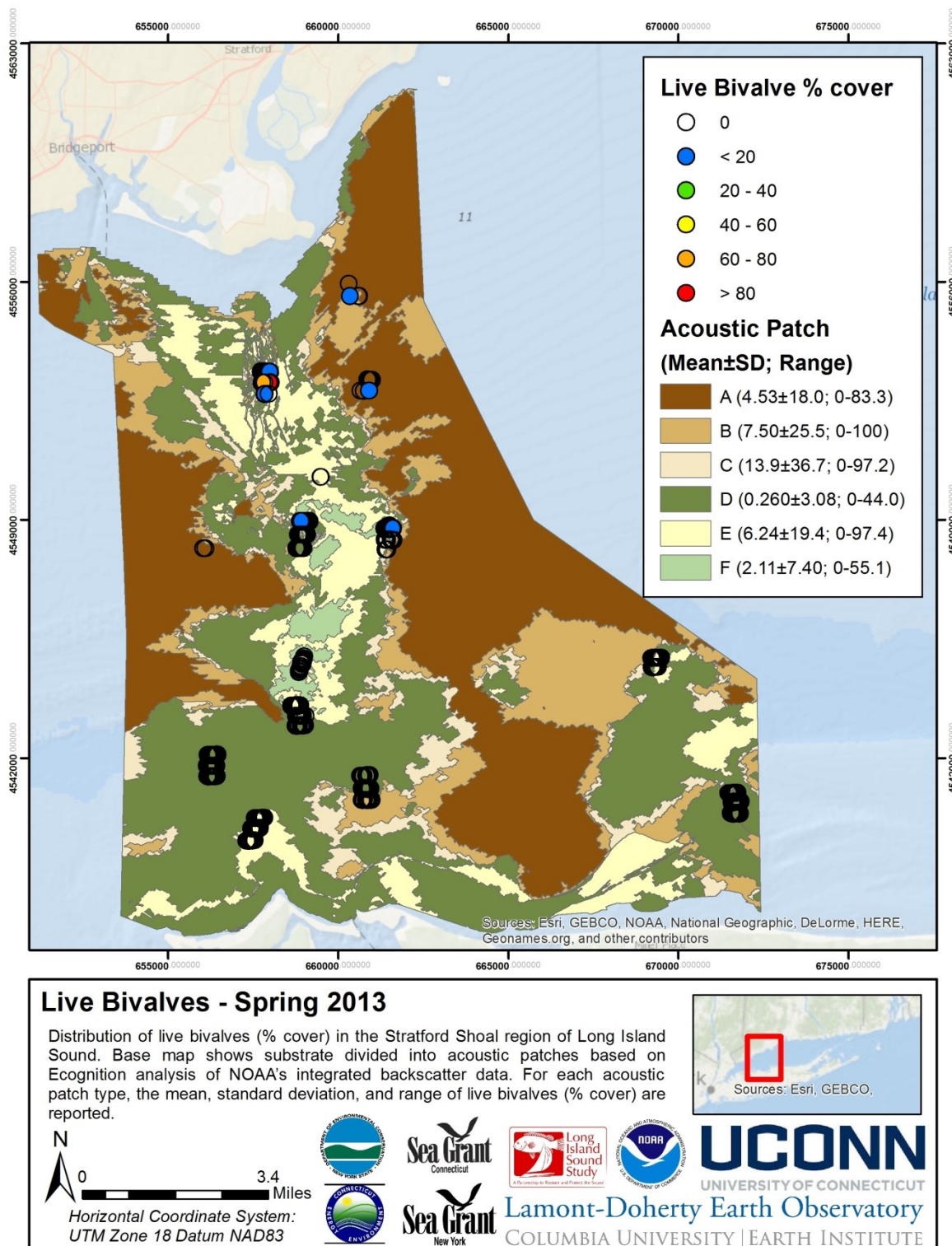


Figure 5.5-39.

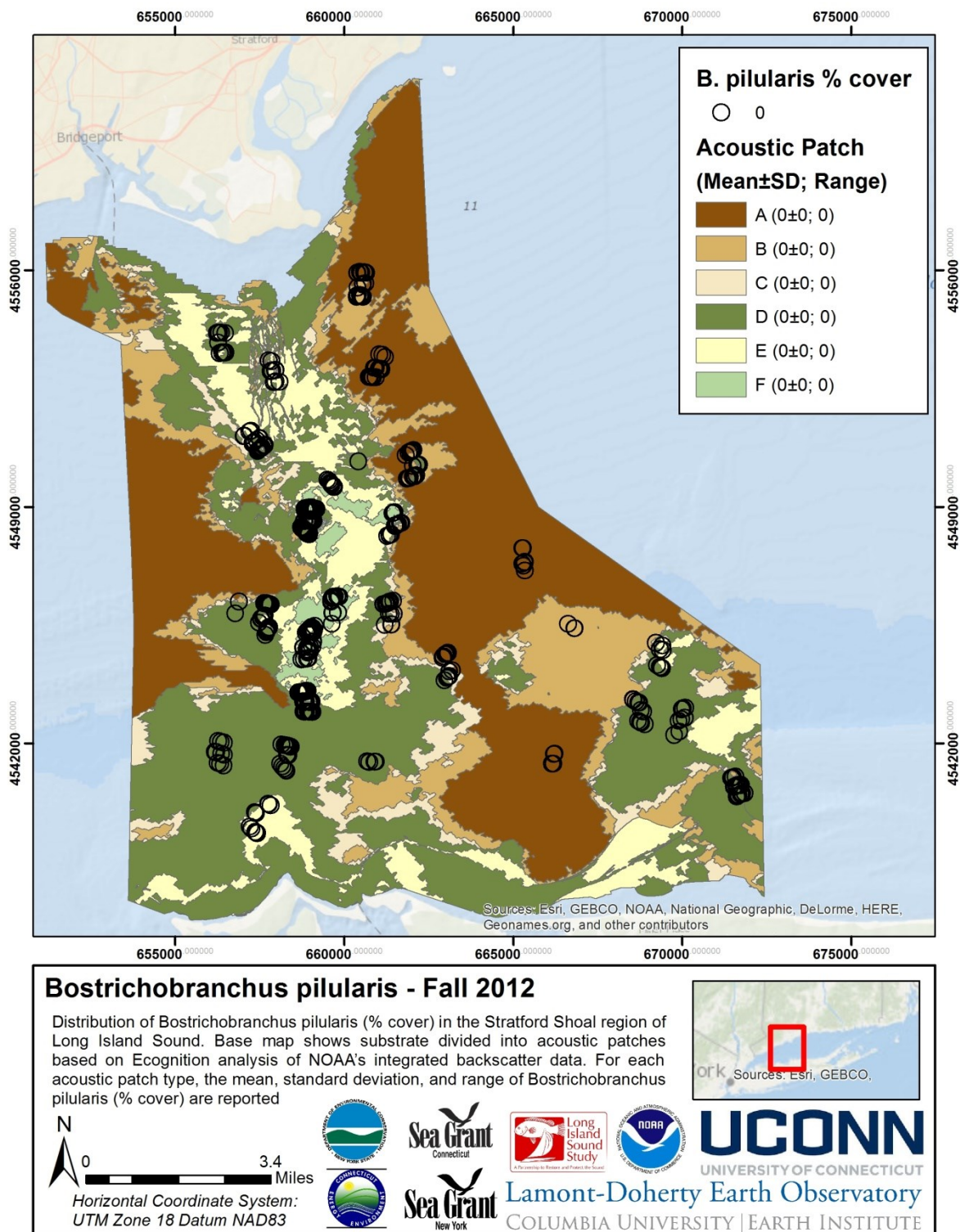


Figure 5.5-40.

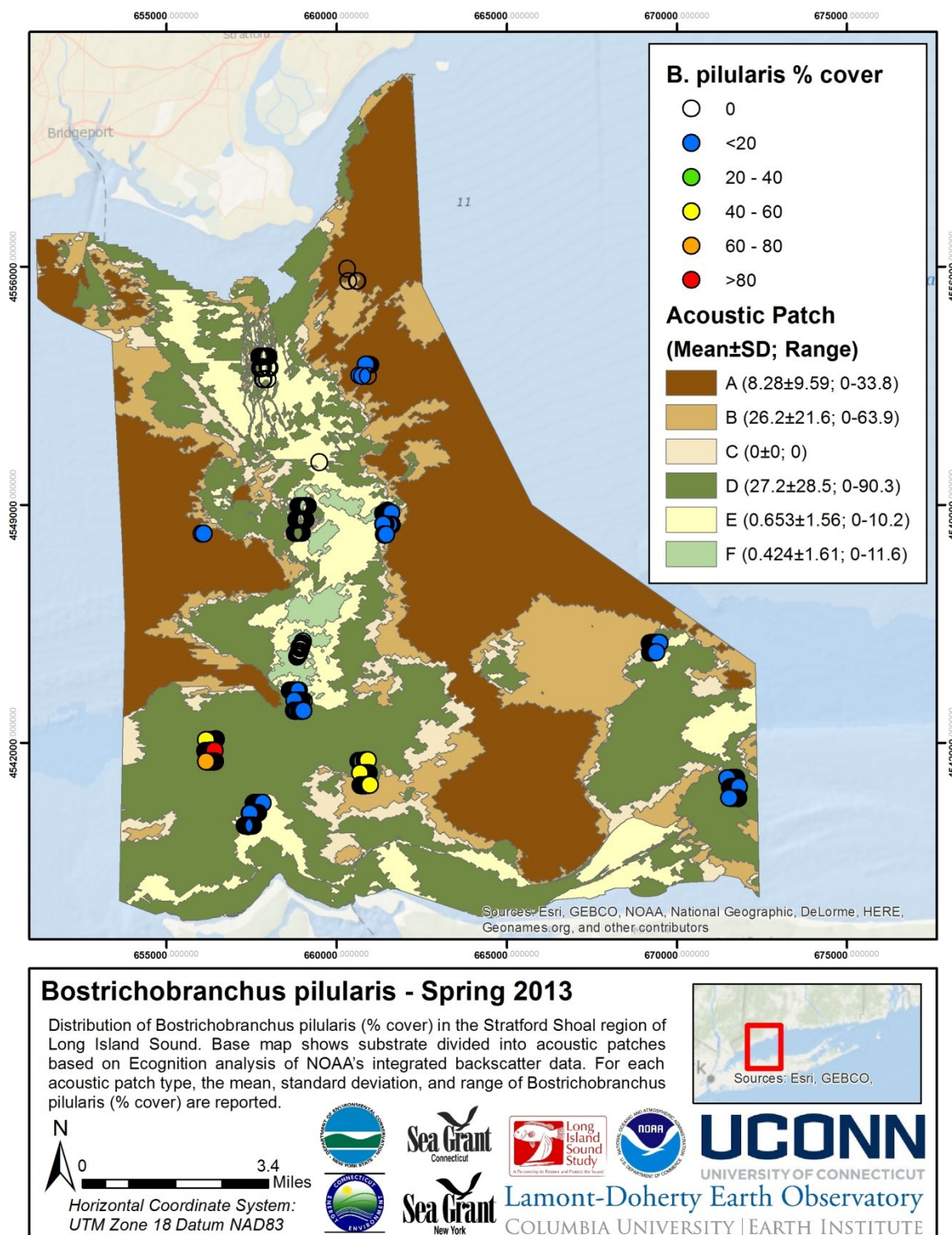


Figure 5.5-41.

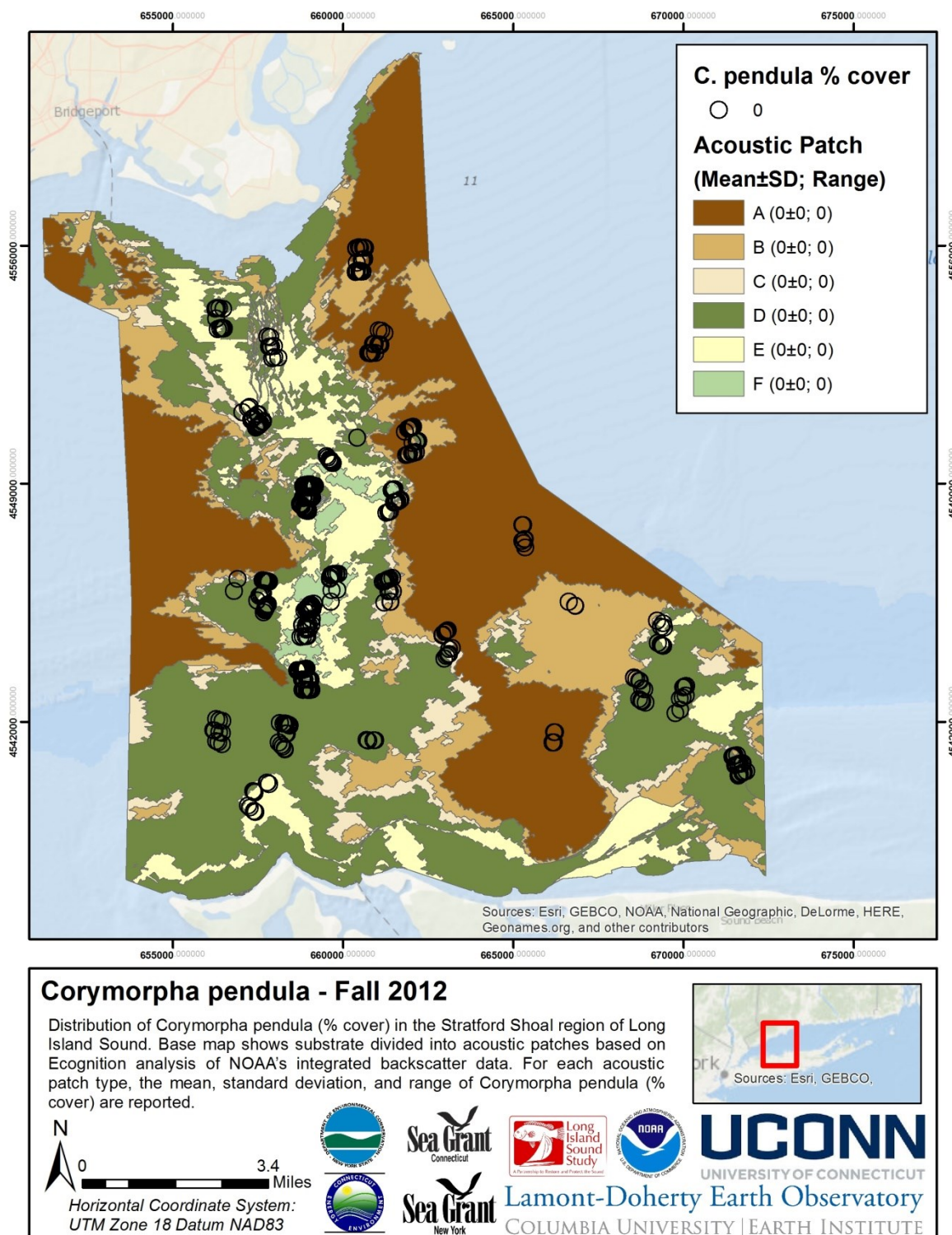


Figure 5.5-42.

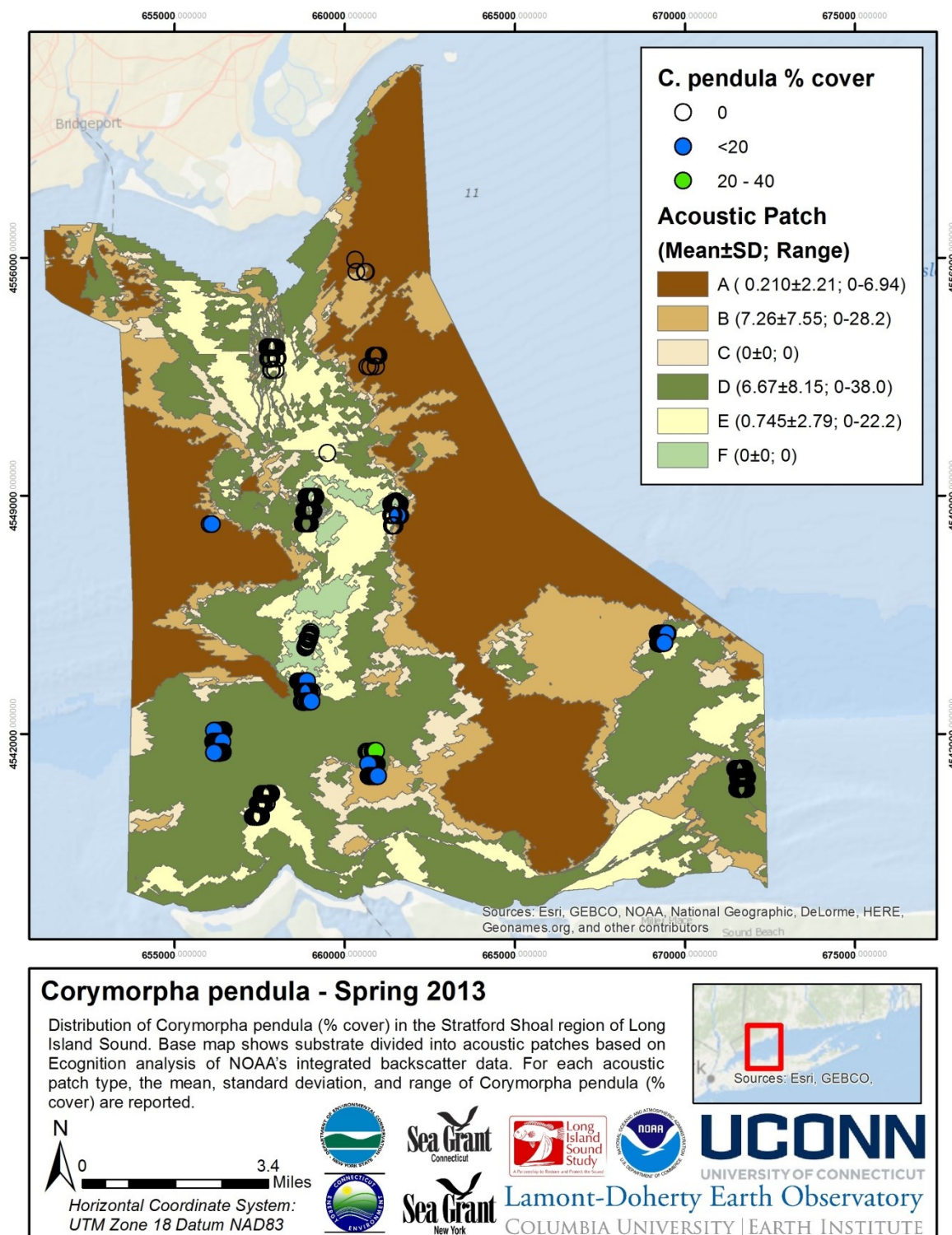


Figure 5.5-43.

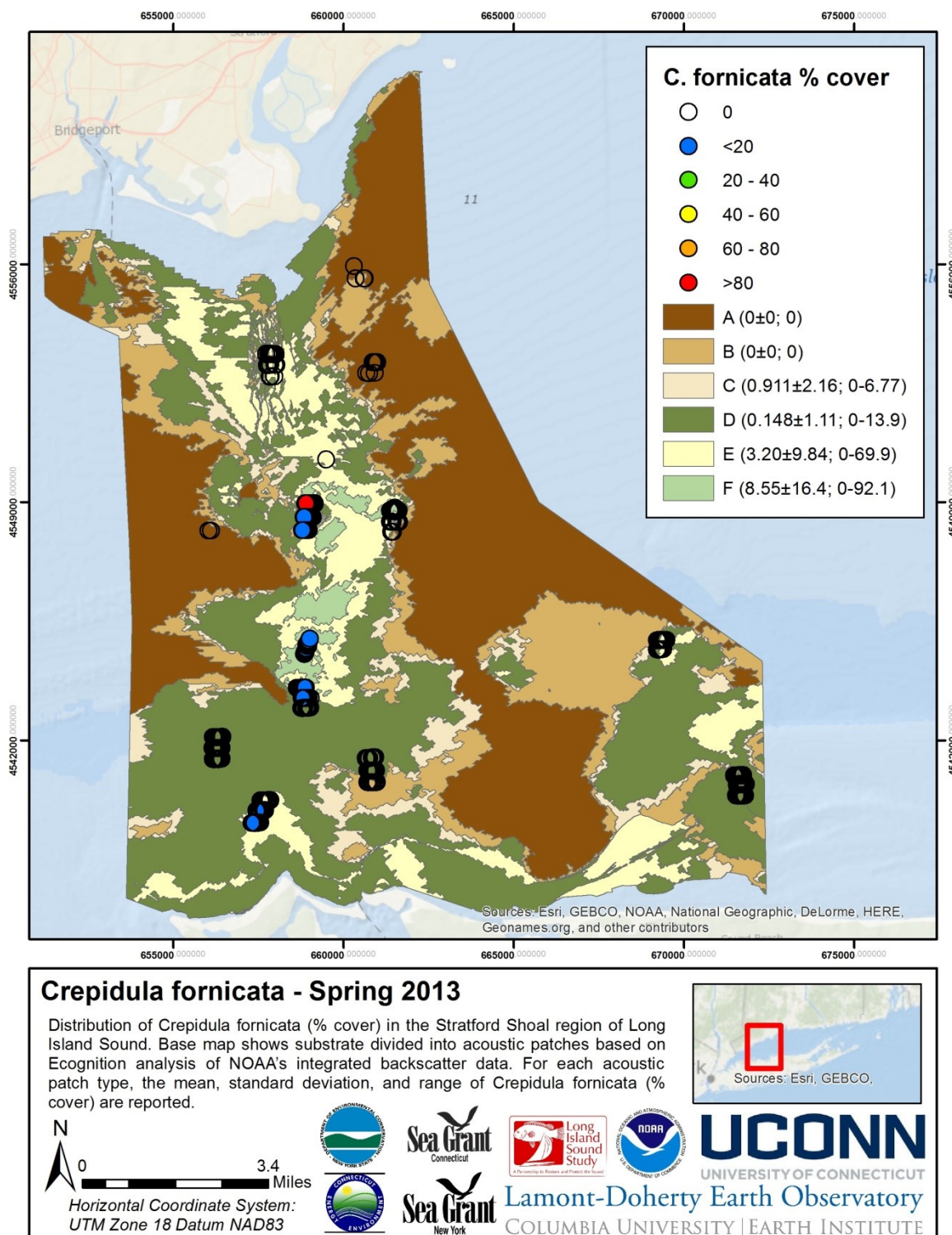


Figure 5.5-45.

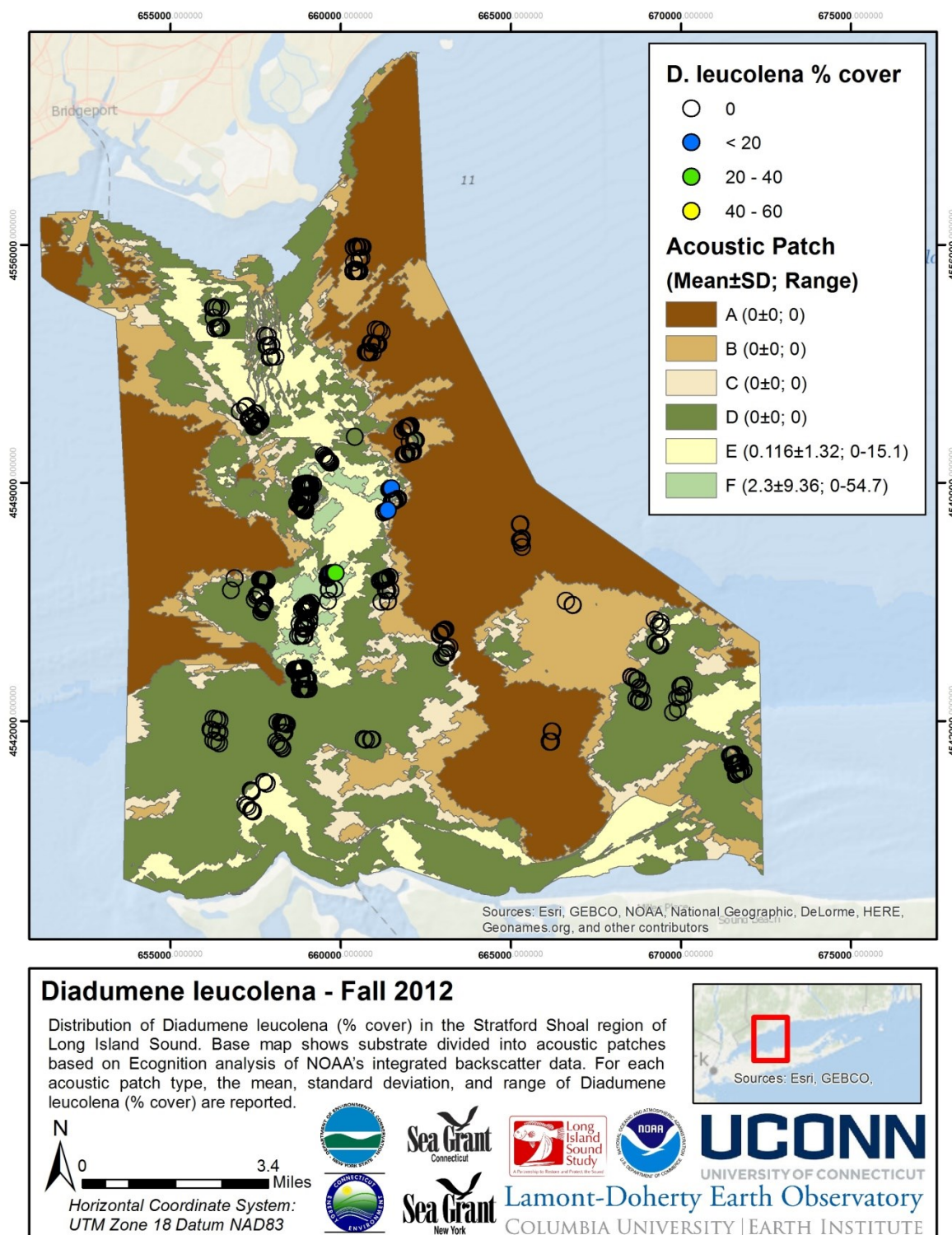


Figure 5.5-46.

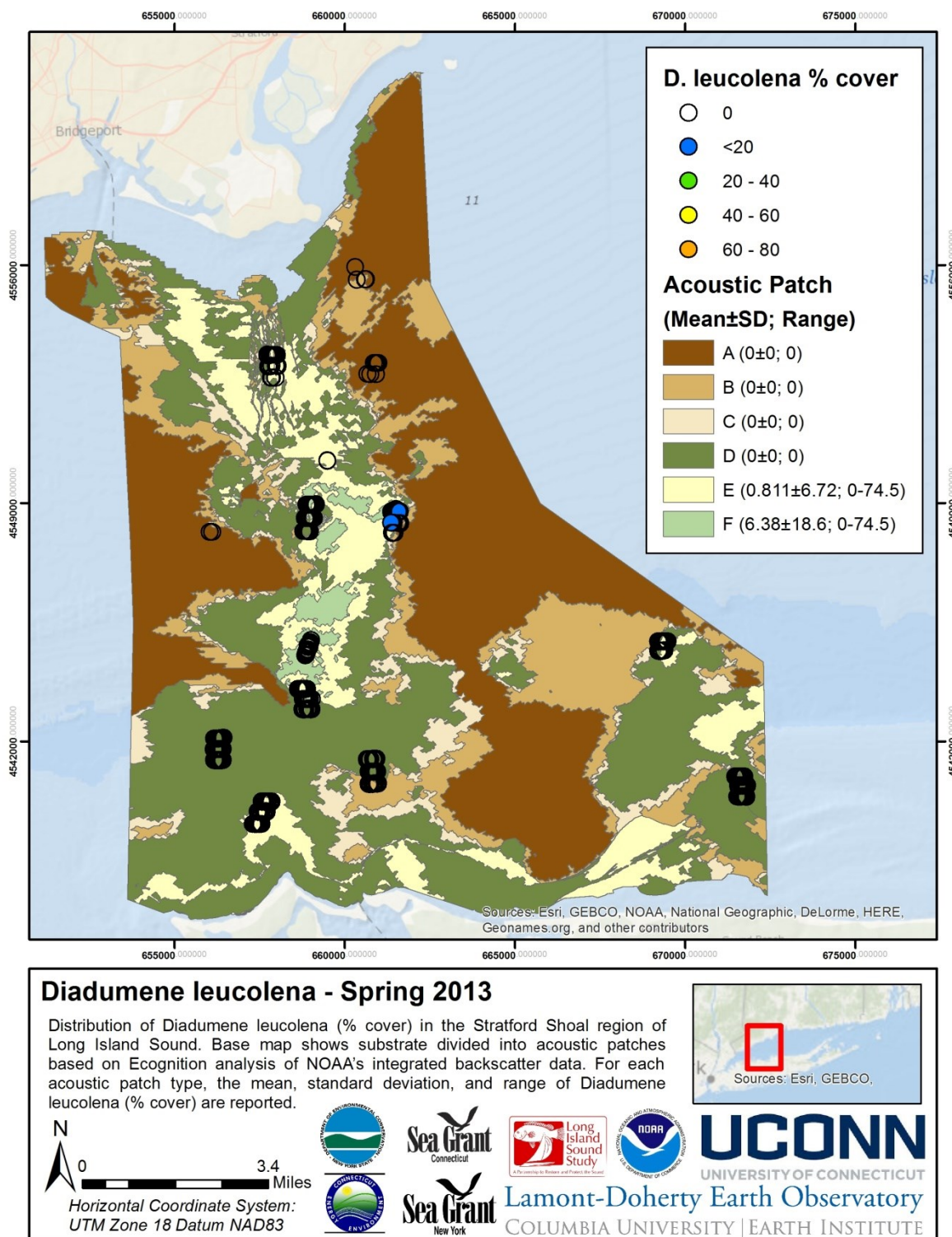


Figure 5.5-47.

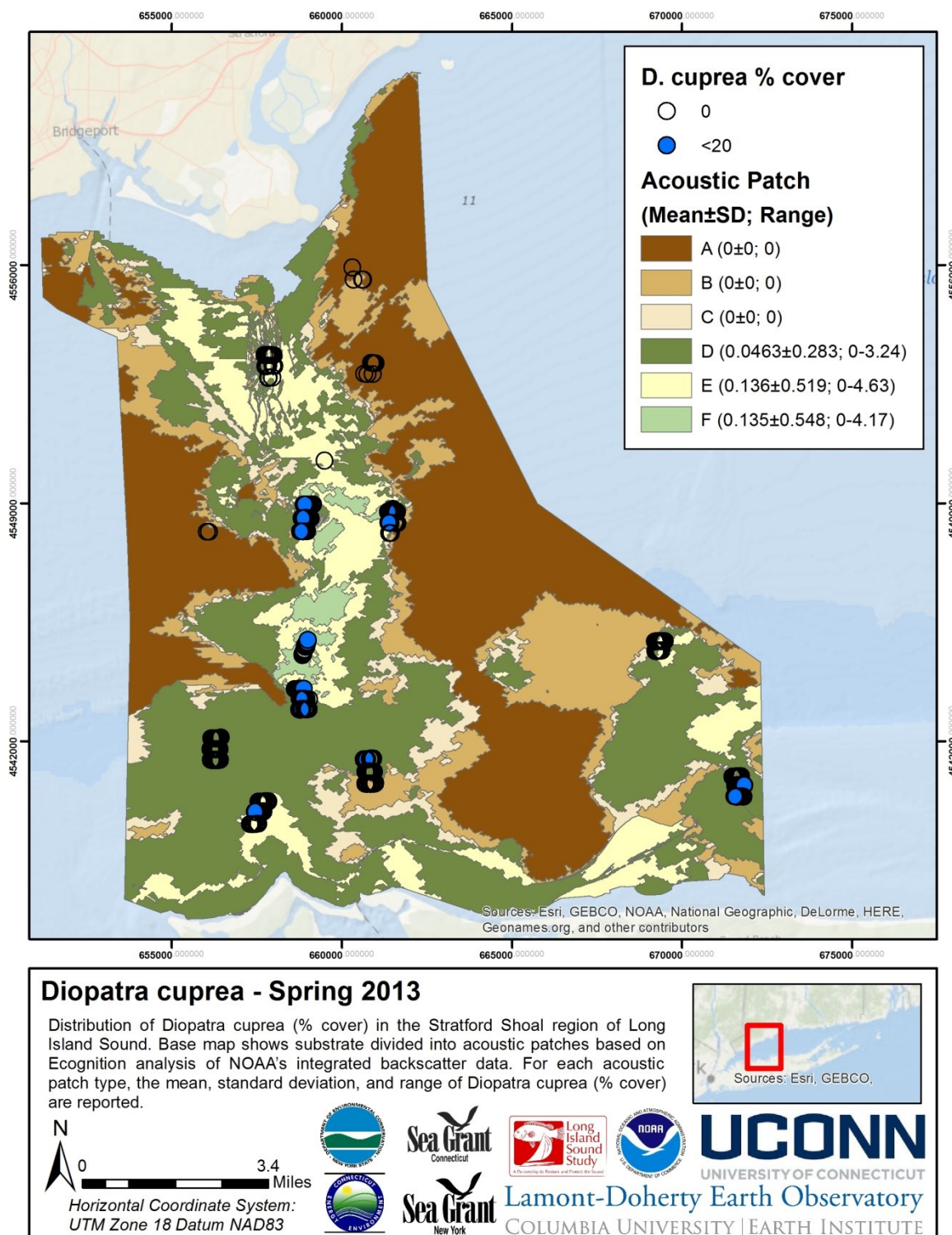


Figure 5.5-48. Figure 5.5-49.

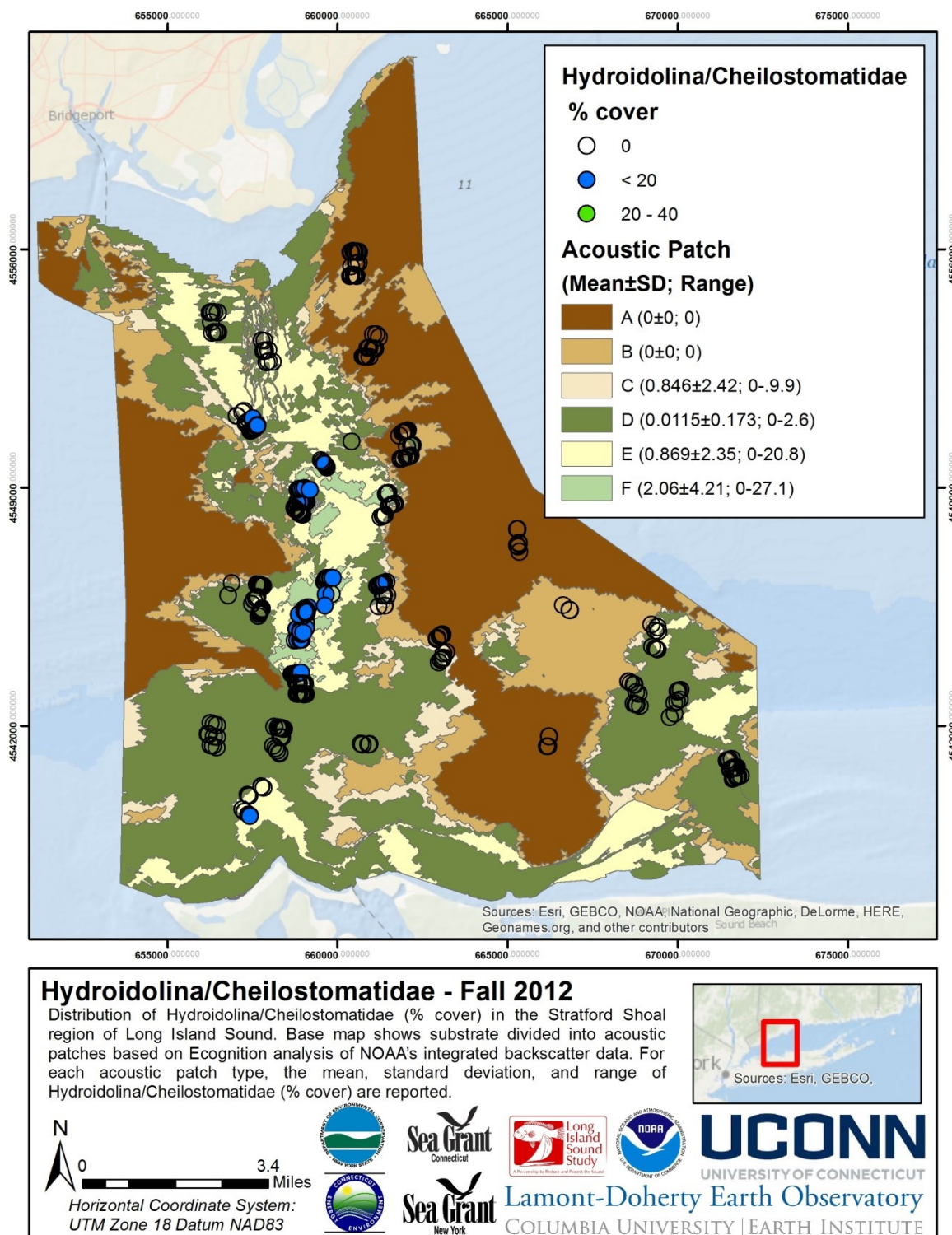


Figure 5.5-50.

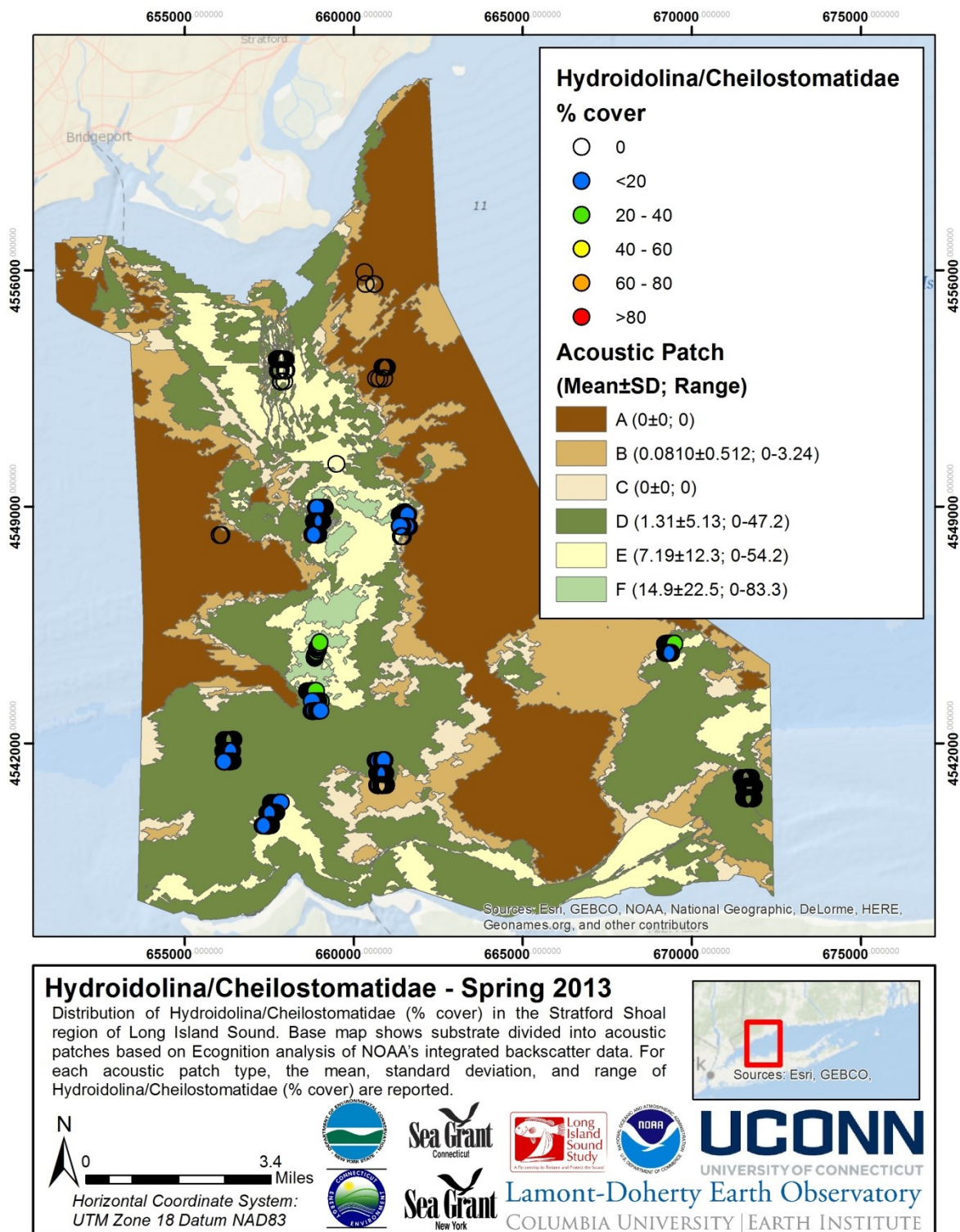


Figure 5.5-51.

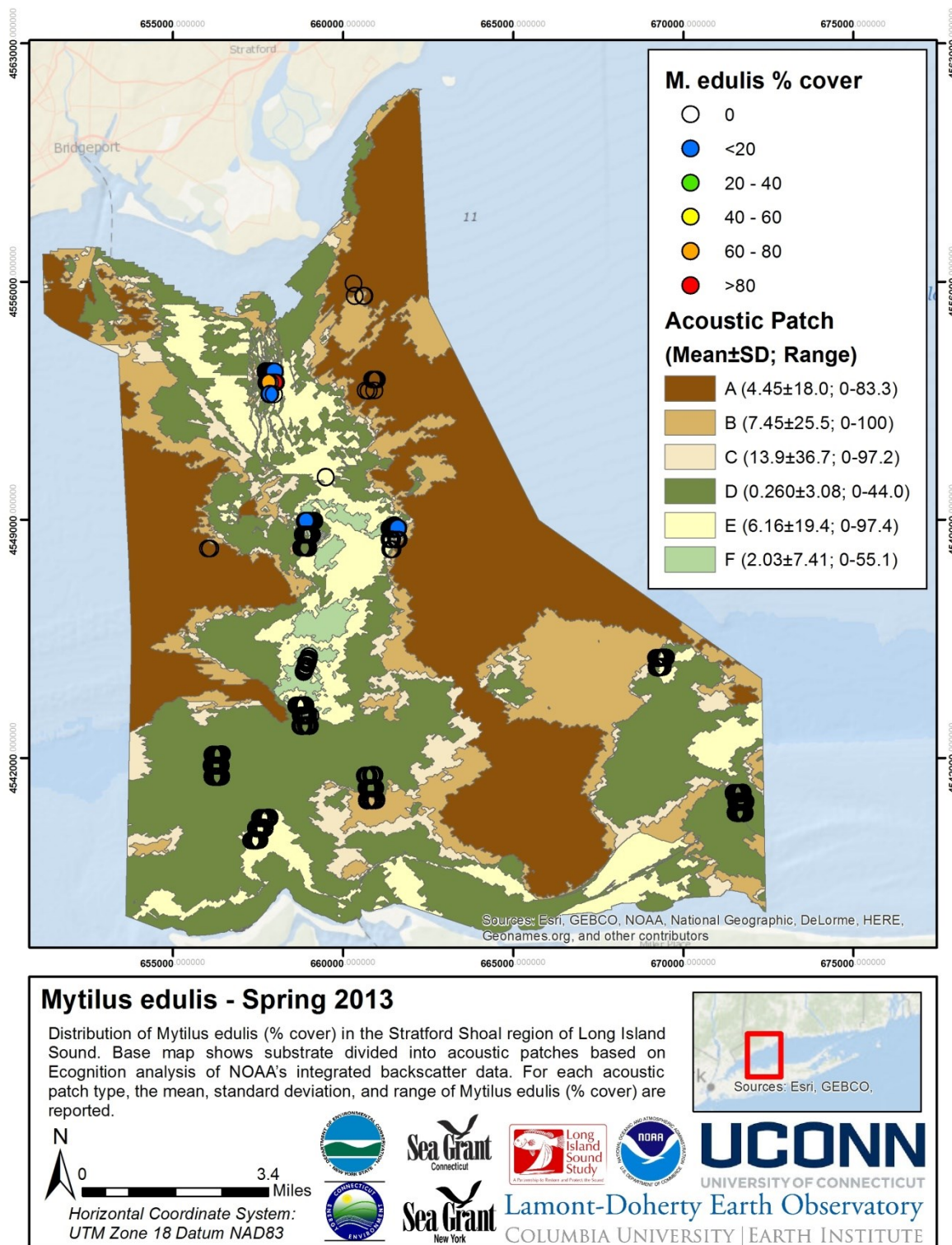


Figure 5.5-53.

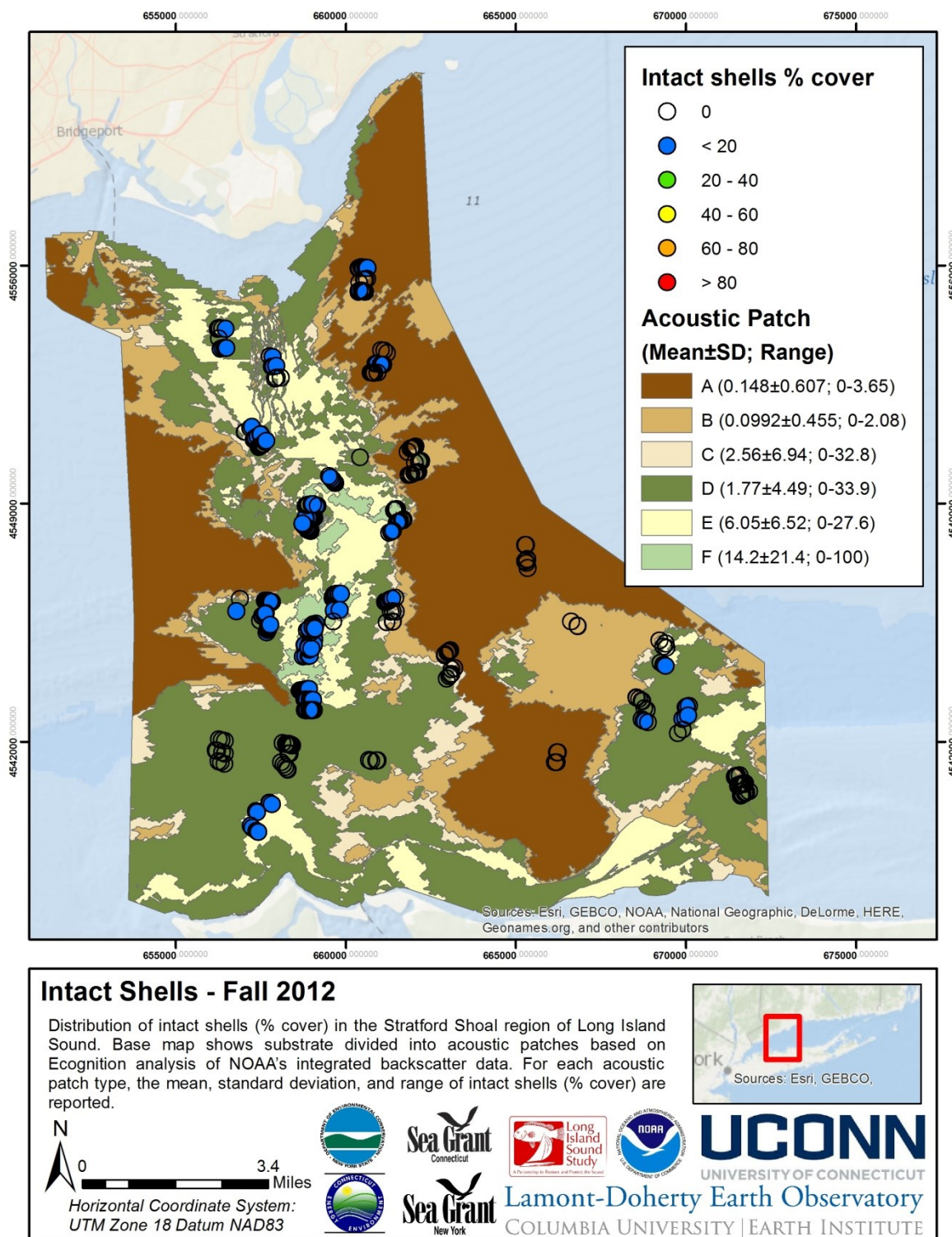


Figure 5.5-54.

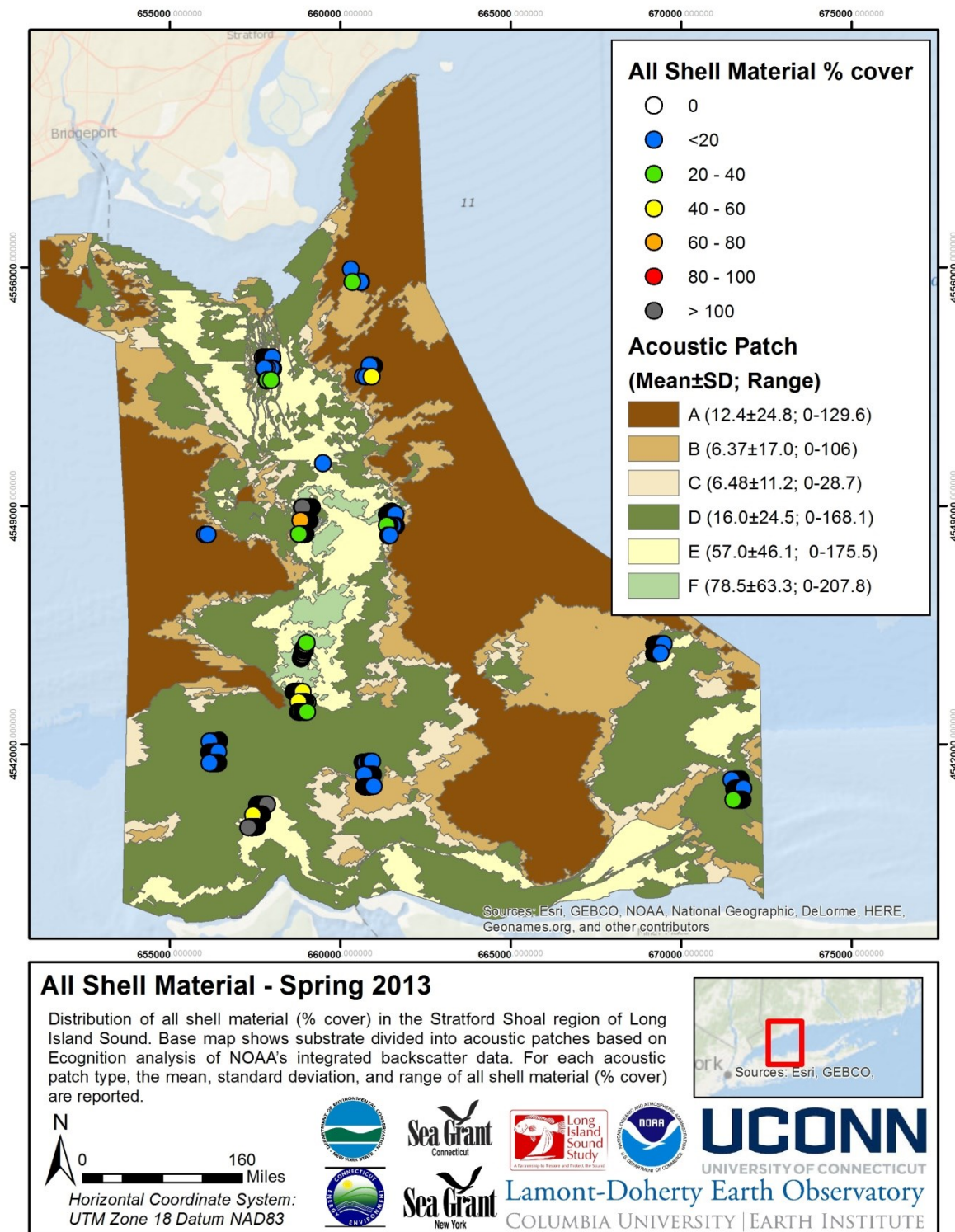


Figure 5.5-57.

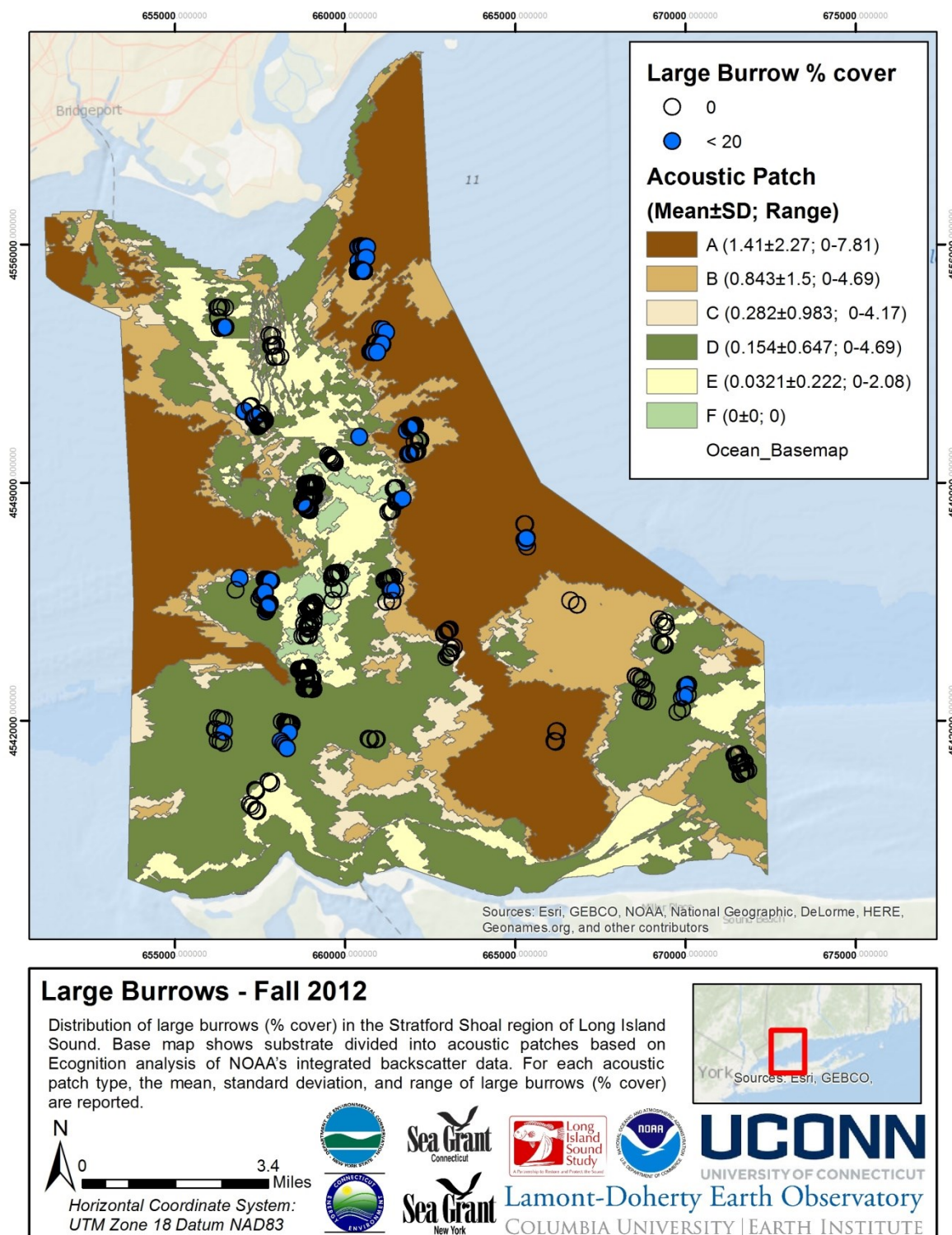


Figure 5.5-58.

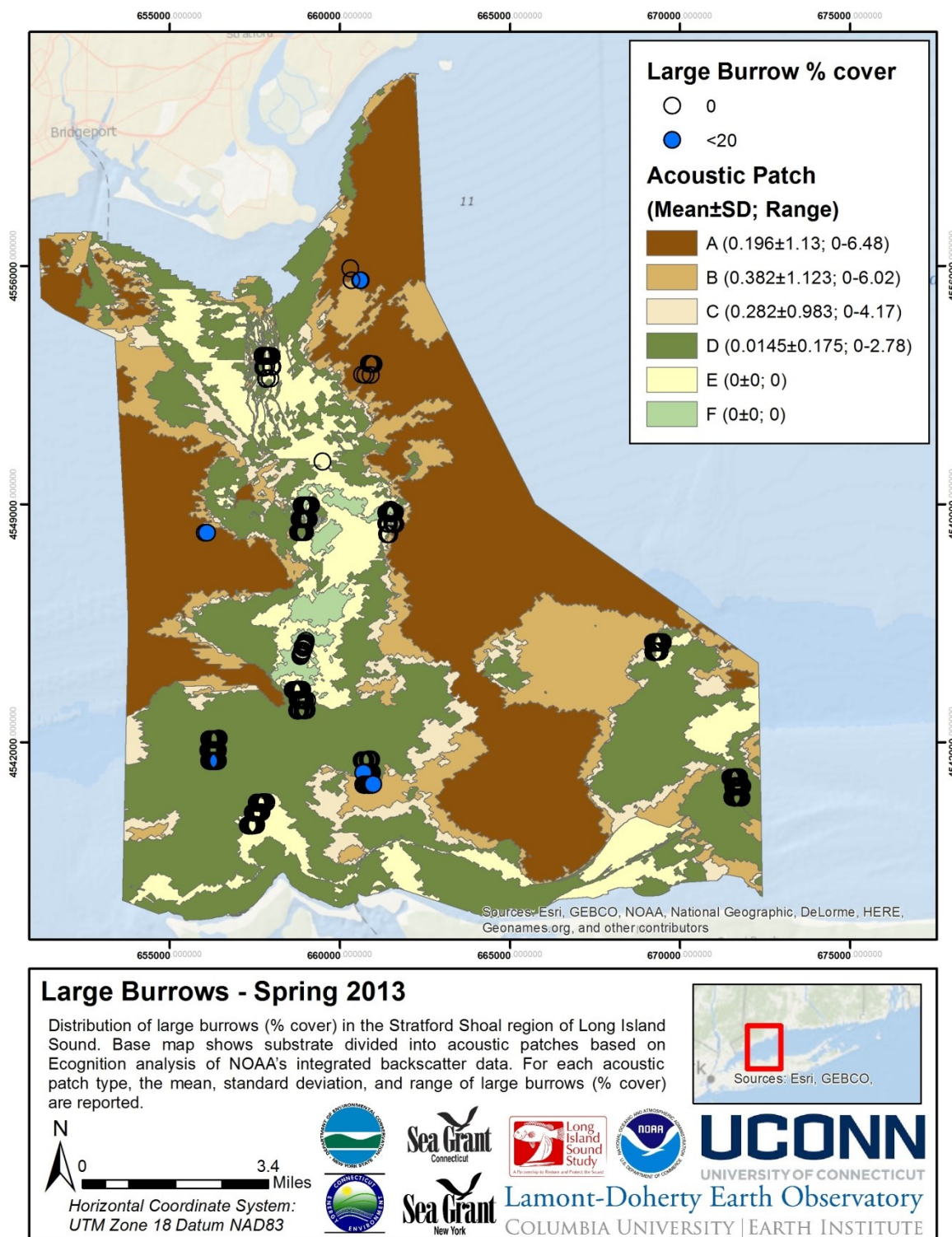


Figure 5.5-59.

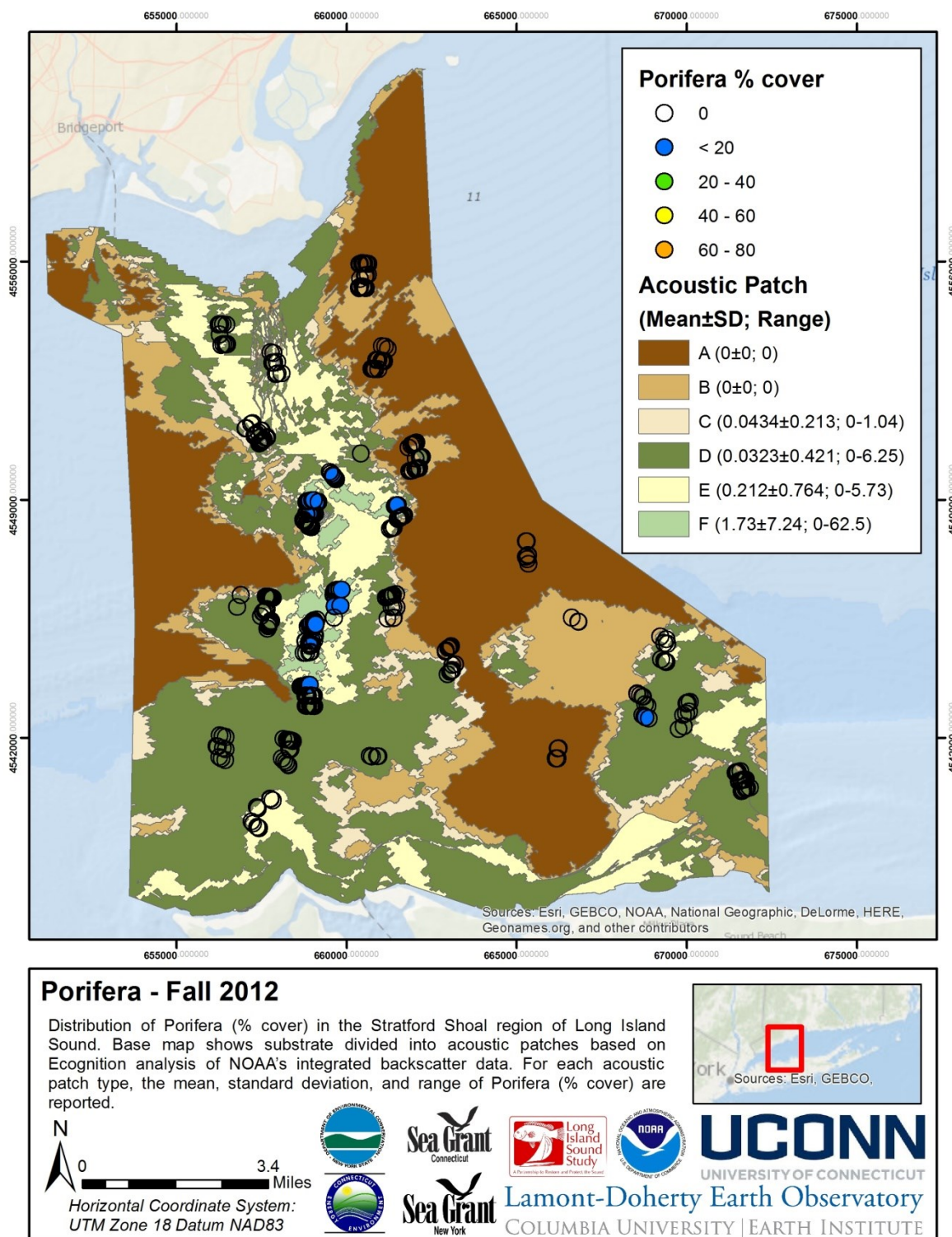


Figure 5.5-60.

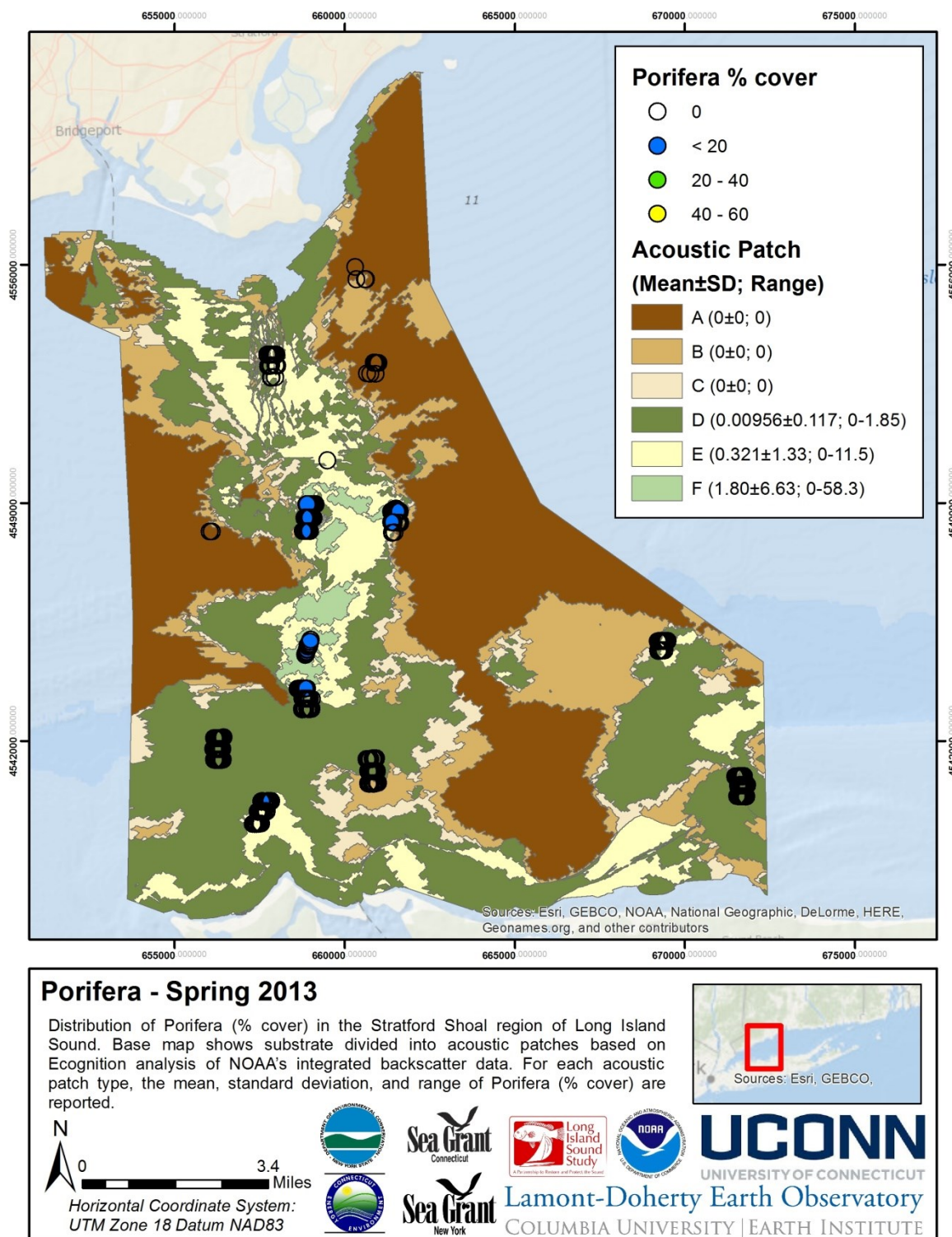


Figure 5.5-61

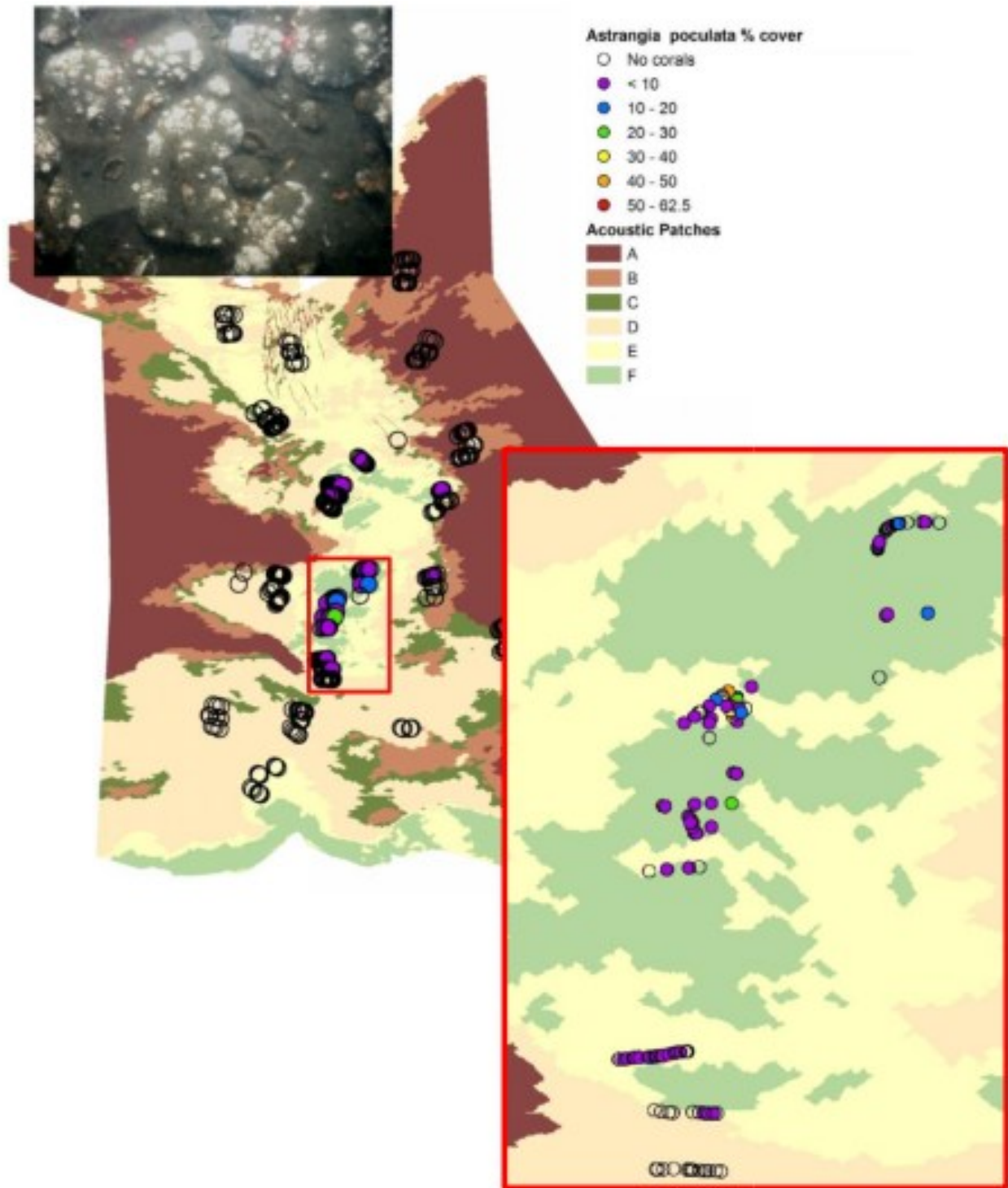


Figure 5.5-62. Northern star coral *Astrangia poculata* exhibits a limited broad scale distribution pattern within the study area has associations with coarse grain substrate types based on Ecognition patch class. As would be predicted with a species that requires a hard surface for attachment, corals in the pilot area are restricted to harder substratum.

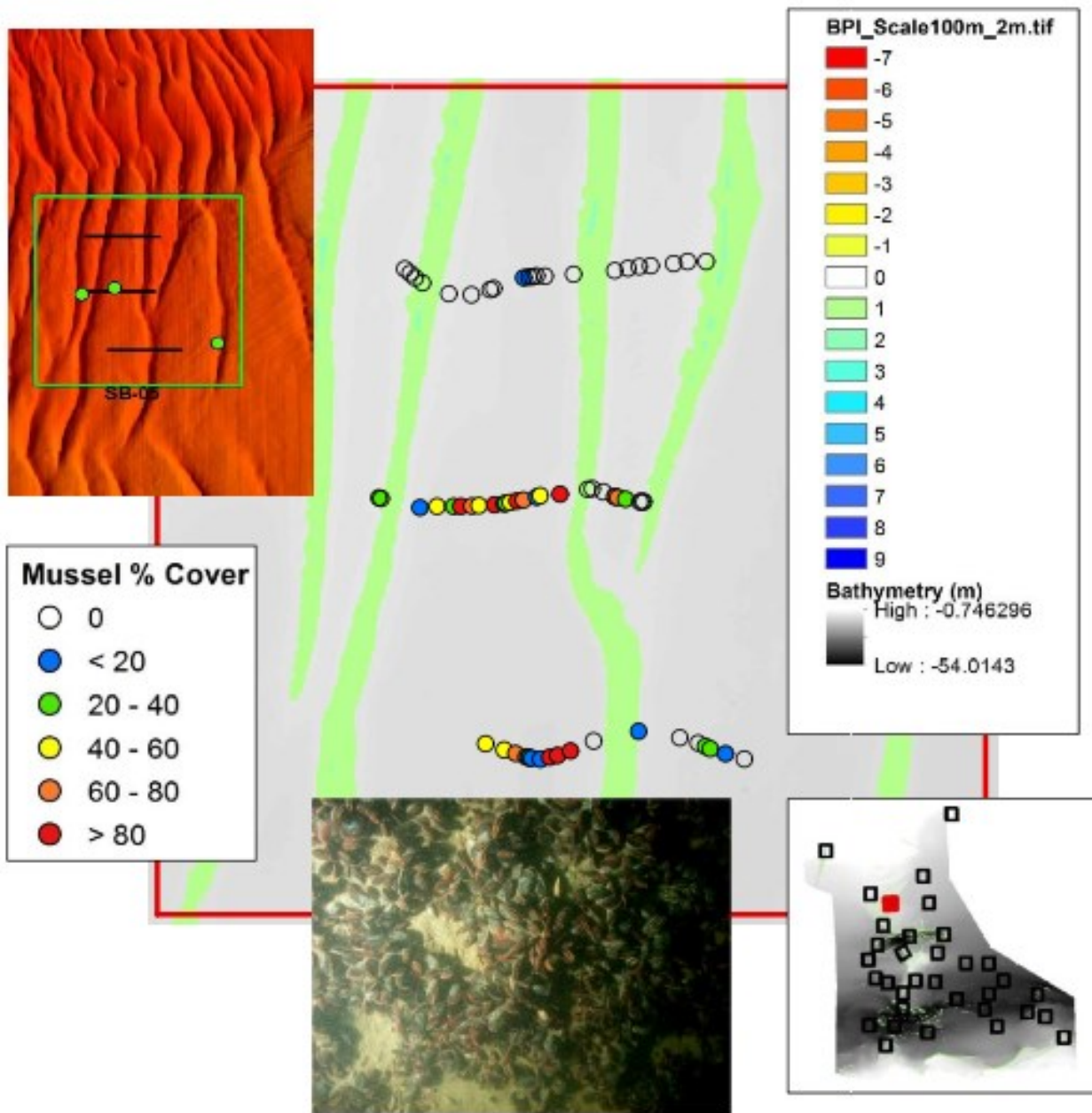


Figure 5.5-63. Fine scale distribution patterns of blue mussel *Mytilus edulis* dominated community in sand waves at the northern end of Stratford Shoal. Here percent cover of blue mussel is plotted over the BPI coverage. Note cover of blue mussel is 40% to over 80% in the troughs of sand waves but is less than 20% or absent on the ridges.

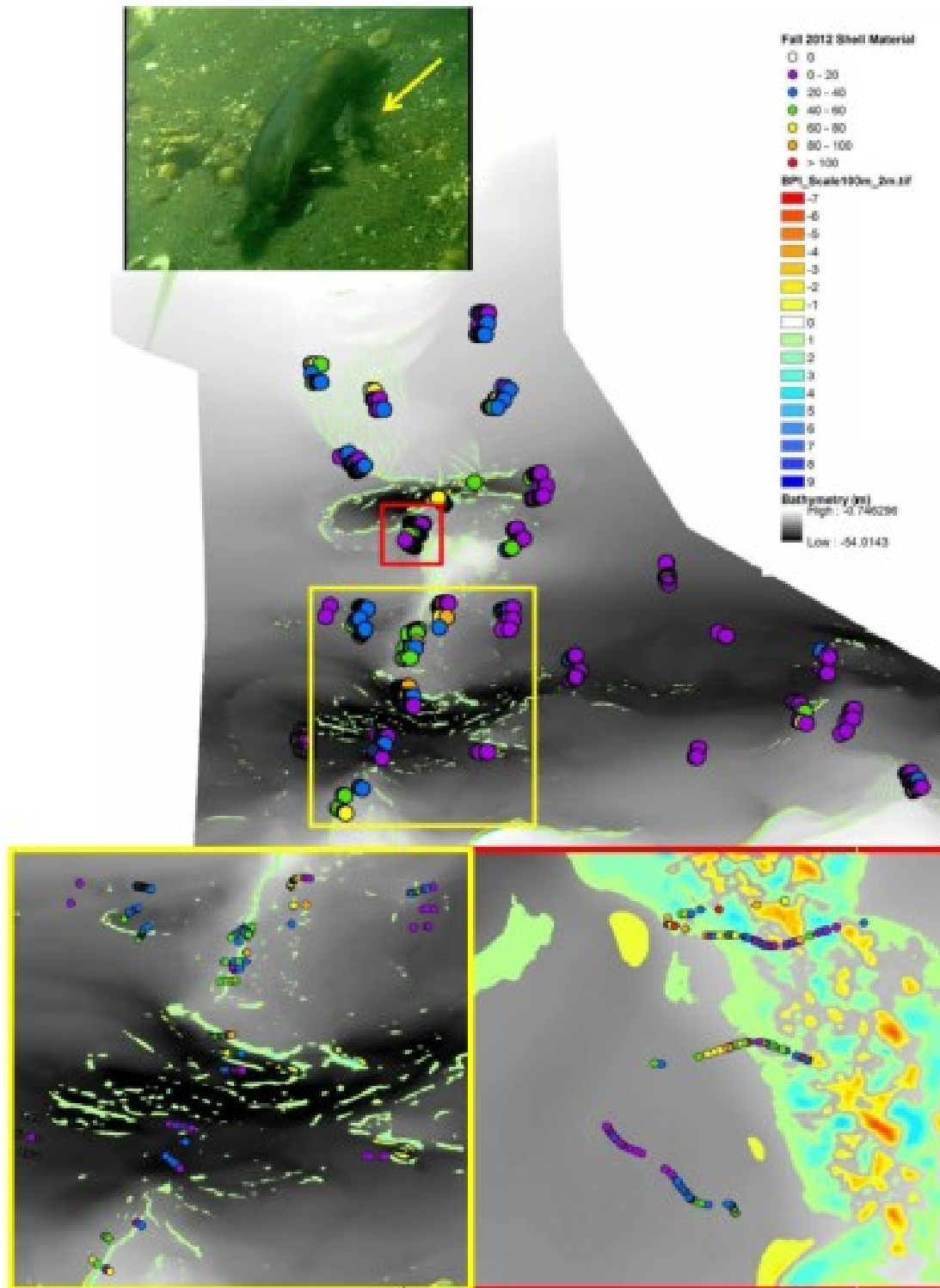


Figure 5.5-64. (Previous page) Shell and shell aggregates provide cover for juveniles of ecologically and economically important species such as the juvenile black sea bass and scup pictured here, using a razor clam shell for shelter. The map integrates three different data sets: bathymetry, percent cover of shell as points, and the bathymetric position index (BPI) on a color ramp where

warm colors indicate depressions and cool colors indicate rises. By mapping the cover data on a BPI coverage, note the higher percent cover of shell is found on flat topographic highs, at the bases of steep slopes, and in local scale depressions.

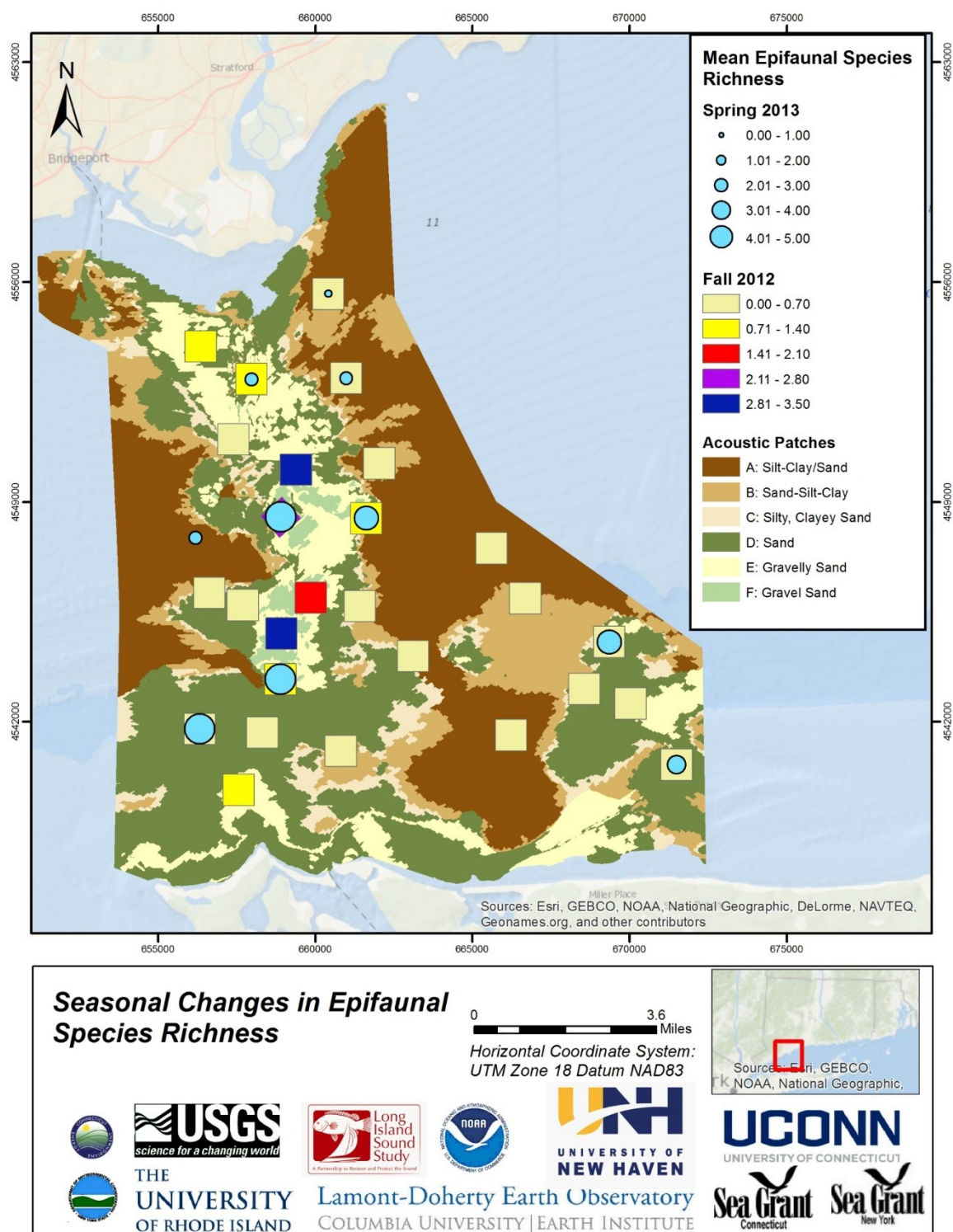


Figure 5.5-65. Contrasts in pattern of species richness (S) within and between seasons based on sampling blocks.

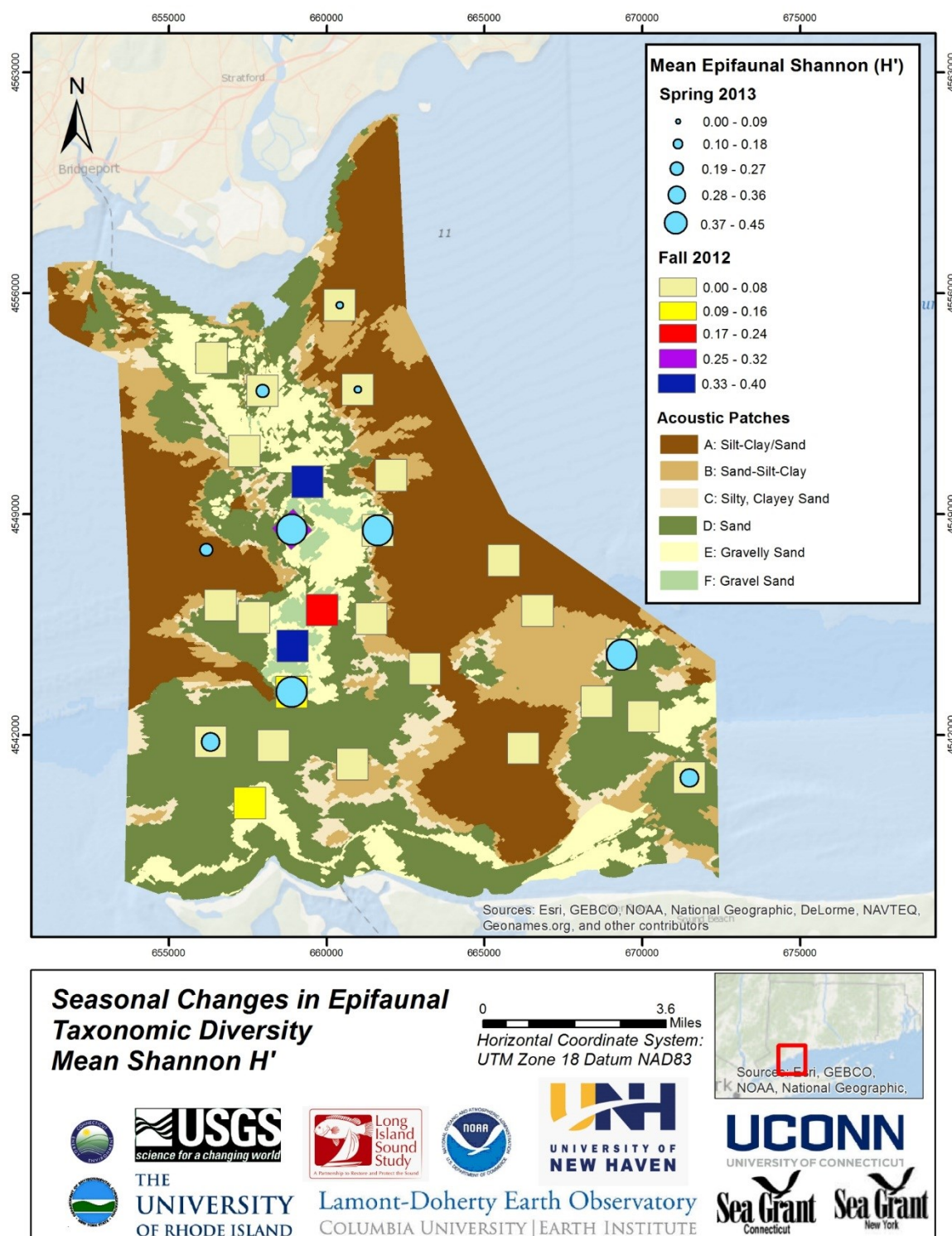


Figure 5.5-66. Contrasts in pattern of species diversity (H') within and between seasons based on sampling blocks.

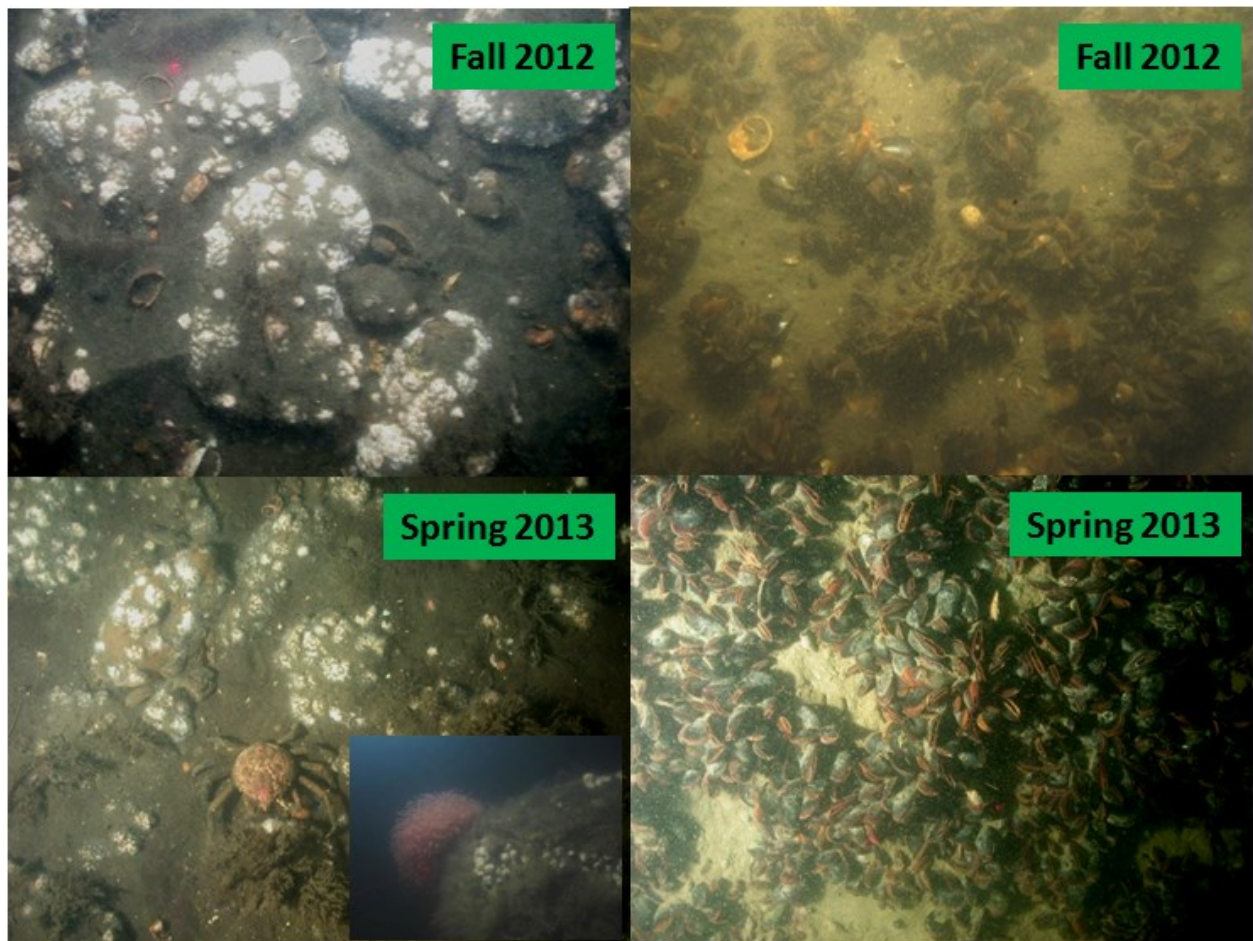


Figure 5.5-67. Interseasonal stability is illustrated by an examination of imagery from the fall and spring along the boulder reef on the ridge of the shoal and the blue mussel dominated communities in sand wave troughs to the north. Both dominant and conspicuous components of the community are present and maintain high cover values in both seasons. It should be noted that mussel communities are subject to a pattern of recruitment and senescence on a 5 to 7 year cycle, so this habitat type may not be stable over longer, such as decadal, time periods.

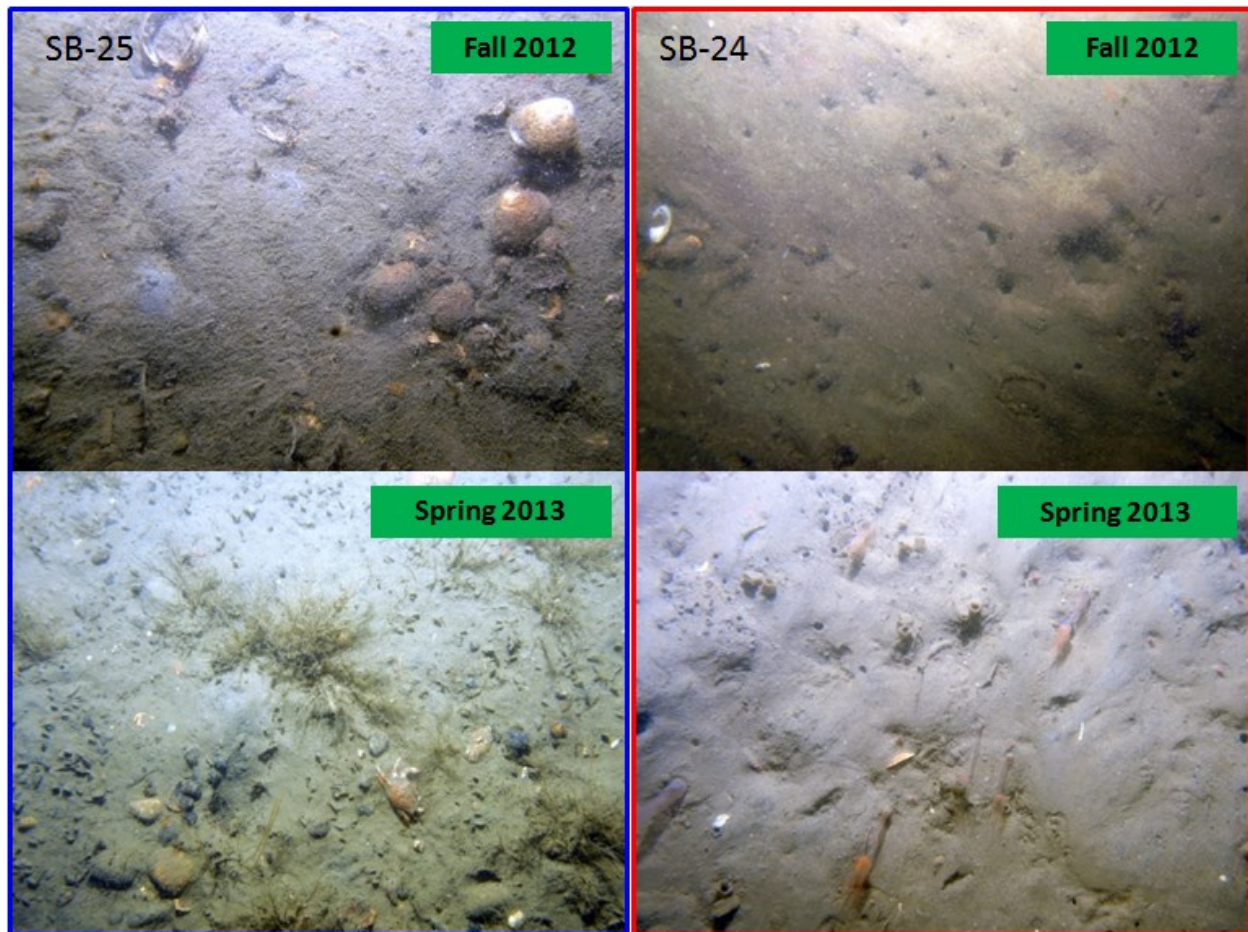


Figure 5.5-68. Interseasonal dynamics are driven primarily by species with short life histories such as amphipods, colonial and solitary hydroids, and ascidians in the spring. These species provide structure in habitats that have minimal emergent structure at other times of year.

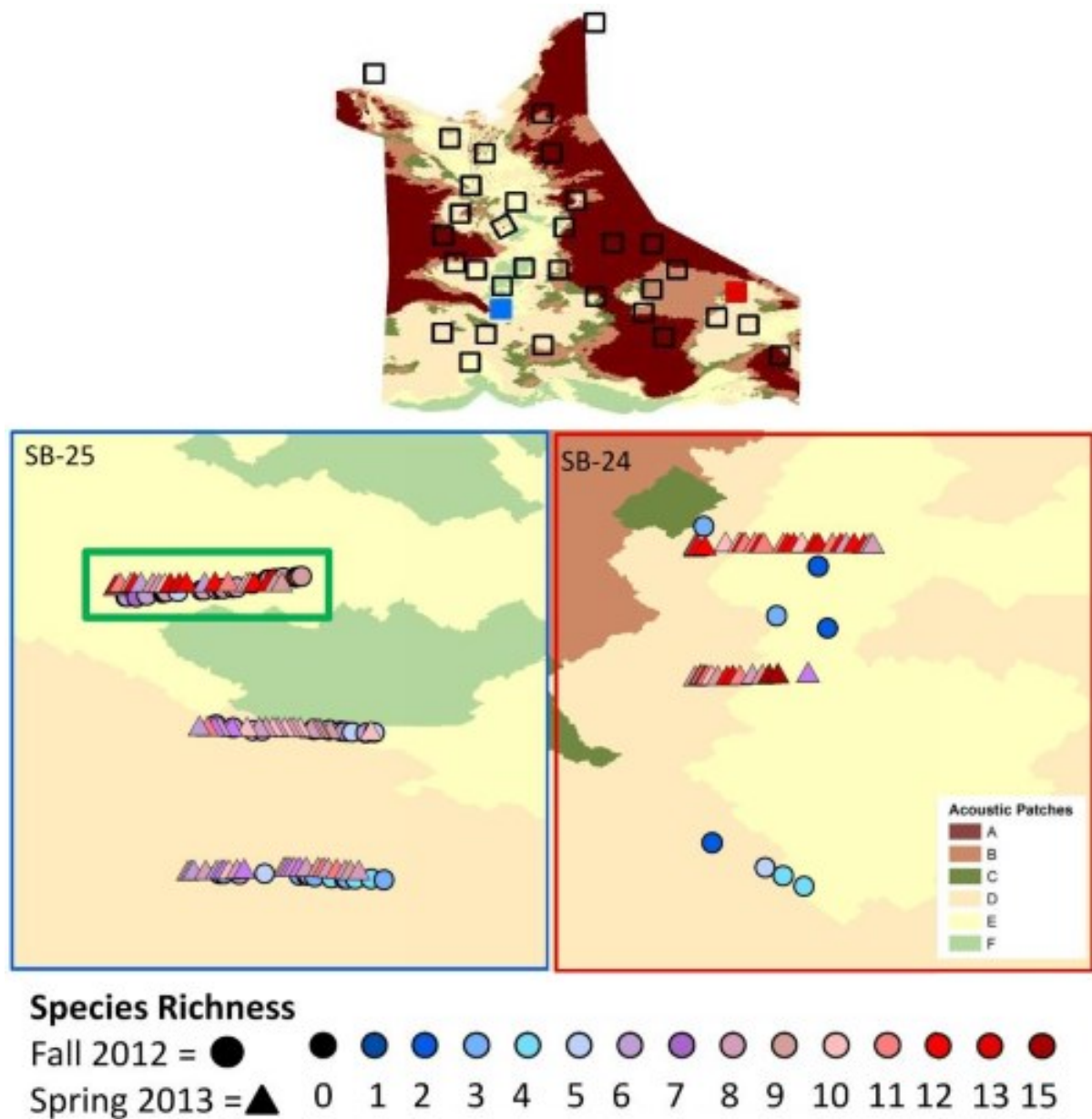


Figure 5.5-69. Transects over harder substratum areas had less inter-seasonal variation. While the imagery from the spring sampling demonstrates the predominance of seasonal dynamics in benthic communities in Long Island Sound. For example, in both sampling blocks 24 and 25 above, species and biogenic feature richness in images taken in the fall (circles) is lower than images taken in Spring 2013 (triangles). In sampling block 25, the transect conducted on harder substrate exhibits less interseasonal variation than those on softer substrates.

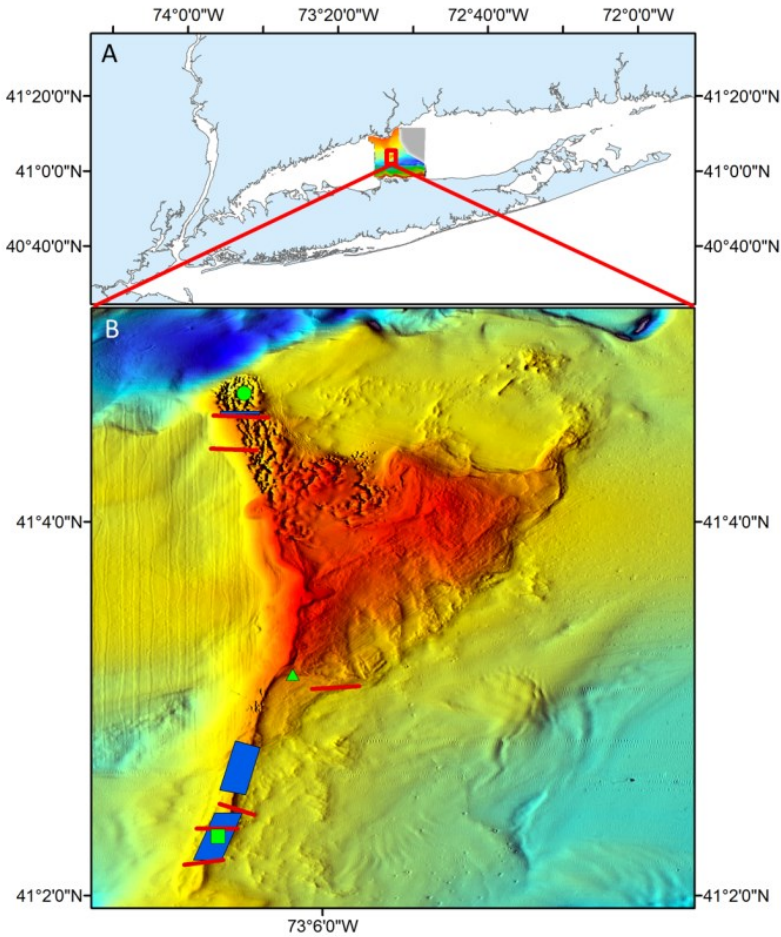


Figure 5.5-70. (A) Long Island Sound showing the location of Stratford Shoal; (B) Bathymetry of southern half of Stratford Shoal showing survey locations. Green triangle = June 1991, MiniRover MkII ROV; Green square = May 2007, ISIS towed camera platform and divers; Green circle = April 2010, Hela ROV; Red lines = October 2012, SEABOSS camera-grab system; Blue lines = December 2012, ISIS towed camera platform. (Bathymetry map modified from Poppe *et al.*, 2006)

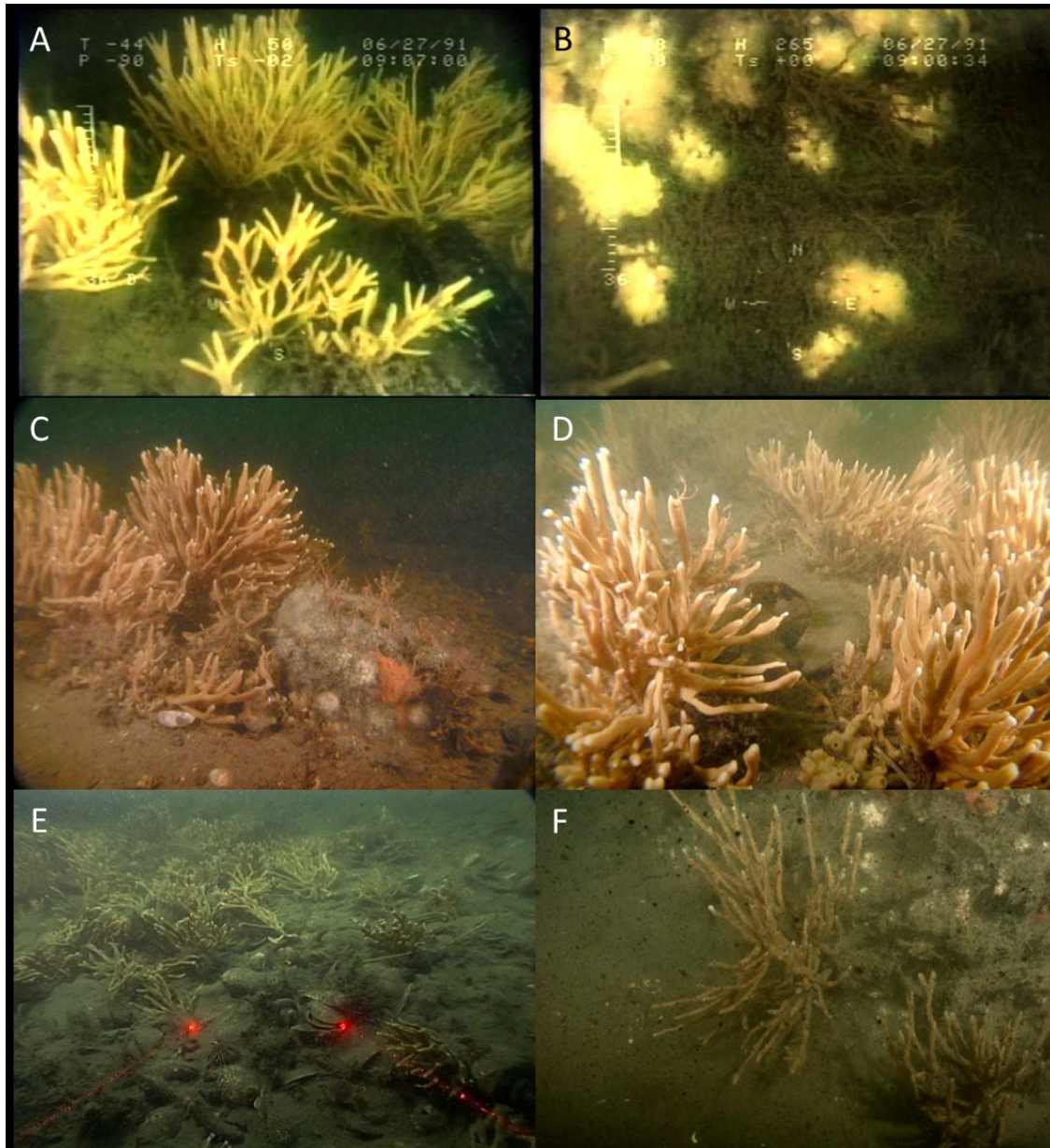


Figure 5.5-71. Exemplary benthic community at Stratford Shoal boulder reefs illustrating dominance of *H. oculata* (height range: 10-40 cm): June 1991 (A & B); May 2007 (C & D); April 2010 (E & F). Other species present include: *Astrangia poculata* (B, C, F) and *Halichondria* sp. (D).

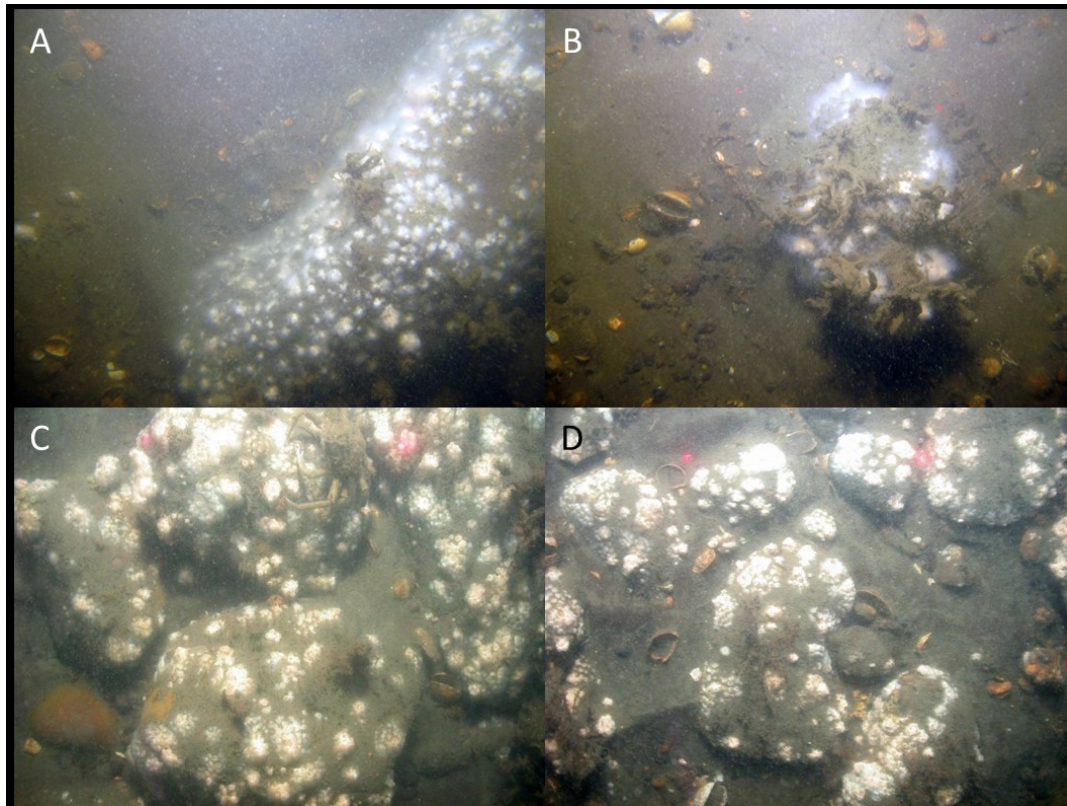


Figure 5.5-72. Exemplar benthic community at Stratford Shoal boulder reefs demonstrating the loss of *H. oculata*: October 2012 (A & B); December 2012 (C & D). Distance between laser points in the center of panels B, C and D are 20 cm.

Table 5.5-1. Lists of all benthic invertebrates and biogenic features, based on lowest identifiable taxon, enumerated from seafloor images. Habitat forming species are a subset of all invertebrates. See Appendix 5.5-1 for a list of taxa and associated common names.

Invertebrates	Biogenic features	Habitat forming species
Arbacia_punctulata	Crepidula fornicata (Dead)	Astrangia_poculata
Astrangia_poculata	Ilyanassa trivittata (dead)	Balanomorpha_Barnacle
Balanomorpha_Barnacle	Mercenaria shells (Dead)	Cliona spp.
Cancer irroratus	Euspira_spp_dead	Crepidula fornicata (Live)
Cliona spp.	Mytilus edulis (dead shell)	Demospongiae_1
Crab_Brachyura	Ensis_directus	Hydroides_dianthus
Crepidula fornicata (Live)	Mud_tube	Hydroidolina_Cheilostomatidae
Demospongiae_1	Worm_mound	Mytilus edulis
Pagurus_spp_small	Worm_castings	Diopatra_cuprea
Pagurus_spp_large	Carapace_fragment	Demospongiae_2
Hydroides_dianthus	Crassostrea_virginica_dead	Bivalve_siphons_1
Hydroidolina_Cheilostomatidae	Mud_tube_on_surface	Bivalve_siphons_2
Libinia spp	Andara_spp_dead	Ceriantheopsis_americanana
Mytilus edulis	Astarte_undata_dead	Diadumene_leucolena
Demospongiae_2	Mucus_strands	Demospongiae_3
Bivalve_siphons_1	Astrangia_poculata_dead	Crassostrea_virginica

Invertebrates	Biogenic features	Habitat forming species
Bivalve_siphons_2	Aoridae_tubes	Bostrichobanchus_pilularis
Ceriantheopsis_americana	Terrestrial_vegetation	Corymorpha_pendula
Diadumene_leucolena	Anomia_spp_dead	Bryozoa_encrusting
Demospongiae_3	Algal_debris	Halichondria_sp
Limulus_polyphemus	Libinia_spp_dead	Worm_pink
Crassostrea_virginica	Shell_hash	Astarte_undata
Henricia_sanguinolenta	Shells_intact	Styela_canopus
Bostrichobanchus_pilularis	Biogenic_depression	Rhodophyta_filamentus
Polychaeta_tentacles	Burrow_medium	Perophora_sp
Corymorpha_pendula	Burrow_large	Ectopleura_spp
Crustacea_shrimp	Burrow_wide	
Aoridae_amphipod	Burrows_small	
Nudibranchia_1		
Bryozoa_encrusting		
Halichondria_sp		
Worm_pink		
Astarte_undata		
Pycnogonida		
Styela_canopus		
Euspira_spp		
Perophora_sp		
Euspira_spp_egg_case		
Asterias_forbesi		
Busycotypus_canaliculatus		
Nudibranchia_2		
Ectopleura_spp		
Gastropoda_small		

Table 5.5-2. Multivariate dispersion indices calculated for community composition attributed to each Ecognition patch type for each season.

Fall 2012		Spring 2013	
Global Analysis			
Factor value	Dispersion	Factor value	Dispersion
F	0.902	A	0.853
B	0.953	D	0.927
D	0.981	B	1.014
A	1.023	F	1.238
E	1.093	E	1.277
C	1.35	C	1.472

Pairwise Comparisons			
Factor values	IMD	Factor values	IMD
E, F	0.187	A, B	-0.146
E, C	-0.27	A, D	-0.085
E, D	0.114	A, E	-0.384
E, A	0.067	A, C	-0.531
E, B	0.143	A, F	-0.352
F, C	-0.408	B, D	0.081
F, D	-0.081	B, E	-0.238
F, A	-0.115	B, C	-0.41
F, B	-0.062	B, F	-0.199
C, D	0.372	D, E	-0.351
C, A	0.321	D, C	-0.523
C, B	0.398	D, F	-0.309

D, A	-0.042	E, C	-0.279
D, B	0.029	E, F	0.03
A, B	0.069	C, F	0.312

Table 5.5-3. Richness estimators from images derived from sampling blocks during fall 2012 cruise using all species and biogenic features. Estimators based on 999 permutations of sample order from the sample-species matrix (habitat forming species and biogenic features). N = number of images per block. S(obs)=cumulative observed richness. A multi-model approach was taken to account for differences in how species richness estimators are calculated. See Clark and Warwick (2001) for a discussion of richness estimators.

SB	N	S(obs)	Chao2	Chao2(SD)	Jackknife1	Jackknife2	Bootstrap
Fall 2012							
SB-03	24	8	8.000	0.000	8.000	8.000	8.085
SB-04	14	15	18.125	3.658	19.643	20.764	17.280
SB-05	10	13	19.250	7.552	17.500	20.078	15.018
SB-06	19	8	9.000	1.871	9.895	9.994	8.958
SB-07	31	18	24.250	7.552	22.839	25.708	20.218
SB-08	11	11	11.000	0.000	11.000	9.527	11.223
SB-09	19	8	16.000	11.662	11.789	14.523	9.591
SB-11	111	43	92.000	43.994	56.874	68.676	48.589
SB-12	16	16	19.600	3.851	21.625	22.792	18.801
SB-15	7	6	8.250	3.396	8.571	9.524	7.209
SB-16	2	8	17.000	10.173	11.000	11.000	9.500
SB-17	39	11	11.000	4.182	13.923	16.769	12.107
SB-18	31	33	61.167	23.167	45.581	55.029	38.150
SB-19	16	16	36.250	20.187	24.438	30.679	19.479
SB-20	3	3	3.000	0.486	3.667	4.000	3.296
SB-21	58	28	36.167	8.277	34.879	38.792	30.952
SB-22	14	4	4.000	1.006	4.929	5.786	4.389
SB-24	8	6	6.500	1.323	6.875	6.982	6.490
SB-25	48	26	34.167	8.277	32.854	36.749	28.960
SB-27	11	13	29.000	16.492	20.273	25.345	16.024
SB-28	10	7	15.000	11.662	10.600	13.089	8.503
SB-29	18	8	8.500	1.323	8.944	8.997	8.526
SB-30	4	5	5.000	0.000	5.000	4.667	5.066
SB-31	4	4	4.000	0.000	4.000	3.333	4.129
SB-32	12	12	12.000	9.496	16.583	20.750	13.816
SB-33	11	16	26.667	10.270	23.273	27.609	19.134
SB-34	23	6	6.000	0.883	6.957	7.870	6.456
All blocks	574	63	91.125	20.900	77.974	88.942	69.307

Table 5.5-4a. Diversity measures based on Ecognition patch types from fall 2012.

Diversity metric/Patch	Size	Mean	Std Dev	SE	Range	Max	Min	Median
Patch A								
S_Invert_Biogenic	60	2.667	1.145	0.148	4	5	1	2.5
H_Invert_Biogenic	60	0.256	0.168	0.0217	0.619	0.619	0	0.263
S_Habitat_Biogenic	60	2.65	1.147	0.148	4	5	1	2
H_Habitat_Biogenic	60	0.255	0.169	0.0218	0.619	0.619	0	0.256
S_Biogenic	60	2.583	1.109	0.143	4	5	1	2
H_Biogenic	60	0.245	0.16	0.0207	0.619	0.619	0	0.249
S_Invert	60	0.0667	0.252	0.0325	1	1	0	0
H_Invert	60	0	0	0	0	0	0	0
S_Habitat	60	0.0667	0.252	0.0325	1	1	0	0
H_Habitat	60	0	0	0	0	0	0	0
Patch B								
S_Invert_Biogenic	21	3.238	1.411	0.308	6	6	0	3
H_Invert_Biogenic	21	0.357	0.17	0.0371	0.553	0.553	0	0.392
S_Habitat_Biogenic	21	3.238	1.411	0.308	6	6	0	3
H_Habitat_Biogenic	21	0.357	0.17	0.0371	0.553	0.553	0	0.392
S_Biogenic	21	3.048	1.284	0.28	5	5	0	3
H_Biogenic	21	0.332	0.168	0.0366	0.553	0.553	0	0.361
S_Invert	21	0.143	0.359	0.0782	1	1	0	0
H_Invert	21	0	0	0	0	0	0	0
S_Habitat	21	0.19	0.402	0.0878	1	1	0	0
H_Habitat	21	0	0	0	0	0	0	0
Patch C								
S_Invert_Biogenic	24	3.667	1.993	0.407	8	9	1	3.5
H_Invert_Biogenic	24	0.366	0.196	0.0401	0.715	0.715	0	0.384
S_Habitat_Biogenic	24	3.667	1.993	0.407	8	9	1	3.5
H_Habitat_Biogenic	24	0.366	0.196	0.0401	0.715	0.715	0	0.384
S_Biogenic	24	2.625	0.97	0.198	3	4	1	3
H_Biogenic	24	0.263	0.149	0.0304	0.485	0.485	0	0.272
S_Invert	24	1.042	1.681	0.343	5	5	0	0
H_Invert	24	0.0997	0.203	0.0414	0.555	0.555	0	0
S_Habitat	24	1.042	1.681	0.343	5	5	0	0
H_Habitat	24	0.0997	0.203	0.0414	0.555	0.555	0	0
Patch D								
S_Invert_Biogenic	226	3.491	1.86	0.124	11	11	0	3
H_Invert_Biogenic	226	0.33	0.178	0.0118	0.745	0.745	0	0.347
S_Habitat_Biogenic	226	3.319	1.795	0.119	11	11	0	3
H_Habitat_Biogenic	226	0.317	0.184	0.0122	0.745	0.745	0	0.343
S_Biogenic	226	2.956	1.414	0.094	7	7	0	3
H_Biogenic	226	0.293	0.171	0.0114	0.631	0.631	0	0.306
S_Invert	226	0.473	0.849	0.0565	4	4	0	0
H_Invert	226	0.0365	0.103	0.00687	0.475	0.475	0	0
S_Habitat	226	0.363	0.749	0.0498	4	4	0	0
H_Habitat	226	0.0257	0.0861	0.00573	0.42	0.42	0	0
Patch E								
S_Invert_Biogenic	130	5.492	2.519	0.221	13	14	1	5
H_Invert_Biogenic	130	0.43	0.181	0.0159	0.912	0.912	0	0.427
S_Habitat_Biogenic	130	5.254	2.531	0.222	13	14	1	5
H_Habitat_Biogenic	130	0.417	0.185	0.0162	0.912	0.912	0	0.415
S_Biogenic	130	3.177	1.315	0.115	6	7	1	3

Diversity metric/Patch	Size	Mean	Std Dev	SE	Range	Max	Min	Median
H_Biogenic	130	0.256	0.138	0.0121	0.598	0.598	0	0.266
S_Invert	130	2.185	1.706	0.15	7	7	0	2
H_Invert	130	0.228	0.213	0.0187	0.667	0.667	0	0.253
S_Habitat	130	2.077	1.755	0.154	7	7	0	2
H_Habitat	130	0.219	0.214	0.0187	0.693	0.693	0	0.248
Patch F								
S_Invert_Biogenic	112	6.364	2.229	0.216	10	11	1	7
H_Invert_Biogenic	112	0.499	0.173	0.0167	0.834	0.834	0	0.508
S_Habitat_Biogenic	112	6.028	2.03	0.196	9	10	1	6
H_Habitat_Biogenic	112	0.488	0.169	0.0163	0.834	0.834	0	0.497
S_Biogenic	112	3.047	1.208	0.117	5	6	1	3
H_Biogenic	112	0.222	0.131	0.0126	0.524	0.524	0	0.241
S_Invert	112	3.047	1.538	0.149	7	7	0	3
H_Invert	112	0.321	0.19	0.0183	0.718	0.718	0	0.353
S_Habitat	112	2.981	1.414	0.137	6	6	0	3
H_Habitat	112	0.321	0.178	0.0172	0.718	0.718	0	0.349

Table 5.5-4b. Diversity measures based on Ecognition patch types from spring 2013.

Diversity metric / Patch	Size	Mean	Std Dev	SE	Range	Max	Min	Median
Patch A								
S_Invert_Biogenic	33	3	1.031	0.179	4	5	1	3
H_Invert_Biogenic	33	0.283	0.172	0.03	0.661	0.661	0	0.303
S_Habitat_Biogenic	33	2.242	1.226	0.213	5	5	0	2
H_Habitat_Biogenic	33	0.201	0.201	0.0351	0.661	0.661	0	0.102
S_Biogenic	33	1.303	0.984	0.171	3	3	0	1
H_Biogenic	33	0.109	0.154	0.0268	0.432	0.432	0	0
S_Invert	33	1.697	0.81	0.141	3	3	0	2
H_Invert	33	0.11	0.127	0.0221	0.439	0.439	0	0.0576
S_Habitat	33	0.909	0.459	0.0798	2	2	0	1
H_Habitat	33	0.0174	0.0694	0.0121	0.292	0.292	0	0
Patch B								
S_Invert_Biogenic	40	4.575	1.852	0.293	7	8	1	5
H_Invert_Biogenic	40	0.363	0.182	0.0288	0.761	0.761	0	0.394
S_Habitat_Biogenic	40	3.725	1.585	0.251	6	7	1	4
H_Habitat_Biogenic	40	0.315	0.177	0.0279	0.692	0.692	0	0.32
S_Biogenic	40	2.05	1.176	0.186	5	5	0	2
H_Biogenic	40	0.232	0.179	0.0284	0.537	0.537	0	0.284
S_Invert	40	2.525	1.219	0.193	5	5	0	3
H_Invert	40	0.229	0.138	0.0219	0.565	0.565	0	0.261
S_Habitat	40	1.65	0.802	0.127	3	3	0	2
H_Habitat	40	0.162	0.123	0.0194	0.458	0.458	0	0.179
Patch C								
S_Invert_Biogenic	7	4.143	1.864	0.705	6	7	1	4
H_Invert_Biogenic	7	0.424	0.196	0.0739	0.58	0.58	0	0.485
S_Habitat_Biogenic	7	3	1.732	0.655	5	6	1	3
H_Habitat_Biogenic	7	0.308	0.225	0.085	0.588	0.588	0	0.382
S_Biogenic	7	2	1.291	0.488	4	4	0	2
H_Biogenic	7	0.2	0.145	0.0547	0.357	0.357	0	0.252

Diversity metric / Patch	Size	Mean	Std Dev	SE	Range	Max	Min	Median
S_Invert	7	2.143	0.69	0.261	2	3	1	2
H_Invert	7	0.204	0.113	0.0428	0.368	0.368	0	0.204
S_Habitat	7	1	0.577	0.218	2	2	0	1
H_Habitat	7	0.0356	0.0942	0.0356	0.249	0.249	0	0
Patch D								
S_Invert_Biogenic	320	6.991	2.804	0.157	13	14	1	7
H_Invert_Biogenic	320	0.53	0.213	0.0119	0.993	0.993	0	0.486
S_Habitat_Biogenic	320	5.55	2.48	0.139	11	12	1	6
H_Habitat_Biogenic	320	0.454	0.225	0.0126	0.938	0.938	0	0.405
S_Biogenic	320	3.406	1.871	0.105	9	9	0	3
H_Biogenic	320	0.351	0.225	0.0126	0.842	0.842	0	0.37
S_Invert	320	3.584	1.425	0.0797	8	8	0	4
H_Invert	320	0.314	0.165	0.00923	0.788	0.788	0	0.292
S_Habitat	320	2.131	1.039	0.0581	5	5	0	2
H_Habitat	320	0.181	0.156	0.00875	0.616	0.616	0	0.192
Patch E								
S_Invert_Biogenic	146	7.068	3.115	0.258	12	13	1	7
H_Invert_Biogenic	146	0.516	0.208	0.0172	0.857	0.857	0	0.562
S_Habitat_Biogenic	146	6.171	3.079	0.255	12	13	1	6
H_Habitat_Biogenic	146	0.465	0.233	0.0193	0.831	0.831	0	0.527
S_Biogenic	146	3.644	1.999	0.165	8	8	0	4
H_Biogenic	146	0.273	0.192	0.0159	0.654	0.654	0	0.323
S_Invert	146	3.425	1.871	0.155	10	10	0	3
H_Invert	146	0.333	0.204	0.0169	0.865	0.865	0	0.36
S_Habitat	146	2.486	1.843	0.153	8	8	0	2
H_Habitat	146	0.23	0.204	0.0169	0.798	0.798	0	0.248
Patch F								
S_Invert_Biogenic	84	7.262	2.395	0.261	12	13	1	7
H_Invert_Biogenic	84	0.54	0.193	0.021	0.899	0.899	0	0.559
S_Habitat_Biogenic	84	5.964	2.142	0.234	10	11	1	6
H_Habitat_Biogenic	84	0.491	0.19	0.0207	0.854	0.854	0	0.525
S_Biogenic	84	2.56	1.459	0.159	7	7	0	2
H_Biogenic	84	0.191	0.198	0.0216	0.72	0.72	0	0.119
S_Invert	84	4.702	1.974	0.215	8	8	0	5
H_Invert	84	0.433	0.176	0.0192	0.766	0.766	0	0.468
S_Habitat	84	3.405	1.599	0.174	7	7	0	3
H_Habitat	84	0.343	0.183	0.02	0.694	0.694	0	0.378

Table 5.5-5. Estimates of species and feature richness based on Ecognition patch types.

Patch	N	S(obs)	Chao2	Chao2(SD)	Jackknife1	Jackknife2	Bootstrap
Fall 2012							
A	60	13	14.500	2.291	15.950	15.999	14.549
B	21	10	14.500	7.194	12.857	14.712	11.239
C	24	18	18.900	1.464	20.875	19.241	19.814
D	226	32	34.500	2.958	36.978	37.000	34.720
E	130	39	57.000	14.387	50.908	58.815	44.102
F	112	39	54.125	12.470	49.902	56.812	43.706

Spring 2013

A	33	15	23.167	8.277	21.788	25.634	17.921
B	40	24	34.125	9.018	32.775	37.622	27.886
C	7	13	13.000	20.573	19.857	25.571	15.747
D	320	45	53.000	7.483	52.975	56.962	48.761
E	146	44	45.333	1.846	47.973	46.041	46.406
F	84	38	44.250	7.552	42.940	45.893	40.238

Table 5.5-6a: Species descriptive stats by Ecognition patch type for fall 2012.

Species/Patch	Size	Mean	Std Dev	Std. Error	Range	Max	Min	Median
Patch A								
Diopatra_cuprea	60	0.000434	0.00336	0.000434	0.026	0.026	0	0
Shell_hash	60	0.146	0.161	0.0207	0.641	0.641	0	0.0964
Burrow_medium	60	0.00122	0.00511	0.000659	0.0313	0.0313	0	0
Burrow_large	60	0.0141	0.0227	0.00293	0.0781	0.0781	0	0
Shells_intact_all	60	0.00148	0.00607	0.000784	0.0365	0.0365	0	0
Burrows_small	60	0.0329	0.0336	0.00434	0.135	0.135	0	0.026
Bivalves_Live	60	0.0026	0.0133	0.00171	0.0885	0.0885	0	0
All_shell_material	60	0.148	0.162	0.0209	0.661	0.661	0	0.0964
Worm_evidence	60	0.00295	0.00751	0.00097	0.0313	0.0313	0	0
Patch B								
Diopatra_cuprea	21	0.000744	0.00341	0.000744	0.0156	0.0156	0	0
Shell_hash	21	0.0774	0.0892	0.0195	0.328	0.328	0	0.0521
Burrow_medium	21	0.000248	0.00114	0.000248	0.00521	0.00521	0	0
Burrow_large	21	0.00843	0.015	0.00326	0.0469	0.0469	0	0
Shells_intact_all	21	0.000992	0.00455	0.000992	0.0208	0.0208	0	0
Burrows_small	21	0.0387	0.0311	0.00679	0.115	0.115	0	0.0365
Bivalves_Live	21	0.00446	0.0117	0.00255	0.0417	0.0417	0	0
All_shell_material	21	0.0784	0.0922	0.0201	0.349	0.349	0	0.0521
Worm_evidence	21	0.0124	0.0199	0.00433	0.0677	0.0677	0	0
Patch C								
Astrangia_poculata	24	0.0258	0.066	0.0135	0.245	0.245	0	0
Balanomorpha_Barnacle	24	0.0293	0.0723	0.0148	0.328	0.328	0	0
Crepidula_fornicata_Live	24	0.00911	0.0216	0.0044	0.0677	0.0677	0	0
Hydroidolina_Cheilostomati	24	0.00846	0.0242	0.00495	0.099	0.099	0	0
Mytilus_edulis	24	0.0501	0.193	0.0393	0.911	0.911	0	0
Shell_hash	24	0.134	0.139	0.0284	0.693	0.693	0	0.112
Burrow_medium	24	0.00109	0.00434	0.000886	0.0208	0.0208	0	0
Burrow_large	24	0.00282	0.00983	0.00201	0.0417	0.0417	0	0
Shells_intact_all	24	0.0256	0.0694	0.0142	0.328	0.328	0	0
Burrows_small	24	0.0352	0.0448	0.00915	0.125	0.125	0	0.0026
Sponges_all	24	0.000434	0.00213	0.000434	0.0104	0.0104	0	0
Bivalves_Live	24	0.0501	0.193	0.0393	0.911	0.911	0	0

Species/Patch	Size	Mean	Std Dev	Std. Error	Range	Max	Min	Median
All_shell_material	24	0.16	0.205	0.0417	1.021	1.021	0	0.112
Worm_evidence	24	0.00738	0.0133	0.00271	0.0469	0.0469	0	0
Patch D								
Astrangia_poculata	226	0.000438	0.00309	0.000206	0.0365	0.0365	0	0
Balanomorpha_Barnacle	226	0.0107	0.0447	0.00297	0.38	0.38	0	0
Crepidula_forficata_Live	226	0.00744	0.0441	0.00293	0.443	0.443	0	0
Hydroidolina_Cheilostomati	226	0.000115	0.00173	0.000115	0.026	0.026	0	0
Diopatra_cuprea	226	0.000714	0.00409	0.000272	0.0521	0.0521	0	0
Ceriantheopsis_america	226	0.000161	0.00211	0.00014	0.0313	0.0313	0	0
Shell_hash	226	0.207	0.178	0.0119	0.891	0.891	0	0.172
Burrow_medium	226	0.000622	0.00333	0.000221	0.026	0.026	0	0
Burrow_large	226	0.00154	0.00647	0.00043	0.0469	0.0469	0	0
Shells_intact_all	226	0.0177	0.0449	0.00298	0.339	0.339	0	0
Burrows_small	226	0.112	0.113	0.00751	0.521	0.521	0	0.0833
Sponges_all	226	0.000323	0.00421	0.00028	0.0625	0.0625	0	0
Bivalves_Live	226	0.000023	0.00034	0.000023	0.00521	0.00521	0	0
All_shell_material	226	0.225	0.202	0.0135	0.99	0.99	0	0.174
Worm_evidence	226	0.0153	0.0308	0.00205	0.177	0.177	0	0
Patch E								
Astrangia_poculata	130	0.0427	0.11	0.00965	0.578	0.578	0	0
Balanomorpha_Barnacle	130	0.0661	0.119	0.0104	0.87	0.87	0	0.0234
Crepidula_forficata_Live	130	0.0421	0.118	0.0103	0.969	0.969	0	0
Hydroidolina_Cheilostomati	130	0.00869	0.0235	0.00206	0.208	0.208	0	0
Mytilus_edulis	130	0.0268	0.103	0.00906	0.719	0.719	0	0
Diopatra_cuprea	130	0.00208	0.00727	0.000637	0.0625	0.0625	0	0
Diadumene_leucolena	130	0.00116	0.0132	0.00116	0.151	0.151	0	0
Astrangia_poculata_dead	130	0.00288	0.0108	0.000943	0.0781	0.0781	0	0
Bryozoa_encrusting	130	0.00012	0.00137	0.00012	0.0156	0.0156	0	0
Shell_hash	130	0.414	0.234	0.0205	0.974	0.995	0.020	0.391
Burrow_medium	130	0.000441	0.0029	0.000255	0.0208	0.0208	0	0
Burrow_large	130	0.000321	0.00222	0.000195	0.0208	0.0208	0	0
Shells_intact_all	130	0.0605	0.0652	0.00572	0.276	0.276	0	0.0417
Burrows_small	130	0.0646	0.102	0.00894	0.391	0.391	0	0
Sponges_all	130	0.00212	0.00764	0.00067	0.0573	0.0573	0	0
Bivalves_Live	130	0.0269	0.103	0.00906	0.719	0.719	0	0
All_shell_material	130	0.474	0.274	0.024	1.125	1.146	0.020	0.451
Worm_evidence	130	0.00132	0.00768	0.000674	0.0625	0.0625	0	0
Patch F								
Astrangia_poculata	112	0.0456	0.0886	0.00856	0.625	0.625	0	0.0156
Balanomorpha_Barnacle	112	0.118	0.151	0.0146	0.573	0.573	0	0.0365

Species/Patch	Size	Mean	Std Dev	Std. Error	Range	Max	Min	Median
Crepidula_fornicata_Live	112	0.0765	0.124	0.012	0.547	0.547	0	0.0052
Hydroidolina_Cheilostomati	112	0.0206	0.0421	0.00407	0.271	0.271	0	0
Mytilus_edulis	112	0.00915	0.0497	0.0048	0.453	0.453	0	0
Diopatra_cuprea	112	0.0036	0.00795	0.000768	0.0417	0.0417	0	0
Ceriantheopsis_americana	112	0.000292	0.00224	0.000217	0.0208	0.0208	0	0
Diadumene_leucolena	112	0.023	0.0936	0.00905	0.547	0.547	0	0
Astrangia_poculata_dead	112	0.00326	0.0115	0.00111	0.0781	0.0781	0	0
Crassostrea_virginica	112	0.000097	0.00101	0.000097	0.0104	0.0104	0	0
Aoridae_tubes	112	0.00141	0.0146	0.00141	0.151	0.151	0	0
Bryozoa_encrusting	112	0.000097	0.00101	0.000097	0.0104	0.0104	0	0
Shell_hash	112	0.422	0.262	0.0253	0.964	0.974	0.010	0.396
Shells_intact_all	112	0.142	0.214	0.0207	1	1	0	0.0469
Burrows_small	112	0.00316	0.0153	0.00148	0.125	0.125	0	0
Sponges_all	112	0.0173	0.0724	0.007	0.625	0.625	0	0
Bivalves_Live	112	0.00954	0.0496	0.0048	0.453	0.453	0	0
All_shell_material	112	0.564	0.368	0.0356	1.5	1.51	0.010	0.5
Worm_evidence	112	0.00531	0.019	0.00183	0.13	0.13	0	0

Table 5.5-6b. Species descriptive stats by Ecognition patch type for spring 2013.

Species/Patch	Size	Mean	Std Dev	SE	Range	Max	Min	Median
Patch A								
Mytilus_edulis	33	0.0445	0.18	0.0313	0.833	0.833	0	0
Ceriantheopsis_americana	33	0.000561	0.00322	0.000561	0.0185	0.0185	0	0
Bostrichobanchus_pilularis	33	0.0828	0.0959	0.0167	0.338	0.338	0	0.037
Corymorpha_pendula	33	0.0021	0.0121	0.0021	0.0694	0.0694	0	0
Shell_hash	33	0.0614	0.124	0.0215	0.648	0.648	0	0.0139
Burrow_large	33	0.00196	0.0113	0.00196	0.0648	0.0648	0	0
Shells_intact_all	33	0.0628	0.125	0.0217	0.648	0.648	0	0.0139
Burrows_small	33	0.0132	0.0219	0.00381	0.0741	0.0741	0	0
Bivalves_Live	33	0.0453	0.18	0.0312	0.833	0.833	0	0
All_shell_material	33	0.124	0.248	0.0432	1.296	1.296	0	0.0278
Worm_evidence	33	0.00505	0.0142	0.00247	0.0648	0.0648	0	0
Patch B								
Balanomorpha_Barnacle	40	0.000926	0.00586	0.000926	0.037	0.037	0	0
Hydroidolina_Cheilostomatidae	40	0.00081	0.00512	0.00081	0.0324	0.0324	0	0
Mytilus_edulis	40	0.0745	0.255	0.0404	1	1	0	0
Ceriantheopsis_americana	40	0.00382	0.0139	0.00219	0.0648	0.0648	0	0
Bostrichobanchus_pilularis	40	0.262	0.216	0.0341	0.639	0.639	0	0.317
Corymorpha_pendula	40	0.0726	0.0755	0.0119	0.282	0.282	0	0.0718
Shell_hash	40	0.0296	0.0747	0.0118	0.463	0.463	0	0.00926
Burrow_medium	40	0.000347	0.0022	0.000347	0.0139	0.0139	0	0
Burrow_large	40	0.00382	0.0123	0.00195	0.0602	0.0602	0	0
Shells_intact_all	40	0.034	0.0953	0.0151	0.597	0.597	0	0.00926
Burrows_small	40	0.0166	0.0187	0.00296	0.0602	0.0602	0	0.0139
Bivalves_Live	40	0.075	0.255	0.0404	1	1	0	0

Species/Patch	Size	Mean	Std Dev	SE	Range	Max	Min	Median
All_shell_material	40	0.0637	0.17	0.0269	1.06	1.06	0	0.0185
Worm_evidence	40	0.00475	0.00822	0.0013	0.0324	0.0324	0	0
Patch C								
Balanomorpha_Barnacle	7	0.00132	0.0035	0.00132	0.00926	0.00926	0	0
Mytilus_edulis	7		0.367	0.139	0.972	0.972	0	0
Bostrichobranchnus_pilularis	7	0.0317	0.0449	0.017	0.111	0.111	0	0.00926
Corymorpha_pendula	7	0.00397	0.0105	0.00397	0.0278	0.0278	0	0
Aoridae_tubes	7	0.000661	0.00175	0.000661	0.00463	0.00463	0	0
Shell_hash	7	0.0304	0.0544	0.0206	0.144	0.144	0	0.00463
Burrow_medium	7	0.00265	0.007	0.00265	0.0185	0.0185	0	0
Shells_intact_all	7	0.0344	0.0579	0.0219	0.144	0.144	0	0.00463
Burrows_small	7	0.0351	0.0339	0.0128	0.0787	0.0787	0	0.0509
Bivalves_Live	7	0.139	0.367	0.139	0.972	0.972	0	0
All_shell_material	7	0.0648	0.112	0.0423	0.287	0.287	0	0.00926
Worm_evidence	7	0.00728	0.0106	0.00402	0.0278	0.0278	0	0
Patch D								
Astrangia_poculata	320	0.0000579	0.00104	0.0000579	0.0185	0.0185	0	0
Balanomorpha_Barnacle	320	0.00273	0.0123	0.000686	0.102	0.102	0	0
Crepidula_fornicata_Live	320	0.00148	0.0111	0.000618	0.139	0.139	0	0
Hydroidolina_Cheilostomatidae	320	0.0131	0.0513	0.00287	0.472	0.472	0	0
Mytilus_edulis	320	0.0026	0.0308	0.00172	0.44	0.44	0	0
Diopatra_cuprea	320	0.000463	0.00283	0.000158	0.0324	0.0324	0	0
Ceriantheopsis_americana	320	0.0126	0.024	0.00134	0.157	0.157	0	0
Bostrichobranchnus_pilularis	320	0.272	0.285	0.0159	0.903	0.903	0	0.144
Corymorpha_pendula	320	0.0667	0.0815	0.00455	0.38	0.38	0	0.037
Aoridae_tubes	320	0.0293	0.0805	0.0045	0.625	0.625	0	0
Bryozoa_encrusting	320	0.000391	0.00296	0.000166	0.037	0.037	0	0
Perophora_sp	320	0.000116	0.00151	0.0000842	0.0231	0.0231	0	0
Shell_hash	320	0.0745	0.11	0.00615	0.69	0.69	0	0.0278
Burrow_medium	320	0.0000289	0.000518	0.0000289	0.00926	0.00926	0	0
Burrow_large	320	0.000145	0.00175	0.0000979	0.0278	0.0278	0	0
Shells_intact_all	320	0.0852	0.136	0.0076	0.991	0.991	0	0.0278
Burrows_small	320	0.0506	0.0743	0.00415	0.352	0.352	0	0.0162
Sponges_all	320	0.0000956	0.00117	0.0000652	0.0185	0.0185	0	0
Bivalves_Live	320	0.0026	0.0308	0.00172	0.44	0.44	0	0
All_shell_material	320	0.16	0.245	0.0137	1.681	1.681	0	0.0556
Worm_evidence	320	0.0437	0.0506	0.00283	0.269	0.269	0	0.0324
Patch E								
Astrangia_poculata	146	0.01	0.0318	0.00263	0.204	0.204	0	0
Balanomorpha_Barnacle	146	0.0309	0.0702	0.00581	0.532	0.532	0	0
Crepidula_fornicata_Live	146	0.032	0.0984	0.00815	0.699	0.699	0	0
Hydroidolina_Cheilostomatidae	146	0.0719	0.123	0.0102	0.542	0.542	0	0
Mytilus_edulis	146	0.0616	0.194	0.0161	0.974	0.974	0	0
Diopatra_cuprea	146	0.00136	0.00519	0.00043	0.0463	0.0463	0	0
Ceriantheopsis_americana	146	0.00164	0.00896	0.000742	0.0833	0.0833	0	0
Diadumene_leucolena	146	0.00811	0.0672	0.00556	0.745	0.745	0	0
Astrangia_poculata_dead	146	0.00119	0.00622	0.000515	0.0556	0.0556	0	0
Bostrichobranchnus_pilularis	146	0.00653	0.0156	0.00129	0.102	0.102	0	0
Corymorpha_pendula	146	0.00745	0.0279	0.00231	0.222	0.222	0	0
Aoridae_tubes	146	0.0515	0.127	0.0105	0.815	0.815	0	0
Bryozoa_encrusting	146	0.0027	0.00718	0.000595	0.0324	0.0324	0	0

Species/Patch	Size	Mean	Std Dev	SE	Range	Max	Min	Median
Perophora_sp	146	0.00336	0.0192	0.00159	0.199	0.199	0	0
Ectopleura_spp	146	0.000492	0.00522	0.000432	0.0625	0.0625	0	0
Shell_hash	146	0.26	0.208	0.0172	0.815	0.815	0	0.234
Shells_intact_all	146	0.31	0.257	0.0213	1.056	1.056	0	0.292
Burrows_small	146	0.0469	0.0994	0.00822	0.454	0.454	0	0
Sponges_all	146	0.00321	0.0133	0.0011	0.115	0.115	0	0
Bivalves_Live	146	0.0624	0.194	0.0161	0.974	0.974	0	0
All_shell_material	146	0.57	0.461	0.0382	1.755	1.755	0	0.539
Worm_evidence	146	0.0196	0.0441	0.00365	0.269	0.269	0	0
Patch F								
Astrangia_poculata	84	0.0769	0.156	0.0171	0.719	0.719	0	0
Balanomorpha_Barnacle	84	0.0524	0.0976	0.0106	0.481	0.481	0	0
Crepidula_fornicata_Live	84	0.0855	0.164	0.0179	0.921	0.921	0	0.0026
Hydrodolina_Cheilostomatidae	84	0.149	0.225	0.0245	0.833	0.833	0	0.0139
Mytilus_edulis	84	0.0203	0.0741	0.00809	0.551	0.551	0	0
Diopatra_cuprea	84	0.00135	0.00548	0.000598	0.0417	0.0417	0	0
Ceriantheopsis_americana	84	0.00391	0.0145	0.00158	0.115	0.115	0	0
Diadumene_leucolena	84	0.0638	0.186	0.0203	0.745	0.745	0	0
Astrangia_poculata_dead	84	0.00109	0.00538	0.000587	0.0365	0.0365	0	0
Bostrichobranchus_pilularis	84	0.00424	0.0161	0.00175	0.116	0.116	0	0
Aoridae_tubes	84	0.0202	0.0805	0.00879	0.551	0.551	0	0
Bryozoa_encrusting	84	0.00439	0.0119	0.0013	0.0833	0.0833	0	0
Perophora_sp	84	0.0192	0.0566	0.00618	0.333	0.333	0	0
Ectopleura_spp	84	0.0046	0.0231	0.00252	0.148	0.148	0	0
Shell_hash	84	0.373	0.301	0.0328	0.979	0.979	0	0.341
Burrow_medium	84	0.00022	0.00202	0.00022	0.0185	0.0185	0	0
Shells_intact_all	84	0.413	0.34	0.0371	1.324	1.324	0	0.382
Burrows_small	84	0.00997	0.0279	0.00304	0.19	0.19	0	0
Sponges_all	84	0.018	0.0663	0.00723	0.583	0.583	0	0
Bivalves_Live	84	0.0211	0.074	0.00807	0.551	0.551	0	0
All_shell_material	84	0.785	0.633	0.0691	2.078	2.078	0	0.722
Worm_evidence	84	0.0153	0.0375	0.00409	0.208	0.208	0	0

Table 5.5-7. List of all taxa and biogenic features enumerated from seafloor imagery during fall 2012 and spring 2013 surveys with associated common name.

Taxon	Common name	Taxon	Common name
Arbacia_punctulata	Purple sea urchin	Astrangia_poculata_dead	Northern star coral
Astrangia_poculata	Northern star coral	Crassostrea_virginica	Northern oyster
Balanomorpha_Barnacle	Barnacle	Henricia_sanguinolenta	Blood star
Cancer_irroratus	Rock crab	Bostrichobranchus_pilularis	Sea squirt
Cliona_spp.	Boring sponge	Polychaeta_tentacles	Polychaete worm
Crab_Brachyura	Brachyuran crab	Corymorpha_pendula	Stalked hydroid
Crepidula_fornicata (Dead)	Common slipper shell	Aoridae_tubes	Amphipod tubes

Taxon	Common name	Taxon	Common name
Crepidula fornicata (Live)	Common slipper shell	Crustacea shrimp	Shrimp
Demospongiae_1	Sponge species 1	Aoridae amphipod	Amphipod
Pagurus spp_small	Hermit crab	Nudibranchia_1	Nudibranch species 1
Pagurus spp_large	Hermit crab	Bryozoa encrusting	
Hydroides dianthus	Carnation worm	Halichondria_sp	Sponge
Hydroidolina_Cheilostomatidae	Encrusting bryozoan	Terrestrial vegetation	
Ilyanassa trivittata (dead)	Eastern mudsnail	Worm_pink	
Libinia spp	Spider crab	Astarte_undata	Bivalve mollsc
Mercenaria shells (Dead)	Hard clam	Pycnogonida	Sea spider
Euspira spp_dead	Moon snail	Styela canopus	Rough sea squirt
Mytilus edulis	Blue mussel	Anomia spp_dead	Bivalve mollusc
Mytilus edulis (dead shell)	Blue mussel	Euspira spp	Moon snail
Ensis directus	Razor clam	Rhodophyta filamentus	Red filamentous algae
Prionotus spp.	Sea robin	Algal debris	Algae
Loligo pealeii	Longfinned squid	Perophora_sp	Sea squirt
Menidia spp_juvenile	Silverside	Pleuronectes_americanus	Winter flounder
Urophycis spp	Hake	Euspira spp_egg_case	Moon snail egg case
Stenotomus chrysops juvenile	Scup	Asterias forbesi	Forbes sea star
Centropristis striata juvenile	Black sea bass	Libinia spp_dead	Spider crab
Tautogolabrus adspersus	Cunner	Busycotypus canaliculatus	Channeled whelk
Actinopterygii_unidentified	Fish unidentified	Nudibranchia_2	Nudibranch species 2
Diopatra cuprea	Plumed worm	Ectopleura spp	Hydroid
Mud tube		Shell hash	
Worm mound		Shells intact	
Worm castings		Biogenic depression	
Carapace_fragment		Burrow_medium	
Demospongiae_2	Sponge species 2	Burrow_large	
Bivalve siphons_1		Burrow_wide	
Bivalve siphons_2		Shells intact_all	
Crassostrea virginica_dead	Northern oyster	Burrows_small	
Mud tube on surface		Gastropoda_small	Snail
Andara spp_dead	Bivalve mollusc	Mucus strands	
Astarte_undata_dead	Bivalve mollusc	Limulus polyphemus	Horseshoe crab
Ceriantheopsis americana	Burrowing anemone		
Diadumene leucolena	Ghost anemone		
Demospongiae_3	Sponge species 3		

Table 5.5-7a: Fall 2012 results of SIMPER procedure based on community composition in Ecognition patch types.

Groups F & E

Average dissimilarity = 51.86

Species	Group F Av.Abund	Group E Av.Abund	Av.Diss	Diss/SD	Contrib%	Cum.%
shell hash	0.65	0.69	9.35	1.28	18.02	18.02
Barnacles	0.3	0.18	7.66	1.27	14.78	32.8
All dead shells	0.31	0.2	7.27	1.03	14.01	46.81
Crepidula fornicata (Live)	0.2	0.11	6.04	1.05	11.66	58.46
Astrangia	0.16	0.11	5.34	0.97	10.3	68.76
Burrows - Small	0.01	0.16	5.25	0.78	10.13	78.89
Hydroids/Bryozoan	0.07	0.04	2.56	0.78	4.93	83.83
Mytilus edulis	0.01	0.05	1.8	0.35	3.48	87.3
Diadumene leucolena	0.04	0	1.37	0.24	2.64	89.94
Diopatra cuprea	0.03	0.02	1.22	0.61	2.36	92.3

Groups F & A

Average dissimilarity = 75.96

Species	Group F Av.Abund	Group A Av.Abund	Av.Diss	Diss/SD	Contrib%	Cum.%
shell hash	0.65	0.33	16.62	1.39	21.87	21.87
All dead shells	0.31	0.01	11.22	1.12	14.77	36.64
Barnacles	0.3	0	11.14	1.32	14.66	51.31
Crepidula fornicata (Live)	0.2	0	7.28	0.96	9.59	60.9
Astrangia	0.16	0	6.62	0.97	8.71	69.61
Burrows - Small	0.01	0.15	6.52	1.16	8.58	78.19
Hydroids/Bryozoan	0.07	0	2.8	0.62	3.69	81.88
Burrow - large	0	0.07	2.57	0.65	3.38	85.26
Depression in sea floor	0	0.06	2.04	0.54	2.68	87.94
Diadumene leucolena	0.04	0	1.89	0.23	2.48	90.43

Groups E & A

Average dissimilarity = 66.27

Species	Group E Av.Abund	Group A Av.Abund	Av.Diss	Diss/SD	Contrib%	Cum.%
shell hash	0.69	0.33	19.83	1.42	29.93	29.93
Burrows - Small	0.16	0.15	9.16	1.12	13.83	43.76
All dead shells	0.2	0.01	8	1.37	12.07	55.83
Barnacles	0.18	0	6.84	0.94	10.33	66.16
Astrangia	0.11	0	4.24	0.57	6.41	72.56
Crepidula fornicata (Live)	0.11	0	3.94	0.64	5.94	78.51
Burrow - large	0	0.07	2.92	0.66	4.4	82.91
Depression in sea floor	0.01	0.06	2.44	0.56	3.68	86.6
Mytilus edulis	0.05	0	2.35	0.32	3.55	90.14

Groups F & B

Average dissimilarity = 79.56

Species	Group F Av.Abund	Group B Av.Abund	Av.Diss	Diss/SD	Contrib%	Cum.%
shell hash	0.65	0.25	16.91	1.56	21.26	21.26
All dead shells	0.31	0.01	11.1	1.13	13.95	35.21

Barnacles	0.3	0	10.97	1.32	13.79	49
Burrows - Small	0.01	0.18	7.39	1.48	9.29	58.3
Crepidula fornicata (Live)	0.2	0	7.18	0.96	9.03	67.32
Astrangia	0.16	0	6.51	0.97	8.18	75.5
Depression in sea floor	0	0.09	3.41	0.59	4.28	79.79
worm castings (thin)	0.01	0.07	2.87	0.73	3.61	83.39
Hydroids/Bryozoan	0.07	0	2.76	0.63	3.47	86.86
Burrow - large	0	0.05	2.09	0.63	2.63	89.49
Diadumene leucolena	0.04	0	1.85	0.23	2.32	91.81

Groups E & B

Average dissimilarity = 70.06

Species	Group E Av.Abund	Group B Av.Abund	Av.Diss	Diss/SD	Contrib%	Cum.%
shell hash	0.69	0.25	20.56	1.69	29.35	29.35
Burrows - Small	0.16	0.18	9.12	1.23	13.02	42.37
All dead shells	0.2	0.01	7.89	1.37	11.27	53.64
Barnacles	0.18	0	6.74	0.94	9.62	63.26
Astrangia	0.11	0	4.18	0.57	5.97	69.23
Depression in sea floor	0.01	0.09	3.91	0.61	5.58	74.81
Crepidula fornicata (Live)	0.11	0	3.89	0.64	5.55	80.36
worm castings (thin)	0.01	0.07	3.07	0.7	4.38	84.74
Burrow - large	0	0.05	2.4	0.64	3.42	88.16
Mytilus edulis	0.05	0	2.31	0.32	3.3	91.46

Groups A & B

Average dissimilarity = 54.03

Species	Group A Av.Abund	Group B Av.Abund	Av.Diss	Diss/SD	Contrib%	Cum.%
shell hash	0.33	0.25	18.13	1.43	33.56	33.56
Burrows - Small	0.15	0.18	10.09	1.08	18.67	52.23
Depression in sea floor	0.06	0.09	7.61	0.78	14.09	66.31
Burrow - large	0.07	0.05	6.26	0.88	11.59	77.9
worm castings (thin)	0.02	0.07	5.29	0.76	9.8	87.7
Bivalve siphons 2	0.01	0.03	2.34	0.45	4.32	92.02

Groups F & D

Average dissimilarity = 67.72

Species	Group F Av.Abund	Group D Av.Abund	Av.Diss	Diss/SD	Contrib%	Cum.%
shell hash	0.65	0.44	12.36	1.24	18.26	18.26
Burrows - Small	0.01	0.3	10.44	1.38	15.42	33.68
Barnacles	0.3	0.04	9.68	1.28	14.3	47.98
All dead shells	0.31	0.07	9.49	1.06	14.02	62
Crepidula fornicata (Live)	0.2	0.02	6.62	0.97	9.78	71.77
Astrangia	0.16	0	5.81	0.95	8.58	80.35
worm castings (thin)	0.01	0.07	2.56	0.68	3.78	84.13
Hydroids/Bryozoan	0.07	0	2.5	0.62	3.69	87.82
Diadumene leucolena	0.04	0	1.62	0.23	2.39	90.21

Groups E & D

Average dissimilarity = 56.86

Species	Group E Av.Abund	Group D Av.Abund	Av.Diss	Diss/SD	Contrib%	Cum.%
shell hash	0.69	0.44	14.26	1.23	25.08	25.08

Burrows - Small	0.16	0.3	10.54	1.26	18.55	43.62
All dead shells	0.2	0.07	6.84	1.32	12.04	55.66
Barnacles	0.18	0.04	6.27	0.98	11.03	66.69
Crepidula fornicata (Live)	0.11	0.02	3.85	0.68	6.77	73.46
Astrangia	0.11	0	3.82	0.58	6.72	80.18
worm castings (thin)	0.01	0.07	2.69	0.65	4.74	84.92
Mytilus edulis	0.05	0	2.06	0.31	3.63	88.55
Hydroids/Bryozoan	0.04	0	1.53	0.52	2.69	91.24

Groups A & D

Average dissimilarity = 55.51

Species	Group A Av.Abund	Group D Av.Abund	Av.Diss	Diss/SD	Contrib%	Cum.%
shell hash	0.33	0.44	19.02	1.29	34.26	34.26
Burrows - Small	0.15	0.3	14.06	1.31	25.34	59.59
worm castings (thin)	0.02	0.07	4.45	0.71	8.01	67.6
Depression in sea floor	0.06	0.03	4.11	0.68	7.41	75.01
Burrow - large	0.07	0.01	4.09	0.68	7.36	82.38
All dead shells	0.01	0.07	3.74	0.68	6.74	89.12
Barnacles	0	0.04	1.55	0.4	2.8	91.92

Groups B & D

Average dissimilarity = 55.15

Species	Group B Av.Abund	Group D Av.Abund	Av.Diss	Diss/SD	Contrib%	Cum.%
shell hash	0.25	0.44	16.93	1.39	30.71	30.71
Burrows - Small	0.18	0.3	12.95	1.29	23.48	54.18
Depression in sea floor	0.09	0.03	5.82	0.71	10.56	64.74
worm castings (thin)	0.07	0.07	5.82	0.9	10.55	75.3
All dead shells	0.01	0.07	3.57	0.67	6.48	81.78
Burrow - large	0.05	0.01	3.44	0.67	6.24	88.02
Barnacles	0	0.04	1.53	0.4	2.77	90.79

Groups F & C

Average dissimilarity = 67.15

Species	Group F Av.Abund	Group C Av.Abund	Av.Diss	Diss/SD	Contrib%	Cum.%
shell hash	0.65	0.34	13.5	1.38	20.1	20.1
All dead shells	0.31	0.08	10.01	1.08	14.9	35
Barnacles	0.3	0.09	9.76	1.28	14.53	49.53
Crepidula fornicata (Live)	0.2	0.04	6.79	0.99	10.11	59.64
Astrangia	0.16	0.07	6.54	1.03	9.73	69.37
Burrows - Small	0.01	0.13	5.48	0.83	8.15	77.52
Hydroids/Bryozoan	0.07	0.03	2.98	0.71	4.44	81.96
Mytilus edulis	0.01	0.08	2.44	0.32	3.63	85.59
Diadumene leucolena	0.04	0	1.69	0.23	2.52	88.12
worm castings (thin)	0.01	0.03	1.64	0.58	2.44	90.56

Groups E & C

Average dissimilarity = 61.33

Species	Group E Av.Abund	Group C Av.Abund	Av.Diss	Diss/SD	Contrib%	Cum.%
shell hash	0.69	0.34	16.2	1.46	26.42	26.42
Burrows - Small	0.16	0.13	8.51	1.01	13.87	40.28

All dead shells	0.2	0.08	7.35	1.32	11.98	52.26
Barnacles	0.18	0.09	6.95	1.04	11.34	63.6
Astrangia	0.11	0.07	5.18	0.71	8.44	72.04
Mytilus edulis	0.05	0.08	4.18	0.42	6.82	78.86
Crepidula fornicata (Live)	0.11	0.04	4.15	0.73	6.77	85.62
Hydroids/Bryozoan	0.04	0.03	2.16	0.64	3.53	89.15
worm castings (thin)	0.01	0.03	1.65	0.55	2.69	91.84

Groups A & C

Average dissimilarity = 60.38

Species	Group A	Group C	Av.Diss	Diss/SD	Contrib%	Cum.%
	Av.Abund	Av.Abund				
shell hash	0.33	0.34	16.59	1.33	27.48	27.48
Burrows - Small	0.15	0.13	11.01	1.11	18.24	45.72
Burrow - large	0.07	0.02	4.54	0.7	7.53	53.24
Barnacles	0	0.09	4.44	0.63	7.35	60.59
All dead shells	0.01	0.08	3.96	0.63	6.56	67.15
Depression in sea floor	0.06	0.01	3.61	0.62	5.97	73.13
worm castings (thin)	0.02	0.03	3.09	0.63	5.12	78.24
Mytilus edulis	0	0.08	3.09	0.29	5.12	83.36
Astrangia	0	0.07	3.05	0.45	5.05	88.41
Crepidula fornicata (Live)	0	0.04	1.56	0.43	2.59	91

Groups B & C

Average dissimilarity = 59.62

Species	Group B	Group C	Av.Diss	Diss/SD	Contrib%	Cum.%
	Av.Abund	Av.Abund				
shell hash	0.25	0.34	12.55	1.35	21.05	21.05
Burrows - Small	0.18	0.13	10.67	1.18	17.9	38.95
Depression in sea floor	0.09	0.01	5.6	0.65	9.4	48.35
worm castings (thin)	0.07	0.03	5.1	0.83	8.56	56.9
Barnacles	0	0.09	4.35	0.63	7.3	64.2
Burrow - large	0.05	0.02	3.89	0.68	6.53	70.73
All dead shells	0.01	0.08	3.77	0.62	6.33	77.06
Mytilus edulis	0	0.08	3.04	0.29	5.11	82.16
Astrangia	0	0.07	2.99	0.45	5.02	87.18
Crepidula fornicata (Live)	0	0.04	1.54	0.43	2.58	89.76
Bivalve siphons 2	0.03	0	1.52	0.4	2.54	92.3

Groups D & C

Average dissimilarity = 56.56

Species	Group D	Group C	Av.Diss	Diss/SD	Contrib%	Cum.%
	Av.Abund	Av.Abund				
shell hash	0.44	0.34	13.88	1.23	24.54	24.54
Burrows - Small	0.3	0.13	13.4	1.27	23.69	48.22
All dead shells	0.07	0.08	5.12	0.85	9.06	57.28
Barnacles	0.04	0.09	4.63	0.73	8.18	65.46
worm castings (thin)	0.07	0.03	4.39	0.79	7.76	73.23
Astrangia	0	0.07	2.76	0.46	4.88	78.11
Mytilus edulis	0	0.08	2.75	0.29	4.86	82.97
Depression in sea floor	0.03	0.01	2.18	0.5	3.86	86.83
Crepidula fornicata (Live)	0.02	0.04	1.99	0.51	3.52	90.35

Table 5.5-7b: Spring 2013 results of SIMPER procedure based on community composition in Ecognition patch types.

Groups A & B

Average dissimilarity = 64.79

Species	Group A Av.Abund	Group B Av.Abund	Av.Diss	Diss/SD	Contrib%	Cum.%
Bostrichobranchus_pilularis	0.25	0.45	18.86	1.53	29.11	29.11
Corymorpha_pendula	0.01	0.22	10.21	1.19	15.76	44.87
Shells_intact_all	0.19	0.13	8.15	1.07	12.58	57.45
Shell_hash	0.19	0.12	7.99	1.09	12.33	69.78
Mytilus edulis	0.07	0.12	7.28	0.39	11.23	81.01
Burrows_small	0.07	0.1	5.37	1.11	8.28	89.29
Worm_castings	0.02	0.03	2.25	0.63	3.48	92.77

Groups A & D

Average dissimilarity = 63.24

Species	Group A Av.Abund	Group D Av.Abund	Av.Diss	Diss/SD	Contrib%	Cum.%
Bostrichobranchus_pilularis	0.25	0.48	15.32	1.34	24.22	24.22
Shells_intact_all	0.19	0.23	8.58	1.13	13.57	37.79
Shell_hash	0.19	0.22	8.14	1.16	12.87	50.66
Corymorpha_pendula	0.01	0.19	6.89	1.03	10.89	61.56
Burrows_small	0.07	0.16	6.09	1.08	9.63	71.19
Worm_castings	0.02	0.14	4.97	1.17	7.85	79.04
Aoridae_tubes	0	0.08	2.55	0.54	4.03	83.07
Ceriantheopsis_americana	0	0.06	2.24	0.65	3.55	86.62
Mytilus edulis	0.07	0	2.2	0.27	3.47	90.09

Groups B & D

Average dissimilarity = 59.57

Species	Group B Av.Abund	Group D Av.Abund	Av.Diss	Diss/SD	Contrib%	Cum.%
Bostrichobranchus_pilularis	0.45	0.48	15.07	1.33	25.3	25.3
Corymorpha_pendula	0.22	0.19	7.38	1.15	12.38	37.68
Shells_intact_all	0.13	0.23	6.55	1.05	10.99	48.67
Shell_hash	0.12	0.22	6.16	1.11	10.34	59.01
Burrows_small	0.1	0.16	5.07	1.17	8.52	67.53
Worm_castings	0.03	0.14	4.2	1.2	7.05	74.58
Mytilus edulis	0.12	0	4.07	0.31	6.83	81.41
Aoridae_tubes	0	0.08	2.25	0.54	3.77	85.18
Ceriantheopsis_americana	0.02	0.06	2.19	0.69	3.68	88.86
Mud_tube_on_surface	0.01	0.04	1.34	0.59	2.25	91.12

Groups A & E

Average dissimilarity = 74.72

Species	Group A Av.Abund	Group E Av.Abund	Av.Diss	Diss/SD	Contrib%	Cum.%
Shells_intact_all	0.19	0.55	15.27	1.53	20.44	20.44
Shell_hash	0.19	0.49	13.58	1.55	18.17	38.6
Bostrichobranchus_pilularis	0.25	0.04	9.57	1.06	12.81	51.41
Mytilus edulis	0.07	0.1	5.64	0.4	7.55	58.97
Burrows_small	0.07	0.12	5.45	0.77	7.29	66.26
Hydroidolina_Cheilostomatidae	0	0.17	5.39	0.75	7.21	73.47
Aoridae_tubes	0	0.12	4.05	0.53	5.42	78.89

Balanomorpha_Barnacle	0	0.1	2.82	0.69	3.77	82.66
Worm_castings	0.02	0.05	2.47	0.61	3.31	85.96
Crepidula fornicata (Live)	0	0.07	1.95	0.45	2.61	88.58
Corymorpha_pendula	0.01	0.03	1.28	0.38	1.72	90.29

Groups B & E

Average dissimilarity = 79.74

Species	Group B Av.Abund	Group E Av.Abund	Av.Diss	Diss/SD	Contrib%	Cum.%
Bostrichobranchus_pilularis	0.45	0.04	13.71	1.33	17.2	17.2
Shells_intact_all	0.13	0.55	13.52	1.67	16.96	34.16
Shell_hash	0.12	0.49	12.05	1.71	15.12	49.27
Corymorpha_pendula	0.22	0.03	6.61	1.16	8.28	57.56
Mytilus edulis	0.12	0.1	6.5	0.44	8.15	65.71
Burrows_small	0.1	0.12	4.92	0.9	6.18	71.88
Hydroidolina_Cheilostomatidae	0	0.17	4.77	0.76	5.99	77.87
Aoridae_tubes	0	0.12	3.53	0.52	4.42	82.29
Balanomorpha_Barnacle	0	0.1	2.56	0.7	3.21	85.5
Worm_castings	0.03	0.05	2.21	0.67	2.78	88.27
Crepidula fornicata (Live)	0	0.07	1.75	0.44	2.2	90.47

Groups D & E

Average dissimilarity = 71.81

Species	Group D Av.Abund	Group E Av.Abund	Av.Diss	Diss/SD	Contrib%	Cum.%
Bostrichobranchus_pilularis	0.48	0.04	12.77	1.24	17.78	17.78
Shells_intact_all	0.23	0.55	10.98	1.41	15.29	33.07
Shell_hash	0.22	0.49	9.59	1.45	13.36	46.43
Burrows_small	0.16	0.12	5.25	0.97	7.31	53.73
Corymorpha_pendula	0.19	0.03	4.93	1.03	6.87	60.6
Hydroidolina_Cheilostomatidae	0.04	0.17	4.55	0.79	6.34	66.94
Aoridae_tubes	0.08	0.12	4.18	0.69	5.82	72.76
Worm_castings	0.14	0.05	3.67	1.1	5.12	77.88
Mytilus edulis	0	0.1	3.17	0.33	4.42	82.3
Balanomorpha_Barnacle	0.01	0.1	2.42	0.72	3.37	85.67
Crepidula fornicata (Live)	0.01	0.07	1.7	0.46	2.37	88.03
Ceriantheopsis_americana	0.06	0.01	1.64	0.66	2.29	90.32

Groups A & C

Average dissimilarity = 67.62

Species	Group A Av.Abund	Group C Av.Abund	Av.Diss	Diss/SD	Contrib%	Cum.%
Bostrichobranchus_pilularis	0.25	0.12	14.01	1.24	20.72	20.72
Mytilus edulis	0.07	0.2	11.43	0.47	16.91	37.63
Shells_intact_all	0.19	0.12	11.29	1.18	16.69	54.33
Shell_hash	0.19	0.11	10.83	1.18	16.02	70.35
Burrows_small	0.07	0.14	9.64	1	14.25	84.6
Worm_castings	0.02	0.05	4.35	0.84	6.43	91.02

Groups B & C

Average dissimilarity = 72.40

Species	Group B Av.Abund	Group C Av.Abund	Av.Diss	Diss/SD	Contrib%	Cum.%
Bostrichobranchus_pilularis	0.45	0.12	19.32	1.65	26.68	26.68
Mytilus edulis	0.12	0.2	11.97	0.51	16.53	43.22

Corymorpha_pendula	0.22	0.02	9.75	1.26	13.46	56.68
Shells_intact_all	0.13	0.12	7.86	1.08	10.86	67.54
Shell_hash	0.12	0.11	7.29	1.05	10.07	77.6
Burrows_small	0.1	0.14	7.07	1.09	9.77	87.37
Worm_castings	0.03	0.05	3.34	0.86	4.61	91.98

Groups D & C

Average dissimilarity = 70.66

Species	Group D Av.Abund	Group C Av.Abund	Av.Diss	Diss/SD	Contrib%	Cum.%
Bostrichobranchus_pilularis	0.48	0.12	16.52	1.33	23.38	23.38
Shells_intact_all	0.23	0.12	8.62	1.2	12.2	35.58
Shell_hash	0.22	0.11	8.02	1.23	11.35	46.94
Burrows_small	0.16	0.14	7.14	1.11	10.11	57.04
Mytilus edulis	0	0.2	7.01	0.4	9.93	66.97
Corymorpha_pendula	0.19	0.02	6.77	1.1	9.59	76.56
Worm_castings	0.14	0.05	4.87	1.25	6.89	83.45
Aoridae_tubes	0.08	0.01	2.72	0.61	3.85	87.3
Ceriantheopsis_americana	0.06	0	2.14	0.64	3.03	90.32

Groups E & C

Average dissimilarity = 77.34

Species	Group E Av.Abund	Group C Av.Abund	Av.Diss	Diss/SD	Contrib%	Cum.%
Shells_intact_all	0.55	0.12	15.69	1.75	20.29	20.29
Shell_hash	0.49	0.11	14.05	1.81	18.16	38.46
Mytilus edulis	0.1	0.2	9.32	0.51	12.06	50.51
Burrows_small	0.12	0.14	6.99	1.04	9.04	59.55
Hydroidolina_Cheilostomatidae	0.17	0	5.31	0.75	6.87	66.42
Bostrichobranchus_pilularis	0.04	0.12	4.96	0.92	6.41	72.83
Aoridae_tubes	0.12	0.01	4.11	0.56	5.32	78.15
Worm_castings	0.05	0.05	3.15	0.82	4.07	82.22
Balanomorpha_Barnacle	0.1	0.01	3.01	0.78	3.89	86.11
Crepidula fornicata (Live)	0.07	0	1.93	0.45	2.5	88.61
Corymorpha_pendula	0.03	0.02	1.71	0.5	2.21	90.82

Groups A & F

Average dissimilarity = 80.20

Species	Group A Av.Abund	Group F Av.Abund	Av.Diss	Diss/SD	Contrib%	Cum.%
Shells_intact_all	0.19	0.66	15.76	1.5	19.65	19.65
Shell_hash	0.19	0.62	14.68	1.47	18.31	37.95
Hydroidolina_Cheilostomatidae	0	0.27	8.03	0.79	10.02	47.97
Bostrichobranchus_pilularis	0.25	0.02	7.74	1.27	9.65	57.63
Crepidula fornicata (Live)	0	0.19	5.11	0.8	6.37	64
Astrangia_poculata	0	0.16	4.19	0.61	5.22	69.22
Balanomorpha_Barnacle	0	0.14	3.63	0.78	4.53	73.75
Diadumene_leucolena	0	0.1	3.35	0.37	4.17	77.92
Mytilus edulis	0.07	0.06	3.12	0.45	3.88	81.8
Burrows_small	0.07	0.05	2.86	0.77	3.56	85.37
Worm_castings	0.02	0.06	2.42	0.59	3.01	88.38
Aoridae_tubes	0	0.05	1.99	0.34	2.49	90.86

Groups B & F

Average dissimilarity = 85.24

Species	Group B	Group F	Av.Diss	Diss/SD	Contrib%	Cum.%
	Av.Abund	Av.Abund				
Shells_intact_all	0.13	0.66	14.46	1.6	16.97	16.97
Shell_hash	0.12	0.62	13.53	1.56	15.87	32.84
Bostrichobranchnus_pilularis	0.45	0.02	11.63	1.39	13.65	46.49
Hydroidolina_Cheilostomatidae	0	0.27	7.13	0.8	8.36	54.85
Corymorpha_pendula	0.22	0	5.64	1.2	6.62	61.47
Crepidula fornicata (Live)	0	0.19	4.56	0.8	5.35	66.83
Mytilus edulis	0.12	0.06	4.21	0.43	4.94	71.76
Astrangia_poculata	0	0.16	3.75	0.61	4.4	76.17
Balanomorpha_Barnacle	0	0.14	3.29	0.78	3.85	80.02
Diadumene_leucolena	0	0.1	2.93	0.37	3.44	83.46
Burrows_small	0.1	0.05	2.86	1.03	3.35	86.81
Worm_castings	0.03	0.06	2.18	0.64	2.56	89.37
Aoridae_tubes	0	0.05	1.7	0.34	2	91.37

Groups D & F

Average dissimilarity = 77.72

Species	Group D	Group F	Av.Diss	Diss/SD	Contrib%	Cum.%
	Av.Abund	Av.Abund				
Shells_intact_all	0.23	0.66	11.99	1.43	15.43	15.43
Shell_hash	0.22	0.62	11.11	1.41	14.3	29.73
Bostrichobranchnus_pilularis	0.48	0.02	11.1	1.31	14.28	44.01
Hydroidolina_Cheilostomatidae	0.04	0.27	6.55	0.81	8.42	52.43
Corymorpha_pendula	0.19	0	4.22	1.02	5.43	57.86
Crepidula fornicata (Live)	0.01	0.19	4.17	0.79	5.37	63.23
Burrows_small	0.16	0.05	3.66	1.04	4.71	67.94
Astrangia_poculata	0	0.16	3.42	0.6	4.4	72.34
Worm_castings	0.14	0.06	3.31	1.09	4.26	76.6
Balanomorpha_Barnacle	0.01	0.14	3.05	0.8	3.92	80.53
Aoridae_tubes	0.08	0.05	2.73	0.57	3.52	84.04
Diadumene_leucolena	0	0.1	2.63	0.36	3.39	87.43
Ceriantheopsis_america	0.06	0.02	1.58	0.73	2.03	89.46
Mytilus edulis	0	0.06	1.42	0.39	1.83	91.29

Groups E & F

Average dissimilarity = 60.48

Species	Group E	Group F	Av.Diss	Diss/SD	Contrib%	Cum.%
	Av.Abund	Av.Abund				
Shells_intact_all	0.55	0.66	9.71	1.38	16.05	16.05
Shell_hash	0.49	0.62	8.77	1.36	14.49	30.54
Hydroidolina_Cheilostomatidae	0.17	0.27	6.7	0.97	11.08	41.62
Crepidula fornicata (Live)	0.07	0.19	4.34	0.88	7.18	48.8
Astrangia_poculata	0.04	0.16	3.51	0.69	5.8	54.6
Balanomorpha_Barnacle	0.1	0.14	3.46	0.98	5.72	60.32
Aoridae_tubes	0.12	0.05	3.35	0.62	5.54	65.86
Mytilus edulis	0.1	0.06	3.29	0.46	5.44	71.3
Burrows_small	0.12	0.05	3.18	0.73	5.26	76.56
Diadumene_leucolena	0.01	0.1	2.67	0.39	4.42	80.98
Worm_castings	0.05	0.06	2.17	0.69	3.59	84.57
Perophora_sp	0.01	0.05	1.45	0.44	2.4	86.97
Bostrichobranchnus_pilularis	0.04	0.02	1.28	0.56	2.11	89.08
Bryozoa_encrusting	0.02	0.03	0.8	0.6	1.33	90.41

Groups C & F

Average dissimilarity = 83.36

Species	Group C	Group F	Av.Diss	Diss/SD	Contrib%	Cum.%
	Av.Abund	Av.Abund				
Shells_intact_all	0.12	0.66	16.31	1.66	19.56	19.56
Shell_hash	0.11	0.62	15.31	1.63	18.36	37.92
Hydroidolina_Cheilostomatidae	0	0.27	7.94	0.8	9.52	47.45
Mytilus edulis	0.2	0.06	6.5	0.51	7.8	55.24
Crepidula fornicata (Live)	0	0.19	5.05	0.81	6.06	61.31
Burrows_small	0.14	0.05	4.5	1.14	5.4	66.71
Astrangia_poculata	0	0.16	4.15	0.61	4.97	71.68
Bostrichobranchus_pilularis	0.12	0.02	4	0.97	4.8	76.49
Balanomorpha_Barnacle	0.01	0.14	3.67	0.84	4.4	80.89
Diadumene_leucolena	0	0.1	3.3	0.37	3.96	84.85
Worm_castings	0.05	0.06	2.86	0.81	3.44	88.28
Aoridae_tubes	0.01	0.05	2.13	0.39	2.55	90.84

5.5.9 References

- Auster, P.J., R.J. Malatesta, S.C. LaRosala. 1995. Patterns of microhabitat utilization by mobile megafauna on the southern New England (USA) continental shelf and slope. *Marine Ecology Progress Series*. 127: 77-85.
- Auster, P.J., Malatesta, R.J. and Donaldson C.L.S. (1997) Distributional responses to small-scale habitat variability by early juvenile silver hake, *Merluccius bilinearis*. *Environmental Biology of Fishes* 50:195-200.
- Auster, P.J., Michalopoulos, C., Valentine, P.C. and Malatesta, R.J. (1998) Delineating and monitoring habitat management units in a temperate deep-water marine protected area. p. 169-185 in N.W.P. Munro and J.H.M. Willison, editors. *Linking Protected Areas with Working Landscapes, Conserving Biodiversity*. Science and Management of Protected Areas Association, Wolfville, Nova Scotia.
- Auster, P.J., Heinonen, K.B., Witharana, C. and McKee, M. (2009) A habitat classification scheme for the Long Island Sound region. Long Island Sound Study Technical Report. EPA Long Island Sound Office, Stamford, Connecticut.
- Abramoff, M.D., Magalhaes, P.J. and Ram, S.J. (2004) Image processing with ImageJ. *Biophotonics International* 11(7):36-42.
- Barnes R.S.K., Coughlan J. and Holmes N.J. (1973) A preliminary survey of the macroscopic bottom fauna of the Solent, with particular reference to *Crepidula fornicata* and *Ostrea edulis*. *Proceedings of the Malacological Society of London* 40, 253–275.
- Bell J.J. (2004) Evidence for morphology-induced sediment settlement prevention on the tubular sponge *Haliclona urceolus*. *Marine Biology* 146, 29–38.

- Bell J.J. (2007) The ecology of sponges in Lough Hyne Marine Nature Reserve (south-west Ireland): past, present and future perspectives. *Journal of the Marine Biological Association of the United Kingdom* 87, 1655–1668.
- Bell J.J., Burton M., Bullimore B., Newman P.B. and Lock K. (2006) Morphological monitoring of subtidal sponge assemblages. *Marine Ecology Progress Series* 311, 79–91.
- Chase B.C. (2002) Differences in diet of Atlantic Bluefin tuna (*Thunnus thynnus*) at five seasonal feeding grounds on the New England continental shelf. *Fisheries Bulletin* 100, 168–180.
- Clarke, K. R., and Warwick, R.M. (2001) Change in Marine Communities: an Approach to Statistical Analysis and Interpretation. PRIMER-E Ltd, Plymouth, U.K.
- CT DEEP (2011) 2011 Long Island Sound Hypoxia Season Review. *Connecticut Department of Energy and Environmental Protection*, 25 pp.
- Dijkstra J.A., Lambert W.J. and Harris L.G. (2012) Introduced species provide a novel temporal resource that facilitates native predator population growth. *Biological Invasions* DOI 10.1007/s10530-012-0339-1.
- Ellis J. and Solander D. (1786) *The natural history of many curious and common zoophytes collected from various parts of the globe*. London: Benjamin White and Son.
- Fell P.E. (1974) Diapause in the gemmules of the marine sponge *Haliclona loosanoffi* with a note on the gemmules of *Haliclona oculata*. *Biological Bulletin* 147, 333–351.
- Fell P.E. (1978) Variation in the time of annual degeneration of the estuarine sponge, *Haliclona loosanoffi*. *Estuaries* 1(4), 261–264.
- Fell P.E., Parry E.H. and Balsamo A.M. (1984) The life histories of sponges in the Mystic and Thames estuaries (Connecticut), with emphasis on larval settlement and post larval reproduction. *Journal of Experimental Marine Biology and Ecology* 78, 127–141.
- Ginn B.K. (1997) *Ecology, systematics, and feeding rate of sponges on subtidal hard substrates in Little Letite Passage, Deer Island, New Brunswick*. Masters Thesis, University of New Brunswick, Fredericton, Canada.
- Grant R.E. (1826) Notice of a New Zoophyte (*Cliona celata* Gr.) from the Firth of Forth. *Edinburgh New Philosophical Journal* 1, 78–81.
- Gray, J.S. (2000) The measurement of marine species diversity, with an application to the benthic fauna of the Norwegian continental shelf. *Journal of Experimental Marine Biology and Ecology* 250:23-49.

- Hartman W.D. (1958) Natural history of the marine sponges of southern New England. *Bulletin of the Peabody Museum Yale University* 12, 1–155.
- Houziaux J., Haelters J. and Kerckhof F. (2007) Facts from history – the former ecological value of the gravel grounds in Belgian marine waters: their importance for biodiversity and relationship with fisheries. *ICES SGBIODIV Report, Annex 4: Biodiversity science: a case study from Belgian marine waters*, 8 pp.
- Howell P. and Auster P.J. (2012) Phase shift in a estuarine finfish community associated with warming temperatures. *Marine and Coastal Fisheries: Dynamics, Management, and Ecosystem Science* 4(1), 481–495.
- Jaques T.G., Marshall N. and Pilson M.E.Q. (1983) Experimental ecology of the temperate scleractinian coral *Astrangia danae* II. *Marine Biology* 76, 135–148.
- Kaandorp J.A. (1999) Morphological analysis of growth forms of branching marine sessile organisms along environmental gradients. *Marine Biology* 134, 295–306.
- Knebel H.J. and Poppe L.J. (2000) Sea-floor environments within Long Island Sound: a regional overview. *Journal of Coastal Research* 16, 533–550.
- Kluijver M.J. de and Leewis R.J. (1994) Changes in the sublittoral hard substrate communities in the Oosterschelde estuary (SW Netherlands), caused by changes in the environmental parameters. *Hydrobiologia* 282/283, 265–280.
- Koopmans M. and Wijffels R.H. (2008) Seasonal growth rate of the sponge *Haliclona oculata* (Demospongiae: Haplosclerida). *Marine Biotechnology* 10, 502–510.
- Koopmans M., Martens D. and Wijffels R.H. (2009) Towards commercial production of sponge medicines. *Marine Drugs* 7, 787–802.
- Langton, R.W., Auster, P.J. and Schneider, D.C. (1995) A spatial and temporal perspective on research and management of groundfish in the northwest Atlantic. *Reviews in Fisheries Science* 3:201-229.
- Linnaeus C. (1758). *Systema Naturae per regna tria naturae, secundum classes, ordines, genera, species, cum characteribus, differentiis, synonymis, locis. Tomus I. Editio decima, reformata*. Holmiae: Laurentius Salvius.
- Linnaeus C. (1759). *Systema Naturae per regna tria naturae, secundum classes, ordines, genera, species, cum characteribus, differentiis, synonymis, locis. Tomus II. Editio decima, reformata*. Holmiae: Laurentius Salvius.

- Lough R.G., Valentine P.C., Potter D.C., Auditore P.J., Bolz G.R. Neilson J.D. and Perry R.I. (1989) Ecology and distribution of juvenile cod and haddock in relation to sediment type and bottom currents on eastern Georges Bank. *Marine Ecology Progress Series* 56:1-12.
- Malatesta, R.J. and Auster, P.J. (1999) The importance of habitat features in low-relief continental shelf environments. *Oceanologica Acta* 22:623-626.
- Miller A.N., Strychar K.B., Shirley T.C. and Rüzler K. (2010) Effects of heat and salinity stress on the sponge *Cliona celata*. *International Journal of Biology* 2, 3–16.
- Müller O.F. (1776) *Zoologiae Danicae prodromus: seu Animalium Daniae et Norvegiae indigenarum ; characteres, nomina, et synonyma imprimis popularium* Havniae: Typis Hallageriis.
- NASA (2013) <http://earthobservatory.nasa.gov/IOTD/view.php?id=52059&src=eorss-iotd> (downloaded 7 March 2013)
- Patrizzzi B.J. (2010) *The distribution and diet of the scleractinian coral Astrangia poculata in Long Island Sound*. Masters Thesis, Southern Connecticut State University, New Haven, USA.
- Poppe L.J., Knebel H.J., Mlodzinska Z.J., Hastings, M.E. and Seekins B.A. (2000) Distribution of surficial sediment in Long Island Sound and adjacent waters: texture and total organic carbon. *Journal of Coastal Research* 16, 567–574.
- Poppe L.J., Ackerman, S.D., Doran E.F., Beaver A.L., Crocker J.M. and Schattgen P.T. (2006) Interpolation of Reconnaissance Multibeam Bathymetry from North-Central Long Island Sound. *U.S. Geological Survey Open-File Report 2005-1145*.
- Shield C. and Witman J. (1993) The impact of *Henricia sanguinolenta* predation on the finger sponges, *Isodictya* spp. *Journal of Experimental Marine Biology and Ecology* 166, 107–133.
- USGS (2013) Waterdata <http://waterdata.usgs.gov/nwis/rt> (downlaoded 7 March 2013)
- Wang Y., Bohlen W.F. and O'donnell J. (2000) Storm enhanced bottom shear stress and associated sediment entrainment in a moderate energetic estuary. *Journal of Oceanography* 56, 311–317.
- Webster N.S. (2007) Sponge disease: a global threat? *Environmental Microbiology* 9, 1363–1375.
- Whitney M.M. (2010) A study on river discharge and salinity variability in the Middle Atlantic Bight and Long Island Sound. *Continental Shelf Research* 30, 305–318.

Wulff J.L. (2006) Ecological interactions of marine sponges. *Canadian Journal of Zoology* 84, 146–166.

Xavier J.R., Rachello-Dolmen P.G., Parra-Velandia F., Schönberg C.H.L., Breeuwer J.A.J. and van Soest R.W.M. (2010) Molecular evidence of cryptic speciation in the “cosmopolitan” excavating sponge *Cliona celata* (Porifera, Clionaidae). *Molecular Phylogenetics and Evolution* 56, 13–20.

5.6 *Integrated Ecological Characterization and Habitat Classification*

Integrating the analyses of spatial and seasonal variation of infaunal and epifaunal communities produced notable results. Of particular interest is the consistent patterns in high diversity of both infaunal and epifaunal taxa along the crest and slopes of Stratford Shoal as well as sloping environments to the southwest and southeast off the north shore of Long Island. This pattern persists using simple species richness (S) and Shannon diversity (H') across seasons (Figures 5.6-1 to 5.6-4) and despite sampling at fewer targeted blocks in the spring.

An integrated habitat map (Figure 5.6-5) links acoustic patch types to mean bottom tidal stress and the defining ecological characteristics of infauna, epifauna, and biogenic features. Notable is the faunal response to the general gradient in grain size from patch types A to F (i.e., fine to coarse) along with the concomitant gradient of increasing tidal stress. The ecological pattern here comports those characteristics of the physical environment with the shifts in the composition and diversity of infaunal taxa, the shift from short-lived to long-lived fragile (i.e., easily damaged or dislodged by minimal direct forces) epifaunal species, and the shift from burrowed sediments to high coverage patches of biogenic shell. While shell can be dispersed by storm energy and direct disturbance (e.g., mobile fishing gear), the bathymetric characteristics that are correlated with the tidal stress measures appear to mediate processes that aggregate shell debris, as long as source populations are maintained along upslope and crest environments. Tidal stress and related measures have been used to characterize and contrast ecological disturbance to human-caused impacts and patterns of resilience (e.g., Grabowski et al. 2014). Future studies may support the development of a resilience map that could be used by managers to weigh risks of particular activities (e.g., acute versus chronic stresses; Auster and Langton 1999).

It is important to acknowledge that data to characterize infaunal and epifaunal communities was collected in fundamentally different ways (i.e., grabs versus imagery). Therefore, comparisons between diversity measures for infauna and epifauna are relative. Future sampling effort should incorporate an element to better integrate epifauna with infauna for statistical comparisons, such as replicate airlift sampling of patch sizes comparable to grabs within each sampling block.

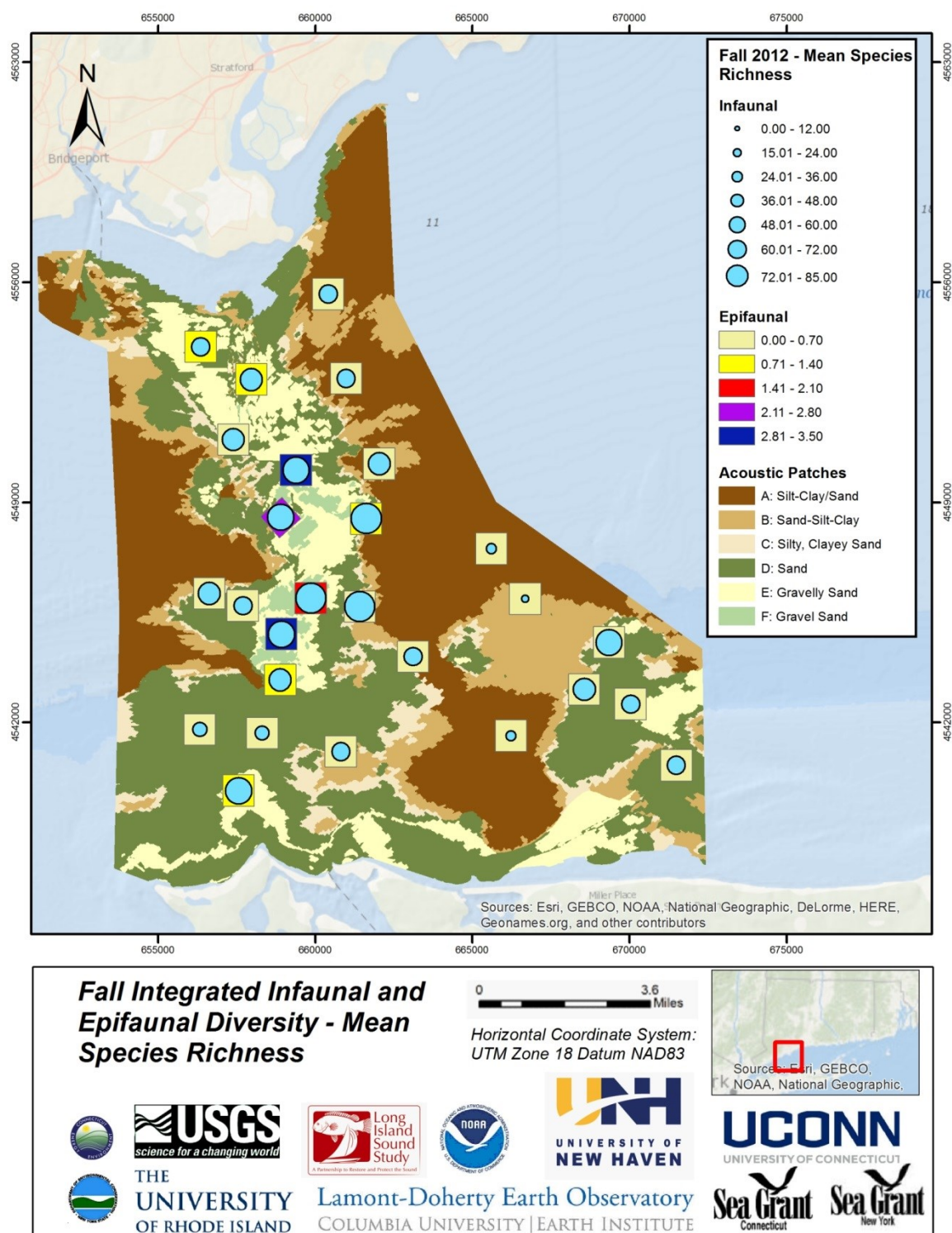


Figure 5.6-1. Integrated infaunal and epifaunal species richness map based on October 2012 samples.

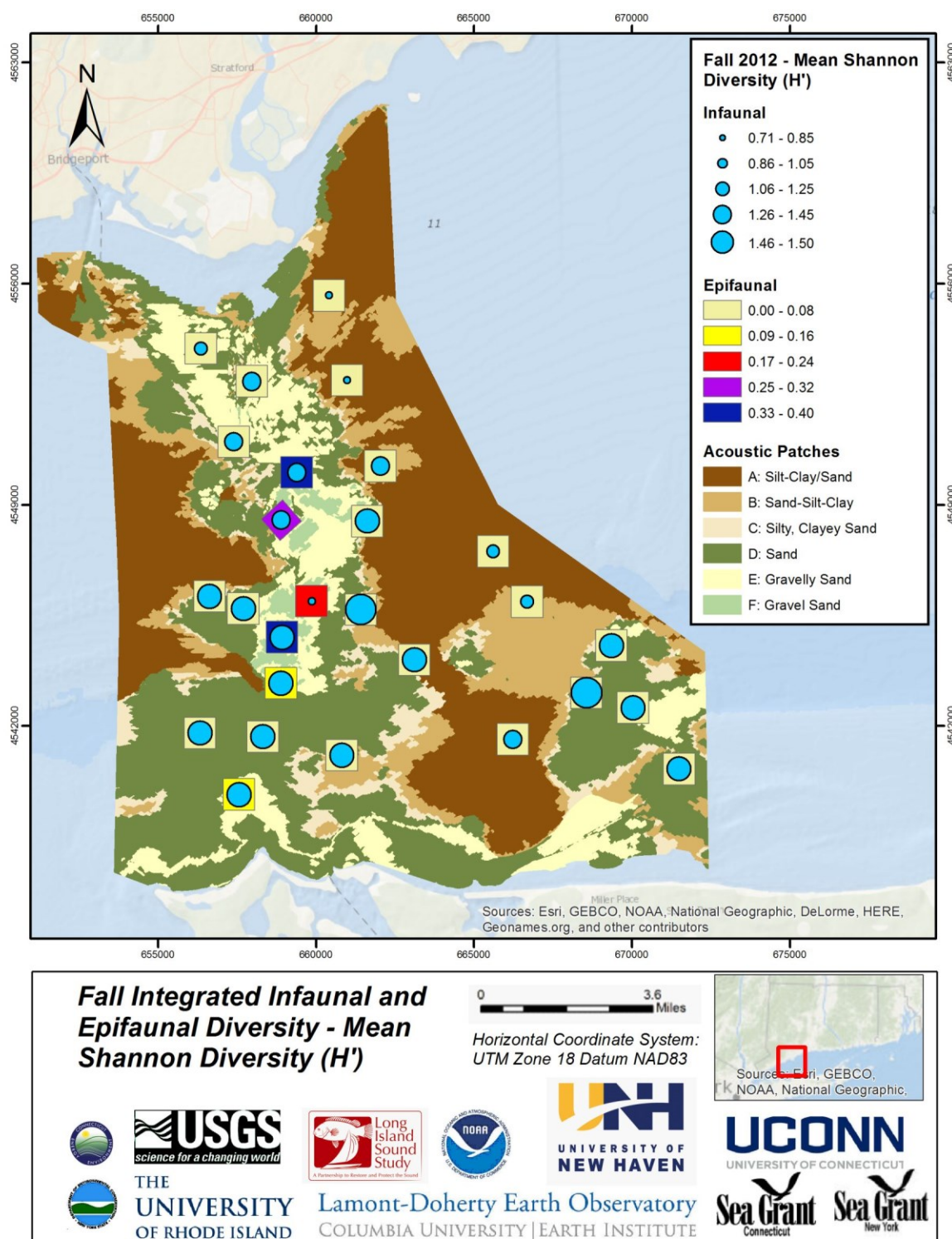


Figure 5.6-2. Integrated infaunal and epifaunal species Shannon diversity map based on October 2012 samples

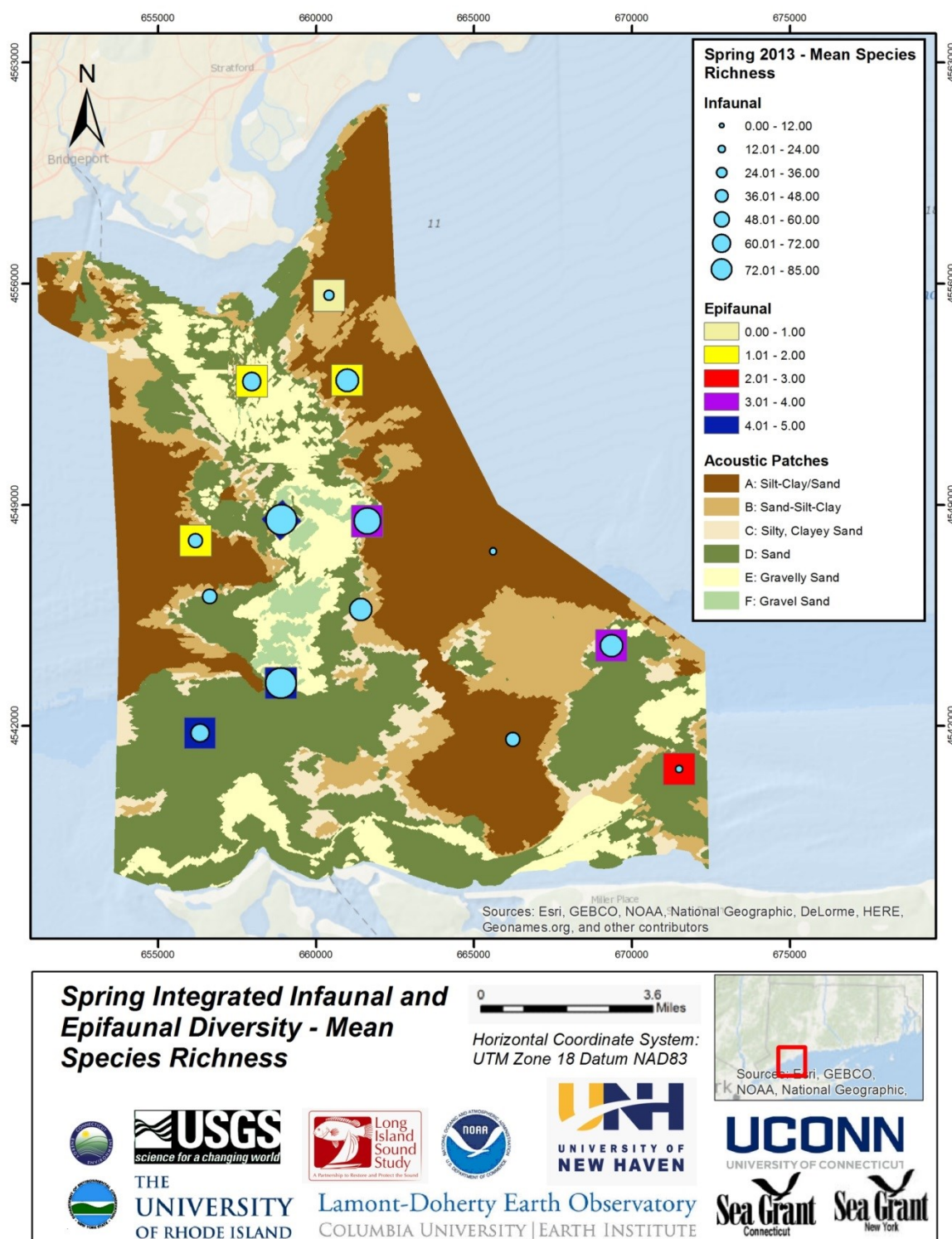


Figure 5.6-3. Integrated infaunal and epifaunal species richness map based on May 2013 samples

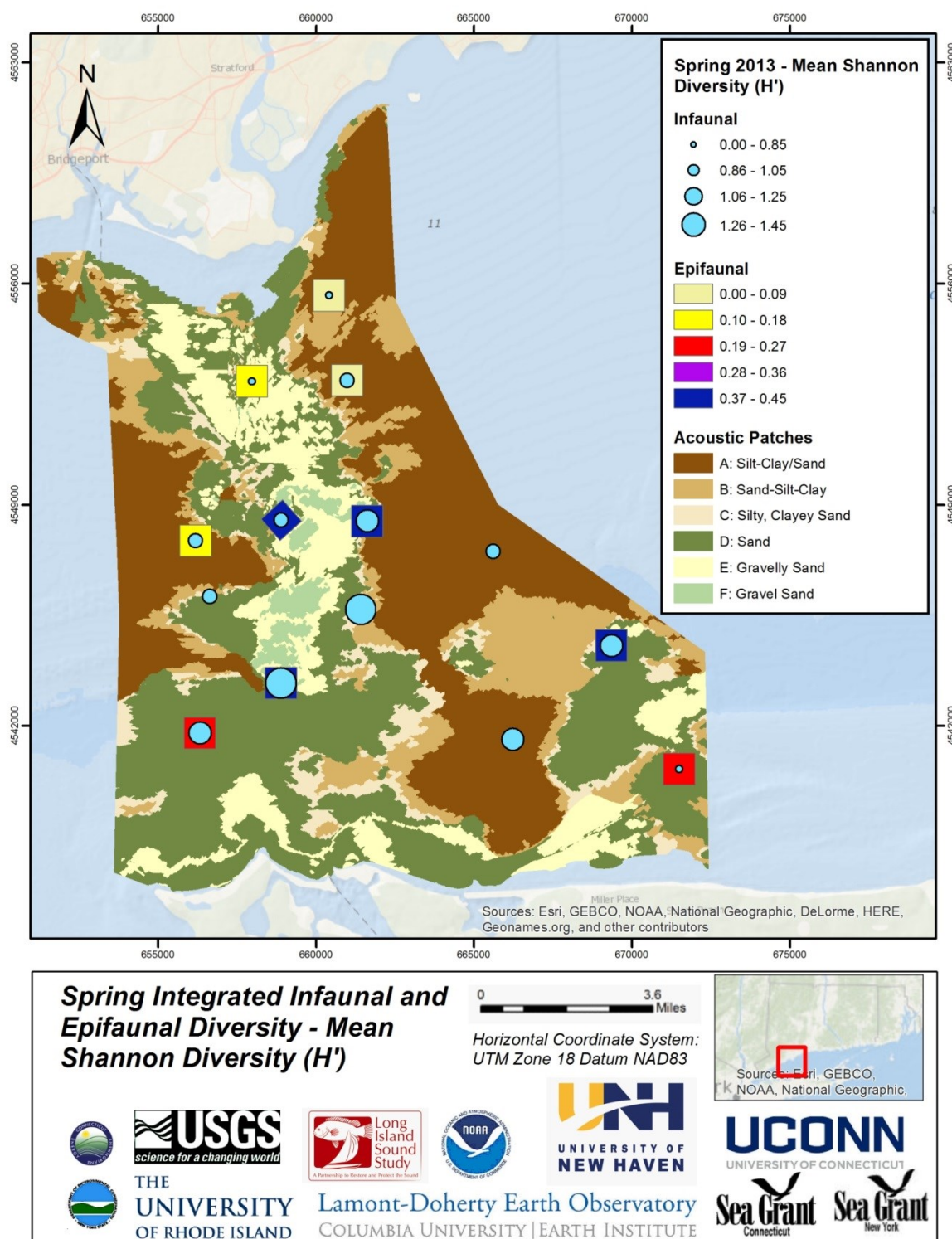
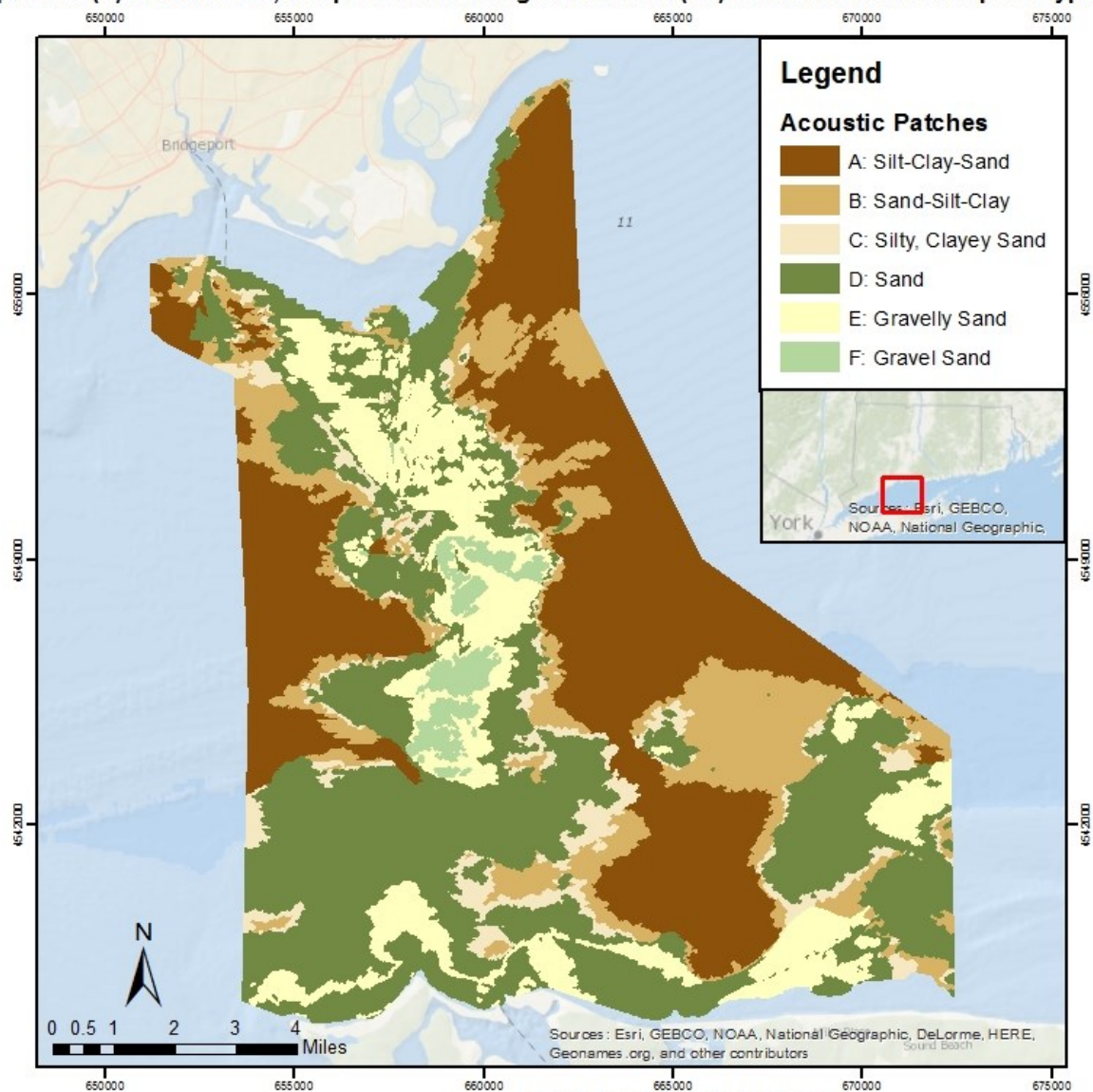


Figure 5.6-4. Integrated infaunal and epifaunal species Shannon diversity map based on May 2013 samples.

Integrated Habitat Map

Based on mean bottom tidal stress, defining ecological characteristics of infaunal (I) and epifaunal (E) communities, and predominant biogenic features (BF) in relation to acoustic patch types.



Patch type A: low-medium stress

I: Mixed burrowing and tubiculous taxa
E: Solitary ascidians, *Mytilus*
BF: Shell, burrows

Patch type B: low-high stress

I: Tubiculous taxa, motile surface feeders
E: Bivalve, *Corymorpha*, solitary ascidian
BF: Shell

Patch type C: predominantly medium stress

I: Variable mix of tubiculous taxa and burrowers
E: *Mytilus*, *Corymorpha*, solitary ascidian
BF: Burrows, shell

Patch type D: high-medium stress

I: Small tubiculous taxa (polychaetes and amphipods);
High density of bivalves
E: Hydroids, *Mytilus*, barnacle
BF: High coverage of shell patches and burrows

Patch type E: predominantly high stress

I: Oligochaetes and archiannelids, small tubiculous taxa,
deep burrowing taxa
E: Hydroids, *Mytilus*, *Astrangia*
BF: High coverage of shell patches

Patch type F: predominantly high stress

I: Oligochaetes and archiannelids, small tubiculous taxa
(polychaetes and amphipods), moderate bivalve abundances
E: *Crepidula*, *Diadumene*, *Astrangia*
BF: High coverage of shell patches

Figure 5.6-5.

6 Physical Characterization

Recommended Citations:

- O'Donnell, J., G. McCardell, and T. Fake. (2015). Objective. Section 6.1, p. 383 in: "Seafloor Mapping of Long Island Sound – Final Report: Phase 1 Pilot Project." (Unpublished project report). U. S. Environmental Protection Agency, Long Island Sound Study, Stamford, CT.
- O'Donnell, J., G. McCardell, and T. Fake. (2015). Historical Context. Section 6.2, p. 383-384 in: "Seafloor Mapping of Long Island Sound – Final Report: Phase 1 Pilot Project." (Unpublished project report). U. S. Environmental Protection Agency, Long Island Sound Study, Stamford, CT.
- O'Donnell, J., G. McCardell, and T. Fake. (2015). Physical Characterization. Section 6.3, p. 384-388 in: "Seafloor Mapping of Long Island Sound – Final Report: Phase 1 Pilot Project." (Unpublished project report). U. S. Environmental Protection Agency, Long Island Sound Study, Stamford, CT.
- O'Donnell, J., G. McCardell, and T. Fake. (2015). Physical Oceanographic Modeling. Section 6.4, p. 388-397 in: "Seafloor Mapping of Long Island Sound – Final Report: Phase 1 Pilot Project." (Unpublished project report). U. S. Environmental Protection Agency, Long Island Sound Study, Stamford, CT.
- O'Donnell, J., G. McCardell, and T. Fake. (2015). Physical Oceanographic Products. Section 6.5, p. 397-426 in: "Seafloor Mapping of Long Island Sound – Final Report: Phase 1 Pilot Project." (Unpublished project report). U. S. Environmental Protection Agency, Long Island Sound Study, Stamford, CT.
- O'Donnell, J., G. McCardell, and T. Fake. (2015). Summary and Conclusions. Section 6.6, p. 427 in: "Seafloor Mapping of Long Island Sound – Final Report: Phase 1 Pilot Project." (Unpublished project report). U. S. Environmental Protection Agency, Long Island Sound Study, Stamford, CT.

6.1 *Objective*

Long Island Sound (LIS) is a region of complex bathymetry that was created by the tectonic and glacial history of the region. The water LIS is in constant motion as a consequence of tidal forcing by the adjacent shelf waters, wind, and the density field created by fresh water delivered by rivers and uneven distributions of surface heating and vertical mixing. The dominant freshwater sources are the Connecticut and the East River. These are almost at opposite ends of the Sound and create a complicated circulation pattern.

These distribution and variability of salinity, temperature, DO, currents, and bottom stresses created by the complex interaction of geometry and forcing effects the biological communities on the bottom. Characterization of the seasonal evolution of these fields with limited resources requires the combination of observations and a model that interpolates in space and time between the measurements in a manner that is consistent with our understanding of the physical processes that determine and constrain changes. This Chapter describes the field work and the model employed to develop maps of bottom stress, temperature, and salinity in the study area.

6.2 *Historical Context*

A comprehensive review of the physical oceanography of LIS has recently been presented by O'Donnell et al. (2013) so only a short summary of previous observations and models is appropriate here.

The western end of LIS is freshened by waters originating in the Hudson River watershed that are transported through New York harbor to the East River by both natural processes and engineered water systems (sewage treatment plants). Kaputa and Olsen (2000) describe an extensive data set obtained by an ongoing survey program that allows a comprehensive view of the seasonal variation of the along-Sound and vertical structure of salinity (S), temperature (T) and density fields (σ_T) and this is summarized by O'Donnell et al. (2013). However, the lateral structure and detail within the study area is much less well resolved. There is strong evidence that the inflow of brackish water to LIS from the East River is generally found on the southern side of the Sound.

The principle tidal constituent in LIS is the M2; Swanson (1976) first described the variation of phase and amplitude of the sea level variations. More sophisticated two-dimensional numerical models were developed by Murphy (1979) and Kenefick (1985). Practical demands for predictions of the transport and fate of materials in the Sound prompted the development of three-dimensional circulation models: see Valle-Levinson and Wilson (1994a,b), Valle-Levinson et al. (1995), Schmalz et al. (1993), Blumberg et al. (1999), and Signell et al. (2000). Recently, Hao (2008) extended the study of Crowley's (2005) and Wilson et al. (2005) who implemented the ROMS model (see Shchepetkin and McWilliams, 2005) for LIS and reported the results of a comprehensive study of the dynamics of the tidal circulation.

Observations were recently acquired and analyzed by Bennett et al. (2010) that described the vertical structure of the M2 in LIS using long-term deployments of Acoustic Doppler Current Profilers (ADCPs) at 11 sites. They identified the tidal constituents that were dominant at each station and described their vertical structure. Recently, NOAA (2010) added to this data set. The available data is, however, inadequate to resolve the spatial structure of currents in the study area.

The non-tidal currents in the Sound are also difficult to measure and the data archive is limited. The three-dimensional models of Blumberg and Pritchard (1997), Crowley (2005) and Hao (2008) have provided estimates of the along-Sound volume fluxes at several across-Sound sections and recent ship survey programs by O'Donnell and Bohlen (2003), Bennett et al. (2010) and Friess et al. (2013) have provided measurements that are generally consistent with the volume flux estimate of the models. However, detailed comparisons remain to be conducted.

Wind velocity and wave height and period observations in the Sound have been measured for more than a decade at a few locations on the shoreline and at buoys. O'Donnell et al. (2013) report that the coastal site measurements of the daily mean stress magnitude are 1/3 to 1/2 of that measured at buoys. They also show that buoy observations demonstrate that at frequencies higher than approximately 1/day, the winds at the two sites have low coherence but that at lower frequencies the coherence is high. This suggests that dense local observations will be required in applications where short time-scale meteorological events are important. Model calculations that don't have realistic wind forcing should therefore only be expected to represent larger scale changes.

By examining the time series of wind stress and wave parameters during large events, and the dependence of the differences in the observations of significant wave height buoys in the eastern and western ends of the Sound, O'Donnell et al. (2013) showed the significant wave heights were sensitive to the direction of the winds. When the wind blows from the east, waves in the western Sound are similar to those in the east. But when winds blow from the west, the waves in the eastern Sound are significantly larger than those in the west. This asymmetry is consistent with the idea that waves in LIS are fetch limited as proposed by Bokuniewicz and Gordon (1980), Signell (2000), and Rivera Lemus (2008).

6.3 *Physical Characterization*

To acquire data that will allow the evaluation of a model with sufficient resolution to describe the expected variability within the study area, we executed two ship surveys in which we measured salinity, temperature, density structure and current patterns, and executed 6 deployments of a bottom tripod with an array of instruments measuring temperature, salinity, currents, and stresses.

6.3.1 Physical Oceanographic Data Collection – Time Series Observations

The moored instruments were all mounted on specially constructed tripods as shown in Figure 6.3.1.1. The location of the six tripod deployments are listed in Table 6.3.1.1 and plotted in Figure 6.3.1.2. Instrumentation on each frame included a downward looking Nortek Aquadopp HR 2Hz pulse coherent current profiler (see Figure 2) with two Campbell Scientific OBS3+ optical backscatter units, an upward-looking RDI acoustic Doppler current profiler (ADCP) with waves array sampling enabled, and a Sea-Bird Electronics Model SMP37 conductivity/temperature sensor. The base of the RDI ADCP was located 1.5 meters above-bottom and the height of the Nortek Aquadopp sensors was 0.75 meters above-bottom. The OBS3+ backscatter units were mounted at 30cm and 80 cm above-bottom.

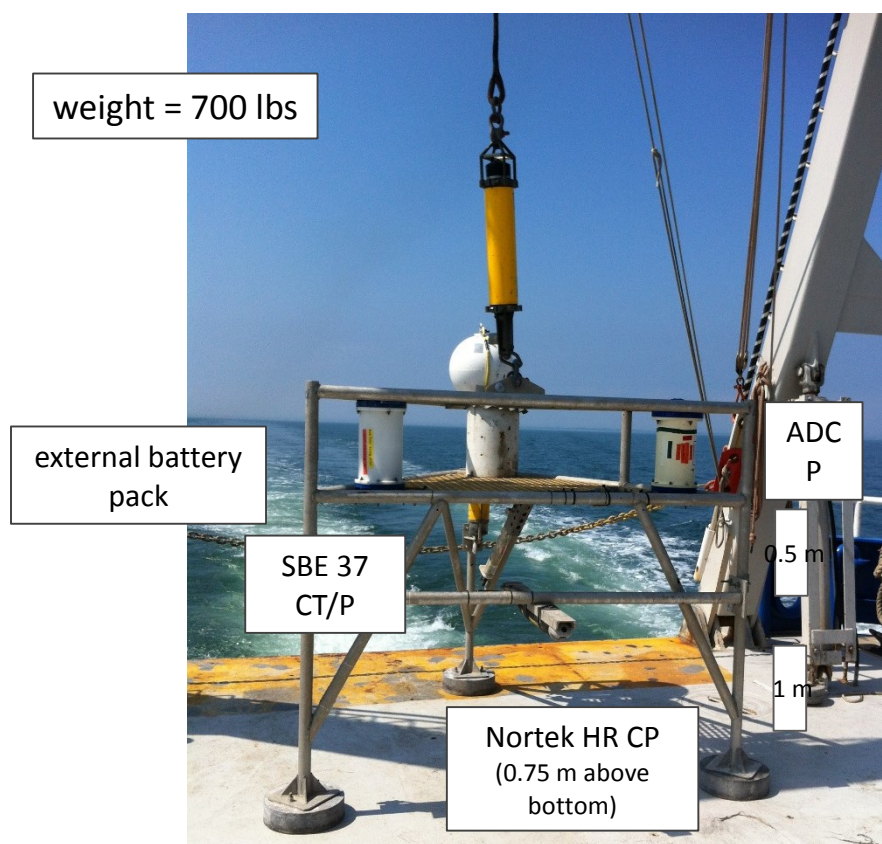


Figure 6.3.1.1. Instrument array for measuring currents and bottom stress.

Table 6.3.1.1 Instrument Deployment locations, durations, and instruments.

Location	Time Period	Duration (days)	Depth (m)	ADCP / Waves	SBE 37 CTP	AQD HR
41 06.805N, 073 04.956W	2012, Dec 7-20	13	14.6	Y	Y	Y

Location	Time Period	Duration (days)	Depth (m)	ADCP / Waves	SBE 37 CTP	AQD HR
41 05.149N, 073 04.261W	2013, Sep 18 -		34.0			
41 07.311N, 073 08.089W	2012-2013, Dec 20 - Jan 11	22	8.0	Y	Y	X
41 04.258N, 073 06.395W	2013, Jan 11-15	4	16.7	Y	Y	Y
41 03.153N, 073 05.805W	2013, Feb 26 - Apr 10	44	18.5	Y	Y	Y
40 59.759N, 073 07.571W	2013, Apr 10 - May 9	30	22.5	Y	Y	Y
41 04.267N, 073 04.588W	2013, Aug 20 - Sep 18	29	22.0	Y	Y	Y



Figure 6.3.1.2. Location of bottom tripod instrument frames deployments.

6.3.2 Physical Oceanographic Data Collection – Ship Board Observations

To complement the observations of the moored instruments, ship surveys were conducted to characterize the vertical structure of the temperature, salinity, density, and the character of the flow in the study area. The ship survey included the deployment of a profiling CTD and the continuous operation of a downward looking ADCP. On each survey cruise the stations were visited four times in each 12 hour interval. A SeaBird Electronics Model 9 CTD with a Model 11 deck unit was used for the collection of the salinity and temperature profiles.

The ship-board ADCP (RD Instruments, 600 kHz Broadband) was logged by the software VmDas (RD Instruments, Vessel Mounted Data Acquisition System) and was run continuously throughout the survey cruise. To provide the most accurate velocity estimates, the ADCP was configured to ping as fast as possible (0.3 secs/ping), with 50 1m bins. All samples were saved. The transducer depth was at 1.5 meters and the blanking distance was 0.88 meters.

6.3.3 Resulting Physical Oceanographic Data

Two survey cruises were conducted to sample salinity and temperature in the study area. Table 6.3.3.1 lists the locations of the station in the October 2012 cruise and Table 6.3.3.2 lists them for the June 2013 cruise. All data files are available through the project data system at <https://lismapping2.dms.uconn.edu> or via thredds at <http://lismapping.uconn.edu:8080/thredds/catalog.html>.

The NETCDF files are in the directory http://lismapping.uconn.edu:8080/thredds/catalog/stratford_shoals/catalog.html and named [STXXXX-3DEPLOY3SBE9_2735.nc](#) where the XXXX is replaced by the sampling block code, e.g. SB03.

Table 6.3.3.1. Station Locations for October 2012 Survey Cruise.

Polygon ID	Sampling Block	Sample #	DDM Lat	DDM Lon
1	SB-03	2	41 08.05492N	073 05.42561W
1	SB-06	6	41 06.77951N	073 04.96170W
1	SB-09	2	41 05.07053N	073 04.20707W
1	SB-10	2	41 04.91242N	073 08.05659W
1	SB-04	3	41 07.31557N	073 08.04942W
2	SB-11	1	41 04.25308N	073 06.41018W
2	SB-18	2	41 03.05745N	073 05.82326W
2	SB-25	3	41 01.50310N	073 06.81304W
2	SB-33	2	40 59.83400N	073 07.60927W
2	SB-13	3	41 04.01255N	073 08.41581W
3	SB-12	2	41 04.29056N	073 04.60809W
3	SB-15	3	41 03.66076N	073 01.87293W
3	SB-26	2	41 01.47613N	073 02.07550W
3	SB-30	1	41 00.17263N	073 05.17984W
3	SB-19	2	41 02.78168N	073 04.76100W
4	SB-20	2	41 02.77703N	073 00.99047W
4	SB-24	3	41 02.10744N	072 59.21174W
4	SB-34	3	41 00.01847N	072 57.73209W
4	SB-31	3	41 00.61058N	073 01.44413W

Table 6.3.3.2. Station Locations for June 2013 Survey Cruise.

Polygon ID	Sampling Block	Sample #	DDM Lat	DDM Lon
1	SB-03	2	41 08.05492N	073 05.42561W
1	SB-06	6	41 06.77951N	073 04.96170W
1	SB-09	2	41 05.07053N	073 04.20707W
1	SB-04	3	41 07.31557N	073 08.04942W
1	SB-18	2	41 03.05745N	073 05.82326W
1	SB-25	3	41 01.50310N	073 06.81304W
1	SB-33	2	40 59.83400N	073 07.60927W
1	SB-13	3	41 04.01255N	073 08.41581W
2	SB-12	2	41 04.29056N	073 04.60809W
2	SB-15	3	41 03.66076N	073 01.87293W
2	SB-30	1	41 00.17263N	073 05.17984W
2	SB-19	2	41 02.78168N	073 04.76100W
2	SB-20	2	41 02.77703N	073 00.99047W
2	SB-24	3	41 02.10744N	072 59.21174W
2	SB-34	3	41 00.01847N	072 57.73209W
2	SB-31	3	41 00.61058N	073 01.44413W

6.3.4 *Physical Oceanographic Analyses*

The main analysis of data that was performed was for the calculation of tidal harmonic coefficients during the testing and evaluation of the model. The approach employed was that of Pawlowicz (2002) and implemented in MATLAB. The rest of the analysis is described in the next section.

6.4 *Physical Oceanographic Modeling*

6.4.1 *The Model and Calibration*

We have employed a high resolution model of the circulation and hydrography in the LIS and BIS that was developed with support from the Connecticut Sea Grant College Program and the collaboration of Prof. C. Chen of University of Massachusetts, Dartmouth. The domain of the model and the resolution in the study area are shown in Figure 6.4.1.1. The model is an implementation of FVCOM (Chen et al., 2007) and is designed to exploit forecasts of the northwest Atlantic regional model operated as the Northeast Coastal Forecast System. This approach is computationally efficient since it allows the effect of the larger-scale processes to be simulated at coarse resolution and allows UConn's computing resources to focus on the smaller scale structures in LIS and BIS. In this section we outline the model forcing, the process of

model calibration, and the assessment of model performance by comparison to measurements collected in the study.

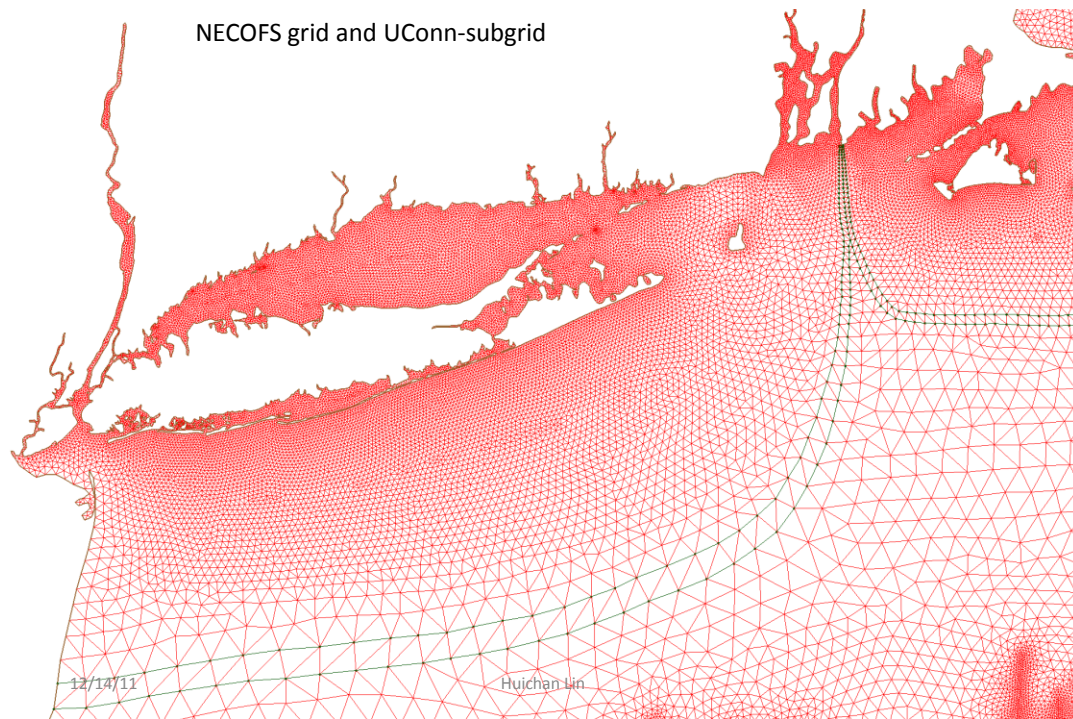


Figure 6.4.1.1. Map of southern New England shore showing the model grid (red). Blue cells show the boundary locations where the regional model NECOFS and the nested LIS-BIS sub-domain overlap.

FVCOM was initialized using a temperature and salinity climatology dataset derived via objective interpolation (OI) from CTDEEP station and offshore buoy records. This climatology has been constructed for times representing four seasons: 15 Oct, 15 Jan, 15 Apr, and 15 Jul. In order to be input into FVCOM, these OI fields are interpolated from sigma level depths to a set of standard depth levels. The standard depths were chosen as: [0. -2. -4. -6. -8. -10. -12. -15. -20. -25. -30. -40. -60. -80. -100.m]. The model simulations are started in the fall for the subsequent year in order to provide an adjustment period.

FVCOM is forced at the open boundaries by sea level variations. We employ constituents derived from the from the TOPEX model using the Foreman algorithm. These boundary conditions were then iteratively adjusted to achieve an optimal representation of the amplitude and phase at each tidal frequency using NOAA tidal height observations from 2012 at Montauk, New London, CT, New Haven, CT, Bridgeport, CT, and King's Point, NY. Each constituent amplitude was adjusted by the mean error of the relative amplitudes. The mean tidal height skill, defined as the model tidal height error normalized by the tidal height amplitude, was improved from 88% to better than 96%. Figure 6.4.1.2 show a comparison of the predicted and observed sea level variation at a NOAA ADCP near Hammonasset Point.

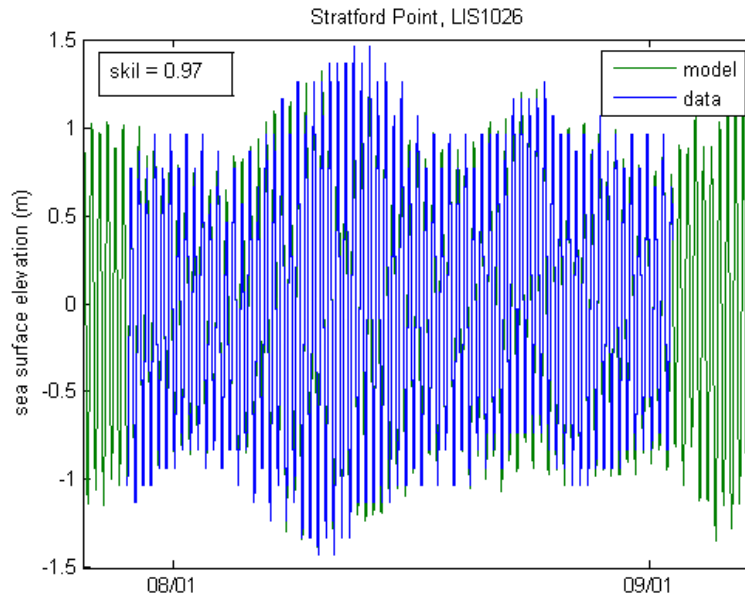


Figure 6.4.1.2. Comparison of model prediction and observation of sea level at the NOAA ADCP LIS1026.

Although the calibration procedure used tidal heights and did not involve ADCP current observations, the calibrated model captures tidal currents and tidal constituents of depth-averaged currents well. Minor differences appear where the topography is steep or the data did not cover a full spring-neap tidal cycle. Time series comparisons between field measurements and model simulations of the same time period demonstrate the model successfully predicts tidal currents. (See Fig. 6.4.1.3.)

Heat fluxes in the version of FVCOM used for these simulations are prescribed via an input file; the model makes no internal calculations of these fluxes. FVCOM can be linked to an atmospheric model and thereby calculate surface heat fluxes in a coupled ocean/ atmosphere manner, but we have not implemented this capability yet. The model is therefore sensitive to the heat fluxes imposed. Domain-uniform fluxes were derived using the WHOI/USGS air-sea toolbox, and then iteratively tuned so as to reproduce the water temperature climatology. The heat flux forcing used is thus neither year nor location specific, but replicates the annual warming and cooling cycle near Stratford Shoals well. Figure 6.4.1.4 shows a comparison of the FVCOM prediction for bottom temperature in the study area for the interval Oct 2012 - Oct 2013 and compares it to the temperatures measured by the bottom frames.

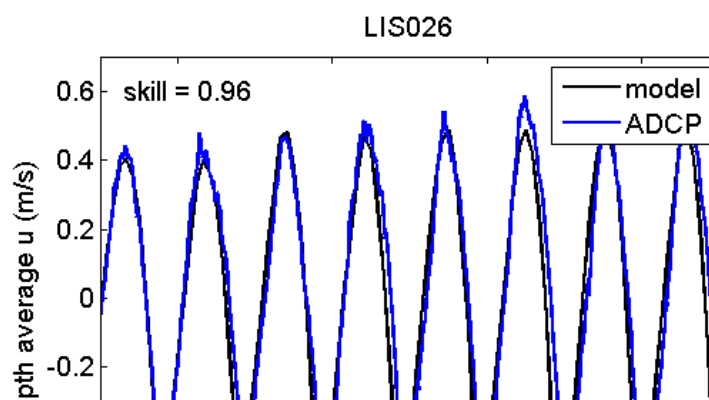


Figure 6.4.1.3 Comparison of depth-averaged currents from an ADCP deployment (blue) compared to those predicted by the FVCOM model (black).

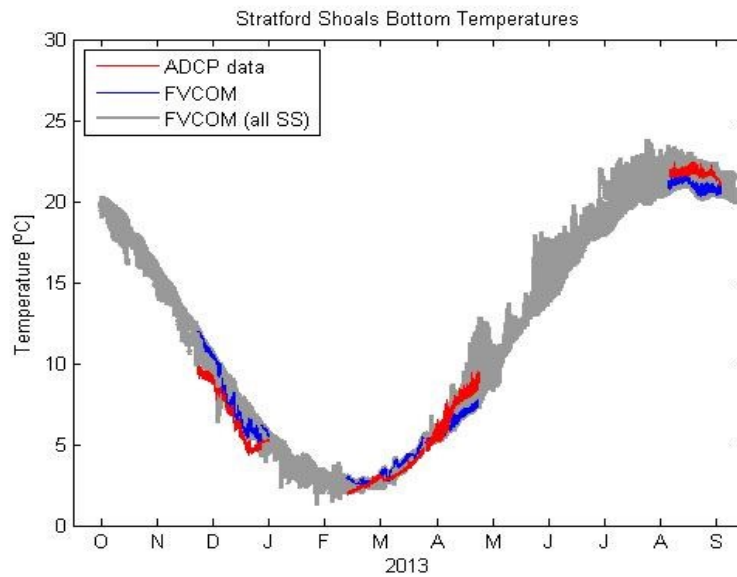


Fig. 6.4.1.4. Comparison of bottom temperatures (°C) in the FVCOM model with those measured during the six ADCP deployments at Stratford Shoals (SS). The temperatures measured by the ADCP sensors are shown in red; shown in grey are the FVCOM model solutions for the entire year at all six SS deployment sites; the FVCOM results at the individual sites for each deployment period are shown in blue. Based on these six data sets, the overall model skill with respect to bottom temperatures in this region is 98%.

Freshwater is input into the LIS FVCOM domain at 5 points corresponding to the locations of the Rivers Thames, Niantic, Quinnipiac, Housatonic, and Hudson rivers. The fluxes are based on gauged flows measured by USGS increased by 20% to account for below-gauge watershed. The gauged flows Thompsonville are lagged by one day to account for the distance between the gauge and the head of the Connecticut River in our model. The flux for each river is calculated proportionate to its mean flow using the Thompsonville data. An additional fixed input of $40 \text{ m}^3\text{s}^{-1}$ was added to the East River to represent the freshwater fluxes from the Bronx River and

New York City Sewage Treatment Plants. Fig.6.4.1.5 shows a comparison of the model salinity in the western LIS at the LISICOS ARTG buoy location (near CTDEEP station E1) with climatology derived from the CTDEEP surveys and with the 2013 buoy measurements. Note that the model results is able to reproduce not only the mean annual cycle (as shown in green), but is able to closely match the individual year data (shown in blue).

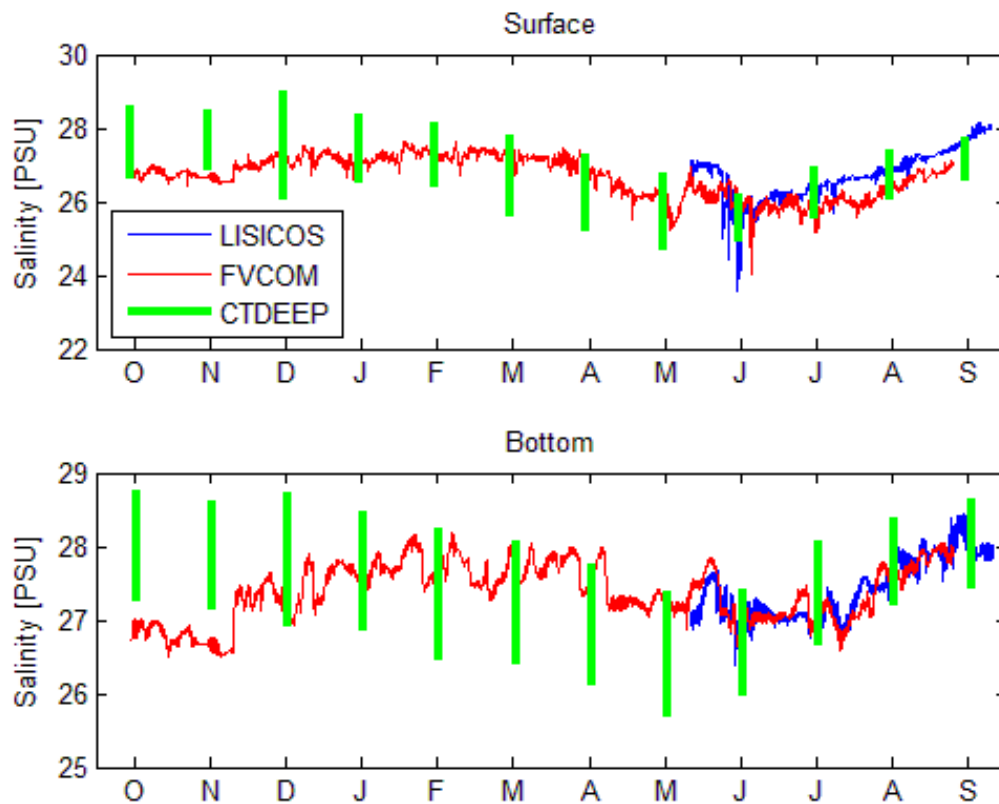


Fig.6.4.1.5. 2012-2013 salinity at ARTG/ E1 for the near surface (top panel) and near-bottom (bottom panel). The FVCOM model predictions are shown in red. Shown by the green bars are the means \pm one standard deviation of the CTDEEP data at station E1 binned by month for 1993-2012. Shown in blue are the salinities measured by the LISICOS ARTG buoy for water year 2013.

The model is forced with domain-uniform winds obtained from the LISICOS Western Sound Buoy. Because FVCOM inputs are expected to be 10 m wind speeds, while the buoy winds are measured at 3.5 m, the wind speeds in the buoy record were converted to W_{10} values using “law of the wall” with $z_0=0.01$ m. Gaps in the buoy record were then filled in using W_{10} data from Bridgeport/ Sikorsky airport (BDR). Because of the disparity in the observational locations, contemporaneous data from both the buoy and BDR were regressed using a total least squares methodology and the regression results were applied to the BDR data for those periods where the buoy data was missing. Fig. 6.4.1.6 shows a comparison of the subtidal bed stresses predicted by

the model during two wind events in 2013 with those calculated from the ADCP deployment data.

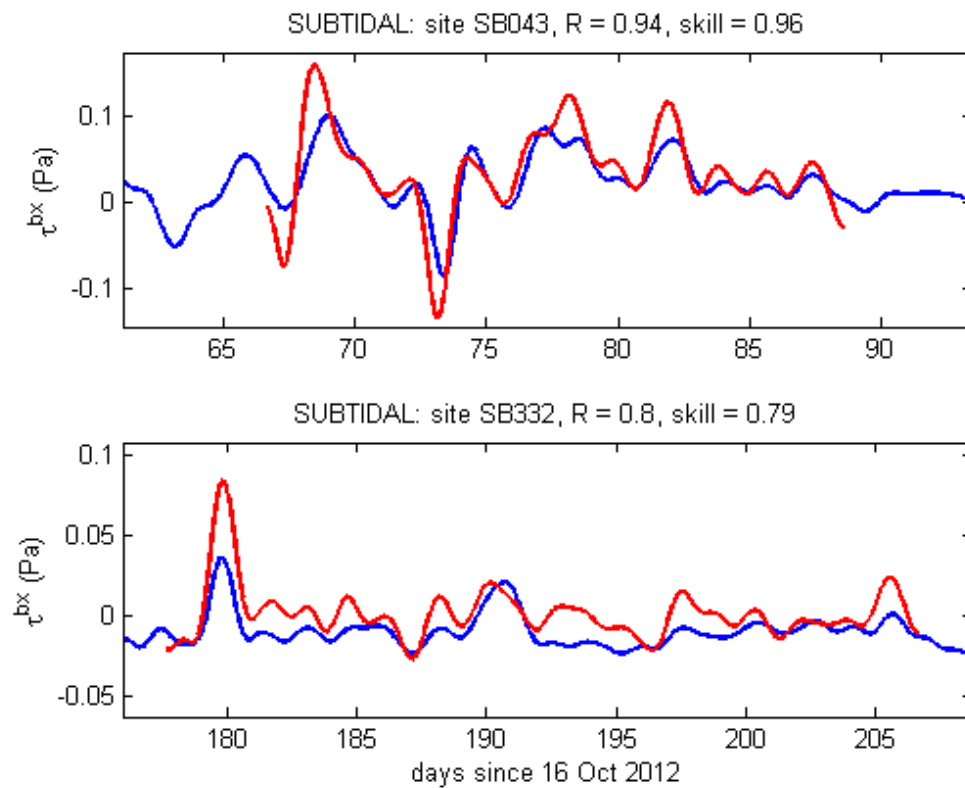


Fig. 6.4.1.6. Subtidal bottom stresses calculated from ADCP records (red) using the SB043 (top) and SB332 deployment data compared with those calculated from the FVCOM model predictions (blue) during wind events (wind speed $> 15 \text{ m s}^{-1}$).

6.4.2 Simulations of the Stratford Shoals Area

To evaluate the performance of the model in the prediction of currents and stress in the study area, in Figure 6.4.2.1 we compare the M2 tidal current ellipses for the vertically averaged flow computed from the data acquired by the moored RDI ADCPs, to that estimated from the model. These ellipses show the results of a harmonic analysis of the primary tidal current component and indicate the magnitude and direction of the semi-diurnal M2 tide. Note that the northern (SB043) and southern (SB332) most deployments are in excellent agreement with the observation-based ellipses and that the discrepancies in direction and amplitude are slightly larger at the stations in the regions of the most complex bathymetry.

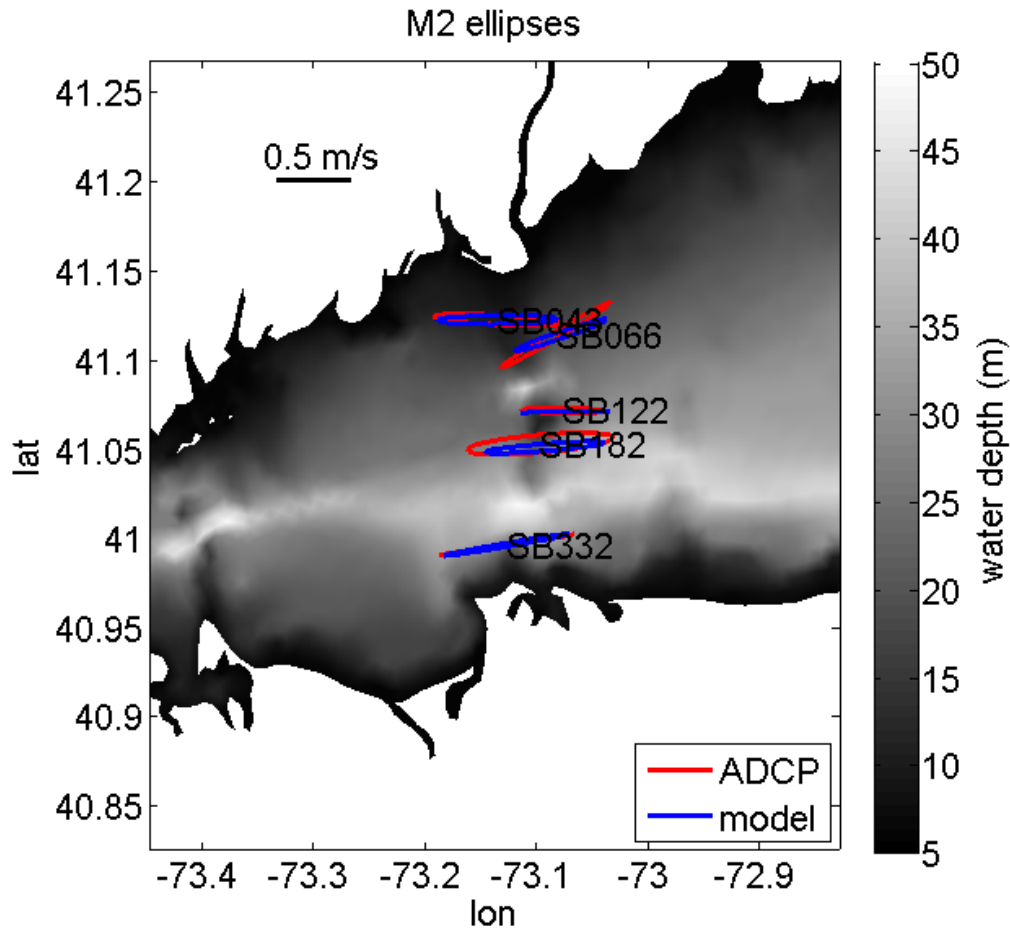


Figure 6.4.2.1. M2 ellipses for depth-average velocities from ADCP measurements (red) and FVCOM model (blue) at 5 sites on Stratford Shoals. ADCP deployments ranged from 13-44 days duration in the summer of 2013. Model ran from fall 2012 to fall 2013. The grey shading represents mean water depth.

Perhaps the most ecologically relevant parameter after temperature is the bottom stress. In Figure 6.4.2.2 we compare the model's estimate of the near bottom stress at the semi-diurnal M2 frequency to that estimated by the moored instruments. The agreement at the northern and southern boundaries of the study area are within 10%, however, in the center the error is closer to 20%. This is clearer in Figure 6.4.2.3 which shows a comparison of the time series of the stress components in the principle axis directions. Their scale is chosen to clarify the intra-tidal variations. Stress magnitudes vary from $\pm 0.5\text{Pa}$ at the northern station and by substantially less at the central stations. The model resolves this spatial structure well. Skills are all over 90% and correlations vary from 80 to 92%. It is, however, clear that the model is underestimating tidal peak currents, and is failing to fully capture the higher frequency tidal components.

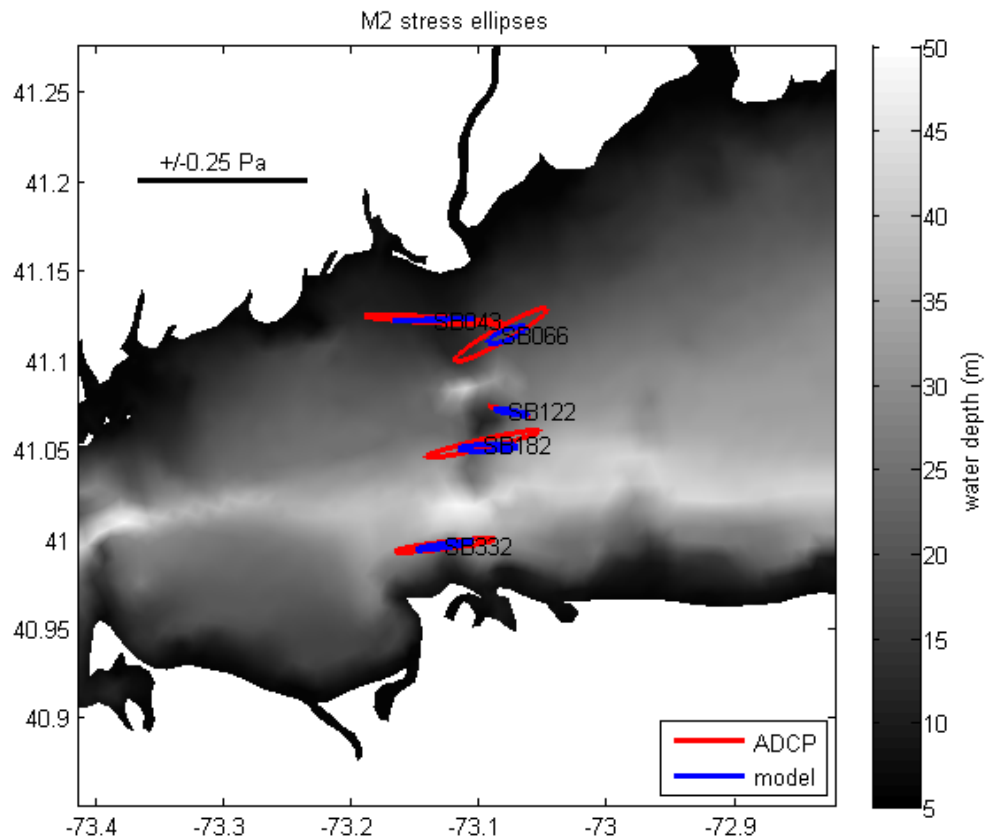


Figure 6.4.2.2 M2 ellipses for bottom stresses, calculated from lowest ADCP velocity measurement (red) and FVCOM model at similar elevation (blue) at 5 sites on Stratford Shoals. ADCP deployments ranged from 13-44 days duration in the summer of 2013. Model ran from fall 2012 to fall 2013.

The performance of the model in simulation of the longer term evolution of the bottom stress is demonstrated in previous Figure 6.4.1.6 which compares the low pass filtered observation and predictions at SB043 (northern station) and SB332 (southern station) during times when the wind was strong (greater than 15 m/s). The results are very good in that the correlations are high and the magnitude as very close. There appears to be a slight low bias in the southern station.

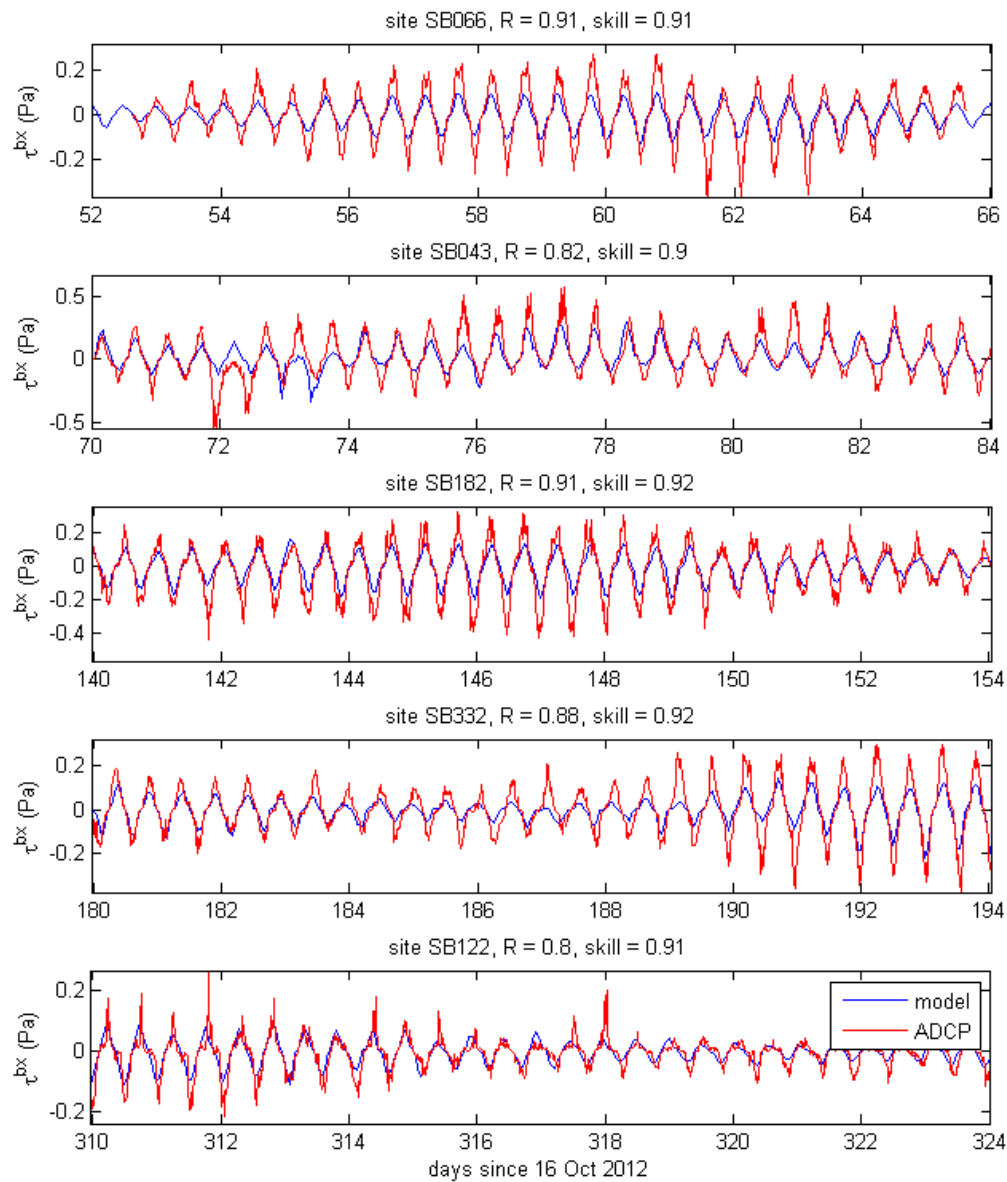


Figure 6.4.2.3. Time series of bottom stresses (by model-day) at 5 sites on Stratford Shoals from the summer of 2013 calculated from ADCP (red) and FVCOM model (blue) velocity data.

6.4.3 Model Performance Summary

The comparison of the model simulations to temperature, salinity, current and bottom stress measurements all show excellent agreement. In the study region, model temperatures were generally within $\pm 1^{\circ}\text{C}$ of measured values, salinities within ± 0.25 ppt, and stresses within $\pm 30\%$. Note, however, that the estimation of stresses through measurements is also imprecise and that

discrepancies between predictions and observations in the stresses may arise from the model's underestimation (or inability to represent) higher frequency and finer scale motions. This issue could be improved upon by running a higher resolution model in a particular area of interest. The spatial and temporal structures of the temperature, salinity, and stress fields captured by the model show excellent agreement with the field studies and this clearly support the model's use as a tool to interpolate spatially between the observations for the purpose of making maps of the characteristics of the bottom environment that are ecologically important.

6.5 *Physical Oceanographic Products*

The model is used to produce maps of:

1. the bottom temperature distributions throughout the study area for each month
2. the bottom salinity distributions throughout the study area for each month
3. the spatial structure of the maximum bottom stress magnitude due to (mainly) tidal currents
4. the spatial structure of the mean bottom stress magnitude due to (mainly) tidal currents
5. the spatial structure of the maximum bottom stress magnitude during a simulation of super Storm Sandy
6. the spatial structure of the maximum bottom stress magnitude during the entire simulation period excluding those during super Storm Sandy

These fields were contoured and transferred to the map server to distribute the results. Products are best viewed through that interface.

Though there is no data with which to evaluate the predictions, the model allows the estimation of the bottom stress at the bottom during a severe storm like Sandy. Figure 6.5.1 shows the distribution of the maximum magnitude of the stress. Largest values exceed 1.5 Pa and appear over the shoals near the mouth of the Housatonic River. Figure 6.5.2 shows the distribution of the near bottom currents in the study area viewed in GoogleEarth with a dynamic slider that allows the evolution of the current pattern to be visualized. Figures 6.5.3 – 6.5.29 depict monthly mean values for bottom temperature (degrees Celsius), bottom salinity (parts per thousand), and maximum bottom stress (pascals.)

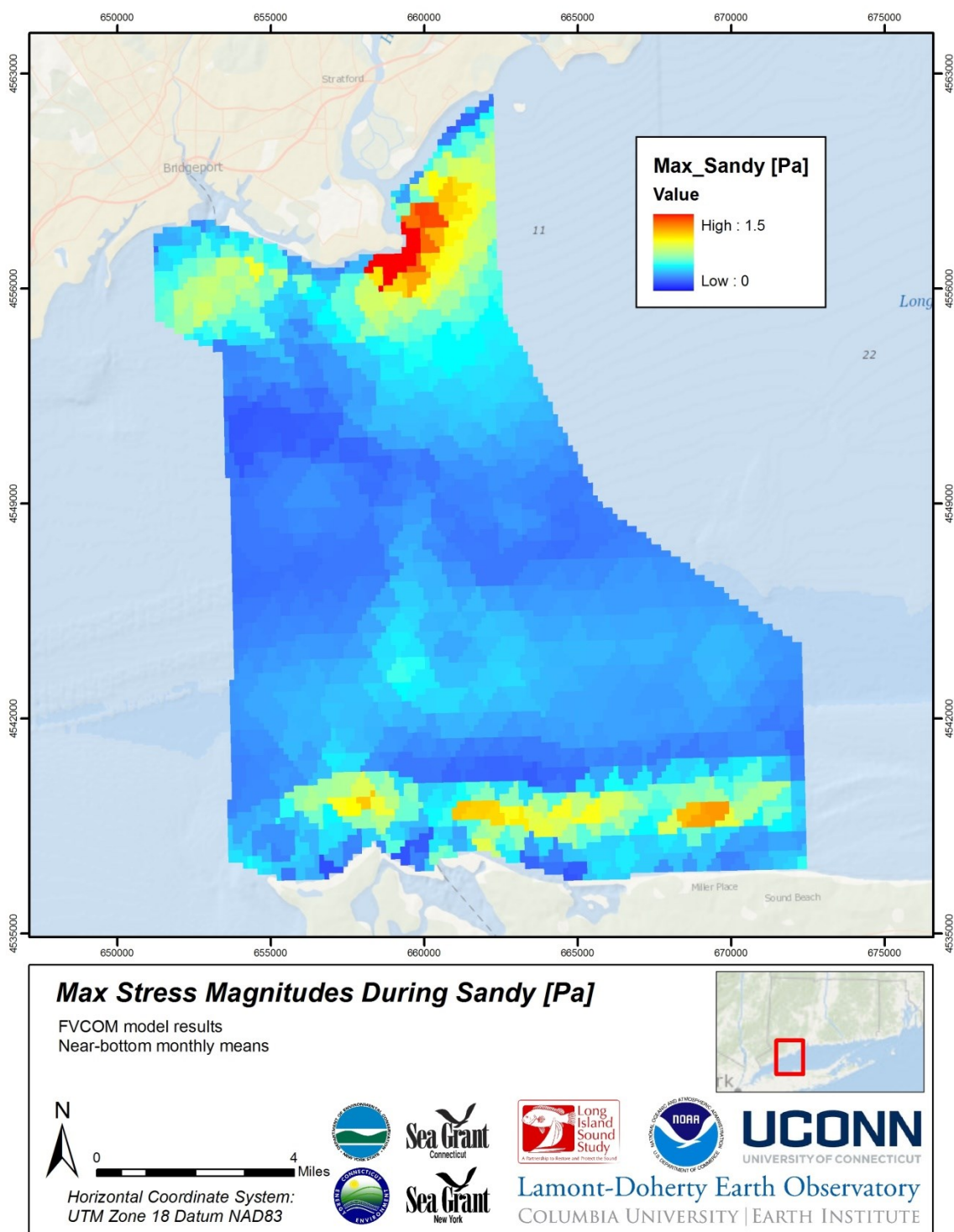


Figure 6.5.1. Map product showing maximum bottom stress magnitude computed during a simulation of Super Storm Sandy. Maximum stress is found over the shallow areas.

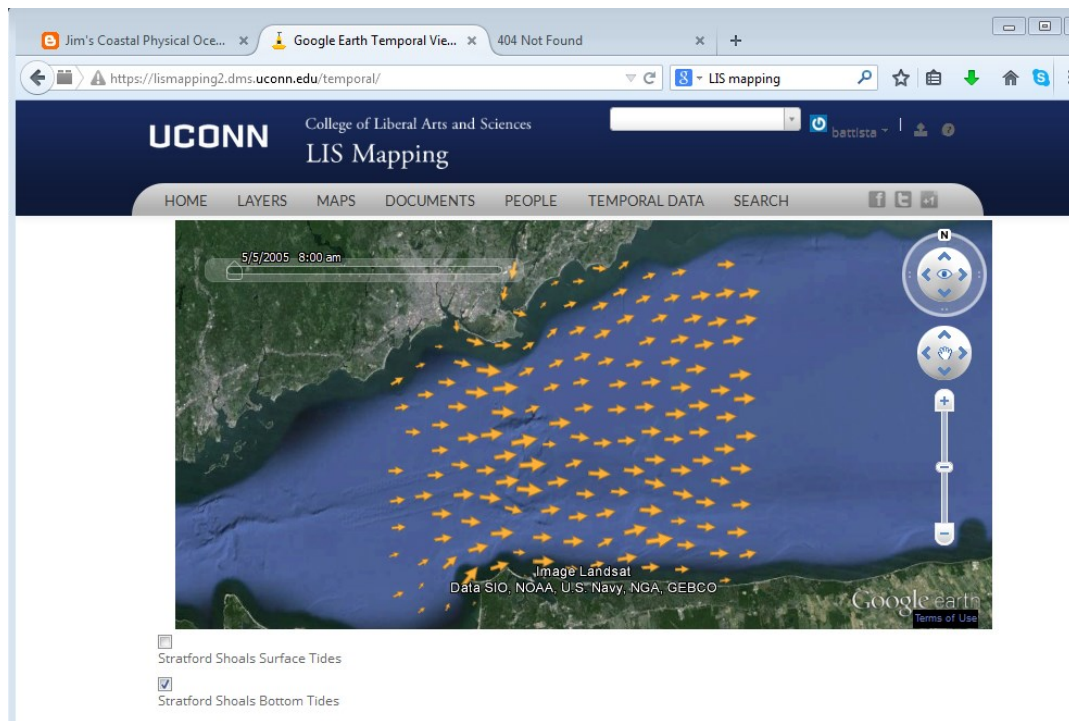


Figure 6.5.2. The on-line display of the evolution of the model current distribution.

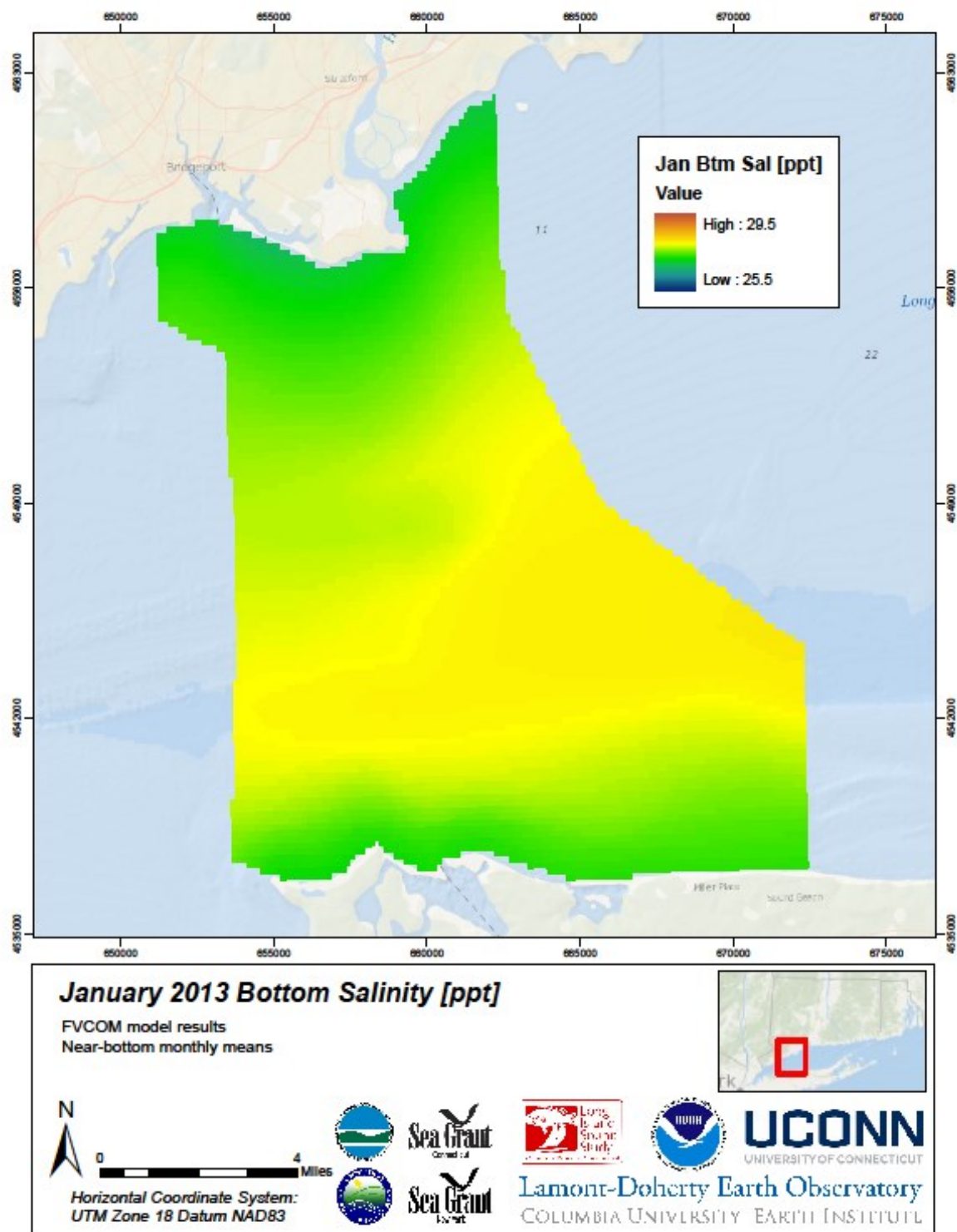


Figure 6.5.3

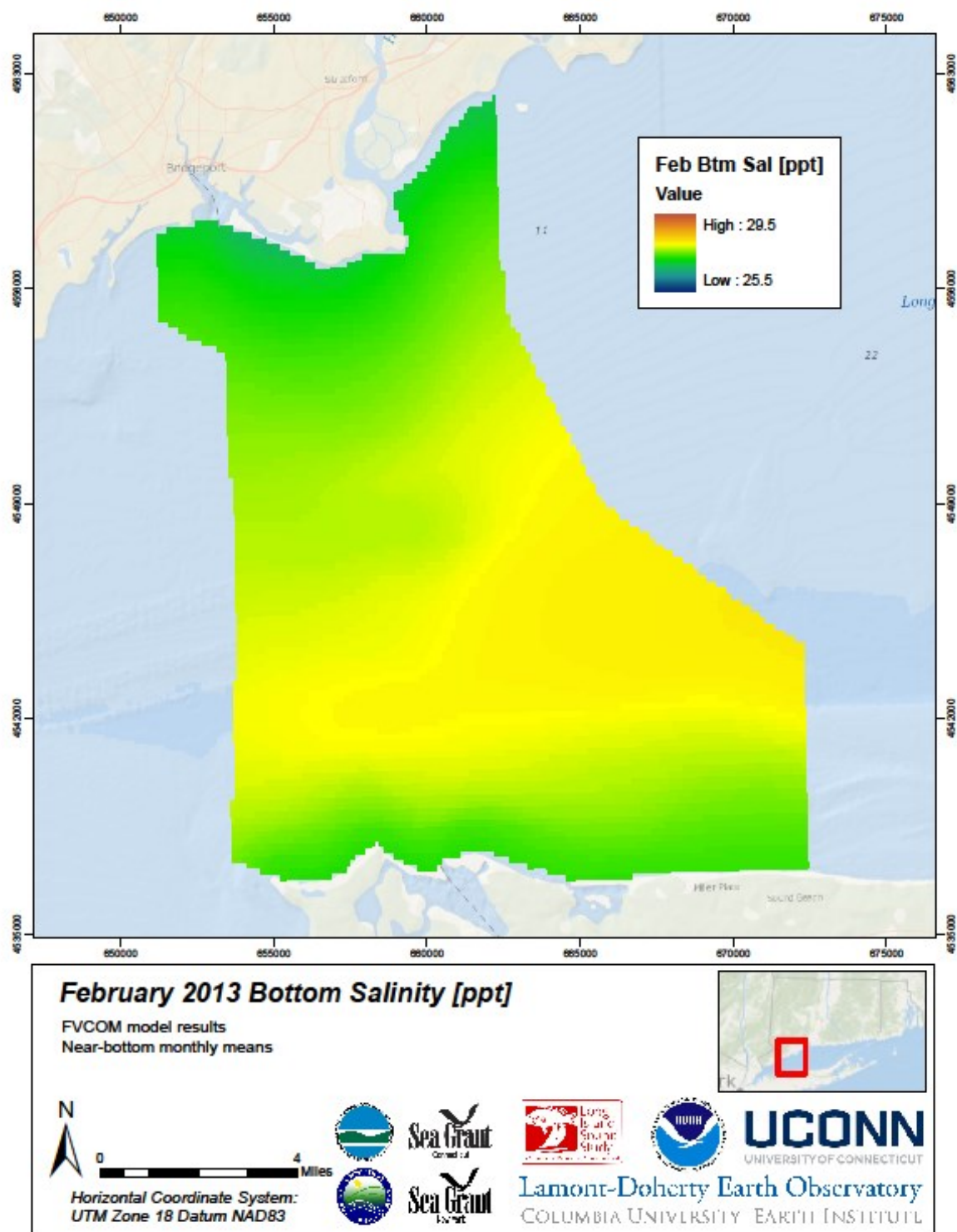


Figure 6.5.4

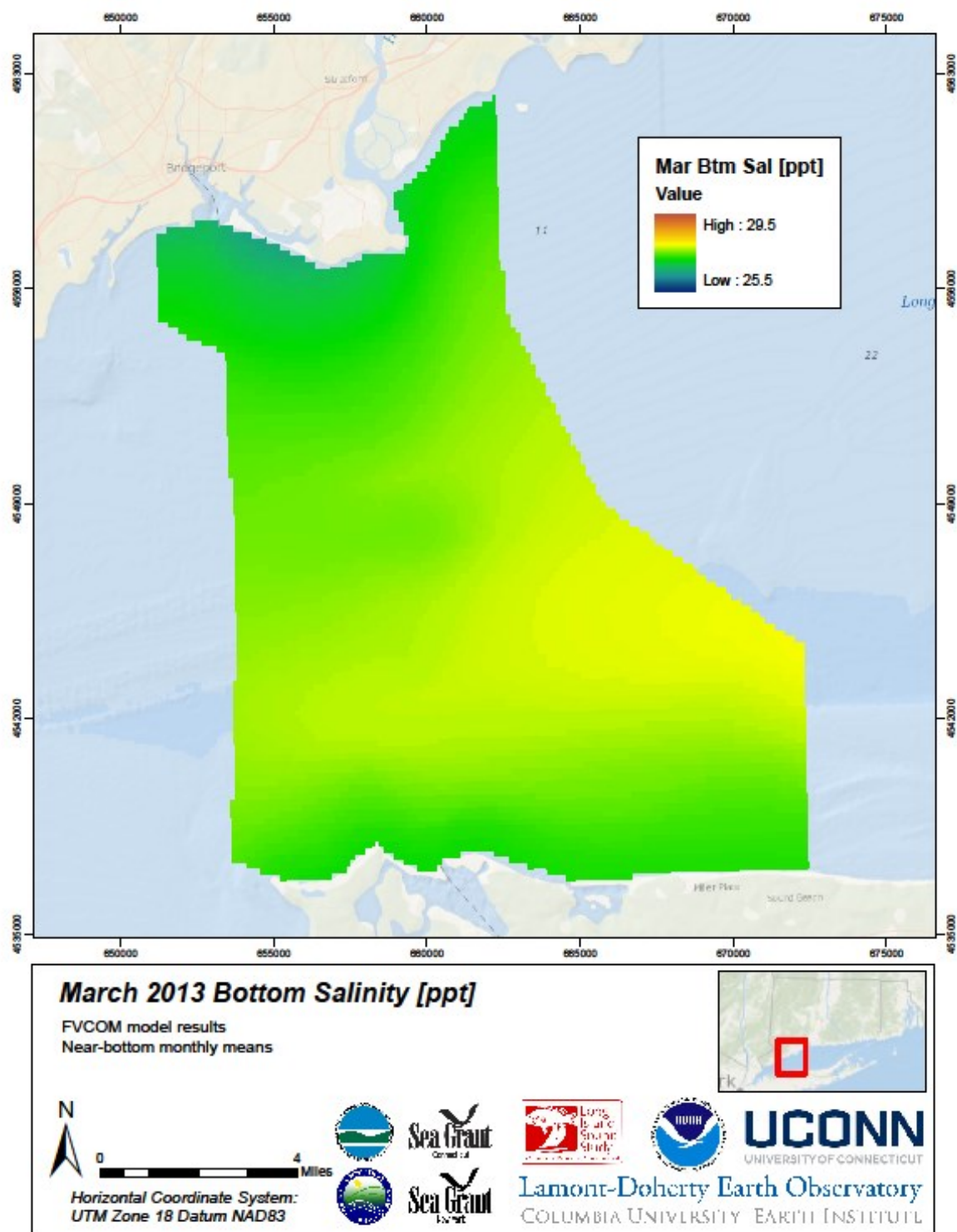


Figure 6.5.5

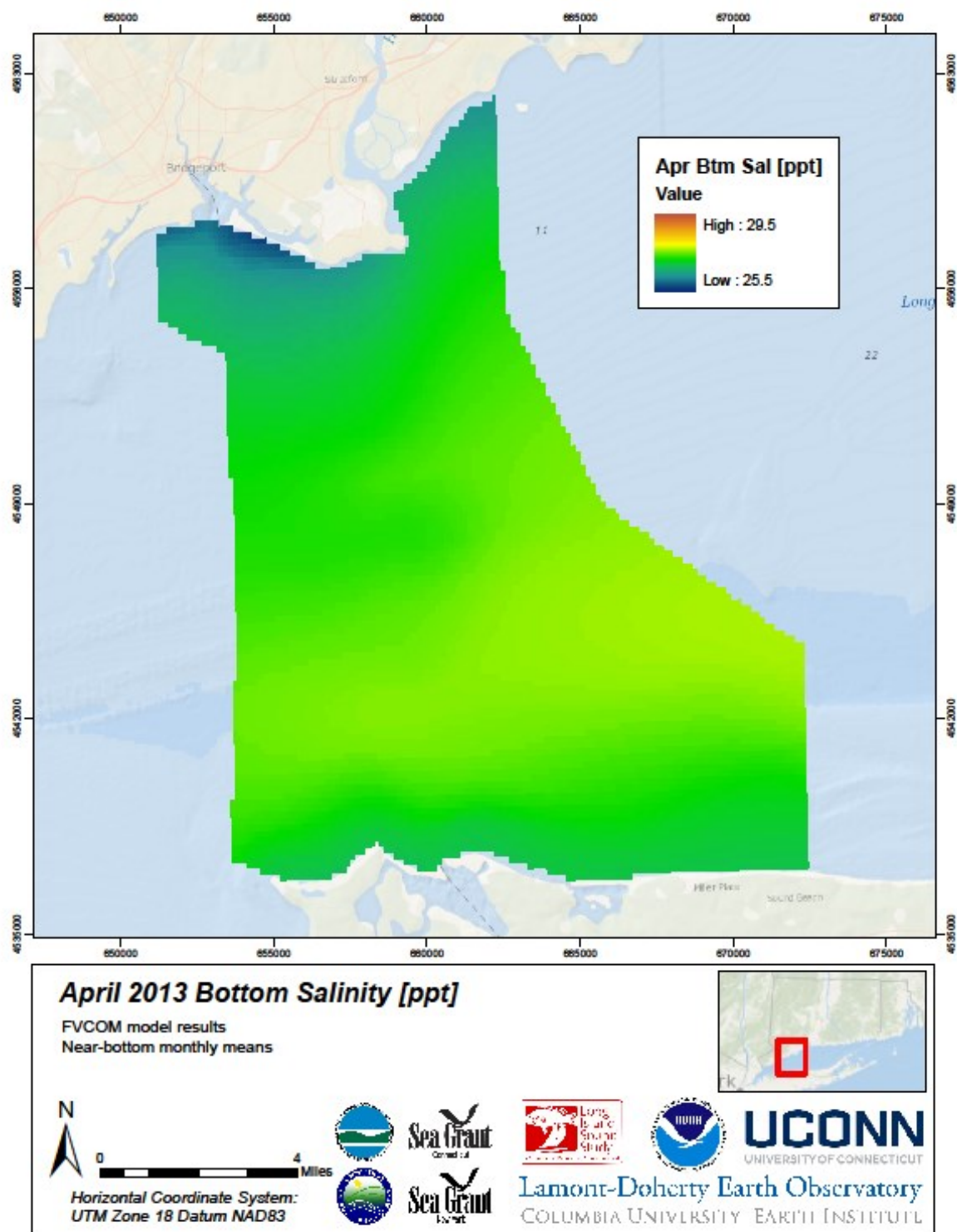


Figure 6.5.6

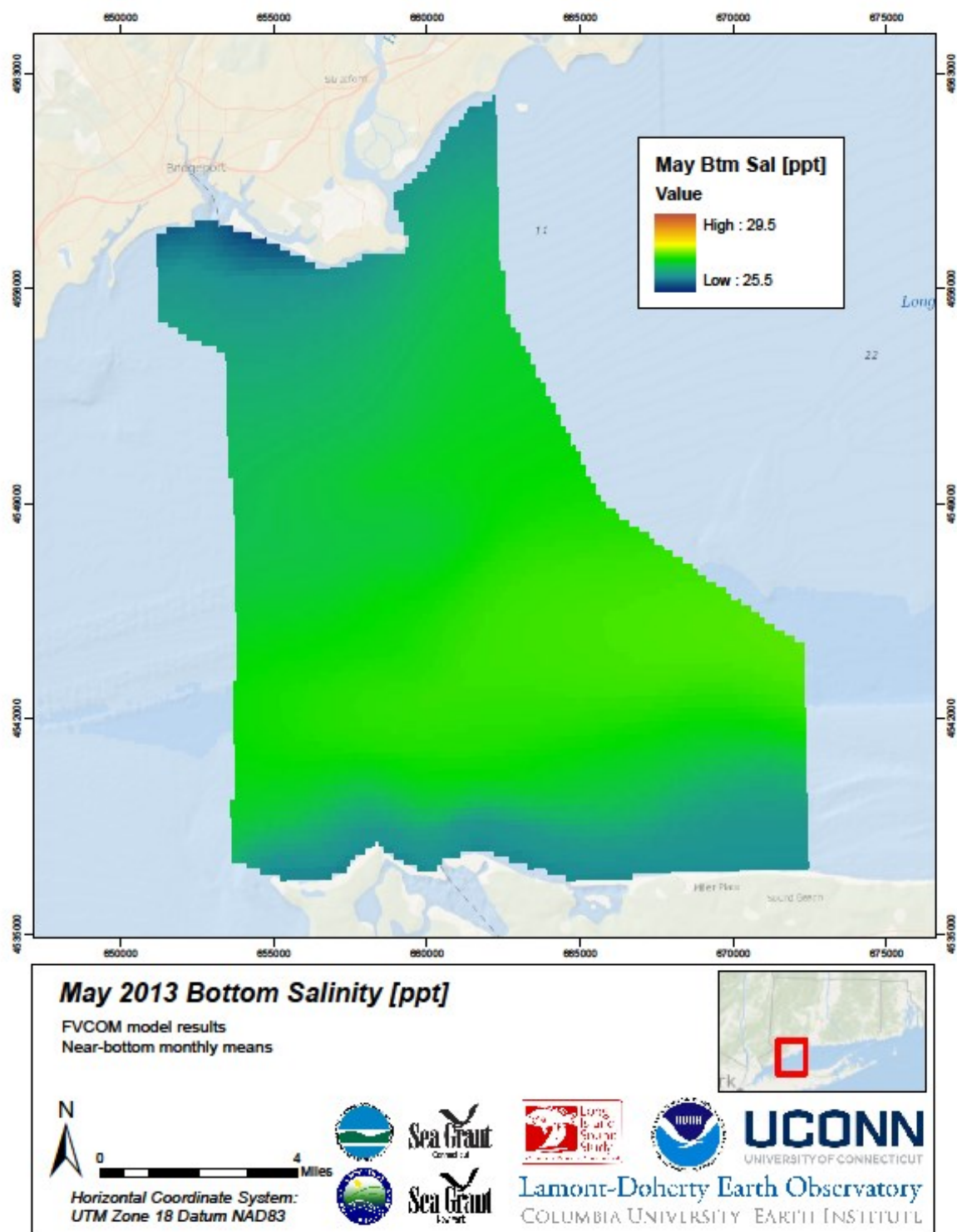


Figure 6.5.7

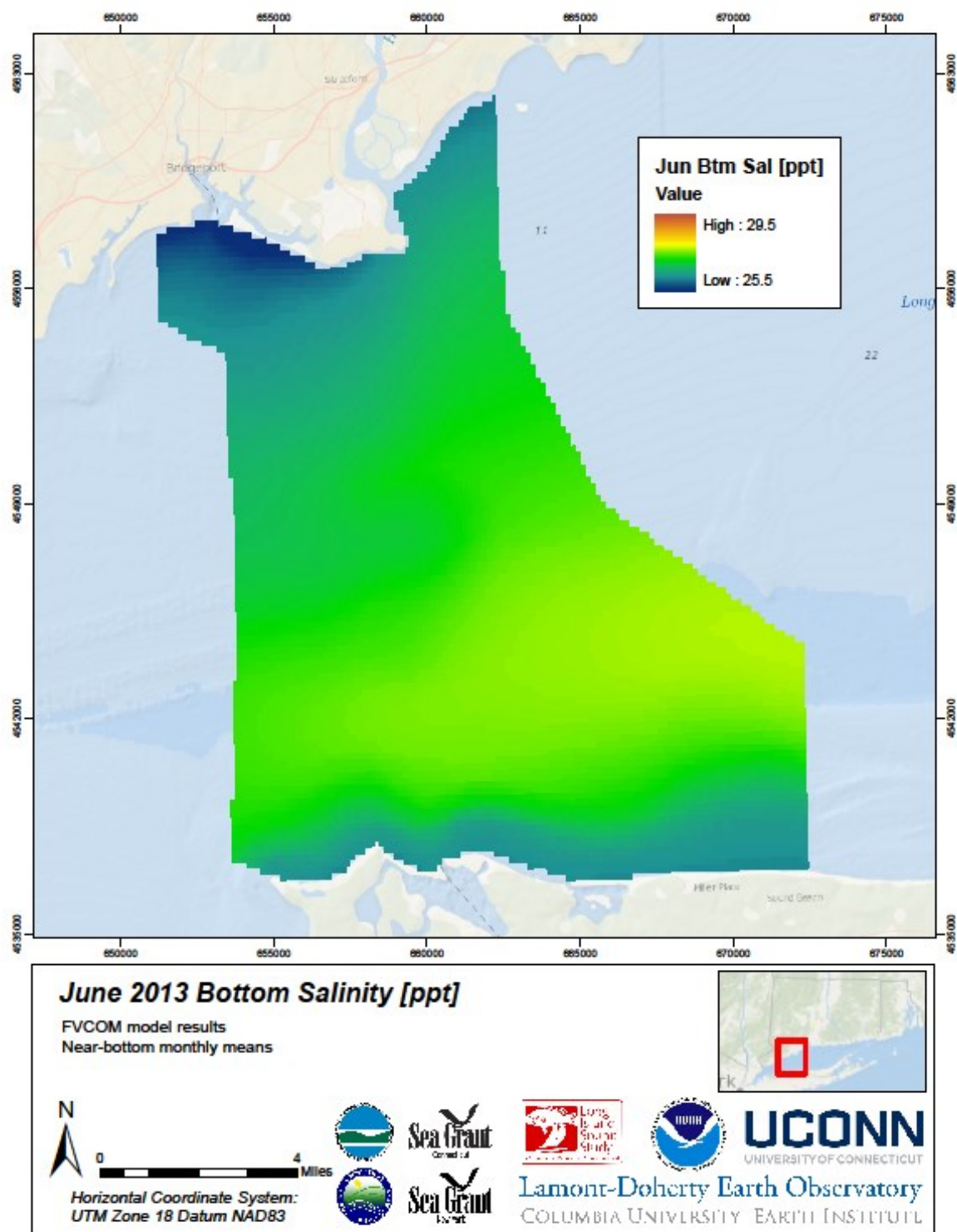


Figure 6.5.8

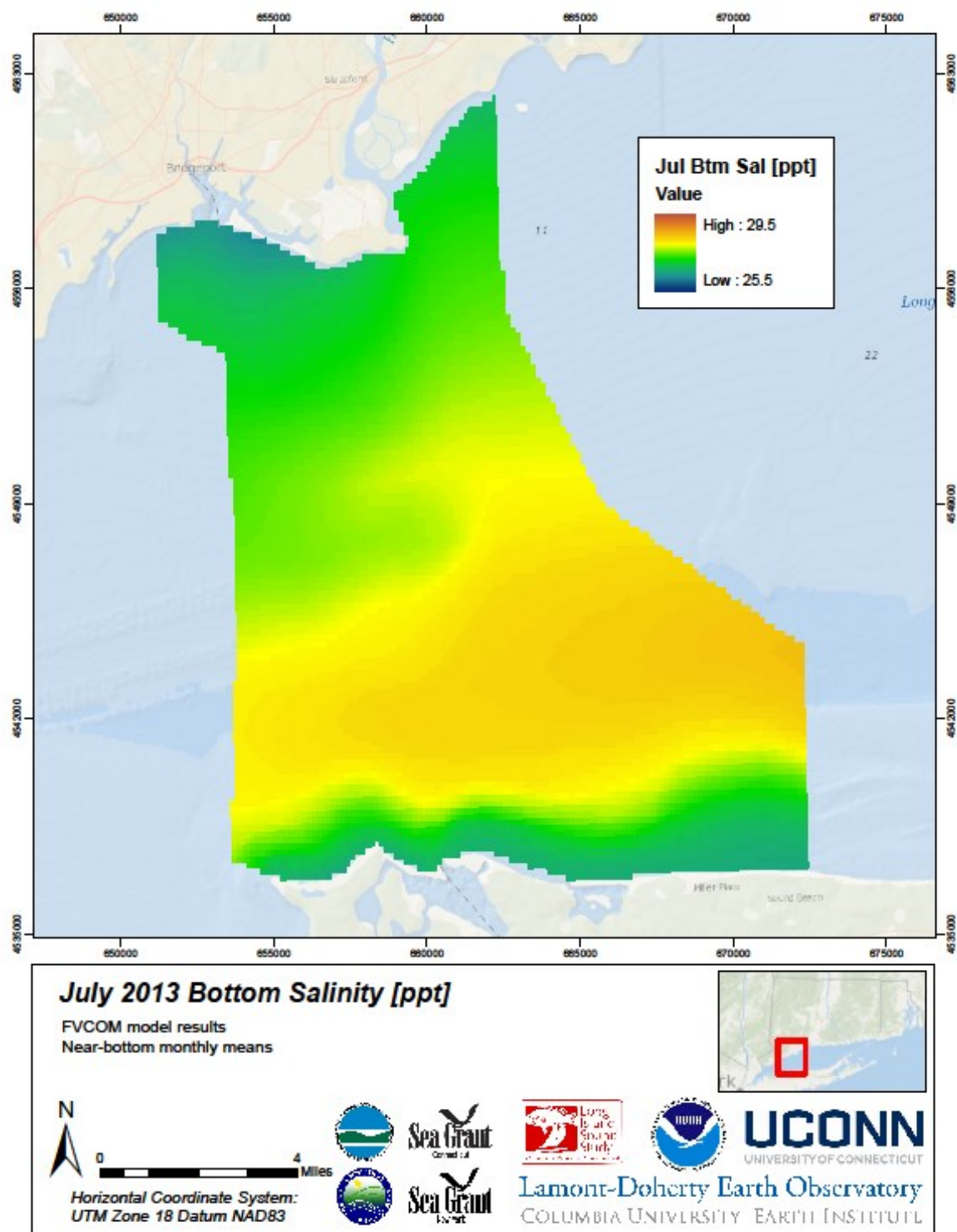


Figure 6.5.9

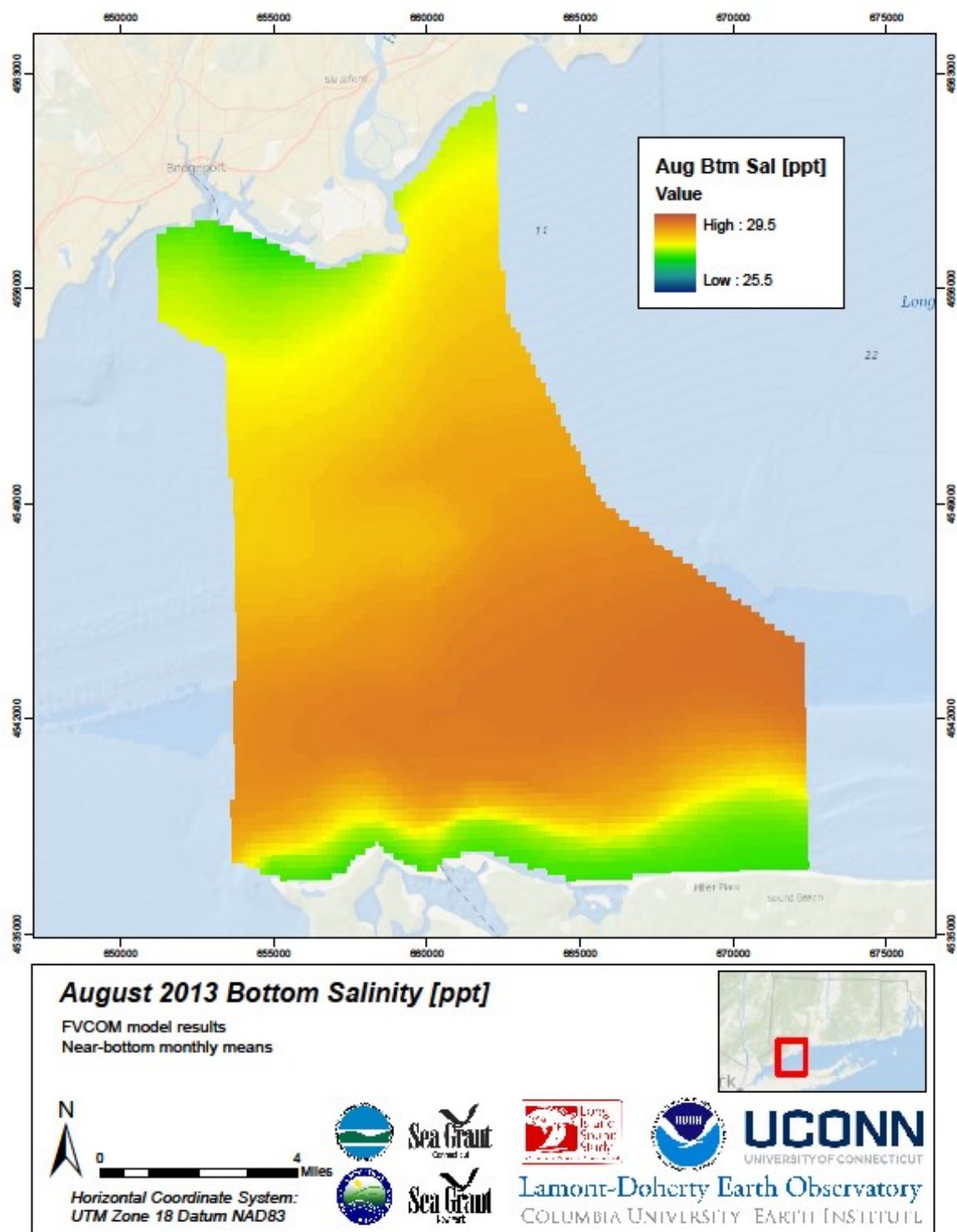


Figure 6.5.10

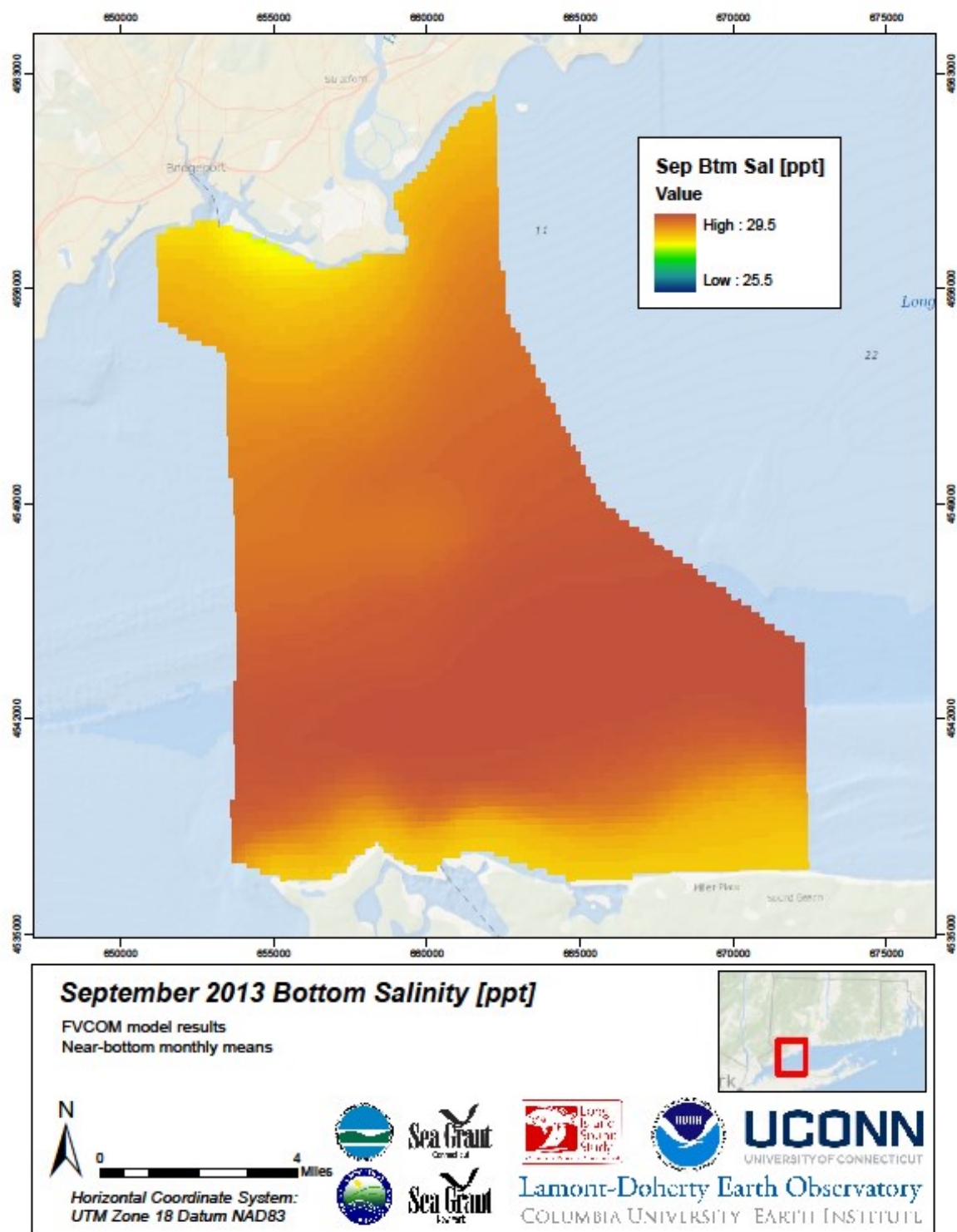


Figure 6.5.11

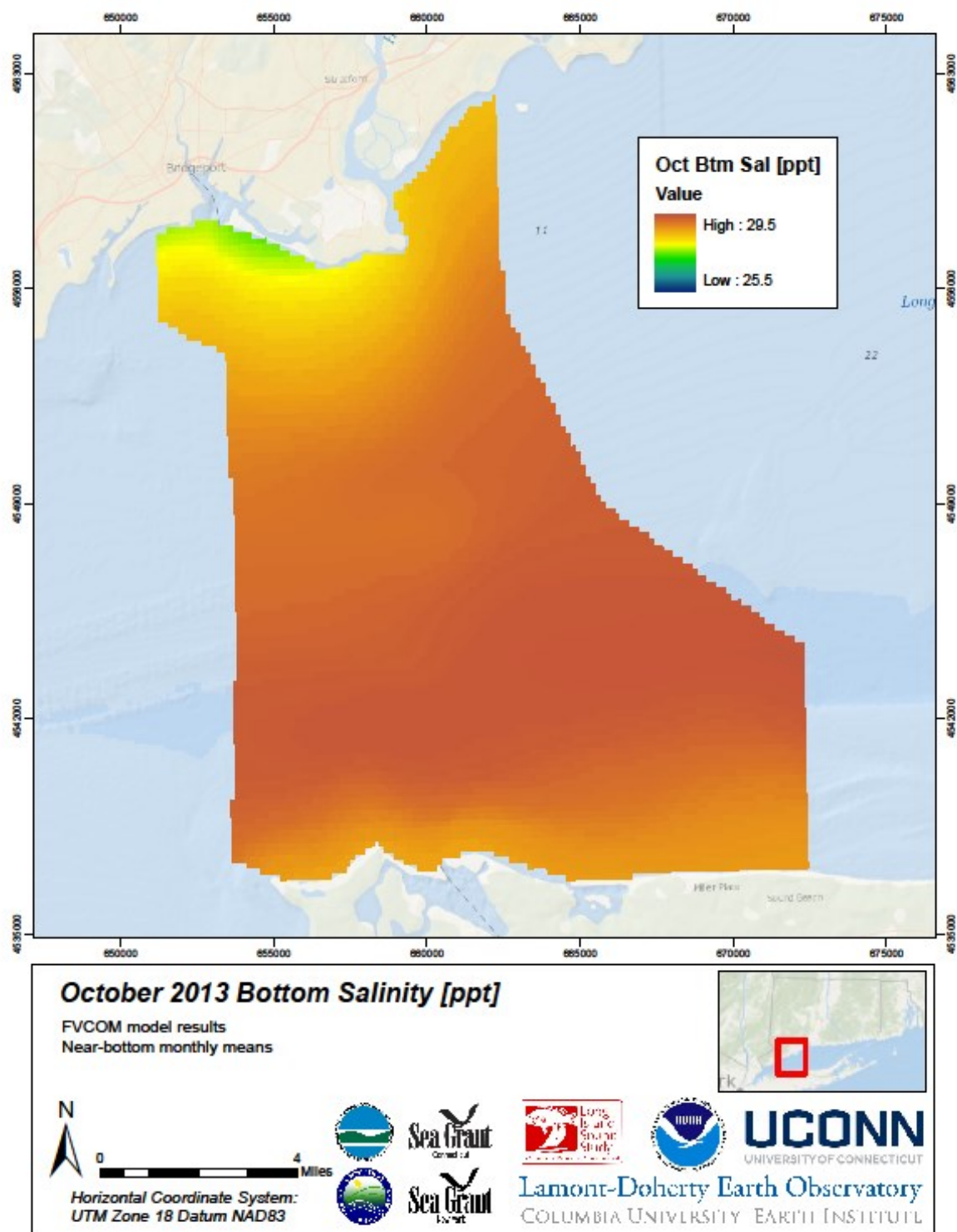


Figure 6.5.12

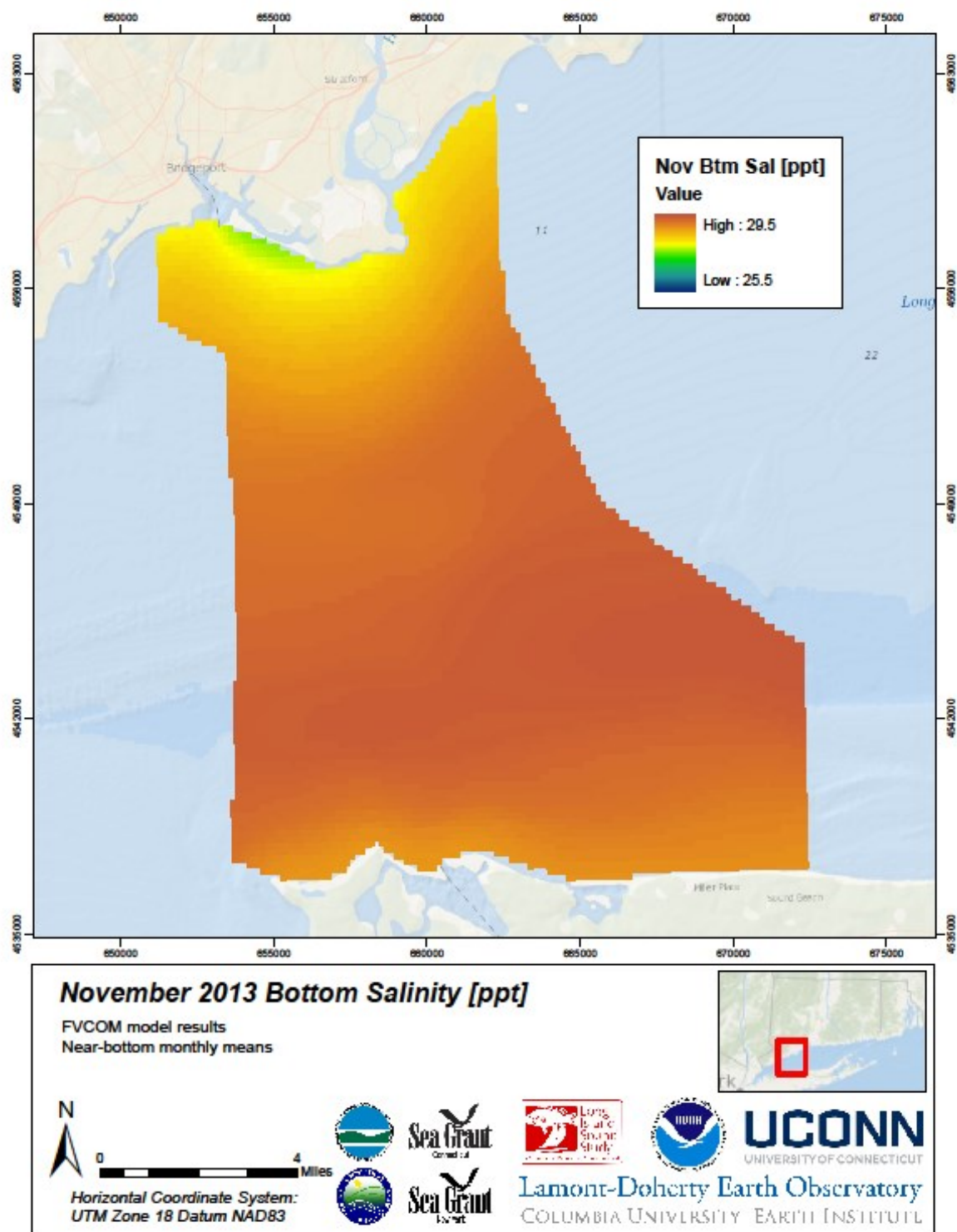


Figure 6.5.13

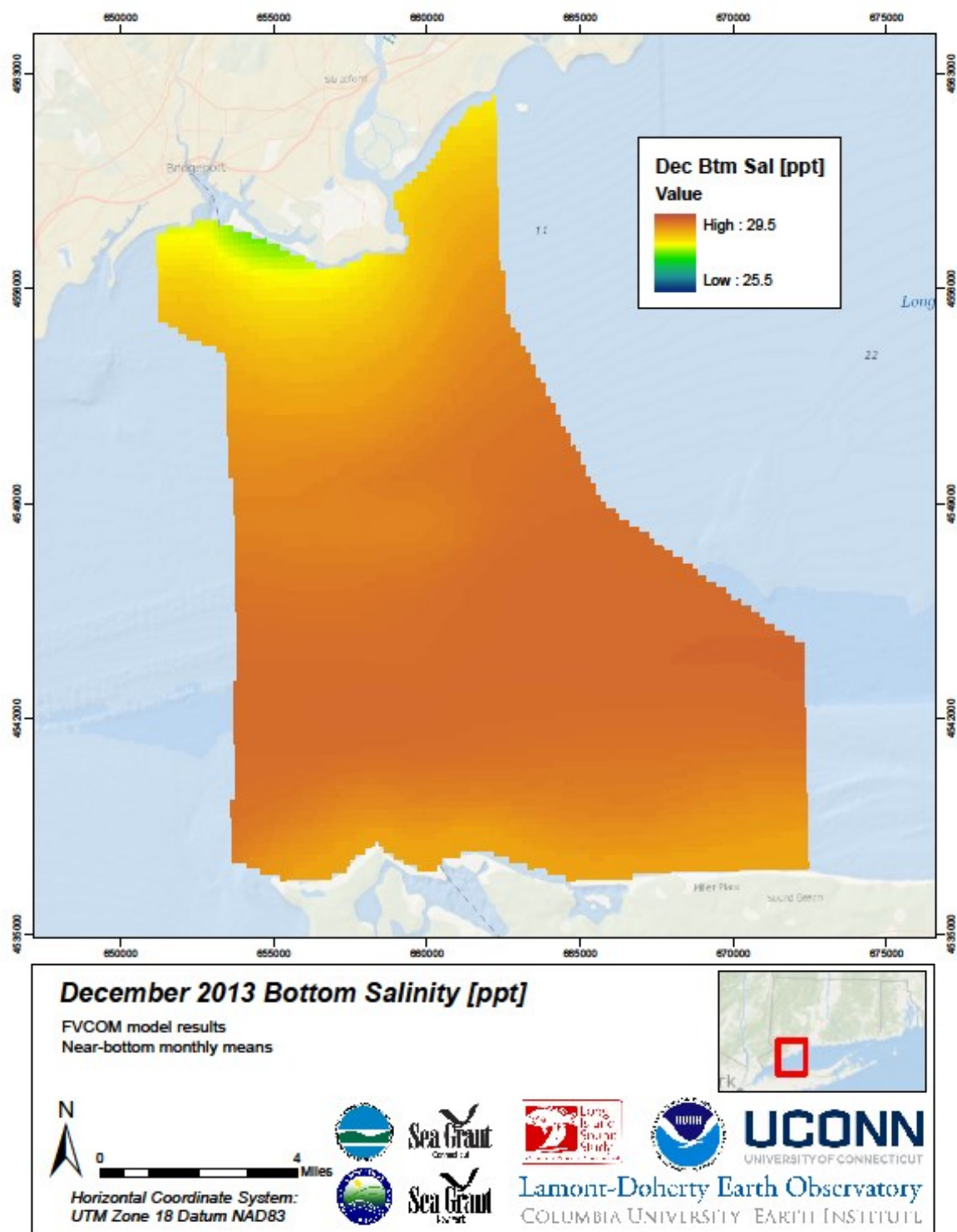


Figure 6.5.14

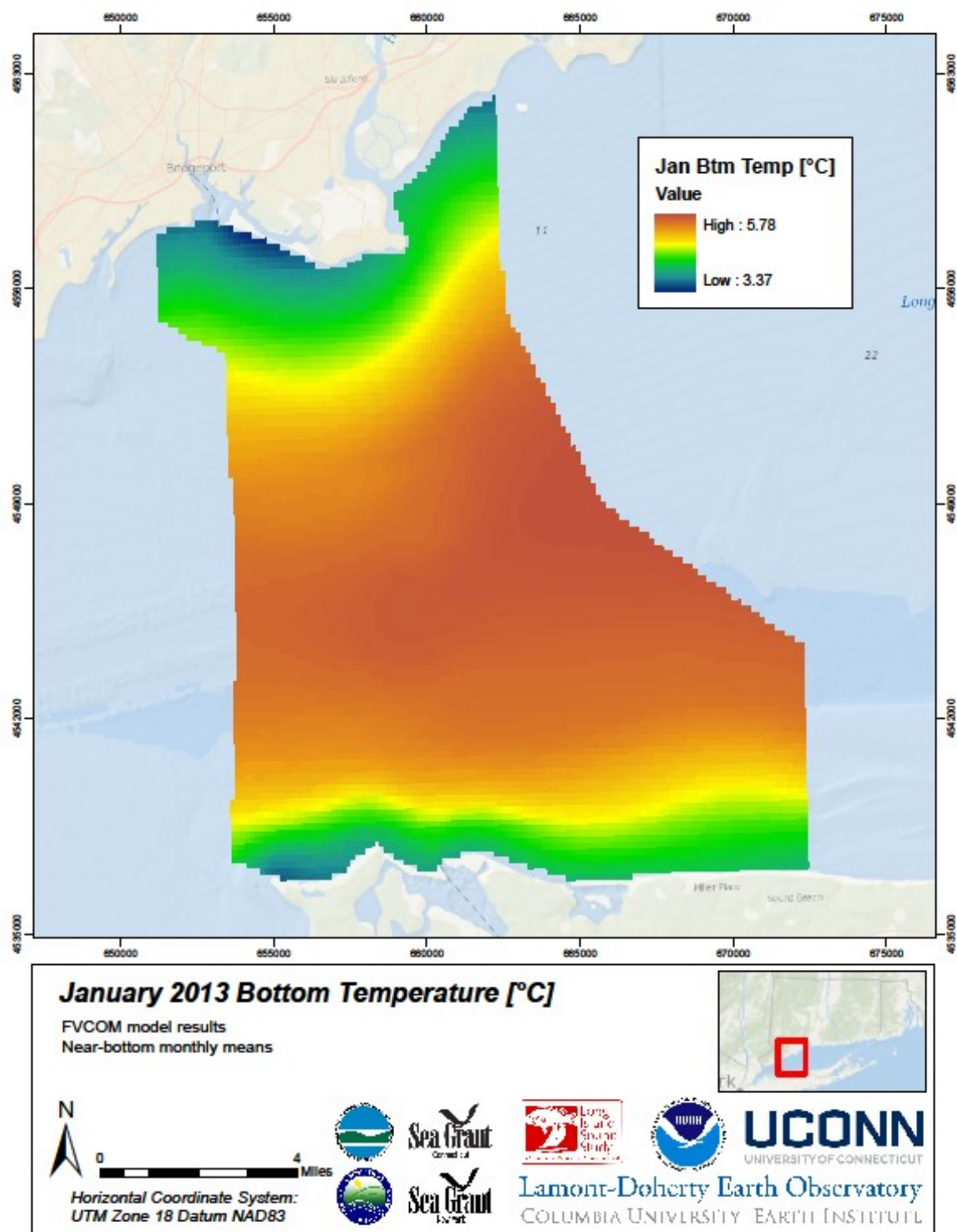


Figure 6.5.15

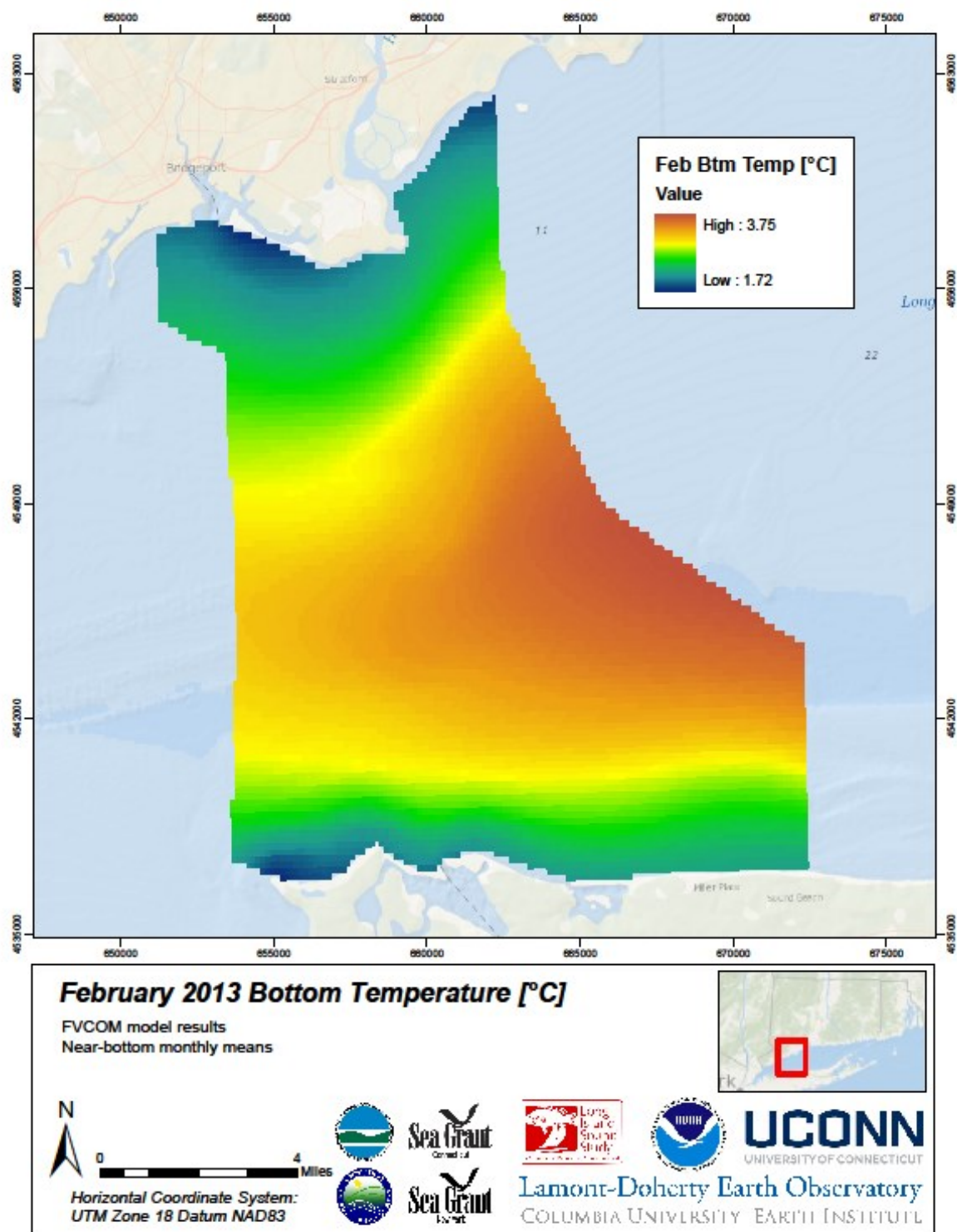


Figure 6.5.16

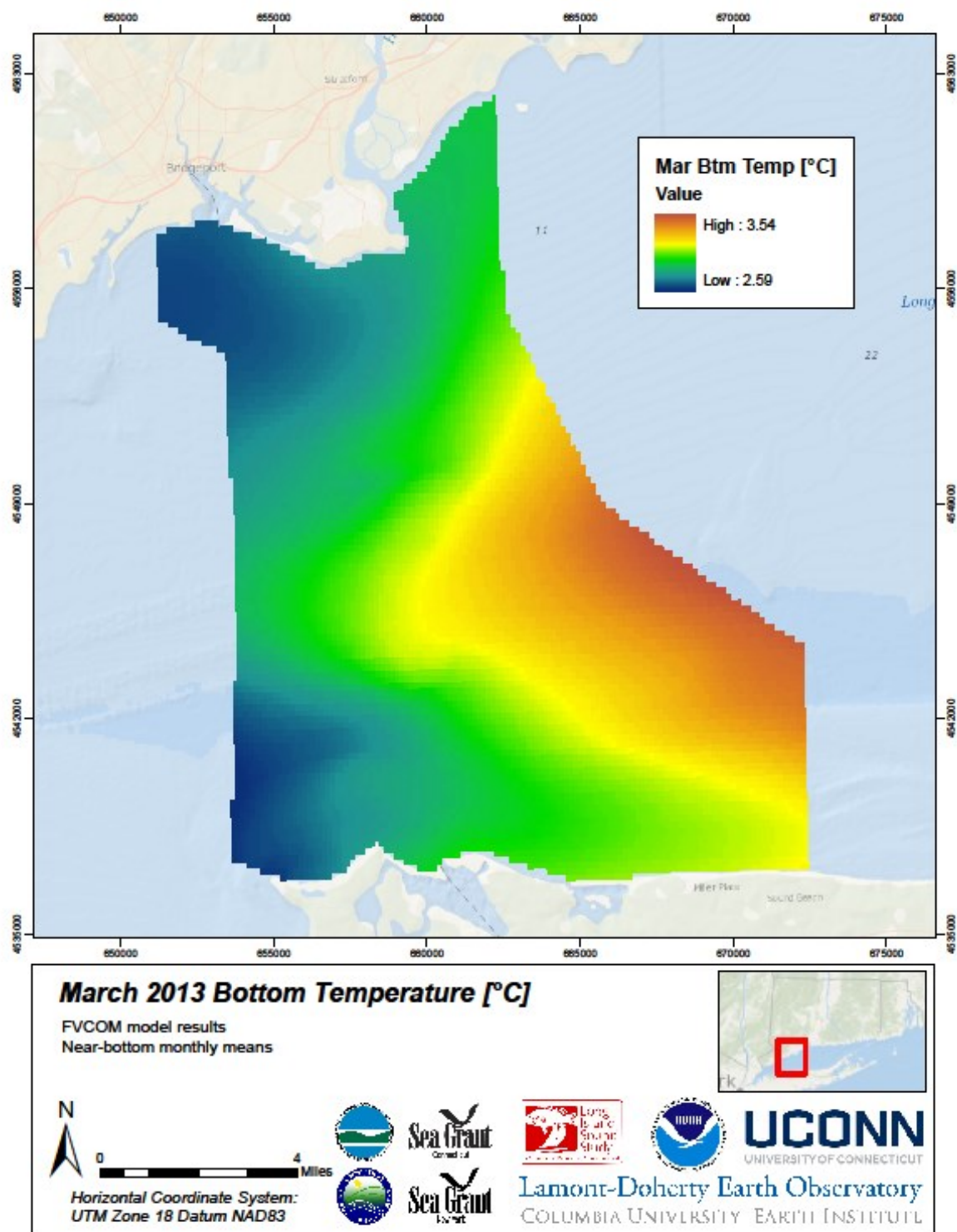


Figure 6.5.17

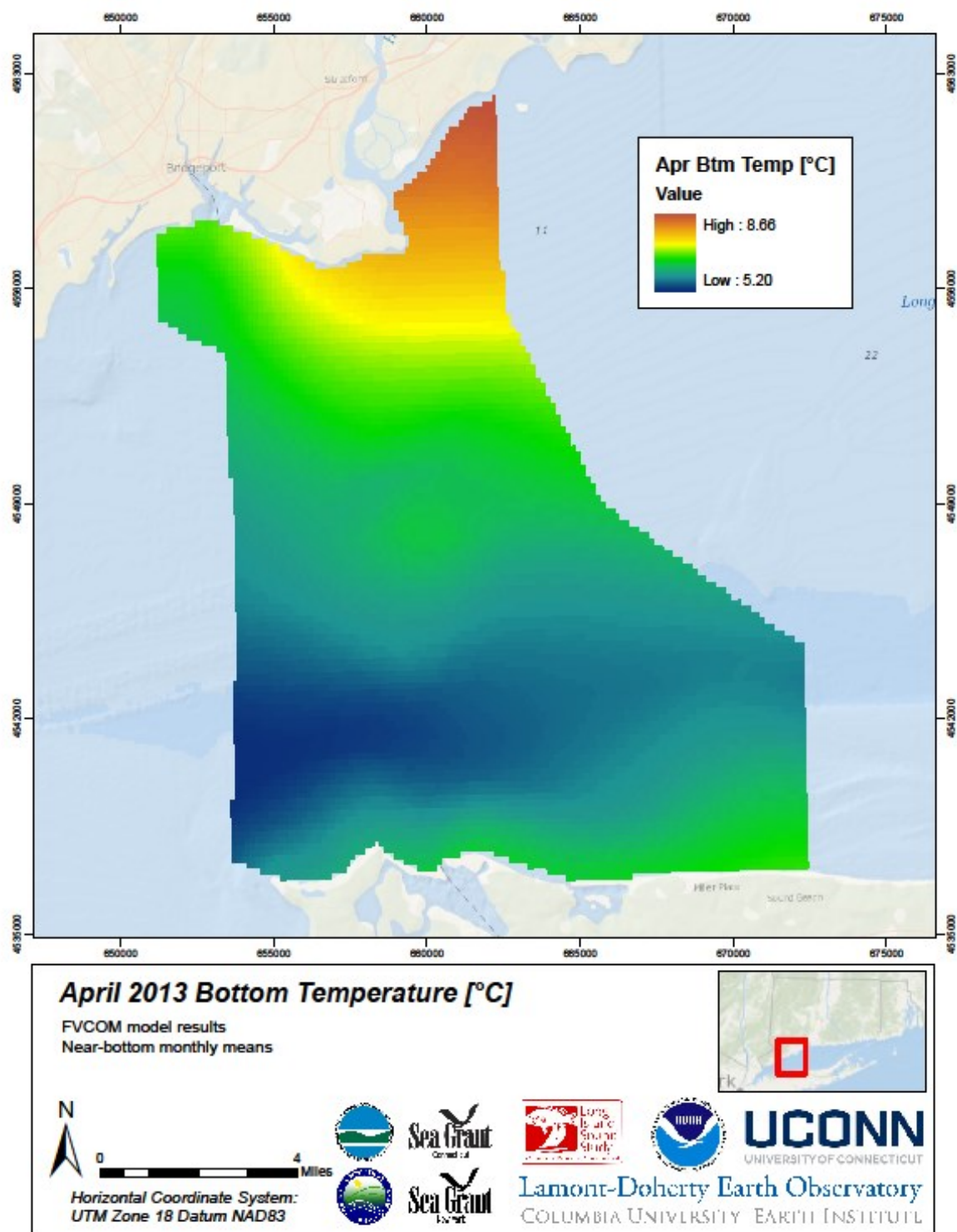


Figure 6.5.18

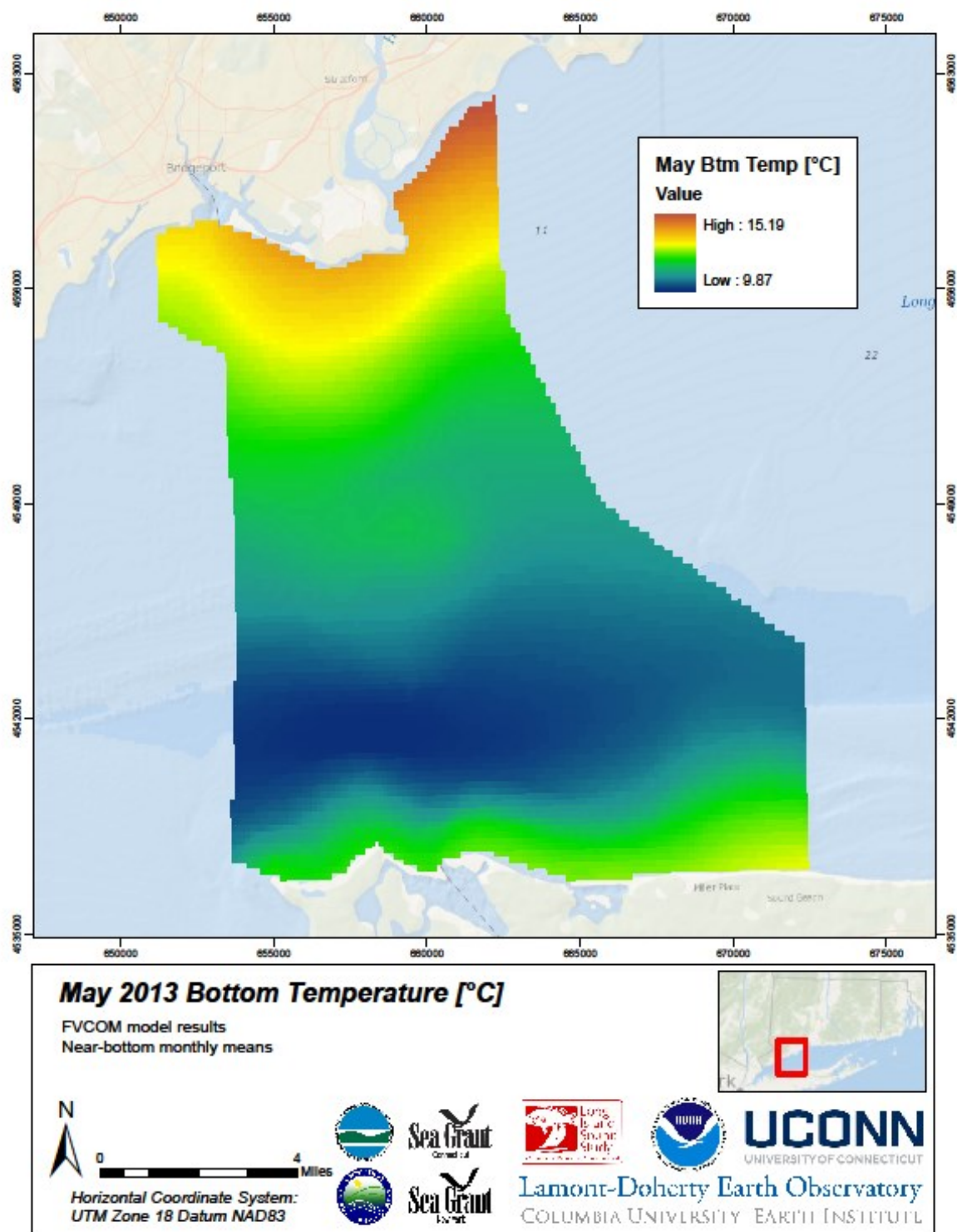


Figure 6.5.19

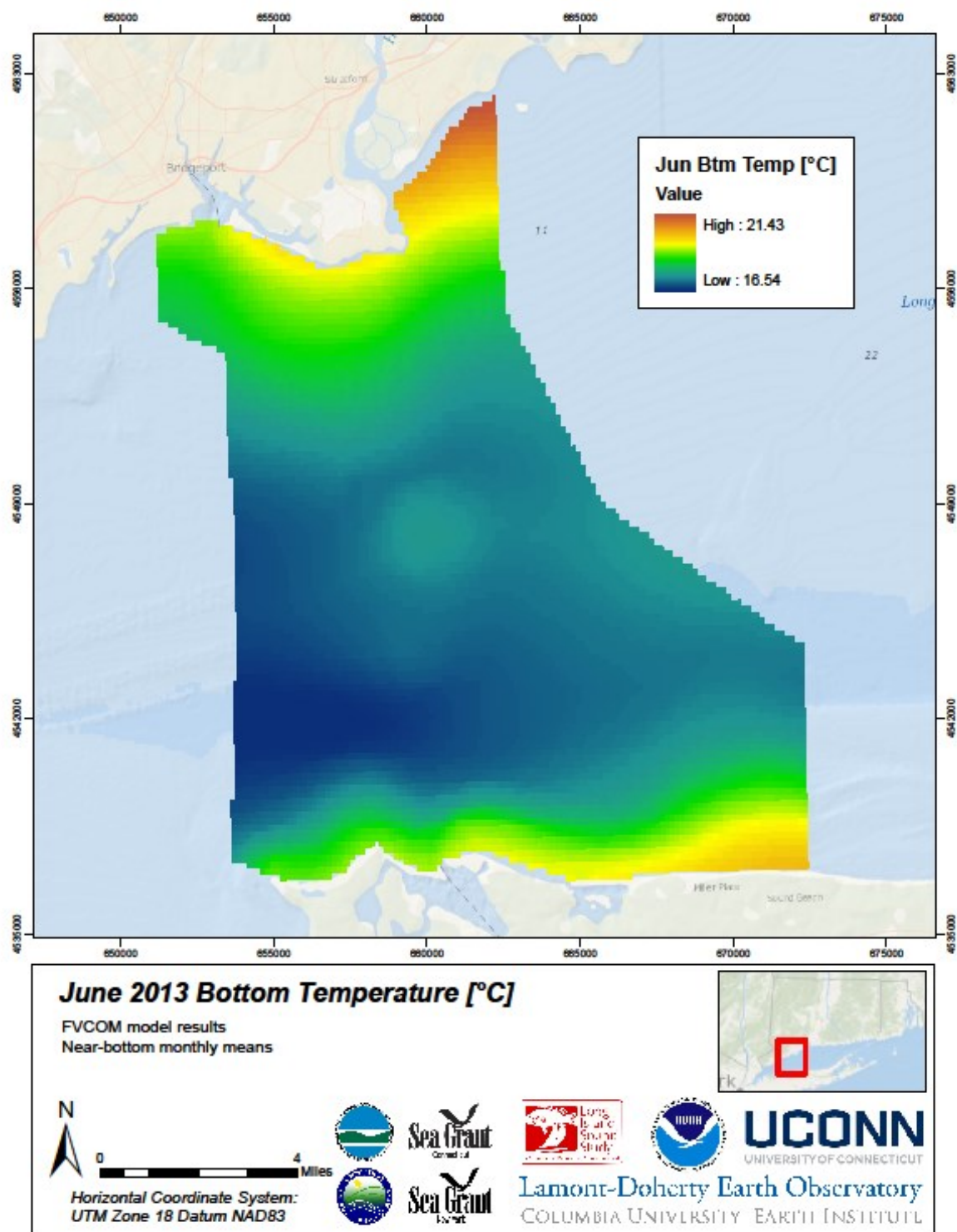


Figure 6.5.20

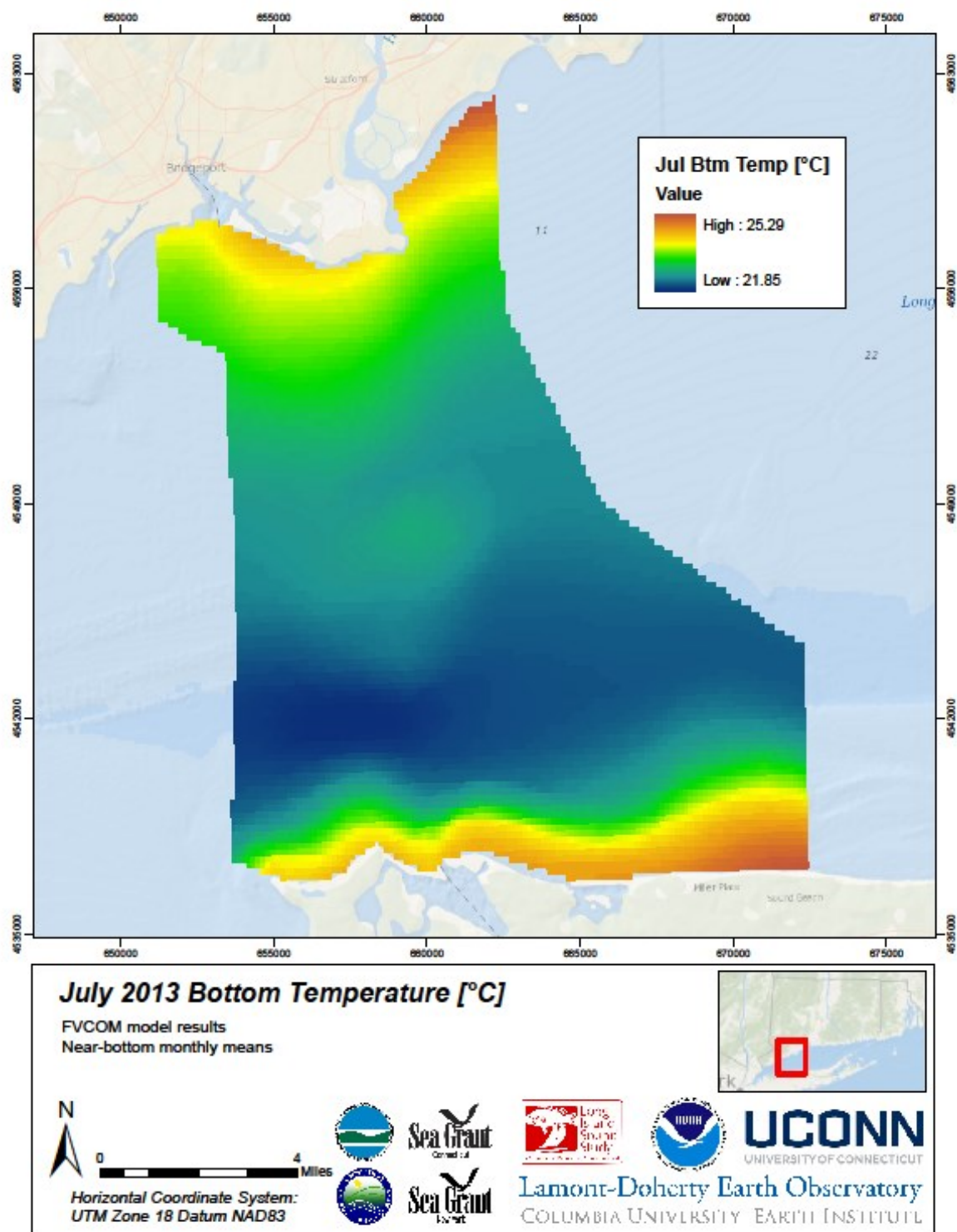


Figure 6.5.21

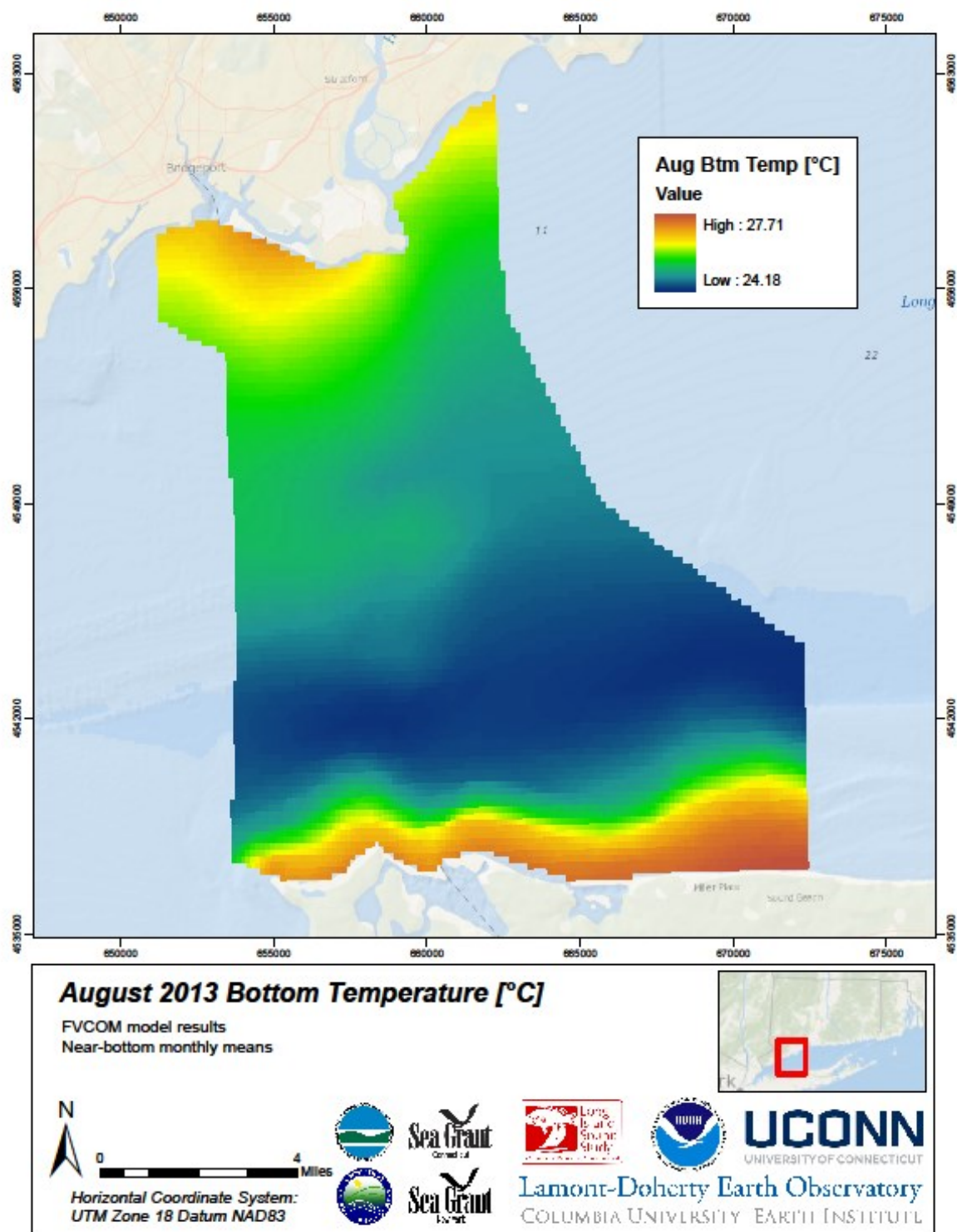


Figure 6.5.22

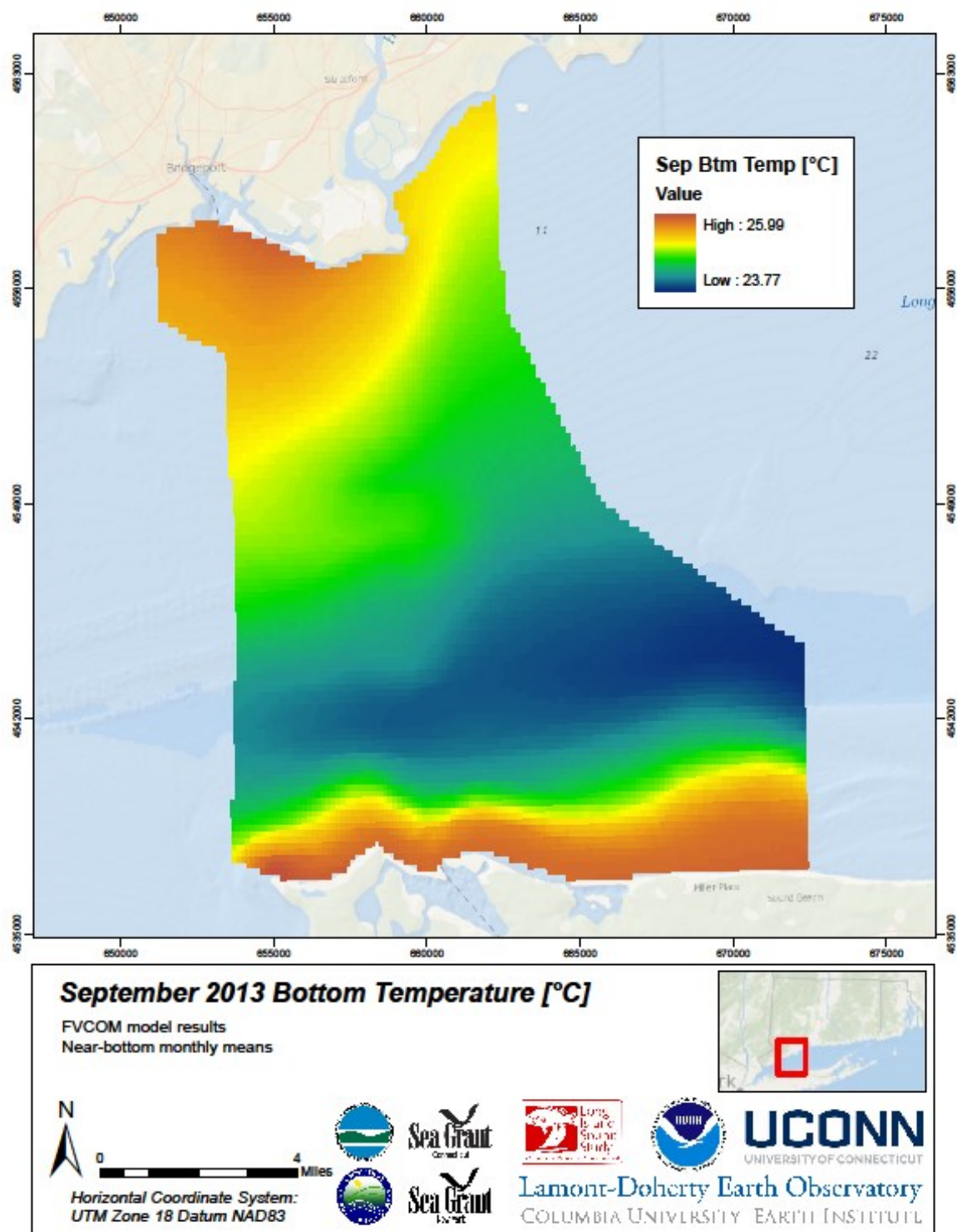


Figure 6.5.23

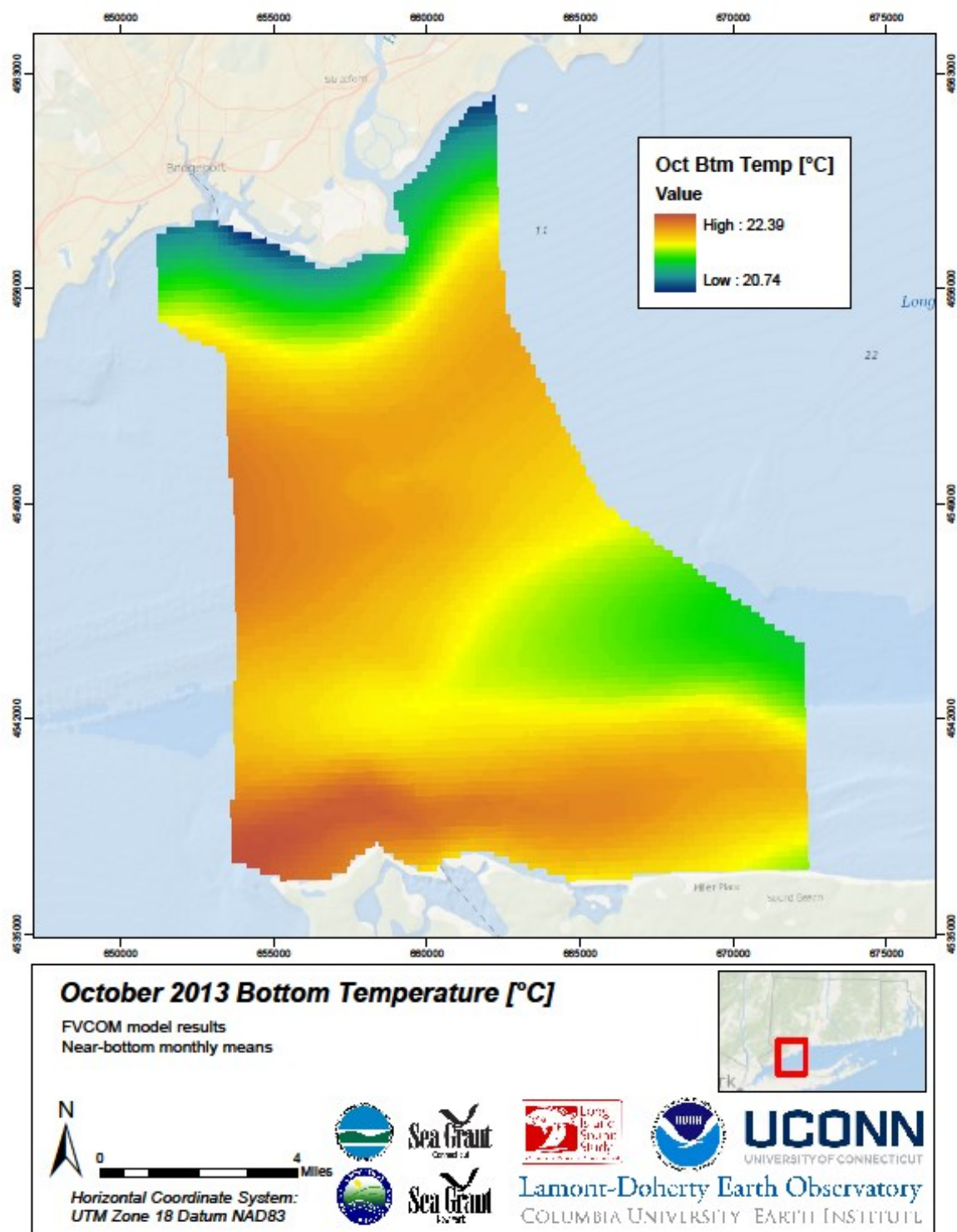


Figure 6.5.24

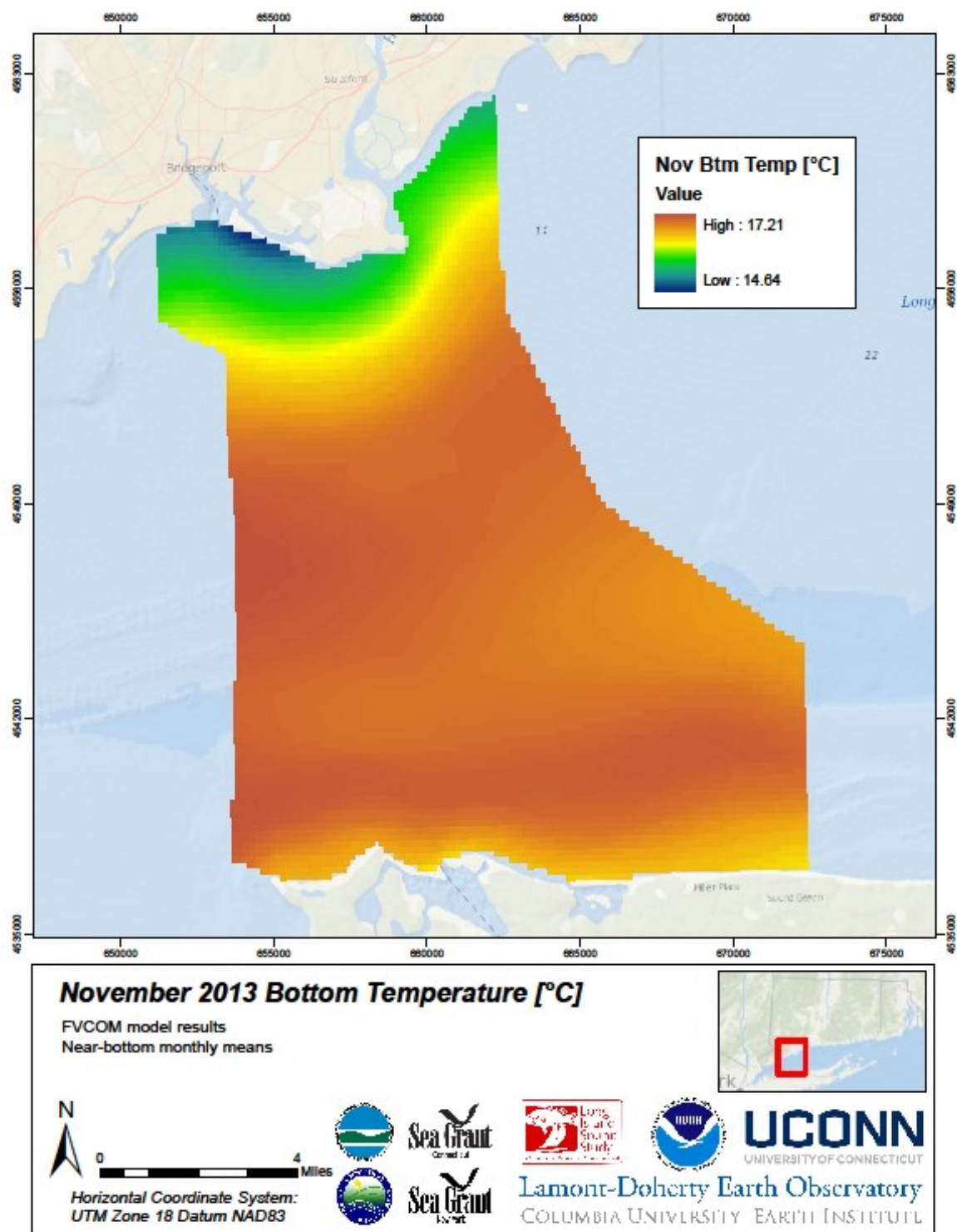


Figure 6.5.25

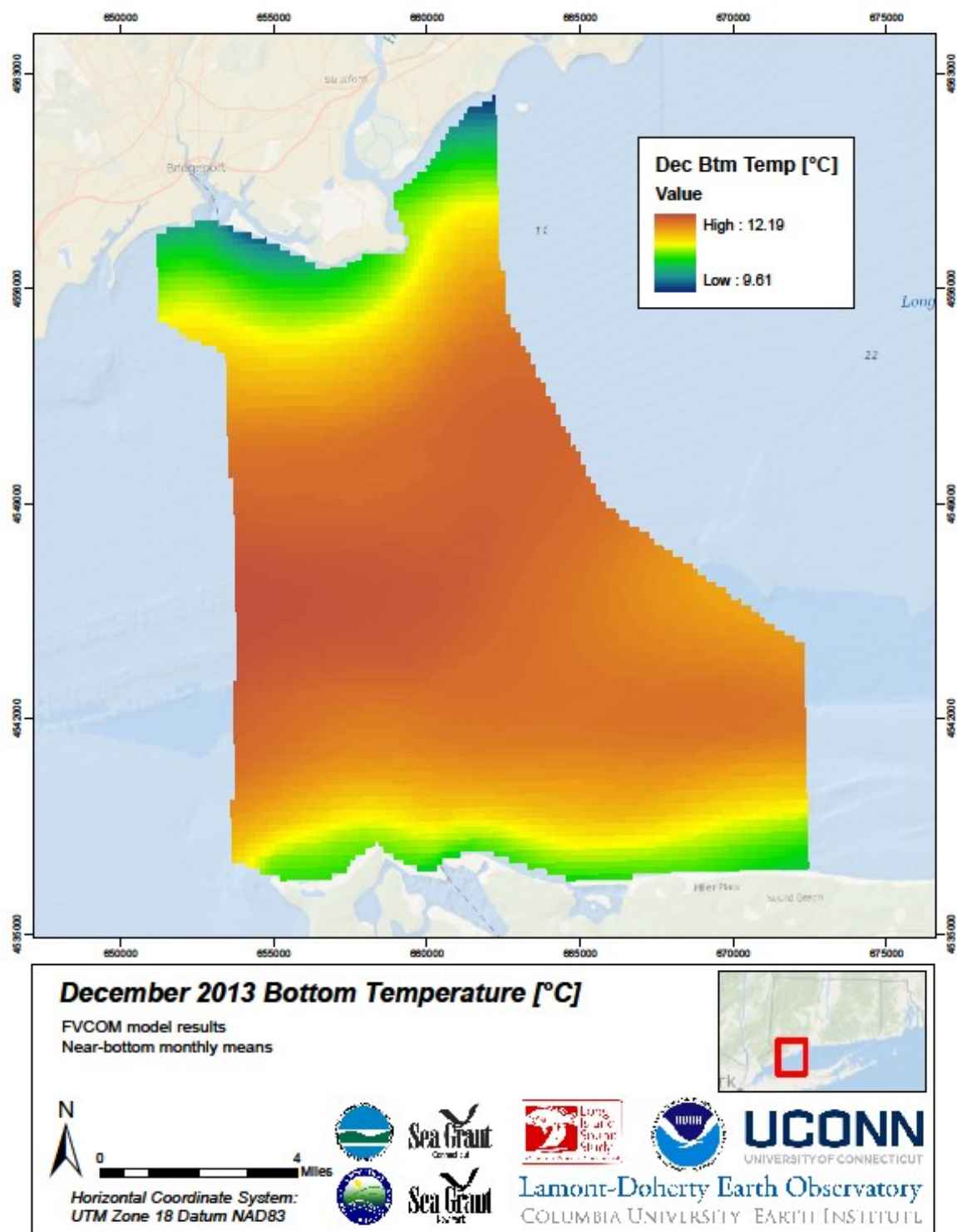


Figure 6.5.26

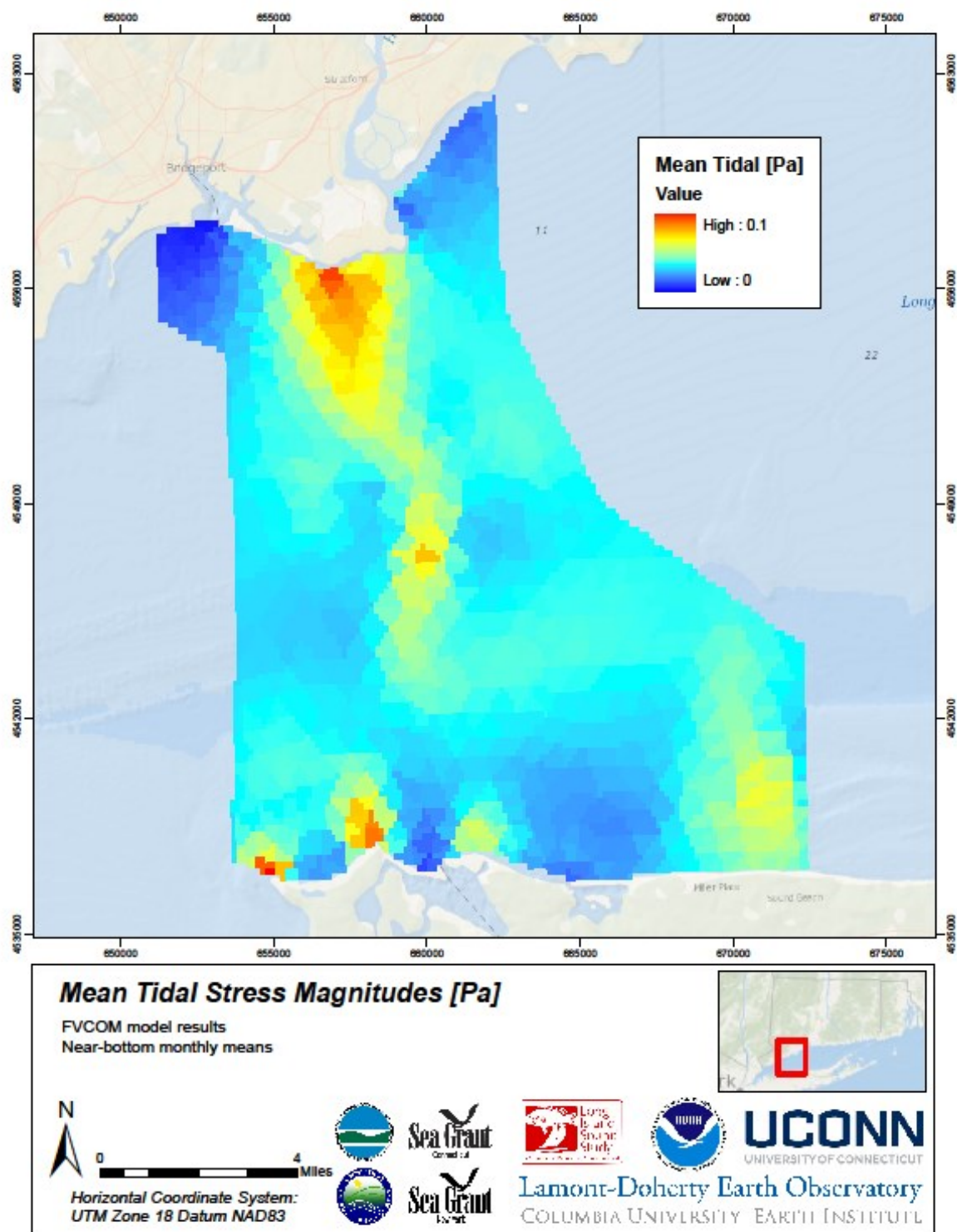


Figure 6.5.27

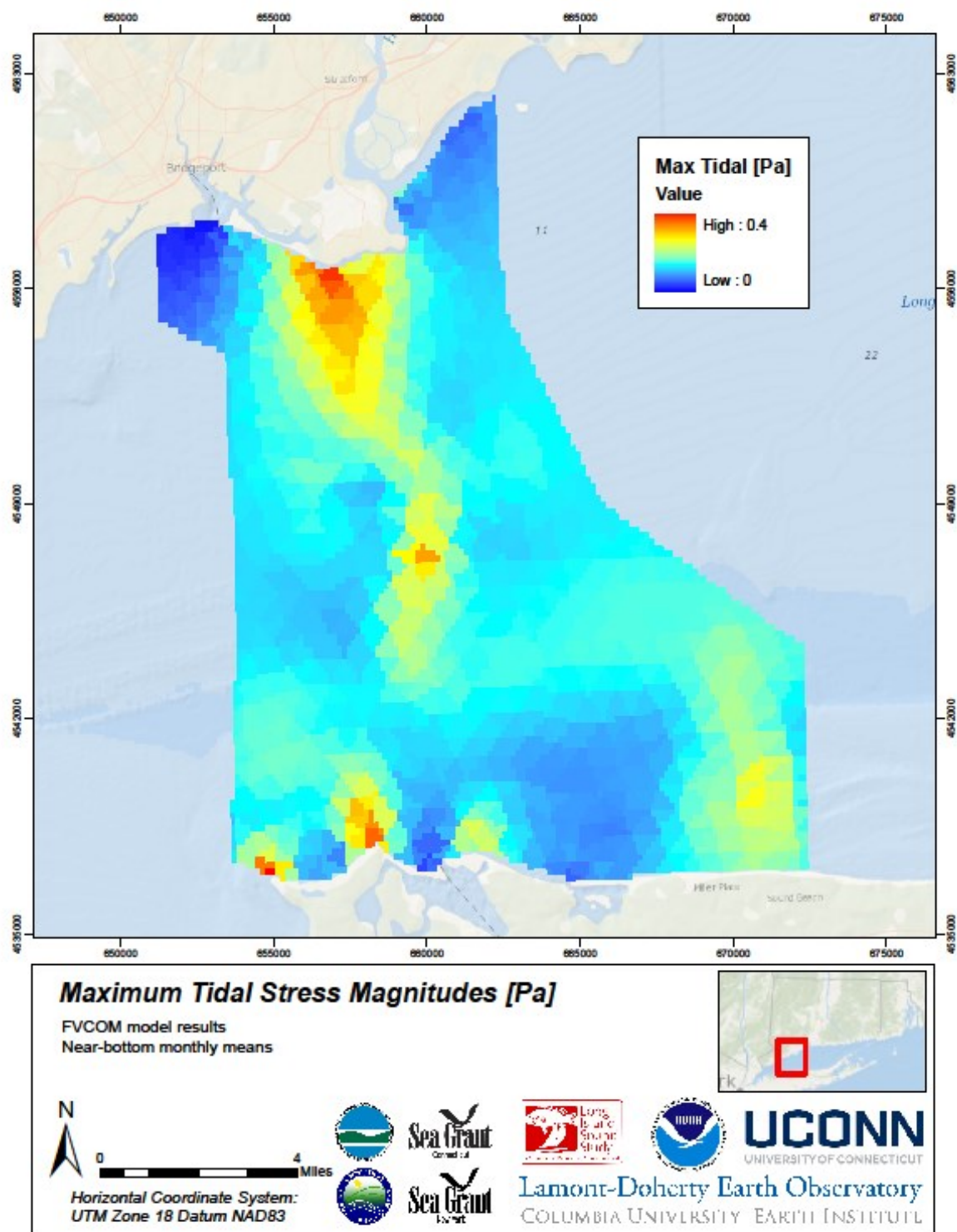


Figure 6.5.28

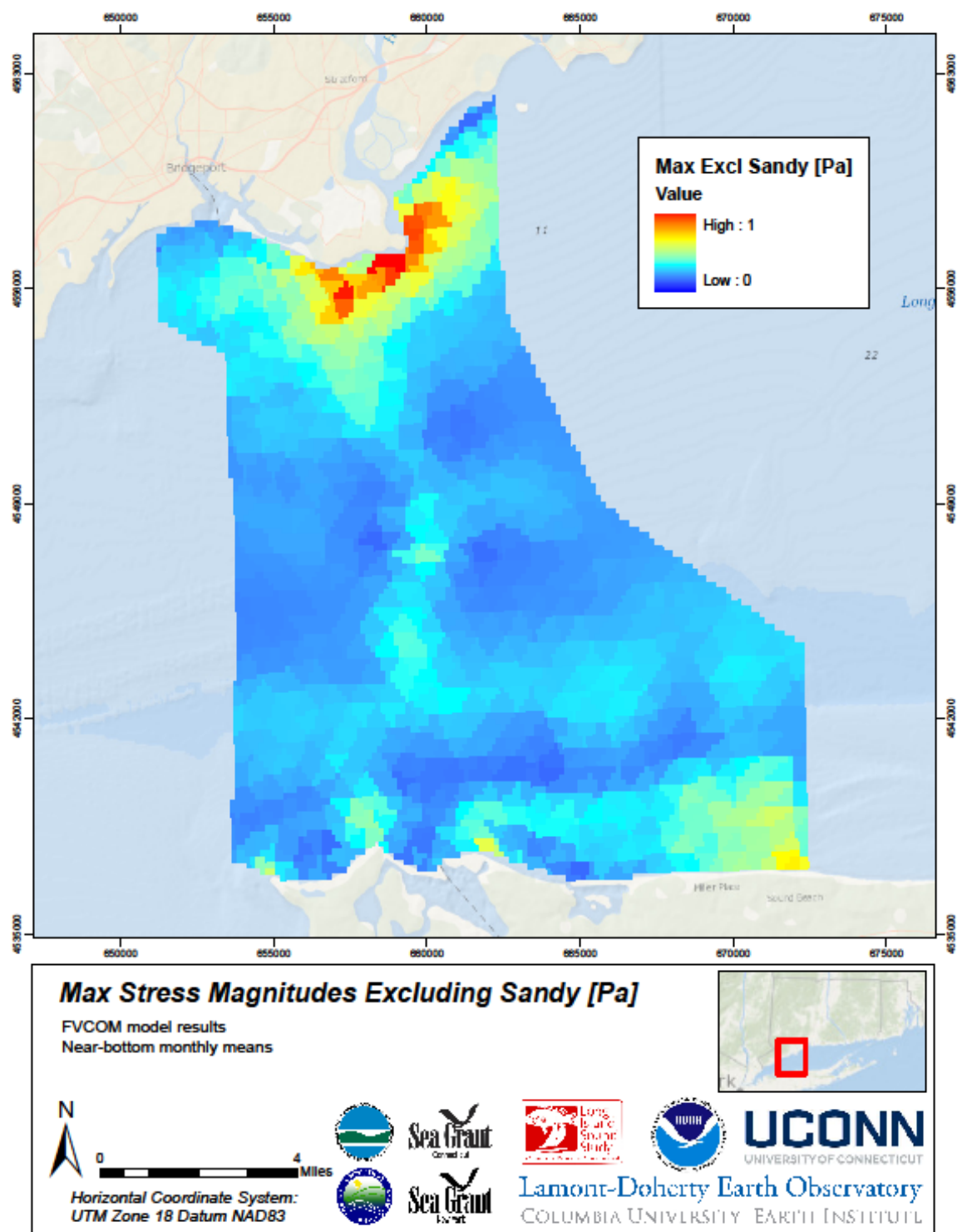


Figure 6.5.29

6.6 Summary and Conclusions

We report the results of the development and testing of a numerical model developed to estimate the distributions of ecologically relevant characteristics of the near bottom environment. A limited measurement program was executed to acquire salinity, temperature, bottom stress and current distributions so that the performance of the model in describing the small scale spatial variations and the seasonal scale evolution of the variables could be critically assessed.

We demonstrate that the model resolves the spatial and temporal structure well. The bottom stress and current estimates are generally within 30% of the measured values. Temperature and salinity distributions are also consistent.

Using the model we developed GIS-format map products with information that span the domain. Figure 6.5.1 shows an example.

6.7 References

- Bennett, D. C., J. O'Donnell, W.F. Bohlen and A.E. Houk, 2010. Tides and Overtides in Long Island Sound. *Journal of Marine Research*, Volume 68, Number 1, January 2010, pp. 1-35.
- Blumberg, A.F., L.A. Khan and J. P. St. John, 1999. *Three-Dimensional Hydrodynamic Simulations of the New York Harbor, Long Island Sound and the New York Bight*, *Journal of Hydraulic Engineering*, 125 799-816
- Bogden, P. S., O'Donnell, J., 1998. Generalized inverse with shipboard current measurements: Tidal and nontidal flows in Long Island Sound. *Journal of Marine Research* 56 (5), 995(3).
- Bokuniewicz, H. J. and R. B. Gordon, 1980a: Sediment transport and deposition in Long Island Sound. *Advances in Geophysics*, 22, 69-106.
- Chen, C.H. Huang, R.C. Beardsley, H. Liu, Q. Xu and G. Cowles, 2007. A finite-volume numerical approach for coastal ocean circulation studies: comparisons with finite difference models. *J. Geophys. Res.*, v. 112, C03018, doi: 10.1029/2006JC003485.
- Crowley, H., 2005. The seasonal evolution of thermohaline circulation in Long Island Sound. PhD Dissertation, Marine Sciences Research Center, Stony Brook University, Stony Brook, NY, 142 pp.
- Fribance, D. B., J. O'Donnell, and A. Houk (2013), Residual circulation in western Long Island Sound, *J. Geophys. Res. Oceans*, 118, 4727–4745, doi: [10.1002/jgrc.20329](https://doi.org/10.1002/jgrc.20329).
- Hao, Y., 2008. Tidal and residual circulation in Long Island Sound. PhD Dissertation, Marine Sciences Research Center, Stony Brook University, Stony Brook, NY, 70 pp.

- Kaputa, N. P. and C. B. Olsen, 2000. State of CT. Dept. of Env. Protection, Long Island Sound Ambient Water Quality Monitoring Program: Summer Hypoxia Monitoring Survey '91-'98 Data Review
- Kenefick, A.M., 1985. Barotropic M2 tides and tidal currents in Long Island Sound: a numerical model: *Journal of Coastal Research*, v. 1, p. 117-128.
- Murphy, D.L., 1979. A Numerical Investigation into the Physical Parameters which Determine the Residual Drift in Long Island Sound. Ph.D. Dissertation, Dept. of Marine Sciences, The University of Connecticut.
- O'Donnell, J. and W.F. Bohlen, 2003. The structure and variability of the residual circulation in Long Island Sound. Final Report, Connecticut Department of Environmental Protection, Hartford, CT. Grant CWF 325-R, 303 p.
http://www.lisrc.uconn.edu/DataCatalog/DocumentImages/pdf/Odonnell_Bohlen_2003.pdf
http://www.lisrc.uconn.edu/DataCatalog/DocumentImages/pdf/Odonnell_Bohlen_2003.pdf
- O'Donnell, J., R. E. Wilson, K. Lwiza, M. Whitney, W. F. Bohlen, D. Codiga, T. Fake, D. Friance, M. Bowman, and J. Varekamp (2013). The Physical Oceanography of Long Island Sound. In *Long Island Sound: Prospects for the Urban Sea*. Latimer, J.S., Tedesco, M., Swanson, R.L., Yarish, C., Stacey, P., Garza, C. (Eds.), ISBN-13: 978-1461461258
- R. Pawlowicz, B. Beardsley, and S. Lentz, (2002), Classical tidal harmonic analysis including error estimates in MATLAB using T_TIDE, *Computers and Geosciences* 28 929-937.
- Rivera Lemus, E. R., 2008. *Wind waves in central Long Island Sound : a comparison of observations to an analytical expression*. Masters Thesis, Department of Marine Sciences, University of Connecticut, 77 pp.
- Schmalz, R.A., Devine, M.F., and Richardson, P.H., 1994. Residual circulation and thermohaline structure, Long Island Sound Oceanography Project Summary Report, Volume 2, NOAA Technical Report NOS-OES-003, National Oceanic and Atmospheric Administration, Rockville, MD, 199 pages.
- Shchepetkin, A. F. and J. C. McWilliams, 2005. Regional Ocean Model System: a split-explicit ocean model with a free-surface and topography-following vertical coordinate. *Ocean Modelling*, 9, 347–404.
- Signell, R., J. List and A. Farris, 2000. Bottom currents and sediment transport in Long Island Sound: a modeling study, *Journal of Coastal Research* **16**, pp. 551–566.
- Swanson, R.L., 1976. Tides. MESA New York Bight Atlas Monograph, 4. New York Sea Grant Institute. Albany, New York.

- Valle-Levinson, A. and R.E. Wilson, 1994a. Effects of Sill Bathymetry, oscillating barotropic forcing and vertical mixing on estuary ocean exchange, J. Geophys. Res., 99(C6), 12667-12681.
- Valle- Levinson, A., and R. E. Wilson, 1994b. Effects of sill processes and tidal forcing on exchange in eastern Long Island Sound, J. Geophys. Res., 99(C6), 12667-12681Valle-Levinson et al. (1995)
- Wilson, R.E. and R.L. Swanson. 2005. A perspective on bottom water temperature anomalies in Long Island Sound during the 1999 Lobster Mortality event. Journal of Shellfish Research, 24: 825–830.

7 Data Management

Recommended Citations:

Fake, T. and V. Ferrini. (2015). Objective. Section 7.1, p. 431-432 in: “Seafloor Mapping of Long Island Sound – Final Report: Phase 1 Pilot Project.” (Unpublished project report). U. S. Environmental Protection Agency, Long Island Sound Study, Stamford, CT.

Fake, T. (2015). LISMARC Data Portal. Section 7.2, p. 432-440 in: “Seafloor Mapping of Long Island Sound – Final Report: Phase 1 Pilot Project.” (Unpublished project report). U. S. Environmental Protection Agency, Long Island Sound Study, Stamford, CT.

Ferrini, V. (2015). Data Portal and Archive @ LDEO. Section 7.3, p. 440-448 in: “Seafloor Mapping of Long Island Sound – Final Report: Phase 1 Pilot Project.” (Unpublished project report). U. S. Environmental Protection Agency, Long Island Sound Study, Stamford, CT.

7.1 Objective

The data management efforts of the Pilot Project are intended to (1) ensure that partners have access to data during the project to facilitate the creation of final data products, (2) ensure long-term preservation and open access to data generated during the Pilot Project, and (3) establish and refine procedures and protocols for documenting, sharing and archiving data that may be acquired during subsequent efforts. To meet the specific needs of the Pilot Project the 2012 Scope of Work (SOW) defined the following data system design requirements:

- a data portal that meets the needs of the user community;
- a search interface based on keywords, parameters, or categories;
- map-based data discovery (e.g. geospatially enabled);
- archival of and access to raw and derived data products, project documentation, & FGDC metadata (Table 7.1);
- web services for access, discovery and interoperability;
- a system for easy cost-effective ingestion of data/metadata/documentation;
- verification of data system integrity;
- the ability to provide access to derived products to other systems; and
- the ability to link to related data housed at other repositories.

Table 7.1 Summary of diverse anticipated data products, types and file formats

Category	Product	Data Type	Preferred Format
Cruise Info	Cruise Tracks	GIS layer(s)	ESRI Geodatabase Feature Class (point/line)
	Cruise Reports/Logs	Digital Documents	PDF
Acoustic	Acoustic Intensity mosaics (composition/roughness/texture)	Rasters	ESRI Grid, GeoTiff
	Topographic mosaics (bathymetry)	Rasters	ESRI Grid, GeoTiff
	Sub-Bottom images	GIS layer(s) & images subbottom data	ESRI Geodatabase Feature Class (line), JPEG, SEG Y
Sampling	Station Data (Biology/Geology/Chemical/Physical)	GIS layer(s)	ESRI Geodatabase Feature Class (point/line/poly)
	Video	Digital Movies	MOV
	Photos	Digital Photos	JPEG
Geospatial Interpretations	Ecological/Habitat Data	GIS layer(s)	ESRI Geodatabase Feature Class (point/line/poly)
	Sediment Texture/Grain Size	GIS layer(s)	ESRI Geodatabase Feature Class (point/poly)
	Sedimentary Environments (Chem/Organic/Inorganic)	GIS layer(s)	ESRI Geodatabase Feature Class (poly)
Maps/Reports	Analysis Reports/Summaries	Digital Documents	PDF
	Cartographic Maps	Digital Documents	GeoPDF

In order to meet the needs of all partners with respect to access to data, two parallel data management efforts were undertaken. While these two efforts share some common elements,

they provide technical solutions for two different use-cases. The LISMARC data portal (Section 7.2) provides infrastructure for direct machine access to a subset of data with a focus on data access by numerical models. The LIS Data Portal at LDEO (Section 7.3) provides a comprehensive metadata catalog and long-term data stewardship solution focused on open access and preservation of all data products (raw and derived) and metadata, ensures compliance with metadata standards, and includes links to related content in distributed data systems. The details of each system are described in detail in the following sections.

7.2 LISMARC Data Portal

The Long Island Sound Mapping initiative uses the open source geospatial content management system GeoNode to facilitate the sharing of geospatial data and any associated documentation such as field notes from various agencies. GeoNode is built atop a number of other robust open source components including Django, PostgreSQL, PostGIS, GeoServer, GeoExt, and OpenLayers.

Django drives much of the front end and back end configuration, dispatching and serving as the “glue” for the other components present in GeoNode's stack. Additionally, it controls the user authentication which in turn allows individuals to publish and modify their data without the need to implement a new administrative backend for handling groups, users, and associated data uploads. The templates for the frontend are served through an Apache webserver. Currently all data is password protected through this management system requiring a user to authenticate with provided credentials in order to access any information.

The map data for the project itself is stored either in a PostGIS database for vector data formats such as ESRI shapefiles, or as files for raster data. PostGIS is a spatial data extension for PostgreSQL which implements a superset of the OGC Simple Features Specification. Currently, GeoTIFF files and ESRI shapefiles are supported for uploading through GeoNode's interface. Other file formats can also be used if uploaded via GeoServer, or alternatively files may be converted to a format which is uploadable through use of geospatial conversion tools such as those present in the GDAL libraries. As vector files are stored in the database, they are not retained as shapefiles. However, the original shapefiles can be obtained via GeoServer's WFS without loss of data. Additionally the shapefile and associated metadata can be obtained in a zipped file format through GeoNode. Additionally, a number of file formats such as .doc, .docx, PDF, JPEG, and PNG can be uploaded and through GeoNode's “Documents” interface and optionally associated with a particular layer which has been uploaded.

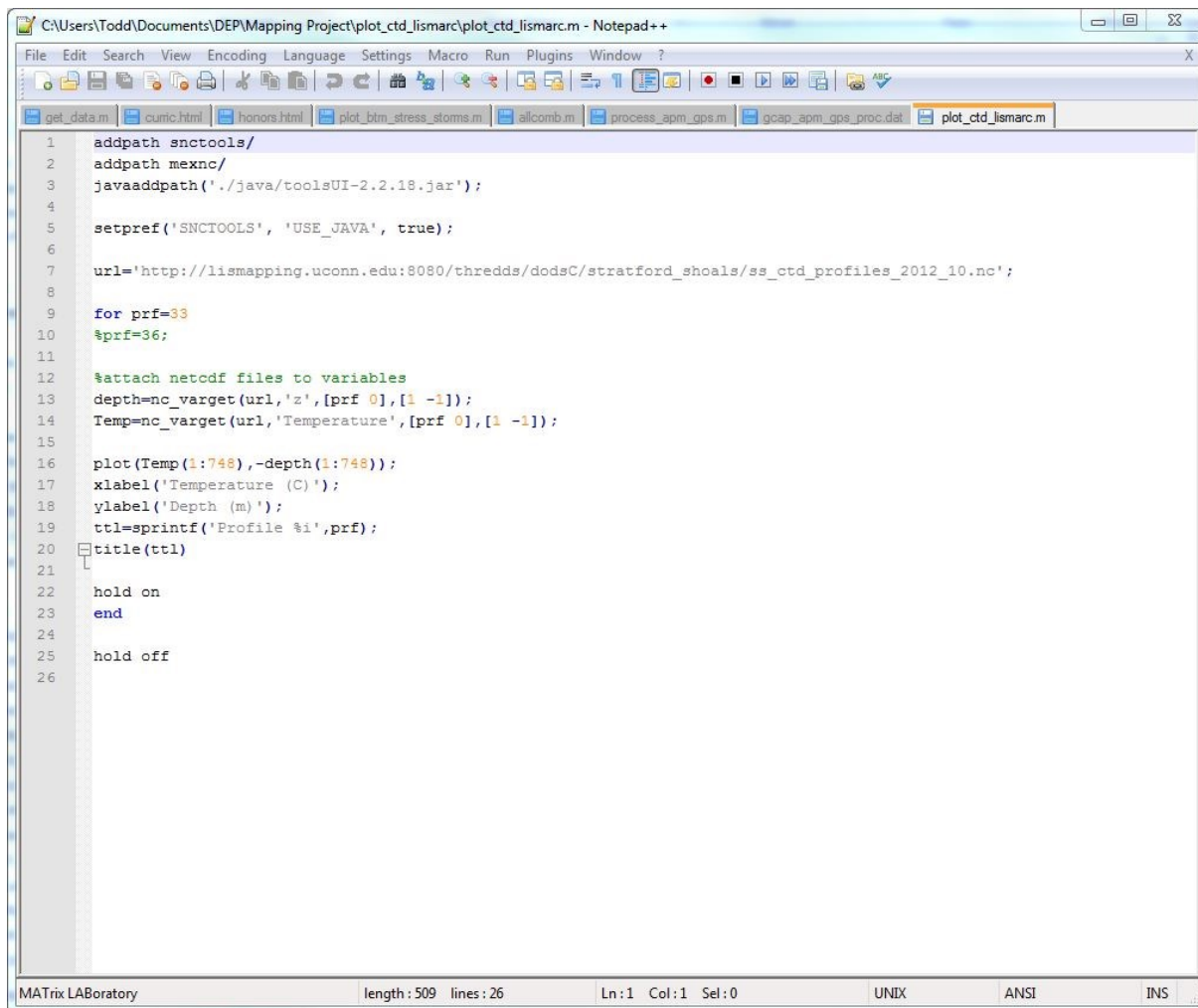
This data is then served through a GeoServer instance exposing multiple OGC Web Services (OWS) including WMS, WCS, WFS, and WPS. Users can view the data through the GeoExplorer client, which leverages OpenLayers and the geospatial user interface library GeoExt for viewing and interacting with the data in the interactive map interface. Users can also create maps from existing layers and create basic cartographic modifications to symbology.

More advanced symbology changes can be achieved through directly modifying the Styled Layer Document (SLD) through GeoServer's administration interface. Conversion to SLD from proprietary cartography formats such as those used by ArcGIS remains somewhat of an issue. In the particular case of ArcGIS's cartography formats, there exist a number of commercial tools to convert to SLD format such as Arc2Earth.

Metadata is sent to a PyCSW backend communicating with the GeoNode database. This backend can then interoperate with other cataloguing services which can harvest CSW records. Metadata can be requested in a number of standard formats, including ISO 19139 and FGDC.

The mapping project also contains links to a number of CT and CTD casts taken near Stratford Shoals and Eastern Long Island Sound, respectively. The datasets are in NetCDF format and while not currently supported by GeoNode, they are linked to externally through a THREDDS Data Server catalog, from which the data can be accessed via the OPeNDAP protocol. The THREDDS server version is 4.3.2 and runs atop an Apache Tomcat 7 server instance. Because of the prevalence of the Climate and Forecast (CF) conventions in the meteorological and oceanographic communities, the CF-1.6 standard has been adopted as the target metadata specification for datasets being hosted through the THREDDS server.

CTD casts from the hydrographic surveys are available through the map interface which points to the Thredds service hosting the CTD data. The map interface allows a user to graphically select a location of interest and view details about the cast and get the link to access the data. The Thredds service provides an interoperable platform to access these data. Matlab is used widely to analyze scientific data and also is an ideal software platform to interface with Thredds. Figure 7.1 details an example matlab script accessing data through this Thredds service and generating a graphic of a CTD cast (see figure 7.2).



```
1  addpath snctools/
2  addpath mexnc/
3  javaaddpath('./java/toolsUI-2.2.18.jar');
4
5  setpref('SNCTOOLS', 'USE_JAVA', true);
6
7  url='http://lismapping.uconn.edu:8080/thredds/dodsC/stratford_shoals/ss_ctd_profiles_2012_10.nc';
8
9  for prf=33
10     $prf=36;
11
12     %attach netcdf files to variables
13     depth=nc_varget(url,'z',[prf 0],[1 -1]);
14     Temp=nc_varget(url,'Temperature',[prf 0],[1 -1]);
15
16     plot(Temp(1:748),-depth(1:748));
17     xlabel('Temperature (C)');
18     ylabel('Depth (m)');
19     ttl=sprintf('Profile %i',prf);
20     title(ttl)
21
22     hold on
23     end
24
25     hold off
26
```

MATrix Laboratory length: 509 lines: 26 Ln: 1 Col: 1 Sel: 0 UNDX ANSI INS

Figure 7.1. Example Matlab script to access data from Thredds

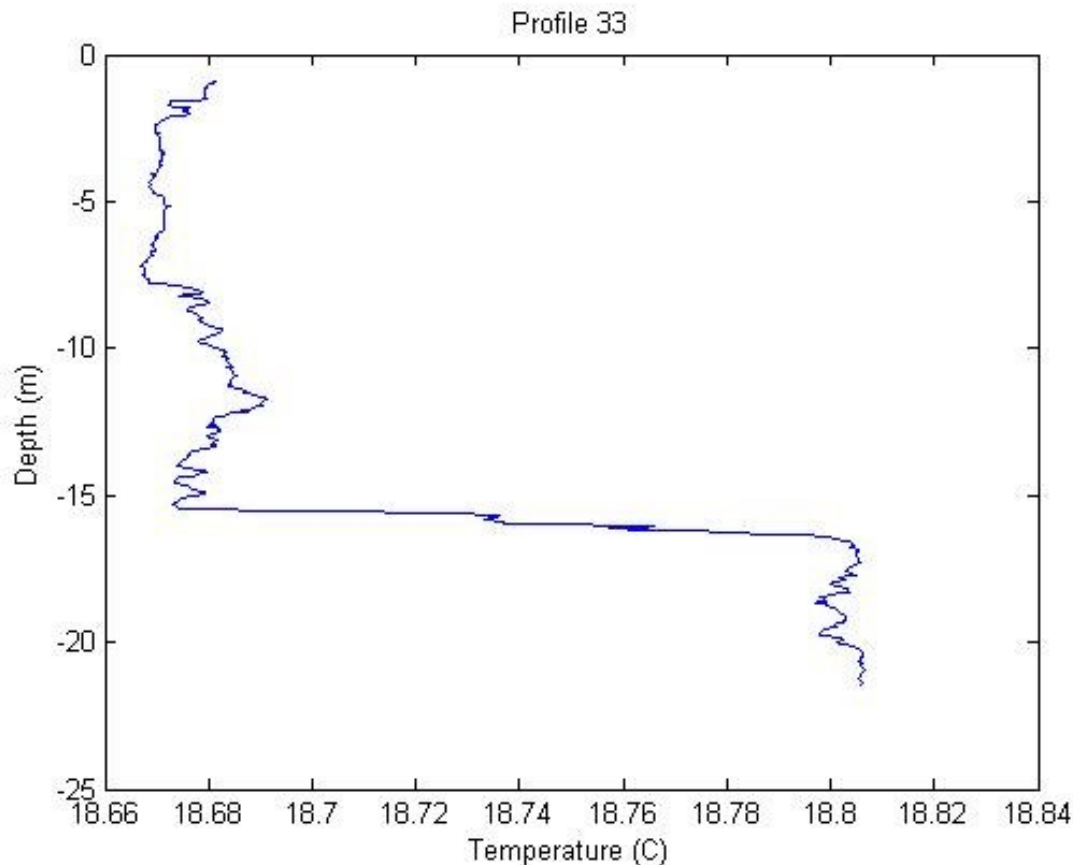


Figure 7.2. Matlab generate graphic of a CTD cast from data served from Thredds.

All model generated products have been created using model output from an implementation of FVCOM for Long Island Sound, which is run at the University Of Connecticut Department Of Marine Sciences. This FVCOM implementation has been calibrated for simulating hydrography and circulation as part of this pilot study focused around Stratford shoals.

FVCOM is a prognostic, unstructured-grid, finite-volume, free-surface, 3-D primitive equation coastal ocean circulation model developed by UMASSD-WHOI joint efforts. The model consists of momentum, continuity, temperature, salinity and density equations and is closed physically and mathematically using turbulence closure submodels. The horizontal grid is comprised of unstructured triangular cells and the irregular bottom is presented using generalized terrain-following coordinates. The General Ocean Turbulent Model (GOTM) developed by Burchard's research group in Germany (Burchard, 2002) has been added to FVCOM to provide optional vertical turbulent closure schemes. FVCOM is solved numerically by a second-order accurate discrete flux calculation in the integral form of the governing equations over an unstructured triangular grid. This approach combines the best features of finite-element methods (grid flexibility) and finite-difference methods (numerical efficiency and code simplicity) and provides a much better numerical representation of both local and global momentum, mass, salt, heat, and

tracer conservation. The ability of FVCOM to accurately solve scalar conservation equations in addition to the topological flexibility provided by unstructured meshes and the simplicity of the coding structure has made FVCOM ideally suited for many coastal and interdisciplinary scientific applications.

Bottom Stress maps for various conditions have been generated from the calibrated model runs for the Stratford shoals pilot region. These maps have been made available through available layers on this system. Maps of the typical maximum wave height, monthly mean bottom salinity and temperature are also available at the same location under the physical environment section (see Figure 7.3). A complete inventory of available data through the Long Island Sound Mapping site is detailed in Table 7.2.

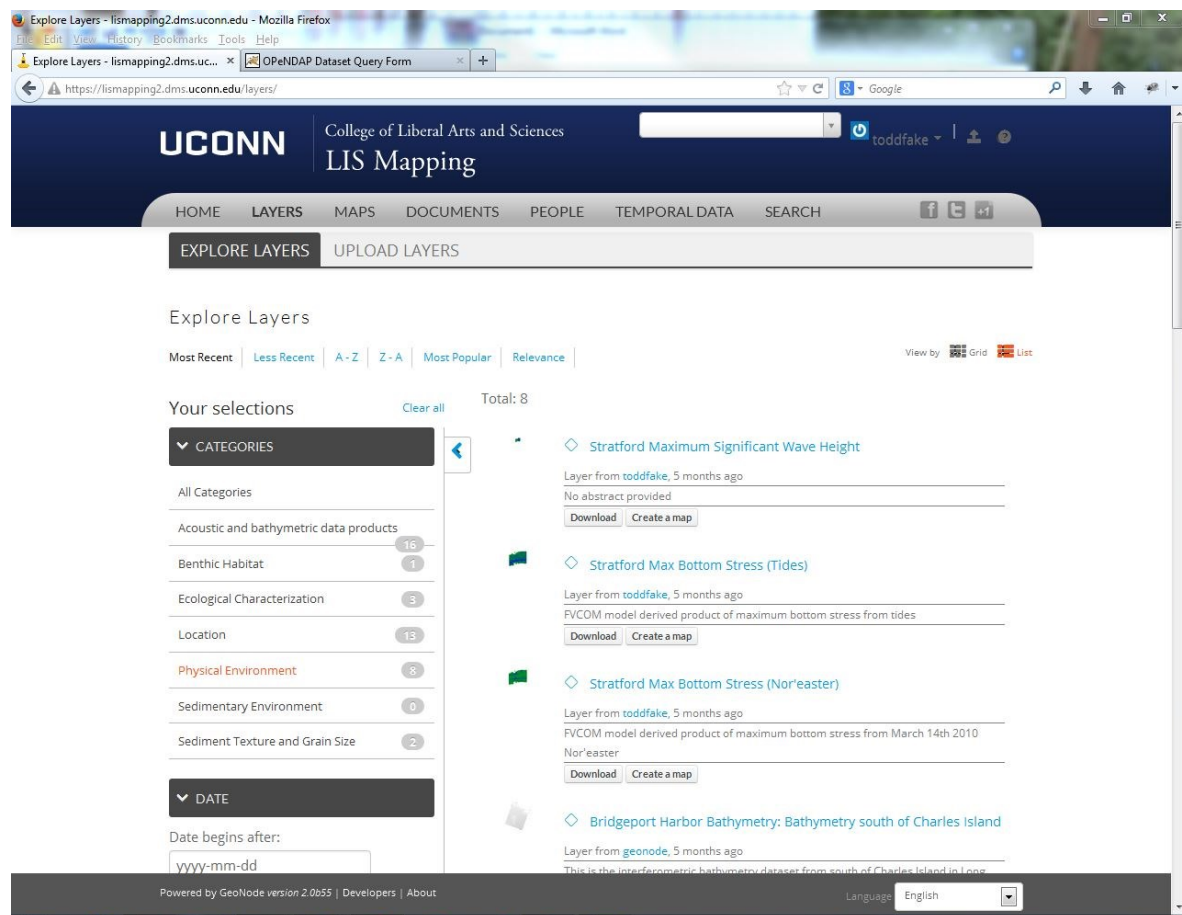


Figure 7.3. LIS Mapping Data System Physical Environment Layers

Table 7.2. Inventory of layers available through the UCONN Long Island Sound Mapping site

Layer Names	Description
stratford_temp_mean_1	FVCOM model derived product of mean January bottom temperature

Layer Names	Description
stratford_temp_mean_2	FVCOM model derived product of mean February bottom temperature
stratford_temp_mean_3	FVCOM model derived product of mean March bottom temperature
stratford_temp_mean_4	FVCOM model derived product of mean April bottom temperature
stratford_temp_mean_5	FVCOM model derived product of mean May bottom temperature
stratford_temp_mean_6	FVCOM model derived product of mean June bottom temperature
stratford_temp_mean_7	FVCOM model derived product of mean July bottom temperature
stratford_temp_mean_8	FVCOM model derived product of mean August bottom temperature
stratford_temp_mean_9	FVCOM model derived product of mean September bottom temperature
stratford_temp_mean_10	FVCOM model derived product of mean October bottom temperature
stratford_temp_mean_11	FVCOM model derived product of mean November bottom temperature
stratford_temp_mean_12	FVCOM model derived product of mean December bottom temperature
stratford_salt_mean_1	FVCOM model derived product of mean January bottom salinity
stratford_salt_mean_2	FVCOM model derived product of mean February bottom salinity
stratford_salt_mean_3	FVCOM model derived product of mean March bottom salinity
stratford_salt_mean_4	FVCOM model derived product of mean April bottom salinity
stratford_salt_mean_5	FVCOM model derived product of mean May bottom salinity
stratford_salt_mean_6	FVCOM model derived product of mean June bottom salinity
stratford_salt_mean_7	FVCOM model derived product of mean July bottom salinity
stratford_salt_mean_8	FVCOM model derived product of mean August bottom salinity
stratford_salt_mean_9	FVCOM model derived product of mean September bottom salinity
stratford_salt_mean_10	FVCOM model derived product of mean October bottom salinity
stratford_salt_mean_11	FVCOM model derived product of mean November bottom salinity
stratford_salt_mean_12	FVCOM model derived product of mean December bottom salinity
stratford_bstress_mean_tides	FVCOM model derived product of mean bottom stress due to tides
stratford_bstress_max_storms_sandy	FVCOM model derived product of max bottom stress during hurrican Sandy
Stratford Max Bottom Stress (Nor'easter)	FVCOM model derived product of maximum bottom stress from March 14th 2010 Nor'easter

Layer Names	Description
Stratford Max Bottom Stress (Waves)	FVCOM model product derived from running model with wave current interaction.
Stratford Max Bottom Stress (Tides)	FVCOM model derived product of maximum bottom stress due to tides
Stratford Maximum Significant Wave Height	FVCOM model derived product of max significant wave height
Pilot Area 4 26 12	Location of Pilot study area
H11044-11045_BPI_3x3Neighborhood_1m	BPI near LIS priority area near H11044 and H11045.
Bridgeport Harbor Bathymetry: Sidescan sonar north of Charles Island	This is the interferometric side scan backscatter dataset from north of Charles Island in Long Island Sound resulting from the URI shallow water mapping initiative associated with the Long Island Sound Mapping and Research Collaborative.
H12416_3101_0.5mBS_Version1	
H12416_S222_0.5mBS_Version1	
H12417_S222_0.5mBS_Version1	
H11044-11045_BPI_15x15Neighborhood_1m	BPI near LIS priority area near H11044 and H11045.
H12417_3101_0.5mBS_Version1	
Bridgeport Harbor Bathymetry: Bathymetry near Bridgeport Harbor	This is the interferometric bathymetry dataset from Bridgeport Harbor in Long Island Sound resulting from the URI shallow water mapping initiative associated with the Long Island Sound Mapping and Research Collaborative.
Bridgeport Harbor Bathymetry: Sidescan Sonar near Bridgeport Harbor	This is the interferometric side scan backscatter dataset from Bridgeport Harbor in Long Island Sound resulting from the URI shallow water mapping initiative associated with the Long Island Sound Mapping and Research Collaborative.
H11044-11045_Bathymetry_Uncertainty_50m	Bathymetry uncertainty over 50 meters.
H12417_3102_0.5mBS_Version1	1 meter bathymetry data near the LIS Priority area (around H11044-H11045).
Bridgeport Harbor Bathymetry: Bathymetry south of Charles Island	This is the interferometric bathymetry dataset from south of Charles Island in Long Island Sound resulting from the URI shallow water mapping initiative associated with the Long Island Sound Mapping and Research Collaborative.
H11044-11045_CurvaturePlan_1m	Curvature metrics near H11044-H11045.
Bridgeport Harbor Bathymetry: Bathymetry north of Charles Island	This is the interferometric bathymetry dataset from north of Charles Island in Long Island Sound resulting from the URI shallow water mapping initiative associated with the Long Island Sound Mapping and Research Collaborative.
dec2012_isis_nav	
2012-028Stationvideonav	

Layer Names	Description
Stratford Shoals CTD Profiles 2012 10	
Lis12Sr Allnav	Cruise paths for URI's R/V Shanna Rose for LIS Shallow Water Mapping pilot project.
Eastern Long Island Sound CTD Data taken March 2013	
lismarc_sampling_blocks	Sampling blocks delineated for the LISMaRC project.
LISMaRC Bottom Frames	Bottom Frames deployed as part of the LISMaRC project
2013-009_bphotolocsa1	
2013-009STATIONPHOTONAV: Navigation For Bottom Photographs Collected At Sampling Stations During Seaboss Operations Aboard the LISMaRC RV Connecticut Cruise (USGS Cruise ID 2013-009-FA) From May 21 to May 24, 2012 (Geographic, WGS84)	A benthic mapping survey cruise was conducted from the Research Vessel Connecticut from May 21-24, 2013 as part of the Long Island Sound Mapping and Research Collaborative (LISMaRC) contribution to the larger Long Island Sound Mapping effort. In addition to LISMaRC, other participants in this larger mapping effort include NOAA and another collaborative led by Lamont Doherty Earth Observatory at Comumbia University.
2012-028STATIONPHOTONAV: Navigation For Bottom Photographs Collected At Sampling Stations During Seaboss Operations Aboard the LISMaRC RV Connecticut Cruise (USGS Cruise ID 2012-028-FA) From October 10 to October 17, 2012 (Geographic, WGS84)	A benthic mapping survey cruise was conducted from the Research Vessel Connecticut from October 10-17, 2012 as part of the Long Island Sound Mapping and Research Collaborative (LISMaRC) contribution to the larger Long Island Sound Mapping effort. In addition to LISMaRC, other participants in this larger mapping effort include NOAA and another collaborative led by Lamont Doherty Earth Observatory at Comumbia University.
LISMaRC Sample Fixes	
2013-009CHNDATA.SHP: Total Organic Carbon, Hydrogen, and Nitrogen Data From Sediment Collected During the May 2013 RV Connecticut LISMaRC Cruise 2013-009-FA in Central Long Island Sound (Geographic, WGS84)	A benthic mapping survey cruise was conducted from the Research Vessel Connecticut from May 21-24, 2013 as part of the Long Island Sound Mapping and Research Collaborative (LISMaRC) contribution to the larger Long Island Sound Mapping effort. In addition to LISMaRC, other participants in this larger mapping effort include NOAA and another collaborative led by Lamont Doherty Earth Observatory at Comumbia University.
2012-028CHNDATA.SHP: Total Organic Carbon, Hydrogen, and Nitrogen Data From Sediment Collected During the October 2012 RV Connecticut LISMaRC Cruise 2012-028-FA in Central Long Island Sound (Geographic, WGS84)	A benthic mapping survey cruise was conducted from the Research Vessel Connecticut from October 10-17, 2012 as part of the Long Island Sound Mapping and Research Collaborative (LISMaRC) contribution to the larger Long Island Sound Mapping effort. In addition to LISMaRC, other participants in this larger mapping effort include NOAA and another

Layer Names	Description
	collaborative led by Lamont Doherty Earth Observatory at Comumbia University.
2013-009SEDDATA.SHP: Surficial Sediment Data Collected During the May 2013 RV Connecticut LISMaRC Cruise 2013-009-FA in Central Long Island Sound (Geographic, WGS84)	A benthic mapping survey cruise was conducted from the Research Vessel Connecticut from May 21-24, 2013 as part of the Long Island Sound Mapping and Research Collaborative (LISMaRC) contribution to the larger Long Island Sound Mapping effort. In addition to LISMaRC, other participants in this larger mapping effort include NOAA and another collaborative led by Lamont Doherty Earth Observatory at Comumbia University.
2012-028SEDDATA.SHP: Surficial Sediment Data Collected During the October 2012 RV Connecticut LISMaRC Cruise 2012-028-FA in Central Long Island Sound (Geographic, WGS84)	A benthic mapping survey cruise was conducted from the Research Vessel Connecticut from October 10-17, 2012 as part of the Long Island Sound Mapping and Research Collaborative (LISMaRC) contribution to the larger Long Island Sound Mapping effort. In addition to LISMaRC, other participants in this larger mapping effort include NOAA and another collaborative led by Lamont Doherty Earth Observatory at Comumbia University.

These map layers are available through the Long Island Sound Mapping GeoNode website (<https://lismapping2.dms.uconn.edu>). CTD data are available through the Long Island Sound Mapping THREDDS server (<http://lismapping.uconn.edu:8080/thredds/catalog.html>).

Temporal animations of surface and bottom tides are also available for viewing within this architecture. A google earth animated representation of the model output surface and bottom tides has been uploaded to the mapping website and is accessible under the Temporal Data section. This particular data is served using the Google Earth API which allows the time slider option for viewing temporal data which is represented in kmz format.

7.3 LIS Data Portal and Archive @ LDEO

The LIS Data Portal (<http://lis.marine-geo.org>, Figure 7.4) deployed at LDEO leverages the technical infrastructure of the Marine Geoscience Data System (MGDS; <http://www.marine-geo.org>), which is part of the NSF-Supported IEDA Data Facility (<http://www.iedadata.org>). MGDS is a well-established digital data repository and integrated data system (Carbotte et al., 2004) that provides a suite of tools and services for a diverse community of marine scientists, policy makers, educators and the general public. The MGDS team curates a metadata catalog and digital data repository that serves over 45 TB of data files, and provides links to data at over 30 external data systems and institutions.

MGDS/IEDA provides investigator-focused data stewardship support through the entire data life cycle – from the planning phase through acquisition to long-term data archiving, dissemination and publication. A variety of online tools are available through MGDS/IEDA to facilitate Data Management Planning, Data Submission, Data Search and Discovery, Data Visualization and Analysis, Data Publication, and Data Compliance Reporting. The LIS Data Portal @ LDEO (<http://lis.marine-geo.org>) hosted within the MGDS not only provides a solution for long-term archiving of metadata and data, but also provides full access to the suite of MGDS/IEDA services.

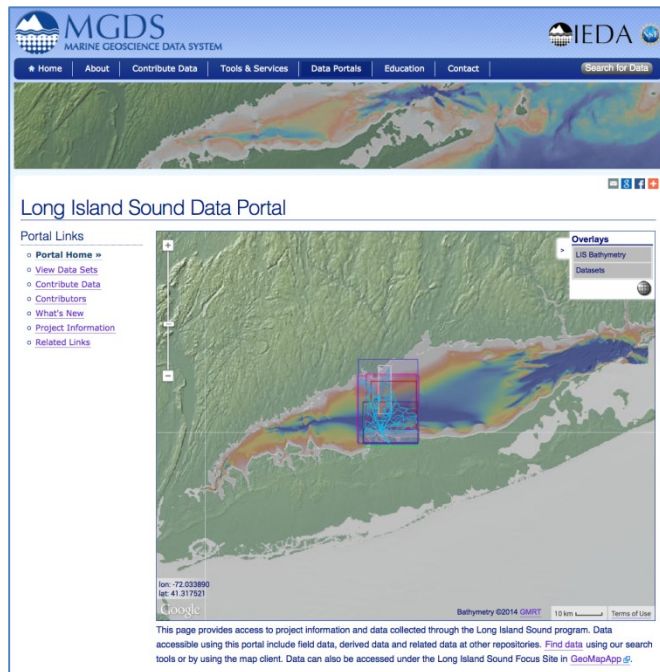


Figure 7.4 Long Island Sound Data Portal @ LDEO (<http://lis.marine-geo.org>) provides access to metadata, data and related documents.

7.3.1 *Technical Overview*

MGDS is supported by enterprise-level IT infrastructure ensuring that data are multiply replicated and systems are monitored to ensure the integrity and security of data holdings. All data files curated by MGDS are stored locally on our servers, with the data system backed up in triplicate, and long-term (100-year) preservation of data handled through agreements with the National Data Centers operated by NOAA for appropriate data types and formats, and through Columbia University Libraries for long-tail data that is not handled by NOAA Data Centers.

MGDS data cataloging, archiving and discovery services are driven by a geospatially-enabled PostgreSQL relational database backend, which is a rich metadata catalog that describes and provides access to data files and complementary descriptive metadata and related documents. For more details about the data model, please see: <http://www.marine-geo.org>

geo.org/about/datamodel.php. In addition to PostgreSQL, the data system makes use of PostGIS, MapServer, Google Maps API, GDAL, MB-System, GMT, and OpenLayers, as well as a suite of software tools developed in-house.

Data system design allows for three modes of data release: (1) fully open access with creative commons attribution (2) full proprietary hold until a date based on the funding agency's requirements, or (3) authenticated user access to data not yet publicly released. Regardless of release status, upon ingestion MGDS displays basic metadata (e.g. data type, device make/model, primary point of contact, file names and sizes) describing all datasets cataloged in the system in an effort to promote collegial sharing of data and to foster collaboration. Data release is typically done quarterly using a standard procedure of notifying contributors by email in advance of release, providing an opportunity to adjust release dates if necessary.

7.3.2 Data System Requirements Described in LIS SOW

The Scope of Work defined several system requirements for the data portal to ensure that it both meets the needs of the project teams and ensures long-term preservation and access. This section describes how the LIS Data Portal @ LDEO addresses each of those system requirements.

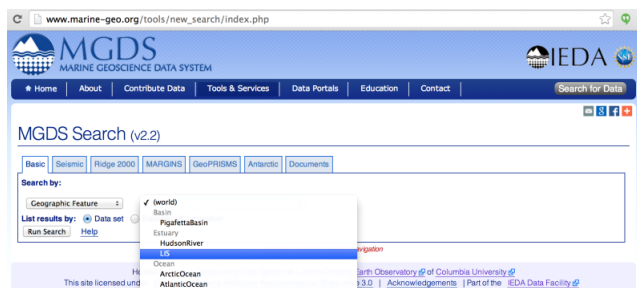
7.3.2.1 Search Interface

The MGDS Search interface (<http://www.marine-geo.org/tools/search>) leverages the rich metadata catalog to provide comprehensive searching across all data curated within MGDS based on a variety of parameters including Data Type, Device Type, Investigator, Cruise ID, Date, and Citation. A custom Search URL that shows all data sets cataloged in the LIS Data Portal is provided on the data portal page: http://www.marine-geo.org/tools/new_search/index.php?a=1&funding=LISS&output_info_all=on

Search results can be refined using the pull-down menus on the search results page.

7.3.2.2 Map-based data discovery

Geospatial information that is extracted from data curated by MGDS as part of the data ingestion process enables geospatial search options as well as map-based data discovery. Each data file, data set, and parent project has an associated geometry that is used for display and discovery. The LIS Data Portal page (<http://lis.marine-geo.org>) includes a Google Maps interface that provides basic map-based access to data (Figure 7.5). In addition, two geospatial options are provided within the search interface: (1) user-defined geographic extent defined in a map interface or by inputting coordinates, or (2) selecting an identified feature (Figure 7.5). All search results pages include an interactive map powered by the Google Maps API, which shows the spatial extent of data sets listed in the search results and provides links to access data and metadata (Figure 7.5b). In the coming months, MGDS will be augmenting its map displays system-wide to provide enhanced data discovery functionality. These system enhancements will automatically be applied to data curated within the LIS Data Portal.



MGDS: Map View

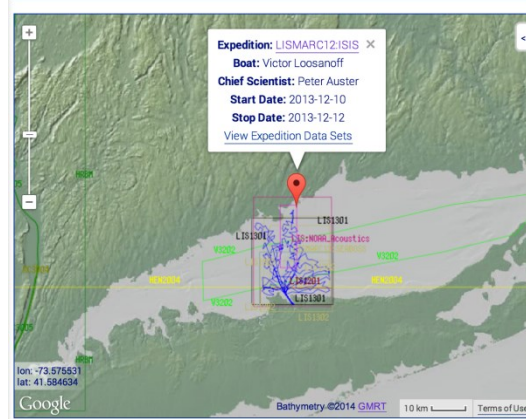


Figure 7.5 (Left) An interactive map client that is part of the LIS Data Portal page shows the geospatial extent of data sets and provides links for accessing metadata and datasets. A similar map interface is provided as part of the search results interface. **(Right)** MGDS search interface that includes a search by “Geographic Feature” option including Long Island Sound (LIS).

7.3.2.3 Data Archival

The MGDS data model accommodates raw and derived data products, project documentation, and links to data at distributed data centers. The metadata that is ingested into the relational database enables the rapid programmatic creation of a variety of formats of metadata records (e.g. ISO, FGDC). This functionality both optimizes the creation of required documentation for submitting data to the National Data Centers, and also enables interoperability with other data systems providing programmatic access data curated by MGDS. No data are only passed on to National Data Centers until after the proprietary release period has passed.

The MGDS metadata catalog also enables data publication through the creation of a Data Digital Object Identifier (DOI) metadata record, which ensures long-term preservation, access, and attribution. The Data DOI provides a unique identifier and permanent URL that is guaranteed to always resolve to a specific data set. Should a data set be moved from one repository to another, the Data DOI metadata would be updated and the DOI would continue to resolve to the exact set of data originally published with that DOI. A Data DOI has been issued for one data set from the LIS Mapping Project to demonstrate this functionality (Figure 7.6), see:

- <http://dx.doi.org/10.1594/IEDA/100433>
- http://www.marine-geo.org/tools/search/Files.php?data_set_uid=20099



Figure 7.6 – Data DOI issued for a data set – the data DOI is provided at the top of the page, and when the link is clicked on the “Data Citation Information” Tab (left) is activated showing users how to format the data citation. Data citation information is also included in data download packages.

7.3.2.4 Web Services & Interoperability

MGDS offers several OGC-Compliant web services including Web Feature Services (WFS), and Web Map Services (WMS). Development is currently underway expand MGDS Web Services and to set up Web Coverage Services (WCS). In addition, a new service that publishes ISO records (similar to FGDC) for all datasets will further enhance interoperability with other data systems by providing rapid machine access to the entire MGDS metadata catalog. Data and metadata at remote data centers are integrated into the system in two ways. First, in cases where a page exists within another system that contains cruise-level information, a link can be made at the cruise level. For example, see link to related data at USGS in the “Related Information” tab here: <http://www.marine-geo.org/tools/search/entry.php?id=LISMARC13:SEABOSS>. If data files exist within a different system, basic high-level metadata can be added to the system along with a link to the data, and the data set will be integrated within the list of data sets in search results and on relevant cruise pages and data compliance reports. An example of this is the link to raw data at NGDC here:

http://www.marine-geo.org/tools/search/entry.php?id=LIS:NOAA_Acoustics.

7.3.2.5 Cost-effective Ingestion of Data

Data ingested into the data system are vetted by data managers to ensure that metadata are complete and of high quality. An online data submission interface is available to facilitate

contribution of data and metadata to the MGDS (<http://www.marine-geo.org/submit/>), but data can also be submitted by FTP, rsync, or can be transferred by hard drive or DropBox. All data and metadata contributed to MGDS are integrated into the data system through the use of in-house software tools that assemble and validate metadata. Coupled with basic metadata supplied by contributors, these tools enable the rapid and consistent integration of data into the system with minimal impact on contributors and data managers.

7.3.2.6 Verification of data system integrity;

In addition to the enterprise-level IT monitoring and routine backups that are part of the core infrastructure, data system metadata and data file integrity are routinely monitored. This is done through the use of scripts that verify the consistency of metadata, check for broken URLs within the metadata catalog and on all public-facing webpages, and verify the integrity of data files on the file system.

7.3.3 Suggested Guidelines and Workflows to Facilitate Data Management

In order to facilitate data management efforts, Data Guidelines were assembled early in the project to promote consistent naming conventions for data files, sampling efforts, and field programs, and facilitate data documentation and management efforts. The guidelines were circulated by email and are posted on the LIS Data Portal: <http://www.marine-geo.org/portals/lis/SuggestedDataGuidelines.pdf>. A proposed workflow was put forth prior to data acquisition that was intended to promote contemporaneous data documentation, and optimize data flow and integration within the LIS Data Portal @ LDEO with an eye toward long-term curation (Figure 7.7). In addition, a “data matrix” was circulated in Fall 2013 to help provide a detailed list of anticipated data products (both raw and derived data) and create a roadmap to assist in data management efforts. When used, these documents and guidelines can significantly increase efficiency for data producers and data managers alike.

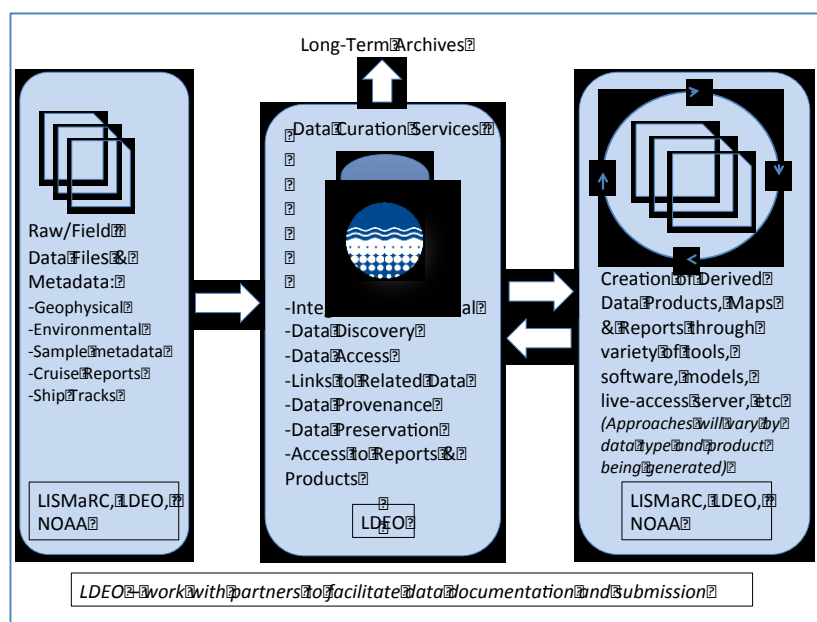


Figure 7.7 – Proposed data flow showing relationship of data management efforts at LDEO and LISMARC, and the Data Portal @ LDEO as the conduit for long-term data preservation

7.3.4 How to Browse and Access Data in the LIS Data Portal @ LDEO

Data can be accessed in a variety of ways through the LIS Data Portal @ LDEO. Visiting <http://lis.marine-geo.org>, and clicking on “View Data Sets” link will perform a query of the database and return all data sets currently cataloged in the system that are associated with this LIS mapping effort. Clicking on any data type in the resulting list will route the user to a webpage that lists all data files for each data set.

If authentication is required to download data (a feature that is typically in place prior to data being in “final release” status,) users must click on the “Login” button in the top right corner of the webpage (Figure 7.8). New users will be required to follow the instructions in the Authenticated Access section below. Note that once a user enters goes through the process of registering and entering the passkey for the LIS Data Portal, they will be granted access to all project related data sets. Once logged in the user can select and download files of interest (Figure 7.9)



Figure 7.8 Appearance of data set page to a non-authenticated user, or when an authenticated user is not logged in. Note the red lock symbol indicates that data are not released. The release date is also shown for each data file. The Login button, for authenticated users to login to the system, is located at the top right of the page.



Figure 7.9 Appearance of data set page once an authenticated user is logged in. Note that the lock is now green indicated that access is granted. Check boxes are also now displayed next to each data file name, as is a “Select All” box above the list of data files. To download data, select the files of interest, and press “Download Selected Data Files” just below the green unlocked symbol.

7.3.5 Data Download Statistics

When users download data from MGDS, they are required to state their intended purpose (Education, Research, Personal, Other). Intended purpose and details of specific files download are logged in a statistics database, which is used to generate data download reports. Twice each year, emails are sent to all data contributors who have had data downloaded over the past six months to inform them of download activity. These reports could also be copied to members of

the Steering Committee, if desired. An example data download report for data contributed is shown in Figure 7.10. Note that the statistics database also tracks users being re-routed to data at remote repositories that are cataloged in the system (e.g. raw swath bathymetry data at NGDC).

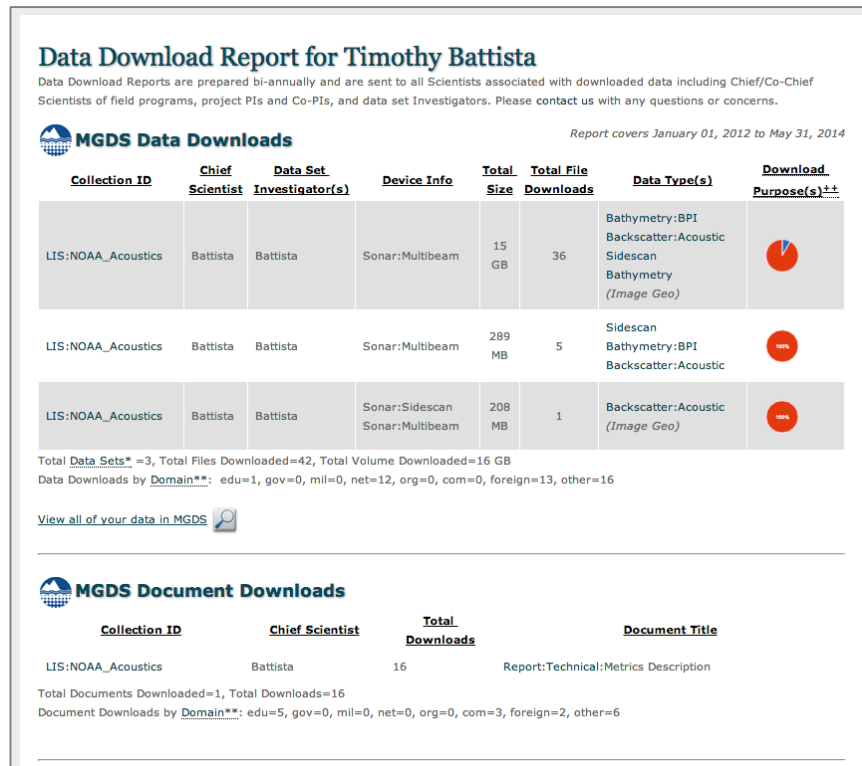


Figure 7.10 Example data download report for data contributor Tim Battista. Report shows intended use, total number of downloads and total volume downloaded. To view this report online, see:

http://www.marine-geo.org/about/stats/reports/DownloadReport.php?person_id=Battista_Timothy&start_date=2012-01-01&stop_date=2014-05-31